NanoScience and Technology

Peter Gehr
Reinhard Zellner *Editors*

Biological Responses to Nanoscale Particles

Molecular and Cellular Aspects and Methodological Approaches

Springer

NanoScience and Technology

The series NanoScience and Technology is focused on the fascinating nano-world, mesoscopic physics, analysis with atomic resolution, nano and quantum-effect devices, nanomechanics and atomic-scale processes. All the basic aspects and technology-oriented developments in this emerging discipline are covered by comprehensive and timely books. The series constitutes a survey of the relevant special topics, which are presented by leading experts in the field. These books will appeal to researchers, engineers, and advanced students.

More information about this series at http://www.springer.com/series/3705

Peter Gehr · Reinhard Zellner
Editors

Biological Responses to Nanoscale Particles

Molecular and Cellular Aspects and Methodological Approaches

Springer

Editors
Peter Gehr
Institute of Anatomy
University of Bern
Bern, Switzerland

Reinhard Zellner
Institute of Physical Chemistry
University of Duisburg-Essen
Essen, Germany

ISSN 1434-4904 ISSN 2197-7127 (electronic)
NanoScience and Technology
ISBN 978-3-030-12460-1 ISBN 978-3-030-12461-8 (eBook)
https://doi.org/10.1007/978-3-030-12461-8

Library of Congress Control Number: 2018968395

This Springer imprint is published by the registered company Springer Nature Switzerland AG
The registered company address is: Gewerbestrasse 11, 6330 Cham, Switzerland

Foreword

Engineered nanoparticles, as one of the principal components of the twenty-first-century nanomaterials toolbox, have had a transformative impact on research, research translation, and development of a wide range of applications in physics, optics, electronics, and medicine. The research interest in nanoparticles is intense as a result of the emergence and use of newly acquired size-dependent properties, including quantum confinement in semiconductor particles, photoactivation in TiO_2 and ZnO, surface plasmon resonance in metals and metal oxides, super-hydrophobicity from surface coatings with organic molecules, super-paramagnetism of magnetic materials, a dynamic range of surface redox active properties, oxidative/reductive surface dissolution with the release of reactive ionic groups, or controllable colloidal behaviors (aggregation, dispersion, diffusion, sorption). These nanoscale properties can be introduced into new nanoparticles by bottom-up synthetic techniques, including hydrothermal synthesis, pyrolysis, chemical precipitation, ion implantation, gas condensation, supramolecular assembly, etc. Moreover, it is also possible to use top-down methods for the size reduction of macroscale or microscale particles through techniques such as ball milling. While pristine nanoparticles may be used as such in the form of powders or suspensions, these materials are often embedded, conjugated, or incorporated into more complex matrices such as polymers, clothes, building materials, cosmetics, foods, polymers, electronic circuits, etc.

From the perspective of material properties and functions, nanoparticles can be thought of as a link between bulk materials and atomic or molecular structures. A key consideration for the use of nanoparticles in a wide range of industrial and biomedical applications is the interfacial properties of the particle surface in relation to the surrounding medium. While the interfacial layer characteristically consists of metallic surfaces, ions, and organic and inorganic molecules, inorganic particle surfaces are frequently coated by organic molecules, which serve as capping agents, stabilizers, surface ligands, or passivating agents. In order to fully understand the use and interfacial behavior of nanoparticles, it is necessary to characterize newly emerging materials by an array of physicochemical techniques such as microscopy (e.g., optical microscopy, transmission electron microscopy, scanning probe microscopy), elemental analysis, spectroscopy (e.g., X-ray, UV-Vis, infrared and nuclear magnetic resonance spectroscopy, mass spectroscopy), light scattering methods (e.g., laser,

X-ray or neutron scattering), electrophoresis (e.g., zeta potential and charge), the Brunauer–Emmett–Teller method (to assess surface area), and X-ray diffraction analysis (to assess crystal structure).

In this challenging book project by Gehr and Zellner, the Biological Responses to Nanoscale Particles, a number of leading scientists have combined expertise to delineate the behavior of nanoparticles on a wide range of nano/bio-interfaces, which ranges from the effects on biomolecules (e.g., the protein corona) to interactions with cells, tissue barriers, and organs. The authors delineate the importance of a variety of intrinsic nanomaterial properties (such as chemical composition, size, shape, dimensions, zeta potential), which are dynamically altered in the presence of biological media to acquire an additional set of extrinsic material properties (e.g., a protein corona, colloidal stability, hydrodynamic diameter, charge, dissolution properties) to shape the outcome at the nano/bio-interface. The various chapters lead us through the cellular uptake mechanisms for nanoparticles, subcellular localization and processing, as well as interactions with cell biology and signaling pathways. The spectrum of interactions includes the catalysis of biological advantageous outcomes as well as the generation of adverse cellular effects through the generation of oxidative stress and genotoxicity. Interestingly, while the generation of danger signals in the immune system could result in adverse outcomes, it is equally possible to use these danger signals gainfully to improve vaccination responses, in addition to the use of nanoparticles to improve antigen delivery. There is also a delineation of the use of nanoscale properties to study cellular structure and function, including to develop novel advanced cellular imaging techniques such as optical microscopy, Raman microscopy, optical near-field microscopy, X-ray microscopy, and spectral microscopy. We also obtain new insight into the use of nanoparticle physicochemical properties to control fate and transport in the gastrointestinal tract, with applications in the food industry and food processing. There is also a description of the nanoparticle interactions with the skin, including the ability to penetrate into the stratum corneum and the follicular ducts, but not into the deeper layers. Turning to the use of nanoparticles for therapeutic purposes, we learn about the versatility of the design, synthesis, and characterization of polymeric nanocarriers for drug delivery applications, including the use of nanoscale design features for stimulus–response coupling leading to drug release.

I appreciate the hard work of the editors, who spared no effort in the development and successful conclusion of an exciting book project. The readers will receive an excellent overview of new ideas, findings, and applications of nanoparticle physicochemical properties in shaping biological outcomes and possible effects on human health.

Andre Nel
Distinguished Professor of Medicine
and Director of Research, California
NanoSystems Institute (CNSI),
School of Medicine, University of
California, Los Angeles (UCLA)

Preface

The topics of nano-science and nanotechnology and the associated fields of research applications like nano-biology, nano-toxicology, and nano-medicine have evolved quickly in recent years. In all these fields, the nature and outcome of the interaction of nanoparticles with the biological system is of key interest. With all the exciting applications of nanomaterials in chemistry, physics, electronics, optics, material science, biology, medicine, and many other fields in mind, one should also carefully investigate the potential risk, i.e., the adverse health impact of nanomaterials upon interaction with the organism. There is, therefore, an urgent need for a detailed understanding of the mechanisms and outcomes of the interaction of nanoparticles with the biological system including the cellular and even molecular level.

The rapid development of nanotechnology has resulted in increased technical applications of a variety of nanoparticles, which may be released into the environment and to which humans may be exposed accidentally, either at the workplace or in the ambient environment. A special situation becomes apparent when nanoparticle is being used in medicine. In this special field of nanotechnology, called nano-medicine, nanoparticles are designed for diagnostic as well as for therapeutic applications. Moreover, this field has lately also advanced in a combination of a specific and targeted therapy with specific targeted diagnostic tests, called theranostics. With these advances, it became imperative to obtain a better understanding of how and on which sites nanoparticles interact with organs and the organism. It is expected that with an improved and elementary understanding of this interaction the risk and the impact of nanomaterials on human health will be better understood. The present book serves this purpose. It covers our current knowledge on the interaction of nanoparticles with our organism, nanoparticles which may be toxic or pathogenic in nature as well as the promising beneficial aspects of nanoparticles applied in diagnostics or therapeutics or in a combination of the two.

Nanoparticles can enter the body primarily via three different pathways: inhalation, ingestion, and uptake via the skin. While the intact skin seems to efficiently prevent nanoparticles from entering our organism, the gastrointestinal tract and probably even more the lungs allow nanoparticles to access the inside of our organism. After deposition on the inner surface of the gastrointestinal tract and the

lung, they penetrate through liquid layers, cells, and tissues and eventually enter the capillary network in the sub-epithelial regions. With the blood, these minuscule particles will translocate into the other organs and may be distributed throughout the whole organism.

It is our intention to present with this book to the reader the events that nanoparticles encounter when interacting with our organism, when moving from the internal surfaces where they had been deposited through tissue into the blood-stream. In order to understand these pathways, we first need to know the physical, chemical, and biological properties of individual types of nanomaterials and how these are manufactured in a reproducible way. In the first part of the book, therefore, the synthesis and characterization of nanoparticles are presented including their physical behavior in biologically relevant environments. In the second part, the mechanisms of interaction with our organism on a cellular and molecular level including the methodology of investigation are described. In the third part, the cellular responses and possible health effects are discussed.

We invited experts for each of these topics to cover these sequences of events, and we were very pleased that many of the scientists we had contacted accepted our invitation. The different chapters had been thoroughly reviewed by the editors as well as by external reviewers to ensure the quality of each chapter with the most updated and comprehensive knowledge.

Finally, we are indebted to the people who were responsible for producing this book. Foremost we are grateful to the chapter authors for their passionate and very valuable contributions to this book. We would also like to thank the external reviewers. Finally, we would like to express our appreciation to the staff of Springer Nature for their patient and invaluable professional assistance in producing this book.

Bern, Switzerland — Peter Gehr
Essen, Germany — Reinhard Zellner

Contents

Contributors

Sandor Balog BioNanomaterials, Adolphe Merkle Institute, Fribourg, Switzerland

Denise Bargheer Institute of Biochemistry and Molecular Cell Biology, University Medical Center Eppendorf, Hamburg, Germany

Fabian Blank Respiratory Medicine, Department of BioMedical Research (DBMR), University of Bern, Bern, Switzerland

Ulrike Blume-Peytavi Department of Dermatology, Venerology and Allergology, Charité – Universitätsmedizin Berlin, Berlin, Germany

Joël Bourquin BioNanomaterials, Adolphe Merkle Institute, Fribourg, Switzerland

Martin J. D. Clift In Vitro Toxicology Group, Swansea University Medical School, Institute of Life Sciences, Swansea, Wales, UK

Shareen H. Doak In Vitro Toxicology Group, Swansea University Medical School, Institute of Life Sciences, Swansea, Wales, UK

Matthias Epple Inorganic Chemistry, University of Duisburg-Essen, Essen, Germany

Stephen J. Evans In Vitro Toxicology Group, Swansea University Medical School, Institute of Life Sciences, Swansea, Wales, UK

Alexander Eychmüller Physical Chemistry, Technical University of Dresden, Dresden, Germany

Wye-Khay Fong BioNanomaterials, Adolphe Merkle Institute, Fribourg, Switzerland

Andreas Frey Division of Mucosal Immunology and Diagnostics, Research Center Borstel, Borstel, Germany

Kleanthis Fytianos Respiratory Medicine, Department of BioMedical Research (DBMR), University of Bern, Bern, Switzerland

Nikolai Gaponik Physical Chemistry, Technical University of Dresden, Dresden, Germany

Gabriella Gébel Institute of Biochemistry and Molecular Cell Biology, University Medical Center Eppendorf, Hamburg, Germany

Artur Giemsa Institute of Biochemistry and Molecular Cell Biology, University Medical Center Eppendorf, Hamburg, Germany

Christina Graf Department of Chemistry and Biotechnology, University of Applied Sciences Darmstadt, Darmstadt, Germany

Markus Heine Institute of Biochemistry and Molecular Cell Biology, University Medical Center Eppendorf, Hamburg, Germany

Marius Hittinger Helmholtz Institute for Pharmaceutical Research Saarland (HIPS), Saarbrücken, Germany;
PharmBioTec GmbH, Saarbrücken, Germany

Banu Iyisan Max Planck Institute for Polymer Research, Mainz, Germany

Gareth J. Jenkins In Vitro Toxicology Group, Swansea University Medical School, Institute of Life Sciences, Swansea, Wales, UK

Fanny Knorr Department of Dermatology, Venerology and Allergology, Charité – Universitätsmedizin Berlin, Berlin, Germany

Jürgen Lademann Department of Dermatology, Venerology and Allergology, Charité – Universitätsmedizin Berlin, Berlin, Germany

Katharina Landfester Max Planck Institute for Polymer Research, Mainz, Germany

Marco Lattuada International Iberian Nanotechnology Laboratory, Water Quality Group, Braga, Portugal

Ingmar Lautenschläger Clinic for Anesthesiology and Operative Intensive Care Medicine, University Hospital Schleswig-Holstein, Kiel, Germany

Claus-Michael Lehr Helmholtz Institute for Pharmaceutical Research Saarland (HIPS), Saarbrücken, Germany;
PharmBioTec GmbH, Saarbrücken, Germany

Kateryna Loza Inorganic Chemistry, University of Duisburg-Essen, Essen, Germany

Volker Mailänder Department of Dermatology, University Medical Center of the Johannes Gutenberg-University Mainz, Mainz, Germany;
Max-Planck-Institute for Polymer Research, Mainz, Germany

Michael Maskos Fraunhofer-Institute for Microengineering and Microsystems (IMM), Mainz, Germany

Martina Claudia Meinke Department of Dermatology, Venerology and Allergology, Charité – Universitätsmedizin Berlin, Berlin, Germany

Lorna Moll Department of Dermatology, University Medical Center of the Johannes Gutenberg-University Mainz, Mainz, Germany;
Max-Planck-Institute for Polymer Research, Mainz, Germany

Thomas L. Moore BioNanomaterials, Adolphe Merkle Institute, Fribourg, Switzerland

Loretta Müller University Children's Hospital Basel, Basel, Switzerland;
Department of Pediatrics, Inselspital, Bern University Hospital, Bern, Switzerland

Xabier Murgia Helmholtz Institute for Pharmaceutical Research Saarland (HIPS), Saarbrücken, Germany

Peter Nielsen Institute of Biochemistry and Molecular Cell Biology, University Medical Center Eppendorf, Hamburg, Germany

Alexa Patzelt Department of Dermatology, Venerology and Allergology, Charité – Universitätsmedizin Berlin, Berlin, Germany

Alke Petri-Fink BioNanomaterials, Adolphe Merkle Institute, Fribourg, Switzerland;
Department of Chemistry, University of Fribourg, Fribourg, Switzerland

Katrin Ramaker Divison of Mucosal Immunology and Diagnostics, Research Center Borstel, Borstel, Germany

Christin Rengers Physical Chemistry, Technical University of Dresden, Dresden, Germany

Niels Röckendorf Division of Mucosal Immunology and Diagnostics, Research Center Borstel, Borstel, Germany

Laura Rodriguez-Lorenzo BioNanomaterials, Adolphe Merkle Institute, Fribourg, Switzerland;
International Iberian Nanotechnology Laboratory, Water Quality Group, Braga, Portugal

Barbara Rothen-Rutishauser BioNanomaterials, Adolphe Merkle Institute, Fribourg, Switzerland

Eckart Rühl Physical Chemistry, Institute of Chemistry and Biochemistry, Free University of Berlin, Berlin, Germany

Nicole Schneider-Daum Helmholtz Institute for Pharmaceutical Research Saarland (HIPS), Saarbrücken, Germany

Dimitri Vanhecke BioNanomaterials, Adolphe Merkle Institute, Fribourg, Switzerland

Anika Vogt Department of Dermatology, Venerology and Allergology, Charité – Universitätsmedizin Berlin, Berlin, Germany

Barbara Wollenberg Department of Ear, Nose and Throat, University Hospital Schleswig-Holstein, Lübeck, Germany

Part I
Manufacturing and Characterization of Materials

Chapter 1
Synthesis of Metallic and Metal Oxide Particles

Kateryna Loza and Matthias Epple

Abstract The diversity of applications in catalysis, energy storage and medical diagnostics utilizes unique and fascinating properties of metal and metal oxide nanostructures. Confined to the nanometer scale, materials may display properties that are different from the equivalent bulk compounds. To meet the requirements for various applications, numerous production techniques were developed to control particle size, morphology, aggregation state, crystal structure, surface charge and composition. This chapter presents an overview of the preparation of metallic and metal oxide nanoparticles by bottom-up and top-down approaches. We describe basic synthetic routes for prominent cases of metals (gold, silver, platinum and copper) and metal oxides (zinc oxide, titania, and silica).

1.1 Introduction

Metal nanostructures attract particular interest because of their unique and fascinating properties compared to their bulk counterparts. The variety of applications comprises biological sensing [1, 2], imaging [3–9], medical diagnostics [10–12], cancer therapy [13, 14], catalysis [15, 16], and energy storage [17, 18]. The observed new chemical, optical, and thermal properties of metallic nanoparticles occur when the size is confined to the nanometer length scale [19]. Numerous techniques were developed to produce metal nanoparticles to meet the requirements for various applications. In general, there are two strategies to manufacture materials on the nanoscale: "Top-down" and "bottom-up" (Fig. 1.1) [20, 21]. The first method is based on breaking down a system (i.e., the bulk material) into smaller units. Common "top-down" techniques are lithography, milling, ultrasound treatment, and laser ablation. These processes

K. Loza (✉) · M. Epple
Inorganic Chemistry, University of Duisburg-Essen, Universitätsstrasse 2, 45141, Essen, Germany
e-mail: Kateryna.Loza@uni-due.de

M. Epple
e-mail: Matthias.epple@uni-due.de

P. Gehr and R. Zellner (eds.), *Biological Responses to Nanoscale Particles*, NanoScience and Technology, https://doi.org/10.1007/978-3-030-12461-8_1

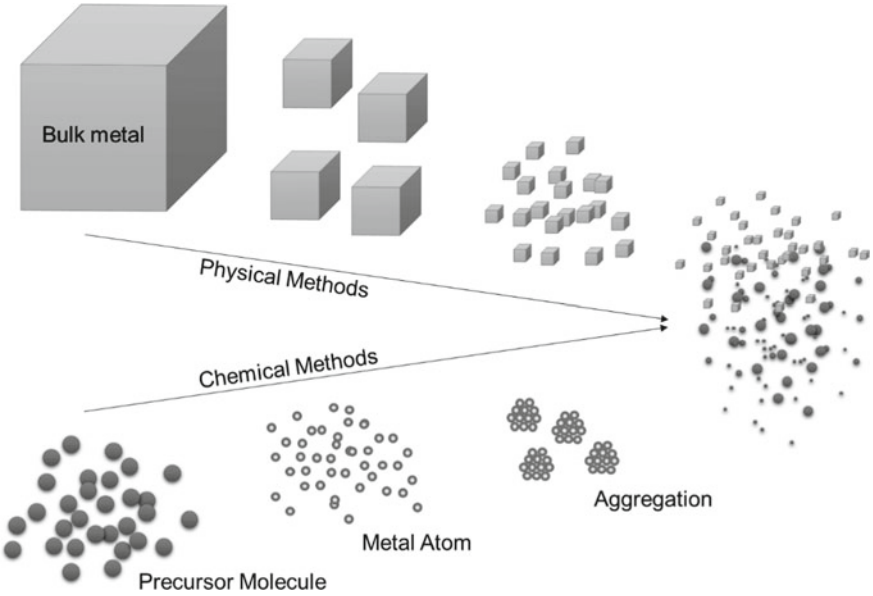

Fig. 1.1 Schematic illustration of synthetic methods for metal nanoparticles. (Adapted with permission from New J. Chem., 1998, 1179–1201. Copyright 1969 The Royal Society of Chemistry) [22]

are comparatively simple and usually lead to ligand-free ("naked") nanoparticles. However, there is a limited control over the manufacturing process, e.g., an exact size or shape adjustment of resulting particles. The "bottom-up" method relies on material synthesis from atomic or molecular species via a suitable chemical reaction, allowing the particles to grow from smaller units. This approach uses the chemical properties of single molecules or atoms to cause self-organization into the desired particle shape.

The "bottom-up" approach is commonly associated with wet-chemical methods, because colloidal metallic particles are commonly produced by chemical reduction of metal salts dissolved in a suitable solvent in the presence of surfactants or ligands that cover the surface [23]. A wide range of reducing agents have been used in the colloid-chemical synthesis of metal nanoparticles [24]. For example, H_2, hydrazine, hydroxylamine, hydrides (e.g. $NaBH_4$ or B_2H_6), ascorbic acid or ascorbate, citric acid or citrate, reducing polymers (e.g., PVA) and solvents (like alcohols, diols, aldehydes, and DMF) have been used to prepare metal nanoparticles [25–29]. Reduction can take place at room temperature or at elevated temperatures, depending on the relative reduction potentials of the precursor and the reducing agents [30–33].

In the following, we discuss the cases of gold, silver, copper, and platinum as representative examples, and also the preparation of alloyed nanoparticles by various synthetic methods. The described methods can typically be transposed to other kinds of nanoparticles, typically of noble metals.

1.2 Metals (Gold, Silver, Platinum and Copper)

1.2.1 Gold

The first systematic synthesis of Au colloids was reported 160 years ago by Michael Faraday using phosphorus to reduce $AuCl_4^-$ ions [34]. In the 1950s, an easier approach was established and standardized by Turkevich [35]. He used the mildly reducing agent trisodium citrate, added to a boiling aqueous solution of $HAuCl_4$, to obtain monodisperse gold nanoparticles in the size range from 10 to 40 nm. Due to its simplicity, this synthesic method was adapted in many variations [36, 37]. For example, switching to a mixture of reducing agents (e.g. citrate and tannine) allows to clearly shorten the reaction time and to enhance the stability of the formed colloid [38, 39].

The reduction of tetrachloroauric acid in an aqueous medium is a versatile synthetic route and possible with many different reducing agents like sodium borohydride ($NaBH_4$), ascorbic acid, and hydroquinone [40–42]. The use of $NaBH_4$ as reducing agent results in a fast reduction and a gold particle size of 1–5 nm [29, 43, 44]. In general, the choice of the reducing agent has a strong influence on the resulting particle size, since with increasing reduction potential the number of the formed nuclei increases and the growth of particles is limited. On the nanometer scale, metals tend to nucleate and grow into multiply twinned particles with their surfaces defined by the lowest-energy facets [45]. Anisotropic gold nanoparticles (rod-, rectangle-, hexagon-, cube-, triangle- and star-like shapes) with less stable facets were kinetically achieved by adding chemical capping reagents, i.e. agents that selectively block certain crystal faces, to the reaction mixture [25, 46, 47].

The previously described methods are based on a synthesis from atomic or molecular species by chemical reaction, so called “bottom-up” approach. In liquid media, dispersed metallic nanoparticles can be generated by the pulsed laser ablation process, a “top down” technique [48]. This method provides ligand-free nanoparticles [49]. The size of obtained particles can be varied to some extent by the laser parameters and by subsequent laser fragmentation steps [50, 51]. Furthermore, an in situ conjugation of nanoparticles with biomolecules by laser ablation in an aqueous medium is a highly promising one-step method for the production of functional nanoparticles [52].

The polydispersity of nanoparticles is a key concern in nanoscience research. Even though reasonably monodisperse nanoparticles can be produced, usually not all nanoparticles are fully identical (see Fig. 1.2 for an example). This fact leads to the ultimate aim for a synthesis of atomically precise nanoparticles [53]. In the case of gold, this was accomplished for ultrasmall gold nanoparticles (containing 10–300 atoms, often called nanoclusters) [54, 55]. Several groups established synthetic routes to produce a gold core in the size range of 1–3 nm. Such ultrasmall nanoparticles are typically formed by metal salt reduction in the presence of phosphanes (PR_3) [56, 57] or thiols (HS–R) [44]. Exerting a strict control over the size of a cluster strongly affects the activity and the selectivity in a catalytic process [58]. Furthermore, a

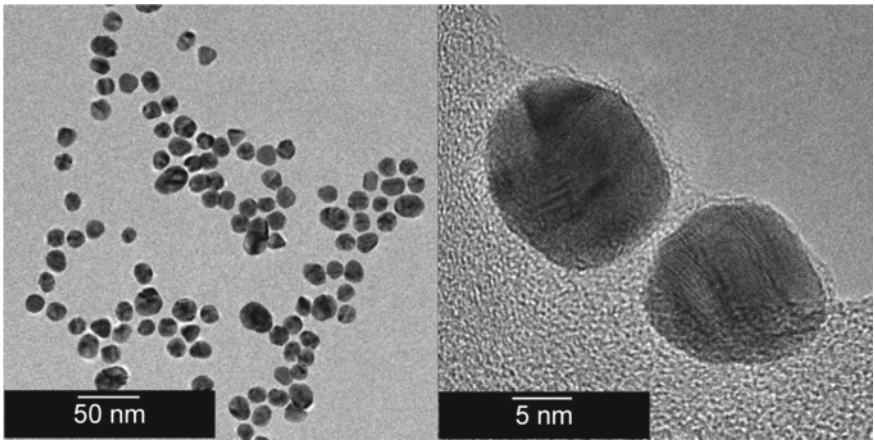

Fig. 1.2 Transmission electron micrographs of PVP-stabilized gold nanoparticles, prepared by the standard citrate method after Turkevich. (Reproduced from the dissertation of D. Mahl, 2011, University of Duisburg-Essen) [60]

supracolloidal self-assembly of atomically precise nanoparticles is a promising platform for novel 2D and 3D materials with additional plasmonic functionalities, novel mechanical properties, and inherent flexibility [59].

1.2.2 Silver

Colloidal silver is known since about 120 years [61]. The manufacturing of silver nanoparticles can be done by physical processes such as ultrasonication, chemical vapor deposition, or pulsed laser ablation in liquids [62–64]. However, wet-chemical "bottom-up" syntheses offer more possibilities for the variation of particle size, morphology and functionalization. The most commonly used precursor for preparing silver nanoparticles in wet-chemical reductions is silver nitrate ($AgNO_3$) because of its high solubility in many polar solvents and dispersability in less polar solvents, sometimes after adding surfactants and/or using ultrasonication. The reducing agents used in the synthesis of nanoparticles from silver(I) ions are comparable to those used for gold nanoparticle preparation. Already in 1889, M. C. Lea published the synthesis of citrate-stabilized silver nanoparticles [65]. In general, one-pot methods for the reduction of silver nitrate have evolved, where different reducing agents such as sodium citrate [66], glucose [67], ascorbate [68], sodium borohydride [69, 70], polyols [71, 72], and ammonium formiate were used [73]. Typically, the reactions are performed at elevated temperatures by conventional heating in an oil bath. Alternatively, microwave-assisted syntheses can increase the reaction rates and yields as well as selectivity and reproducibility [30].

The particle properties depend not only on their size but also on their morphology. As a result, a shape-controlled synthesis of silver nanoparticles is of special

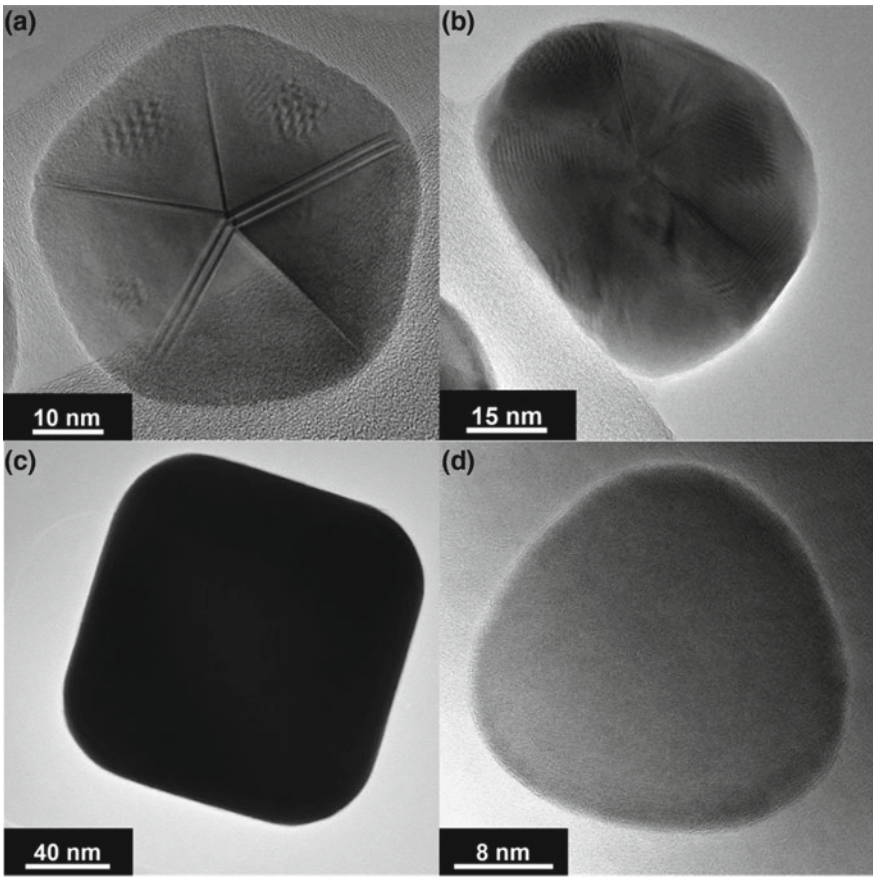

Fig. 1.3 Transmission electron micrographs of different kinds of PVP-stabilized silver nanoparticles, prepared by glucose reduction (**a**) [67], a microwave-assisted reduction (**b**) [30], a modified polyol synthesis (**c**) [79], and a microwave-assisted modified polyol process (**d**) [80]. (Adapted with permission from Cryst. Growth Des. 16, 7, 3677–3687. Copyright 2016 American Chemical Society) [81]

interest. Xia et al. and others described the structural evolution of silver nanoseeds to nanoparticles with defined shapes like platelets [74], cubes [75], rods [76], rings [77], and bipyramids [78] (Fig. 1.3).

It is critical to understand not only the growth mechanism of nanostructures, but the process of seed formation, because the number of twin planes in the initial stage is the key factor for determining the shape of the final product (single-crystal seeds form cubes, multiply-twinned decahedral seeds form wires) [82].

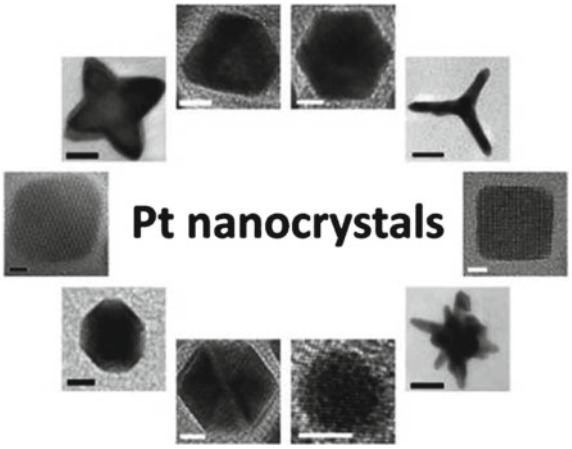

Fig. 1.4 Transmission electron micrographs of platinum nanoparticles, prepared by solution-phase synthesis using metal carbonyls as reducing agents. This synthetic method produces highly monodisperse Pt octahedral, icosahedra, cubes, truncated cubes, cuboctahedra, spheres, tetrapods, star-shaped octapods, multipods, and hyper-branched structures. (Reproduced with permission from ACS Nano 7, 1, 645–653. Copyright 2012 American Chemical Society) [89]

1.2.3 Platinum

Platinum nanostructures are of particular interest for many industrial applications due to their extraordinary catalytic properties in various industrial syntheses like petrochemistry or energy conversion [83–86]. Conventional techniques to prepare platinum nanoparticles are based on wet-chemical methods [87–89]. Typically, the reaction involves the reduction of a Pt(II) precursor (like K_2PtCl_4 or $Pt(acac)_2$) or a Pt(IV) precursor (like K_2PtCl_6) in the presence of a stabilizing polymer by reducing agents such as hydrogen [90], carbon monoxide [91], sodium borohydride [92], lithium borohydride [93], and ethylene glycol [94]. The resulting nanoparticles may be considered as monodisperse in size, but they are often irregular in shape and lack well-defined facets [95]. Further modifications may include sonication during the reaction [96] or microwave-assisted heating [94]. Because the reactivity and the selectivity of Pt nanoparticles are highly dependent on the exposed facets [97], the synthesis of uniformly shaped particles is decisive for high catalytic performance [98]. Their morphological evolution is often controlled by the reduction kinetics of the platinum precursor [95], the reaction temperature [98], or the use of shape-directing reagents [99, 100] (Fig. 1.4).

The previously syntheses were based on the “bottom-up” approach. However, chemical synthesis methods often lead to impurities of the nanoparticle colloids caused by additives and precursor reaction products [101]. In contrast, Barcikowski et al. demonstrated the preparation of ligand-free platinum nanoparticles by laser

ablation in liquids ("top-down" technique) for the surface modification of electrodes for neural stimulation [102].

1.2.4 Copper

Since the ninth century, copper nanoparticles are known as coloring agents in Mesopotamia [103]. Nowadays the application range comprises biomedicine [104, 105], sensors [106], conductive inks [107], and organic catalysis [108–110]. Being inexpensive and rather abundant in nature, copper is utilized in large scale for the fabrication of plasmonic solar cells [111]. Recently established methods for copper nanoparticle synthesis include laser ablation [112], thermal decomposition [113], the polyol process [114, 115], and other chemical reduction methods [116]. Typical precursors for copper nanoparticle wet-chemical syntheses are $CuSO_4$, copper acetylacetonate ($Cu(acac)_2$), $CuCl_2$, and $Cu(NO_3)_2$ [117]. Reducing agents comprise ascorbic acid [118], sodium borohydride [119], and hypophosphite [120]. It should be mentioned that the preparation of Cu nanoparticles is challenging due to its high sensitivity to air because copper is easily oxidized to copper oxides, being less noble than silver, gold, or platinum metals [121]. The oxidation of copper nanoparticles can be avoided if the synthesis is conducted in non-aqueous media (sometimes under inert gas) and in the presence of CO or H_2. Previously described synthetic routes result in spherical multi-twinned nanoparticles in the size range between 10 and 70 nm. As shown in Fig. 1.5, by variation of the ratio of copper acetylacetonate to oleylamine, different particle size distributions can be achieved. If a hydrothermal treatment is applied, anisotropic copper particles such as nanowires or nanorods can be produced [110].

1.3 Alloyed Nanoparticles

The properties of metallic systems can be significantly extended by mixing elements to generate intermetallic compounds and alloys. Due to synergetic effects, an enhancement in desired properties is possible. The diversity of compositions, structural organizations, and tunable properties of metallic alloys makes them suitable for a wide range of applications in electronics, engineering, biomedicine, and heterogeneous catalysis [123–126]. For example, alloyed silver and gold nanoparticles utilize the physicochemical properties of both metals, e.g., the optical properties of gold and the toxicity towards bacteria or cells of silver [127, 128]. Surface structure, composition, and segregation properties [129] of nanoalloys are of great importance for the chemical reactivity and the selectivity in catalysis [130, 131]. If confined to the nanometer scale, they may display properties that are different from the equivalent bulk compounds. For example, iron and silver are immiscible in the bulk, but can be mixed in nanoparticles [132] (Fig. 1.6).

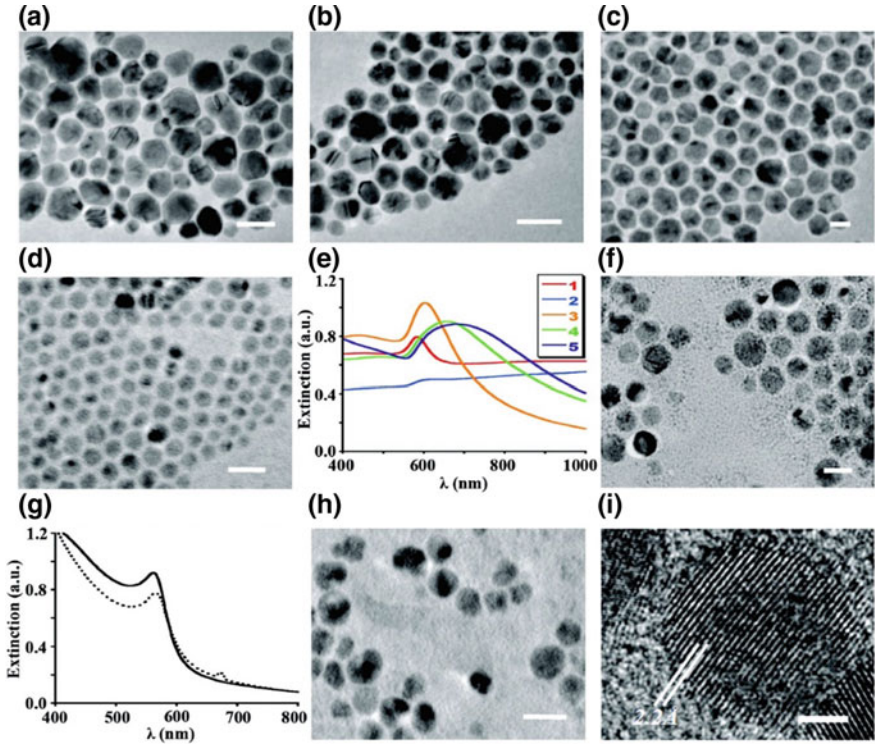

Fig. 1.5 Transmission electron micrographs and UV/VIS spectra of copper nanoparticles, prepared with different ratios of copper acetylacetonate and oleylamine. Scale bars in **a** and **b** are 50 nm, those in **c**, **d**, **f**, and **h** are 20 nm, and that in **i** is 2 nm. (Reproduced with permission from J. Phys. Chem. C, 2010, 114 (37), pp 15612–15616. Copyright 2010 American Chemical Society) [122]

Due to the heterogeneity of different properties of individual components (e.g., crystal system, redox potential, crystal symmetry, or surface charge), the successful mixture of these materials into a finite nanoparticle is challenging [123, 133]. In general, the methods for preparation of nanoalloys are the same as for single metal nanoparticles. Ligand-free manufacturing methods of nanoparticles are based on laser ablation of solids in liquid environment [134, 135], pulsed arc discharge, and sputtering techniques [123]. These approaches start with single, bimetallic or ternary targets or mixed metallic powders. Figure 1.7 shows a typical setup and the obtained alloyed Ag/Au nanoparticles by laser ablation in liquids.

Bimetallic colloids can be generated by chemical reduction of a suitable mixture of salts (metal precursor) in the solution, using appropriate reducing agent. To avoid the formation of core-shell structures due to the difference in redox potentials, different ligands can be used [137]. Another variation is based on the reduction of double metal complexes [22]. Instead of chemical reduction, an electrochemical process can be

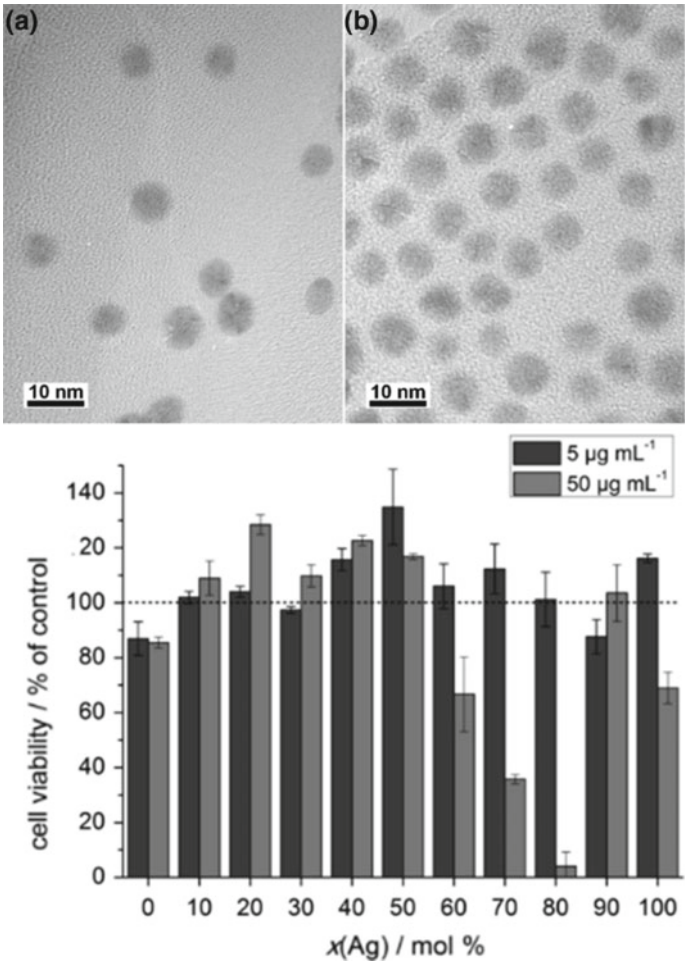

Fig. 1.6 Transmission electron micrographs of PVP-functionalized Ag/Au alloyed nanoparticles and the viability of HeLa cells after incubation with alloyed nanoparticles. Note that the cytotoxicity is not proportional to the relative silver amount, pointing to special effects that occur in the alloyed nanoparticle beyond a mere additivity of the metal properties. (Adapted from Beilstein J. Nanotechnol. 2015, 6, 1212–1220; © 2015 Ristig et al.; licensee Beilstein-Institut) [127]

used to create metal atoms from bulk metal. The particle size was be controlled by the current density [138].

Seeded-growth techniques permit the synthesis of core-shell nanoparticles [139]. As seen from Fig. 1.8, Pd–Au core-shell nanoparticles can be prepared by a water-based one-pot synthesis, followed by a stabilization with poly(N-vinyl pyrrolidone). Here, a sequential metal deposition with a distinct boundary between both metals was achieved [140].

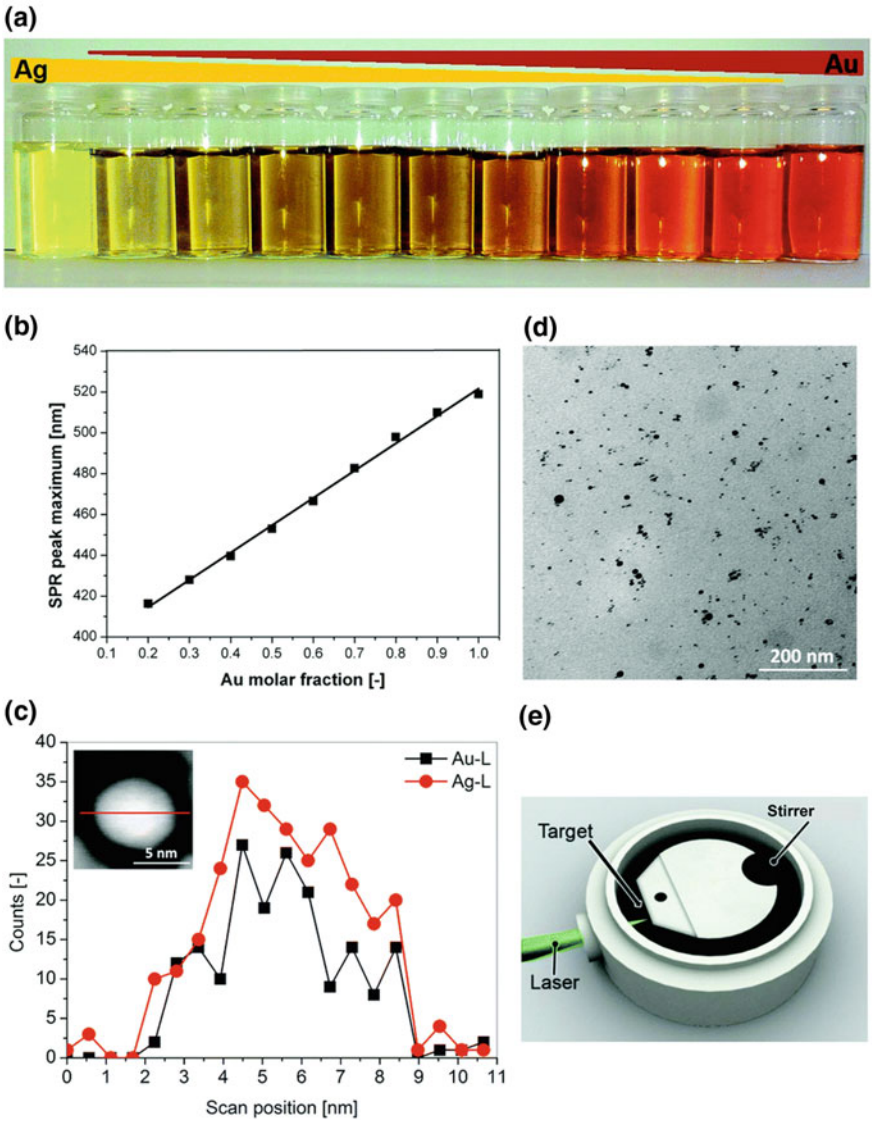

Fig. 1.7 **a** Representative AuAg nanoparticles with different molar fractions. **b** Correlation of the gold molar fraction with a maximum surface plasmon resonance extinction peak. **c** TEM-EDX line scan with an inset, showing a high-angular annular dark field micrograph. **d** TEM micrograph of Ag50Au50 nanoparticle dispersion after stabilisation with BSA. **e** Aluminum batch chamber for the synthesis of silver and gold-silver alloyed nanoparticles. (Reproduced with permission from Analyst, 2014, 139, 931–942. Copyright 2014 The Royal Society of Chemistry) [136]

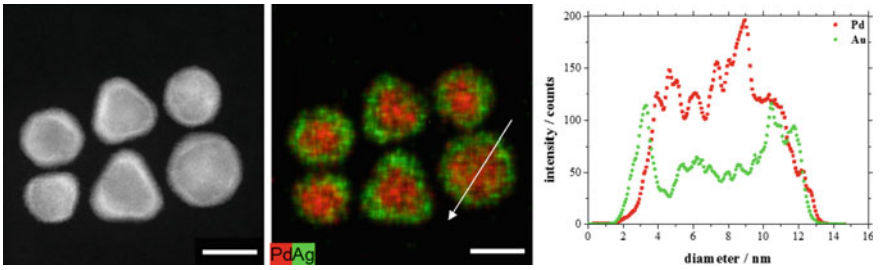

Fig. 1.8 HAADF-STEM image and corresponding EDX map with an additional line scan (white arrow) of Pd–Au core-shell nanoparticles. The EDX maps and line scans clearly show the presence of a core-shell structure with a palladium core (red) and a gold shell (green). The scale bars are 7 nm. (Reproduced with permission from ChemistrySelect 2018, 3, 4994. Copyright 2018, John Wiley and Sons)

The synthesis of alloyed nanoparticles with non-spherical morphology can lead to specific optical properties like plasmonic resonances and surface-enhanced Raman scattering (SERS) [141, 142].

1.4 Nanoscale Oxide Particles

Due to their intrinsic properties, metal oxide nanoparticles strongly contribute to a variety of applications in chemistry, physics, and materials science [143, 144]. A large diversity of oxide compounds with many structural geometries and various electronic structure (metals, semiconductors, or insulators) is known. They are widely applicable in the fabrication of sensors [145], microelectronic circuits [146], piezoelectric devices [147], fuel cells [148, 149], passivation coatings [150], water treatment agents [151], bactericides [152], sun screen [153], and as heterogeneous catalysts [154]. Almost all active phases, promoters, or "supports" in industrial catalytic reactions are based on oxides. The entanglement of size, shape, morphology, crystal structure, and surface chemistry requires a fundamental understanding and rational design for technologically relevant areas. In the following, we will discuss the prominent cases of zinc oxide, titanium dioxide (titania), and silicon dioxide (silica).

1.4.1 Zinc Oxide Nanoparticles

Zinc oxide (ZnO) is extensively utilized in everyday applications, like transparent electronics, smart windows, piezoelectric devices, chemical sensors, biosensors and dye-sensitized solar cells [155, 156]. However, zinc oxide is used at least since 2000 BC as component of therapeutic creams for skin medication [157]. Registered as safe material by the Food and Drug Administration (FDA) [158], it is used as food additive and inorganic antimicrobial additive in polymeric matrices for the packaging material, e.g. the incorporation of ZnO into the coatings of containers for meat, fish, corn and peas can retain the food color and avoid degradation [159]. Today, the commercial production of ZnO nanoparticles is realized by mechanochemical processing and physical vapor synthesis [160]. The first method is based on physical size reduction in a conventional ball mill with additives that are activated during grinding. The reaction comprises the mechanical activation of precursors ($ZnCl_2$ and Na_2CO_3) with a further thermal decomposition to ZnO [161]. The typical size range of the produced nanoparticles is 20–30 nm. The particle size can be varied by milling time and the heat treatment temperature. Physical vapor syntheses use the plasma arc energy intake by a solid precursor to generate a vapor at high temperature. Being decomposed into atoms, gases can react or condense to form particles when cooled [162].

Wet-chemical methods include hydrothermal/solvothermal processes, solution-liquid-solid, and surfactant-assisted synthesis. These methods provide a convenient and facile platform for a low-temperature fabrication of the desired ZnO nanostructures [163–165]. Typical precursors for ZnO nanocrystal preparation are zinc nitrate [166], metallic zinc [167], zinc chloride [168], zinc acetate [169, 170], and zinc sulfate [171]. If an anisotropic growth of ZnO nanoparticles is desired, surfactants such as hexamethylenetetramine [172], ammonia [173], ascorbic acid [174], and sodium hydroxide [175] can be added. Most reactions are performed at elevated temperatures up to 180 °C [165]. As shown in Fig. 1.9, different kinds of ZnO nanoparticles are obtained by adjusting the hydrolysis ratio. The nature of the protective agent added during ZnO formation and hydrolysis ratio are two major handles for size and shape control [176].

1.4.2 Titanium Dioxide Nanoparticles

Titanium dioxide nanoparticles are among the most frequently used metal oxide nanoparticles in industrial products and consumer goods [177]. Due to its very high refractive index and brightness, TiO_2 is extensively utilized as a white pigment with an annual consumption of almost four million tons worldwide [178]. Typical applications comprise paints [179, 180], coatings [181], plastics [182], papers [183], inks [184], pharmaceuticals [185], food products [186], cosmetics [187, 188], sun screens [189], and toothpaste [190]. Rompelberg et al. estimated the oral intake of TiO_2 from

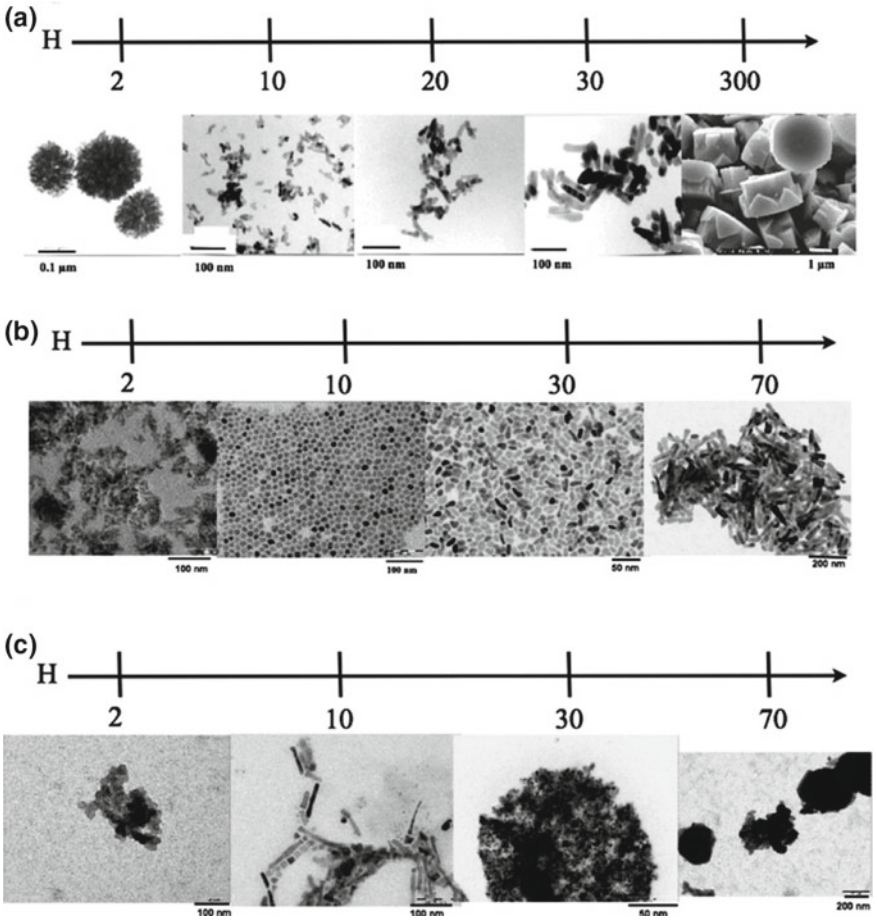

Fig. 1.9 TEM micrographs of ZnO nanoparticles synthesized in diethylene glycol (DEG) by variation of the hydrolysis ratio (*H*): **a** ZnO without addition of protective agents, **b** ZnO- tri-*n*-octylphosphine oxide, and **c** ZnO-polyoxyethylene stearyl ether. (Reproduced with permission from Langmuir 26, 9, 6522–6528. Copyright 2010 American Chemical Society) [176]

food, food supplements and toothpaste by measuring the total titanium concentrations and subsequently calculated the TiO_2 concentrations in selected representative Dutch food products (see Table 1.1) [186].

Several processes have been developed for the preparation of nanostructured TiO_2 with distinct characteristics. Commercial powders are typically prepared by the so-called chloride-process from $TiCl_4$ using hydrocarbon-assisted flame synthesis [191]. In the sulfate-process, ilmenite ($FeTiO_3$) is treated with concentrated sulfuric acid, and the titanium oxygen sulfate ($TiOSO_4$) is extracted and converted into titanium dioxide [192].

Table 1.1 Average measured total titanium concentrations and subsequently calculated TiO_2 concentrations in selected representative Dutch food products, raw (cow) milk, and food supplements. Samples rich in calcium were analyzed by ICP-HRMS, others by ICP-QMS. Limit of quantitation 0.05 mg Ti/kg product. (Reproduced from Rompelberg et al., 2016, Nanotoxicology, 10:10, 1404–1414 © 2016 National Institute for Public Health and the Environment. Published by Informa UK Limited, trading as Taylor & Francis Group) [187]

	Number of samples	Mean total-Ti (mg/kg product) (± SD)	Min total-Ti (mg/kg product)	Max total-Ti (mg/kg product)	Mean TiO_2 (mg/kg product)
Samples analysed by ICP-HRMS					
Raw (cow) milk	6 (6)	0.31(±0.23)	0.05	0.63	0.51
Regular dairy products (i.e. milk, yoghurt)	11 (10)	0.47(±0.46)	<LOQ	1.46	0.79
Processed dairy products	10 (5)	0.12(±0.17)	<LOQ	0.57	0.21
Soy milk	2 (2)	0.33(±0.01)	0.32	0.34	0.55
Dutch cake with icing and cream	1 (1)	0.23	0.23	0.23	0.38
Coffee creamer (powdered)	1 (1)	1640	1640	1640	2739
Samples analysed by ICP-QMS					
Energy drink (containing caffeine)	1 (1)	0.07	0.07	0.07	0.11
Soft drink	2 (2)	0.06 (±0.00)	0.06	0.07	0.11
Sports drink	2 (2)	0.09 (±0.05)	0.05	0.12	0.14
Syrup	2 (2)	0.17 (±0.00)	0.17	0.17	0.28
Ice (water-based)	1 (1)	0.16	0.16	0.16	0.26
Wine gums	1 (1)	0.25	0.25	0.25	0.42
Salad dressing	1 (1)	0.43	0.43	0.43	0.72
Food supplement (multivitamin)	2 (2)	744 (±1009)	31	1458	1242

The wet-chemical fabrication of TiO_2 nanoparticles allows to control the stoichiometry, homogeneity, and morphology of the resulting materials. Nevertheless, the drawbacks are expensive precursors, long processing times, the nanoparticle isolation/purification after the synthesis, and the presence of impurities. The sol-gel technique is based on the hydrolysis of the precursors of the metal alkoxides ($Ti(OR)_4$) with further thermal decomposition [193]. By controlling solution composition, pH, and temperature, the particle size can be tuned [194]. The precipitation process involves the addition of NaOH, NH_4OH, or urea to metal precursors (e.g., $TiCl_4$), followed by thermal treatment to crystallize the oxide [195]. The hydrothermal method can be started from metallic Ti, oxidized by H_2O_2 [196]. Nanocrystalline TiO_2 can be prepared by mechanical alloying from a metastable intermediate phase, i.e. $TiO(OH)_2$ powder [197]. By in-flight oxidation of titanium nitride powder in an r.f. thermal plasma reactor, the formation of core-shell structured composites (with TiN cores and oxide shells) was realized [198].

1.4.3 Silica Nanoparticles

Silicon dioxide (SiO_2) nanoparticles are extensively used since the 1950s in numerous applications like additives for rubber (also in tires) and plastics [199–201], strengthening filler for concrete [202, 203], abrasives in toothpaste [204], thickeners in foods [205], and anti-caking agents in foods (E551) [206, 207]. Due its excellent biocompatibility, low toxicity, easy surface modification, and facile synthetic routes, silica nanoparticles are suitable for biological applications as grafting platform for imaging, detecting, drug loading, and site-specific targeting [208–210]. Their particle size, crystallinity, porosity, and shape can be accurately controlled, enabling a fine-tuning of silica nanoparticles for the intended application.

The large scale production of silica nanoparticles is performed by flame aerosol technology [211]. Developed by Kloepfer [212], this fabrication method is based on the continuous flame pyrolysis of vaporized silicon tetrachloride ($SiCl_4$) [213]. The produced silica forms branched aggregates, with the primary amorphous particles in the size range from 5 to 50 nm [214]. The particle size and the particle size distribution can be modified varying the concentration of the reactants, the flame temperature, and the gas dwell time in the combustion [211].

Established in 1968, the Stöber method is a widely used sol-gel process for silica nanoparticle synthesis [215]. This reaction permits a controlled evolution of spherical silica particles of uniform size in the size range of 50 nm to 2 μm. Catalyzed by ammonia, it is based on the hydrolysis of alkyl silicates (e.g., tetraethoxysilane (TEOS)), and the subsequent condensation of silicic acid in alcoholic solutions. The control of the ratio of solvent to TEOS permits a fine control of particle size in the Stöber method [216]. As shown in Fig. 1.10, the diameter of the synthesized particle decreases as the ratio of solvent to TEOS is increased. The method can be modified for the incorporation of organic dyes and other nanosized materials [217].

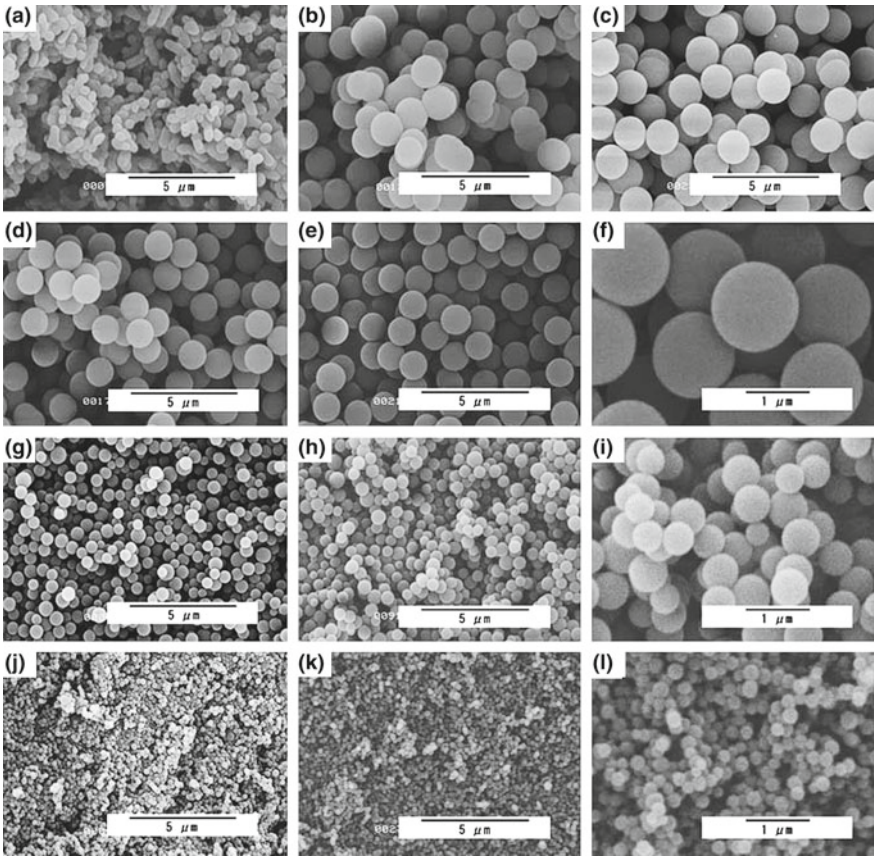

Fig. 1.10 Silica nanoparticles synthesized by the Stöber method with variable methanol/TEOS ratios before and after calcination. The MeOH/TEOS synthesis ratios and calcined versus noncalcined status are as follows: **a** 300/noncalcined, **b** 750/noncalcined, **c** 1125/noncalcined, **d** 1500/noncalcined, **e** and **f** 1500/calcined, **g** 2250/noncalcined, **h** and **i** 2250/calcined, **j** 3000/noncalcined, and **k** and **l** 3000/calcined. As the ratio of methanol/TEOS increases from 300 to 1125, the particle size increases. However, from 1125 to 6000, the particle size decreased from 1500 to 10 nm in diameter [216]. (Reproduced with permission from Shimura, N. & Ogawa, M. J Mater Sci (2007) 42:5299 Copyright © 2007, Springer Nature)

Another important technique for silica nanoparticle preparation is the reverse microemulsion. Established by Arriagada and Osseo-Asare in the early 1990s, this method utilizes the ammonia-catalyzed polymerization of tetraethoxysilane in a reverse phase (water-in-oil microemulsion) [218]. The dispersion of nanodroplets leads to nanoreactors to form nanoparticles. The size of the colloids depends on the intrinsic properties of a surfactant and the molar ratio of water to surfactant [210]. The variation of the nanoparticle morphology can drastically affect their biodistribution, bioavailability, and toxicity [219, 220]. For instance, Trewyn et al. demonstrated the

effect of organic C_n-methylimidazolium ($n = 14,16,18$) derivatives on the modified Stöber synthesis [221]. The particles derived from modifications with C18MIM and C14OCMIM exhibited a rod- or worm-like structure.

References

1. Elghanian, R., et al.: Selective colorimetric detection of polynucleotides based on the distance-dependent optical properties of gold nanoparticles. Science **277**(5329), 1078 (1997)
2. Haes, A.J., Van Duyne, R.P.: A nanoscale optical biosensor: sensitivity and selectivity of an approach based on the localized surface plasmon resonance spectroscopy of triangular silver nanoparticles. J. Am. Chem. Soc. **124**(35), 10596–10604 (2002)
3. Sokolov, K., et al.: Real-time vital optical imaging of precancer using anti-epidermal growth factor receptor antibodies conjugated to gold nanoparticles. Cancer Res. **63**(9), 1999–2004 (2003)
4. El-Sayed, I.H., Huang, X., El-Sayed, M.A.: Surface plasmon resonance scattering and absorption of anti-EGFR antibody conjugated gold nanoparticles in cancer diagnostics: applications in oral cancer. Nano Lett. **5**(5), 829–834 (2005)
5. Alivisatos, P.: The use of nanocrystals in biological detection. Nat. Biotechnol. **22**, 47 (2003)
6. Li, Y.Y., et al.: Targeted polydopamine nanoparticles enable photoacoustic imaging guided chemo-photothermal synergistic therapy of tumor. Acta Biomater. **47**, 124–134 (2017)
7. Liu, J.N., Bu, W.B., Shi, J.L.: Chemical design and synthesis of functionalized probes for imaging and treating tumor hypoxia. Chem. Rev. **117**(9), 6160–6224 (2017)
8. Liu, G.L., et al.: Fluorescence enhancement of terminal amine assembled on gold nanoclusters and its application to ratiometric lysine detection. Langmuir **33**(51), 14643–14648 (2017)
9. Ricciardi, L., et al.: Plasmon-mediated cancer phototherapy: the combined effect of thermal and photodynamic processes. Nanoscale **9**(48), 19279–19289 (2017)
10. Chen, Y.P., Xianyu, Y.L., Jiang, X.Y.: Surface modification of gold nanoparticles with small molecules for biochemical analysis. Acc. Chem. Res. **50**(2), 310–319 (2017)
11. Xiang, Y., Lu, Y.: Using personal glucose meters and functional DNA sensors to quantify a variety of analytical targets. Nat. Chem. **3**(9), 697–703 (2011)
12. Hahn, M.A., et al.: Nanoparticles as contrast agents for in-vivo bioimaging: current status and future perspectives. Anal. Bioanal. Chem. **399**(1), 3–27 (2011)
13. Sailor, M.J., Park, J.H.: Hybrid nanoparticles for detection and treatment of cancer. Adv. Mater. **24**(28), 3779–3802 (2012)
14. Zhang, P.C., et al.: Recent progress in light-triggered nanotheranostics for cancer treatment. Theranostics **6**(7), 948–968 (2016)
15. Yang, Q.H., Xu, Q., Jiang, H.L.: Metal-organic frameworks meet metal nanoparticles: synergistic effect for enhanced catalysis. Chem. Soc. Rev. **46**(15), 4774–4808 (2017)
16. Jiang, K.Z., et al.: Efficient oxygen reduction catalysis by subnanometer Pt alloy nanowires. Sci. Adv. **3**(2), 8 (2017)
17. Eftekhari, A.: Electrocatalysts for hydrogen evolution reaction. Int. J. Hydrogen Energy **42**(16), 11053–11077 (2017)
18. Xu, H., et al.: Facile synthesis of Pd-Ru-P ternary nanoparticle networks with enhanced electrocatalytic performance for methanol oxidation. Int. J. Hydrogen Energy **42**(16), 11229–11238 (2017)
19. El-Sayed, M.A.: Some interesting properties of metals confined in time and nanometer space of different shapes. Acc. Chem. Res. **34**(4), 257–264 (2001)
20. Shenhar, R., Rotello, V.M.: Nanoparticles: scaffolds and building blocks. Acc. Chem. Res. **36**(7), 549–561 (2003)

21. Eustis, S., el-Sayed, M.A.: Why gold nanoparticles are more precious than pretty gold: noble metal surface plasmon resonance and its enhancement of the radiative and nonradiative properties of nanocrystals of different shapes. Chem. Soc. Rev. **35**(3), 209–217 (2006)
22. Toshima, N., Yonezawa, T.: Bimetallic nanoparticles-novel materials for chemical and physical applications. New J. Chem. **22**(11), 1179–1201 (1998)
23. Johnston, R.L.: Atomic and Molecular Clusters. Taylor & Francis (2002)
24. Sau, T.K., Rogach, A.L.: Nonspherical noble metal nanoparticles: colloid-chemical synthesis and morphology control. Adv. Mater. **22**(16), 1781–1804 (2010)
25. Sau, T.K., Murphy, C.J.: Room temperature, high-yield synthesis of multiple shapes of gold nanoparticles in aqueous solution. J. Am. Chem. Soc. **126**(28), 8648–8649 (2004)
26. Lee, H., et al.: Localized Pd overgrowth on cubic Pt nanocrystals for enhanced electrocatalytic oxidation of formic acid. J. Am. Chem. Soc. **130**(16), 5406–5407 (2008)
27. Zhang, J., et al.: Shape-selective synthesis of gold nanoparticles with controlled sizes, shapes, and plasmon resonances. Adv. Funct. Mater. **17**(16), 3295–3303 (2007)
28. Yu, Y.-T., Xu, B.-Q.: Shape-controlled synthesis of Pt nanocrystals: an evolution of the tetrahedral shape. Appl. Organomet. Chem. **20**(10), 638–647 (2006)
29. Schuetze, B., et al.: Conjugation of thiol-terminated molecules to ultrasmall 2 nm-gold nanoparticles leads to remarkably complex 1H-NMR spectra. J. Mater. Chem. B **4**(12), 2179–2189 (2016)
30. Helmlinger, J., et al.: A rapid, high-yield and large-scale synthesis of uniform spherical silver nanoparticles by a microwave-assisted polyol process. RSC Adv. **5**(112), 92144–92150 (2015)
31. Sajanlal, P.R., Pradeep, T.: Electric-field-assisted growth of highly uniform and oriented gold nanotriangles on conducting glass substrates. Adv. Mater. **20**(5), 980–983 (2008)
32. Wang, L., et al.: Synthesis of gold nano- and microplates in hexagonal liquid crystals. J. Phys. Chem. B **109**(8), 3189–3194 (2005)
33. Djalali, R., Chen, Y.F., Matsui, H.: Au nanowire fabrication from sequenced histidine-rich peptide. J. Am. Chem. Soc. **124**(46), 13660–13661 (2002)
34. Faraday, M.: *X. The Bakerian Lecture. —Experimental relations of gold (and other metals) to light.* Philos. Trans. R. Soc. Lond. **147**, 145–181 (1857)
35. Turkevich, J., Stevenson, P.C., Hillier, J.: A study of the nucleation and growth processes in the synthesis of colloidal gold. Discuss. Faraday Soc. **11**, 55–75 (1951)
36. Frens, G.: Particle size and sol stability in metal colloids. Kolloid-Zeitschrift und Zeitschrift für Polymere **250**(7), 736–741 (1972)
37. Frens, G.: Controlled nucleation for the regulation of the particle size in monodisperse gold suspensions. NPhS **241**, 20 (1973)
38. Huang, X., et al.: One-step, size-controlled synthesis of gold nanoparticles at room temperature using plant tannin. Green Chem. **12**(3), 395–399 (2010)
39. Mahl, D., et al.: Silver, gold, and alloyed silver–gold nanoparticles: characterization and comparative cell-biologic action. J. Nanopart. Res. **14**(10), 1153 (2012)
40. Shang, L., et al.: One-pot synthesis of near-infrared fluorescent gold clusters for cellular fluorescence lifetime imaging. Small **7**(18), 2614–2620 (2011)
41. Jana, N.R., Gearheart, L., Murphy, C.J.: Seeding growth for size control of 5–40 nm diameter gold nanoparticles. Langmuir **17**(22), 6782–6786 (2001)
42. Perrault, S.D., Chan, W.C.W.: Synthesis and surface modification of highly monodispersed, spherical gold nanoparticles of 50–200 nm. J. Am. Chem. Soc. **131**(47), 17042–17043 (2009)
43. Ristig, S., et al.: An easy synthesis of autofluorescent alloyed silver-gold nanoparticles. J. Mater. Chem. B **2**(45), 7887–7895 (2014)
44. Brust, M., et al.: Synthesis of thiol-derivatised gold nanoparticles in a two-phase liquid-liquid system. J. Chem. Soc. Chem. Commun. 7, 801–802 (1994)
45. Allpress, J.G., Sanders, J.V.: The structure and orientation of crystals in deposits of metals on mica. Surf. Sci. **7**(1), 1–25 (1967)
46. Structural studies of trigonal lamellar particles of gold and silver. Proc. R. Soc. Lond. Ser. A: Math. Phys. Sci. **440**(1910), 589–609 (1993)

47. Sun, Y., Xia, Y.: Shape-controlled synthesis of gold and silver nanoparticles. Science **298**(5601), 2176 (2002)
48. Rehbock, C., et al.: Size control of laser-fabricated surfactant-free gold nanoparticles with highly diluted electrolytes and their subsequent bioconjugation. PCCP **15**(9), 3057–3067 (2013)
49. Semaltianos, N.G.: Nanoparticles by laser ablation. Crit. Rev. Solid State Mater. Sci. **35**(2), 105–124 (2010)
50. Popovic, D.M., et al.: Continuous wave laser for tailoring the photoluminescence of silicon nanoparticles produced by laser ablation in liquid. J. Appl. Phys. **122**(11), 113107 (2017)
51. Tsuji, T., et al.: Preparation of silver nanoparticles by laser ablation in solution: influence of laser wavelength on particle size. Appl. Surf. Sci. **202**(1), 80–85 (2002)
52. Walter, J.G., et al.: Laser ablation-based one-step generation and bio-functionalization of gold nanoparticles conjugated with aptamers. J. Nanobiotechnol. **8**(1), 21 (2010)
53. Jin, R., et al.: Atomically precise colloidal metal nanoclusters and nanoparticles: fundamentals and opportunities. Chem. Rev. **116**(18), 10346–10413 (2016)
54. Schmid, G.: The relevance of shape and size of Au55 clusters. Chem. Soc. Rev. **37**(9), 1909–1930 (2008)
55. Hakkinen, H.: Atomic and electronic structure of gold clusters: understanding flakes, cages and superatoms from simple concepts. Chem. Soc. Rev. **37**(9), 1847–1859 (2008)
56. Schmid, G., et al.: Au55[P(C6H5)3]12CI6—ein Goldcluster ungewöhnlicher Größe. Chem. Ber. **114**(11), 3634–3642 (1981)
57. Newton, M.G., et al.: Symmetrical and unsymmetrical bridging carbonyl groups in binuclear molybdenum carbonyl complexes of alkylaminobis(difluorophosphines); X-ray crystal structures of two of the complexes. J. Chem. Soc. Chem. Commun. (3), 201–203 (1982)
58. Tyo, E.C., Vajda, S.: Catalysis by clusters with precise numbers of atoms. Nat. Nanotechnol. **10**, 577 (2015)
59. Nonappa, et al., Template-free supracolloidal self-assembly of atomically precise gold nanoclusters: from 2D Colloidal crystals to spherical capsids. Angew. Chem. Int. Ed. **55**(52), 16035–16038 (2016)
60. Mahl, D.: Synthese, Löslichkeit und Stabilität von Gold-Nanopartikeln in biologischen Medien. University of Duisburg-Essen, Essen (2011)
61. Nowack, B., Krug, H.F., Height, M.: 120 years of nanosilver history: implications for policy makers. Environ. Sci. Technol. **45**(4), 1177–1183 (2011)
62. Xu, H., Suslick, K.S.: Sonochemical synthesis of highly fluorescent Ag nanoclusters. ACS Nano **4**(6), 3209–3214 (2010)
63. Chen, J., et al.: A simple and versatile mini-arc plasma source for nanocrystal synthesis. J. Nanopart. Res. **9**(2), 203–213 (2007)
64. Wagener, P., et al.: Dynamics of silver nanoparticle formation and agglomeration inside the cavitation bubble after pulsed laser ablation in liquid. PCCP **15**(9), 3068–3074 (2013)
65. Lea, M.C.: Allotropic forms of silver. Am. J. Sci. (Series 3) **37**(222), 476–491 (1889)
66. Kittler, S., et al.: Toxicity of silver nanoparticles increases during storage because of slow dissolution under release of silver ions. Chem. Mater. **22**(16), 4548–4554 (2010)
67. Banerjee, S., et al.: Structural evolution of silver nanoparticles during wet-chemical synthesis. Chem. Mater. **26**(2), 951–957 (2014)
68. Firdhouse, M.J., Lalitha, P.: Biosynthesis of silver nanoparticles and its applications. J. Nanotechnol. **2015**, 18 (2015)
69. Prabhu, S., Poulose, E.K.: Silver nanoparticles: mechanism of antimicrobial action, synthesis, medical applications, and toxicity effects. Int. Nano Lett. **2**(1), 32 (2012)
70. Mavani, K., Shah, M.: Synthesis of silver nanoparticles by using sodium borohydride as a reducing agent (2013)
71. Kim, D., Jeong, S., Moon, J.: Synthesis of silver nanoparticles using the polyol process and the influence of precursor injection. Nanotechnology **17**(16), 4019–4024 (2006)
72. Zhao, T., et al.: Size-controlled preparation of silver nanoparticles by a modified polyol method. Colloid Surf A: Physicochem. Eng. Aspects **366**(1), 197–202 (2010)

73. Won, H., et al.: Preparation of porous silver particles using ammonium formate and its formation mechanism. Chem. Eng. J. **156,** 459–464 (2010)
74. Chen, S., Fan, Z., Carroll, D.L.: Silver nanodisks: synthesis, characterization, and self-assembly. J. Phys. Chem. B **106**(42), 10777–10781 (2002)
75. Rycenga, M., McLellan, J.M., Xia, Y.: Controlling the assembly of silver nanocubes through selective functionalization of their faces. Adv. Mater. **20**(12), 2416–2420 (2008)
76. Schuette, W.M., Buhro, W.E.: Silver chloride as a heterogeneous nucleant for the growth of silver nanowires. ACS Nano **7**(5), 3844–3853 (2013)
77. Zinchenko, A.A., Yoshikawa, K., Baigl, D.: DNA-templated silver nanorings. Adv. Mater. **17**(23), 2820–2823 (2005)
78. Wiley, B.J., et al.: Right bipyramids of silver: a new shape derived from single twinned seeds. Nano Lett. **6**(4), 765–768 (2006)
79. Im, S.H., et al.: Large-scale synthesis of silver nanocubes: the role of hcl in promoting cube perfection and monodispersity. Angew. Chem. Int. Ed. **44**(14), 2154–2157 (2005)
80. Darmanin, T., et al.: Microwave-assisted synthesis of silver nanoprisms/nanoplates using a "modified polyol process". Colloids Surf. Physicochem. Eng. Aspects **395**, 145–151 (2012)
81. Helmlinger, J., et al.: On the crystallography of silver nanoparticles with different shapes. Cryst. Growth Des. **16**(7), 3677–3687 (2016)
82. Wiley, B., et al.: Shape-controlled synthesis of metal nanostructures: the case of silver. Chem. – A Eur. J. **11**(2), 454–463 (2005)
83. Ye, X., et al.: Morphologically controlled synthesis of colloidal upconversion nanophosphors and their shape-directed self-assembly. Proc. Natl. Acad. Sci. USA **107**(52), 22430–22435 (2010)
84. Bratlie, K.M., et al.: Platinum nanoparticle shape effects on benzene hydrogenation selectivity. Nano Lett. **7**(10), 3097–3101 (2007)
85. Tian, N., et al.: Synthesis of tetrahexahedral platinum nanocrystals with high-index facets and high electro-oxidation activity. Science **316**(5825), 732–735 (2007)
86. Roldan Cuenya, B.: Metal nanoparticle catalysts beginning to shape-up. Acc. Chem. Res. **46**(8), 1682–1691 (2013)
87. Schmid, G.: Large clusters and colloids. Metals in the embryonic state. Chem. Rev. **92**(8), 1709–1727 (1992)
88. Song, H., et al.: Pt nanocrystals: shape control and langmuir–blodgett monolayer formation. J. Phys. Chem. B **109**(1), 188–193 (2005)
89. Kang, Y., et al.: Shape-controlled synthesis of Pt nanocrystals: the role of metal carbonyls. ACS Nano **7**(1), 645–653 (2013)
90. Henglein, A., Ershov, B.G., Malow, M.: Absorption spectrum and some chemical reactions of colloidal platinum in aqueous solution. J. Phys. Chem. **99**(38), 14129–14136 (1995)
91. Kang, Y., Ye, X., Murray, C.B.: Size- and shape-selective synthesis of metal nanocrystals and nanowires using CO as a reducing agent. Angew. Chem. Int. Ed. Engl. **49**(35), 6156–6159 (2010)
92. Zhao, S.-Y., et al.: Preparation, phase transfer, and self-assembled monolayers of cubic Pt nanoparticles. Langmuir **18**(8), 3315–3318 (2002)
93. Lee, S.-A., et al.: Nanoparticle synthesis and electrocatalytic activity of Pt alloys for direct methanol fuel cells. J. Electrochem. Soc. **149**(10), A1299–A1304 (2002)
94. Liu, Z., et al.: Nanosized Pt and PtRu colloids as precursors for direct methanol fuel cell catalysts. J. Mater. Chem. **13**(12), 3049–3052 (2003)
95. Herricks, T., Chen, J., Xia, Y.: Polyol synthesis of platinum nanoparticles: control of morphology with sodium nitrate. Nano Lett. **4**(12), 2367–2371 (2004)
96. Fujimoto, T., et al.: Sonochemical preparation of single-dispersion metal nanoparticles from metal salts. Chem. Mater. **13**(3), 1057–1060 (2001)
97. Falicov, L.M., Somorjai, G.A.: Correlation between catalytic activity and bonding and coordination number of atoms and molecules on transition metal surfaces: theory and experimental evidence. Proc. Natl. Acad. Sci. USA **82**(8), 2207–2211 (1985)

98. Wang, C., et al.: A general approach to the size- and shape-controlled synthesis of platinum nanoparticles and their catalytic reduction of oxygen. Angew. Chem. Int. Ed. **47**(19), 3588–3591 (2008)
99. Teng, X., Yang, H.: Synthesis of platinum multipods: an induced anisotropic growth. Nano Lett. **5**(5), 885–891 (2005)
100. Chen, J., et al.: Single-crystal nanowires of platinum can be synthesized by controlling the reaction rate of a polyol process. J. Am. Chem. Soc. **126**(35), 10854–10855 (2004)
101. Barcikowski, S., Compagnini, G.: Advanced nanoparticle generation and excitation by lasers in liquids. PCCP **15**(9), 3022–3026 (2013)
102. Angelov, S.D., et al.: Electrophoretic deposition of ligand-free platinum nanoparticles on neural electrodes affects their impedance in vitro and in vivo with no negative effect on reactive gliosis. J. Nanobiotechnology **14**(1), 3 (2016)
103. Khan, F.A.: Biotechnology Fundamentals. CRC Press, Boca Raton (2011)
104. Seku, K., et al.: Hydrothermal synthesis of Copper nanoparticles, characterization and their biological applications. Int. J. Nano Dimens. **9**(1), 7–14 (2018)
105. Sanchez-Sanhueza, G., et al.: Synthesis of Copper nanowires and their antimicrobial activity on strains isolated persistent endodontic infections. J. Nanosci. Nanotechnol. **18**(7), 4507–4514 (2018)
106. Shabnam, L., et al.: Doped graphene/Cu nanocomposite: a high sensitivity non-enzymatic glucose sensor for food. Food Chem. **221**, 751–759 (2017)
107. Lee, Y., et al.: Large-scale synthesis of Copper nanoparticles by chemically controlled reduction for applications of inkjet-printed electronics. Nanotechnology **19**(41), 415604 (2008)
108. Ranu, B.C., et al.: Copper nanoparticle-catalyzed carbon-carbon and carbon-heteroatom bond formation with a greener perspective. ChemSusChem **5**(1), 22–44 (2012)
109. Allen, S.E., et al.: Aerobic copper-catalyzed organic reactions. Chem. Rev. **113**(8), 6234–6458 (2013)
110. Kaur, R., Pal, B.: Cu nanostructures of various shapes and sizes as superior catalysts for nitroaromatic reduction and co-catalyst for Cu/TiO2 photocatalysis. Appl. Catal. A **491**, 28–36 (2015)
111. Parveen, F., et al.: Copper nanoparticles: synthesis methods and its light harvesting performance. Sol. Energy Mater. Sol. Cells **144**, 371–382 (2016)
112. Tilaki, R.M., Iraji zad, A., Mahdavi, S.M.: Size, composition and optical properties of copper nanoparticles prepared by laser ablation in liquids. Appl. Phys. A **88**(2), 415–419 (2007)
113. Salavati-Niasari, M., Fereshteh, Z., Davar, F.: Synthesis of oleylamine capped copper nanocrystals via thermal reduction of a new precursor. Polyhedron **28**(1), 126–130 (2009)
114. Park, B.K., et al.: Direct writing of copper conductive patterns by ink-jet printing. Thin Solid Films **515**(19), 7706–7711 (2007)
115. Woo, K., et al.: Ink-jet printing of Cu-Ag-based highly conductive tracks on a transparent substrate. Langmuir **25**(1), 429–433 (2009)
116. Khan, A., et al.: A chemical reduction approach to the synthesis of copper nanoparticles. Int. Nano Lett. **6**(1), 21–26 (2016)
117. Gawande, M.B., et al.: Cu and Cu-based nanoparticles: synthesis and applications in catalysis. Chem. Rev. **116**(6), 3722–3811 (2016)
118. Wu, C., Mosher, B.P., Zeng, T.: One-step green route to narrowly dispersed copper nanocrystals. J. Nanopart. Res. **8**(6), 965–969 (2006)
119. Thi My Dung, D., et al.: Synthesis and optical properties of copper nanoparticles prepared by a chemical reduction method. Adv. Nat. Sci.: Nanosci. Nanotechnol. **2**(1), 015009 (2011)
120. Chernogorenko, V.B., Tasybaeva, S.T.: Mechanism of chemical, reduction of copper(II) by hypophosphite ion. Russ. J. Appl. Chem. **68**(4), 461–464 (1995)
121. Jeong, S., et al.: Controlling the thickness of the surface oxide layer on Cu nanoparticles for the fabrication of conductive structures by Ink-jet printing. Adv. Funct. Mater. **18**(5), 679–686 (2008)
122. Wei, Y., et al.: Synthesis of stable, low-dispersity copper nanoparticles and nanorods and their antifungal and catalytic properties. J. Phys. Chem. C **114**(37), 15612–15616 (2010)

123. Ferrando, R., Jellinek, J., Johnston, R.L.: Nanoalloys: from theory to applications of alloy clusters and nanoparticles. Chem. Rev. **108**(3), 845–910 (2008)
124. Wanjala, B.N., et al.: Nanoscale alloying, phase-segregation, and core–shell evolution of gold–platinum nanoparticles and their electrocatalytic effect on oxygen reduction reaction. Chem. Mater. **22**(14), 4282–4294 (2010)
125. Tahir, M., Tahir, B., Amin, N.A.S.: Synergistic effect in plasmonic Au/Ag alloy NPs co-coated TiO2 NWs toward visible-light enhanced CO2 photoreduction to fuels. Appl. Catal. B **204**, 548–560 (2017)
126. Bennett, E., et al.: A synthetic route for the effective preparation of metal alloy nanoparticles and their use as active electrocatalysts. ACS Catal. **6**(3), 1533–1539 (2016)
127. Ristig, S., et al.: Synthesis, characterization and in vitro effects of 7 nm alloyed silver–gold nanoparticles. Beilstein J. Nanotechnol. **6**, 1212–1220 (2015)
128. Taylor, U., et al.: Influence of gold, silver and gold–silver alloy nanoparticles on germ cell function and embryo development. Beilstein J. Nanotechnol. **6**, 651–664 (2015)
129. Ruban, A.V., Skriver, H.L., Nørskov, J.K.: Surface segregation energies in transition-metal alloys. PhRvB **59**(24), 15990–16000 (1999)
130. Molenbroek, A.M., Haukka, S., Clausen, B.S.: Alloying in Cu/Pd Nanoparticle Catalysts. J. Phys. Chem. B **102**(52), 10680–10689 (1998)
131. Nanosized clusters on and in supports—perspectives for future catalysis, in metal clusters in chemistry
132. Andrews, M.P., O'Brien, S.C.: Gas-phase "molecular alloys" of bulk immiscible elements: iron-silver (FexAgy). J. Phys. Chem. **96**(21), 8233–8241 (1992)
133. Cortie, M.B., McDonagh, A.M.: Synthesis and optical properties of hybrid and alloy plasmonic nanoparticles. Chem. Rev. **111**(6), 3713–3735 (2011)
134. Zhang, D., Gökce, B., Barcikowski, S.: Laser synthesis and processing of colloids: fundamentals and applications. Chem. Rev. **117**(5), 3990–4103 (2017)
135. Simakin, A.V., et al.: Nanoparticles produced by laser ablation of solids in liquid environment. Appl. Phys. A **79**(4), 1127–1132 (2004)
136. Tiedemann, D., et al.: Reprotoxicity of gold, silver, and gold-silver alloy nanoparticles on mammalian gametes. Analyst **139**(5), 931–942 (2014)
137. Goia, D.V., Matijevic, E.: Preparation of monodispersed metal particles. New J. Chem. **22**(11), 1203–1215 (1998)
138. Reetz, M.T., Helbig, W.: Size-selective synthesis of nanostructured transition metal clusters. J. Am. Chem. Soc. **116**(16), 7401–7402 (1994)
139. Tan, C., et al.: A self-supporting bimetallic Au@Pt core-shell nanoparticle electrocatalyst for the synergistic enhancement of methanol oxidation. Sci. Rep. **7**, 6347 (2017)
140. Rostek, A., Breisch, M., Loza, K., Garcia, P.R.A.F., Oliveira, C.L.P., Prymak, O., Heggen, M., Köller, M., Sengstock, C., Epple, M.: ChemistrySelect **3**, 4994 (2018)
141. Schlücker, S.: Surface-enhanced raman spectroscopy: concepts and chemical applications. Angew. Chem. Int. Ed. **53**(19), 4756–4795 (2014)
142. Rodriguez-Gonzalez, B., et al.: Multishell bimetallic AuAg nanoparticles: synthesis, structure and optical properties. J. Mater. Chem. **15**(17), 1755–1759 (2005)
143. Lintz, H.G., Kung, H.H.: Transition Metal Oxides: Surface Chemistry and Catalysis, Vol. 45, Studies in Surface Science and Catalysis, Elsevier, Amsterdam, Oxford, New York, Tokyo (1989)
144. Fernández-García, J.A.R.: Synthesis, Properties, and Applications of Oxide Nanomaterials. Wiley, New York (2006)
145. Miller, D.R., Akbar, S.A., Morris, P.A.: Nanoscale metal oxide-based heterojunctions for gas sensing: a review. Sensors Actuators B: Chem. **204**, 250–272 (2014)
146. Cui, T.H., Hua, F., Lvov, Y.: FET fabricated by layer-by-layer nanoassembly. IEEE Trans. Electron Devices **51**(3), 503–506 (2004)
147. Jeong, S.J., et al.: Characteristics of piezoelectric multilayer devices containing metal-oxide multicomponent electrode. Ferroelectrics **338**, 425- + (2006)

148. Winter, M., Brodd, R.J.: What are batteries, fuel cells, and supercapacitors? Chem. Rev. **104**(10), 4245–4270 (2004)
149. Hu, J.S., et al.: Synthesis of hierarchically structured metal oxides and their application in heavy metal ion removal. Adv. Mater. **20**(15), 2977–2982 (2008)
150. Wang, F.Y., et al.: Manipulating III–V nanowire transistor performance via surface decoration of metal-oxide nanoparticles. Adv. Mater. Interfaces **4**(12), 1700260 (2017)
151. Kumar, K.Y., et al.: Low-cost synthesis of metal oxide nanoparticles and their application in adsorption of commercial dye and heavy metal ion in aqueous solution. Powder Technol. **246**, 125–136 (2013)
152. Stoimenov, P.K., et al.: Metal oxide nanoparticles as bactericidal agents. Langmuir **18**(17), 6679–6686 (2002)
153. Serpone, N., Dondi, D., Albini, A.: Inorganic and organic UV filters: their role and efficacy in sunscreens and suncare product. Inorg. Chim. Acta **360**(3), 794–802 (2007)
154. Wang, H.T., et al.: Bifunctional non-noble metal oxide nanoparticle electrocatalysts through lithium-induced conversion for overall water splitting. Nat. Commun. **6**, 7261 (2015)
155. Wang, Z.L.: Zinc oxide nanostructures: growth, properties and applications. J. Phys.: Condens. Matter **16**(25), R829 (2004)
156. Moezzi, A., McDonagh, A.M., Cortie, M.B.: Zinc oxide particles: synthesis, properties and applications. Chem. Eng. J. **185–186**, 1–22 (2012)
157. Frederickson, C.J., Koh, J.-Y., Bush, A.I.: The neurobiology of zinc in health and disease. Nat. Rev. Neurosci. **6**, 449 (2005)
158. Code of Federal Regulations Title 21 (2017). https://www.accessdata.fda.gov/scripts/cdrh/cfdocs/cfcfr/CFRSearch.cfm?fr=182.8991
159. Espitia, P.J.P., et al.: Zinc oxide nanoparticles: synthesis, antimicrobial activity and food packaging applications. Food Bioprocess Technol. **5**(5), 1447–1464 (2012)
160. Casey, P.: 1—Nanoparticle technologies and applications. In: Nanostructure Control of Materials, pp. 1–31. Woodhead Publishing (2006)
161. Aghababazadeh, R., et al.: ZnO nanoparticles synthesised by mechanochemical processing. J. Phys: Conf. Ser. **26**(1), 312 (2006)
162. Swihart, M.T.: Vapor-phase synthesis of nanoparticles. Curr. Opin. Colloid Interface Sci. **8**(1), 127–133 (2003)
163. Willander, M., et al.: ZnO nanowires: chemical growth, electrodeposition, and application to intracellular nano-sensors. Phys. Status Solidi C **5**(9), 3076–3083 (2008)
164. Hu, H., Deng, C., Huang, X.: Hydrothermal growth of center-hollow multigonal star-shaped ZnO architectures assembled by hexagonal conic nanotubes. Mater. Chem. Phys. **121**(1), 364–369 (2010)
165. Arya, S.K., et al.: Recent advances in ZnO nanostructures and thin films for biosensor applications: review. Anal. Chim. Acta **737**, 1–21 (2012)
166. Zhao, J., Wu, L., Zhi, J.: Fabrication of micropatterned ZnO/SiO2 core/shell nanorod arrays on a nanocrystalline diamond film and their application to DNA hybridization detection. J. Mater. Chem. **18**(21), 2459–2465 (2008)
167. Zeng, H., et al.: Microstructure control of Zn/ZnO core/shell nanoparticles and their temperature-dependent blue emissions. J. Phys. Chem. B **111**(51), 14311–14317 (2007)
168. Wei, A., et al.: Enzymatic glucose biosensor based on ZnO nanorod array grown by hydrothermal decomposition. Appl. Phys. Lett. **89**(12), 123902 (2006)
169. Yu, L., Qu, F., Wu, X.: Solution synthesis and optimization of ZnO nanowindmills. Appl. Surf. Sci. **257**(17), 7432–7435 (2011)
170. Daumann, S., et al.: Water-free synthesis of ZnO quantum dots for application as an electron injection layer in light-emitting electrochemical cells. J. Mater. Chem. C **5**(9), 2344–2351 (2017)
171. Dai, Z., et al.: Immobilization and direct electrochemistry of glucose oxidase on a tetragonal pyramid-shaped porous ZnO nanostructure for a glucose biosensor. Biosens. Bioelectron. **24**(5), 1286–1291 (2009)

172. Lei, Y., et al.: Improved glucose electrochemical biosensor by appropriate immobilization of nano-ZnO. Colloids Surf. B. Biointerfaces **82**(1), 168–172 (2011)
173. Liu, J., et al.: Vertically aligned 1D ZnO nanostructures on bulk alloy substrates: direct solution synthesis, photoluminescence, and field emission. J. Phys. Chem. C **111**(13), 4990–4997 (2007)
174. Xia, C., et al.: Synthesis of nanochain-assembled ZnO flowers and their application to dopamine sensing. Sensors Actuators B: Chem. **147**(2), 629–634 (2010)
175. Zhang, Y., et al.: An enzyme immobilization platform for biosensor designs of direct electrochemistry using flower-like ZnO crystals and nano-sized gold particles. J. Electroanal. Chem. **627**(1), 9–14 (2009)
176. Brayner, R., et al.: ZnO nanoparticles: synthesis, characterization, and ecotoxicological studies. Langmuir **26**(9), 6522–6528 (2010)
177. Shukla, R.K., et al.: ROS-mediated genotoxicity induced by titanium dioxide nanoparticles in human epidermal cells. Toxicol. In Vitro **25**(1), 231–241 (2011)
178. Ortlieb, M.: White giant or white dwarf?: particle size distribution measurements of TiO2. GIT Lab. J. Eur. **14**, 42–43 (2010)
179. Taheri, M., Jahanfar, M., Ogino, K.: Self-cleaning traffic marking paint. Surf. Interfaces **9**, 13–20 (2017)
180. Fadhilah, N., et al.: Self-cleaning limestone paint modified by nanoparticles TiO2 synthesized from TiCl3 as precursors and PEG6000 as dispersant. Bull. Chem. React. Eng. Catal. **12**(3), 351–356 (2017)
181. Du, Z.F., et al.: Enhanced photocatalytic activity of Bi2WO6/TiO2 composite coated polyester fabric under visible light irradiation. Appl. Surf. Sci. **435**, 626–634 (2018)
182. Olariu, M.A., et al.: Electrical properties of polyimide composite films containing TiO2 nanotubes. Polym. Compos. **38**(11), 2584–2593 (2017)
183. Xu, W.J., et al.: Superhydrophobic titania nanoparticles for fabrication of paper-based analytical devices: an example of heavy metals assays. Talanta **181**, 333–339 (2018)
184. Imran, M., et al.: Oxygen-deficient TiO(2-x)methylene blue colloids: highly efficient photoreversible intelligent ink. Langmuir **32**(35), 8980–8987 (2016)
185. Ruiz, P.A., et al.: Titanium dioxide nanoparticles exacerbate DSS-induced colitis: role of the NLRP3 inflammasome. Gut **66**(7), 1216–1224 (2017)
186. Rompelberg, C., et al.: Oral intake of added titanium dioxide and its nanofraction from food products, food supplements and toothpaste by the Dutch population. Nanotoxicology **10**(10), 1404–1414 (2016)
187. Choi, S., et al.: A seasonal observation on the distribution of engineered nanoparticles in municipal wastewater treatment systems exemplified by TiO2 and ZnO. Sci. Total Environ. **625**, 1321–1329 (2018)
188. Nohynek, G.J., et al.: Grey goo on the skin? Nanotechnology, cosmetic and sunscreen safety. Crit. Rev. Toxicol. **37**(3), 251–277 (2007)
189. Lewicka, Z.A., et al.: Photochemical behavior of nanoscale TiO2 and ZnO sunscreen ingredients. Journal of Photochemistry and Photobiology a-Chemistry **263**, 24–33 (2013)
190. de la Calle, I., et al.: Screening of TiO2 and Au nanoparticles in cosmetics and determination of elemental impurities by multiple techniques (DLS, SP-ICP-MS, ICP-MS and ICP-OES). Talanta **171**, 291–306 (2017)
191. Titanium Compounds, Inorganic, in Kirk-Othmer Encyclopedia of Chemical Technology
192. G¨¢zquez, M.J.s., et al.: A review of the production cycle of titanium dioxide pigment. Mater. Sci. Appl. **05**(07), 18 (2014)
193. Behnajady, M.A., et al.: Investigation of the effect of sol–gel synthesis variables on structural and photocatalytic properties of TiO2 nanoparticles. Desalination **278**(1), 10–17 (2011)
194. Burda, C., et al.: Chemistry and properties of nanocrystals of different shapes. Chem. Rev. **105**(4), 1025–1102 (2005)
195. Carp, O., Huisman, C.L., Reller, A.: Photoinduced reactivity of titanium dioxide. Prog. Solid State Chem. **32**(1), 33–177 (2004)

196. Qian, Y., et al.: Preparation of ultrafine powders of TiO2 by hydrothermal H2O2 oxidation starting from metallic Ti. J. Mater. Chem. **3**(2), 203–205 (1993)
197. Kim, D.H., et al.: Photocatalytic behaviors and structural characterization of nanocrystalline Fe-doped TiO2 synthesized by mechanical alloying. J. Alloys Compd. **375**(1), 259–264 (2004)
198. Oh, S.-M., Ishigaki, T.: Preparation of pure rutile and anatase TiO2 nanopowders using RF thermal plasma. Thin Solid Films **457**(1), 186–191 (2004)
199. Susanna, A., et al.: Catalytic effect of ZnO anchored silica nanoparticles on rubber vulcanization and cross-link formation. Eur. Polym. J. **93**, 63–74 (2017)
200. Liu, Z.J., Zhang, Y.: Enhanced mechanical and thermal properties of SBR composites by introducing graphene oxide nanosheets decorated with silica particles. Compos. Part A-Appl. Sci. Manuf. **102**, 236–242 (2017)
201. Zhao, X.L., et al.: Surface modification of ultra-high molecular weight polyethylene fiber by different kinds of SiO2 nanoparticles. Polym. Compos. **38**(9), 1928–1936 (2017)
202. Mosquera, M.J., Carrascosa, L.A.M., Badreldin, N.: Producing superhydrophobic/oleophobic coatings on cultural heritage building materials. Pure Appl. Chem. **90**(3), 551–561 (2018)
203. Bernal, J., et al.: Fresh and mechanical behavior of a self-compacting concrete with additions of nano-silica, silica fume and ternary mixtures. Constr. Build. Mater. **160**, 196–210 (2018)
204. Wiilknitz, P.: Cleaning power and abrasivity of European toothpastes. Adv. Dental Res. **11**(4), 576–579 (1997)
205. Younes, M., et al.: Re-evaluation of silicon dioxide (E 551) as a food additive. EFSA J. **16**(1), e05088 (2018)
206. Athinarayanan, J., et al.: Presence of nanosilica (E551) in commercial food products: TNF-mediated oxidative stress and altered cell cycle progression in human lung fibroblast cells. Cell Biol. Toxicol. **30**(2), 89–100 (2014)
207. Peters, R., et al.: Presence of nano-sized silica during in vitro digestion of foods containing silica as a food additive. ACS Nano **6**(3), 2441–2451 (2012)
208. Taylor-Pashow, K.M.L., et al.: Hybrid nanomaterials for biomedical applications. Chem. Commun. **46**(32), 5832–5849 (2010)
209. Wang, L., Zhao, W., Tan, W.: Bioconjugated silica nanoparticles: development and applications. Nano Research **1**(2), 99–115 (2008)
210. Shirshahi, V., Soltani, M.: Solid silica nanoparticles: applications in molecular imaging. Contrast Media Mol. Imaging **10**(1), 1–17 (2015)
211. Teoh, W.Y., Amal, R., Madler, L.: Flame spray pyrolysis: an enabling technology for nanoparticles design and fabrication. Nanoscale **2**(8), 1324–1347 (2010)
212. Wolf, M.: Immer eine Idee besser: Forscher und Erfinder der Degussa. Degussa AG, Frankfurt am Main (1998)
213. Garrett, P.: Defoaming. CRC Press, Boca Raton (1992)
214. EVONIK. AEROSIL® – Fumed Silica. http://www.aerosil.com/product/aerosil/downloads/technical-overview-aerosil-fumed-silica-en.pdf
215. Stöber, W., Fink, A., Bohn, E.: Controlled growth of monodisperse silica spheres in the micron size range. J. Colloid Interface Sci. **26**(1), 62–69 (1968)
216. Shimura, N., Ogawa, M.: Preparation of surfactant templated nanoporous silica spherical particles by the Stöber method. Effect of solvent composition on the particle size. JMatS **42**(14), 5299–5306 (2007)
217. Ow, H., et al.: Bright and stable core-shell fluorescent silica nanoparticles. Nano Lett. **5**(1), 113–117 (2005)
218. Arriagada, F.J., Osseo-Asare, K.: Phase and dispersion stability effects in the synthesis of silica nanoparticles in a non-ionic reverse microemulsion. ColSu **69**(2), 105–115 (1992)
219. Huang, X., et al.: The effect of the shape of mesoporous silica nanoparticles on cellular uptake and cell function. Biomaterials **31**(3), 438–448 (2010)
220. Diagnosis and initial management of nonmalignant diseases related to asbestos. Am. J. Respir. Crit. Care Med. **170**(6), 691–715 (2004)
221. Trewyn, B.G., Whitman, C.M., Lin, V.S.Y.: Morphological control of room-temperature ionic liquid templated mesoporous silica nanoparticles for controlled release of antibacterial agents. Nano Lett. **4**(11), 2139–2143 (2004)

Chapter 2
Quantum Dots and Quantum Rods

Christin Rengers, Nikolai Gaponik and Alexander Eychmüller

Abstract Quantum Dots are tiny nanocrystals of a few nanometers in size. Due to their unique optical and electronic properties they are one of the core issues in the field of nanotechnology. This chapter will cover fundamental facts of Quantum Dots and the state of research of preparation methods and surface architectures. Section 2.1 will summarize the historical development of the field of nanotechnology and give a short introduction on Quantum Dots. The electronic structure and resultant optical properties are discussed in Sect. 2.2. The importance of the surface chemistry on the Quantum Dots functionality and optical properties will be explained in Sect. 2.3. Section 2.3.1 outlines the fundamental preparation methods and state of the art techniques in aqueous media and in organic solvents. Nanostructures of other geometries including their optical and electronic characteristic will be described in Sect. 2.4.

2.1 Introduction

The foundation for the development of the field of nanotechnology was laid by the speech of Richard Feynman "There is plenty of room at the bottom" in 1959, in which he spoke about the principles of miniaturization as low as to the atomic level. The term "nanotechnology" itself was first introduced by Taniguchi 1974, whereas first attempts towards the synthesis of semiconductor nanomaterials were done by Ekimov [1], Grätzel [2], Henglein [3] as well as Rosetti and Brus [4] in the early 1980s. In 1982, Efros and Efros [5] developed an idealized model to study the light absorption in semiconductor spheres. Postulating that the quantum size effect could be used to control the colour of the crystallites by changing their size or stoichiometry,

C. Rengers · N. Gaponik · A. Eychmüller (✉)
Physical Chemistry, Technical University of Dresden, Bergstrasse 66b,
01069 Dresden, Germany
e-mail: Alexander.eychmueller@chemie.tu-dresden.de

C. Rengers
e-mail: Christin.Rengers@gmx.de

N. Gaponik
e-mail: nikolai.gaponik@chemie.tu-dresden.de

P. Gehr and R. Zellner (eds.), *Biological Responses to Nanoscale Particles*,
NanoScience and Technology, https://doi.org/10.1007/978-3-030-12461-8_2

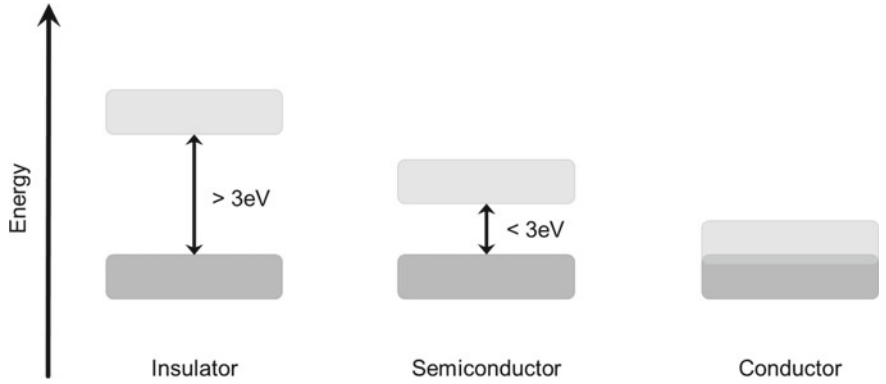

Fig. 2.1 Schematic illustration of the band structure of a semiconductor in comparison to insulators and conductors. The band gap of a semiconductor, which is the distance between the electron filled valence band (dark grey) and the empty conduction band (light grey) can be overcome by an electron upon absorption of a photon. A positively charged hole is left in the valence band, when the electron is excited to the conduction band. In the case of insulators, the band gap is unsurmountable high for electrons, whereas the valence band and conduction band of conductors overlap resulting in permanent electrical conductivity

they laid the foundation for the research on semiconductor quantum dots (QDs). The field of light-emitting semiconductor nanoparticles has experienced an enormous development over the past three decades and as a result the extent of the literature dealing with this topic has become virtually unmanageable.

QDs are colloidal nanocrystals, usually made from semiconductor materials, that possess particle diameters in the range of typically 1–20 nm. This corresponds to only some hundreds to a few thousands of atoms per particle, giving rise to the dominance of quantum mechanical effects in these structures. Generally, QDs are composed of an inorganic core capped by a surrounding organic surfactant layer, so-called ligands. The ligands, which are bound to surface atoms coordinatively, electrostatically or via van der Waals interactions, provide sufficient repulsion in order to prevent agglomeration of the QDs. Typically, QDs present different physical properties in comparison with the semiconductor bulk material that they are made of. One example for this behavior is the melting point depression. Another more interesting observation is the change of the semiconductor band gap energy, which is the reason for the unique optical properties of the QDs. In the case of bulk semiconductors, the band gap is a material specific constant and describes the energy difference between the electron-filled valence band and the empty conduction band (see Fig. 2.1). The change of the physical properties in nanometer-sized QDs results from the confinement of the charge carriers (electrons and holes) in all three spatial dimensions. Thus, their energies do not exhibit continuous but discrete values. The electronic and optical properties are strongly dependent on the nanocrystal dimension, shape and material of which the QDs are made of and can thus be tailored specifically.

2.2 Quantum-Size-Effect (and Optical Properties)

The electronic properties of QDs lie between those of the macroscopic expanded bulk and discrete molecules and are strongly dependent on the nanocrystal size. In a bulk semiconductor an electron can be excited from the valence band to the conduction band upon absorption of a photon with the energy at least as high as the band gap energy. The elevation of the electron evokes that a hole is left behind in the valence band. Due to Coulomb attractions the electron and the hole do not move independently from each other. One can say, they "feel" each other's charge and form an electron-hole pair, a so-called "exciton". However, the effective masses of the charge carriers are small and the dielectric constant is high so that the exciton's wave function ranges over a large region of several lattice spacings and the Bohr exciton radius is also large, i.e. approximately 3 and 5 nm for CdS and CdSe respectively. When the particle size is reduced to a few nanometers, such as in semiconductor QDs, the nanocrystal dimension may be smaller than the Bohr exciton radius. As a consequence, the exciton is confined in all three spatial dimensions (particle-in-a-box model) entailing higher kinetic energies of the charge carriers and an increasing band gap accompanied by quantization of the energy levels to discrete values. A mathematical description for this phenomenon, which is called the quantum-size-effect, was formulated in the above mentioned article by Efros and Efros and by Brus in 1986. He described the mathematical term for the band gap energy E_{QD} as a function of nanocrystal radius r, today known as the Brus-equation [6]:

$$E_{\mathrm{QD}} = E_g + \frac{h^2}{8m_e r^2}\left(\frac{1}{m_e^*} + \frac{1}{m_h^*}\right) - \frac{1,8e^2}{4\pi\varepsilon\varepsilon_0 r} \tag{2.1}$$

Here E_{g} is the band gap energy of the bulk material, h is the Planck constant, m_e is the electron mass, $\mathrm{m_e^*}$ and $\mathrm{m_h^*}$ are the effective masses of the electron and the hole, e is the elementary charge, ε is the relative permittivity and ε_0 the vacuum permittivity. The equation allows the calculation of E_{QD} starting from the band gap of the bulk semiconductor E_g, considering the repulsive impact of exciton formation in the quantum mechanical term and the attraction of the charge carriers by the coulomb term.

According to this formulation, the larger the QD, the smaller its band gap energy. Or conversely, smaller QDs possess a higher band gap energy (see Fig. 2.2). A photon with a certain energy E_P can be absorbed if its energy is exceeding the band gap energy of the QD, i.e. $E_P > \mathrm{E_{QD}}$. Hence, larger QDs are allowed to absorb photons with lower energy than smaller QDs. An electron that was elevated from the valence band to the conduction band upon absorption of a photon can relax radiatively to the ground state by emitting another photon. The energy of the emitted photon is thereby equal to the difference of the band gap energy of the QD and the Stokes shift and thus a function of QD size as well. Accordingly, using QDs of one material, it is possible to redshift the colour of the emitted photons with increasing particle size.

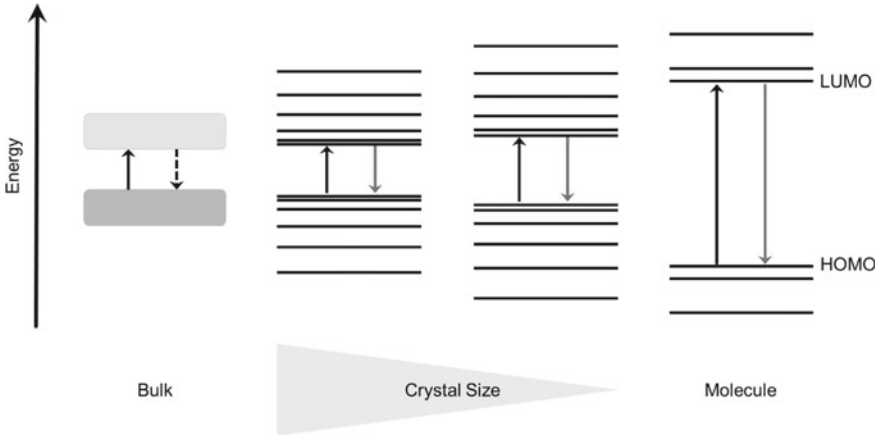

Fig. 2.2 Scheme of the quantum-size-effect. Due to the quantum confinement the semiconductor band gap increases and the density of states decreases with decreasing nanocrystal size

Electron-hole recombination in direct band gap colloidal QDs can occur through radiative band-to-band transition. Owing to their defined and discrete electronic structure, the emission spectrum of QDs is typically very narrow with full widths at half-maximum (FWHM) of about 15–40 nm. The observed peak broadening is mainly the result of the particle size distribution. Furthermore, QDs possess a high extinction coefficient and, when assuming appropriate surface capping, great stability against photobleaching and high photoluminescence intensity and lifetime. However, when the surface is not well passivated, dangling bonds may contribute additional electronic states lying within the bandgap of the QDs. These so-called trap states introduce competitive nonradiative pathways for the electron-hole recombination and thus undesirably alter the optical properties. Another nonradiative relaxation pathway is the Auger recombination. This process occurs when an exciton recombines, but instead of emitting a photon, the electron-hole recombination energy is transferred to a neighboring charge carrier (electron or hole), which is brought to a "hot" state. The Auger recombination is typically very fast with recombination times below 1 ns and quenches the radiative recombination [7]. Appropriate surface passivation can inhibit the nonradiative processes and is thus very important for the preservation of the unique optical properties of QDs.

Their superior size-dependent, tailorable optical properties make QDs a promising class of materials in various fields, where they provide an alternative to traditional organic luminophores. The latter often lack in photo-stability and have only a narrow absorption spectrum hindering efficient simultaneous multi-colour excitation. Promising application fields for QDs are for example: light emitting devices (LEDs), optical sensors, photocatalysis and photovoltaics [8–10].

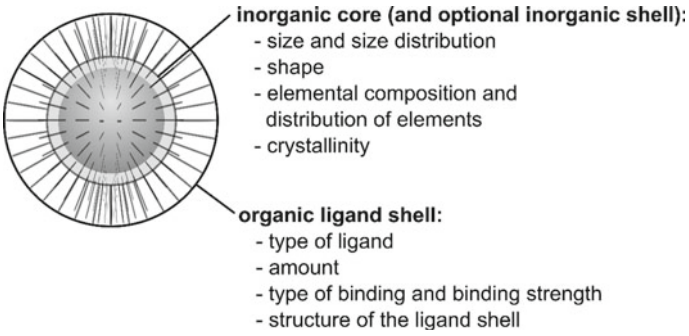

Fig. 2.3 Scheme of the core/shell architecture of a colloidal QD. In general, a colloidal QD consists of an inorganic core (frequently covered with an inorganic shell) and an organic ligand shell. Nature and properties of both parts have substantial influence on the characteristics of the final material

2.3 Surface Chemistry

Colloidal QDs are core/shell architectures that comprise a small inorganic core of a few nm in diameter, frequently covered with a wider-bandgap inorganic shell, and a coating with organic passivating surface ligands, also known as capping molecules, stabilizers or surfactants [11]. Whereas the optical properties, such as the spectral position and bandwidth of the first excitonic absorption maximum, the emission band, the fluorescence quantum yield, and fluorescence dynamics are mainly determined by the core, the surface chemistry has a substantial influence on the functionality of the QDs as well as the optical properties. The influence of both parts on the QD characteristics is displayed in Fig. 2.3.

As follows from the quantum-size-effect, the optical properties strongly depend on the nanocrystal size. Other parameters, however, should not be neglected in this context, such as the semiconductor material, the nanocrystal shape and the particle size distribution. Another influencing parameter to alter the optical properties is the elemental composition and element distribution in a nanocrystal in form of core/shell, alloyed or doped QDs. Furthermore, numerous studies for various materials show that the occurrence and amount of lattice defects in a QD strongly affect its properties as well [8, 10].

Nevertheless, the surface chemistry also plays an important role, although it is often neglected. The large surface-to-volume ratio in QDs implies at the same time a large number of surface atoms in comparison to the total amount of atoms in a NC. Therefore, the nature of the surface gains substantially more importance in nanocrystalline objects. Undercoordinated surface atoms lead to the presence of dangling bonds. These unsaturated atoms contribute electronic states lying between the valence and the conduction band of the QD and may, thus, alter its electronic and optical properties. To give an example, low-energy states may serve as dopants, whereas deeper band-tail and mid-gap states may act as trap states for charge carriers

and provide a path for fast electron-hole recombination, mostly non-radiatively [6]. Saturation of undercoordinated surface atoms can be done by the attachment of surface ligands. By this, energy states between the band gap of the QD are eliminated as the energy levels of occupied surface states are pushed below the valence band and the levels of the unoccupied surface states above the conduction band [12, 13]. Consequently, surface capping with a ligand shell provides a sufficient passivation of the QD surface by influencing the electronic structure resulting in improved optical properties.

The organic ligand shell is characterized by the type and amount of molecules on the NC surface, the exact structure of the shell as well as the type of chemical bonding and the bond strength. The ligands primarily determine the solubility of the QDs in different solvents and their colloidal stability. Additionally, the possibility of further functionalization enables various processing strategies. The choice of ligands is therefore a powerful tool to control design parameters such as the solubility in different matrices and routes to subsequent (bio)functionalization of QDs. Moreover, the ligands also play an important role during the QD synthesis as they provide control of the nucleation and growth kinetics [14–17].

The control of the surface chemistry is at least as important as the control of the particle size and dispersity. Although there have been significant improvements in understanding and the controlling of the interface between the NC and its ligand shell in the recent years [18], it is not entirely understood so far. Various characterization techniques have been used in order to investigate the arrangement of surface atoms, amount of ligands in the surrounding shell and its structure and the influence of the ligands on the electronic structure of the QDs [19], such as optical and vibrational spectroscopy [20–22], NMR spectroscopy [21–23], X-ray absorption [21] and UV photoelectron spectroscopy [24] and high resolution electron microscopy [25]. The combination of these experimental techniques with theoretical methods, such as DFT and molecular dynamics, provides more thorough insight into the surface structure and binding conditions and allows for the development of models to describe the QD/ligand core/shell structure [26, 27].

A second strategy to passivate the QD surface is the formation of an inorganic, epitaxial shell. Depending on the bandgaps and relative positions of the electronic energy levels of the involved semiconductors, the resulting nano-heterostructures can be classified into three different configurations, i.e. type I, type II (see Fig. 2.4) and reverse type I [28]. Upon excitation of a core/shell QD, the electron and the hole are confined in different regions of the core/shell structure according to the QD configuration. In type I heterostructures, the bandgap of the shell material is larger than that of the core and the valence and conduction band edges of the core lie between the band edges of the shell resulting in complete confinement of the charge carriers in the core. In reverse type I core/shell particles, the band gap of the shell material is smaller than that of the core and the valence and conduction band edges of the shell lie between the band edges of the core. In this configuration the electrons and the holes are, depending on the shell thickness, partially or completely confined within the shell. In type II heterostructures either the valence band edge or the conduction band edge is located in the band gap of the core. This configuration results in partial

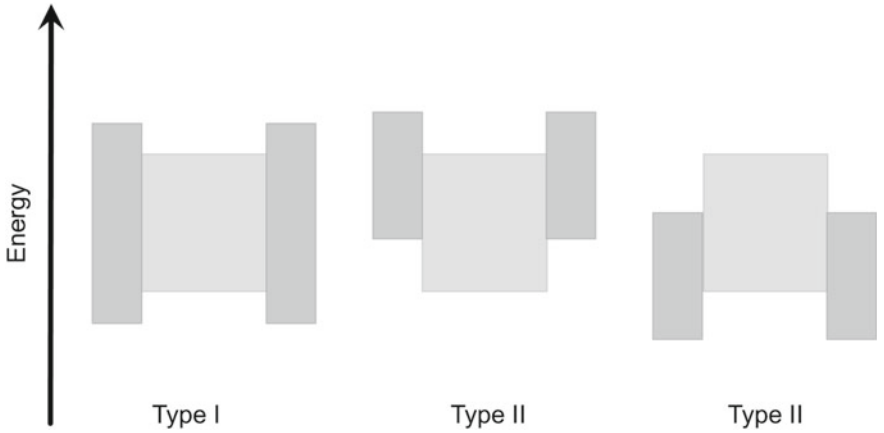

Fig. 2.4 Scheme of the band alignments for type I and type II core/shell heterostructures. The conduction and valence band edges correspond to the upper and lower edges of the rectangles

(quasi-type II) or complete (type II) separation of the charge carriers by extension of one charge carrier into the shell. Whereas the type I core/shell structure is the most beneficial configuration to passivate the QD surface and achieve high photoluminescence quantum yields (PL QYs), type II QDs are advantageous for electrical devices, such as photovoltaic devices or photodetectors, as they provide effective spatial separation of the charge carriers and decreased radiative recombination rates. The good passivation in type I QDs results on the one hand from the confinement of the charge carriers in the core and on the other hand from the physical separation of the optically active core from the exterior environment. The optical properties of the QDs are thus less sensitive to changes in the local environment of the NC's surface, such as induced by the presence of oxygen or water molecules. In general the optical properties of type I core/shell QDs are characterized by enhanced stability against photodegradation due to the just explained reason and at the same time enhanced PL QYs as the amount of surface dangling bonds is significantly reduced in this core/shell structures. After first successful type I prototype systems were introduced [29] a nicely characterized example was described by Hines and Guyot-Sionnest in 1996 [29]. They presented a CdSe/ZnS core/shell heterostructure, which displayed dramatically enhanced and long-time stable PL QY of 50%. The ZnS capping was accompanied by a slight red-shift of approximately 5 nm of the fluorescence peak, which can be explained by a partial leakage of the exciton into the shell. Furthermore, broad tails at higher wavelengths (700–800 nm) due to surface traps, which were observable in the fluorescence spectrum of CdSe QDs, were absent in the case of CdSe/ZnS.

In contrast to small spectral red-shifts in type I heterostructures, type II systems aim at significant red-shifts. By increasing the shell thickness, the emission colour can be tuned towards spectral ranges, which cannot be easily attained with other materials. Therefore, type II QDs such as CdTe/CdSe or CdSe/ZnTe are particularly

of interest for near-infrared emission. The PL decay is strongly prolonged in type II structures due to the lower overlap of the electron and the hole wavefunctions, however the PL QY and photostability is usually poor [29]. In order to enhance the PL QY and photostability of these heterostructures, an additional shell of an appropriate material can be added in the same way as in type I structures.

2.3.1 Synthesis Methods

2.3.1.1 Aqueous Synthesis

From a historical point of view, the first successful attempts of colloidal QD preparation were performed in aqueous media. In these early methods, colloidal NCs were synthesized from suitable reagents in homogeneous aqueous solution in the presence of surface-active or polymeric stabilizers [30–32], which bind to the NC surface and thus provide colloidal stability of the particles by steric inhibition and/or electrostatic repulsion. Amongst other capping agents, thiol ligands became widely popular in the beginning of the 1990s. 1993, the Nozik group reported on the controlled synthesis of quantized colloidal CdTe nanocrystals in aqueous solutions with narrow size distributions achieved by capping the QD particles with 3-mercapto-1,2-propanediol [33]. Nanocrystals with mean diameters of 20, 25, 35, and 40 Å were produced. Vossmeyer et al. [34] reported on CdS cluster-like species with low particle dispersity synthesized in DMF and water in 1994. "Ultrasmall CdS particles" from cadmium complexes of 2-mercaptoethanol were reported by Nosaka et al. in 1995 [35]. The relationship between the wavelength of the absorption peak and the size of clusters was discussed.

Another approach that was developed in parallel is a bi-phase technique, wherein NCs are grown in the nanoreactors of an inverse emulsion [36]. In these systems, nanometer-sized water droplets are dispersed in a continuous phase of an organic solvent. The droplets, commonly called micelles, are stabilized by amphiphilic surfactants.

Both methods substantially contributed to the development of QD synthesis providing low experimental complexity as well as the use of standard reagents and conditions. Although there have been great advances using other preparation techniques, for some materials such as mercury chalcogenides the aqueous synthesis approach remains the most successful preparation method until today [37–39]. However, nanometer-sized particles (except for magic-sized clusters) prepared from aqueous approaches generally display a broad size distribution. The size distribution results in large peak broadening so that individual transitions from quantized states cannot be observed in the optical spectra. For example, the size distribution of nanoparticles prepared inside inverse micelles is still 10–25% [40] despite the spatial limitation of the particle growth in the micellar cavity. In order to optimize this issue, many efforts have been pursued to develop suitable post-preparative methods, such as size-selective precipitation, size-selective photo etching [41], exclusion chromato-

graphy [42] and gel electrophoresis [43]. Probably the most important and nowadays most frequently used technique amongst them is the size-selective precipitation. This method, which is not restricted to aqueous-based QDs, was firstly introduced in 1993 by Chemseddine and Weller [44]. The separation according to particles size is based on the difference in solubility of differently sized particles in the same solvent [44, 45] and can be performed in large scale in contrast to other size-selective separation techniques like chromatography or electrophoresis [44]. Typically, size-selective precipitation of nanoparticles from colloidal dispersions is performed as follows: starting from as-prepared nanoparticle dispersions with broad size-distributions, a non-solvent is added dropwise until the optically clear solution turns slightly turbid. The turbidity indicates the beginning destabilization of the nanoparticles. Due to their higher attractive van-der-Waals forces, the largest nanoparticles tend to aggregate before the smaller particles. The aggregates formed in this manner can be isolated from the solution by centrifugation or filtration and then be re-dissolved in a suitable solvent. By this, the fraction of the largest particles will be separated from the original nanoparticle suspension. Repeating this procedure several times allows to isolate several size-selected fractions from one as-prepared nanoparticle dispersion resulting in size distributions for each fraction of 5–10% [44, 46].

Besides the efforts in the development of post-preparative methods, remarkable progress has also been made in the preparation and surface tailoring of thiol-capped water-soluble QDs during the last two decades. Depending on the semiconductor material and nanocrystal size, the photoluminescence of these QDs can cover a broad spectral range from the UV/Vis to the near infrared region. Nowadays, reliable aqueous synthesis approaches using different short-chained thiol stabilizers exist for many II–V and IV–VI semiconductor QDs such as CdTe [14, 15, 33, 47, 48], CdS [31, 34, 49], CdSe [50–52], HgTe [37], PbS [53–57] and ZnSe [58–60] as well as alloyed particles such as CdHgTe [61–64], CdSeTe [65], ZnSeS [58], ZnCdSe [60, 66–68] ZnHgSe [69] and ZnSeTe [70, 71]. These approaches provide QDs of high quality with PL QYs of up to 80% [72] and, thus, represent suitable alternatives to organic based synthesis routes. Thereby, the choice of the thiol ligand is a useful tool to exert influence on the surface functionality, stability and solubility of the nanocrystals, the passivation of surface dangling bonds and the kinetic control during the QD synthesis. Due to their excellent tuneable photoluminescence and high extinction coefficients, these nanocrystals provide application potential in the fields of light emitting diodes [73], colour conversion [74], energy scavenging [75, 76], fluorescence sensing [77–79], bioimaging [80] and biosensing [81].

The synthesis of water-based QDs from different semiconductor materials generally follows the same preparative approach, wherein molecules or complexes introducing species, also referred to as precursors, are decomposed to reactive species, so-called monomers, followed by nucleation and growth of the final colloidal nanocrystals from the monomers. As compared to organic based syntheses, the aqueous approach provides several advantages such as the use of water as a widespread, environmentally friendly and biocompatible solvent, which allows for an easy fabrication and processing in solution while avoiding the use of highly toxic organometallic. Furthermore, the cheap, simple and reproducible approach is not restricted to inert

atmosphere, allows easy up-scaling to industrial requirements, can yield versatile materials in terms of composition, size and shape, and provides various functionalization possibilities due to a large number of appropriate surface capping ligands, which also may be further manipulated by electrostatic or covalent linking [82].

A scheme of the synthesis of thiol capped semiconductor QDs in aqueous media is shown in Fig. 2.5. In a typical synthesis, a salt of the desired metal ion (Zn^{2+}, Cd^{2+}, Hg^{2+}) is dissolved in water in the presence of a thiol ligand such as thioglycolic acid (TGA), 3-mercaptopropionic acid (MPA), 1-thio-glycerol, 2-mercaptoethanol, L-cysteine, 2-(dimethylamino)ethanethiol or 2-mercaptoethylamine. The list of the thiol-stabilizers can be easily extended in order to achieve specific functionalities of the finally resulting QDs, e.g. 2-mercaptopropionic acid (2MPA), L-glutathione (GSH), dihydrolipoic acid (DHLA), 5-mercaptomethyltetrazole, mPEG-SH, mercaptosuccinic acid, etc. [82, 83]. Upon adjusting the pH, metal ion-thiolate complexes of various composition form. The adjustment of the pH to an appropriate value is as important as the proper choice of absolute and relative concentrations of the reaction components in order to efficiently control the reaction rate and the quality of the resulting QDs. H_2X (X = Te, Se, S) gas is then injected into the well deaerated metal ion-thiolate solution under inert atmosphere leading to the formation of precursors containing the metal cation, the chalcogenide anion and thiolates. Nucleation and growth of the nanocrystals finally proceed upon heating reflux to 100 °C or in the case of HgTe upon mixing at room temperature. The formation of nanoparticles is a dynamic process which usually is explained by an Ostwald ripening mechanism, wherein the growth of larger particles is realized at the expense of smaller ones present in the reaction solution. The growth of the QDs can be easily monitored by absorption and PL spectroscopy during the synthesis.

Whereas CdS was the first semiconductor QD compound synthesized in water [3], CdTe is the most successful example. Nowadays, CdTe and its optical properties are very well studied as is reflected by a large number of reviews on this material class [14, 15, 47, 82, 83]. The PL of CdTe QDs capped with different thiols and diameters of up to 6 nm can cover most of the visible spectrum up to the NIR region providing at the same time high PL QYs. Furthermore, by introducing Hg into the compound, alloyed CdHgTe QDs can be obtained whose photoluminescence is shifted towards the IR region up to 1600 nm [62]. It should be emphasized that up to now, these are the only nanocrystal compounds emitting in the NIR and IR region that can be synthesized in water with high quality using a one-pot reaction.

As outlined above, the aqueous approach for the synthesis of colloidal QDs can be performed by applying mild preparative conditions with no need for temperatures higher than 100 °C or environmental critical organometallics. However, the use of these mild conditions also holds some drawbacks. Since the temperature is not high enough, the perfect structural localization of atoms in the crystal lattice is disabled. The degree of crystallinity of QDs synthesized via the aqueous approach is therefore usually lower as compared to QDs from organic syntheses, where much higher temperatures of 200–360 °C are applied. Furthermore, the direct efficient control of size and shape is limited during the growth due to the relatively low temperature. For example, CdTe QDs synthesized in water show an isotropic zinc blende cubic crystal

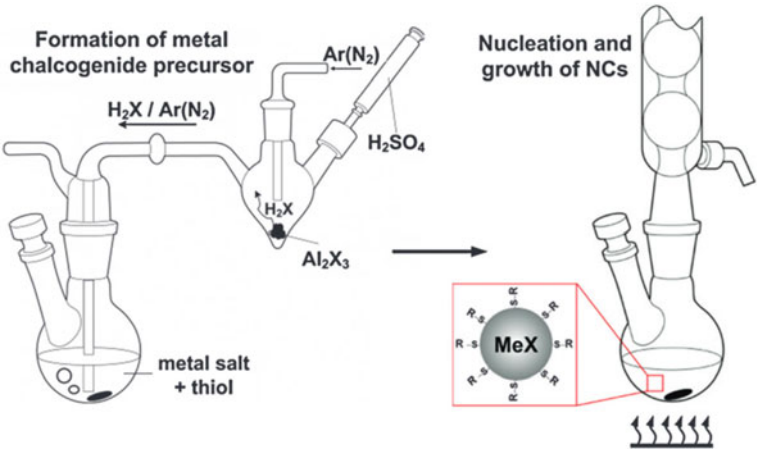

Fig. 2.5 Scheme of the synthesis of thiol-capped binary semiconductor QDs (ZnSe, CdSe, CdTe, HgTe) using aluminum chalcogenides (Al_2Se_3, Al_2Te_3) as the chalcogen source in aqueous medium. Involved are two reaction steps: (I) the precursor formation and (II) the NC nucleation and growth upon heating to reflux. Courtesy of A. Dubavik

structure and a mainly spherical or quasi-spherical shape as the applied temperature of 100 °C is not high enough to overcome the energy barrier of transforming zinc blende to wurtzite which is thermodynamically the most stable phase [84]. Although the aqueous approach typically allows the preparation of smaller nanocrystals, much narrower size-distributions can be achieved with the organic hot-injection technique owing to the effective separation the nucleation and growth stages. However, a fortunate fact is that the post-preparative size-selective precipitation is more reliable in the case of aqueous colloidal solutions in terms of preservation of the optical properties.

2.3.1.2 Synthesis in Organic Solvents

An important step towards the synthesis of CdE (E = S, Se, Te) QDs with low size dispersity ("monodisperse particles") was achieved in 1993 by Murray, Norris and Bawendi who reported on a high temperature preparation method using organic solvents [45]. Nowadays, among the so-called "bottom-up" colloidal approaches, the hot-injection method is a well-established procedure for the preparation of highly monodisperse spherical semiconductor nanocrystals. It earned its name from the typical synthetic procedure, wherein a chalcogenide precursor is injected into a hot solution of metal precursor in a high-boiling solvent. The precursors are decomposed due to the high temperature to highly reactive species leading to the formation of metal chalcogenide semiconductor NCs. According to LaMer and Dinegar, the degree of monodispersity of the resulting NCs originates from the homogeneous nucleation process, wherein nucleation and growth are separated [85].

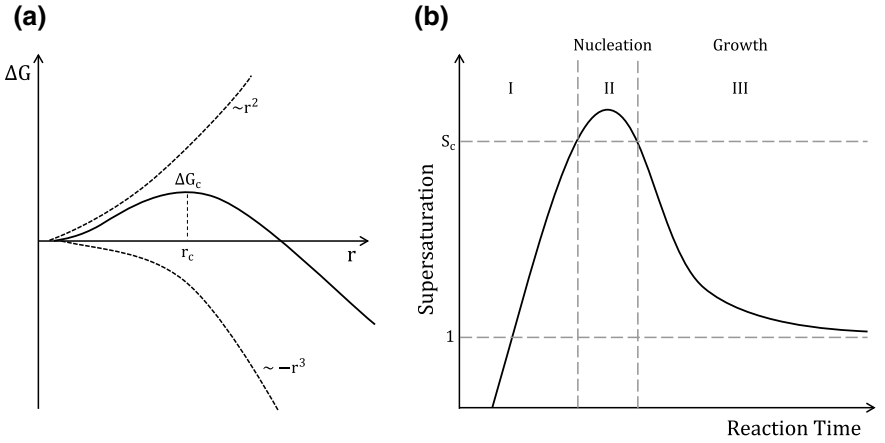

Fig. 2.6 **a** Plot of the Gibbs free energy for homogeneous nucleation and **b** LaMer plot for the change of supersaturation

The homogeneous nuclei formation has a high energy barrier, because of the higher surface energy of small NPs compared to the bulk. This energy barrier can be explained by regarding the Gibbs free energy change ΔG for the formation of a spherical nucleus with radius r. It is composed of the energy which is needed to form the new interface and the lattice energy that is released upon solid formation [17]:

$$\Delta G = 4\pi r^2 \gamma + \frac{4}{3}\pi r^3 \Delta \mathrm{G}_v \tag{2.2}$$

where γ is the surface free energy per unit area and ΔG_v is the free energy change per unit volume. Because the surface energy term is always positive and ΔG_v is negative as long as the solution is supersaturated, the plot of ΔG versus r has a maximum at r_c (see Fig. 2.6a). The critical radius r_c is the minimum radius of a nucleus which can be formed spontaneously. If nuclei with $r < r_c$ are formed, ΔG is mainly determined by the surface energy. In this case, nucleation is thermodynamically unfavourable and the nuclei will dissolve. In the case of $r > r_c$, the released lattice energy makes the nucleation more favorable and the stable nuclei formed will begin to grow. The critical free energy ΔG_c, which is needed to form a stable nucleus can be regarded as the activation energy.

In order to overcome this energy barrier and allow a spontaneous, homogeneous nucleation, a high supersaturation is needed. The supersaturation is induced by the rapid injection of the precursor into the hot solution. As demonstrated in Fig. 2.6b, the monomer concentration strongly increases during period I upon the thermal decomposition of the precursors until the critical supersaturation level S_c is reached. Exceeding S_c in period II, the energy barrier for homogeneous nucleation can be overcome. Thus, numerous nuclei are formed simultaneously, which consequently leads to a decrease of the monomer supersaturation. When the supersaturation is

decreased below S_c, further nucleation does not occur. In period III, the systems enters the growth stage and the particles keep growing as long as the solution is supersaturated. However, once the supersaturation is sufficiently depleted, further growth can proceed by Ostwald ripening, whereby larger particles grow at the expense of smaller ones. The smaller particles dissolve due to their higher surface energy resulting in a reduction of the total amount of particles in the system.

The original work of Bawendi and coworkers [45] described the hot-injection preparation of CdE (E = S, Se, Te) QDs with an emphasis on CdSe. The publication attracted much attention although this is rarely the case for new synthesis methods of already existing compounds. The widespread success of this preparation technique can be ascribed to its versatility, its reproducibility and the well-developed crystallinity and uniformity of the resulting high quality nanocrystals. Many adaptions of the synthesis were done including the variation of the temperature of injection and growth [86–88], the substitution of TOP and TOPO with other organic ligands [86, 89, 90], the growth of inorganic shells around the CdE core [29, 91–93] and the preparation of nanocrystals with non-spherical shape [94, 95]. Nowadays, also other compounds such as ZnE (E = S, Se, Te) materials can be prepared with good optical properties (ZnS [96], ZnSe [97], ZnTe [98]) using similar high temperature syntheses such as those employed for the CdE QDs. Furthermore, it became apparent that the preparation procedure using organometallic precursors and high temperatures is appropriate for the synthesis of semiconductor materials beyond II–VI compounds namely III–V (e.g. InAs, InP, GaP) and IV–VI (e.g. PbS, PbSe, PbTe) semiconductor compounds as well as metal nanocrystals.

A major disadvantage of the initially reported synthesis methods was the usage of pyrophoric organometallic precursors, which required special experimental precautions and limited the batch size to laboratory scale due to their extremely high reactivity. These hazardous organometallic precursors were gradually replaced by less hazardous compounds, which are much easier to handle. The preparation of CdE QDs for example is nowadays usually based on CdO [99, 100] or Cd salts of weak acids such as Cd-acetate [101, 102] instead of the former used extremely toxic dimethyl cadmium. Further modification of the high temperature method has been achieved by an appropriate selection of coordinating and non-coordinating ligands. It was demonstrated that coordinating ligands are not necessarily needed, since size and shape control of the QDs can also be achieved when high-boiling non-coordinating solvents such as octadecene are used in the presence of small amounts of coordinating agents in the reaction mixture, e.g. carboxylic acids, phosphonic acids or amines [103]. Owing to these modifications, the preparation of QDs has become cheaper, easier and less hazardous and enabled the possibility for large-scale syntheses, such as a multigram scale synthesis of CdSe/CdS [91].

Usually, a shell coating is required as the PL QY of core-only CdE QDs is comparatively low since the optical properties are strongly dependent on the nanocrystal surface and, thus, are easily affected by surface defects and poor surface passivation through organic molecules. As emphasized above, a type I heterostructure by coating with a larger bandgap semiconductor is a suitable measure to improve the PL QY and simultaneously protect the core from influences of the surrounding media. To

give an example, CdS and ZnS are isostructural materials for CdSe and have been applied to form shells and heterostructures with alloyed or graded composition [29, 104–106]. The PL QY of the resulting QDs was several times reported to be near 100%. A further undesired characteristic of many semiconductor core-only QDs is the on-off blinking behavior of their photoluminescence. The blinking is generally considered to arise from charging processes of the QD in which an electron (or hole) is temporarily lost to the surrounding matrix, e.g. by Auger ejection or charge tunneling, or captured to surface-related trap states [106]. When the QD is charged the emission is turned "off" and turns "on" again once the particle regains neutrality. The charged QD is susceptible to non-radiative Auger recombination, whereby the energy of an exciton is transferred to the extra carrier (electron in the case of a negatively charged QD, hole in the case of a positively charged QD), rather than recombining radiatively. Blinking is very unfavorable for many applications, such as single-photon light sources or biolabels for real-time monitoring of biomolecules. With respect to blinking suppression, type I core-shell structures have also been proven to be very promising as a decreased Auger recombination was reported in these heterostructures [107–109].

Several approaches have been developed for the synthesis of core-shell QDs, such as continuous or layer-by-layer shell growth [91, 100]. Amongst these, the most widespread technique is the layer-by-layer approach SILAR (successive ion layer adsorption and reaction process), which allows for stepwise tuning of the shell thickness. In this procedure, which was originally developed for the growth of high-quality thin films, the cation and anion precursor of the desired shell are alternately injected to a colloidal solution of QD cores allowing for controlled growth of a desired amount of monolayers of the shell material. In this way, the preparation of so-called giant CdSe/CdS QDs with more than 10 monolayers of CdS has been reported [106]. However, the SILAR method is quite time-consuming and complex, as it requires different growth temperatures and annealing times for the anion and cation precursor species, respectively, as well as different precursor amounts depending on the core size and/or number of coated layer. A recently reported alternative method to SILAR for the preparation of CdSe/CdS core-shell QDs is the "flash" synthesis, which is a seeded growth at relatively high temperatures of approximately 330 °C [110]. The temperatures during SILAR coating usually do not exceed 250 °C. The "flash" synthesis, which was adapted from the literature for the synthesis of anisotropic heterostructures, was reported to be a very fast and efficient method for the controlled growth of CdS on CdSe. CdS shells with up to 7 nm thickness were grown in only 3 min while preserving state-of-the-art optical properties.

As already stated above, the hot-injection preparation technique has been successfully adapted to other semiconductor compounds, such as the IV–VI compounds of lead chalcogenide. Lead chalcogenide QDs offer attractive optical properties due to their strong confinement and their narrow direct band gap (PbS 0.41 eV, PbSe 0.28 eV) [111]. Their high dielectric constants and small effective electron and hole masses result in large exciton Bohr radii, e.g. 20 nm for PbS and 46 nm for PbSe, which is about 4 respectively 9 times larger than that of CdSe [112]. Consequently, size quantization effects are more pronounced in lead chalcogenide QDs as compared

to cadmium chalcogenides QDs. Furthermore, the narrow band gap allows them to absorb and emit photons in the near-infrared and mid-infrared region. Combined with the large exciton Bohr radius this means that their size-dependent bandgaps can be tuned between 500 and 3000 nm [112, 113]. Potential applications of lead chalcogenide QDs can be found as optically active components in a wide range of devices, such as solar cells, IR lasers, IR detectors and fluorophores in the telecommunication field [114, 115]. With respect to photovoltaic applications, another beneficial property of lead chalcogenides is the possibility of multiple exciton generation (MEG) [116, 117].

Murray et al. firstly reported the synthesis of high quality PbSe nanocrystals using the hot-injection method in 2001. The QDs were obtained by rapidly injecting lead oleate and trioctylphosphine selenide into diphenylether at 90–220 °C [118]. Depending on the temperature, different QD sizes ranging from 3.5 nm to 15 nm with size distributions ~10% were obtained, whereby higher temperatures were used to prepare larger crystal sizes. The size distribution was further narrowed to 5% or better by size-selective precipitation. The resulting PbSe QDs had a pronounced first absorption maximum from ~1200 nm for 3 nm particles to 2200 nm for 9 nm particles. Later on, the study of the optical properties and the interband and intraband transitions in PbSe revealed high PL QYs of up to 85% [119, 120]. Similar to II–VI compounds, the synthetic protocol was later modified by the replacement of the coordinating solvent with the non-coordinating solvent octadecene.

Based on the hot-injection synthesis of PbSe, the first published and most commonly cited method for the preparation of PbS QDs was published by Hines and Scholes in 2003 [115]. They applied lead (II) oxide and bis(trimethylsilyl)sulfide as lead and sulfur sources and chose the non-coordinating solvent octadecene in combination with the stabilizer oleic acid as reaction medium. The synthesis reliably yields PbS QDs with pronounced absorption ranging from 800 to 1800 nm and narrow emission with small Stokes shifts. Numerous adaptions of the synthetic protocols have been made since then, including the variation of precursors, stabilizers and solvent. The procedures developed for PbSe and PbS have also been successfully adapted for the preparation of PbTe with narrow size distributions of ~5% [116, 121]. PbTe is particularly of interest for thermolelectric applications.

II–VI semiconductor QDs based on Cd have been the most investigated QD material for years due to their excellent optical properties referring to high PL QYs near unity [122], photostability and tunability of the emission wavelength over the entire visible spectrum. But besides these various favourable properties, one of the main disadvantages of these materials is the heavy metal compound cadmium. Due to the harmful impact and the cytotoxic potential of heavy metals, their use in household goods or consumer goods has been restricted in many regions of the world. The European Commission for example has therefore implemented several directives (EG) including the restriction of cadmium in accumulators 2006/66/EG or heavy metals in food 2001/466/EG and lighting equipment 2011/65/EU. Therefore, the usage of Cd-based QDs may not have a promising future. Detailed investigations in aqueous and biological media have revealed that oxidation through a variety of pathways leads to the formation of Cd^{2+} on the nanocrystal surface which can be

released to the surrounding media. The concentration of released Cd^{2+} was found to be directly correlated to the cytotoxic effect. Although appropriate shell coatings, such as ZnS, additional organic ligand shells or inorganic silica or polymer shells [123–125] significantly reduced the heavy metal ion release in some cases, a complete inhibition cannot be guaranteed.

The development of appropriate Cd-free alternatives is therefore essential. The new materials must meet the standards of their Cd-based references. NCs, such as ZnO, carbon dots or indirect band gap semiconductors imposed with non-toxic behaviour and wide abundance, but they do not represent an alternative for Cd-based QDs due to their low PL QY [126]. The following classes are therefore considered as suitable alternatives: III–V (e.g. InP), I–III–VI_2 compounds (e.g. $CuInS_2$, $CuInSe_2$) or doped II–VI semiconductor NCs (e.g. Mn^{2+} doped ZnS or ZnSe). Setting the stage for this class of materials, a number of difficulties require further research and development. Synthetic procedures, such as nanocrystal preparation, ligand exchanges or incorporation techniques, and processing techniques optimized for Cd-based QDs have to be adapted, due to the different surface chemistry and bonding strengths. Thus, changes with respect to altered solubility, impact of surface ligands and stability require for modified or new approaches. For example, the bonding of III–V semiconductors and their precursors is more covalent compared to the rather ionic bonding of their II–VI analogues [127]. Therefore, the separation of nucleation and growth is more difficult and requires higher reaction temperatures and prolonged reaction times. In fact, these conditions propagate Ostwald ripening, leading to a broader particle size distribution and FWHM. Consequently, modified synthetic procedures or highly reactive precursors have to be found.

So far, progresses in the synthesis of Cd-free QDs [128, 129] with QYs comparable to Cd-based QDs have been made and practical application in light conversion [130] or biological media [131] has been demonstrated.

A promising material for the replacement of Cd-based QDs is the low-toxic III–V semiconductor InP. By now, InP QDs have been under investigation for almost three decades. First reports were the publications of Uchida in 1990 and Mićić in 1994 on the synthesis of InP nanostructures in tectosilicates such as zeolites [132] and the synthesis of InP NPs respectively [133]. Based on the knowledge collected for CdSe QD synthesis, air-stable InP QDs were prepared using TOP/TOPO as the stabilizer. However, long reaction times of several days resulted in broad particle size distributions and very low PL QYs of only a few percent. With reference to their former work, Mićić et al. demonstrated the significant improvement of the PL QY of InP QDs up to 30% by etching the particle surface with hydrofluoric acid or ammonium fluoride in order to reduce surface defects in 1996 [134]. Nevertheless, long reaction times still had to be taken into account until Yu and Peng [103] proposed the usage of non-coordinating solvents in 2002, such as octadecene (ODE).

Subsequent studies were mainly focused on the improvement of surface passivation by encapsulation with appropriate shells in order to increase the PL QY of the InP QDs. Organic ligand shells, e.g. aliphatic acids [135], were found to improve the optical properties of the QDs as well as their stability. The same trend was encountered for inorganic shell coatings, such as ZnS [136], ZnSe [137] or ZnSSe [138],

resulting in core-shell QDs. However, high PL QYs comparable to Cd-based QDs were not accessible. The large lattice mismatch between the QD core and the shell material was considered as the most obvious reason for this. Hereof, a great progress was achieved by Kim et al. in 2012 [128]. Using GaP as a lattice adapter between the InP core and a ZnS shell, they were able to synthesize very bright and stable type-I structured InP-based core/shell/shell QDs with PL QYs up to 85%.

While possessing comparable optical properties by now, the in vitro and in vivo toxicity of InP-based QDs is much lower as compared to Cd-containing QDs. This was carefully investigated by Brunetti et al. in 2013 by a direct comparison of the toxicity of InP/ZnS and CdSe/ZnS particles in cells and animals [139]. Both QD species were adjusted to have similar properties known to affect cellular responses, i.e. size and size distributions, inorganic shell and surface chemistry in terms of ligand shell and surface charge. It was found that comparable ion leaching and cell uptake take place in in vitro cultures. However, the damage caused by InP QDs was greatly reduced to about 30% of the toxicity of CdSe QDs in in vivo necrosis tests. InP-based QDs as an environmentally friendly alternative to Cd-based QDs are therefore a relevant material for further research.

2.4 Nanostructures of Other Geometries

QDs are a special case of quantum particles, where all three spatial dimensions are in the size range of 1–100 nm. Quantum particles in general exhibit at least one dimension in the mentioned order, where quantum confinement effects may occur and lead to unique size-dependent optical, electronic, mechanical and chemical properties. Quantum particles can be classified into 0, 1 and 2 dimensional (D) particles, depending on the number of spatial dimensions in which charge carriers are confined. 0D particles represent QDs, where confinement occurs in three spatial dimensions, whereas 2D and 1D confinement is found in nanorods/-wires/-tubes and quantum wells, respectively. The electronic and opto-electronic properties of a quantum particle are primarily determined by its dimensionality and length of confinement as these parameters prevail the density of states for charge carriers. The density of electron and hole states changes from discrete levels for 0D quantum particles, to a saw-like quasicontinuum for 1D quantum particles and finally to a step-like quasicontinuum for 2D quantum particles. Furthermore, the quantum particle shape influences the Coulomb coupling between the electron and the hole resulting in higher exciton binding energies in 1D and 2D nanostructures. In the case of 0D QDs this results in their typical properties, such as the spectral width of the absorption band, the size-tunability of the PL emission, the symmetry of the emission bands and high PL intensity. An exceptional property that can be found in 1D nanorods/-wires/-tubes is anisotropic (or polarized) absorption and emission. Several potential application fields arise from this behavior, e.g. the usage for polarization sensitive devices such as optical switches and interconnects, integrated circuits and high-resolution detectors.

Quantum rods (QRs) are elongated 1D nanostructures that display confinement in two spatial dimensions. Unlike spherical QDs, which emit plane-polarized light, light emitted perpendicular to the long axis of QRs is linearly polarized due to their intrinsic anisotropy [140]. Moreover, the degree of polarization can be tuned by the aspect ratio of the QR [141]. On the contrary, light emitted parallel to the long axis of QRs is plane-polarized just like in the case of QDs. QRs are desirable building blocks for nanoscale materials and devices based on their linearly polarized absorption and emission but also other properties such as a large absorption cross section, low lasing threshold, improved charge separation and transport as compared to their QD counterparts and novel assembly opportunities for elongated nanoparticles originating from their intrinsic geometry [142]. With respect to their application potential reliable synthetic strategies for the preparation of monodisperse QRs with controlled aspect ratios are required. The development of such strategies is therefore highly important. Pioneering works on the preparation of colloidal semiconductor QRs by nucleation of precursors and selective monomer attachment [16, 94] were subsequently modified by the dot in rod seeded-growth approach [143, 144] and other approaches such as oriented attachment of spherical particles [145–147], catalyst-assisted nanorod growth [148, 149] and a recently developed thermodynamically driven material diffusion ripening process [150, 151]. These strategies already demonstrated great advances in terms of precise control of length, diameter and aspect ratio of the resulting QRs, however none of the mentioned strategies is versatile for the synthesis of all types of semiconductor QRs. Currently existing synthetic approaches for the synthesis of QRs from a certain semiconductor material are not necessarily applicable to other semiconductor materials. As the growth habit and influencing parameters are not sufficiently understood yet, further research needs to focus on the intrinsic properties of the semiconductor materials in combination with the control of the synthetic conditions, such as the type and amount of ligands, the monomer concentration, the growth temperature and the kinetic and thermodynamic of the chemical reaction.

A representative of 2D quantum particles are nanoplatelets, which are colloidal analogues to quantum well films known from lasing and light-harvesting layers in optoelectronic devices. Nanoplatelets can be synthesized with atomic layer precision. For CdS, CdSe or CdTe precise thickness control of 4–11 monolayers and a widely tunable lateral dimension ranging from ~10 nm to more than 100 nm are reported [152, 153]. Due to the large number of atoms in these quantum particles and the atomic homogeneity in the dimension of confinement, exceptionally narrow excitation and emission bands can be found in nanoplatelets, which offers them a high application potential e.g. for multiplexed bioimaging of several spectrally distinct signals. Similar to carbon-based graphene sheets, thin nanoplatelets with a large lateral dimension tend to roll themselves into helical tubes [154]. Thicker nanoplatelets with a smaller lateral dimension usually possess larger quantum yields and are thus currently preferred for physical studies.

References

1. Ekimov, A.I., Onushchenko, A.A.: JETP Lett. **34**(6), 345–349 (1981)
2. Kalyanasundaram, K., Borgarello, E., Duonghong, D., Grätzel, M.: Angew. Chem. Int. Ed. Engl. **20**(11), 987–988 (1981)
3. Henglein, A.: Ber. Bunsenges. Phys. Chem. **86**(4), 301–305 (1982)
4. Rossetti, R., Brus, L.: J. Phys. Chem. **86**(23), 4470–4472 (1982)
5. Efros, A.L., Efros, A.: Sov. Phys. Semicond **16**, 772 (1982)
6. Brus, L.: J. Phys. Chem. **90**(12), 2555–2560 (1986)
7. Klimov, V.I., Mikhailovsky, A.A., McBranch, D.W., Leatherdale, C.A., Bawendi, M.G.: Science **287**(5455), 1011–1013 (2000)
8. Rogach, A.: Semiconductor Nanocrystal Quantum Dots: Synthesis, Assembly, Spectroscopy and Applications. Springer, Berlin (2008)
9. Talapin, D.V., Lee, J.-S., Kovalenko, M.V., Shevchenko, E.V.: Chem. Rev. **110**(1), 389–458 (2010)
10. Schmid, G.: Nanoparticles: From Theory to Application. Wiley, New York (2011)
11. Shirasaki, Y., Supran, G.J., Bawendi, M.G., Bulovic, V.: Nat. Photonics **7**(1), 13–23 (2013)
12. Trotzky, S., Kolny-Olesiak, J., Falke, S.M., Hoyer, T., Lienau, C., Tuszynski, W., Parisi, J.: J. Phys. D Appl. Phys. **41**(10), 102004 (2008)
13. Kilina, S., Ivanov, S., Tretiak, S.: J. Am. Chem. Soc. **131**(22), 7717–7726 (2009)
14. Rogach, A.L., Franzl, T., Klar, T.A., Feldmann, J., Gaponik, N., Lesnyak, V., Shavel, A., Eychmüller, A., Rakovich, Y.P., Donegan, J.F.: J. Phys. Chem. C **111**(40), 14628–14637 (2007)
15. Gaponik, N., Talapin, D.V., Rogach, A.L., Hoppe, K., Shevchenko, E.V., Kornowski, A., Eychmüller, A., Weller, H.: J. Phys. Chem. B **106**(29), 7177–7185 (2002)
16. Yin, Y., Alivisatos, A.P.: Nature **437**(7059), 664–670 (2005)
17. Park, J., Joo, J., Kwon, S.G., Jang, Y., Hyeon, T.: Angew. Chem. **119**(25), 4714–4745 (2007)
18. Boles, M.A., Ling, D., Hyeon, T., Talapin, D.V.: Nat. Mater. **15**(2), 141–153 (2016)
19. Guyot-Sionnest, P., Wehrenberg, B., Yu, D.: J. Chem. Phys. **123**(7), 074709 (2005)
20. Leubner, S., Hatami, S., Esendemir, N., Lorenz, T., Joswig, J.-O., Lesnyak, V., Recknagel, S., Gaponik, N., Resch-Genger, U., Eychmüller, A.: Dalton Trans. **42**(35), 12733–12740 (2013)
21. Protesescu, L., Nachtegaal, M., Voznyy, O., Borovinskaya, O., Rossini, A.J., Emsley, L., Copéret, C., Günther, D., Sargent, E.H., Kovalenko, M.V.: J. Am. Chem. Soc. **137**(5), 1862–1874 (2015)
22. Badia, A., Cuccia, L., Demers, L., Morin, F., Lennox, R.B.: J. Am. Chem. Soc. **119**(11), 2682–2692 (1997)
23. Hens, Z., Martins, J.C.: Chem. Mater. **25**(8), 1211–1221 (2013)
24. Brown, P.R., Kim, D., Lunt, R.R., Zhao, N., Bawendi, M.G., Grossman, J.C., Bulović, V.: ACS Nano **8**(6), 5863–5872 (2014)
25. Panthani, M.G., Hessel, C.M., Reid, D., Casillas, G., José-Yacamán, M., Korgel, B.A.: J. Phys. Chem. C **116**(42), 22463–22468 (2012)
26. Zherebetskyy, D., Scheele, M., Zhang, Y., Bronstein, N., Thompson, C., Britt, D., Salmeron, M., Alivisatos, P., Wang, L.-W.: Science **344**(6190), 1380–1384 (2014)
27. Schapotschnikow, P., Hommersom, B., Vlugt, T.J.H.: J. Phys. Chem. C **113**(29), 12690–12698 (2009)
28. (a) Dorfs, D., Eychmüller, A., Z. Phys. Chem. **220**(12), 1539–1552 (2006); (b) Reiss, P., Protière, M., Li, L.: Small **5**(2), 154–168 (2009)
29. (a) Hässelbarth, A., Eychmüller, A., Eichberger, R., Giersig, M., Mews, A., Weller, H.: J. Phys. Chem. **97**(20), 5333–5340 (1993); (b) Hines, M.A., Guyot-Sionnest, P.: J. Phys. Chem. **100**(2), 468–471 (1996); (c) Dorfs, D., Franzl, T., Osovsky, R., Brumer, M., Lifshitz, E., Klar, T.A., Eychmüller, A.: Small **4**(8), 1148–1152 (2008)
30. Fojtik, A., Weller, H., Koch, U., Henglein, A.: Ber. Bunsenges. Phys. Chem. **88**(10), 969–977 (1984)

31. Spanhel, L., Haase, M., Weller, H., Henglein, A.: J. Am. Chem. Soc. **109**(19), 5649–5655 (1987)
32. Rossetti, R., Nakahara, S., Brus, L.E.: J. Chem. Phys. **79**(2), 1086–1088 (1983)
33. Rajh, T., Micic, O.I., Nozik, A.J.: J. Phys. Chem. **97**(46), 11999–12003 (1993)
34. Vossmeyer, T., Katsikas, L., Giersig, M., Popovic, I.G., Diesner, K., Chemseddine, A., Eychmueller, A., Weller, H.: J. Phys. Chem. **98**(31), 7665–7673 (1994)
35. Nosaka, Y., Shigeno, H., Ikeuchi, T.: J. Phys. Chem. **99**(20), 8317–8322 (1995)
36. Lianos, P., Thomas, J.K.: Chem. Phys. Lett. **125**(3), 299–302 (1986)
37. Rogach, A., Kershaw, S.V., Burt, M., Harrison, M.T., Kornowski, A., Eychmüller, A., Weller, H.: Adv. Mater. **11**(7), 552–555 (1999)
38. Kuno, M., Higginson, K.A., Qadri, S.B., Yousuf, M., Lee, S.H., Davis, B.L., Mattoussi, H.: J. Phys. Chem. B **107**(24), 5758–5767 (2003)
39. Shen, G., Guyot-Sionnest, P.: J. Phys. Chem. C **120**(21), 11744–11753 (2016)
40. Steigerwald, M.L., Alivisatos, A.P., Gibson, J.M., Harris, T.D., Kortan, R., Muller, A.J., Thayer, A.M., Duncan, T.M., Douglass, D.C., Brus, L.E.: J. Am. Chem. Soc. **110**(10), 3046–3050 (1988)
41. van Dijken, A., Janssen, A.H., Smitsmans, M.H.P., Vanmaekelbergh, D., Meijerink, A.: Chem. Mater. **10**(11), 3513–3522 (1998)
42. Fischer, C.H., Weller, H., Katsikas, L., Henglein, A.: Langmuir **5**(2), 429–432 (1989)
43. Eychmueller, A., Katsikas, L., Weller, H.: Langmuir **6**(10), 1605–1608 (1990)
44. Chemseddine, A., Weller, H.: Ber. Bunsenges. Phys. Chem. **97**(4), 636–638 (1993)
45. Murray, C.B., Norris, D.J., Bawendi, M.G.: J. Am. Chem. Soc. **115**(19), 8706–8715 (1993)
46. Norris, D.J., Bawendi, M.G.: Phys. Rev. B **53**(24), 16338–16346 (1996)
47. Li, Y., Jing, L., Qiao, R., Gao, M.: Chem. Commun. **47**(33), 9293–9311 (2011)
48. Rogach, A.L., Katsikas, L., Kornowski, A., Su, D., Eychmüller, A., Weller, H.: Ber. Bunsenges. Phys. Chem. **100**(11), 1772–1778 (1996)
49. Weller, H.: Angew. Chem. Int. Ed. Engl. **32**(1), 41–53 (1993)
50. Rogach, A.L., Kornowski, A., Gao, M., Eychmüller, A., Weller, H.: J. Phys. Chem. B **103**(16), 3065–3069 (1999)
51. Bäumle, M., Stamou, D., Segura, J.-M., Hovius, R., Vogel, H.: Langmuir **20**(10), 3828–3831 (2004)
52. Kalasad, M.N., Rabinal, M.K., Mulimani, B.G.: Langmuir **25**(21), 12729–12735 (2009)
53. Gallardo, S., Gutiérrez, M., Henglein, A., Janata, E.: Ber. Bunsenges. Phys. Chem. **93**(10), 1080–1090 (1989)
54. Zhao, X., Gorelikov, I., Musikhin, S., Cauchi, S., Sukhovatkin, V., Sargent, E.H., Kumacheva, E.: Langmuir **21**(3), 1086–1090 (2005)
55. Bakueva, L., Gorelikov, I., Musikhin, S., Zhao, X.S., Sargent, E.H., Kumacheva, E.: Adv. Mater. **16**(11), 926–929 (2004)
56. Deng, D., Zhang, W., Chen, X., Liu, F., Zhang, J., Gu, Y., Hong, J.: Eur. J. Inorg. Chem. **2009**(23), 3440–3446 (2009)
57. Levina, L., Sukhovatkin, V., Musikhin, S., Cauchi, S., Nisman, R., Bazett-Jones, D.P., Sargent, E.H.: Adv. Mater. **17**(15), 1854–1857 (2005)
58. Shavel, A., Gaponik, N., Eychmüller, A.: J. Phys. Chem. B **108**(19), 5905–5908 (2004)
59. Li, C.L., Nishikawa, K., Ando, M., Enomoto, H., Murase, N.: Colloids Surf. A: Physicochem. Eng. Aspects **294**(1–3), 33–39 (2007)
60. Zheng, Y., Yang, Z., Ying, J.Y.: Adv. Mater. **19**(11), 1475–1479 (2007)
61. Harrison, M.T., Kershaw, S.V., Burt, M.G., Eychmüller, A., Weller, H., Rogach, A.L.: Mater. Sci. Eng.: B **69–70**, 355–360 (2000)
62. Lesnyak, V., Lutich, A., Gaponik, N., Grabolle, M., Plotnikov, A., Resch-Genger, U., Eychmüller, A.: J. Mater. Chem. **19**(48), 9147–9152 (2009)
63. Rogach, A.L., Harrison, M.T., Kershaw, S.V., Kornowski, A., Burt, M.G., Eychmüller, A., Weller, H.: Phys. Status Solidi (B) **224**(1), 153–158 (2001)
64. Sun, H., Zhang, H., Ju, J., Zhang, J., Qian, G., Wang, C., Yang, B., Wang, Z.Y.: Chem. Mater. **20**(21), 6764–6769 (2008)

65. Piven, N., Susha, A.S., Döblinger, M., Rogach, A.L.: J. Phys. Chem. C **112**(39), 15253–15259 (2008)
66. Liu, F.-C., Cheng, T.-L., Shen, C.-C., Tseng, W.-L., Chiang, M.Y.: Langmuir **24**(5), 2162–2167 (2008)
67. Lesnyak, V., Plotnikov, A., Gaponik, N., Eychmüller, A.: J. Mater. Chem. **18**(42), 5142–5146 (2008)
68. Deng, Z., Lie, F.L., Shen, S., Ghosh, I., Mansuripur, M., Muscat, A.J.: Langmuir **25**(1), 434–442 (2009)
69. Liu, F.-C., Chen, Y.-M., Lin, J.-H., Tseng, W.-L.: J. Colloid Interface Sci. **337**(2), 414–419 (2009)
70. Li, C., Nishikawa, K., Ando, M., Enomoto, H., Murase, N.: J. Colloid Interface Sci. **321**(2), 468–476 (2008)
71. Lesnyak, V., Dubavik, A., Plotnikov, A., Gaponik, N., Eychmüller, A.: Chem. Commun. **46**(6), 886–888 (2010)
72. He, Y., Sai, L.-M., Lu, H.-T., Hu, M., Lai, W.-Y., Fan, Q.-L., Wang, L.-H., Huang, W.: Chem. Mater. **19**(3), 359–365 (2007)
73. Rogach, A L., Gaponik, N., Lupton, J.M., Bertoni, C., Gallardo, D.E., Dunn, S., Li Pira, N., Paderi, M., Repetto, P., Romanov, S.G., O'Dwyer, C., Sotomayor Torres, C.M., Eychmüller, A.: Angew. Chem. Int. Ed. **47**(35), 6538–6549 (2008)
74. Cicek, N., Nizamoglu, S., Ozel, T., Mutlugun, E., Karatay, D.U., Lesnyak, V., Otto, T., Gaponik, N., Eychmüller, A., Demir, H.V.: Appl. Phys. Lett. **94**(6), 061105 (2009)
75. Franzl, T., Klar, T.A., Schietinger, S., Rogach, A.L., Feldmann, J.: Nano Lett. **4**(9), 1599–1603 (2004)
76. Rakovich, A., Sukhanova, A., Bouchonville, N., Lukashev, E., Oleinikov, V., Artemyev, M., Lesnyak, V., Gaponik, N., Molinari, M., Troyon, M., Rakovich, Y.P., Donegan, J.F., Nabiev, I.: Nano Lett. **10**(7), 2640–2648 (2010)
77. Mohamed Ali, E., Zheng, Y., Yu, H.-H., Ying, J.Y.: Anal. Chem. **79**(24), 9452–9458 (2007)
78. Susha, A.S., Javier, A.M., Parak, W.J., Rogach, A.L.: Colloids Surf. A: Physicochem. Eng. Aspects **281**(1–3), 40–43 (2006)
79. Xu, S., Wang, C., Zhang, H., Sun, Q., Wang, Z., Cui, Y.: J. Mater. Chem. **22**(18), 9216–9221 (2012)
80. Nabiev, I., Mitchell, S., Davies, A., Williams, Y., Kelleher, D., Moore, R., Gun'ko, Y.K., Byrne, S., Rakovich, Y.P., Donegan, J.F., Sukhanova, A., Conroy, J., Cottell, D., Gaponik, N., Rogach, A., Volkov, Y.: Nano Lett. **7**(11), 3452–3461 (2007)
81. Yuan, J., Gaponik, N., Eychmüller, A.: Anal. Chem. **84**(11), 5047–5052 (2012)
82. Gaponik, N., Rogach, A.L.: Phys. Chem. Chem. Phys. **12**(31), 8685–8693 (2010)
83. Lesnyak, V., Gaponik, N., Eychmüller, A.: Chem. Soc. Rev. **42**(7), 2905–2929 (2013)
84. Smith, A.M., Nie, S.: Acc. Chem. Res. **43**(2), 190–200 (2010)
85. LaMer, V.K., Dinegar, R.H.: J. Am. Chem. Soc. **72**(11), 4847–4854 (1950)
86. Talapin, D.V., Rogach, A.L., Kornowski, A., Haase, M., Weller, H.: Nano Lett. **1**(4), 207–211 (2001)
87. de Mello Donegá, C., Hickey, S.G., Wuister, S.F., Vanmaekelbergh, D., Meijerink, A.: J. Phys. Chem. B **107**(2), 489–496 (2003)
88. Katari, J.E.B., Colvin, V.L., Alivisatos, A.P.: J. Phys. Chem. **98**(15), 4109–4117 (1994)
89. Qu, L., Peng, X.: J. Am. Chem. Soc. **124**(9), 2049–2055 (2002)
90. Bullen, C.R., Mulvaney, P.: Nano Lett. **4**(12), 2303–2307 (2004)
91. Li, J.J., Wang, Y.A., Guo, W., Keay, J.C., Mishima, T.D., Johnson, M.B., Peng, X.: J. Am. Chem. Soc. **125**(41), 12567–12575 (2003)
92. Dabbousi, B.O., Rodriguez-Viejo, J., Mikulec, F.V., Heine, J.R., Mattoussi, H., Ober, R., Jensen, K.F., Bawendi, M.G.: J. Phys. Chem. B **101**(46), 9463–9475 (1997)
93. Talapin, D.V., Mekis, I., Götzinger, S., Kornowski, A., Benson, O., Weller, H.: J. Phys. Chem. B **108**(49), 18826–18831 (2004)
94. Manna, L., Scher, E.C., Alivisatos, A.P.: J. Am. Chem. Soc.s **122**(51), 12700–12706 (2000)
95. Peng, X.: Adv. Mater. **15**(5), 459–463 (2003)

96. Li, Y., Li, X., Yang, C., Li, Y.: J. Phys. Chem. B **108**(41), 16002–16011 (2004)
97. Hines, M.A., Guyot-Sionnest, P.: J. Phys. Chem. B **102**(19), 3655–3657 (1998)
98. Xie, R., Zhong, X., Basché, T.: Adv. Mater. **17**(22), 2741–2745 (2005)
99. Peng, Z.A., Peng, X.: J. Am. Chem. Soc. **123**(1), 183–184 (2001)
100. Mekis, I., Talapin, D.V., Kornowski, A., Haase, M., Weller, H.: J. Phys. Chem. B **107**(30), 7454–7462 (2003)
101. Liu, H., Owen, J.S., Alivisatos, A.P.: J. Am. Chem. Soc. **129**(2), 305–312 (2007)
102. Qu, L., Peng, Z.A., Peng, X.: Nano Lett. **1**(6), 333–337 (2001)
103. Yu, W.W., Peng, X.: Angew. Chem. Int. Ed. **41**(13), 2368–2371 (2002)
104. Peng, X., Schlamp, M.C., Kadavanich, A.V., Alivisatos, A.P.: J. Am. Chem. Soc. **119**(30), 7019–7029 (1997)
105. Xie, R., Kolb, U., Li, J., Basché, T., Mews, A.: J. Am. Chem. Soc. **127**(20), 7480–7488 (2005)
106. Chen, Y., Vela, J., Htoon, H., Casson, J.L., Werder, D.J., Bussian, D.A., Klimov, V.I., Hollingsworth, J.A.: J. Am. Chem. Soc. **130**(15), 5026–5027 (2008)
107. Hollingsworth, J.A.: Chem. Mater. **25**(8), 1318–1331 (2013)
108. Wang, X., Ren, X., Kahen, K., Hahn, M.A., Rajeswaran, M., Maccagnano-Zacher, S., Silcox, J., Cragg, G.E., Efros, A.L., Krauss, T.D.: Nature **459**(7247), 686–689 (2009)
109. Mahler, B., Spinicelli, P., Buil, S., Quelin, X., Hermier, J.-P., Dubertret, B.: Nat. Mater. **7**(8), 659–664 (2008)
110. Cirillo, M., Aubert, T., Gomes, R., Van Deun, R., Emplit, P., Biermann, A., Lange, H., Thomsen, C., Brainis, E., Hens, Z.: Chem. Mater. **26**(2), 1154–1160 (2014)
111. Brumer, M., Kigel, A., Amirav, L., Sashchiuk, A., Solomesch, O., Tessler, N., Lifshitz, E.: Adv. Func. Mater. **15**(7), 1111–1116 (2005)
112. Wise, F.W.: Acc. Chem. Res. **33**(11), 773–780 (2000)
113. Hickey, S.G., Gaponik, N., Eychmüller, A.: Photonics Nanostruct. Fundam. Appl. **5**(2–3), 113–118 (2007)
114. Nagel, M., Hickey, S.G., Frömsdorf, A., Kornowski, A., Weller, H.: Z. Phys. Chem. **221**(3), 427–437 (2007)
115. Hines, M.A., Scholes, G.D.: Adv. Mater. **15**(21), 1844–1849 (2003)
116. Murphy, J.E., Beard, M.C., Norman, A.G., Ahrenkiel, S.P., Johnson, J.C., Yu, P., Micic, O.I., Ellingson, R.J., Nozik, A.J.: J. Am. Chem. Soc. **128**(10), 3241–3247 (2006)
117. Ellingson, R.J., Beard, M.C., Johnson, J.C., Yu, P., Micic, O.I., Nozik, A.J., Shabaev, A., Efros, A.L.: Nano Lett. **5**(5), 865–871 (2005)
118. Murray, C.B., Sun, S., Gaschler, W., Doyle, H., Betley, T.A., Kagan, C.R.: IBM J. Res. Dev. **45**(1), 47–56 (2001)
119. Du, H., Chen, C., Krishnan, R., Krauss, T.D., Harbold, J.M., Wise, F.W., Thomas, M.G., Silcox, J.: Nano Lett. **2**(11), 1321–1324 (2002)
120. Wehrenberg, B.L., Wang, C., Guyot-Sionnest, P.: J. Phys. Chem. B **106**(41), 10634–10640 (2002)
121. Lu, W., Fang, J., Stokes, K.L., Lin, J.: J. Am. Chem. Soc. **126**(38), 11798–11799 (2004)
122. Greytak, A.B., Allen, P.M., Liu, W., Zhao, J., Young, E.R., Popovic, Z., Walker, B.J., Nocera, D.G., Bawendi, M.G.: Chem. Sci. **3**(6), 2028–2034 (2012)
123. Derfus, A.M., Chan, W.C.W., Bhatia, S.N.: Nano Lett. **4**(1), 11–18 (2004)
124. Kirchner, C., Liedl, T., Kudera, S., Pellegrino, T., Muñoz Javier, A., Gaub, H.E., Stölzle, S., Fertig, N., Parak, W.J.: Nano Lett. **5**(2), 331–338 (2005)
125. Selvan, S.T., Tan, T.T., Ying, J.Y.: Adv. Mater. **17**(13), 1620–1625 (2005)
126. Anc, M.J., Pickett, N.L., Gresty, N.C., Harris, J.A., Mishra, K.C.: ECS J. Solid State Sci. Technol. **2**(2), R3071–R3082 (2013)
127. Bharali, D.J., Lucey, D.W., Jayakumar, H., Pudavar, H.E., Prasad, P.N.: J. Am. Chem. Soc. **127**(32), 11364–11371 (2005)
128. Kim, S., Kim, T., Kang, M., Kwak, S.K., Yoo, T.W., Park, L.S., Yang, I., Hwang, S., Lee, J.E., Kim, S.K., Kim, S.-W.: J. Am. Chem. Soc. **134**(8), 3804–3809 (2012)
129. De Trizio, L., Prato, M., Genovese, A., Casu, A., Povia, M., Simonutti, R., Alcocer, M.J.P., D'Andrea, C., Tassone, F., Manna, L.: Chem. Mater. **24**(12), 2400–2406 (2012)

130. Lim, J., Park, M., Bae, W.K., Lee, D., Lee, S., Lee, C., Char, K.: ACS Nano **7**(10), 9019–9026 (2013)
131. Akkerman, Q.A., Genovese, A., George, C., Prato, M., Moreels, I., Casu, A., Marras, S., Curcio, A., Scarpellini, A., Pellegrino, T., Manna, L., Lesnyak, V.: ACS Nano **9**(1), 521–531 (2015)
132. Uchida, H., Ogata, T., Yoneyama, H.: Chem. Phys. Lett. **173**(1), 103–106 (1990)
133. Micic, O.I., Curtis, C.J., Jones, K.M., Sprague, J.R., Nozik, A.J.: J. Phys. Chem. **98**(19), 4966–4969 (1994)
134. Mićić, O.I., Sprague, J., Lu, Z., Nozik, A.J.: Appl. Phys. Lett. **68**(22), 3150–3152 (1996)
135. Battaglia, D., Peng, X.: Nano Lett. **2**(9), 1027–1030 (2002)
136. Gao, S., Zhang, C., Liu, Y., Su, H., Wei, L., Huang, T., Dellas, N., Shang, S., Mohney, S.E., Wang, J.: Opt. Express **19**(6), 5528–5535 (2011)
137. Kim, M.R., Chung, J.H., Lee, M., Lee, S., Jang, D.-J.: J. Colloid Interface Sci. **350**(1), 5–9 (2010)
138. Lim, J., Bae, W.K., Lee, D., Nam, M.K., Jung, J., Lee, C., Char, K., Lee, S.: Chem. Mater. **23**(20), 4459–4463 (2011)
139. Brunetti, V., Chibli, H., Fiammengo, R., Galeone, A., Malvindi, M.A., Vecchio, G., Cingolani, R., Nadeau, J.L., Pompa, P.P.: Nanoscale **5**(1), 307–317 (2013)
140. Chen, X., Nazzal, A., Goorskey, D., Xiao, M., Peng, Z.A., Peng, X.: Phys. Rev. B **64**(24), 245304 (2001)
141. Hu, J., Li, L.-S., Yang, W., Manna, L., Wang, L.-W., Alivisatos, A.P.: Science **292**(5524), 2060–2063 (2001)
142. Jia, G., Xu, S., Wang, A.: J. Mater. Chem. C **3**(32), 8284–8293 (2015)
143. Carbone, L., Nobile, C., De Giorgi, M., Sala, F.D., Morello, G., Pompa, P., Hytch, M., Snoeck, E., Fiore, A., Franchini, I.R., Nadasan, M., Silvestre, A.F., Chiodo, L., Kudera, S., Cingolani, R., Krahne, R., Manna, L.: Nano Lett. **7**(10), 2942–2950 (2007)
144. Sitt, A., Salant, A., Menagen, G., Banin, U.: Nano Lett. **11**(5), 2054–2060 (2011)
145. Pacholski, C., Kornowski, A., Weller, H.: Angew. Chem. Int. Ed. **41**(7), 1188–1191 (2002)
146. Liao, H.-G., Cui, L., Whitelam, S., Zheng, H.: Science **336**(6084), 1011–1014 (2012)
147. Evers, W.H., Goris, B., Bals, S., Casavola, M., de Graaf, J., Roij, R.v., Dijkstra, M., Vanmaekelbergh, D.: Nano Lett. **13**(6), 2317–2323 (2013)
148. Shen, H., Shang, H., Niu, J., Xu, W., Wang, H., Li, L.S.: Nanoscale **4**(20), 6509–6514 (2012)
149. Kan, S., Mokari, T., Rothenberg, E., Banin, U.: Nat. Mater. **2**(3), 155–158 (2003)
150. Jia, G., Banin, U.: J. Am. Chem. Soc. **136**(31), 11121–11127 (2014)
151. Jia, G., Sitt, A., Hitin, G.B., Hadar, I., Bekenstein, Y., Amit, Y., Popov, I., Banin, U.: Nat. Mater. **13**(3), 301–307 (2014)
152. Ithurria, S., Dubertret, B.: J. Am. Chem. Soc. **130**(49), 16504–16505 (2008)
153. Son, J.S., Wen, X.-D., Joo, J., Chae, J., Baek, S.-I., Park, K., Kim, J.H., An, K., Yu, J.H., Kwon, S.G., Choi, S.-H., Wang, Z., Kim, Y.-W., Kuk, Y., Hoffmann, R., Hyeon, T.: Angew. Chem. Int. Ed. **48**(37), 6861–6864 (2009)
154. Hutter, E.M., Bladt, E., Goris, B., Pietra, F., van der Bok, J.C., Boneschanscher, M.P., de Mello Donegá, C., Bals, S., Vanmaekelbergh, D.: Nano Lett. **14**(11), 6257–6262 (2014)

Chapter 3
Polymeric Nanocarriers

Banu Iyisan and Katharina Landfester

Abstract Control over the nanoscopic scale opens nearly endless opportunities for many scientific areas. In particular, polymeric nanoparticles offer the versatility to cover a wide range of mesoscopic properties for sophisticated applications. However, making and applying smart nanoparticles is inevitably linked to a deep understanding of the overall physico-chemical principle of their formation and their interaction with their surroundings.

3.1 Introduction

Control over the nanoscopic scale opens nearly endless opportunities for many scientific areas. In particular, polymeric nanoparticles offer the versatility to cover a wide range of mesoscopic properties for sophisticated applications. However, making and applying smart nanoparticles is inevitably linked to a deep understanding of the overall physico-chemical principle of their formation and their interaction with their surroundings.

The ideal nanocarrier for biomedical application would be biodegradable and shall circulate freely in the blood until it reaches selectively its place of action, is incorporated and selectively releases the drug or allows diagnostics only at this point with finally being cleared from the body without any trace. To reach this ideal case, key characteristics of the nanocarriers including composition, size, biocompatibility, colloidal stability, targeting ability and control over the diffusion mechanism of the loaded drugs should be precisely engineered.

In this context, the aim of this chapter is to discuss various types of polymeric nanocarriers from the perspective of their formation, design, and characterization for drug delivery applications. Therefore, the chapter starts with the classification of the nanocarriers, which is then followed by the description of advanced preparation techniques. Furthermore, the requirement and possible ways of encapsulation and release methods for drugs and reporter molecules in terms of stimuli-responsivity

B. Iyisan · K. Landfester (✉)
Max Planck Institute for Polymer Research, Ackermannweg 10, 55128 Mainz, Germany
e-mail: landfester@mpip-mainz.mpg.de

P. Gehr and R. Zellner (eds.), *Biological Responses to Nanoscale Particles*,
NanoScience and Technology, https://doi.org/10.1007/978-3-030-12461-8_3

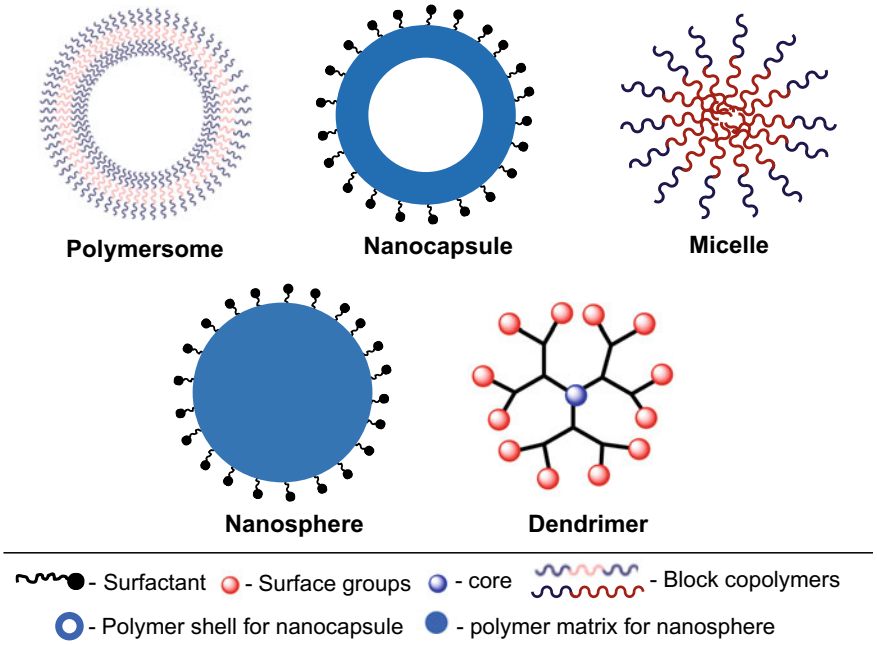

Fig. 3.1 Schematic illustration of various polymeric nanocarriers

and multifunctionality are described in detail before finalizing the chapter with the focus of widely used characterization tools for nanocarriers.

3.1.1 Classification and Types of Polymeric Nanocarriers

The International Union of Pure and Applied Chemistry (IUPAC) defines nanoparticles as particles of any shape in the nanometer size range [1]. By keeping this definition as a base for the nomenclature of this chapter, the term polymeric nanocarriers covers various types of colloidal particles, which differ by their size, structure and morphology. Figure 3.1 outlines these nanoparticles that are classified as (i) nanospheres, (ii) nanocapsules, (iii) polymersomes, (iv) micelles, and (v) dendrimers including their diameter scale ranging from 1 nm to 1000 nm. They all have different advantages depending on their physicochemical characteristics that leads to varied applications in drug delivery field.

3.1.1.1 Nanospheres

Nanospheres are solid particles in spherical shape that are composed of a polymer matrix having one single phase. The drugs can be incorporated to the matrix by embedding them either physically or covalently and can be then released depending on the polymer nature as being biodegradable or stimuli-responsive.

3.1.1.2 Nanocapsules

Nanocapsules are defined by IUPAC as a "hollow nanoparticle composed of a solid shell that surrounds a core-forming space available to entrap substances [1]." They can be described as container systems where the hydrophobic or hydrophilic drugs are placed in the core covered by a polymer shell layer. Nanocapsules enable optimized drug encapsulation with the aid of a large selection of the core material whereas the polymeric shell enhances the lifetime of the drugs by protection from the factors such as pH value and tissue irritation. Besides, the polymeric shell also prevents the side effects of the drugs or marker molecules that is the case most of the time in nanomedicine. For example, to investigate individual organs with nuclear magnetic resonance tomography, a contrast medium is injected into the patient that consists in many cases of magnetite nanoparticles containing iron oxide. The disadvantage of pure magnetite nanoparticles is that they do not remain stable in water and therefore not in blood either, and can even dissolve; this can lead in turn to iron shock. To avoid this, these substances need a protective shell. In comparison to commercially available particles thus far, it was possible to envelop these marker particles in miniemulsions to be hydrophobic first, rather than hydrophilic [2–4]. In addition, the dense hydrophobic polymer shell prevents the encapsulated substance from chemically reacting with the dispersion medium, i.e. first with the water and then with the blood, thus protecting it. This underlines the importance and benefits of container like structures as nanocapsules in nanomedicine.

3.1.1.3 Polymersomes

Polymersomes can be classified in the nanocapsule group, as they are also container like systems having an aqueous core surrounded by a polymeric bilayer. In contrary to bulk nanocapsule structures, the formation is triggered by the self assembly of amphiphilic block copolymers designed with a suitable hydrophilic/hydrophobic balance. They are analogous to liposomes that are self-assembled natural phospholipids. However, many promising properties including higher mechanical strength, enhanced stability as well wide range of chemical versatility make polymersomes advantageous over their lipid counterparts. Besides, encapsulation of both hydrophilic and hydrophobic drugs simultaneously to the core and membrane of the polymersomes is another promising property that increase the drug delivery applications of these particles over the past decades.

3.1.1.4 Micelles

Polymeric micelles are typically spherical nanosized particles with a core-shell structure formed by the self-assembled amphiphilic block copolymers. They are formed in aqueous solution when the concentration of the amphiphilic block copolymers is above the critical micelle concentration (CMC) in which thermodynamic stabilization against disassembly is provided. By this, the hydrophobic regions of the amphiphiles are accumulated in the core that serves a space for lipophilic drugs whereas the hydrophilic parts of the block copolymers tend to place towards the water as a brush like corona. Although polymeric micelles have a better stability in comparison to micelles of small surfactants, they are relatively instable in bloodstream leading to rapid disassembly and drug release [5]. In order to avoid this obstacle, the corona of the micelles are usually formed by poly (ethylene oxide) (PEO) polymers that provides a steric stabilization to the core. Additionally, the thermal- or photo-crosslinking of the core helps to keep them intact as shown in cross-linked PEO-PLA based micelles by Kataoka et al. [6, 7].

3.1.1.5 Dendrimers

Dendrimers are perfectly branched macromolecules that are grown from a functional core through subsequent branching units. These tree-like structures are spherical particles having a diameter range of about 1–20 nm. The size and molecular weight varies depending on the generation number which is a term to define the amount of dendritic arms from the core towards to the particle periphery. The potential of dendrimers are lying down in their multivalent surface where the high amount of functional groups exist. By this way, various drugs or marker molecules like dyes can be covalently bound to use them in delivery and diagnostic applications. In addition, the drugs can also be placed into their core and cavity through non-covalent interactions, which enables the loading of many drugs simultaneously. One obstacle of these particles can be their smaller size that can lead to a relatively fast clearance from the bloodstream. Apart from that, they have gained an increased interest with their uniform size distribution and ease of multifunctionalization since their discovery by Vögtle et al. [8]. Some of the common dendritic particles are poly(propylene) imine (PPI) [9] and poly(amido) amine (PAMAM) [10] dendrimers as studied by various research groups.

3.2 Preparation Methods

3.2.1 Nanocapsules and Nanospheres

3.2.1.1 Emulsion Polymerization

Emulsion polymerization is a type of heterogeneous polymerization process that is divided into three groups: (macro)emulsion, microemulsion, and miniemulsion polymerizations [11]. The first two types are described in the following whereas miniemulsion polymerization will be discussed in detail in the next part.

In (macro)emulsion polymerization, the micron-sized monomer droplets

(1–10 μm in diameter) are dispersed in a continuous phase and are stabilized by surfactant molecules. At first, the emulsion comprises the surfactant micelles and the large monomer droplets. The polymerization starts with the initiation step where the water soluble initiator forms oligoradicals from slightly water soluble monomer units. Afterwards, the obtained oligoradicals enter to the surfactant micelles to form the particles. The particle growth continues along with the diffusion of the monomer from the large droplets to the micelles through the water phase. Commonly, particles larger than 100 nm are formed by using this type of conventional Emulsion Polymerization. Monomers such as vinyl acetate, vinyl chloride, acrylamine acrylates and methacrylates can be polymerized by this way.

In microemulsion polymerization, thermodynamically stable dispersions are spontaneously formed from mixtures of water and an organic phase. The precondition for microemulsions is to use large amount of surfactant molecules that results with the complete coverage of the particles. This is the reason why interfacial tension between organic and water phases are close to zero in microemulsions. In addition to the surfactant molecule often cosurfactants such as hexanol or pentanol are used to obtain the low interfacial tension. The polymerization starts when the thermodynamic equilibrium is reached. Then polymer chain growth proceeds solely in some of the droplets because the initiation does not take place simultaneously at all microdroplets. This type of microemulsion polymerization leads to the particles having a size range of 10–100 nm.

3.2.1.2 Miniemulsion polymerization

By means of the miniemulsion process, it is possible to design custom-made nanoparticles and nanocapsules for nearly any purpose. This is facilitated by the enormous versatility of the miniemulsion process that has been developed and conceptually understood. The concept of the miniemulsion process was first described in 1973 by Ugelstad, ElAasser and Vanderhoff [12]. The accumulation of understanding the formation process has led to successful and precise control of important nanoparticle parameters such as size, shape, morphology, degradation, release kinetics and surface functionalization [11, 13–15]. This degree of control is unique and allows one to

tune specific properties tailored to particular applications; the successful up-scaling of the process is of technical relevance. Furthermore, the encapsulation and release of a great variety of payloads, ranging from hydrophobic to hydrophilic substances has been successfully achieved in a highly controlled manner and with unmatched high encapsulation efficiency. The continuous progress in understanding the detailed properties of nanosized objects and their interactions in materials as well as in biomedical applications or with electromagnetic radiation opens new opportunities.

The Miniemulsion Process

A child hardly sees the light of this world before becoming acquainted with a vital emulsion: milk. Later on, most people come into contact with emulsions and dispersion systems often on a given day, whether in the bathroom in the form of liquid soaps, skin creams, and toothpastes, in the kitchen as dairy cream, margarine or mayonnaise, or working with paint (from water-based to latex paint) and adhesives. Using a special form of emulsion, known as the miniemulsion, nanoparticles and nanocontainers can be formed, and supply them with a broad palette of functions which can not be obtained in this perfection by other means: tunable size, high homogeneity of the particle size and structure, high stability in a liquid environment, high solid content, high loading capacity for many materials, adjustable interactions to synthetic and biological materials, upscalable to ton scale.

How to Understand Stability of Emulsions

By emulsions, we mean systems of two immiscible liquids, where one liquid—we refer to this as a phase—is distributed in the form of droplets into a second liquid that is called a continuous phase. For milk, liquid soaps, skin creams, and mayonnaise, small droplets of fat are suspended in water. Solid particles distributed in a liquid is called a suspension. In paints, the pigments and polymer particles are finely distributed in water; in adhesives, they are sticky polymer particles. Emulsions, considered as liquid droplets in a liquid, and suspensions, considered as solid particles in a liquid, are also labelled dispersions, and droplets or particles dispersed within them as colloids. As a rule, surfactants maintain the droplets and particles in their form within the continuous phase. For the miniemulsions, the oil droplets were only stable when very specific conditions were maintained. Therefore, it was first needed to understand what prevents two liquids such as oil and water from exsolving or unmixing.

Anyone who cooks knows how difficult it can be to make a stable emulsion. Vinegar and oil separate immediately and again even when you thoroughly shake them. Two processes are involved here. One is coalescence: droplets merge when you disturb them. This process can be suppressed quite well by using surfactants.

In the other process, Ostwald ripening destabilizes emulsions. This process is based upon the curvature strain in a droplet, which strongly depends on its size. The more tightly the surface of the droplet is curved, the higher the pressure inside the droplet. Since in practice the droplets of an emulsion are not all exactly the same size, the curvature strain in them also varies: it is higher in the smaller droplets than in the larger ones. Since the high pressure within small drops is energetically less favourable, larger ones grow at the expense of the smaller ones. This ripening process can begin if molecules from the smaller drop are able to diffuse through the

continuous phase into the larger drops. The process is called Ostwald ripening and continues until the liquids have totally separated.

Both processes are effectively suppressed in miniemulsions so they remain stable. Therefore, it is now possible to manufacture nanospheres and nanocapsules from the droplets and thus design vehicles for diverse applications.

The Importance of the Third Component

For obtaining a stability of miniemulsion, a third component, known as a co-stabilizer or osmotic agent, can be used to suppress the diffusion in simple one-component miniemulsions. The co-stabilizer accomplishes this by building up an osmotic pressure in opposition to the curvature strain. In the case of oil-in-water miniemulsion, the osmotic agent is an (ultra)hydrophobic agent and needs to be even less soluble in water than the oil droplets so that itself cannot diffuse. In the mixing process, droplets develop having the identical concentration as the (ultra)hydrophobic reagent. If the larger oil droplets begin to grow due to the Ostwald ripening, the concentration of the ultrahydrophobic reagent rises in the shrinking droplets, while it decreases in the expanding droplets. Such a difference in concentration leads to differential osmotic pressures and is thermodynamically very unfavourable, particularly as the osmotic pressures were previously equal. Therefore, the oil molecules diffuse from the large droplets back into the smaller ones. Hence, effectively no diffusion takes place, since the mechanisms of Ostwald ripening and the osmotic pressure equalization at equilibrium exactly equal one another. Thus, the droplets remain stable. To reach this equilibrium, the droplets may not be too different in size from one another at the beginning, however. It was found that the size of the droplets can be easily adjusted, using for instance a high-pressure homogenizer or ultrasound device, to diameters of between 30 and 500 nm.

On the one hand, fundamental physical knowledge with this setup have been obtained about these kinds of complex mixtures, and on the other hand, the stabilized droplets in the miniemulsions have facilitated many modern applications in various areas of research and technology, since they are very small and permit diverse materials to be combined inside them. Effectively transporting drugs to desired locations in the body is one of the most prominent applications of such nanoparticles, which significantly reduces the side effects.

Platform for Particle Formation

By suppressing the Ostwald ripening, is it possible to obtain stable miniemulsions and to make use of them in synthesising diverse nanoparticles. Miniemulsion technology thus represents a versatile platform for producing (polymer) nanoparticles. It is based on the ability to distribute the chemical components of the desired colloidal mixtures into individual emulsion droplets actually prior to polymerization. This allows one to carry out many different reactions in spatially and chemically isolated compartments, i.e. the droplets, without the components diffusing. In this way, every drop represents an independent "nanoreactor" with the identical size and identical composition.

It has not only be possible to transform smaller organic and inorganic molecules and substances in numerous reactions within the nanoreactors, it has also been possible over the past years to transfer the conceptual design of the miniemulsion to

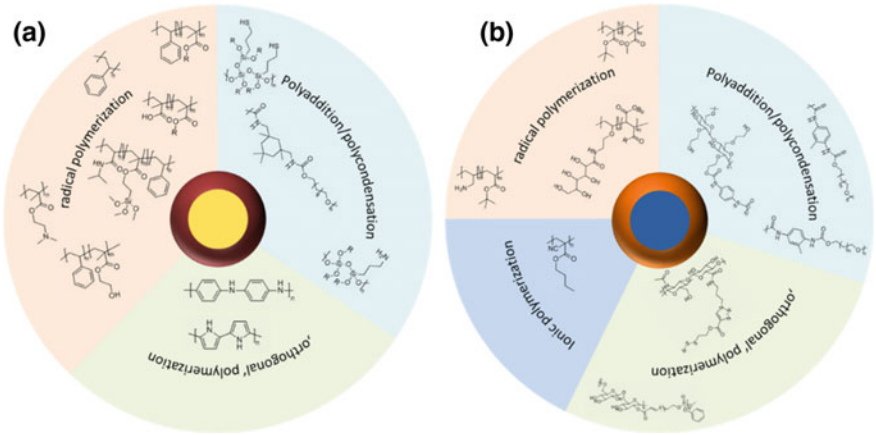

Fig. 3.2 Summary of used polymerization techniques in direct (**a**) or (**b**) inverse miniemulsions to fabricate nanoparticles and nanocapsules

polymer chemistry. In this way, a broad range of different nanoparticles, depending on how the process is carried out and the monomers used, by our polymerizing monomers within the droplets has been very successfully produced. Prior to 2000, only radical polymerization was possible in emulsions and miniemulsions. After having comprehensively investigated and understood the stabilization process, it was possible to carry out for the first time all types of polymerization and create nanoparticles for numerous applications via condensation polymerization, step polymerization, polyaddition, as well as radical, oxidative, and anionic polymerization methods as shown in Fig. 3.2. Depending on the hydrophilicity of the monomer, particles either in direct (oil-in-water) or inverse (water-in-oil) miniemulsion can be performed. Therefore, user-friendly dispersions of the colloids were obtained that enabled them to be easily processed further for coatings, for instance.

A wide range of application areas in technology and the sciences is therefore available for dispersed nanoparticles. This is because the particles can consist of numerous functional materials, while dispersions possess properties that make them particularly interesting for applications. These colloidal systems can be very complex, depending on the combination of the particle material and architecture.

For industrial applications, aqueous dispersions of functional polymers in particular are of great importance since they can be processed with very small amounts of organic solvents or entirely without these expensive and often toxic substances. Thus, dispersions of nanoparticles are suited to obtain particularly soft polymers like polybutadiene or polyisoprene for coatings and adhesives. They can be applied as an aqueous dispersion system to a surface and subsequently simply fused together with one another by heating, for example, so that they form a non-porous film. However, mechanically extra-hard polymers also play a large role in engineering and industry. Nanoparticles could be produced in miniemulsions from polymer resins,

polyurethanes [16], or polyesters [17] that are already found today in applications like automobile coatings. Previously, polyurethanes dispersions could only be made with organic solvent; with miniemulsion processes by contrast, only water is used—an environmentally friendly solvent. Polybenzoxazine particles in an aqueous medium with the help of a miniemulsion were synthesized [18]. The process allows to use such materials in fibre-reinforced composites for very high mechanical loading, for instance in aircraft and in rotor blades for wind turbines.

Furthermore, the miniemulsion technology offers the means of producing nanoparticles from polymers that are already present. In this instance, a solution of the polymer in the continuous phase could be employed, and after evaporating the solvent, a secondary dispersion system of the polymer particles was obtained. In this way, it was possible to successfully create particles of conductive polymers in an aqueous suspension, from which organic light-emitting diodes (OLEDs) and solar cells with excellent optical properties using a conventional inkjet printer could be fabricated [19].

From Nanoparticles to the Construction of Nanocontainers

The great potential of the miniemulsion approach is evident from the ability to produce not just solid nanoparticles with it, but nanocapsules as well having a polymeric jacket and a liquid core. These kinds of nanocapsules are suitable for enclosing functional molecules such as drugs, for example. The first nanocapsules in miniemulsions containing a hydrophobic liquid were obtained in 2001 by the Landfester and coworkers [20]; the monomers for the capsule wall were present in the droplets of the substance to be encapsulated and then polymerized. Because the growing polymer chains are no longer soluble in the non-polar solvent, the polymer separates at the interface and forms a shell around the drop. The advantage of this process in comparison to conventional methods is that a much broader palette of polymers becomes available and additionally, the capsule surface can be designed to carry out virtually limitless reactions.

Even greater possibilities are offered by miniemulsion technology since solid particles in inverse (i.e. a water-in-oil) miniemulsion were created [21]. Later, also nanocapsules in inverse miniemulsions could be created [20]. These nanocapsules have remained unique and can only be fabricated in a miniemulsion. It first became possible to encapsulate hydrophilic substances like salts, biological molecules like DNA, RNA, enzymes, and proteins or active agents like doxorubicin in this manner. Polymerization reactions were used at the droplet's surface. Here, a monomer is in solution within the aqueous droplets, while the continuous hydrophobic phase contains a second monomer or reactive agent. When the components diffuse to the surface of the droplets and encounter one another there, reactions take place and the polymeric shell of the capsules forms. The capsule walls could also be formed by nanoprecipitation [22]. In this case, a polymer insoluble in water is dissolved in the dispersed hydrophobic phase consisting of two solvents, one in which the polymer readily dissolves and in the other hardly at all. When we now evaporate

the effective solvent, the polymer selectively precipitates onto the nanodroplet and forms the capsules.

Tuning the Transport Properties of the Wall: Dense Capsules, Permanent Sieve Capsules, and Capsules with Gateways

After it was possible to package many active substances in a polymer matrix or shell using the nanoreactors of a miniemulsion, the spectrum of potential and already-realized applications has broadened immensely. The identical structure of all the droplets prior to polymerization guarantees that the captive substance is also equally distributed in the nanoparticles or nanocapsules. If the matrix or the shell is produced from an inert polymer, this can serve for instance as a permanent protective shell for sensitive substances, facilitate their processing, or combine their properties with the advantages of dispersed systems.

Packaging substances using miniemulsion polymerization is simple: during the subsequent polymerization, the functional substances are self-sheathing if the material to be encapsulated is at least as hydrophobic as the shell. The first material that was successfully encapsulated was titanium dioxide [23–25] and carbon black [26]. This process is already in large-scale industrial usage to package not just carbon black, but other colour pigments [27] as well. Indeed, this enveloping prevents the pigments from clumping during the manufacture of printing inks, which in turn increases resolution and prevents smearing.

Whereas solid pigments do not tend to escape from their containers, small molecules, liquids and highly volatile molecules use any cavity to escape from their prison. However, a toxic drug should only be released at its final destination and not harm cells during the transport through the body and a highly volatile perfume in detergents should only be released in the washing process and not during storage. Therefore, the first requirement is to construct nanocapsules which keep their content trapped. In polymer-based *micro*capsules, high shell thicknesses greater than one micrometer are the obvious origin for high diffusion barrier. At the *nano*scale, high barrier performance is much more difficult to achieve, which is related to ultra-thin shells. Especially small molecules tend to diffuse quickly through nanocapsule walls. Therefore, the shell has to be tightened by decreasing the mesh size in the thin shell. High barrier nanocapsules have been constructed containing highly volatile substances like perfumes or drugs in miniemulsion [28]. The polymeric shell material includes functions that strongly interact with each other and therefore form a thin, but very dense net which hinders the small molecules from escaping. For very small molecules like oxygen, an even tighter nanoshell had to be constructed. Inspired by leaves in nature, we used cellulose as impermeable nanopaper for the nanocapsule formation. Such nanocapsules can be used to protect oxygen-sensitive food (like fish oil) or in nanomedicine.

For some applications, it is of interest to construct capsules with a sieve shell where some components can freely pass the barrier, but others are captured. For the realization for nanocapsules with a gadolium-based magnetic resonance tomography (MRT) contrast agent, nanocapsules with a wall can be formed selectively allowing a fast passage of water molecules which is important so that the imaging in the MRT

scanner works, but which entraps the contrast agent [29]. That way, the nanocapsules with the contrast agent can be localized in the body [30, 31].

Nanocapsules are not always meant to permanently protect or shield an encapsulated substance from external influences though, because other applications must be able to selectively release a stored substance again. When this happens due to an external stimulus, we speak of smart or stimuli-sensitive transporters. In this way, cytotoxic substances for example can be introduced into cells with these materials, released there, and activated. The protective polymer shell prevents toxic effects in other types of cells and areas of the body that are not exposed to the activation stimulus. This is how chemotherapy side effects in particular are suppressed. For the construction of nanocapsules, valves or gates have to be integrated in the nanocapsule wall. The shell resembles a patchy leopard skin where the patches represent the gateways which can be opened and closed by different stimuli. As the most promising internal cell stimulus, we have shown that cell-own substances open nanocapsules selectively, like the enzyme hepsin in prostate cancers cells [32].

Tuning the Interactions

The miniemulsion technology also allows one to design the surface of the nanocarriers so that interactions between the nanocarriers themselves (flow can be switched on and off) and between nanocarriers and a surface (adhesion can be switched on and off) can be switched. It was shown that the interaction between nanocarriers can be tuned so that well-defined nanofibers or a homogenous network of particles thereby decreasing or stopping the flow of the dispersion were obtained. As a new interaction concept between particles, the tuning of hydrophobic associations was used to obtain stimuli-responsive aqueous adhesives, e.g. to label wet and cold beer bottles at high speed, with low coating weights, high accuracy—and additionally to obtain stronger ice water resistance after drying due to the hydrophobic modification [33].

Today almost no nanoparticular medicine is in clinical use in spite of the high potential for the use of nanocarriers for the development of personalized smart medicine, namely drugs, imaging, diagnostic or therapeutic agents. A major obstacle to their medical application and translation to the clinic is the fact of unknown or unspecific blood interactions of the nanocarriers in vivo leading to aggregation or scavenging by the mononuclear phagocyte system. Therefore, the scope of today's research is to understand step by step the different interactions of the nanocarriers encounter during their journey through the body.

To lead a nanocontainer to a specific type of target cell, a capsule must first interact as little as possible with cells generally; it has to disguise itself. If the capsules are injected into blood, first of all they must not be recognized there by any cell and taken up. We have recently been successful in producing nanocapsules based on hydroxyethyl starch that are not recognized by any cell. Immediately after coming in contact with blood, proteins from the blood will be adsorbed and therefore dress the surface of the nanocarriers. Mass spectrometry was used for the identification of the adsorbed proteins and for the first time for the determination of the change of the dress with time. Light-scattering based methods were developed to be able of performing multi-angle light scattering on concentrated human blood serum to

monitor aggregation events between nanocapsules and proteins in blood [34]. In a next step, the nanocarriers can be functionalized specifically so that can be taken up receptor specifically in cells.

Overall, the miniemulsion process permits highly stable dispersions with uniform particle size (from 50 to 500 nm) and structure to be fabricated. The dispersions can be stored without difficulty. While working in the lab with small volumes (in the millilitre realm), it has been possible to transfer the process to industrial scales. The advantageous continuous processing technique has already been implemented in tubular reactors, for which the heat of the reaction can be led off without difficulty. Besides dispersions having high solid content, dry powder can also be produced for immersion in water when in use and thereby avoid expensive transport of the water.

3.2.1.3 Preparation from Pre-formed Polymers

The combination of miniemulsions with solvent evaporation is another method for the nanocapsule and nanoparticle preparation. The necessity of this technique arises if (i) the polymer synthesis can not be done easily, e.g. requirement of special catalysts, (ii) the encapsulated cargos are interacted with the active reagents, e.g. initiation species formed during the polymerization, (iii) the purification of the particles is difficult [15]. The handling of this technique is easy and fast, therefore it is used in various particle and capsule formation using different polymers such as polystyrene (PS), poly(L-lactide) (PLLA), poly(ε-caprolactone) (PCL), poly(methyl acrylate) (PMA) and poly(methyl methacrylate) (PMMA) [22, 35, 36]. However, the main drawback of the technique is that particles with a lesser solid content and the broader size distribution are obtained. Nevertheless, it is very handy for preparation of the upconversion nanocapsules that can take part in triplet triplet annihilation upconversion (TTA-UC) phenomenon. Wohnhaas et al. [37] showed that the use of miniemulsion polymerizations to prepare PMMA based upconversion (UC) nanocapsules leads to a decrease in the efficiency of the UC dye couples since they were reacted with the formed radicals during polymerization. Similarly, Liu et al. [38] also used the miniemulsion/solvent evaporation technique to develop biocompatible bovine serum albumin based upconversion nanocapsules for triggering TTA-UC processes.

3.2.1.4 Layer by Layer Assembly

Layer by layer assembly (LBL) has gained high interest over the past decades for the fabrication of polymeric hollow capsules through templating method. Herein, inorganic or organic particles are used as a template in which the polymers are either adsorbed or grown by surface initiated polymerization (SIP) on the surface of the particle support [39, 40]. Various silica, gold, carbonate based particles [41] are used for such purpose as the core of the capsules which can be further removed through etching processes like dissolution in acids to form the hollow capsules made of a polymer shell. The use of particle templates enables to control the size easily that is one advantage of LBL assembly. In addition, different stimuli-responsive and func-

tional polymers can be deposited onto the support surface to apply these capsules in various biomedical applications [42]. For instance, recently, pH and temperature responsive, photo-crosslinked hollow capsules with a multilayer shell consist of poly(N-isopropyl acrylamine)-*b*-poly(methacrylate) and polyallylamine polymers made by silica-templated LBL assembly has been reported by Voit and coworkers [43, 44]. These capsules are used for studying glycopolymer or enzyme uptake to construct cellular mimics. Apart from that, SIP methods are also widely applied to form functional hollow capsules with the aid of the developments in polymer chemistry. Various controlled polymerization techniques such as atom transfer radical polymerization (ATRP) [45], revesible addition-fragmentation chain-transfer (RAFT) [46] and nitroxide mediated radical polymerization (NMRP) [47] are favored to grow the polymers on the surface of the supporting particles to form various kinds of hollow capsules.

3.2.2 Polymersomes

The starting point of a polymersome formation is to produce amphiphilic block copolymers that consist of hydrophobic and hydrophilic segments. Depending on the ratio of these two blocks, the amphiphilic copolymers can self-assemble into variety of structures such as spherical micelles, rods and vesicles. Thus, a precise polymer structure is required to obtain the desired morphology that can be provided by applying controlled polymerization techniques in which common approaches are the anionic polymerization and the atom transfer radical polymerization (ATRP).

Synthesis of amphiphilic block copolymers
Anionic polymerization exemplifies the first polymersome forming block copolymer synthesis that is based on the poly(ethylene oxide)-*b*-poly-ethyl ethylene (PEO-*b*-PEE) structure [48–50] whereas ATRP is very efficient to design multifunctional and nanostructured materials in the scope of biomedical applications [51]. This widely usage is simply based on various advantages such as commercially available initiators and precise control over macromolecular structure. In addition, several monomers including styrene, methacrylate and acrylate can be polymerized in a controlled manner with this technique [52]. Since the controlled polymerization techniques are not in the scope of this chapter, detailed synthetic descriptions will not be given as they were extensively discussed in many polymer chemistry books. In this context, self-assembly principles as well as the polymersome formation techniques from the pre-formed polymers will be highlighted in the following parts.

Self-assembly Principles of amphiphilic block copolymers
The self-assembly of amphiphilic block copolymers may result in different morphologies including planar bilayers, micelles and vesicles depending on the relative size of hydrophilic to hydrophobic segments. The curvature of the hydrophobic-hydrophilic interface is described by its mean (H) and Gaussian (K) curvature as shown in Fig. 3.3 [53].

Table 3.1 Packing parameter and hydrophilic fraction of different self-assemblies [56–58]

Shape of the assemblies	Packing parameter (p)	[a]Hydrophilic fraction (f)
Spherical micelle	$p < 1/3$	$f = 0.55–0.70$
Cylindrical micelle	$1/3 < p < 1/2$	$f = 0.45–0.55$
Vesicle	$1/2 < p < 1$	$f = 0.10–0.40$

[a]Hydrophilic fraction of the block copolymers either mass or volume ratios

In this regard, a model developed by Israelachvili et al. is used to define the shape of the self-assembled structures by linking the curvature with the molecular packing parameter (p) (2.1) where v denotes the hydrophobic volume, a is the interfacial area and l represents the hydrophobic chain length [54]. By calculating the p values, the resulting shape of the self-assembled structures can be predicted as seen in Table 3.1 [55].

$$p = \frac{v}{al} = 1 - Hl + \frac{Kl^2}{3} \tag{3.1}$$

However, it should be noted that the packing parameter is defined by means of geometrical aspects and therefore it is not adequate to fully explain the self-assembly of amphiphilic block copolymers. The free energy of the system, which is the combination of the interfacial energy of the hydrophobic-hydrophilic interface and the entropy loss of the polymer chains during vesicle formation, have a considerable effect on the resulting morphologies. In this manner, Disher and Eisenberg reported another parameter known as mass or volume fraction of hydrophilic part of the block copolymer (f) to predict the morphology of the self-assembled structures (Table 3.1) [56–58].

Apart from the above-mentioned parameters, several other factors can also influence the shape of the self-assembled block copolymers. For instance, the nature of the solvent, temperature, amount of water in the medium and the presence of salts,

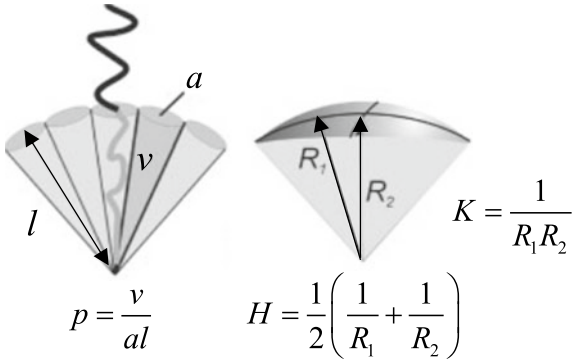

Fig. 3.3 Description of amphiphile shape in terms of molecular packing parameter (p) and its relation to the to the interfacial mean curvature (H) and Gaussian curvature (K) [53]

acids or bases may also have an effect on the final morphologies [59]. It has been reported that PS-PAA copolymer self-assembled into spheres when dimethylformamid (DMF) was used as the dissolution solvent, whereas vesicles can be obtained in the case of tetrahydrofuran (THF) usage [60]. Another example is that the addition of hydrochloric acid (HCl) to PS-PAA spheres led to a decrease in the volume of the corona which resulted in a morphological change into rods and vesicles [61]. Thus, self-assembly of the block copolymers should be always investigated by taking into account all these factors in combination with the preparation method.

Formation Techniques

Numerous techniques exist for preparing polymersomes from the self-assembly of amphiphilic block copolymers. These can be classified into five groups including solvent-switch, film rehydration, electroformation, microfluidic technology and direct dissolution like the pH switch method. The selection of the convenient method is highly dependent on the copolymer structure and the application needs. It should be also noted that the resulting polymersome size can be varied significantly from nanometer to micrometer scale by using different techniques. Therefore, this is also an essential criterion for choosing the most suitable preparation method.

The solvent-switch method, also termed as co-solvent method, is a common polymersome preparation technique for the block copolymers that are not soluble in water. The procedure requires an organic solvent such as THF, chloroform, dichloromethane or ethanol for dissolving all block copolymers which are then gradually mixed with water under vigorous stirring. Subsequently, the organic phase is separated from the mixture by using dialysis against water or ultrafiltration. During this procedure, the hydrophobic blocks of the copolymer are assembled together in the aqueous solution that form the membrane whereas the solvated hydrophilic blocks create the polymersome corona [59, 62]. Although this technique is a simple way of polymersome preparation, the use of organic solvent includes some drawbacks. For instance, the variation of the solvent behavior during the prolonged dialysis period may affect the morphology of the resulting self-assembled structures [63, 64]. In addition, using fully water miscible solvents like acetone and THF led to smaller polymersomes in comparison to the chloroform/water systems when biodegradable PEG-PDLLA polymersomes were formed. A broad size distribution of the resulting polymersomes within the range of 70 nm–50 μm was also reported which points out another drawback of this technique [65].

The film rehydration method starts with the dissolution of the block copolymers in an organic solvent such as chloroform and ethanol. Then the solvent is evaporated under reduced pressure to form the polymeric film on a solid surface like glass or roughened Teflon. Afterwards, the addition of the aqueous buffer solution enables the hydration of the copolymer film and thus, the polymersomes are formed. To support this process, gentle methods such as stirring, sonication or mechanical agitation may be utilized [62]. This method is generally combined with an extrusion step to obtain polymersomes with a narrow size distribution like it was applied for poly(dimethylsiloxane)-block-poly(2-methyloxazoline) based polymersomes reported by Meier et al. [66].

Electroformation is similar to the film hydration method which results in micrometer-sized giant polymersomes. Therein, the copolymers are spread onto an electrode surface followed by the addition of a buffer solution and finally the rehydration process is facilitated by applying the electric current [59]. The used electrodes can be made of indium-tin oxide (ITO) coated glass plates [67], platinum wires [68] or gold wires [69] which have been already applied to form liposomes or polymersomes.

The microfluidic technology is utilized recently to prepare polymersomes in a controllable and reproducible way. This technique is based on two approaches including the formation of a double emulsion template in microchannels [70, 71] or the hydrodynamic flow-focusing in microfluidics [72, 73]. In the former approach, the amphiphilic block copolymers are carried in an organic solvent which is then removed in the case of double emulsion formation at the microchannels to produce the polymersomes. This way of production enables larger polymersomes in the range of micrometer size. An example for the latter approach is the preparation of poly-2-vinylpyridine-b-poly(ethylene oxide) based polymersomes in which the block copolymers were dissolved in ethanol and flowed through the main channel of the microfluidic device. The side channel of the microfluidic device was also filled with Millipore water that was flowing in the perpendicular direction to the block copolymer side. Eventually, these two solutions mixed through diffusion that led to the polymersomes with a controllable size range of 40 nm–2 μm [72]. This result showed that the hydrodynamic-flow based microfluidic production is a feasible preparation technique for nanometer-sized polymersomes as well. However, Braun et al. have shown that there was no difference in the size distribution of pH sensitive poly(2-(methacryloyloxy) ethyl phosphorylcholine)-*b*-poly(2-(diisopropylamino) ethyl methacrylate) based polymersomes formed either using microfluidics or direct bulk production [73].

The direct dissolution method is carried out without the need of an organic solvent. The block copolymers are directly self-assembled in water or aqueous buffer solutions under vigorous stirring. For instance, the poly(ε-caprolactone)-b-poly(2-aminoethyl-methacrylate) and poly(ε-caprolactone)-*b*-poly[2-(methacryloyloxy)ethyl phosphorylcholine] based polymeromes have been successfully prepared in pure water within this technique [74, 75]. In addition, the self-assembly of pH-responsive block copolymers can be easily performed by adjusting the pH of the corresponding polymer solution. The pH-sensitive groups such as 2-(diisopropylamino)ethyl methacrylate enables the direct dissolution of the copolymer in an acidic water by means of protonation. This is followed by adding a base to deprotonate the amino groups that triggers the self-assembly process for the polymersome formation. Nano-sized polymersomes can be obtained using this technique which is advantageous by being practical, clean and fast. Recently, this technique has been widely used by Voit and coworkers to fabricate various photo-crosslinked and functionalized polymersomes for applications in drug delivery [76, 77], biosensing [78] and synthetic biology [79, 80].

3.2.3 Dendrimers and Micelles

Dendrimers are prepared by two common routes known as divergent and convergent methods. In the divergent method, the dendritic molecule is synthesized starting from the core and is growth in a stepwise approach. PAMAM dendrimers reported by Tomalia et al. [10] are a common example prepared by this method. Herein, ethylene diamine (EDA) is used as a core which is followed by alkylation with methyl acrylate through Michael addition and subsequent amidation of the created esters with EDA to end up with the dendritic structures for the applications in gene therapy, controlled drug delivery and in coating technology. In addition, another commercially useful dendrimer as PPI dendrimers were also synthesized divergently by the group of Mülhaupt [9] taking Vögtle's work [8] as a basis. The second preparation way of dendrimers, namely the convergent method is firstly shown by Frechet and coworkers [81] to produce aromatic polyether dendrimers in which the formation is established by synthesizing firstly the branches, which are later connected together to the core focal point. Recently, more complex globular structures with an enhanced biocompatibility and biodegradability are formed by making use of these base dendrimers to form their sugar-decorated versions called glycodendrimers. Introduction of oligosaccharide shells to the PAMAM, PPI, polyester, etc. dendrimers make these particles efficient to be used as drug carriers and to take part in the fabrication of diagnostic devices [82].

Micelle formation is directed by the design of block copolymer structures as likely the polymersomes that is described in the previous section. When the required hydrophilic-hydrophobic balance (Table 3.1) is achieved, the self-assembly process ends up with the spherical micelles. Their formation is possible if the concentration of the amphiphilic block copolymers is above the critical micelle concentration (CMC). Indeed, the preparation of polymeric micelles have common approaches with the polymersomes that can be listed as film rehydration, direct dissolution and solvent switch methods [5] in which the relevant technique is highly dependent on the hydrophilicity of the self-assembling block copolymers.

3.3 Functional Nanocarriers for Applications in Nanomedicine

Employment of nanocarriers in medicine undoubtedly requires the design of nanoparticle surface and the hosting cage with a controlled manner. It is very important how nanoparticles interact with the biological medium surrounding them. The nature of the particle surface is especially of primary importance that can be engineered by the needs of the carrier system. In this context, a good nanocarrier for nanomedicine must have various properties including (i) longevity in the bloodstream, (ii) specific targeting to solely diseased regions of the patient, and (iii) controlled release of the encapsulated payloads. The longevity in the bloodstream can be usually imparted by

selection of the suitable size range (100–300 nm), colloidal stabilizations (surfactant chemistry and/or crosslinking possibilities) to avoid the premature degradation as well as minimizing the tissue irritation by PEGylation of the particle surface. To achieve specific targeting, a common way is to functionalize the nanoparticle surface with recognitive ligands such as antibodies, peptides, folic acid, oligo (mannose) molecules that are active only for certain cells [83]. On the other hand, the way for a controlled release of the loaded payloads is to fabricate stimuli-responsive particles [84, 85] that are sensitive to the variations in biological environments. This leads to the physical or chemical structural changes of the nanoparticle such as morphological transitions, degradation and porous shell formation. By this, release of the payloads can be performed when the target of interest is reached. Various external or internal stimuli like pH, temperature, redox, light, and enzyme can be utilized for designing such systems.

3.3.1 Stimuli-Responsive Nanocarriers

First of all, the payload should stay within the nanocapsules up to the point where a release is desired. The release can be triggered by different stimuli which will be discussed in the following:

pH-Responsive Stimulus
A change of the pH value can be used to trigger opening of the capsules due to hydrophilicity changes or to cleavage. In the case of polyelectrolytes, the polymers are charged at neutral pH value and by lowering the pH value, e.g. within cells protonation, takes place. The charges vanish and therefore, the electrostatic repulsion disappears leading to an opening of the gates with subsequent release of the cargo [86, 87]. In a polypseudorotaxane–based gating system the cargo is released upon protonation of a poly(ethylene-imine) at pH 5.5 [88]. For a release at pH values >7, the ion-dipole interaction between bisammonium and cucurbit [6] uril can be used. Whereas at pH 7 a supramolecular cap is formed, at pH 10, the bisammonium groups become deprotonated and the cap is released together with the cargo [89].

Acid-labile linkers, such as esters [90], acetal groups [91, 92], or boronate esters [93], can also be used as gating systems. Upon acidication, the chemical bonds break up, the gates open and the payload can be released. Inorganic materials such as ZnO are stable at pH 7.4, but dissolve under acid conditions (pH < 5.5) [94].

Temperature-Responsive
By increasing the temperature, chemical bonds such as azogroups [95], peroxides [96], or loosely arranged complexes [97] can be used as degradable units. Another possibility is to use the melting of the material, e.g. as reported in the case of paraffin caps [98]. Some polymers exhibit a lower critical solution temperature and become insoluble under heating, releasing their embedded cargo [99]. However even more interesting is the use of the upper critical solution temperature, since at elevated temperatures, the solubility of the polymer increases and allows a release of the payload.

Very recently, a vesicle-forming polyphosphorester-based copolymer is reported with an upper critical solution temperature [100].

For bioapplications, the temperature for the trigger should be in the physiological range. Only very locally, higher temperatures can be induced using magnetic nanoparticles. Magnetic nanocrystals react to magnetic actuation and can heat up their local environment. The magnetic nanoparticles can be accumulated in the region of interest e.g., a tumor preferentially by magnetic directing the nanoparticles to the tissue of interest [95, 97, 99]. The heat leads to apoptosis of the surrounding cells. In a similar way, the photothermal effect of metallic nanoparticles of e.g. gold nanoparticles can also be used to locally generate heat and kill cells [93].

Light-Responsive

Photo-irradiation can lead to a switching of *trans* to *cis* conformation in molecules and vice versa [101]. The induction of local heating by irradiation of metallic nanoparticles (plasmons) converts irradiation into heat [93]. Mal et al. reported photo-responsive coumarin derivatives grafted onto pores. A reversible intermolecular dimerization of the coumarin derivatives took place upon irradiation; the photocleavage of the dimers leads to a release of the payload [102].

Redox-Responsive

Disulfide groups can be used as redox-responsive units. Disulfide bonds can be found in proteins, defining their supramolecular structure [103–105]. These disulfide bonds or tetrasulfide groups can also be incorporated in the shell of nanocapsules allowing the opening of the gates and releasing the payload. Poly(vinlyferrocene)-based block copolymers [106] or polyaniline as shell material [107] can also be applied for a redox-responsive release of payloads from capsules. Another example is the use of pseudorotaxanes formed of 1,5-dioxynaphthalene derivatives as gateposts and cyclobis(paraquat-p-phenylene), a tetracation, as gate. On reduction of the gate to bisradical di-cations the gates open and the content is released [108].

Enzyme-Responsive

Enzymes are able to disrupt disulfide bonds. Proteins can also be digested by enzymes. In gating systems based on protein caps [109] or whole nanocontainers based on proteins [110], the release is achieved by enzymatic degradation. As degrading enzyme, trypsin is often described as a model system [109, 110]. Other enzymes presented in literature are, for instance, amidase and urease [111].

Apart from that, enzyme responsive nanocarriers were developed. They are dye-containing peptide-based capsules that are cleaved by the enzyme hepsin [32, 112], which occurs exclusively in prostate cancer cells, and then release the dye. This enables the prostate cancer to be easily diagnosed. In addition, it is possible to employ enzyme responsive capsules to fight against bacteria in bandages. For instance, capsules based on hyaluronic acid can be designed that are broken by an enzyme produced by many bacteria called hyaluronidase [113]. The capsules not only release a warning stain, but simultaneously an active agent that combats the bacteria as soon as they appear.

3.3.2 *Functionalization of Nanocarriers*

Nanocarrier functionalization is useful to develop active targeting via specific receptor-ligand interaction for enhanced therapeutic efficiency as well as a diagnostic ability for especially drug delivery purposes. Although the functionalization methods can differ depending on the nanocarrier structure, the common approach for all carriers is to add some biologically useful reactive groups through covalent or noncovalent ways. Common linker groups for further functionalization with targeting ligands are amine moieties, azido groups or alkyne groups to favor esterification and click chemistries. Besides, non-covalent conjugations including biotin-streptavidin binding [114, 115], and adamantane-cyclodextrin binding [76, 116] are also another way of further modification steps.

For instance, Voit and coworkers showed azido and adamantane functionalized pH sensitive polymersomes [76] that can be linked to the cleavable photoactive species and/or onto cyclodextrin modified solid surfaces [78] as well as to the glycodendrimers [116] by use of click chemistry and non-covalent conjugations.

Landfester and coworkers also showed various examples of nanoparticle functionalization. One example is the amino and carboxyl decorated polystyrene nanoparticles fabricated through miniemulsion polymerizations of styrene with 2-aminoethyl methacrylate hydrochloride (AEMH) or acrylic acid (AA) [117]. The amino groups on polystyrene particles were also utilized to modify the surface by maleimide bearing polymers to understand the correlation between hydrophilicity and stealth properties of polyphosphoester-coated nanocarriers [118] Additionally, folic acid [119] and mannose [120] functionalized HES nanocapsules for targeted cell uptake has been also reported.

Another interesting way of particle functionalization is to make use of surfactants that are utilized for colloidal stabilization. By this, it is possible to add reactive groups or physical functions to stabilizers first then to the particle surface. surfactants with polymerizable groups, bioactive surfactants comprising polysaccharides or amino acids, and stimuli-responsive surfactants that are sensitive to triggers like pH, temperature, or redox are considered as 'functional surfactants' favored in particle modification [121].

3.4 Characterization of Nanocarriers

The important parameters that define the characteristics of nanocarriers are their size, shape, surface charge, stability and the mechanical strength. Besides, the encapsulation and release behavior of the loaded cargos needs to be tracked to apply these colloidal dispersions as nanocarriers. In this context, several characterization tools including light scattering methods, imaging techniques and spectroscopic methods are available to monitor such parameters. The selection of the relevant characteriza-

tion tool is highly dependent on the physicochemical properties of the particles that are highlighted in below.

Light Scattering Methods

Light scattering methods are mainly used to gain information about the average size and structural information of the nanocarriers in colloid science. Among the available methods, dynamic light scattering (DLS) and static light scattering (SLS) are the commonly applied techniques that utilizes the laser illumination of a sample.

Dynamic light scattering (*DLS*) is relying on the measurement of translational diffusion coefficient which is then related to the size by using relevant theoretical relations. In brief, the nanoparticles dispersed in a liquid are illuminated by a laser source and use of photodetector enables to detect the fluctuations of the scattered light at a fixed angle which reflects the Brownian motion of the particles. In order to obtain a meaningful information from the collected signal, the correlation function is computed by using an autocorrelator which is shown in below along with the exponential fitting expression (3.2). To have a more comprehensive information on size distribution of particles, multi-angle measurements can also be performed.

$$G(\tau) = < I(t) \cdot I(t+\tau) > = A[1 + B\exp(-2Dq^2\tau)] \tag{3.2}$$

In the above equation, I is the scattering intensity, t is the initial time, τ represents the delay time, A is the intercept and B is the baseline of the correlation function. Additionally, D represents the diffusion coefficient, an important parameter to define the size. The scattering vector (q) is also included in this equation and it is defined by the following relation where n is the refractive index of the medium, Θ is the scattering angle and λ_0 is the wavelength of the laser (3.3).

$$q = (4\pi\eta/\lambda_0)\sin(\theta/2) \tag{3.3}$$

By following this, a common theoretical approach named as Cumulants analysis is used to determine the mean size and polydispersity index of the particles. The principle of this analysis is basically fitting a single exponential to the correlation function to compute the diffusion coefficient (D) from (3.2) which is then related to the radius of diffusing particles by Stokes Einstein equation where R_H is the z-average hydrodynamic radius, T is temperature, k_B is the Boltzmann constant and η is the viscosity of the solvent [122–124].

$$D = \frac{k_B T}{6\pi\eta R_H} \tag{3.4}$$

Static light scattering (SLS) measures the absolute intensity of the scattered light from the particles as a function of the scattering angle when a laser beam illuminates them. By this technique, it is possible to determine weight averaged molar mass, aggregation number, radius of gyration number, shape and particle interactions within each other and with the liquid phase that are dispersed in. The molecular weight (M_w)

is related to light scattering through the following Rayleigh equation (3.5) where c is the sample concentration, Θ is the scattering angle, R_θ is the Rayleigh ratio, K is an optical constant (3.6) and A_2 is the second virial coefficient that defines the interactions between particles. In addition, the $P\theta$ term relates the radius of gyration (R_g) to the fundamental Rayleigh theory (3.7)

$$\frac{Kc}{R_\theta} = \left(\frac{1}{Mw} + 2A_2c\right)\frac{1}{P_\theta} \tag{3.5}$$

$$K = \frac{4\pi^2}{\lambda^4 N_A}\left(n\frac{\mathrm{d}n}{\mathrm{d}c}\right)^2 \tag{3.6}$$

$$\frac{1}{P_\theta} = 1 + \frac{16\pi^2 n^2 R_g^2}{3\lambda^2}\sin^2\left(\frac{\theta}{2}\right) \tag{3.7}$$

where λ = laser wavelength, N_A = Avagadro's constant, n = refractive index of the solvent and $\mathrm{d}n/\mathrm{d}c$ = refractive index increment of the sample.

Once the measured data obtained from SLS system, the desired information can be calculated by simplifying the above mentioned equations through special analysis such as Zimm plot or Guinier plot. For instance, plot of Kc/R_θ to $\sin^2(\Theta/2)$ is the widely used Guinier plot where the slope and intercept helps to calculate the radius of gyration (R_g) and the molecular weight respectively. This also enables to define the shape of the particles in which the R_g can be related with the hydrodynamic radius (R_h) obtained from DLS and the ratio of these two values (R_g/R_h) describes the ρ-ratio that shows the geometry of the particles. For example, the ρ—ratio is 1 for a hollow sphere whereas 1.505 for a random polymer coil [125].

Imaging Techniques

Imaging techniques such as electron microscopy, atomic force microscopy and optical microscopy are widely used to determine morphology, shape, size and mechanical properties of the investigated nanocarriers. The selection of the appropriate method depends highly on the technical constraints. For instance, optical microscopes that employs light to magnify small objects have a lesser resolution than the electron microscopes, which differs the applicability a lot. To explain this more in detail, one should recall the mathematical expression called Abbe's equation (3.8)

$$d = \frac{0.6\lambda}{\sin\alpha} \tag{3.8}$$

that describes the resolution of a microscope in a perfect optical system. Herein, d is the resolution, λ is the wavelength and α is the aperture angle. For optical microscopes containing ideal lenses, the resolution (d) can be 200 nm whereas for an electron microscope it is possible to decrease the wavelength several orders of magnitude leading to a decreased resolution of about 0.3 nm [126]. Thus, standard optical microscopes are more convenient for the particles in micron size range although the recently developed advanced methods like super-resolved fluorescence microscopy [127] enables the nano-scale visualization. In addition, use of conventional fluo-

rescent microcopy or confocal laser scanning microscopy that are in the family of optical microscopes are very useful in imaging fluorescently tagged nanocarriers. By this way, cell uptake behavior of the nanoparticles can be easily tracked.

Electron microscopy techniques include two major methods: transmission electron microscopy (TEM) and scanning electron microscopy (SEM). As already described above, the resolution of this type of microscopy technique fits very well with the nano-scaled nanocarriers. Both of them enables the direct observation of size, size distribution, morphology and shape of the nanocarriers. The main principle is the illumination of the sample by electron beams that are transmitted or scattered through the sample in TEM and SEM operation respectively. Both techniques are complementary to each other, but also include some differences for the nanoparticle characterization. TEM provides 2D projection of the nanoparticle image whereas SEM gives 3D images that is practical when surface characteristics of the nanoparticles needs to be lightened. In this context, SEM is stronger in topographic visualization of the nanocarriers. On the other hand, the resolution and magnification level of TEM (down to 0.2 nm) is much higher than the SEM which is advantageous for tracking smaller nanoparticles in the atomic level. TEM is also more powerful when the internal structure needs to be characterized which can give information about the crystallinity or amorphous properties as well as the magnetic domains of the particles. It is also noteworthy to point that electron microscopy visualization requires the nanoparticles spread on a thin solid layer under vacuum. This can be achieved by different specimen preparation methods but all needs simply drying of the nanoparticles that leads to artifacts. In addition, electron beams and observation under vacuum can damage sensitive polymers during the operation. Therefore, special care has to be done for the specimen preparation and data interpretation although both ways of electron microscopy are very convenient tools for nanoparticle imaging.

Atomic force microscopy (*AFM*) is another tool for characterizing the topography of the nanoparticles. However, more importantly, AFM can provide information about the mechanical properties of the colloidal systems as differently than the other microscopy techniques. Various types of nanoparticles including polymersomes [78, 128], liposomes [129], micelles [130], and polyelectroclyte multilayer capsules [131], are monitored by AFM to understand their mechanical properties.

The precondition for AFM analysis is to fix the nanoparticles onto convenient solid substrate. Basically, this technique allows to measure the interactions between the sample and the sharp tip attached to the cantilever in which the surface is scanned by moving either the tip or the sample. Figure 3.4 shows the components of an AFM when the sample is stationary and the tip is moved over the surface with the aid of a connected piezo scanner. The topography of the sample surface leads to a deflection of the cantilever which is detected through the reflected laser light onto a split photodiode. The converted electrical signal is evaluated by a feedback control system through a given set point. The tapping and non-contact mode of AFM enables a constant cantilever vibration amplitude whereas in contact mode, the cantilever deflection is maintained by moving the piezo scanner at the vertical position. The data at each (x, y) position for any chosen modes of AFM are then stored by the computer software to obtain a three-dimensional surface topography. This operation

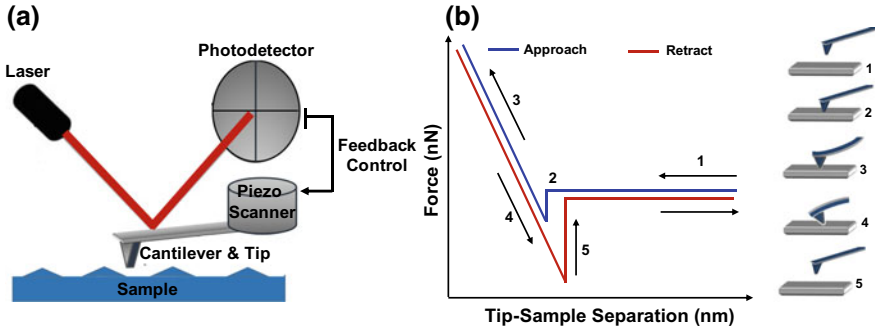

Fig. 3.4 Scheme of the atomic force microscopy setup (**a**) and ideal force-distance curves (**b**) of AFM. Adapted from Leggett et al. [133] and Averett et al. [138]

can take place in both ambient and liquid environments. For the latter case, special cantilever holders are available which is very advantageous to image the nanocarriers under liquid phase to avoid the artifacts caused by drying [132, 133].

Among the different AFM modes, tapping mode or more advanced technologies such as peak force tapping mode are widely used for relatively soft nanoparticles due to the lower applied forces on the sample. By this way, possible deformation during the tip interaction is kept to a minimum. As mentioned earlier, the mechanical properties can be also probed within AFM through individual force curves by monitoring approaching, contacting and withdrawal of tip from the sample surface. In this regard, the measured cantilever deflection versus piezo scanner extension is converted into the force versus tip-sample separation curves [134, 135]. A basic idea of this operation can be seen in Fig. 3.4 in which different analytical models such as Hertz [136] or Reissner Thin Shell Theory [137] are used to evaluate the measured data for acquiring elastic modulus values.

Other Methods

In addition to the characterizations about size, shape, morphology and mechanical strength of the nanoparticles, various methods exist to determine other colloidal and structural characteristics of nanocarriers. Here, the most widely used ones are highlighted.

One essential information about nanocarriers is undoubtedly monitoring the charge of the particles that gives insight both stability and potential interactions with the surroundings. In this regards, zeta potential is a common method for analyzing the particle's charge and colloidal stability. The theoretical background of this technique is based on the particle's interactions with the surrounding liquid phase. The net charge of the particle surface in liquid leads to a change in the distribution of ions covering it. Firstly, the counter ions from the solution is adsorbed on the particle surface to form the "Stern layer". Then "diffusive layer" is formed by covering the Stern layer that consists of the loosely associated ions. Due to an applied electrical field, some ions in diffusive layer move with the particles in the direction of the oppositely charged electrode. However, some ions keep their stationary condition and do

not move at a certain distance from the particle. This boundary layer is known as the slipping plane in which the electrical potential in this region is described as "zeta potential". The determination of the zeta potential is performed by measuring the electrophoretic mobility of the particles in a capillary cell containing two electrodes. In brief, an electrical field is applied to the electrodes and the charged particles move towards the oppositely charged electrode with a velocity known as the electrophoretic mobility (U_E) which is then related to the zeta potential (ζ) by the Henry equation shown in below. Herein, the parameters like viscosity (η) and dielectric constant (ε) is already known whereas the Henry's function, $f(\kappa a)$, is assumed as 1.5 for the aqueous solutions of moderate electrolyte concentration. This is known as the Smoluchowski approximation which is commonly used for nanoparticles [139]. As can be inferred, information about zeta potential is also important for pH responsive nanocarriers where charge of the particles is highly dependent on the working pH value.

$$U_E = \frac{2\,\varepsilon\,\zeta\; f(\kappa a)}{3\eta} \tag{3.9}$$

Spectroscopic methods such as ultraviolet visible spectroscopy (UV-Vis) and fluorescence spectroscopy are other efficient tools for monitoring the encapsulation and release behavior of the nanocarriers when they are tagged with fluorescent or light absorbing compounds. For instance, the encapsulation and further release of a light absorbing cargo such as doxorubicin molecules [140] or enzymatic reactions within the polymersomes [80] can be monitored easily by using these techniques. Indeed, they are also useful naturally for light-responsive particles which can be simply tracked through the chromophore or fluorophore in their structure.

It is also worth to mentioning that the conventional polymer characterization techniques such as nuclear magnetic resonance (NMR), infrared spectroscopy (IR) and size exclusion chromotagrophy (SEC) are also commonly used in the nanoparticle field to perform structural analysis. By this way, it is possible to define the polymeric characteristics like the molecular weight, polydispersity as well as the functional groups placed on the polymer backbone. In addition, thermoanalytical methods including thermogravimetric analysis (TGA) and differential scanning calorimetry (DSC) are also favored for defining the temperature-dependent decay or the crystallinity of the polymer that forms the nanoparticles.

References

1. Vert, M., Doi, Y., Hellwich, K.-H., Hess, M., Hodge, P., Kubisa, P., Rinaudo, M., Schué, F.: Terminology for biorelated polymers and applications (Iupac Recommendations 2012). Pure Appl. Chem. **84**, 377 (2012)
2. Landfester, K., Ramírez, L.P.: Encapsulated magnetite particles for biomedical application. J. Phys.: Condens. Matter 15, S1345 (2003)

3. Mailänder, V., Lorenz, M.R., Holzapfel, V., Musyanovych, A., Fuchs, K., Wiesneth, M., Walther, P., Landfester, K., Schrezenmeier, H.: Carboxylated superparamagnetic iron oxide particles label cells intracellularly without transfection agents. Mol. Imag. Biol. **10**, 138–146 (2008)
4. Bannwarth, M.B., Ebert, S., Lauck, M., Ziener, U., Tomcin, S., Jakob, G., Münnemann, K., Mailänder, V., Musyanovych, A., Landfester, K.: Tailor-Made nanocontainers for combined magnetic-field-induced release and Mri. Macromol. Biosci. **14**, 1205–1214 (2014)
5. Kataoka, K., Harada, A., Nagasaki, Y.: Block copolymer micelles for drug delivery: design, characterization and biological significance. Adv. Drug Deliv. Rev. **47**, 113–131 (2001)
6. Iijima, M., Nagasaki, Y., Okada, T., Kato, M., Kataoka, K.: Core-Polymerized reactive micelles from heterotelechelic amphiphilic block copolymers. Macromolecules **32**, 1140–1146 (1999)
7. Kim, J.H., Emoto, K., Iijima, M., Nagasaki, Y., Aoyagi, T., Okano, T., Sakurai, Y., Kataoka, K.: Core-Stabilized polymeric micelle as potential drug carrier: increased solubilization of taxol. Polym. Adv. Technol. **10**, 647–654 (1999)
8. Buhleier, E., Wehner, W., Vögtle, F.: Synthesis **2**, 155–158 (1978)
9. Wörner, C., Mülhaupt, R.: Polynitrile- and polyamine-functional poly(Trimethylene Imine) dendrimers. Angew. Chem. Int. Edition Engl. **32**, 1306–1308 (1993)
10. Tomalia, D.A., Baker, H., Dewald, J., Hall, M., Kallos, G., Martin, S., Roeck, J., Ryder, J., Smith, P.: A new class of polymers: starburst-dendritic macromolecules. Polym. J. **17**, 117 (1985)
11. Landfester, K.: Polyreactions in miniemulsions. Macromol. Rapid Commun. **22**, 896–936 (2001)
12. Ugelstad, J., El-Aasser, M.S., Vanderhoff, J.W.: Emulsion polymerization: initiation of polymerization in monomer droplets. J. Polym. Sci.: Polym. Lett. Edition **11**, 503–513 (1973)
13. Asua, J.M.: Miniemulsion Polymerization. Prog. Polym. Sci. **27**, 1283–1346 (2002)
14. Schork, F.J., Luo, Y., Smulders, W., Russum, J.P. Butte, A., Fontenot, K.: Miniemulsion polymerization. Adv. Polym. Sci. **175**, 129–255 (2005)
15. Landfester, K.: Miniemulsion polymerization and the structure of polymer and hybrid nanoparticles. Angew. Chem. Int. Edition **48**, 4488–4507 (2009)
16. Barrère, M., Landfester, K.: High molecular weight polyurethane and polymer hybrid particles in aqueous miniemulsion. Macromolecules **36**, 5119–5125 (2003)
17. Barrère, M., Landfester, K.: Polyester synthesis in aqueous miniemulsion. Polymer **44**, 2833–2841 (2003)
18. Sawaryn, C., Landfester, K., Taden, A.: Benzoxazine miniemulsions stabilized with polymerizable nonionic benzoxazine surfactants. Macromolecules **43**, 8933–8941 (2010)
19. Landfester, K., Montenegro, R., Scherf, U., Güntner, R., Asawapirom, U., Patil, S., Neher, D., Kietzke, T.: Semiconducting polymer nanospheres in aqueous dispersion prepared by a miniemulsion process. Adv. Mater. **14**, 651–655 (2002)
20. Tiarks, F., Landfester, K., Antonietti, M.: Preparation of polymeric nanocapsules by miniemulsion polymerization. Langmuir **17**, 908–918 (2001)
21. Landfester, K., Willert, M., Antonietti, M.: Preparation of polymer particles in nonaqueous direct and inverse miniemulsions. Macromolecules **33**, 2370–2376 (2000)
22. Paiphansiri, U., Tangboriboonrat, P., Landfester, K.: Polymeric nanocapsules containing an antiseptic agent obtained by controlled nanoprecipitation onto water-in-oil miniemulsion droplets. Macromol. Biosci. **6**, 33–40 (2006)
23. Erdem, B., Sudol, E.D., Dimonie, V.L., El-Aasser, M.S.: Encapsulation of inorganic particles via miniemulsion polymerization. I. Dispersion of titanium dioxide particles in organic media using Oloa 370 as stabilizer. J. Polym. Sci. Part A: Polym. Chem. **38**, 4419–4430 (2000)
24. Erdem, B., Sudol, E.D., Dimonie, V.L., El-Aasser, M.S.: Encapsulation of inorganic particles via miniemulsion polymerization. Ii. Preparation and characterization of styrene miniemulsion droplets containing Tio2 particles. J. Polym. Sci. Part A: Polym. Chem. **38**, 4431–4440 (2000)
25. Erdem, B., Sudol, E.D., Dimonie, V.L., El-Aasser, M.S.: Encapsulation of inorganic particles via miniemulsion polymerization. Iii. Characterization of encapsulation. J. Polym. Sci. Part A: Polym. Chem. **38**, 4441–4450 (2000)

26. Tiarks, F., Landfester, K., Antonietti, M.: Encapsulation of carbon black by miniemulsion polymerization. Macromol. Chem. Phys. **202**, 51–60 (2001)
27. Steiert, N., Landfester, K.: Encapsulation of organic pigment particles via miniemulsion polymerization. Macromol. Mater. Eng. **292**, 1111–1125 (2007)
28. Hofmeister, I., Landfester, K., Taden, A.: Controlled formation of polymer nanocapsules with high diffusion-barrier properties and prediction of encapsulation efficiency. Angew. Chem. Int. Edition **54**, 327–330 (2015)
29. Jagielski, N., Sharma, S., Hombach, V., Mailänder, V., Rasche, V., Landfester, K.: Nanocapsules synthesized by miniemulsion technique for application as new contrast agent materials. Macromol. Chem. Phys. **208**, 2229–2241 (2007)
30. Malzahn, K., Ebert, S., Schlegel, I., Neudert, O., Wagner, M., Schütz, G., Ide, A., Roohi, F., Münnemann, K., Crespy, D., Landfester, K.: Design and control of nanoconfinement to achieve magnetic resonance contrast agents with high relaxivity. Adv. Healthc. Mater. **5**, 567–574 (2016)
31. Schlegel, I., Renz, P., Simon, J., Lieberwirth, I., Pektor, S., Bausbacher, N., Miederer, M., Mailänder, V., Muñoz-Espí, R., Crespy, D., Landfester, K.: Highly loaded semipermeable nanocapsules for magnetic resonance imaging. Macromol. Biosci. **18**, 1700387 (2018)
32. Andrieu, J., Kotman, N., Maier, M., Mailänder, V., Strauss, W.S.L., Weiss, C.K., Landfester, K.: Live monitoring of cargo release from peptide-based hybrid nanocapsules induced by enzyme cleavage. Macromol. Rapid Commun. **33**, 248–253 (2012)
33. Dundua, A., Landfester, K., Taden, A.: Water-Based adhesives with tailored hydrophobic association: dilution resistance and improved setting behavior. Macromol. Rapid Commun. **35**, 1872–1878 (2014)
34. Rausch, K., Reuter, A., Fischer, K., Schmidt, M.: Evaluation of nanoparticle aggregation in human blood serum. Biomacromol **11**, 2836–2839 (2010)
35. Wohnhaas, C., Friedemann, K., Busko, D., Landfester, K., Baluschev, S., Crespy, D., Turshatov, A.: All organic nanofibers as ultralight versatile support for triplet-triplet annihilation upconversion. ACS Macro Lett. **2**, 446–450 (2013)
36. Musyanovych, A., Schmitz-Wienke, J., Mailänder, V., Walther, P., Landfester, K.: Preparation of biodegradable polymer nanoparticles by miniemulsion technique and their cell interactions. Macromol. Biosci. **8**, 127–139 (2008)
37. Wohnhaas, C., Mailänder, V., Dröge, M., Filatov, M.A., Busko, D., Avlasevich, Y., Baluschev, S., Miteva, T., Landfester, K., Turshatov, A.: Triplet-Triplet annihilation upconversion based nanocapsules for bioimaging under excitation by red and deep-red light. Macromol. Biosci. **13**, 1422–1430 (2013)
38. Liu, Q., Yin, B., Yang, T., Yang, Y., Shen, Z., Yao, P., Li, F.: A general strategy for biocompatible, high-effective upconversion nanocapsules based on triplet-triplet annihilation. J. Am. Chem. Soc. **135**, 5029–5037 (2013)
39. Cui, J., van Koeverden, M.P., Müllner, M., Kempe, K., Caruso, F.: Emerging methods for the fabrication of polymer capsules. Adv. Colloid Interface Sci. **207**, 14–31 (2014)
40. Gaitzsch, J., Huang, X., Voit, B.: Engineering functional polymer capsules toward smart nanoreactors. Chem. Rev. **116**, 1053–1093 (2016)
41. Parakhonskiy, B.V., Yashchenok, A.M., Konrad, M., Skirtach, A.G.: Colloidal micro- and nano-particles as templates for polyelectrolyte multilayer capsules. Adv. Colloid Interface Sci. **207**, 253–264 (2014)
42. del Mercato, L.L., Ferraro, M.M., Baldassarre, F., Mancarella, S., Greco, V., Rinaldi, R., Leporatti, S.: Biological applications of Lbl multilayer capsules: from drug delivery to sensing. Adv. Colloid Interface Sci. **207**, 139–154 (2014)
43. Liu, X., Appelhans, D., Wei, Q., Voit, B.: Photo-Cross-Linked dual-responsive hollow capsules mimicking cell membrane for controllable cargo post-encapsulation and release. Adv. Sci. **4**, 1600308 (2017)
44. Liu, X., Formanek, P., Voit, B., Appelhans, D.: Functional cellular mimics for the spatiotemporal control of multiple enzymatic cascade reactions. Angew. Chem. **129**, 16451–16456 (2017)

45. Morinaga, T., Ohkura, M., Ohno, K., Tsujii, Y., Fukuda, T.: Monodisperse silica particles grafted with concentrated oxetane-carrying polymer brushes: their synthesis by surface-initiated atom transfer radical polymerization and use for fabrication of hollow spheres. Macromolecules **40**, 1159–1164 (2007)
46. Huang, X., Appelhans, D., Formanek, P., Simon, F., Voit, B.: Synthesis of well-defined photo-cross-linked polymeric nanocapsules by surface-initiated raft polymerization. Macromolecules **44**, 8351–8360 (2011)
47. Blomberg, S., Ostberg, S., Harth, E., Bosman, A.W., Horn, B.V., Hawker, C.J.: Production of crosslinked, hollow nanoparticles by surface-initiated living free-radical polymerization. J. Polym. Sci. Part A: Polym. Chem. **40**, 1309–1320 (2002)
48. Discher, B.M., Won, Y.-Y., Ege, D.S., Lee, J.C.-M., Bates, F.S., Discher, D.E., Hammer, D.A.: Polymersomes: tough vesicles made from diblock copolymers. Science **284**, 1143–1146 (1999)
49. Hillmyer, M.A., Bates, F.S.: Synthesis and characterization of model Polyalkane–Poly(Ethylene Oxide) block copolymers. Macromolecules **29**, 6994–7002 (1996)
50. Hillmyer, M.A., Bates, F.S., Almdal, K., Mortensen, K., Ryan, A.J., Fairclough, J.P.A.: Complex phase behavior in solvent-free nonionic surfactants. Science **271**, 976–978 (1996)
51. Siegwart, D.J., Oh, J.K., Matyjaszewski, K.: Atrp in the design of functional materials for biomedical applications. Prog. Polym. Sci. **37**, 18–37 (2012)
52. Braunecker, W.A., Matyjaszewski, K.: Controlled/Living radical polymerization: features, developments, and perspectives. Prog. Polym. Sci. **32**, 93–146 (2007)
53. Antonietti, M., Förster, S.: Vesicles and liposomes: a self-assembly principle beyond lipids. Adv. Mater. **15**, 1323–1333 (2003)
54. Israelachvili, J.N., Mitchell, D.J., Ninham, B.W.: Theory of self-assembly of hydrocarbon amphiphiles into micelles and bilayers. J. Chem. Soc. Faraday Trans. 2: Mol. Chem. Phys. **72**, 1525–1568 (1976)
55. Zhang, J., Li, X., Li, X.: Stimuli-Triggered structural engineering of synthetic and biological polymeric assemblies. Prog. Polym. Sci. **37**, 1130–1176 (2012)
56. Discher, D.E., Eisenberg, A.: Polym. Vesicles. Science **297**, 967–973 (2002)
57. Le Meins, J.F., Sandre, O., Lecommandoux, S.: Recent trends in the tuning of polymersomes' membrane properties. Eur. Phys. J. E **34**, 1–17 (2011)
58. Lee, J.S., Feijen, J.: Polymersomes for drug delivery: design, formation and characterization. J. Control. Release **161**, 473–483 (2012)
59. Balasubramanian, V., Herranz-Blanco, B., Almeida, P.V., Hirvonen, J., Santos, H.A.: Multifaceted polymersome platforms: spanning from self-assembly to drug delivery and protocells. Prog. Polym. Sci. **60**, 51–85 (2016)
60. Yu, Y., Eisenberg, A.: Control of morphology through polymer–solvent interactions in crew-cut aggregates of amphiphilic block copolymers. J. Am. Chem. Soc. **119**, 8383–8384 (1997)
61. Zhang, L., Eisenberg, A.: Morphogenic effect of added ions on crew-cut aggregates of Polystyrene-B-Poly(Acrylic Acid) block copolymers in solutions. Macromolecules **29**, 8805–8815 (1996)
62. Kita-Tokarczyk, K., Grumelard, J., Haefele, T., Meier, W.: Block copolymer vesicles—using concepts from polymer chemistry to mimic biomembranes. Polymer **46**, 3540–3563 (2005)
63. Zhang, L., Eisenberg, A.: Multiple morphologies and characteristics of "Crew-Cut" Micelle-Like aggregates of Polystyrene-B-Poly(Acrylic Acid) diblock copolymers in aqueous solutions. J. Am. Chem. Soc. **118**, 3168–3181 (1996)
64. Won, Y.-Y., Davis, H.T., Bates, F.S.: Giant wormlike rubber micelles. Science **283**, 960–963 (1999)
65. Meng, F., Hiemstra, C., Engbers, G.H.M., Feijen, J.: Biodegradable polymersomes. Macromolecules **36**, 3004–3006 (2003)
66. Egli, S., Nussbaumer, M.G., Balasubramanian, V., Chami, M., Bruns, N., Palivan, C., Meier, W.: Biocompatible functionalization of polymersome surfaces: a new approach to surface immobilization and cell targeting using polymersomes. J. Am. Chem. Soc. **133**, 4476–4483 (2011)

67. Dimitrov, D.S., Angelova, M.I.: Lipid swelling and liposome formation on solid surfaces in external electric fields. In: Hoffmann, H. (ed.) New Trends in Colloid Science, Darmstadt, vol. 1987, pp 48–56. Steinkopff, Darmstadt (1987)
68. Bucher, P., Fischer, A., Luisi, P.L., Oberholzer, T., Walde, P.: Giant vesicles as biochemical compartments: the use of microinjection techniques. Langmuir **14**, 2712–2721 (1998)
69. Sauer, M., Haefele, T., Graff, A., Nardin, C., Meier, W.: Ion-Carrier controlled precipitation of calcium phosphate in giant aba triblock copolymer vesicles. Chem. Commun. 2452–2453 (2001)
70. Shum, H.C., Kim, J.-W., Weitz, D.A.: Microfluidic fabrication of monodisperse biocompatible and biodegradable polymersomes with controlled permeability. J. Am. Chem. Soc. **130**, 9543–9549 (2008)
71. Perro, A., Nicolet, C., Angly, J., Lecommandoux, S., Le Meins, J.-F., Colin, A.: Mastering a double emulsion in a simple co-flow microfluidic to generate complex polymersomes. Langmuir **27**, 9034–9042 (2011)
72. Thiele, J., Steinhauser, D., Pfohl, T., Förster, S.: Preparation of monodisperse block copolymer vesicles via flow focusing in microfluidics. Langmuir **26**, 6860–6863 (2010)
73. Brown, L., McArthur, S.L., Wright, P.C., Lewis, A., Battaglia, G.: Polymersome production on a microfluidic platform using ph sensitive block copolymers. Lab Chip **10**, 1922–1928 (2010)
74. Du, J., Armes, S.P.: Preparation of primary amine-based block copolymer vesicles by direct dissolution in water and subsequent stabilization by Sol–Gel Chemistry. Langmuir **24**, 13710–13716 (2008)
75. Du, J., Armes, S.P.: Preparation of biocompatible zwitterionic block copolymer vesicles by direct dissolution in water and subsequent silicification within their membranes. Langmuir **25**, 9564–9570 (2009)
76. Iyisan, B., Kluge, J., Formanek, P., Voit, B., Appelhans, D.: Multifunctional and dual-responsive polymersomes as robust nanocontainers: design, formation by sequential post-conjugations, and ph-controlled drug release. Chem. Mater. **28**, 1513–1525 (2016)
77. Yassin, M.A., Appelhans, D., Wiedemuth, R., Formanek, P., Boye, S., Lederer, A., Temme, A., Voit, B.: Overcoming concealment effects of targeting moieties in the peg corona: controlled permeable polymersomes decorated with folate-antennae for selective targeting of tumor cells. Small **11**, 1580–1591 (2015)
78. Iyisan, B., Janke, A., Reichenbach, P., Eng, L.M., Appelhans, D., Voit, B.: Immobilized multifunctional polymersomes on solid surfaces: infrared light-induced selective photochemical reactions, ph responsive behavior, and probing mechanical properties under liquid phase. ACS Appl. Mater. Interfaces **8**, 15788–15801 (2016)
79. Gaitzsch, J., Appelhans, D., Wang, L., Battaglia, G., Voit, B.: Synthetic Bio-Nanoreactor: mechanical and chemical control of polymersome membrane permeability. Angew. Chem. Int. Edition **51**, 4448–4451 (2012)
80. Grafe, D., Gaitzsch, J., Appelhans, D., Voit, B.: Cross-linked polymersomes as nanoreactors for controlled and stabilized single and cascade enzymatic reactions. Nanoscale **6**, 10752–10761 (2014)
81. Hawker, C.J., Frechet, J.M.J.: Preparation of polymers with controlled molecular architecture. A new convergent approach to dendritic macromolecules. J. Am. Chem. Soc. **112**, 7638–7647 (1990)
82. Voit, B., Haag, R., Appelhans, D., Welzel, P.B.: Bio- and Multifunctional Polymer Architectures. Wiley (2016)
83. Landfester, K., Mailänder, V.: Nanocapsules with specific targeting and release properties using miniemulsion polymerization. Expert Opin. Drug. Deliv. **10**, 593–609 (2013)
84. Zhao, Y., Lv, L.-P., Jiang, S., Landfester, K., Crespy, D.: Advanced stimuli-responsive polymer nanocapsules with enhanced capabilities for payloads delivery. Polym. Chem. **6**, 4197–4205 (2015)
85. Che, H., van Hest, J.C.M.: Stimuli-Responsive polymersomes and nanoreactors. J. Mater. Chem. B **4**, 4632–4647 (2016)

86. Casasús, R., Marcos, M.D., Martínez-Máñez, R., Ros-Lis, J.V., Soto, J., Villaescusa, L.A., Amorós, P., Beltrán, D., Guillem, C., Latorre, J.: Toward the development of ionically controlled nanoscopic molecular gates. J. Am. Chem. Soc. **126**, 8612–8613 (2004)
87. Casasús, R., Climent, E., Marcos, M.D., Martínez-Máñez, R., Sancenón, F., Soto, J., Amorós, P., Cano, J., Ruiz, E.: Dual aperture control on ph- and anion-driven supramolecular nanoscopic hybrid gate-like ensembles. J. Am. Chem. Soc. **130**, 1903–1917 (2008)
88. Park, C., Oh, K., Lee, S.C., Kim, C.: Controlled release of guest molecules from mesoporous silica particles based on a ph-responsive polypseudorotaxane motif. Angew. Chem. Int. Edition **46**, 1455–1457 (2007)
89. Angelos, S., Yang, Y.-W., Patel, K., Stoddart, J.F., Zink, J.I.: Ph-Responsive supramolecular nanovalves based on cucurbit [6] uril pseudorotaxanes. Angew. Chem. **120**, 2254–2258 (2008)
90. Zhang, Q., Ariga, K., Okabe, A., Aida, T.: A condensable amphiphile with a cleavable tail as a "Lizard" template for the Sol−Gel synthesis of functionalized mesoporous silica. J. Am. Chem. Soc. **126**, 988–989 (2004)
91. Schlossbauer, A., Dohmen, C., Schaffert, D., Wagner, E., Bein, T.: Ph-Responsive release of acetal-linked melittin from Sba-15 mesoporous silica. Angew. Chem. Int. Edition **50**, 6828–6830 (2011)
92. Liu, R., Zhang, Y., Zhao, X., Agarwal, A., Mueller, L.J., Feng, P.: Ph-Responsive nanogated ensemble based on gold-capped mesoporous silica through an acid-labile acetal linker. J. Am. Chem. Soc. **132**, 1500–1501 (2010)
93. Aznar, E., Marcos, M.D., Martínez-Máñez, R., Sancenón, F., Soto, J., Amorós, P., Guillem, C.: Ph- and photo-switched release of guest molecules from mesoporous silica supports. J. Am. Chem. Soc. **131**, 6833–6843 (2009)
94. Muhammad, F., Guo, M., Qi, W., Sun, F., Wang, A., Guo, Y., Zhu, G.: Ph-Triggered controlled drug release from mesoporous silica nanoparticles via intracellular dissolution of zno nanolids. J. Am. Chem. Soc. **133**, 8778–8781 (2011)
95. Riedinger, A., Guardia, P., Curcio, A., Garcia, M.A., Cingolani, R., Manna, L., Pellegrino, T.: Subnanometer local temperature probing and remotely controlled drug release based on Azo-Functionalized iron oxide nanoparticles. Nano Lett. **13**, 2399–2406 (2013)
96. McClure, J.H., Robertson, R.E., Cuthbertson, A.C.: The decomposition of benzoyl peroxide in benzene. Can. J. Res. 20b, 103–113 (1942)
97. Thomas, C.R., Ferris, D.P., Lee, J.-H., Choi, E., Cho, M.H., Kim, E.S., Stoddart, J.F., Shin, J.-S., Cheon, J., Zink, J.I.: Noninvasive remote-controlled release of drug molecules in vitro using magnetic actuation of mechanized nanoparticles. J. Am. Chem. Soc. **132**, 10623–10625 (2010)
98. Aznar, E., Mondragón, L., Ros-Lis, J.V., Sancenón, F., Marcos, M.D., Martínez-Máñez, R., Soto, J., Pérez-Payá, E., Amorós, P.: Finely tuned temperature-controlled cargo release using paraffin-capped mesoporous silica nanoparticles. Angew. Chem. Int. Edition **50**, 11172–11175 (2011)
99. Zhang, J., Misra, R.D.K.: Magnetic drug-targeting carrier encapsulated with thermosensitive smart polymer: core-shell nanoparticle carrier and drug release response. Acta Biomater. **3**, 838–850 (2007)
100. Wolf, T., Rheinberger, T., Simon, J., Wurm, F.R.: Reversible self-assembly of degradable polymersomes with upper critical solution temperature in water. J. Am. Chem. Soc. **139**, 11064–11072 (2017)
101. Ferris, D.P., Zhao, Y.-L., Khashab, N.M., Khatib, H.A., Stoddart, J.F., Zink, J.I.: Light-Operated mechanized nanoparticles. J. Am. Chem. Soc. **131**, 1686–1688 (2009)
102. Mal, N.K., Fujiwara, M., Tanaka, Y.: Photocontrolled reversible release of guest molecules from coumarin-modified mesoporous silica. Nature **421**, 350–353 (2003)
103. Fujiwara, M., Terashima, S., Endo, Y., Shiokawa, K., Ohue, H.: Switching catalytic reaction conducted in pore void of mesoporous material by redox gate control. Chem. Commun. 4635–4637 (2006)

104. Lai, C.-Y., Trewyn, B.G., Jeftinija, D.M., Jeftinija, K., Xu, S., Jeftinija, S., Lin, V.S.Y.: A mesoporous silica nanosphere-based carrier system with chemically removable cds nanoparticle caps for stimuli-responsive controlled release of neurotransmitters and drug molecules. J. Am. Chem. Soc. **125**, 4451–4459 (2003)
105. Behzadi, S., Steinmann, M., Estupiñán, D., Landfester, K., Crespy, D.: The pro-active payload strategy significantly increases selective release from mesoporous nanocapsules. J. Control. Release **242**, 119–125 (2016)
106. Staff, R.H., Gallei, M., Mazurowski, M., Rehahn, M., Berger, R., Landfester, K., Crespy, D.: Patchy nanocapsules of Poly(Vinylferrocene)-Based block copolymers for redox-responsive release. ACS Nano **6**, 9042–9049 (2012)
107. Lv, L.-P., Zhao, Y., Vilbrandt, N., Gallei, M., Vimalanandan, A., Rohwerder, M., Landfester, K., Crespy, D.: Redox responsive release of hydrophobic self-healing agents from polyaniline capsules. J. Am. Chem. Soc. **135**, 14198–14205 (2013)
108. Hernandez, R., Tseng, H.-R., Wong, J.W., Stoddart, J.F., Zink, J.I.: An operational supramolecular nanovalve. J. Am. Chem. Soc. **126**, 3370–3371 (2004)
109. Schlossbauer, A., Kecht, J., Bein, T.: Biotin-Avidin as a protease-responsive cap system for controlled guest release from colloidal mesoporous silica. Angew. Chem. Int. Edition **48**, 3092–3095 (2009)
110. Piradashvili, K., Fichter, M., Mohr, K., Gehring, S., Wurm, F.R., Landfester, K.: Biodegradable protein nanocontainers. Biomacromol **16**, 815–821 (2015)
111. Agostini, A., Mondragón, L., Coll, C., Aznar, E., Marcos, M.D., Martínez-Máñez, R., Sancenón, F., Soto, J., Pérez-Payá, E., Amorós, P.: Dual enzyme-triggered controlled release on capped nanometric silica mesoporous supports. ChemistryOpen **1**, 17–20 (2012)
112. Fuchs, A.V., Kotman, N., Andrieu, J., Mailander, V., Weiss, C.K., Landfester, K.: Enzyme cleavable nanoparticles from peptide based triblock copolymers. Nanoscale **5**, 4829–4839 (2013)
113. Baier, G., Cavallaro, A., Vasilev, K., Mailänder, V., Musyanovych, A., Landfester, K.: Enzyme responsive hyaluronic acid nanocapsules containing polyhexanide and their exposure to bacteria to prevent infection. Biomacromol **14**, 1103–1112 (2013)
114. Brož, P., Benito, S.M., Saw, C., Burger, P., Heider, H., Pfisterer, M., Marsch, S., Meier, W., Hunziker, P.: Cell Targeting by a generic receptor-targeted polymer nanocontainer platform. J. Control. Release **102**, 475–488 (2005)
115. Rigler, P., Meier, W.: Encapsulation of fluorescent molecules by functionalized polymeric nanocontainers: investigation by confocal fluorescence imaging and fluorescence correlation spectroscopy. J. Am. Chem. Soc. **128**, 367–373 (2006)
116. Iyisan, B., Siedel, A.C., Gumz, H., Yassin, M., Kluge, J., Gaitzsch, J., Formanek, P., Moreno, S., Voit, B., Appelhans, D.: Dynamic docking and undocking processes addressing selectively the outside and inside of polymersomes. Macromol. Rapid Commun. **38**, 1700486 (2017)
117. Musyanovych, A., Rossmanith, R., Tontsch, C., Landfester, K.: Effect of hydrophilic comonomer and surfactant type on the colloidal stability and size distribution of carboxyl- and amino-functionalized polystyrene particles prepared by miniemulsion polymerization. Langmuir **23**, 5367–5376 (2007)
118. Simon, J., Wolf, T., Klein, K., Landfester, K., Wurm, F.R., Mailänder, V.: Hydrophilicity regulates the stealth properties of polyphosphoester-coated nanocarriers. Angew. Chem. Int. Edition **57**, 5548–5553 (2018)
119. Baier, G., Baumann, D., Siebert, J.M., Musyanovych, A., Mailänder, V., Landfester, K.: Suppressing unspecific cell uptake for targeted delivery using hydroxyethyl starch nanocapsules. Biomacromol **13**, 2704–2715 (2012)
120. Freichels, H., Wagner, M., Okwieka, P., Meyer, R.G., Mailander, V., Landfester, K., Musyanovych, A.: (Oligo)Mannose functionalized hydroxyethyl starch nanocapsules: en route to drug delivery systems with targeting properties. J. Mater. Chem. B **1**, 4338–4348 (2013)
121. Bijlard, A.C., Wald, S., Crespy, D., Taden, A., Wurm, F.R., Landfester, K.: Functional Colloidal Stabilization. Adv. Mater. Interfaces **4**, 1600443 (2017)

122. Hallett, F.R., Watton, J., Krygsman, P.: Vesicle sizing: number distributions by dynamic light scattering. Biophys. J. **59**, 357–362 (1991)
123. Pencer, J., Hallett, F.R.: Effects of vesicle size and shape on static and dynamic light scattering measurements. Langmuir **19**, 7488–7497 (2003)
124. Pecora, R.: Dynamic light scattering measurement of nanometer particles in liquids. J. Nanopart. Res. **2**, 123–131 (2000)
125. Schärtl, W.: Light Scattering from Polymer Solutions and Nanoparticle Dispersions. Springer Science & Business Media (2007)
126. Williams, D.B., Carter, C.B: Transmission Electron Microscopy, pp. 3–17. Springer, Boston, MA, (1996)
127. Möckl, L., Lamb, D.C., Bräuchle, C.: Super-Resolved fluorescence microscopy: nobel prize in chemistry 2014 for Eric Betzig, Stefan Hell, and William E. Moerner. Angew. Chem. Int. Edition **53**, 13972–13977 (2014)
128. Jaskiewicz, K., Makowski, M., Kappl, M., Landfester, K., Kroeger, A.: Mechanical properties of Poly(Dimethylsiloxane)-Block-Poly(2-Methyloxazoline) polymersomes probed by atomic force microscopy. Langmuir **28**, 12629–12636 (2012)
129. Delorme, N., Fery, A.: Direct method to study membrane rigidity of small vesicles based on atomic force microscope force spectroscopy. Phys. Rev. E **74**, 030901 (2006)
130. Li, S., Palmer, A.F.: Structure and mechanical response of Self-Assembled Poly(Butadiene)-B-Poly(Ethylene Oxide) colloids probed by atomic force microscopy. Macromolecules **38**, 5686–5698 (2005)
131. Fery, A., Weinkamer, R.: Mechanical properties of micro- and nanocapsules: single-capsule measurements. Polymer **48**, 7221–7235 (2007)
132. Shan, Y., Wang, H.: The structure and function of cell membranes examined by atomic force microscopy and single-molecule force spectroscopy. Chem. Soc. Rev. **44**, 3617–3638 (2015)
133. Leggett, G.J.: pp. 470–562. Wiley (2009)
134. Alsteens, D., Dupres, V., Yunus, S., Latgé, J.-P., Heinisch, J.J., Dufrêne, Y.F.: High-Resolution imaging of chemical and biological sites on living cells using peak force tapping atomic force microscopy. Langmuir **28**, 16738–16744 (2012)
135. Heu, C., Berquand, A., Elie-Caille, C., Nicod, L.: Glyphosate-Induced stiffening of hacat keratinocytes, a peak force tapping study on living cells. J. Struct. Biol. **178**, 1–7 (2012)
136. Hertz, H.: On the contact of elastic solids. Z. Reine Angew. Mathematik **92**, 156–171 (1881)
137. Taber, L.A.: Large deflection of a fluid-filled spherical shell under a point load. J. Appl. Mech. **49**, 121–128 (1982)
138. Averett, L.E., Schoenfisch, M.H.: Atomic force microscope studies of fibrinogen adsorption. Analyst **135**, 1201–1209 (2010)
139. Schmitz, K.S.: Introduction to Dynamic Light Scattering by Macromolecules, pp. 319–376. Academic Press, Oxford (1990)
140. Nahire, R., Haldar, M.K., Paul, S., Ambre, A.H., Meghnani, V., Layek, B., Katti, K.S., Gange, K.N., Singh, J., Sarkar, K., Mallik, S.: Multifunctional polymersomes for cytosolic delivery of gemcitabine and doxorubicin to cancer cells. Biomaterials **35**, 6482–6497 (2014)

Chapter 4
Stability of Nanoparticle Dispersions and Particle Agglomeration

Kateryna Loza, Matthias Epple and Michael Maskos

Abstract The stability of colloids is an important issue of colloid-based processes and formulations. Due to the large specific surface area, particles have a low thermodynamic stability and tend to agglomerate over time. Furthermore, the physicochemical properties of nanomaterials depend on the size, morphology, and surface state of the system, therefore in-depth characterization techniques are essential to predict the degree of variation in properties. In this chapter, the colloidal stability of nanoparticle dispersions as well as the basic stabilization mechanisms will be discussed both at the theoretical and at the experimental level. Relevant characterization methods will be presented and illustrated with suitable examples, including their limitations.

4.1 Introduction

The term "colloid" was introduced by Graham, "the founder of colloid chemistry", in 1861, from Greek meaning glue-like [1]. The word "colloidal" refers to disperse systems of distributed molecules or particles in a continuous medium. Thus, on the physical-chemical level colloids are between the molecular dimensions of real solutions and macroscopic dimensions of heterogeneous mixtures [2]. The basics of colloid science were established by Francesco Selmi in 1845. He studied the aggregation of pseudo-solutions of silver iodide and sulphur in water [3]. In 1857, Michael Faraday reported the experimental relationship of gold colloid and light (today known as surface plasmon resonance) [4]. Current definitions of colloids describe the par-

K. Loza (✉) · M. Epple
Inorganic Chemistry, University of Duisburg-Essen, Universitätsstrasse 2, 45141 Essen, Germany
e-mail: Kateryna.Loza@uni-due.de

M. Epple
e-mail: Matthias.Epple@uni-due.de

M. Maskos
Fraunhofer-Institute for Microengineering and Microsystems (IMM), Carl-Zeiss-Strasse 18-20, 55129 Mainz, Germany
e-mail: michael.maskos@imm.fraunhofer.de

P. Gehr and R. Zellner (eds.), *Biological Responses to Nanoscale Particles*, NanoScience and Technology, https://doi.org/10.1007/978-3-030-12461-8_4

Table 4.1 Examples of colloidal systems [7]

Dispersed phase	Continuous phase	Common name	Examples
Liquid	Gas	Liquid aerosol	Fog
Solid	Gas	Solid aerosol	Smoke
Gas	Liquid	Foam	Whipped cream
Liquid	Liquid	Emulsion	Mayonnaise
Solid	Liquid	Sol	Paint
Gas	Solid	Solid foam	Marshmallow
Liquid	Solid	Solid emulsion	Opal
Solid	Solid	Solid sol	Some alloys

ticles in the dispersed phase in the range of 1 nm–1 μm or 1 nm–500 nm [5]. The International Union of Pure and Applied Chemistry (IUPAC) defines nanoparticles as "microscopic particle whose size is measured in nanometers, often restricted to so-called nanosized particles (<100 nm in aerodynamic diameter), also called ultrafine particles" [6]. Colloids are combinations of two or more components. In biphasic systems, the dispersed phase and the dispersion medium (continuous phase) can exist in numerous combinations. The particles of the dispersed phase can occur as droplets or bubbles (spheres) (diameter d). Solid particles can also be present as rods, cubes, plates. Some examples are listed in Table 4.1.

In real cases, the system may be considerably more complex because all phases (dispersed or continuous) may be multi-component.

This chapter discusses the colloidal stability of nanoparticle dispersions at the theoretical and at the experimental level. The relevant characterization methods will be presented and illustrated with suitable examples, including their limitations.

4.2 Stability of Colloids

In many practical cases, the stability of colloids is an important issue of colloid-based processes and formulations. Due to the large specific surface area, particles have a lower thermodynamic stability and tend to agglomerate over time because the free surface energy is higher in comparison to a system with larger particles. This results in a separation of the dispersed phase from the continuous phase. Figure 4.1 shows models that are able to describe the evolution and transport processes of nanoparticles ("particokinetics") [8]. In terms of biological response for the fields of pharmacology and toxicology, particle sedimentation, diffusion and agglomeration as related to their size, density, and surface properties strongly affect the dose-response concept [9].

In the case of a diluted system, i.e. with particles acting as individual objects, the particles are subject to different forces. The Earth's gravitation field forces the

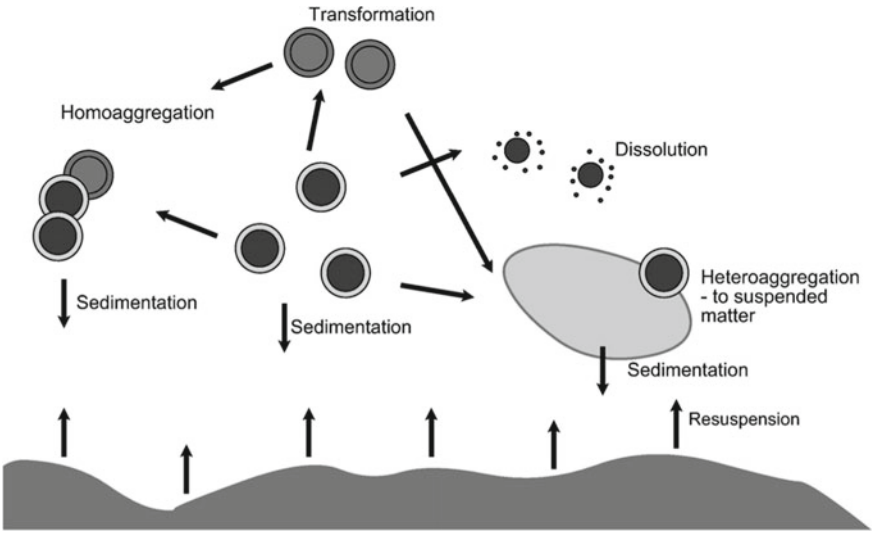

Fig. 4.1 Schematic representation of the various processes nanoparticles are subject to in the aquatic environment (Reproduced from Markus et al. [8] © 2014 Elsevier B.V.) [8]

particles to sediment if the dispersing medium has a lower density. The sedimentation velocity can be estimated with the equation of Stokes drag with gravitational force:

$$v_s = \frac{2}{9}\frac{\Delta\rho g a^2}{\eta_0} \tag{1.1}$$

where v_s is the sedimentation velocity, $\Delta\rho$ is the difference of densities, g is the gravitational constant, a is the particle radius, and η_0 is the medium viscosity. Therefore, larger particles have a greater tendency for sedimentation [10]. It was shown that barium sulphate microparticles (1.3 μm) fully sediment during 8 min, submicroparticles (420 nm) need about 100 min, and nanoparticles (70 nm) need more than 60 h. Aggregates will of course sediment faster [11, 12].

Brownian motion (inertial forces from the solvent molecules) can be described in terms of the diffusion coefficient (D) of the particles:

$$D = \frac{kT}{6\pi\eta a} \tag{1.2}$$

where k is the Boltzmann constant, T is the absolute temperature, η is the solvent viscosity and a is the particle radius [11]. This means that particokinetics for non-interacting spherical particles depend on the media viscosity and the particle dimension [12]. For definition of the nanoparticle dose in an in vitro system, the dynamics in liquids can be approached by describing both diffusion and gravitational settling

[13]. The transport of particles smaller than about 10 nm is principally controlled by diffusion.

A deviation of the colloid properties can be caused by shear forces. However, it is usually not visible for the particles themselves, but by the macroscopic properties of the whole system. For dilute dispersions of spherical particles, the shear viscosity (η) depends on the particle volume fraction (φ):

$$\eta = \eta_0(1 + 2.5\varphi) \tag{1.3}$$

Due to fluidic stimulation, the shear stress can affect an intracellular uptake of nanoparticles during drug delivery. Thus, a dynamic physical environment exerting forces on cells in vivo can cause a difference between the in vitro and in vivo cellular distribution of drugs and nanoparticles [14, 15].

The colloidal stability in terms of inter-particle forces (van der Waals attraction, double-layer repulsion and steric interaction) was described on the fundamental level by Deryaguin and Landau [16], and Verwey and Overbeek [17] (DLVO theory). This model of the stability of charge-stabilized particulate dispersions considers the balance of forces acting between interfaces and explains the particle deposition to planar substrates. It assumes that the surface charge can originate from contact with the electrolyte. Van der Waals forces are the attractive forces, and electrostatic forces act as repulsive forces. The van der Waals energy of attraction (G_A) between two equal particles, each of radius R, at a distance h is given by

$$G_A = -\frac{A_{11}}{6}\left[\frac{2}{s^2-4} + \frac{2}{s^2} + \ln\left(\frac{s^2-4}{s^2}\right)\right] \tag{1.4}$$

where $s = (2R + h)/R$ and A_{11} the Hamaker constant (function of electronic polarizability and the density of the material).

Neutral particles can become charged in contact with an electrolyte. Helmholtz's model describes a rigid layer of solvated ions that carry a counter charge to its surface [18]. Stern, Gouy, and Chapman suggested a bilayer of counter ions adsorbed directly on the particle surface, as well as a diffuse layer of solvated ions that extends beyond the rigid layer over several molecular layers [19, 20]. Due to thermal movements of the ions and solvent molecules in the dispersion medium, the diffuse layer creates a charge balance between the dispersion medium and the rigid layer (Fig. 4.2).

The Stern layer is formed by counter ions attracted to the particle surface and attached by the electrostatic force. A diffuse layer appears as a film of the dispersion medium next to the particle. The diffuse layer contains free ions with a higher concentration of counter ions. The electrical potential within the electric double layer has its maximum on the particle surface (Stern layer). The dimension of the double layer (thickness) depends on the electrolyte concentration and valency of the ions. It can be described by the reciprocal Debye-Hückel parameter:

$$\frac{1}{k} = \left(\frac{\varepsilon_0 \varepsilon_r kT}{2n_0 Z^2 e^2}\right)^{1/2} \tag{1.5}$$

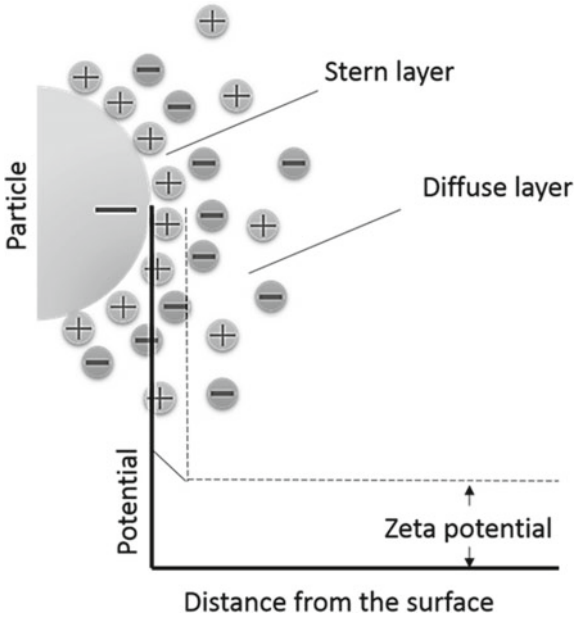

Fig. 4.2 Schematic representation of electrical double layer

where ε_r is the relative permittivity, ε_0 is the permittivity of free space, k is the Boltzmann constant, T is the absolute temperature, n_0 is the number of ions of each type present in the bulk phase, Z is the valency of the ions and e is the electronic charge. Repulsion occurs if two particles with an extended double layer approach a separation distance (double-layer overlap). The electrostatic energy of repulsion G_{el} with the potential ψ_d can be expressed as:

$$G_{el} = \frac{4\pi\varepsilon_0\varepsilon_r R^2 \psi_d^2 \exp(-kh)}{2R + h} \tag{1.6}$$

Equation 1.6 shows that the electrostatic energy of repulsion decays exponentially when the distance between the particles increases. The rate of decrease is affected by the electrolyte concentration and the valence of the ions [21].

The DLVO theory describes the total energy of interaction G_T between two particles by the sum of G_{el} and G_A at each distance value.

Figure 4.3 shows the energy–distance curve for electrostatically stabilized systems. The stability of the dispersion can be estimated from the energy of the local maximum. From the energetic point of view, reversible agglomeration may occur in the secondary minimum. If the energy barrier is exceeded (domination of the attractive van der Waals forces), the particles coagulate irreversibly into the primary energy minimum. An increase of charge density on the particle surface leads to a potential increase of the energy barrier and favours a reversible flocculation over the irreversible aggregation in the secondary energy minimum [22].

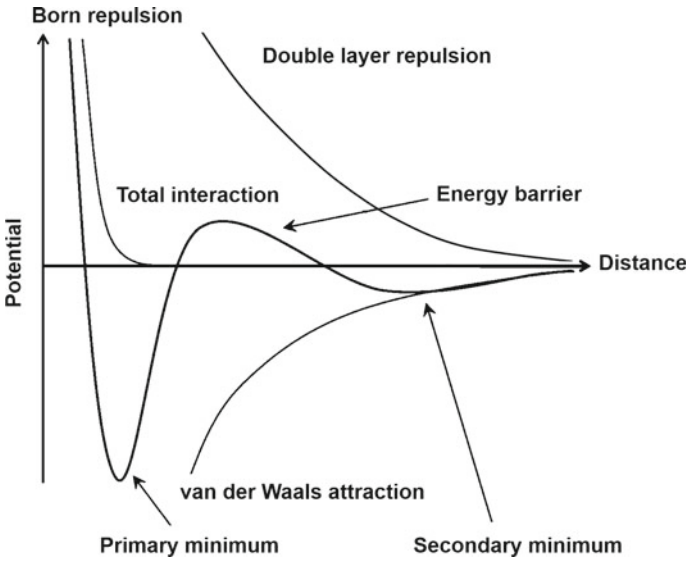

Fig. 4.3 Energy–distance curve for electrostatically stabilized systems according to the DLVO theory

Another aspect of colloidal stability is associated with the imbalance of the intermolecular forces near an interface [11]. In 1896, Ostwald described the dissolution of small particles and the reorganization of the dissolved species on the surfaces of larger particles [23]. This phenomenon is explained by decrease of the chemical potential of the molecules constituting the particles with increasing size. Therefore, particles tend to grow at the expense of smaller particles, if some solubility of these molecules is provided [24]. Figure 4.4 shows electron microscopic studies of a nanoparticle system. The fraction of small sacrificial nanocrystals decreases slowly, leading to the development of octahedral nanoparticles [25].

4.3 Stabilization Effects

Many attempts were devoted to access a rational manufacturing of particles at the nanoscale with desired electronic, catalytic, optical, and biological properties. However, after the preparation, nanoparticles are often exposed to a liquid phase before processing into a final formulation or device. Therefore, a long-term stability of colloids must be ensured. To prevent colloidal systems from changing, they can be improved by steric stabilization or electrosteric stabilization.

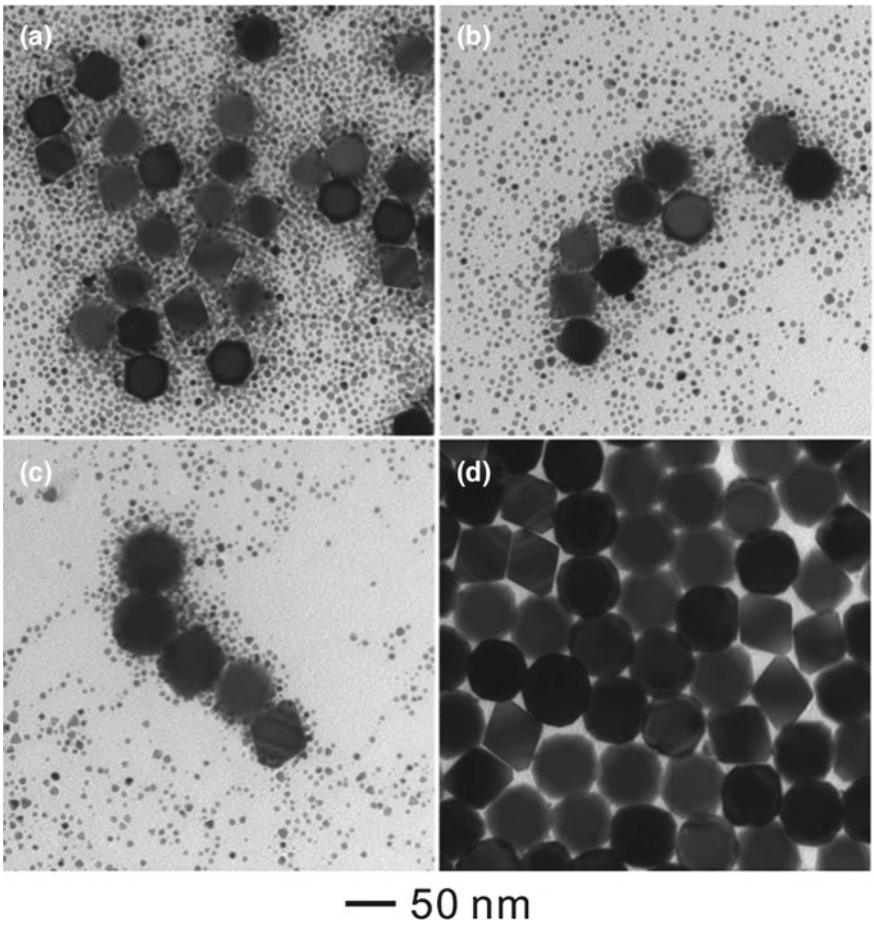

Fig. 4.4 TEM images of palladium octahedra obtained after ripening for different periods of time: **a** 6 h, **b** 24 h, **c** 48 h, and **d** 72 h (Reproduced with permission from (Z. Zhang, Z. Wang, S. He, C. Wang, M. Jin and Y. Yin, Chem. Sci., 2015, 6, 5197 Published by The Royal Society of Chemistry)

4.3.1 Electrostatic Stabilization

Electrostatic (or charge-induced) stabilization can be controlled by variation of the chemical environment (e.g. pH, salt concentration, ion type) or by introducing a surface charge from adsorbing molecules or ions. The basic mechanisms are ion adsorption, ionization of surface groups, ion dissolution, and ion substitution. Particles can be functionalized with appropriate chemical compounds that carry a positive or negative charge. In the case of the reduction of tetrachloroauric acid in an aqueous medium, the reducing agent (e.g. citrate or tannine) simultaneously serves as electrostatic stabilizers, providing a negative charge by citrate and tannine molecules

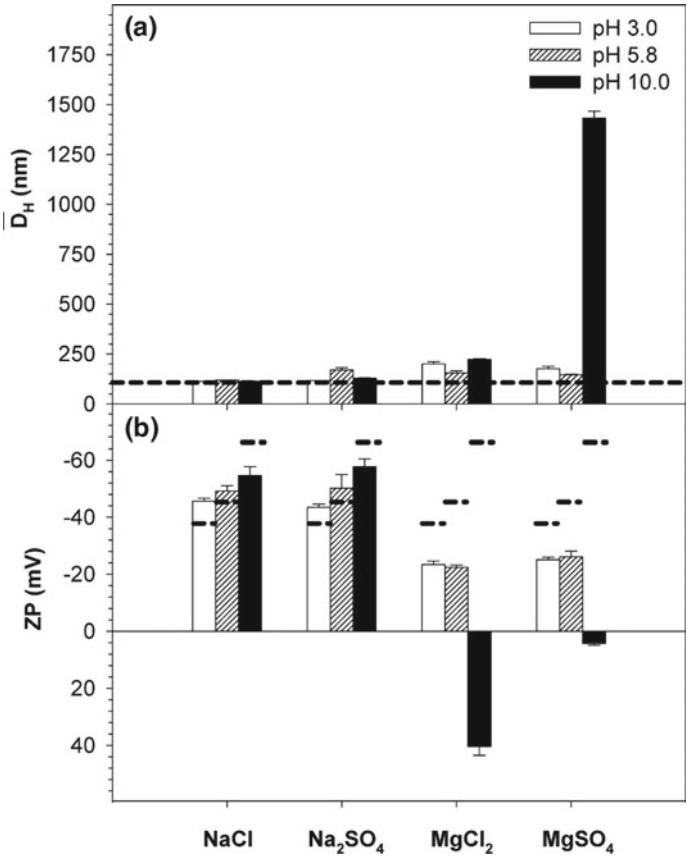

Fig. 4.5 Effect of different electrolytes (NaCl, Na_2SO_4, $MgCl_2$, and $MgSO_4$) on **a** average aggregate size, $\overline{D}H$ and **b** zeta potential, ZP, of fullerene C_{60} NPs as a function of pH (Reproduced with permission from B. Mukherjee; J. W. Weaver; Environ. Sci. Technol. 2010, 44, 3332–3338 Copyright © 2010 American Chemical Society) [28]

[26]. Furthermore, the ionization in aqueous solutions can be controlled by the pH. For example, metal oxides may become charged because of the protonation or the deprotonation of surface groups [27, 28]. When a material cannot be ionized, ionic surfactants may be added to produce charge stabilized suspensions. For example, fullerenes can be colloidally stabilized by introduction of an anionic surfactant [28]. Mukherjee et al. showed that multivalent counter-ions can strongly influence the surface charge properties of C_{60} NPs at higher pH, and even at low concentration can cause charge inversion (Fig. 4.5).

An uneven dissolution of ionic solids can also lead to an electrostatic stabilization and formation of charged colloids. Silver halides are a prominent example from photochemistry. Sparingly soluble silver iodide becomes charged in the presence of an excess of either iodine or silver ions. This phenomenon is used for the titration

of silver and halide ions with organic dyes [29]. Another electrostatic stabilization effect is based on isomorphous substitution. This is possible due to the replacement of one atom by another of similar size in a crystal lattice. For example, clays (naturally occurring colloidal particles) become charged as result of the substitution of Si^{4+} by Al^{3+} in the tetrahedral layers [11, 30].

4.3.2 Steric and Electrosteric Stabilization

The stability of colloids in terms of the electrostatic stabilization was discussed in Sect. 4.3.1. However, electrostatic stabilization is not always successful or robust due to some limitations like the use of a polar solvent or an increased electrolyte concentration (ion strength). The situation can be improved by introducing a steric stabilization. A steric stabilization can be realized by surfactant (polymer) adsorption or attachment onto the particle surface. If two particles covered with a polymer layer approach each other, the polymer chains are forced to overlap or to undergo some compression [21]. A strong repulsion will be caused by local increase in segment density due to change in the osmotic pressure and the configurational entropy of the chains in the interaction zone. A non-adsorbing (unanchored) polymer can be used for depletion stabilization of colloids, creating repulsive forces between the approach-

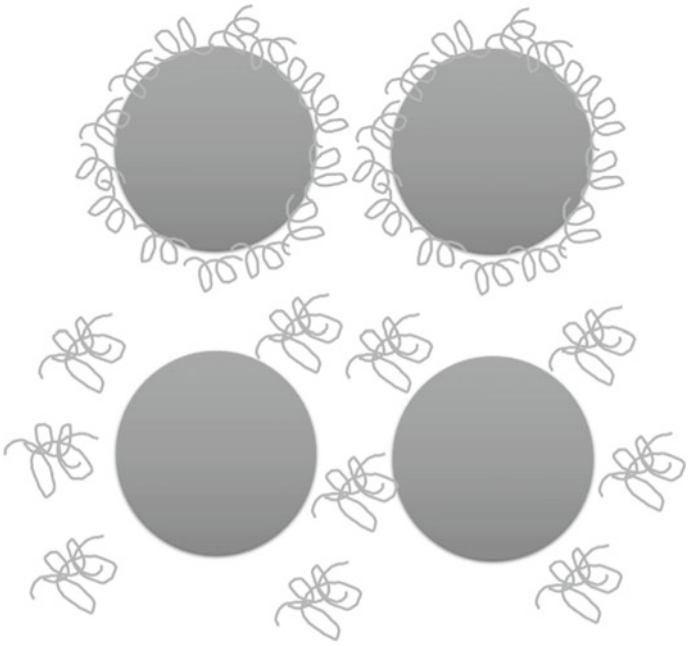

Fig. 4.6 Schematic representation of depletion stabilization of colloids

ing particles [2, 11]. However, depletion phenomenon is also used for flocculation of colloidal particles (i.e., the suspension forms flocs or flakes) by polymers in the dispersion [31]. Increasing concentration of the depletant (e.g., polymers, polyelectrolytes, small or non-spherical particles) causes higher order structural interactions between the particles [32, 33]. Figure 4.6 shows schematic representation of steric stabilization (upper particles) and depletion (lower particles).

Strong repulsions can be realized when stability criteria for steric stabilization (high surface coverage, strong adsorption, rational use of solvent, and low free polymer concentration with polymers) are met.

If polyelectrolytes (carrying a charge) are used, a synergetic effect of electrostatic and steric stabilization can be achieved. Due to their pH sensitivity (charge by protonation or deprotonation), the charge contribution to particle stabilization becomes highly dependent on the solution environment [11, 34].

4.4 Possibilities and Limitations of Analytical Methods to Analyze Nanoparticle Dispersions

As defined previously, colloids are larger than small molecules, but too small to be seen with a conventional optical microscope. Typical dimensions range from 1 nm to 1 μm. The high specific surface area and surface-to-volume ratio lead to an increasing demand for different applications like energy storage, pharmaceuticals, life science applications, optoelectronics, sensing, and heterogeneous catalysis. Because the physicochemical properties of nanomaterials depend on size, morphology, and surface state of the system, in-depth characterization techniques are essential to predict the degree of variation in properties.

A classical example of a colloidal dispersion is milk. Its white turbid appearance results from the ability of colloids to scatter light. Scattering techniques have been used for over 150 years to determine particle sizes. In the dispersion medium, particles move randomly in accordance with the Brownian motion. Upon irradiation, light will be scattered by the colloidal particles. Depending on the position of the individual scatterer, constructive and destructive interference will occur. This leads to time-dependent fluctuations in the scattered light intensity which can be measured by a detector. From the correlation of time and light intensity, an auto-correlation function can be determined [35]. By functional analysis, the diffusion coefficient of the particles can be investigated. If temperature and solvent viscosity are known, the hydrodynamic diameter can be estimated from the Stokes-Einstein equation:

$$D_t = \frac{T k_B}{3\pi \eta d} \tag{1.7}$$

where D_t is the particle diffusion coefficient, T is the temperature, k_B is Boltzmann's constant, η is the solvent viscosity, and d is the hydrodynamic diameter [31]. Further details can be found in [36].

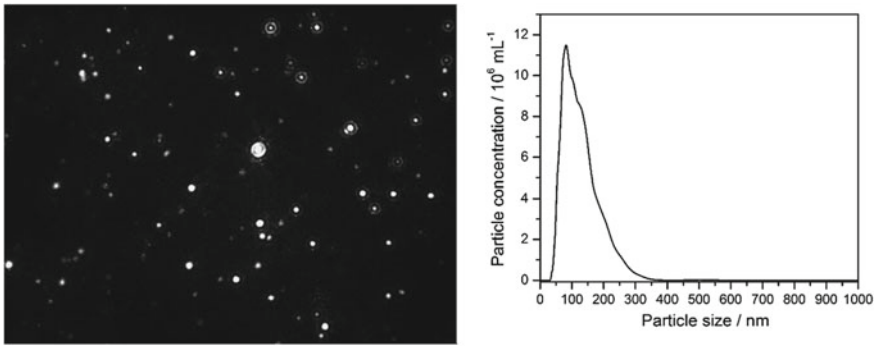

Fig. 4.7 Nanoparticle tracking analysis results of AgCl nanoparticles, formed after the addition of 10 μg mL^{-1} Ag^+ (10 ppm) to RPMI/10% FCS. Left: NTA image of diffusing AgCl particles; right: particle size distribution (by number) from NTA (Reproduced from K. Loza, C. Sengstock, S. Chernousova, M. Köller and M. Epple, RSC Adv., 2014, 4, 35290, Published by The Royal Society of Chemistry)

Particles in liquids can be visualized and analysed by nanoparticle tracking analysis (NTA) [37]. This system is based on the relationship of Brownian motion to particle size as well. Using a microscope, particles moving under Brownian motion can be detected. By image analysis, the average distance travelled by each particle can be determined [38]. The hydrodynamic radius can be calculated with the Stokes–Einstein equation as well. Figure 4.7 shows a nanoparticle tracking analysis of nanoparticles in cell culture medium [39].

Not only diffusion, but also the sedimentation of particles in a fluid can be utilized to determine the particle size distribution of dispersed systems. Differential centrifugal sedimentation (DCS) measures the time that particles with unknown size but known density need to travel a known distance by given viscosity and density. The sedimentation typically occurs during centrifugation [40]. Since the sedimentation time is proportional to the square of the particle diameter, DCS has a very high resolution. This also allows the detection of very small or polydisperse particles [41, 42].

Typical colloids are not suitable for characterization by conventional optical microscopes due to their small size because the resolution limit in light microscopy is about 200 nm (diffraction limit by Abbé). In contrast, modern advanced electron microscopy allows spatial resolution down to 50 pm ($5 \cdot 10^{-11}$ m) [43]. Electrons and not photons are used for imaging and spectroscopy. A scanning electron microscope (SEM) produces images of a sample by scanning it with a focused beam of electrons. The topography of the sample surface (edges are bright, recesses are dark) results from secondary electron signal. Backscattered electrons consist of high-energy electrons that are back-scattered by elastic interactions with sample atoms. This signal is typically used to detect a contrast between areas with different chemical compositions, because heavy elements backscatter electrons more strongly than light

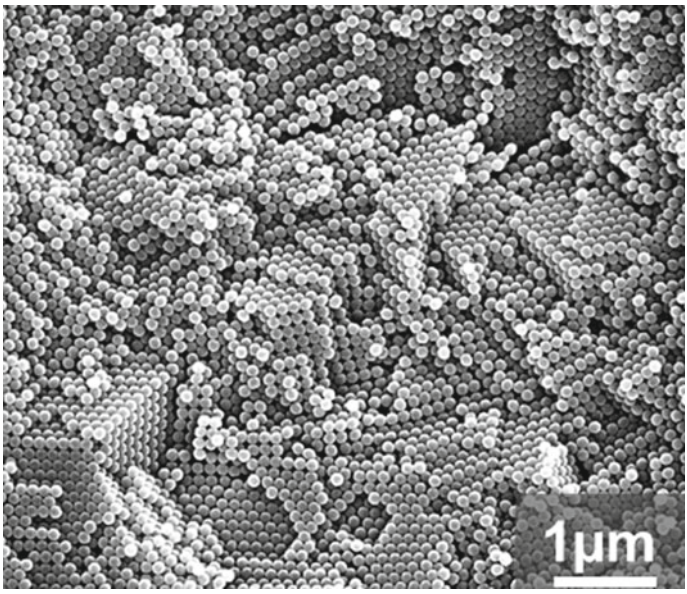

Fig. 4.8 Scanning electron micrograph of closely packed latex nanoparticles

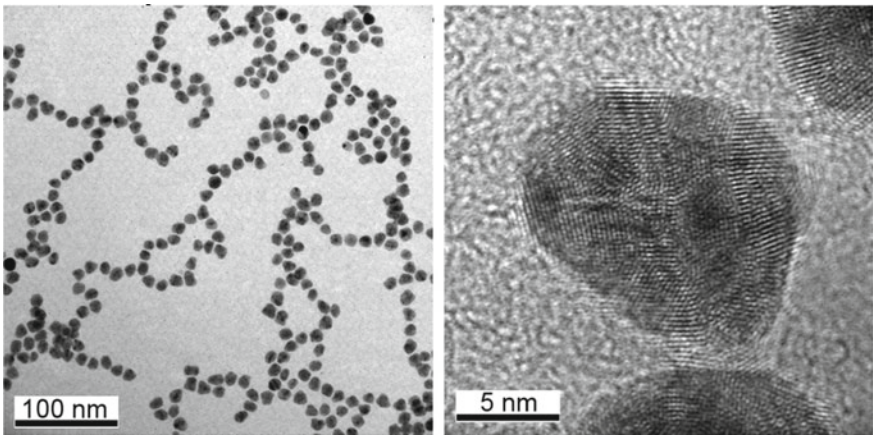

Fig. 4.9 Transmission electron micrograph of PVP-stabilized silver-gold nanoparticles (Reproduced from the dissertation of S. Ristig, University of Duisburg-Essen, 2014)

elements [44]. Figure 4.8 shows scanning electron micrographs (secondary electron signal) of closely packed latex nanoparticles.

Transmission electron microscopy (TEM) is a microscopic technique in which a beam of electrons is transmitted through an ultra-thin specimen, interacting with the specimen as it passes through. An image is obtained by interaction (absorption and diffraction) of electrons transmitted through the specimen [45]. Figure 4.9 shows a transmission electron microscopy image of PVP-stabilized silver-gold nanoparticles [46]. Suspensions of small particles can be dried directly onto grids for examination in the SEM and TEM. By analyzing statically relevant number of objects, particle size distributions can be computed.

The characterization of nanoparticles that are still in dispersion is not as trivial as it may appear. There is a variety of methods that detects a nanoparticle typically as core–shell complex with adsorbed molecules and the hydration layer [47]. Ligand-decorated nanoparticles analysed by hydrodynamic techniques (DLS, NTA) will always show the hydrodynamic radius [47–49]. Nevertheless, the scattering power

Table 4.2 Summary of the results obtained by the different methods for silver nanoparticles (70 nm), gold nanoparticles (15 nm), and the 1:1 mixture of both (Reproduced with the permission from D. Mahl et al., Colloids and Surfaces A: Physicochem. Eng. Aspects 377 (2011) 386–392, Copyright © 2011 Elsevier B.V.)

Method	Diameter	Ag nanoparticles	Au nanoparticles	1:1 mixture of Ag and Au nanoparticles
SEM	By number	70 ± 19 nm	13 nm	72–97 nm (Ag; 5% by number); 12 nm (Au; 95% by number)
TEM	By number	18–72 nm	15 ± 1.5 nm	43–112 nm (Ag; 7% by number); 13 nm (Au; 93% by number)
DLS	By number	63 ± 21 nm	22 ± 7 nm	55 ± 20 nm
	By intensity	124 ± 50 nm	52 ± 23 nm	121 ± 48 nm
	By volume	94 ± 47 nm	30 ± 13 nm	86 ± 41 nm
	z-average	102 nm	42 nm	121 nm
	Zeta potential	−36 ± 2 mV	−57 ± 7 mV	−34 ± 1 mV
	Polydispersity index (PDI)	0.173	0.207	0.171
Nanoparticle tracking analysis	By number	95 ± 36 nm	57 ± 28 nm	87 ± 45 nm (average)
Analytical disc centrifugation	By number	40 ± 19 nm	11 ± 3 nm	
	By weight	48 ± 23 nm	13 ± 3 nm	34 ± 16 nm (Ag; 66% by volume); 13 ± 3 nm (Au; 34% by volume)
	By surface	43 ± 20 nm	12 ± 3 nm	
Theoretical data	By number	15 nm	70 nm	Ag: 1.8%; Au: 98.2%
	By volume	15 nm	70 nm	Ag: 65%; Au: 35%

of dispersed particles increases with the 6th power of the particle diameter. In case of a heterogeneous sample (e.g. when agglomerates are present) this will cause an underestimation of the fraction of small particles and sometimes renders the analysis impossible [49].

Mahl et al. studied the limitations of the detection systems by analysing a known mixture of silver and gold nanoparticles with different methods. The results are summarized in Table 4.2. Dynamic light scattering and nanoparticle tracking analysis were not able to discriminate between large silver particles and small gold particles. Disc centrifugation consistently gave the smallest particle diameter but was able to detect the bimodal particle size distribution in the Au/Ag mixture [49].

Electron microscopic techniques provides a detailed analysis of sample morphology. However, a serious disadvantage is the introduction of drying artefacts during sample preparation. The particle diameters estimated by these methods should be considered as the lower limits of particle size [50]. For heterogeneous samples, the size distribution analysis may deliver poor results due to low number of particles in the observed area. Electron microscopy allows the determination of the fractal dimension during kinetic aggregation of colloids [51, 52].

Additional techniques to analyse nanoparticle dispersions include e.g. field-flow fractionation-based techniques [53, 54]. It is generally recommended to apply several different methods for the characterization of colloidal systems and of nanoparticles to provide adequate conclusions and correlations of suspension state and measured chemical, physical, or biological response.

References

1. Graham, T.: Liquid diffusion applied to analysis. Phil. Trans. R. Soc. 151, 183, 184, 206, 207, 220, 221 (1861)
2. Dörfler, H.D.: Grenzflächen und kolloid-disperse Systeme. Springer, Berlin (2002)
3. Selmi, F.: Azione del latte sulle materie metalliche e reazioni di queste su quello: discorso letto da Francesco Selmi nell'adunanza. Soc. Agr. Reg. (1847)
4. Faraday, M.X.: The Bakerian lecture—experimental relations of gold (and other metals) to light. Philos. Trans. R. Soc. **147**, 145–181 (1857)
5. Hofmann, T.: Kolloide: Die Welt der vernachlässigten Dimensionen. Chem. unserer Zeit **38**, 24–35 (2004)
6. Duffus, J.H., Nordberg, M., Templeton, D.M.: Glossary of Terms Used in Toxicology, 2nd edn. (IUPAC Recommendations 2007). Pure and Applied Chemistry, p. 1153 (2007)
7. Sarquis, J.: Colloidal systems. J. Chem. Educ. **57**, 602–605 (1980)
8. Markus, A.A., Parsons, J.R., Roex, E.W.M., de Voogt, P., Laane, R.W.P.M.: Modeling aggregation and sedimentation of nanoparticles in the aquatic environment. Sci. Total Environ. **506–507**, 323–329 (2015)
9. Teeguarden, J.G., Hinderliter, P.M., Orr, G., Thrall, B.D., Pounds, J.G.: Particokinetics in vitro: Dosimetry considerations for in vitro nanoparticle toxicity assessments. Toxicol. Sci. **95**, 300–312 (2007)
10. Loza, K., Föhring, I., Bünger, J., Westphal, G.A., Köller, M., Epple, M., et al.: Barium sulfate micro- and nanoparticles as bioinert reference material in particle toxicology. Nanotoxicology **10**, 1492–1502 (2016)
11. Cosgrove, T.: Colloid Science: Principles, Methods and Applications. Willey (2010)

12. Hinderliter, P.M., Minard, K.R., Orr, G., Chrisler, W.B., Thrall, B.D., Pounds, J.G., et al.: ISDD: A computational model of particle sedimentation, diffusion and target cell dosimetry for in vitro toxicity studies. Part Fibre Toxicol. **7**, 36 (2010)
13. Mason, M., Weaver, W.: The settling of small particles in a fluid. Phys. Rev. **23**, 412–426 (1924)
14. Kang, T., Park, C., Choi, J.-S., Cui, J.-H., Lee, B.-J.: Effects of shear stress on the cellular distribution of polystyrene nanoparticles in a biomimetic microfluidic system. J. Drug Deliv. Sci. Tech. **31**, 130–136 (2016)
15. Harris, S.S., Giorgio, T.D.: Convective flow increases lipoplex delivery rate to in vitro cellular monolayers. Gene Ther. **12**, 512 (2005)
16. Deryaguin, B., Landau, L.D.: Theory of the stability of strongly charged lyophobic sols and of the adhesion of strongly charged particles in solution of electrolytes. Acta Physicochim. USSR **14** (1941)
17. Verwey, E.W., Overbeek, J.T.G.: Theory of Stability of Lyophobic Colloids. Elsevier, Amsterdam (1948)
18. Helmholtz, H.: Ueber einige Gesetze der Vertheilung elektrischer Ströme in körperlichen Leitern mit Anwendung auf die thierisch-elektrischen Versuche. Ann. Phys. **165**, 211–233 (1853)
19. Stern, O.: The theory of the electrolytic double-layer. Zeit Elektrochem **30**, 508–516 (1924)
20. Gouy, L.G.: Sur la constitution de la charge électrique à la surface d'un electrolyte. J. Phys. **9**, 457–468 (1910)
21. Tadros, T.F.: Colloid Stability: The Role of Surface Forces. WILEY-VCH Verlag GmbH, Weinheim (2007)
22. Kaldasch, J., Laven, J., Stein, H.N.: Equilibrium phase diagram of suspensions of electrically stabilized colloidal particles. Langmuir **12**, 6197–6201 (1996)
23. Ostwald, W.: Lehrbuch der Allgemeinen Chemie. 1st edn. Leipzig (1896)
24. Singh, Y., Meher, J.G., Raval, K., Khan, F.A., Chaurasia, M., Jain, N.K., et al.: Nanoemulsion: concepts, development and applications in drug delivery. J. Control Release **252**, 28–49 (2017)
25. Zhang, Z., Wang, Z., He, S., Wang, C., Jin, M., Yin, Y.: Redox reaction induced Ostwald ripening for size- and shape-focusing of palladium nanocrystals. Chem. Sci. **6**, 5197–5203 (2015)
26. Mahl, D., Diendorf, J., Ristig, S., Greulich, C., Li, Z.-A., Farle, M., et al.: Silver, gold, and alloyed silver–gold nanoparticles: characterization and comparative cell-biologic action. J. Nanopart. Res. **14**, 1153 (2012)
27. Fatehah, M.O., Aziz, H.A., Stoll, S.: Stability of ZnO nanoparticles in solution. Influence of pH, dissolution, aggregation and disaggregation effects. J. Colloid Sci. Biotechnol. **3,** 75–84 (2014)
28. Segets, D., Marczak, R., Schäfer, S., Paula, C., Gnichwitz, J.-F., Hirsch, A., et al.: Experimental and theoretical studies of the colloidal stability of nanoparticles—a general interpretation based on stability maps. ACS Nano **5**, 4658–4669 (2011)
29. Fajans, K., Hassel, O.: Eine neue Methode zur Titration von Silber- und Halogenionen mit organischen Farbstoffindikatoren. Z. Anorg. Allg. Chem. **137**, 221–245 (1923)
30. Schofield, R.K.: Effect of pH on electric charges carried by clay particles. J. Soil Sci. **1**, 1–8 (1950)
31. Feigin, R.I., Napper, D.H.: Depletion stabilization and depletion flocculation. J. Colloid Interface Sci. **75**, 525–541 (1980)
32. Ji, S., Walz, J.Y.: Depletion forces and flocculation with surfactants, polymers and particles—synergistic effects. Curr. Opin. Colloid In. **20**, 39–45 (2015)
33. Xu, W., Nikolov, A.D., Wasan, D.T.: Role of depletion and surface-induced structural forces in bidisperse suspensions. AIChE J. **43**, 3215–3222 (2004)
34. Ruesing, J., Rotan, O., Gross-Heitfeld, C., Mayer, C., Epple, M.: Nanocapsules of a cationic polyelectrolyte and nucleic acid for efficient cellular uptake and gene transfer. J. Mater. Chem. B **2**, 4625–4630 (2014)
35. Berne, B.J., Pecora, R:. Dynamic Light Scattering. Courier Dover Publications (2000)
36. Schaertl, W.: Light Scattering from Polymer Solutions and Nanoparticle Dispersions. 1st edn. ed: Springer Laboratory, Springer (2007)

37. Filipe, V., Hawe, A., Jiskoot, W.: Critical evaluation of nanoparticle tracking analysis (NTA) by Nanosight for the measurement of nanoparticles and protein aggregates. Pharm. Res. **27**, 796–810 (2010)
38. Defante, A.P., Vreeland, W.N., Benkstein, K.D., Ripple, D.C.: Using image attributes to assure accurate particle size and count using nanoparticle tracking analysis. J. Pharm. Sci. **107**, 1383–1391 (2018)
39. Loza, K., Sengstock, C., Chernousova, S., Koller, M., Epple, M.: The predominant species of ionic silver in biological media is colloidally dispersed nanoparticulate silver chloride. RSC Adv. **4**, 35290–35297 (2014)
40. Fitzpatrick, S.T.: Particle size analysis by differential centrifugal sedimentation: advantages and limitations, recent progress, and future trends. Polym. News. **24**, 42–50 (1999)
41. Johnston, B.D., Kreyling, W.G., Pfeiffer, C., Schäffler, M., Sarioglu, H., Ristig, S., et al.: Colloidal stability and surface chemistry are key factors for the composition of the protein corona of inorganic gold nanoparticles. Adv. Funct. Mater. **27** (2017)
42. Schuetze, B., Mayer, C., Loza, K., Gocyla, M., Heggen, M., Epple, M.: Conjugation of thiol-terminated molecules to ultrasmall 2 nm-gold nanoparticles leads to remarkably complex 1H-NMR spectra. J. Mater. Chem. B **4**, 2179–2189 (2016)
43. Ernst Ruska-Centre for Microscopy and Spectroscopy with Electrons (ER-C). FEI Titan G3 50-300 PICO. J. Large-scale. Res. Facil. **1**, A34 (2015)
44. Reimer, L.: Scanning electron microscopy. In: Physics of Image Formation and Microanalysis. Springer, Berlin, Heidelberg (1998)
45. Hawkes, P.: The Beginnings of Electron Microscopy. Academic Press (1985)
46. Ristig, S.: Bimetallische Silber-Gold-Nanopartikel: Synthese, Charakterisierung und zellbiologische Untersuchungen. Thesis, University of Duisburg-Essen, Essen (2014)
47. Dieckmann, Y., Cölfen, H., Hofmann, H., Petri-Fink, A.: Particle size distribution measurements of manganese-doped ZnS nanoparticles. Anal. Chem. **81**, 3889–3895 (2009)
48. Bootz, A., Vogel, V., Schubert, D., Kreuter, J.: Comparison of scanning electron microscopy, dynamic light scattering and analytical ultracentrifugation for the sizing of poly(butyl cyanoacrylate) nanoparticles. Eur. J. Pharm. Biopharm. **57**, 369–375 (2004)
49. Mahl, D., Diendorf, J., Meyer-Zaika, W., Epple, M.: Possibilities and limitations of different analytical methods for the size determination of a bimodal dispersion of metallic nanoparticles. Coll. Surf. A Physicochem. Eng. Asp **377**, 386–392 (2011)
50. Fissan, H., Ristig, S., Kaminski, H., Asbach, C., Epple, M.: Comparison of different characterization methods for nanoparticle dispersions before and after aerosolization. Anal. Methods **6**, 7324–7334 (2014)
51. Weitz, D.A., Huang, J.S., Lin, M.Y., Sung, J.: Limits of the fractal dimension for irreversible kinetic aggregation of gold colloids. Phys. Rev. Lett. **54**, 1416–1419 (1985)
52. Liu, J., Shih, W.Y., Sarikaya, M., Aksay, I.A.: Fractal colloidal aggregates with finite interparticle interactions: energy dependence of the fractal dimension. Phys. Rev. A **41**, 3206–3213 (1990)
53. Lang, T., Eslahian, K.A., Maskos, M.: Ion effects in field-flow fractionation of aqueous colloidal polystyrene. Macromol. Chem. Phys. **213**, 2353–2361 (2012)
54. Schimpf, M.E., Caldwell, K., Giddings, J.C.: Field-flow fractionation handbook. NY Wiley—Interscience, New York (2000)

Chapter 5
Nanoparticle Behaviour in Complex Media: Methods for Characterizing Physicochemical Properties, Evaluating Protein Corona Formation, and Implications for Biological Studies

Wye-Khay Fong, Thomas L. Moore, Sandor Balog, Dimitri Vanhecke, Laura Rodriguez-Lorenzo, Barbara Rothen-Rutishauser, Marco Lattuada and Alke Petri-Fink

Abstract The transformation of nanoparticles (NPs) in physiological milieu is a dynamic phenomenon that is the subject of intense investigation. When introduced into the body, NPs can undergo a variety of changes, such as, protein adsorption, dissolution, agglomeration/aggregation, structural deformities and redox reactions. It is these changes that subsequently determine the uptake, bioavailability, translocation and fate of NPs, which ultimately determine their therapeutic efficiency, diagnostic efficacy or toxicity. This chapter will consider the colloidal interactions at the interface of NPs with the contents of biological milieu, the practical and theoretical considerations required to modify analytical and imaging techniques to detect and, if possible, quantify NPs in this complex environment, and the requirement for a highly interdisciplinary approach to understand the behaviour at the bio-nano interface.

W.-K. Fong · T. L. Moore · S. Balog · D. Vanhecke · L. Rodriguez-Lorenzo · B. Rothen-Rutishauser · A. Petri-Fink (✉)
BioNanomaterials, Adolphe Merkle Institute, Chemin des Verdiers 4, 1700 Fribourg, Switzerland
e-mail: alke.fink@unifr.ch

L. Rodriguez-Lorenzo · M. Lattuada
International Iberian Nanotechnology Laboratory, Water Quality Group, 4715-330 Braga, Portugal

A. Petri-Fink
Department of Chemistry, University of Fribourg, Chemin du Museé 9, 1700 Fribourg, Switzerland

P. Gehr and R. Zellner (eds.), *Biological Responses to Nanoscale Particles*, NanoScience and Technology, https://doi.org/10.1007/978-3-030-12461-8_5

Abbreviations

AFFF	Asymmetric flow field-flow fractionation
AFM	Atomic force microscopy
AUC	Analytical ultracentrifuge
BSA	Bovine serum albumin
BSE	Backscattered electrons
CD	Circular dichroism
CCM	Cell culture media
DC	Disc centrifuge analysis
DDLS	Depolarized dynamic light scattering
DLS	Dynamic light scattering
DLS-zeta potential	Laser-Doppler velocimetry
EELS	Electron energy loss spectroscopy
ESEM	Environmental scanning electron microscope
EXAFS	Extended X-ray absorption fine structure
FBS	Foetal bovine serum
FCS	Fluorescence correlation spectroscopy
FRET	Förster resonance energy transfer
LIT	Lock in thermography LM: light microscopy
NPs	Nanoparticles
SANS	Small-angle neutron scattering
SAXS	Small-angle X-ray scattering
SE	Secondary electrons
SERS	Surface-enhanced Raman spectroscopy
SLS	Static light scattering
SPIONs	Superparamagnetic iron nanoparticles
sSAXS	Synchrotron small angle X-ray scattering
STEM	Scanning transmission electron microscope
STXM	Scanning transmission X-ray microscopy
TDA	Taylor dispersion analysis
TEM	Transmission electron microscopy
TiO_2	Titanium dioxide
TRPS	Tuneable resistive pulse sensing
UV-Vis	Optical extinction spectroscopy in the UV-Visible range
XAS	X-ray absorption spectroscopy
XANES	X-ray absorption near edge structure
XRD	X-ray diffraction
XRM	X-ray microscopy
ZnO	Zinc oxide

5.1 Introduction

The unique properties of nanoparticles (NPs) have provided the opportunity for the creation of materials with properties that far surpass the bulk material. These materials, in turn, can influence and interact with biological systems on the colloidal (sub-micron) level. The successful application of nanotechnology has can be found in both industrial and biomedical settings, for instance, in the case of nanomedicine the safety and efficacy of the drug is determined by the properties of the NP, not the encapsulated drug [1, 2].

Although the promise and potential of NPs to significantly improve the quality of life is immense, the limited success of NPs from the plethora of academic literature is staggering. Whilst we are able to understand the behaviour of these engineered NPs in ideal conditions, it is more difficult to "observe" NPs behaviour in physiological media. This begs the question, how do we observe and quantify how the NPs are behaving in actuality?

Upon exposure to physiological fluids, NPs undergo a variety of colloidal interactions with different components, specifically, salts, sugars and proteins. This interface between the 'bio-nano' comprises the dynamic physicochemical interactions, kinetics and thermodynamic exchanges between nanomaterial surfaces and biological components. These interactions can have a devastating effect on the stability of the NPs in vivo. Fundamental physical chemical studies are generally performed in ideal conditions in order to maintain the integrity of the particle design and conjugation,

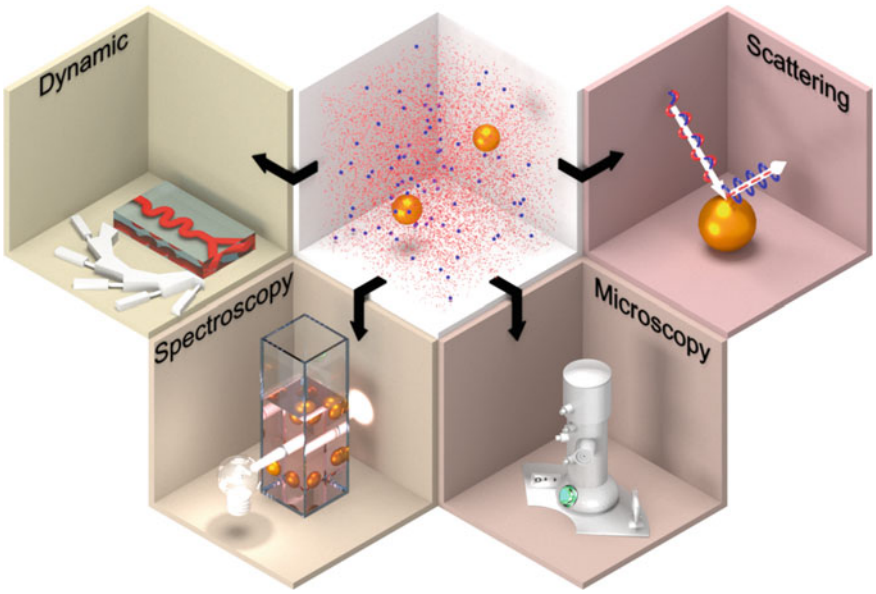

Fig. 5.1 Nanoparticles in complex fluids undergo multiple interactions when they encounter physiological fluids. These interactions can be illuminated and investigated by multiple techniques

however it is the alterations to the particle when exposed to physiological fluids that ultimately determine the biocompatibility and biodistribution of these particles [3].

The purpose of this chapter is to promote interdisciplinary communication between the physical chemistry and the biology communities concerning the development of NPs for bio-applications. In the first instance, the physiological challenges to NP stability will be briefly explored. Then, this chapter will explore the life of NPs in complex media that mimic in vivo environments. Thus, the following topics will be explored: physiological milieu as complex, crowded fluids; the potential influence of complex environments upon NP; current and emerging methods that are available to assess NP stability; and how to translate this data to help develop NPs from bench top to the clinic. Discussion surrounding methods is split into four foci: scattering, spectroscopy and separation, microscopy and dynamic methods (Fig. 5.1).

5.2 Biological Fluids: Composition as Colloids

In a biomedical context, NPs will enter a number of "complex" environments when administered in vitro or in vivo. In vitro, the most common solution NPs will encounter is cell culture media (CCM), which usually contains foetal calf or bovine serum required for optimal cell growth. Depending on the biomedical application of the particle system, it may be necessary to test their performance and behaviour in simulated physiological solutions. Finally, for particles that are introduced into the

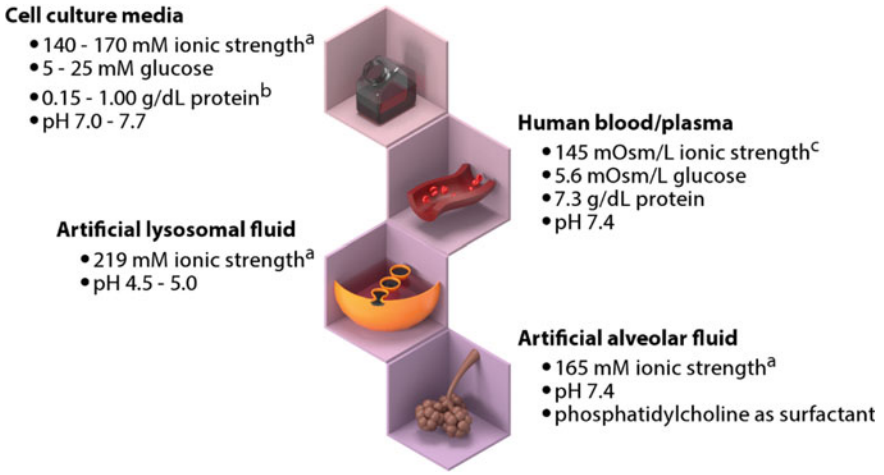

Fig. 5.2 Biological media are comprised of cell culture media, physiological fluids (i.e. human blood or plasma), as well as various synthetic/artificial fluids. These solutions can vary significantly in their composition and thus impact their effects on NP. [a] Estimated based on the inorganic salt concentrations in the media composition assuming no protein interactions in supplemented media; [b] assuming a 5–20× dilution of standard foetal bovine serum into cell culture medium; [c] estimated from the ion concentrations provided by [4]

human circulatory system, understanding what NPs may encounter in whole blood or plasma is critical to inform the rational design of particle systems. The human body comprises many dynamic solutions where biomacromolecules, ionic strength, changes in pH, and active biological processes can act to (de)stabilise, dissolve, and transform particles. In order to assess the effect of biological and physiological fluids on particles, it is therefore important to understand the composition of these fluids, where some of the differences are summarised in Fig. 5.2.

5.2.1 Cell Culture Media

There are a wide range of CCM, where Yao and Asayama have provided an excellent review of their history and use [5]. Synthetic CCM are comprised of a mixture of inorganic salts, amino acids, vitamins, and sugars. Media was initially derived from natural physiological solutions (e.g. blood plasma). The findings that cell proliferation could be improved by exchanging the CCM [6] or adding extracts from physiologically relevant fluids to the growth media [7] instigated a search to understand what biological components led to successful cell culture. Fischer first pioneered a method to understand the necessary components of CCM for cell viability and growth by using a dialysed serum that controlled the amount of low molecular weight components (amino acids, vitamins) added [8].

Initial attempts at CCM were comprised of balanced salt solutions, primarily inorganic salts that were possibly supplemented with glucose [5]. Research in the past century has resulted in the development of numerous "basal" media, that is, CCM containing the minimum essential components to promote cell growth, including proliferation and differentiation. Thus, these balanced salt solutions and basal media are high ionic strength solutions that can have an adverse effect on particle stability. In the presence of high ionic strength solutions, the electrical double layer of NPs can be compressed, resulting in particle colloidal destabilisation and aggregation [3]. If only accounting for the contribution of inorganic salts and not factoring potential interactions of salt ions with biomacromolecules, the ionic strength of basal media can vary between 140 and 170 mM.[1] Thus, NPs need to have mechanisms to prevent aggregation due to high salt content.

These basal media are commercially available, and for conventional cell culture they are traditionally supplemented with protein-rich serum such as foetal bovine serum (FBS) or pooled human serum, generally at a rate of 5–20%. This equates to a protein concentration of approximately 0.15–1.00 g/dL [9].

Generally, basal medias are also buffered to maintain pH of 7.4, but optimal cell growth pH can vary between 7.0 and 7.7 [10]. Changing pH can have dramatic ramifications on particle colloidal stability. Usually, the isoelectric point of the NP material will in part dictate particle surface charge, and changing pH can alter the particle surface charge, which can in turn stabilise or destabilise NPs.

[1]Based on inorganic salt concentrations of several common basal media formulations, such as DMEM, MEM, RPMI-1640, DMEM/F-12, Medium 199 with Earle's salts.

5.2.2 Model Physiological Fluids

In some cases, model physiological fluids are employed in order to mimic certain biological environments. In the context of NPs for biomedical applications, by studying NP behaviour in these fluids, realistic particle behaviour can be examined, such as dissolution/degradation, aggregation, release of active pharmaceutical ingredients, and targeting efficiency. These include artificial lysosomal fluid (ALF), artificial alveolar fluid, artificial synovial fluid, artificial interstitial fluid, and artificial gastric juices. The composition of these artificial biological fluids vary based on pH, inorganic salt concentrations, and presence of other biopolymers [11]. For example, ALF, meant to mimic the endo-lysosomal compartments of cells through which most NPs will be trafficked upon internalization, has a pH from 4.5 to 5.0. Artificial gastric juices, which mimic stomach acid, have a pH even lower at 1.5. These low pH values can severely degrade or dissolve NPs, thereby destabilising them. Moreover, varying salt concentrations can act to destabilise particle solutions.

5.2.3 Human Blood and Plasma

When considering NPs entering the body, blood is the primary tissue with which these particles will first come into contact. Blood comprises of approximately 7% of a person's body weight (~5 L) [4], which is in turn comprised of 60% plasma (water, proteins, glucose, clotting factors, and electrolytes) and 40% red blood cells (RBCs). Plasma contains high concentrations of sodium and chloride ions (142 and 108 mOsm/L, respectively), as well as a mixture of proteins (6.4–8.3 g/dL) [12] that are mostly comprised of serum albumin, immunoglobulins, receptor ligands, and tissue leakage proteins [13]. Blood also contains assorted phospholipids (0.28 g/dL) and cholesterol (0.15 g/dL), macromolecules with the potential to adsorb onto NPs and in part mediate their biological fate [14]. Human blood has a tightly regulated at pH 7.4, however certain pathological conditions can result in acidosis or alkalosis [15].

The cellular component of blood could also factor into particle interactions within this biological space. RBCs vastly outnumber leukocytes, the immune cells responsible for defending against foreign pathogens, at approximately 700–1. However, leukocytes play a major role in mediating NPs fate in the body. The cellular components of blood (e.g. RBCs and leukocytes), may interact with particles that are introduced into intravascular flow. Upon introduction to blood, opsonin proteins can adsorb onto the particle surface—these proteins act as 'flags' for leukocytes to sequester particles from circulation and tissues [16]. Some have even exploited the potential of naturally circulating cells to transport NPs to physiological targets [17, 18].

5.3 Fate of NPs in Electrolyte and Protein Crowded Environments

NPs are similar in size to intra- and extracellular biological species, which can result in interactions with biological components such as cells and proteins, thereby affecting cellular processes. This has two major consequences: firstly, it makes them very attractive candidates for medical applications; secondly, the increasing use of engineered NPs has raised serious concerns about their safety for human health and the environment. Both nanomedicine and nanotoxicology are complementary disciplines aimed at the prevention and treatment of diseases, which require the development and/or study NPs in *physiological environment*s.

The behaviour of the NPs and their potential physiological impact are determined by the physicochemical properties of the particles (such as size, surface, crystallinity, shape etc.) and the interaction with their environment. Due to the complexity of the environment, it is almost impossible to predict particle behaviour in a particular cell or physiological medium [19]. Thus, it is crucial to first discuss the most prominent possible consequences arising from NP incubation in complex biomimetic and/or physiological fluids (Fig. 5.3).

Particle aggregation

Once the NPs are incubated in complex physiological fluids, their surfaces are exposed to significant amounts of salts, proteins, vitamins etc. This encounter can induce NP aggregation (see previous chapter), which is a common phenomenon and has important consequences with for the particles and the cellular dose [3]. In a study comparing carbon nanotube aggregates with bundles of the same carbon nanotubes, Wick et al. has correlated the dispersion state to the cytotoxicity of the material [19]. Teeguarden et al. showed that 15 nm silver NPs appear ca. 4000 times more potent than a micron sized particle on a cm^2/mL media basis [20]. Albanese et al. studied the impact of NP aggregation on particle uptake and cytotoxic behaviour. They could not show unique toxic responses but were able to correlate uptake patterns with particle aggregation [21].

Nanoparticle dissolution

As the size of a material decreases, its surface area and volume decrease. However, the surface area to volume ratio will develop by a ratio of 3/r, with r being the radius. Consequently, an increased number of all atoms that constitute the particle will be surface atoms. NP size and surface area to volume ratio, respectively, influence particle dissolution kinetics. Typically, a decrease in particle size correlates with an increase in particle dissolution [22]. Although the underlying mechanisms responsible for this inverse correlation are not yet fully understood, it is widely accepted that (a) aggregation decreases dissolution and (b) metal NPs can undergo oxidative dissolution [23]. However, several parameters play an important role and are often hard to separate. For example, particle dissolution and consequently ion release was shown to correlate not only with particle size, but also with its shape,

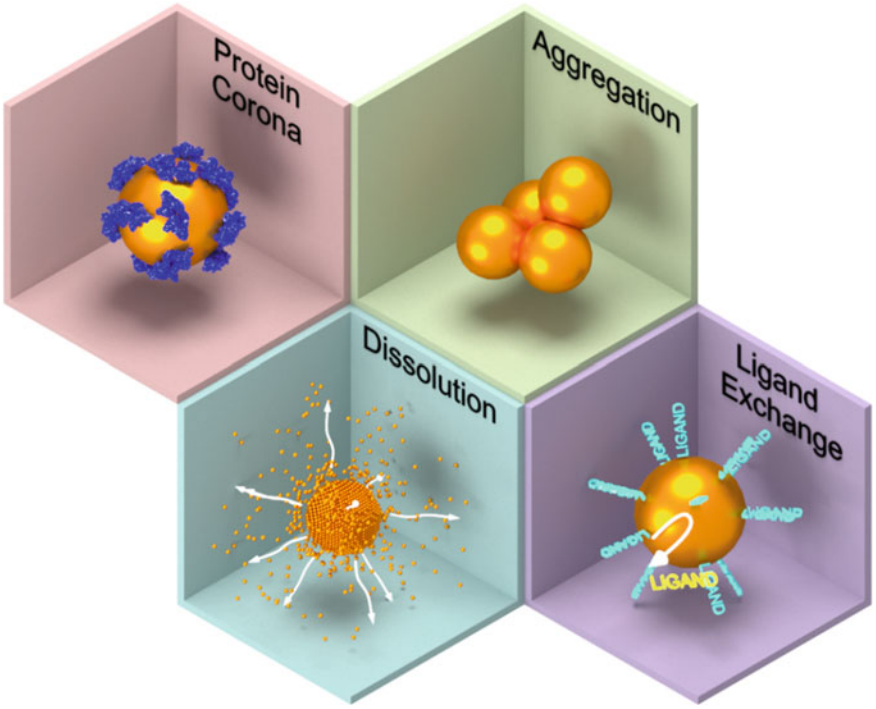

Fig. 5.3 Schematic illustration of possible consequences arising from nanoparticle incubation in physiological fluids. [a] Formation of protein corona which can both shield targeting moieties or antibodies as well as denature proteins; [b] nanoparticle aggregation; [c] nanoparticle dissolution; [d] removal or exchange of surface ligands

surface coating, in addition to environmental factors such as temperature, pH, ionic strength, dissolved oxygen, and the presence of proteins [24].

Removal or exchange of surface ligands

In many cases, anchoring ligands are not firmly chemically bound to the particle surfaces but ligand grafting relies on relatively weak interactions with the surface atoms of the particles. Consequently, it is imaginable that the presence of biomolecules (or high affinity ligands) could remove surface grated ligands. For example, physiological concentrations of thiol-containing molecules such as cysteine have been shown to displace thiolated polyethylene-glycol from the surface of gold NPs [25]. The partial loss of the ligand, however, has far-reaching consequences as it impacts colloidal stability of the NPs, modifies the adsorbed protein profile, and ultimately results in the complete loss of biochemical or analytical function such as targeting ligands (e.g. antibodies), or fluorescent dyes [26]. Kreyling et al. attributed the degradation of a NP grafted polymer coating in vitro and in vivo, on proteolytic enzymes of endosomal and lysosomal cellular compartments [27].

5.4 Interaction with Biomolecules: The Corona of Proteins and More

5.4.1 The "Protein Corona"

The consequent fate of NPs is determined by how they react to biological components they encounter in physiological systems. Upon interaction with biological media (i.e. human blood/plasma, cell culture media, etc.), the surface of a particle will become rapidly opsonised, that is coated with biomacromolecules, in preparation for their removal by immune cells [28]. This forms the "protein corona," a layer of tightly bound and immobile biomacromolecules (e.g. proteins) comprising the hard corona and a weakly associated mobile layer known as the soft corona [29]. The interaction of particles with biological systems is widely attributed to the physicochemical characteristics of the NP; that is, the size, surface charge, surface functionalisation, shape, and material. However, because the protein corona forms a biological layer around particles, it is fair to state that physicochemical characteristics drive nano-bio interactions through the protein corona. In fact, work done by the group of Warren Chan has shown that the protein "fingerprint" (i.e. characteristic NP protein corona) is the optimal indicator for predicting particle-cell interaction [30, 31].

5.4.2 Factors Affecting Protein Corona Formation

The formation of the protein corona is driven by particle physicochemical characteristics at the particle surface [32]. When particles are introduced into a biological fluid, proteins will adsorb rapidly onto their surface due to van der Waals interactions, Columbic forces, hydrophobic interactions, and hydrogen bonding. Protein adsorption can result in changes to the protein conformation or alter protein solubility, which can have major consequences on protein function by altering their secondary and tertiary structures [33–35]. Significant research has been pursued in order to understand how particle physicochemical characteristics influence protein corona formation, and several excellent reviews on the particle protein corona exist [36, 37].

The formation of the corona is not only driven by physicochemical factors, but also experimental conditions such as experimental temperature, exposure time, particle concentration, and method of isolating particles for analysis [37–39]. However, in the most basic sense, the formation of the protein corona is a study of protein interactions with a (nano)surface. An early study by Lück et al. [40] showed that latex particles with different surface charge densities altered protein adsorption, and Gessner et al. [41] likewise investigated the effect of different surface chemistries on corona formation around latex particles. They showed that Columbic interactions between the particle surface functional groups and proteins were a critical in determining protein corona formation. Tenzer et al. [42] investigated the effect of particle

size, surface charge, and incubation time on the formation of protein corona on silica and polystyrene NPs in human plasma. They observed that the protein corona forms rapidly (~30 min) and remains rather consistent over time. Isolating particles at time points earlier than 30 min, where there may be protein exchanging between abundant proteins and higher affinity proteins (i.e. the Vroman effect) [43, 44] is a non-trivial challenge. A study investigating polystyrene particles with different functional groups (carboxy, amino, sulfonate, and phosphonate) showed that amino and sulfonate groups enriched the adsorption of apolipoproteins; proteins that can reduce the uptake by phagocytic cells and so prolong circulation time [45]. Thus, Coloumbic and hydrophobic interactions, dictated by the particle material and surface functionalisation, seem to be the key drivers mediating protein corona formation.

Often, polymers are chemically coupled or adsorbed to particle surfaces to enable a so-called "stealth" effect [46]. Poly(ethylene glycol) (PEG) is the gold standard for particle shielding, reducing particle clearance and prolonging blood circulation time while reducing the adsorption of opsonins (which facilitate particle clearance). Interestingly, it seems that the protein corona, and not merely reducing protein adsorption due to polymer shielding, is responsible in the stealth effect observed with polymers such as PEG or poly(ethyl ethylene phosphate) [47]. It has been shown that PEG conformation on a particle surface in part mediates particle circulation time in vivo [48], and other evidence shows that this could be due to variations on the protein corona based on PEG conformation [49]. Furthermore, PEG chain length and surface coverage dictate protein corona formation (and subsequent biological interactions) in part [50]. The use of other stabilising molecules (e.g. surfactants, which can adsorb onto particles via hydrophobic interactions, electrostatic or van der Waals forces) has also been shown to mediate protein corona formation [51, 52].

Particle size has been investigated for its role in mediating protein corona formation; however, results vary as to what effect size has. Cedervall et al. [29] showed that the total amount of protein adsorption onto polymeric particles was determined by size (scaling with the amount of particle surface available), however the pattern of proteins adsorbed remained consistent. A study on different sized gold NPs (5, 15, 80 nm) showed that protein corona composition changed across the different size regimes [53]. Thus, it appears that particle size (largely due to the amount of surface area and also the material) can play a role in corona formation but the effect is not consistent. Similarly, particle shape may influence protein corona formation. Miclăus et al. [54] showed that protein adsorbed preferentially to silver nanocube faces as opposed to edges at early time points (<1 h), though it is unclear if this difference is due to the particle geometry or due to displacement of particle-stabilising polyvinylpyrrolidone which has a different affinity to the particle surface depending on the crystal plane to which it is adsorbed. However, another study showed via 2D gel electrophoresis that there was a difference in protein adsorption onto titanium dioxide nanoparticles, nanorods, and nanotubes, i.e. due to particle shape [55].

It is difficult to draw any type of universal guiding rule for protein corona formation; rather particles are currently investigated on a case-by-case basis noting the particle material, surface functionalisation/properties, shape, size, etc. However, it

is possible to make some predictions for particle interaction with biological systems based on the bimolecular corona.

5.4.3 Beyond Proteins: Other Components of the Corona

Lipids, sugars, vitamins and other small organic molecules can or may also adsorb on the NP surfaces, thereby affecting immunogenicity and potentially hampering targeting abilities of administrated NPs, and in part mediating nano-bio interactions [51, 56]. For example, Müller et al. [51] showed that the lipid-domains of lipoproteins were also responsible for adsorption processes, indicating that lipid-like molecules can comprise the protein corona. These data are supported by the fact that surfactants and hydrocarbons are often used to adsorb stabilising macromolecules, ligands, and polymers onto particle surfaces [52, 57]. Studies on lipoprotein binding onto hydrogel particles revealed that high-density lipoproteins and, cholesterol, and triglycerides are present in the bimolecular corona, and are speculated to govern particle interaction with, for example, lipid transport pathways [14]. Investigations into the glycosylation of proteins, the natural and frequent modification of proteins with sugar molecules, showed that protein coronas that were deglycosylated (i.e. sugar molecules removed from corona proteins) were less stable and increased the adhesion of particles to cells [58]. It is therefore evident that biomolecules beyond proteins may yet play an important role in our understanding of fundamental bio-nano interactions.

5.4.4 Biological Effects of the Protein Corona

Even after extensive characterisation ex vivo, the eventual biodistribution of the NP plus biomacromolecule corona can result in unexpected in vivo behaviour. This rearrangement has been shown to affect their pharmacological activities, interaction with their environment (i.e. other proteins) and other biological responses [59, 60].

When the NP reach their target, it is the corona that the cells actually ‘see’. The corona may contain opsonins, which can enhance the uptake of the NP-corona-complex by cells of the reticuloendothelial system (RES) [61, 62]. This “molecular signature” is recognised by immune cells and so determines the route of particle internalisation, its pharmacokinetics, namely, volume of distribution, organ disposition, and rate of clearance from the blood and body [63, 64]. Recent studies have also demonstrated that surface adsorbed biomolecules can shield NP functionality, reduce cell selectivity [65] and impact cellular uptake kinetics [45]. Thus, the type and number of proteins that the NP attracts determines its biodistribution. It follows that there have been and continues to be a plethora of studies and reviews into understand exactly what physicochemical properties of different kinds of NPs determines the composition of their protein corona [3, 66].

In terms of biocompatibility, the formation of the corona can be advantageous or disadvantageous [67]. Attached biomacromolecules that are not recognized by any receptors make the particle less attractive to the cell. For example, Salvati et al. demonstrated that proteins can shield NP derivatised transferrin from binding to its receptors on cells end entirely lose its targeting specificity [68]. On the other hand, if a developed corona contains the right biomarkers, they can activate the endocytic pathway of the target cell, where it consequently effects haemolysis, thrombocyte activation, nanoparticle uptake and endothelial cell death [42]. Several studies have demonstrated enhanced biocompatibility of protein coated NPs compared to the originally protein-free synthesised NPs [69]. For instance, the pre-coating of blood proteins on the surface of carbon nanotubes greatly alter their cellular interaction pathways and result in much reduced cytotoxicity [70]. In a landmark study, Wang et al. deliberately manipulated the corona of positively charged polystyrene NPs in order to traffic them into the lysosomal compartments of target cells [71]. In addition to the surface character of the single particles, aggregation also determines their biodistribution. This is elaborated upon in Sect. 6.5. As can be seen, it is insufficient to characterise NP designed for in vivo use solely in pristine conditions as the biological identity conferred onto the surface of the NP by the components of the corona determines their fate. Thus, in the following sections, methods to characterise the protein corona and their changing colloidal identities will be discussed.

5.4.5 Characterising the Protein Corona

Given the importance of the corona surrounding the NP, the investigation of its composition is key to understand the biological impact of nanomaterials. In general, the following processes are taken in order to characterise the NP-corona. Firstly, the NPs are incubated with the representative complex media of choice for a defined period. The complexes then have to be separated from the unbound proteins in the matrix. Different protocols achieve this by initially washing and centrifuging the sample, followed by further processing such as magnetic separation (limited to magnetic NP [72]), microfiltration, ultracentrifugation, chromatography and/or electrophoresis, where the latter two techniques allows for the exquisite and more gentle separation and isolation of NP-biomacromolecule-complexes from unbound components. Protein corona separation and characterisation is summarised below and in Table 5.1, and is reviewed in more detail in these informative references [37, 73–76].

5.4.5.1 Separation

Chromatography separates components based on the differences in their interactions with stationary phase of the column through which they are travelling. The main method to separate unbound biomacromolecules from the NP-corona is size exclusion chromatography (SEC), and to a lesser extent ion exchange chromatography

Table 5.1 Summary of the techniques that can be used to separate NP-corona complexes, characterise protein composition and protein conformation

Function	Technique	Advantages	Disadvantages	References
Isolation of NP-corona	Chromatography Field-flow fractionation Capillary electrophoresis 1D/2D gel electrophoresis	Quantitative Low shear force Quantitative Simple, fast	Limited applicability High complexity Limited sensitivity Limited separation	[29, 77, 78] [39, 79] [80–84] [85–91]
Characterisation of protein composition	Proteomics + mass spectroscopy	Quantitative, high resolution	Time consuming, expensive, significant experimental and theoretical expertise required	[29, 90, 94, 95]
Characterisation of conformational change	Fourier transform infrared spectroscopy Raman spectroscopy Fluorescence spectroscopy Circular dichroism Nuclear magnetic resonance spectroscopy Isothermal titration calorimetry	Identifies amide bands of proteins bound to NP Identifies amide bands of proteins bound to NP in solution Wide range of probes available Identifies secondary structures of proteins Can map site of protein attachment Kinetics and thermodynamics of protein attachment	Sample preparation destroys samples Autofluoresence and Raleigh scattering noise In vivo environment can adversely change signal Limited specificity Line broadening of spectra High sample concentration and user expertise	[96, 97] [98] [101] [103, 104, 110–112] [14, 105–107] [108, 109, 113]

(IEC) and reverse phase liquid chromatography (RPLC). SEC separates components based on size. Larger molecules are unable to interact with the stationary phase and thus move rapidly through the column, whereas smaller molecules such as unbound proteins are able to fall into the pores in the mobile phase and thus move slower through the column [29]. IEC separates components based on their affinity to the ion exchanger, where the elution of components can be easily manipulated by changing the ionic strength of the mobile phase [77]. RPLC separates components based on their polarity through their interaction with the hydrophobic stationary phase [78].

Recent studies have utilised flow field-flow fractionation to separate NP from protein solutions. Field-flow fractionation is a chromatography-like method that separates components in a fluid suspension or solution by applying a field (e.g. temperature, gravity, centrifugal) perpendicular to the direction of flow of the sample in a long and narrow channel. This causes separation of the components present in the fluid depending on their differing mobility under the force exerted by the field. This method allowed for the differentiation of the corona proteins on SPIONS based on their relative dissociation rates from the NPs [79]. A more advanced version of this technique, asymmetric flow field-flow fractionation (AFFF), is described in more detail in the Sect. 5.6.5. This method has a lower shear force on the sample and thus, remarkably, was able to keep the soft protein corona on a polystyrene NP intact for further analysis [39].

Electrophoresis separates proteins by their migration in an electric field depending on their electrophoretic mobility, size or charge. Most commonly, capillary electrophoresis (CE), 1D and 2D gel electrophoresis is used. CE separates components based on charge and friction and is performed in submillimetre diameter capillaries. It has been used to separate polymeric [80–83] and metallic NPs [80, 84] from the different components of plasma. 1D and 2D gel electrophoresis differ in complexity and sensitivity. 1D separation is simpler and faster to run and separates components through a polyacrylamide gel based on molecular weight, 1D gels can be used to detect between 1 and 50 ng for a single protein band. Whereas 2D provides higher separation of components as it separates components in a polyacrylamide gel based on molecular weight and isoelectric point. 2D gel electrophoresis is nominally used when protein mixtures are more complex. Gel electrophoresis has been wildly used in order to separate a wide variety of particles from metallic NP [85, 86], liposomes [87], carbon nanotubes [88, 89] and polymeric particles [90, 91]. Images of the 2D gels can then be analysed via readily available software that compares the image to a 2D master map of human plasma proteins [76, 92] and/or linked with spectroscopic techniques described below.

5.4.5.2 Protein Quantification

Separation techniques are subsequently coupled with mainly spectroscopic methods in order to identify the composition and/or conformation of protein in the corona. Protein identification is achieved by mass spectroscopy (MS) and proteomics. MS ionizes chemical species and then sorts the ions based on their mass-to-charge ratio.

The MS spectra is then analysed and proteins identified via a database search [93]. Following the separation of the NP-corona-complex from free protein, the corona then needs to be separated from the NP. This is achieved by either the use of surfactants and subsequent separation using gel electrophoresis and then MS analysis of the fractions [29, 90, 94]; or by "shotgun proteomics" which is the in situ digestion of the NP-corona-complex by a protease (trypsin) followed by separation of the individual proteins and peptides by liquid chromatography MS [95]. Thus far, MS is the only method that can provide single protein identifications.

5.4.5.3 Protein Conformation

NP bound proteins can change their 3D structure when compared to the native proteins in solution, thus many techniques are used to investigate conformational change as an indication of binding to the NP.

Fourier transform infrared spectroscopy (FTIR) measures the wavelength and intensity of the absorption of infrared (IR) radiation by a sample. The absorption of IR radiation excites vibrational transitions in molecular bonds, where the vibrational frequency depends on the strength and polarity of the vibrating bonds, they are influenced by intramolecular and intermolecular effects. Protein molecules exhibit many vibrational frequencies and it is through identifying these vibrations that proteins conformation can be elucidated [96, 97]. In a similar manner, Raman spectroscopy (RS) identifies protein secondary structure by probing molecular vibrations to provide a molecular fingerprint of biomolecules at the surface of NPs [98]. When these proteins are adsorbed on plasmonic NPs, a surface-enhanced RS (SERS) effect occurs, enhancing the Raman signal, thereby allowing the study of the NP-protein complex at low concentrations. However, Raman and FTIR spectroscopy differ in some key fundamental ways. RS investigates changes in polarisability of a molecule, whereas IR spectroscopy looks at changes in the dipole moment. RS measures relative frequencies at which a sample scatters radiation, whereas FTIR measures absolute frequencies at which a sample absorbs radiation. FTIR spectroscopy is particularly sensitive to heteronuclear functional group vibrations and polar bonds, especially OH stretching in water. Raman on the other hand is sensitive to homonuclear (e.g. C–C, C=C and C≡C) molecular bonds.

Fluorescence spectroscopy is used to look at protein conformation as fluorescent signals are exquisitely sensitive to the immediate environment of the probe, have a high signal to noise ratio, and the time scale of emission is in the nanosecond range [99, 100]. This technique has been used to probe the kinetics of protein attachment [101].

Circular dichroism (CD) occurs as a consequence of the interaction of polarised light with chiral molecules. As proteins are chiral molecules, changes in the secondary structure of proteins can be identified via CD spectroscopy [102]. It is thus utilised for the rapid evaluation of structural and stability changes when the proteins form stable, noncovalent, complexes with NPs [103, 104].

Nuclear magnetic resonance spectroscopy (NMR) observes local magnetic fields around atomic nuclei. The intramolecular magnetic field around an atom in a molecule changes the resonance frequency, thus giving access to details of the electronic structure of a molecule and its individual functional groups, allowing for the observation of not only chemical identity, but also structure, dynamics, reaction state, and chemical environment of molecules. Thus, it has been used to observe the corona of liposomes [105], lipids in the corona surrounding polymeric particles [14], as well as hydroxyapatite surfaces [106]. On the flip side, a recent study has utilised ^{19}F diffusion NMR to look at changes in the hydrodynamic radii of gold NP upon exposure to complex media as opposed to changes in proteins attached to the NP [107].

The kinetics of protein attachment to NPs can be identified by isothermal titration calorimetry (ITC). ITC identifies the thermodynamic parameters (binding affinity, enthalpy changes and binding stoichiometry) of interactions in solution by measuring a change in heat upon the addition of a component to another one in solution. Consequently, it has been used to study the binding of proteins to particles [108, 109].

The protein corona is recognised as a critical factor in understanding fundamental interactions between nanomaterials and biological systems. Whether exposing particles to cells, injecting particles into a living organism, or evaluating the effect of particles on an ecosystem, the biomolecular or protein corona will serve as the interface between nanomaterial and biology. Within this chapter we focus on the characterisation of particles in complex biological media, and there is simply not enough space to cover the complex and nuanced depth of the protein corona topic. For that the readers are directed to several excellent reviews mentioned in the beginning of this section. However, it is important to understand that the protein corona will drive the interaction of particles with a biological system, and so mediate particle colloidal behaviour (i.e. colloidal stability/aggregation, cellular interaction, etc.). One crucial aspect of corona formation is its impact on colloidal stability, where the presence of proteins can either enhance or reduce colloidal stability, the following sections of this chapter will discuss the colloidal behaviour of NP in more detail and how it is analysed.

5.5 Theoretical Considerations with Regards to Colloidal Stability in Physiological Media

5.5.1 Fundamentals of Nanoparticle Aggregation

Given that the behaviour of a NP cannot be decoupled from its surroundings, describing NPs in the context of their actual environment is crucial. For example, while particles may quickly aggregate in water, they may become completely stable in CCM, due to the high excess of proteins that alters particle interactions and stabilises the dispersion [114]. The opposite of this is also frequent, and NP aggregation is immi-

nent as soon as particles dispersed in CCM [115]. In both cases, the resulting protein covered NPs have completely differently physical properties from individual NP. Consequently, experimental characterisation must give an accurate account of several fundamental properties regarding the chemical and physical behaviour of the NPs, as it is these properties that influence their efficacy [116], specifically:

- chemical composition of the core and surface
- surface charge
- density and conformation of functional groups
- phases found in/on the particle (amorphous vs. crystalline phases)
- porosity, structure of porosity (fractal vs. ordered)
- size and its distribution
- shape and its uniformity/heterogeneity
- colloidal stability in terms of aggregation
- physical stability and chemical integrity (dissolution, ligand exchange)
- optical and magnetic properties.

Therefore, characterisation should be performed in both in 'ideal' conditions and in complex CCM. Interested readers are directed to several reviews introducing the available techniques briefly introduced below for the physicochemical characterisation of NPs in complex biological media [117, 118].

5.5.2 Consequences of Nanoparticle Aggregation on Cell Studies: Dosimetry of Single Particles Versus Aggregates

The influence of NPs internalized by cells is frequently studied by using in vitro models. In these models, establishing dose–response relationships are of paramount importance, where the metrics of the administered dose are NP number, mass, volume, and surface area. Due to the nature of cell culture experiments, the dosimetry metrics must be ascertained at three different sites: the dose administered to the cell culture, the dose delivered to the cell surface, and the dose internalised by the cell, whereas the two latter are the most relevant for the subsequent cellular interaction and induction of responses [119, 120]. The measurement of NP properties at these three sites is increasingly difficult, and the achievable accuracy and precision fall quickly with polydispersity, typical for aggregates and agglomerates.

Mathematical models are used to estimate these parameters, assuming that in in vitro models, particle delivery is driven by diffusion and sedimentation [121], regardless of whether the particle is stable or not [122]. The rate of diffusion and sedimentation of a particle are determined by the hydrodynamic radius and effective mass density, where the adsorption of proteins will alter both metrics. The rate of transport, and thus, the rate of particle delivery can be estimated via modelling, provided that these hydrodynamic properties are known [123–127].

The delivery profile of NPs is also determined by the ability of the cell to internalise the particles. From the point of view of the NP, uptake is dependent on size, shape, elasticity, and surface chemistry [126, 128–133]. Thus, the physicochemical characteristics of NPs in CCM strongly impacts their deposition and interactions on the outer cell membrane, as well as the potential induction of cellular responses [134]. From the point of view of the cell, the principal mechanisms whereby NPs interact and impact upon target cells occurs through their interaction with cell membranes, endo-lysosomal vesicles, nucleus and organelles [135–137]. Cell types also different in lipid and receptor composition of the membrane, where modifications have been shown to alter the membrane fluidity and cellular functions and consequently NP uptake [138–140]. Additionally, NPs adhering to the outer cell membrane also can induce adverse responses [141], for instance, a pro-inflammatory response via oxidative means [142], the fibre paradigm [143] and genotoxicity [144]. The use of reliable methods and realistic test conditions to study possible effects of NPs on cells have recently been reviewed in several publications [145, 146] and are covered in the Chapter titled, "Molecular and Cellular Aspects and Methodological Approaches".

The intracellular fate of NPs upon interaction with cells (uptake, retention, release, intracellular degradation, transfer to other cells, and/or translocation across tissue barriers) is still poorly understood but there seems to be an agreement that solubility, size and surface charge are the most important determinants of a material's fate in vitro as well as in vivo [147]. Therefore, it is imperative that the characterisation and understanding of NP in complex media is performed as accurately and realistically as possible in order to understand the physicochemical phenomena driving their interaction with cells.

5.6 Measuring NP in Complex Cell Culture Media: Different Methods, Pitfalls and New Developments

In this section, available methods for the characterisation of NP in complex media will be discussed. It is divided into four parts: **scattering**, **separation**, **imaging** and **dynamic** methods.

5.6.1 Scattering and Spectroscopic Methods

Light scattering instruments are well-established techniques for the characterisation of NP and consequently are the most frequently used to obtain information about the behaviour of NPs in complex media.

The average size (hydrodynamic diameter) of NPs can be characterised by dynamic light scattering (DLS), depolarized dynamic light scattering (DDLS), fluorescence correlation spectroscopy (FCS), small-angle neutron scattering (SANS),

small-angle X-ray scattering (SAXS), static light scattering (SLS), X-ray diffraction (XRD) and UV-Vis spectroscopy in case of plasmonic NPs. Characterizing polydispersity and size distribution is not as straightforward with FCS, XRD, and UV-Vis. DDLS is especially well-suited to studies in CCM when the NPs exhibit optical anisotropy, such as gold, silver, ZnO, TiO_2. In this case, the experimental accuracy benefits from the fact that the scattering of depolarized light from the CCMs is weak, and thus, an excellent 'contrast' in favour of the NPs can be obtained [115, 148]. Information about stability, protein adsorption, aggregation, integrity, such as dissolution and loss of ligands, can be obtained with techniques that are used to measure particle size.

Information about particle shape can be obtained via DLS, DDLS, SANS, SAXS, and SLS. Additionally, plasmonic and anisotropic NPs, such as metallic nanorods and nanostars, have unique signatures in the UV-Vis spectrum. For metallic NPs, the red shift of the plasmon resonance peak in the UV-Vis spectrum can either signal aggregation or the formation of a thick protein or polymer shell around the particle. In the case of particle agglomerates, the "fractal dimension" is a measure of the density of packing of the primary particles that could be redefined as the porosity of the aggregates. This information can be obtained with SLS, SAXS and SANS. Structural information about the protein corona beyond its thickness, (e.g. density as a function of distance from the particle surface), can also be obtained via SANS [148–151].

Another important aspect is that these techniques give a holistic representation of the sample; consequently, the protein-rich background signal must be very carefully and justly addressed. Figure 5.4 compares the dynamic light scattering analysis of silica particles in water to its scattering in complex CCM. While the particles are relatively large (100 nm in diameter) the CCM scatter nearly as much as the particles themselves, and therefore, strongly interfere with the signal (called the correlation function) to be analysed in order to characterise the NPs.

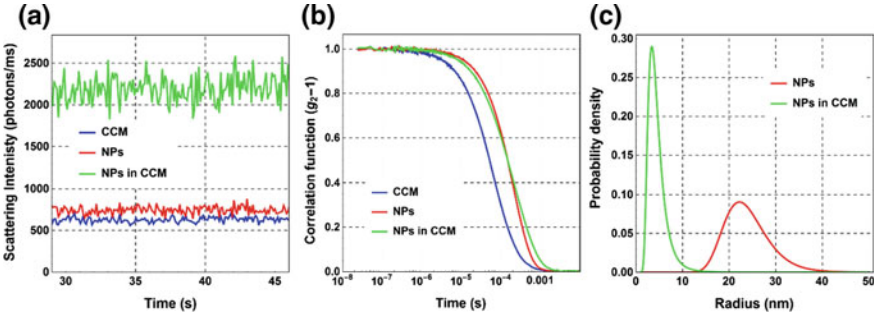

Fig. 5.4 a The intensity of light scattering from silica particles in water, from the CCM, and from the particles in CCM. (SiO_2 NPs, 100 nm, 20 μg/ml, scattering angle: 90°, CCM: RPMI suppl. with 10% foetal calf serum). b The corresponding signals to be analysed (correlation function). c Due to the strong scattering from proteins, the NPs in CCM appear to be smaller than in water

5.6.2 Zeta Potential—Describing the Surface Charge of NP

The surface charge of a particle is usually described by measuring the zeta potential, which is the electrokinetic potential at the slipping plane, not the true potential found at the particle surface itself (Fig. 5.5). Consider a negatively charged NP immersed into a complex media. Due to its charge, ions and molecules with the opposite charge form a strongly adhered layer (Stern layer) around the particle. Beyond the Stern layer, a loosely bound and mobile layer develops, comprised of both negative and positive charges. The edge of this layer is known as the slipping plane. When the particle moves, ions and molecules within this plane move along with the NP, but ions and molecules beyond the slipping plane do not, thus, it is at this point the zeta potential is measured. When NPs enter CCM, different proteins and other organic molecules can adhere to their surfaces. The properties of the corona highly depend on the surface characteristics and on the type of the CCM [90]. As can be seen, the zeta potential is exemplary case demonstrating that this physicochemical property of the NP cannot be decoupled from the context of its actual environment.

5.6.3 Measuring the Effect of Proteins on Zeta Potential

The understanding of the zeta potential of a particle is an important tool for understanding their long term colloidal stability and efficiency on surface functionalisation [152]. However, the zeta potential obtained for NP in CCM can be easily misinter-

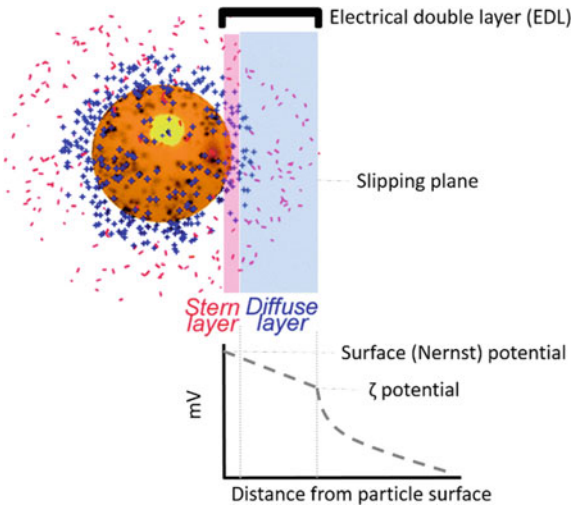

Fig. 5.5 The arrangement of ions surrounding a negatively charged particle. The important parts of the electrical double layer are highlighted. Adapted from [3]

preted. The ideal NP sample for zeta potential analysis using electrophoresis is as follows: (1) monodisperse in size and with high light scattering properties; (2) dispersed at low salt concentration (conductivities (Λ) < 1 mS/cm); and (3) dispersed in a particulate-free, polar dispersant (e.g. high purity water). Particles delivered in CCM clearly do not meet all of these criteria and thus, may not give high quality zeta potential data. Common challenges with this type of sample are:

- CCM contain high salt concentrations and as a consequence high sample conductivity (Λ is 1.5 S/cm) [153], which raises the likelihood of Joule heating (the process where the energy of an electric current is converted into heat as it flows through a resistance) and consequently lead to electrode polarisation and degradation due to the movement of the conductive ions.
- In many cases, NPs selected for biological applications usually have a diameter of <20 nm, which have a high mobility in suspension due to the applied field and Brownian motion [154] and so have very low light scattering properties [155]. Therefore, the electrical field needs to be applied for long integration times to increase the signal-to-noise ratio. Consequently, Joule heating of the sample may also occur. Since the mobility is calculated directly from the sample viscosity, this temperature increase creates a substantial systematic uncertainty in the electrophoretic mobility measurement.
- Proteins can aggregate immediately at the electrodes even at extremely low voltages and due to the integration times required for weakly scattering NPs. These protein aggregates can migrate into the optical detection region of the cell, leading to measurement of the electrophoretic mobility of the aggregates, rather than that of the NPs [156].
- Zeta potential is only obtained by using mathematical models to extract it from the electrophoretic mobility of the particle. In general, a proportionality between electrophoretic mobility and zeta potential is assumed. While this proportionality is dependent on ionic strength, for high values of zeta potential, electrophoretic mobility can either be independent of zeta potential, or non-monotonic behaviours can occur, which limit the accuracy of the obtained zeta potential value.

Due to the aforementioned challenges, it is important to understand the strengths and limitations of zeta potential measurements of NPs in CCM when interpreting results. For this, a "special" sample preparation is recommended in order to improve data quality in terms of accuracy and reproducibility:

- The CCM should be filtered before adding to remove the possible protein aggregates and any visible particulates.
- The dilution of CCM to decrease the conductivity is a way to protect the electrode and typically improves data quality. It is important to re-measure the pH after dilution.
- The characterisation of hydrodynamic size of the NPs before and after measuring zeta potential can reveal any interaction between the sample and the electrode material (e.g. protein and formation of NP aggregates).

- Centrifuging the sample and reconstituting in "clean media" is a method of "washing" the NPs and reducing conductivity. It is worth noting that this procedure should not have an effect on the original colloidal stability and the original pH.

5.6.4 Choosing Scattering Methods for Nanoparticles in Complex Media

Nanoscience is intrinsically an interdisciplinary approach, therefore the range of skills and expertise within a research group are becoming more and more multidisciplinary. Probably the best thing that the typical researcher engaged in nanomedicine and nanotoxicology can do is to collaborate closely with instrument scientists having the necessary theoretical and experimental expertise in the techniques of choice. Basic guidelines that outline the function and utility of scattering techniques are summarised in Table 5.2.

5.6.5 Characterisation Methods Based on Separation

A different approach to extract information about NP is to separate them via external fields and use their response to the field to gain information about their size and size distribution. Three fields are commonly used for this purpose: centrifugal force, flow fields and electrical fields.

5.6.5.1 Analytical Centrifugation

Centrifugal force is used in analytical ultracentrifuge (AUC) and disc centrifuge (DC) analysis [176–180]. The principle of analytical ultracentrifugation is to expose NP to a very strong acceleration (up to a million times that of gravity). Under these conditions, particles and macromolecules experience an enhanced sedimentation velocity, which is proportional to their mass minus their buoyancy, and inversely proportional to their hydrodynamic radius. Therefore, any difference in either their mass or their hydrodynamic radius is enormously amplified in an ultracentrifuge. This permits the separation of particles with differences in mass, in density, or simply in their hydrodynamic radius. In its basic configuration, an analytical ultracentrifuge is coupled to a UV-Vis detector operating at single wavelength, or to a refractive index detector, which allows one the determination concentration of all particles passing through a detection window. Determining the concentration clearly requires the knowledge of the object shape, which defines the amount of light scattered and adsorbed by it. The most advanced versions of the analytical ultracentrifuge can measure full UV-spectra at multiple wavelengths all along the sample tube, thus providing sedimentation pro-

Table 5.2 Summary of the information that can be obtained from scattering, spectroscopic and separation based analysis techniques covered in Sect. 5.6

Technique	Properties of NPs the technique directly based on	Recommended usage	Warnings	Properties derived indirectly	Information deduced	Typical pitfalls and/or benefits	References
DLS	Optical polarisation Translational diffusion due to Brownian motion	Uniform NPs characterised in non-complex matrices, such as water	Presence of proteins may strongly scatter light, which interfere with the analysis, (Fig. 5.4) Polydispersity (apparent particle size may be defined by only a few large NPs)	Hydrodynamic radius	Particle size Polydispersity Colloidal stability Thickness of protein corona	Improper sample prepara-tion/purification Isolation of 'protein signal' is erroneous or forgotten Converting particle size and polydispersity values into number-averaged size distribution is done incorrectly Solution is not dilute enough (multiple scattering, inter-particle interactions)	[157–160]
DLS-Zeta potential	Optical polarizability Electrophoretic mobility: translational motion of NPs in quasi-static electric field	Uniform NPs characterised in non-complex matrices, such as water	Presence of proteins with non-zero electrophoretic mobility may strongly interfere with the signal Polydispersity: surface charge may be curvature dependent [161] Irregular shape	Electric double layer (EDL) describing the interface between NP and solution (solvent)	Potential difference between the slipping plane and solution Predict colloidal stability	Using wrong mathematical model for the type of media (e.g. the limiting cases of Hückel vs. Smoluchowski approximation)	[152]

(continued)

Table 5.2 (continued)

Technique	Properties of NPs the technique directly based on	Recommended usage	Warnings	Properties derived indirectly	Information deduced	Typical pitfalls and/or benefits	References
DDLS	Anisotropic optical polarizability Translational and rotational diffusion due Brownian motion	Both without and in the presence of CCM Uniform and optically anisotropic NPs (gold, silver, nanorods, tubes)	Compared to DLS, roughly three-times more sensitive to polydispersity Polydispersity of non-spherical particles	Hydrodynamic radius	Particle size Polydispersity Colloidal stability Thickness of protein corona	Improper sample prepara-tion/purification Converting particle size and polydispersity values into number-averaged size distribution is done incorrectly Solution is not dilute enough (multiple scattering, inter-particle interactions)	[115, 148, 162–164]
FCS	Fluorescence Translational diffusion due to Brownian motion	Fluorescent labels may provide a high degree of selectivity towards the NPs	Polydispersity [165]	Hydrodynamic radius	Particle size	Stability and integrity of fluorophores Irregular shape and size polydispersity limits the accuracy of models available	[166–168]
SANS	The strength of interaction of neutrons with the atomic nuclei	Soft (light elements) NP Characterising the thickness and density of soft corona (proteins, polymers) around particles [151, 169] Magnetic NP Self-assembly	Presence of proteins in CCM may interfere with the analysis	Particle size and distribution Thickness and density of protein corona Functional layer, polymer coat Superstructure from particle Self-assembly	Particle size Polydispersity Particle shape and morphology (shell vs. sphere) Protein/Polymer corona	Analysis can be model-independent and model based Irregular shape and size polydispersity limits the accuracy of models available	[149, 150]

(continued)

Table 5.2 (continued)

Technique	Properties of NPs the technique directly based on	Recommended usage	Warnings	Properties derived indirectly	Information deduced	Typical pitfalls and/or benefits	References
SAXS	Electron density (number of electrons in each element's electron shells)	Both soft and inorganic NPs Self-assembly	Presence of proteins in CCM may interfere with the analysis	Particle size and its distribution Superstructure from particle self-assembly	Particle size Polydispersity Particle shape and morphology (shell vs. sphere)	Analysis can be both model-independent and model based Irregular shape and size polydispersity limits the accuracy of models available Insufficient information about biological surrounding of the NP	[150, 170, 171]
SLS	Optical polarizability	Both soft and inorganic NPs Self-assembly	Presence of proteins in CCM may interfere with the analysis	Particle size and shape Polydispersity	Particle size Polydispersity Particle shape and morphology (shell vs. sphere)	Analysis can be both model-independent and model based Irregular shape and size polydispersity limits the accuracy of models available	[17]
XRD	Electron density (number of electrons in the electron shells of each element)	Crystalline structure		Crystallinity Crystal structure	Crystallinity Average crystalline size Average particle size	Irregular shape and size polydispersity limits the accuracy of models available Little sensitivity to polydispersity Insufficient information about biological surrounding of the NP	[172]

(continued)

Table 5.2 (continued)

Technique	Properties of NPs the technique directly based on	Recommended usage	Warnings	Properties derived indirectly	Information deduced	Typical pitfalls and/or benefits	References
TDA	Optical extinction. Brownian motion. Dispersion in laminar flow	Poorly purified samples Ultra-small NPs Multimodal suspensions	Hydrodynamic radius Poor time resolution (kinetics)	Particle size Polydispersity	Particle size Polydispersity	Irregular shape and size polydispersity limits the accuracy of models available Microfluidic environment is needed	[173, 174]
UV-Vis	Optical extinction	NPs exhibiting plasmon resonance	In case of protein corona/polymer shell, aggregation is not indicated	Particle size Polydispersity	Average size Concentration	Little sensitivity of analysis to polydispersity	[175]
AUC/DC	Sedimentation velocity, optical extinction	Possibility to resolve the particle size distribution and multimodality Distinguish between different materials	Loosely bound proteins and macromolecules can be detached	Hydrodynamic radius, full characterisation of the size distribution	Separation of particles by population, including clusters	Irregular shape of particles requires advanced modelling	[176–180]
AFFF	Diffusion coefficient	Separation of particles based on size, and their independent characterisation	Loosely bound proteins and macromolecules can be detached. Interaction with membrane might be troublesome	Particle hydrodynamic radius, particle shape (via SLS)	Separation of particles by population, including clusters	Irregular particle shape; interactions with membrane is particle dependent	[79, 181]
TRPS	Particle volume and electrophoretic mobility	Individual particle counting and size/electrophoretic mobility measurement	High ionic strengths are required to measure small particles	Particle volume	Size distribution Zeta potential distribution	Particle colloidal stability Aggregates might cause blockage of the pore	[182–184]

files with full UV-Vis characterisation of the centrifugate [177, 179]. This method has been used to characterise gold NP undergoing aggregation, as well as mixtures of quantum dots.

Disc centrifugation is a cheaper and simpler variation of ultracentrifuge, operating at a much lower number of revolutions per minute, where particles are injected in proximity to the centre of a spinning disk, and a single wavelength detector is used to measure their concentrations at a given passage point [180]. While unable to provide the same amount of information as ultracentrifuge, this technique is highly versatile, and suitable for separation and characterisation of NP covering a broad range of sizes, especially high density inorganic NP. One particularly interesting feature of centrifugation-based characterisation methods is the possibility to separate NP from clusters with two, three, four particles, thus allowing a much more precise assessment of the cluster mass distribution in the case of aggregation. This is one of major advantages compared to scattering techniques, which probe solutions without any separation of the different components.

The disadvantages of centrifugation techniques are that: (1) they usually require dilution of the sample, which could change the quantity and composition of proteins and ions adsorbed on their surface, and (2) quantitative interpretation of the data is only possible when the shape of the particles and clusters is known, which determines their hydrodynamic radius. Except for very simple shapes, the determination of hydrodynamic radius is usually a complicated problem, and irregular particles are characterised by sedimentation velocity that are a function of their orientation.

5.6.5.2 Taylor Dispersion Analysis (TDA)

Taylor dispersion analysis is another method that can be used to determine the size and size distribution of particles [173, 174]. The principle is based on the injection of concentration pulse of particles in an empty capillary, where a parabolic flow profile leads to a dispersion of the particles. Because particles close to the middle of the channel travel faster than those close to the walls, a concentration gradient in the radial direction is created. This concentration gradient is compensated by particles diffusion, which tends to create a uniform concentrations profile in the radial direction. Therefore, a measurement of concentration at two different positions along the channel allow one the determination of the particle diffusion coefficient and its distribution, from which size is extracted. While the technique has been widely used to determine the molecular weight of biological macromolecules, the application to particles is only recent. Some configurations exist, where Taylor dispersion has been used in combination with capillary electrophoresis, which can be used to speed up the analysis. The method represents a reliable alternative to DLS in the determination of particles diffusion coefficient, because it requires a much simpler setup, but suffers from the usual limitations of how to relate the diffusion coefficient to particle shape. In addition, since particles are exposed to a shear rate, adsorption of molecules on their surface could be affected be the flow field. Furthermore, compared to the analytical centrifugation method, TDA cannot fractionate the samples, thus is less accurate in

determining the particle size distribution, even though a recently introduced moment-based method to obtain more accurate size information has been proposed [173, 185, 186].

5.6.5.3 Asymmetric Flow Field-Flow Fractionation (AFFF)

This technique is able to fractionate a sample by exposing it a laminar flow field and perpendicular cross-flow in order to determine particle size distribution in biologically-relevant samples [181]. A small sample of particles in solution is injected in a channel with a laminar parabolic profile. Perpendicularly to the flow direction, another flow filed is applied. As a result, large particles tend to be driven towards the bottom part of the channel, while smaller ones, having larger diffusion coefficients, stay closer to the centre of the channel. Large particles take longer times to flow through the channel than smaller ones. The perpendicular cross flow is obtained by removing part of the main flow in the channel through a membrane positioned on one of the sides of the channel. The cut-off of the membrane determines the minimum size of particles of macromolecules that can be detected. AFFF can be used to separate particles from clusters, to determine the size of particles, including the presence of a coating on the particles. Quite often, is AFFF coupled to detectors, such as DLS and multi-angle light scattering, in addition to more common refractive index detectors, used in chromatographic processes. While in the oldest versions of the methods a calibration of the elution time was necessary to determine the size of the eluting particles, similar to what used in gel permeation chromatography, the use of modern detectors allows one to measure the absolute values of the size of the particles that elute, and also to obtain information about their shape. The elution time of the particles can be further controlled by tuning the flowrate and the extent of crossflow. Therefore, the combination of the fractionation ability of the AFFF with the presence of these advanced detectors, make this method one of the most versatile and powerful in the characterisation of particles.

However, the method has also some limitations. The exposure of particles to shear forces, as well as the intrinsic dilution that the particles are subject to, can easily lead to desorption of proteins from particles exposed to complex media. This has been exploited to distinguish between strongly bound proteins versus weakly bound proteins, which have been both detected separately [79, 178]. In addition, the interaction of particles with the membrane in the channel is one of the major concerns of the AFFF. Depending on the material of the membrane, particles can be repelled, or can adhere to the membrane, thus resulting in partial loss of analyte, and difficulty in assessing whether the analysis of the sample is thorough.

5.6.5.4 Tuneable Resistive Pulse Sensing (TRPS)

A completely different approach is the one used by Tuneable Resistive Pulse Sensing (TRPS) [182]. In this case, particles immersed in an electrolyte solution are exposed

to an electric field and forced to move through a narrow pore. The measurements are done at such a low concentration that only one particle at a time passes through the pore. The presence of electrolytes in the solution leads to a steady passage of electrical current through the pore. However, as one particle passes through the pore, a drop in the electrical current ensues, which is proportional to the volume of the particle. Additionally, the shape of the resistance pulse depends on the electrophoretic mobility (and zeta potential) of the particles. This technique enables not only a precise determination of the particle size, provided that the particles are stable under electrolyte conditions using during the measurement, but also the assessment of the particle concentration. Interestingly, the size determination is independent of particle shape and material. Because the method is based on counting individual particles, an accurate determination of size distribution, even in the case of multimodal distribution of particles, is possible.

The technique can also create maps of particles based on not only their size, but their zeta potential too [183, 184]. This opportunity has been used to characterise particles with a protein corona obtained by exposing them to bovine serum, and the results have been compared to those obtained by DLS and by analytical centrifugation. The main drawbacks of TRPS are the following: (1) particles with a size lower than 30 nm cannot be detected, and, additionally, (2) small sized particles require high electrolyte concentrations, which might hamper their colloidal stability. Additionally, pore size must be not much larger than the particles, otherwise the limits of detection will be hit, and the presence of clusters of particles will result in blocking of the pore.

5.6.6 Microscopic Methods

5.6.6.1 Advancements in Light Microscopy (LM)

The theoretical resolution limit of light (~200 nm) defines the size limit of objects that can be resolved by standard light microscopic methods. The resolution limit can be improved by capturing the absorption/scattering of light by an object in a Fourier plane by the objective lens and converted into a real plane image by the ocular lens, thereby providing additional resolution on nanostructures in a technique called Fourier plane imaging [187]. This requires the use of a rotating grating to obtain inaccessible high-resolution information that are encoded into the Fourier plane. Combining these images in the Fourier space yields information that is converted into a higher resolution of the (real) image [188] and is applicable to a biological complex setting [189]. Such computational approaches push the 200 nm size limit of a standard light microscope to somewhere around 50–100 nm.

Besides computational advancements, additional hardware can provide improvement in resolution. The detection of strongly scattering NPs, such as gold NP and multiwall carbon nanotubes, profits from cardioid condensers provided in enhanced darkfield microscopic imaging [190]. The oblique illumination reaches a resolution

around 90 nm and accentuates the effects of strongly scattering particles and reduces the contribution of the much less strongly light scattering complex environment [191, 192]. With this method, it is also possible to determine the aggregation state of the particles.

If the information on the absorbance and/or reflection of the incoming electromagnetic wave is insufficient, one must rely on a signal inherent and exclusive to the NP. In the case of superparamagnetic iron NP (SPIONs), the inherent ability to convert electromagnetic energy into heat can be exploited for their detection. Hence the usage of such particles in clinical settings as contrast enhancers in magnetic resonance imaging. More recently, lock in thermography (LIT) uses this ability to study the heating power of clinical applications of SPIONs [193].

The bioimaging of NPs rely on an exclusive light signal originating from the particles, typically achieved by covalent bonds with fluorescent dyes [194, 195]. Unfortunately, these approaches are of limited interest to natural NP in complex media since NP in consumer products are seldom tagged with such fluorescent dyes.

5.6.6.2 X-Ray Microscopy

Owing to the smaller wavelength of X-rays, X-ray microscopy (XRM) resolves objects up to a spatial resolution of about 30 nm without the need for a vacuum (as in electron microscopy, see below) [196]. Scanning transmission X-ray microscopy (STXM) has been used, for example, to monitor copper NP in river biofilms [197].

5.6.6.3 Scanning Probe Microscopy

Scanning probe microscopy, especially atomic force microscopy (AFM), is an often-used method to measure NP. AFM provides a three-dimensional surface profile by raster-scanning a sharp tip (few nm to 10s of nm) over a surface with a feedback loop to adjust parameters needed to image a surface. Atomic forces are used to map the tip-sample interaction and can be used for all types of nanomaterials.

Most AFMs use a laser beam deflection system where a laser beam is focused on the back of the reflective AFM lever onto a position-sensitive detector. The acquired height map can provide the height of NP with unprecedented accuracy and precision. Although AFM can operate both in air and in solution, the former procedure is much more present in literature owing to an easier procedure [198].

5.6.6.4 Electron Microscopy

The wavelength of electrons in an electron microscope is another 1000 fold smaller than the wavelength of X-rays in XRM and 10,000 fold smaller than photons in optical light microscopy. Therefore, electrons can convey much smaller information providing sub-Ångstrom resolution. Two types of electron microscopy are commonly

utilised: scanning electron microscopy (SEM) and transmission electron microscopy (TEM).

A scanning electron microscope operates by registering the interaction between the sample and a focused electron beam that scans over the sample. Dedicated detectors can collect back scattered electrons and secondary electrons. Backscattered electrons (BSE) are electrons provided by the focused electron beam that are slingshot back under the influence of positively charged atomic nuclei. The BSE yield relates to the proton density: the heavier the atoms the brighter BSE the signal [199]. This relationship can be used to differentiate between two components, e.g. a metal NP in a carbon-based medium. Secondary electrons (SE) are electrons that derive from the inelastic collision of the electron beam with the electron shell. They originate from the atoms within the samples and will result in ionisation events. SEs mainly contain topographic information on the surface of the object. SEM provides a unique view on the surface of particles and allows for size estimation, surface structural analysis and surface defects detection for particles of a few nm diameter or higher.

In a TEM, the shadow of the object, as witnessed by the electron beam, is imaged. TEM provides the highest resolution of all known microscopic methods: around 0.2 nm in conventional instruments and even 0.05 nm in high-end aberration corrected instruments [200]. Darkfield approaches, similar to in light microscopy, such as scanning transmission electron microscope (STEM) and variants such as high-angle annular darkfield provide high contrast in function of the atomic number thereby permitting differentiation between the signal of non-carbon-based NPs and the typically carbon-based medium in the image [201].

Electrons have a much stronger interaction with matter than the other electromagnetic waves described above. Consequently, electron microscopes must operate under a vacuum as electrons will be scattered by the atmosphere. However, water will evaporate at room temperature in the vacuum of an EM. This implies that aqueous samples require complete dehydration prior to measuring [202]. If removing the aqueous medium is not an option, for example because it is an integral structural component as in liposomal preparations, cryo-electron microscopy can be useful. Water in frozen samples will remain in its solid form at liquid nitrogen temperatures, even at the low pressures inside the electron microscope. Cryo-EM has the additional advantage that drying-induced aggregation or structural changes are prevented. Such low temperature approaches are possible both in SEM, TEM and STEM.

Another possibility to image without removing the aqueous solution is to sacrifice resolution for the presence of water in the sample, a concept which is applied in the environmental scanning electron microscope (ESEM). Differential pumping permits to have the electron optics under high vacuum but the sample chamber under a poorer vacuum: typically around 50–100 mbar, 1/20 of the ambient pressure. A 10-fold reduction in resolution compared to conventional SEM is the main drawback (in the range of 50–100 nm), along with a very limited penetration depth of the beam. Efforts were made to develop sample chambers, WetSEM™ capsules, which enclose the sample including the liquid environment inside the vacuum of the electron microscope. These capsules are equipped with an electron-transparent membrane that allows electrons to pass into the sample. More recently, liquid TEM holders have

been developed, based on a similar principle of shielding the aqueous samples from the vacuum in the instrument by means of silicon nitride windows [203].

5.6.6.5 Analytical Methods

The microscopic approaches discussed above result in images that reflect the absorption, reflection and/or scattering of the incoming electromagnetic waves. Most imaging modalities can be complimented with analytical tools, often of spectroscopic nature. These analytical tools provide a means to characterise the wavelengths present in the image-forming waves, i.e. the spectral fingerprint. The analytical microscopy concept turns the 2D micrographs into 3D data cubes, with the third dimension a spectrum for each pixel that can be matched with existing libraries.

Light microscopic methods can be complemented with visual and infrared range spectroscopy (400–1000 nm). Such spectroscopic analyses have been used in combination with dark field microscopy to study the interaction between cells and NP in the absence of a fluorescent probe [204], where the spectrum can be influenced by the surrounding matrix [205]. Other spectroscopic possibilities, such as Raman spectroscopy or Fourier transformed infrared spectroscopy can be used.

The interaction of an electron beam with the inner shell electrons of atoms can result in the expulsion of X-rays which are characteristic of the atom. The specific X-ray energy can be detected and quantified by a silicon drift detector, an analytical method known as electron dispersive X-ray or EDS. EDS provides the chemical characterisation for each pixel in the image, resulting in elemental maps, and can be found in SEM and STEM setups. A second spectroscopic method in found TEM and STEM based on electron interactions with atoms is called electron energy loss spectroscopy (EELS). Electrons in a high voltage, coherent electron beam hitting outer shell electrons of atoms will lose energy by inelastically scattering electrons in a way that is characteristic for the interacting atom. Peaks in the absence of a specific energy band quantify elements in the sample [206].

5.6.6.6 Advice for Sample Preparation for Imaging Techniques

Unlike scattering methods, microscopy provides results on a per particle basis. This necessitates the creation of proper sampling schemes: each nano-object must have the same chance to be sampled, independent of its size or other characteristics. Omission bias (larger objects are favoured) or convenience sampling (searching for a convenient example) render data unsuitable for generalisation and hence useless to represent the entire nanomaterial. The key to overcome such bias is to record data according to a (computer-) generated randomised scheme [207]. A summary of the discussed techniques can be found in Table 5.3.

Table 5.3 Summary of imaging techniques used in the elucidation of colloidal interactions at the bio-nano interface

Technique	Information	Pro	Cons	Pitfalls
Structured illumination microscopy	Presence of NP	Sub 100 nm resolution	Will not resolve NP	Processing time. Artefacts due poor grating position
Darkfield microscopy imaging	Presence and localization (unresolved) of NP	Light microscopy based, easy sample prep	Only strongly scattering NP	Interpretation of the data can be arduous
Fluorescence microscopy (including laser scanning microscopy and super resolution microscopy (STED, PALM, STORM)	Presence and localisation (unresolved) of NP	Light microscopy based, easy sample prep. <100 nm resolution in super resolution LM	Necessity for fluorescent dyes	Fluorescent staining of NP in complex media can be difficult
Magnetic resonance imaging	Presence and (crude) localisation of NP	Non-invasive, and very specific	Poor resolution, limited to paramagnetic NP	
Lock in thermography	Presence and thermal signature of paramagnetic and plasmonic NP	Sensitive, reliable	Poor resolution, limited to paramagnetic particles	
Atomic force microscopy	Presence, localisation, size	High resolution, in aqueous solutions	Bias in height values due to deformation by the cantilever tip [138]	User influence on the data processing [139]
XRM XRSM	Presence, aggregation, size distribution	No sample prep needed	Synchrotron or advanced light source needed	
Scanning electron microscopy	Presence, aggregation, size distribution, surface analysis, surface defects detection, material contrast information	Resolves single particles, high resolution, Bulk samples	Vacuum needed, meaning drying of the particles, may induce aggregation. Samples may need conductive coating, destructive method (samples cannot be reused)	Size estimation can be complex for non-spherical NPs
Environmental scanning electron microscopy	Presence, aggregation and size of (larger) NP	In situ electron microscopy	Loss of resolution	Complex image interpretation

(continued)

Table 5.3 (continued)

Technique	Information	Pro	Cons	Pitfalls
Transmission electron microscopy	Presence, aggregation, size, morphology, 3D structure	High resolution	Sample preparation: water must be removed	Only thin objects (<200 nm thick)
Scanning transmission electron microscopy	Presence, aggregation, size, morphology, 3D structure	High resolution, thicker samples (up to 1 μm)	Sample preparation: water must be removed	Radiation damage of the sample
wetSEM	Presence, aggregation state, size, morphology	Electron microscopy without the need for dehydration	Loss of resolution	Sensitivity of the membrane to radiation damage
Liquid holders TEM	Presence, aggregation state, size, morphology, 3D structure	Electron microscopy without the need for dehydration	Dedicated chips needed for each sample	Interaction of electron beam on enclosed water complicates interpretation

5.6.7 Dynamic Methods

The interactions of NPs in vivo have been shown to be a dynamic affair, where the faster moving proteins arrive first, forming the 'soft corona', and then are replaced by less motile proteins that have a higher affinity for the surface and become electrostatically bound, forming the 'hard corona', over the course of several hours [208–210]. Full understanding of any dynamic behaviour necessitates its study in space and

Table 5.4 Summary of dynamic techniques

Technique	Information	Pros	Cons	Pitfalls
Synchrotron techniques	NP properties, chemical composition and protein aggregation	High flux allows for excellent resolution in space and time	Samples are easily damaged by synchrotron radiation Beamtime is not easily awarded	Data deconvolution can be complex
Microfluidics	Interfacial phenomena	Can be coupled with scattering and imaging techniques Can overcome sample preparation issues found in bulk	Interdisciplinary knowledge of optics, and fluid mechanics in addition to your own expertise are required	Devices are not 'plug and play' units Resolution is limited to the detection method Detection methods are limited by chip material

in time. As the interaction of NPs with components in physiological media is a dynamic phenomenon, scientists are utilising advanced, high energy synchrotron techniques, coupling microfluidic technologies with scattering or imaging methods, and/or sophisticated software to analyse images in order to obtain time resolved data (Table 5.4).

5.6.7.1 Synchrotron radiation

The brilliance of synchrotron radiation has significantly shortened the analysis time of a multitude of scattering techniques in specialised facilities that can be found around the world. Synchrotron light is produced by the acceleration of electrons under the direction of a magnetic field to 99.9% of the speed of light. This results in the production of radiation that has high flux, a wide energy spectrum, highly collimated and polarised, which can produce short pulses. Such radiation allows for the fast illumination of NP at the bio-nano interface, where data deconvolution allows for the separation of signal between the protein and NP. Because of the advantages of high spatial resolution, high sensitivity, excellent accuracy, low matrix effects and non-destructiveness, synchrotron radiation analytical techniques are increasingly becoming valuable tools for investigating the bio-nano interface.

By selecting and directing specific wavelengths of light to specific instruments, called 'beamlines', one can utilise specific wavelengths of radiation, to analyse the bio-nano interface within one facility. Of particular utility for the dynamic analysis of NP in complex media are the following methods.

Synchrotron Small Angle X-Ray Scattering (SAXS)

High brilliance synchrotron sources coupled with advanced detectors has ensued the adoption of time resolved synchrotron SAXS data to observe a multitude of dynamic processes, thus helping us to understand the link between nanostructure and the properties of the materials [211]. Synchrotron SAXS, coupled with SANS, has been used to observe changes in morphology of gold NP upon interaction with physiological proteins [150]. This detailed study employed complex data deconvolution in order to elucidate protein dissociation constants, and the stoichiometry of the NP-protein complex, where the authors developed their custom built software in order to make this technique accessible to non-experts in small angle scattering. In a more straightforward manner, highly ordered nanomaterials can particularly benefit from dynamic study with synchrotron SAXS, where changes in scattering are more evident. This method has been used in the determination of the kinetics of disorder-order and order-order phase transitions in lipidic liquid crystalline NP, upon exposure to lipases [212, 213].

Synchrotron X-Ray Absorption Spectroscopy (XAS)

X-ray absorption spectroscopy detects change in the local electronic environment, coordination geometry and bond distances of absorbed atoms in materials [214]. Because of its unique chemical sensitivity, synchrotron XAS provides precise fingerprint measurements of the NP structure, shedding light on the molecular mechanism of physicochemical interactions, such as adsorption, dissolution, phase transformation, and oxidative-reductive reactions, at the interface between NP and physiological milieu [215]. Additionally, synchrotron X-ray sources can be focused to spot sizes ranging from mm^2 down to the nm^2 range [216]. XAS reveals specific information of specific sites in three different energy regions: the pre-edge region, which reflects electronic structure and oxidation state; the X-ray absorption near edge structure (XANES) and the extended X-ray absorption fine structure (EXAFS), providing geometry and coordination of the local structure. An important advantage of XAS is that samples of all states of matter (gas, liquid, soft matter and solid) can be analysed.

For instance, XANES has been used to differentiate the chemical states of iron on the surface of two types of Fe_2O_3 NPs (α-Fe_2O_3 and γ-Fe_2O_3) in the presence of biological reducing agents cysteine and NADPH [217]. Binding sites of BSA upon gold nanorods have also been identified via XANES in combination with a least squares linear fitting [218]. XANES experimental data combined with simulations revealed that the hydrophobic interaction between a streptavidin and the hydrophobic surface of single-walled carbon nanotubes induced changes in the C=O double bond of the streptavidin which subsequently led to a small, but relevant structural distortion of the protein [219]. As can be seen, XAS is a powerful tool for characterizing the chemical states of NP and proteins at the interface between NP and biological milieu.

Synchrotron Circular Dichroism (CD)

The main advantage of synchrotron CD over benchtop instruments is that it has the capacity to obtain structural information of proteins with only small sample amounts in a short amount of time. By following the unfolding of different classes of human plasma proteins upon exposure to gold and silver NP at different temperatures, Laera et al. demonstrated that albumin, transtyrethrin and lysozyme are significantly destabilised when interacting with silver NP, whilst its stability is not affected when interacting with gold NP [110]. Time resolved synchrotron CD has been utilised to observe rapid changes in the folding of BSA in the corona, attributed to the transformation of protein disulfide bonds to Au–S coordination [218]. Thus, the rapid acquisition of CD data can be used to reveal the molecular mechanisms of interfacial reactions of proteins.

Advances in Synchrotron Techniques

Recent developments in synchrotron instrumentation have afforded scientists the ability to visualise NP on a single particle level. Coherent X-ray diffraction is a powerful method of measuring the three dimensional structure of NP, where 2D or 3D reconstruction of the scattering pattern allows for the elucidation of an image of nanoscale structures [220]. The most recent advances in this field have been in X-ray free-electron lasers, where femtosecond flashes of X-ray light have been used to provide single particle analysis on nanoscale particles, in this case, a crystalline gold core and a differently shaped palladium shell to a resolution of 7 nm [221]. These advances in synchrotron science will allow for a faster and more focussed understanding of interaction at the bio-nano interface.

5.6.7.2 Microfluidics

Microfluidics has facilitated the development of nanomaterials through the ability to accurately manipulate nanolitre volumes in microscale fluidic channels in turbulence free conditions, resulting in well-defined and well-controlled fluid-fluid interfaces to be made and manipulated [222]. Without agitation or obstacles within the channels, interaction between these interfaces at microfluidic length scales results only in diffusion controlled mixing. Microfluidic devices have thus been used in the creation of nanoscale materials, as fine control of the interfaces can be achieved through the directed introduction of valves, mixers and pumps on the chip in order to form uniform droplets and precipitates, and consequently, the precise control of NP synthesis [223] and separation [224]. In terms of looking at bio-nano interactions, chips can be designed and created in order to accurately mimic in vivo environments and processes, where the flexible and modular nature of microfluidic devices provides opportunities to create increasingly realistic models, including multi-tissue devices, which have been used to assess NP as drug delivery vehicles [225, 226].

Microfluidic chips can be combined with either scattering or optical techniques in order to understand how engineered particles behave in complex environments. Investigating NP dispersions under microfluidic laminar flow conditions coupled with florescence spectroscopy has previously been established as a technique known as flow cytometry [227], however the use of MF chips allows for this investigation in a more complex manner. The integration of sample preparation and delivery with the analytical mechanism results in the synergistic enhancement of function and performance of extremely small detection volumes (femtolitres to nanolitres). In order to monitor intra- and intermolecular reactions occurring in microfluidic reactors, they have been coupled with spectroscopic methods [228], surface-enhanced Raman spectroscopy (SERS) detection [229], Förster resonance energy transfer (FRET) [230], light scattering [231] and small angle x-ray scattering [232]. Thus, the flexibility of microfluidic chips allows them to be coupled to a wide range of characterisation techniques for the dynamic characterisation of NP at the bio-nano interface.

5.7 Conclusions and Future Directions

This chapter has:

- demonstrated that physiological fluids contain elements that alter the stability of NPs in in vivo conditions and that complex CCM have been formulated to reflect these conditions;
- demonstrated that colloidal chemistry phenomena of NPs are altered by elements in complex CCM;
- highlighted analytical techniques that are particularly useful to look at NPs in complex CCM; uncertainty surrounding colloidal interactions requires investigation by multiple techniques in order to get the complete picture;
- provided practical advice as to how these techniques need to be modified in order to take into consideration the effect of naturally occurring salts, surfactants and proteins upon the colloidal stability of NP in vivo;
- given insight into developing techniques that can be used to characterise the chemical and structural changes of the components at bio-nano interface;

In this way, a solid foundation for the long-term advancement of nanotechnology into effective new products both in medicine and industry can be established.

Acknowledgements This work was supported by the Swiss National Science Foundation through the National Center of Competence in Research Bio-Inspired Materials (WKF through the Research Program for Women in Science). The authors acknowledge financial support of the Swiss National Science Foundation (ML through grant number PP00P2_159258, BRR through grant number 310030_159847/1), the Adolphe Merkle Foundation, and the University of Fribourg. LRL acknowledges financial support from the Marie Curie COFUND Action (600375. NanoTRAINforGrowth).

References

1. Kim, B.Y.S., Rutka, J.T., Chan, W.C.W.: Nanomedicine. New Engl. J. Med. **363**(25), 2434–2443 (2010)
2. Bobo, D., Robinson, K.J., Islam, J., Thurecht, K.J., Corrie, S.R.: Nanoparticle-based medicines: a review of FDA-approved materials and clinical trials to date. Pharm. Res. **33**(10), 2373–2387 (2016)
3. Moore, T.L., Rodriguez-Lorenzo, L., Hirsch, V., Balog, S., Urban, D., Jud, C., Rothen-Rutishauser, B., Lattuada, M., Petri-Fink, A.: Nanoparticle colloidal stability in cell culture media and impact on cellular interactions. Chem. Soc. Rev. **44**(17), 6287–6305 (2015)
4. Guyton, A.C., Hall, J.E.: Textbook of Medical Physiology, 11th ed, p XXXV, 1116 p. Elsevier/Saunders, Philadelphia [etc.] (2006)
5. Yao, T., Asayama, Y.: Animal-cell culture media: history, characteristics, and current issues. Reprod. Med. Biol. **16**(2), 99–117 (2017)
6. Carrel, A.: On the permanent life of tissues outside of the organism. J. Exp. Med. **15**(5), 516–528 (1912)
7. Ebeling, A.H.: A ten year old strain of fibroblasts. J. Exp. Med. **35**(6), 755–759 (1922)
8. Fischer, A., Astrup, T., Ehrensvard, G., Oehlenschlager, V.: Growth of animal tissue cells in artificial media. Exp. Biol. Med. **67**(1), 40–46 (1948)

9. Zheng, X., Baker, H., Hancock, W.S., Fawaz, F., McCaman, M., Pungor, E.: Proteomic analysis for the assessment of different lots of fetal bovine serum as a raw material for cell culture. Part IV. Application of proteomics to the manufacture of biological drugs. Biotechnol. Progr. **22**(5), 1294–1300 (2006)
10. Eagle, H., Buffer combinations for mammalian cell culture. **174**, 500–503 (1971)
11. Stopford, W., Turner, J., Cappellini, D., Brock, T.: Bioaccessibility testing of cobalt compounds. J. Environ. Monit. **5**(4), 675–680 (2003)
12. Pagana, K.D., Pagana, T.J.: Mosby's Manual of Diagnostic and Laboratory Tests, 5th ed, pp. 1180. Elsevier Mosby, St. Louis, Missouri (2014)
13. Anderson, N.L., Anderson, N.G.: The human plasma proteome: history, character, and diagnostic prospects. Mol. Cell. Proteomics **1**(11), 845–867 (2002)
14. Hellstrand, E., Lynch, I., Andersson, A., Drakenberg, T., Dahlbäck, B., Dawson, K.A., Linse, S., Cedervall, T.: Complete high-density lipoproteins in nanoparticle corona. FEBS J. **276**(12), 3372–3381 (2009)
15. Kellum, J.A.: Determinants of blood pH in health and disease. Crit. Care **4**(1), 6 (2000)
16. Caracciolo, G., Farokhzad, O.C., Mahmoudi, M.: Biological identity of nanoparticles in vivo: clinical implications of the protein corona. Trends Biotechnol. **35**(3), 257–264
17. Choi, M.-R., Bardhan, R., Stanton-Maxey, K.J., Badve, S., Nakshatri, H., Stantz, K.M., Cao, N., Halas, N.J., Clare, S.E.: Delivery of nanoparticles to brain metastases of breast cancer using a cellular Trojan horse. Cancer Nanotechnol. **3**(1–6), 47–54 (2012)
18. Anselmo, A.C., Kumar, S., Gupta, V., Pearce, A.M., Ragusa, A., Muzykantov, V., Mitragotri, S.: Exploiting shape, cellular-hitchhiking and antibodies to target nanoparticles to lung endothelium: synergy between physical, chemical and biological approaches. Biomaterials **68**, 1–8 (2015)
19. Wick, P., Manser, P., Limbach, L.K., Dettlaff-Weglikowska, U., Krumeich, F., Roth, S., Stark, W.J., Bruinink, A.: The degree and kind of agglomeration affect carbon nanotube cytotoxicity. Toxicol. Lett. **168**(2), 121–131 (2007)
20. Teeguarden, J.G., Hinderliter, P.M., Orr, G., Thrall, B.D., Pounds, J.G.: Particokinetics in vitro: dosimetry considerations for in vitro nanoparticle toxicity assessments. Toxicol. Sci. **95**(2), 300–312 (2007)
21. Albanese, A., Chan, W.C.W.: Effect of gold nanoparticle aggregation on cell uptake and toxicity. ACS Nano **5**(7), 5478–5489 (2011)
22. Singh, A.K.: Physicochemical, electronic, and mechanical properties of nanoparticles. Engineered Nanoparticles, pp. 77–123. Academic Press, Boston (2016)
23. Zhang, Z., Wu, Y.: Investigation of the NaBH4-induced aggregation of Au nanoparticles. Langmuir **26**(12), 9214–9223 (2010)
24. Peretyazhko, T.S., Zhang, Q., Colvin, V.L.: Size-controlled dissolution of silver nanoparticles at neutral and acidic pH conditions: kinetics and size changes. Environ. Sci. Technol. **48**(20), 11954–11961 (2014)
25. Larson, T.A., Joshi, P.P., Sokolov, K.: Preventing protein adsorption and macrophage uptake of gold nanoparticles via a hydrophobic shield. ACS Nano **6**(10), 9182–9190 (2012)
26. Urban, D.A., Rodriguez-Lorenzo, L., Balog, S., Kinnear, C., Rothen-Rutishauser, B., Petri-Fink, A.: Plasmonic nanoparticles and their characterization in physiological fluids. Colloid Surf. B **137**, 39–49 (2016)
27. Kreyling, W.G., Abdelmonem, A.M., Ali, Z., Alves, F., Geiser, M., Haberl, N., Hartmann, R., Hirn, S., de Aberasturi, D.J., Kantner, K., Khadem-Saba, G., Montenegro, J.-M., Rejman, J., Rojo, T., de Larramendi, I.R., Ufartes, R., Wenk, A., Parak, W.J.: In vivo integrity of polymer-coated gold nanoparticles. Nat. Nanotechnol. **10**, 619 (2015)
28. Lynch, I., Langevin, D., Dawson, K.A.: Lessons for bionanointeractions from colloidal science. In: Starov, V.M. (ed.) Nanoscience: Colloidal and Interfacial Aspects, p. 369. Taylor & Francis, London (2010)
29. Cedervall, T., Lynch, I., Lindman, S., Berggård, T., Thulin, E., Nilsson, H., Dawson, K.A., Linse, S.: Understanding the nanoparticle–protein corona using methods to quantify exchange rates and affinities of proteins for nanoparticles. Proc. Natl. Acad. Sci. U. S. A. **104**(7), 2050 (2007)

30. Walkey, C.D., Olsen, J.B., Song, F., Liu, R., Guo, H., Olsen, D.W.H., Cohen, Y., Emili, A., Chan, W.C.W.: Protein corona fingerprinting predicts the cellular interaction of gold and silver nanoparticles. ACS Nano **8**(3), 2439–2455 (2014)
31. Liu, R., Jiang, W., Walkey, C.D., Chan, W.C.W., Cohen, Y.: Prediction of nanoparticles-cell association based on corona proteins and physicochemical properties. Nanoscale **7**(21), 9664–9675 (2015)
32. Ke, P.C., Lin, S., Parak, W.J., Davis, T.P., Caruso, F.: A decade of the protein corona. ACS Nano **11**(12), 11773–11776 (2017)
33. Treuel, L., Docter, D., Maskos, M., Stauber, R.H.: Protein corona—from molecular adsorption to physiological complexity. Beilstein J. Nanotech. **6**, 857–873 (2015)
34. Medintz, I.L., Konnert, J.H., Clapp, A.R., Stanish, I., Twigg, M.E., Mattoussi, H., Mauro, J.M., Deschamps, J.R.: A fluorescence resonance energy transfer-derived structure of a quantum dot-protein bioconjugate nanoassembly. Proc. Natl. Acad. Sci. U. S. A. **101**(26), 9612–9617 (2004)
35. Schein, C.H.: Solubility as a function of protein structure and solvent components. Bio/Technology **8**, 308 (1990)
36. Monopoli, M.P., Åberg, C., Salvati, A., Dawson, K.A.: Biomolecular coronas provide the biological identity of nanosized materials. Nat. Nanotechnol. **7**, 779 (2012)
37. Docter, D., Westmeier, D., Markiewicz, M., Stolte, S., Knauer, S.K., Stauber, R.H.: The nanoparticle biomolecule corona: lessons learned—challenge accepted? Chem. Soc. Rev. **44**(17), 6094–6121 (2015)
38. Monopoli, M.P., Wan, S., Bombelli, F.B., Mahon, E., Dawson, K.A.: Comparisons of nanoparticle protein corona complexes isolated with different methods. Nano Life **03**(04), 1343004 (2013)
39. Weber, C., Simon, J., Mailänder, V., Morsbach, S., Landfester, K.: Preservation of the soft protein corona in distinct flow allows identification of weakly bound proteins. Acta Biomater. **76**, 217–224 (2018)
40. Lück, M., Paulke, B.-R., Schröder, W., Blunk, T., Müller, R.H.: Analysis of plasma protein adsorption on polymeric nanoparticles with different surface characteristics. J. Biomed. Mater. Res. **39**(3), 478–485 (1998)
41. Gessner, A., Lieske, A., Paulke, B.-R., Müller, R.H.: Functional groups on polystyrene model nanoparticles: influence on protein adsorption. J. Biomed. Mater. Res. Part A **65A**(3), 319–326 (2003)
42. Tenzer, S., Docter, D., Kuharev, J., Musyanovych, A., Fetz, V., Hecht, R., Schlenk, F., Fischer, D., Kiouptsi, K., Reinhardt, C., Landfester, K., Schild, H., Maskos, M., Knauer, S.K., Stauber, R.H.: Rapid formation of plasma protein corona critically affects nanoparticle pathophysiology. Nat. Nanotechnol. **8**, 772 (2013)
43. Zhdanov, V.P., Cho, N.-J.: Kinetics of the formation of a protein corona around nanoparticles. Math. Biosci. **282**, 82–90 (2016)
44. Vroman, L., Adams, A.L.: Identification of rapid changes at plasma–solid interfaces. J. Biomed. Mater. Res. **3**(1), 43–67 (1969)
45. Ritz, S., Schöttler, S., Kotman, N., Baier, G., Musyanovych, A., Kuharev, J., Landfester, K., Schild, H., Jahn, O., Tenzer, S., Mailänder, V.: Protein corona of nanoparticles: distinct proteins regulate the cellular uptake. Biomacromolecules **16**(4), 1311–1321 (2015)
46. Owens, D.E., Peppas, N.A.: Opsonization, biodistribution, and pharmacokinetics of polymeric nanoparticles. Int. J. Pharmaceut. **307**(1), 93–102 (2006)
47. Schöttler, S., Becker, G., Winzen, S., Steinbach, T., Mohr, K., Landfester, K., Mailänder, V., Wurm, F.R.: Protein adsorption is required for stealth effect of poly(ethylene glycol)- and poly(phosphoester)-coated nanocarriers. Nat. Nanotechnol. **11**, 372 (2016)
48. Perry, J.L., Reuter, K.G., Kai, M.P., Herlihy, K.P., Jones, S.W., Luft, J.C., Napier, M., Bear, J.E., DeSimone, J.M.: PEGylated PRINT nanoparticles: the impact of PEG density on protein binding, macrophage association, biodistribution, and pharmacokinetics. Nano Lett. **12**(10), 5304–5310 (2012)

49. Sacchetti, C., Motamedchaboki, K., Magrini, A., Palmieri, G., Mattei, M., Bernardini, S., Rosato, N., Bottini, N., Bottini, M.: Surface polyethylene glycol conformation influences the protein corona of polyethylene glycol-modified single-walled carbon nanotubes: potential implications on biological performance. ACS Nano **7**(3), 1974–1989 (2013)
50. Gref, R., Lück, M., Quellec, P., Marchand, M., Dellacherie, E., Harnisch, S., Blunk, T., Müller, R.H.: 'Stealth' corona-core nanoparticles surface modified by polyethylene glycol (PEG): influences of the corona (PEG chain length and surface density) and of the core composition on phagocytic uptake and plasma protein adsorption. Colloids Surf. B Biointerfaces **18**(3–4), 301–313 (2000)
51. Müller, J., Simon, J., Rohne, P., Koch-Brandt, C., Mailänder, V., Morsbach, S., Landfester, K.: Denaturation via surfactants changes composition of protein corona. Biomacromolecules **19**(7), 2657–2664 (2018)
52. Müller, J., Bauer, K.N., Prozeller, D., Simon, J., Mailänder, V., Wurm, F.R., Winzen, S., Landfester, K.: Coating nanoparticles with tunable surfactants facilitates control over the protein corona. Biomaterials **115**, 1–8 (2017)
53. Schäffler, M., Semmler-Behnke, M., Sarioglu, H., Takenaka, S., Wenk, A., Schleh, C., Hauck, S.M., Johnston, B.D., Kreyling, W.G.: Serum protein identification and quantification of the corona of 5, 15 and 80 nm gold nanoparticles. Nanotechnology **24**(26), 265103 (2013)
54. Micläuş, T., Bochenkov, V.E., Ogaki, R., Howard, K.A., Sutherland, D.S.: Spatial mapping and quantification of soft and hard protein coronas at silver nanocubes. Nano Lett. **14**(4), 2086–2093 (2014)
55. Zhou, J.D., Gysell, M., Tara, S., Anthony, M., Darren, M., Rodney, F.M.: Differential plasma protein binding to metal oxide nanoparticles. Nanotechnology **20**(45), 455101 (2009)
56. Feiner-Gracia, N., Beck, M., Pujals, S., Tosi, S., Mandal, T., Buske, C., Linden, M., Albertazzi, L.: Super-resolution microscopy unveils dynamic heterogeneities in nanoparticle protein corona. Small 13(41), 1701631–n/a (2017)
57. Welsher, K., Liu, Z., Sherlock, S.P., Robinson, J.T., Chen, Z., Daranciang, D., Dai, H.: A route to brightly fluorescent carbon nanotubes for near-infrared imaging in mice. Nat. Nanotechnol. **4**, 773 (2009)
58. Wan, S., Kelly, P.M., Mahon, E., Stöckmann, H., Rudd, P.M., Caruso, F., Dawson, K.A., Yan, Y., Monopoli, M.P.: The "Sweet" side of the protein corona: effects of glycosylation on nanoparticle-cell interactions. ACS Nano **9**(2), 2157–2166 (2015)
59. Lynch, I., Dawson, K.A.: Protein-nanoparticle interactions. Nano Today **3**(1), 40–47 (2008)
60. Nguyen, V.H., Lee, B.-J.: Protein corona: a new approach for nanomedicine design. Int. J. Nanomed. **12**, 3137–3151 (2017)
61. Patel, H.M.: Serum opsonins and liposomes: their interaction and opsonophagocytosis. Crit. Rev. Ther. Drug Carrier Syst. **9**(1), 39–90 (1992)
62. Chonn, A., Semple, S.C., Cullis, P.R.: Association of blood proteins with large unilamellar liposomes in vivo. Relation to circulation lifetimes. J. Biol. Chem. 267(26), 18759–19765 (1992)
63. Tyrrell, D.A., Richardson, V.J., Ryman, B.E.: The effect of serum protein fractions on liposome-cell interactions in cultured cells and the perfused rat liver. Biochim. Biophys. Acta (BBA) Gen. Subj. 497(2), 469–480 (1977)
64. Göppert, T.M., Müller, R.H.: Polysorbate-stabilized solid lipid nanoparticles as colloidal carriers for intravenous targeting of drugs to the brain: comparison of plasma protein adsorption patterns. J. Drug Target. **13**(3), 179–187 (2005)
65. Mirshafiee, V., Kim, R., Park, S., Mahmoudi, M., Kraft, M.L.: Impact of protein pre-coating on the protein corona composition and nanoparticle cellular uptake. Biomaterials **75**, 295–304 (2016)
66. Moghimi, S.M., Hunter, A.C., Murray, J.C.: Long-circulating and target-specific nanoparticles: theory to practice. Pharmacol. Rev. **53**(2), 283–318 (2001)
67. Corbo, C., Molinaro, R., Parodi, A., Toledano Furman, N.E., Salvatore, F., Tasciotti, E.: The impact of nanoparticle protein corona on cytotoxicity, immunotoxicity and target drug delivery. Nanomedicine **11**(1), 81–100 (2016)

68. Salvati, A., Pitek, A.S., Monopoli, M.P., Prapainop, K., Bombelli, F.B., Hristov, D.R., Kelly, P.M., Åberg, C., Mahon, E., Dawson, K.A.: Transferrin-functionalized nanoparticles lose their targeting capabilities when a biomolecule corona adsorbs on the surface. Nat. Nanotechnol. **8**, 137 (2013)
69. Landgraf, L., Christner, C., Storck, W., Schick, I., Krumbein, I., Dähring, H., Haedicke, K., Heinz-Herrmann, K., Teichgräber, U., Reichenbach, J.R., Tremel, W., Tenzer, S., Hilger, I.: A plasma protein corona enhances the biocompatibility of Au@Fe3O4 Janus particles. Biomaterials **68**, 77–88 (2015)
70. Ge, C., Du, J., Zhao, L., Wang, L., Liu, Y., Li, D., Yang, Y., Zhou, R., Zhao, Y., Chai, Z., Chen, C.: Binding of blood proteins to carbon nanotubes reduces cytotoxicity. Proc. Natl. Acad. Sci. U. S. A. **108**(41), 16968–16973 (2011)
71. Wang, F., Yu, L., Monopoli, M.P., Sandin, P., Mahon, E., Salvati, A., Dawson, K.A.: The biomolecular corona is retained during nanoparticle uptake and protects the cells from the damage induced by cationic nanoparticles until degraded in the lysosomes. Nanomedicine Nanotechnol. Biol. Med. 9(8), 1159–1168 (2013)
72. Lee, I.S., Lee, N., Park, J., Kim, B.H., Yi, Y.-W., Kim, T., Kim, T.K., Lee, I.H., Paik, S.R., Hyeon, T.: Ni/NiO core/shell nanoparticles for selective binding and magnetic separation of histidine-tagged proteins. JACS **128**(33), 10658–10659 (2006)
73. Capriotti, A.L., Caracciolo, G., Cavaliere, C., Colapicchioni, V., Piovesana, S., Pozzi, D., Laganà, A.: Analytical methods for characterizing the nanoparticle-protein corona. Chromatographia **77**(11), 755–769 (2014)
74. Li, L., Mu, Q., Zhang, B., Yan, B.: Analytical strategies for detecting nanoparticle-protein interactions. The Analyst **135**(7), 1519–1530 (2010)
75. Mahmoudi, M., Lynch, I., Ejtehadi, M.R., Monopoli, M.P., Bombelli, F.B., Laurent, S.: Protein–nanoparticle interactions: opportunities and challenges. Chem. Rev. **111**(9), 5610–5637 (2011)
76. Aggarwal, P., Hall, J.B., McLeland, C.B., Dobrovolskaia, M.A., McNeil, S.E.: Nanoparticle interaction with plasma proteins as it relates to particle biodistribution, biocompatibility and therapeutic efficacy. Adv. Drug Deliv. Rev. **61**(6), 428–437 (2009)
77. Levy, R., Thanh, N.T.K., Doty, R.C., Hussain, I., Nichols, R.J., Schiffrin, D.J., Brust, M., Fernig, D.G.: Rational and combinatorial design of peptide capping Ligands for gold nanoparticles. JACS **126**(32), 10076–10084 (2004)
78. Aubin-Tam, M.-E., Hamad-Schifferli, K.: Gold nanoparticle–cytochrome c complexes: the effect of nanoparticle ligand charge on protein structure. Langmuir **21**(26), 12080–12084 (2005)
79. Ashby, J., Schachermeyer, S., Pan, S., Zhong, W.: Dissociation-based screening of nanoparticle-protein interaction via flow field-flow fractionation. Anal. Chem. **85**(15), 7494–7501 (2013)
80. Aleksenko, S.S., Shmykov, A.Y., Oszwaldowski, S., Timerbaev, A.R.: Interactions of tumour-targeting nanoparticles with proteins: potential of using capillary electrophoresis as a direct probe. Metallomics **4**(11), 1141–1148 (2012)
81. Kim, H.R., Andrieux, K., Delomenie, C., Chacun, H., Appel, M., Desmaele, D., Taran, F., Georgin, D., Couvreur, P., Taverna, M.: Analysis of plasma protein adsorption onto PEGylated nanoparticles by complementary methods: 2-DE, CE and protein Lab-on-chip((R)) system. Electrophoresis **28**(13), 2252–2261 (2007)
82. Brambilla, D., Verpillot, R., Taverna, M., De Kimpe, L., Le Droumaguet, B., Nicolas, J., Canovi, M., Gobbi, M., Mantegazza, F., Salmona, M., Nicolas, V., Scheper, W., Couvreur, P., Andrieux, K.: New method based on capillary electrophoresis with laser-induced fluorescence detection (CE-LIF) to monitor interaction between nanoparticles and the amyloid-beta peptide. Anal. Chem. **82**(24), 10083–10089 (2010)
83. Brambilla, D., Verpillot, R., Le Droumaguet, B., Nicolas, J., Taverna, M., Kona, J., Lettiero, B., Hashemi, S.H., De Kimpe, L., Canovi, M., Gobbi, M., Nicolas, V., Scheper, W., Moghimi, S.M., Tvaroska, I., Couvreur, P., Andrieux, K.: PEGylated nanoparticles bind to and alter amyloid-beta peptide conformation: toward engineering of functional nanomedicines for Alzheimer's disease. ACS Nano **6**(7), 5897–5908 (2012)

84. Chang, C.W., Tseng, W.L.: Gold nanoparticle extraction followed by capillary electrophoresis to determine the total, free, and protein-bound aminothiols in plasma. Anal. Chem. **82**(7), 2696–2702 (2010)
85. Chen, F., Wang, G., Griffin, J.I., Brenneman, B., Banda, N.K., Holers, V.M., Backos, D.S., Wu, L., Moghimi, S.M., Simberg, D.: Complement proteins bind to nanoparticle protein corona and undergo dynamic exchange in vivo. Nat. Nanotechnol. **12**, 387 (2016)
86. García-Álvarez, R., Hadjidemetriou, M., Sánchez-Iglesias, A., Liz-Marzán, L.M., Kostarelos, K.: In vivo formation of protein corona on gold nanoparticles. The effect of their size and shape. Nanoscale 10(3), 1256–1264 (2018)
87. Caracciolo, G., Pozzi, D., De Sanctis, S.C., Capriotti, A.L., Caruso, G., Samperi, R., Lagana, A.: Effect of membrane charge density on the protein corona of cationic liposomes: interplay between cationic charge and surface area. Appl. Phys. Lett. 99(3) (2011)
88. Dutta, D., Sundaram, S.K., Teeguarden, J.G., Riley, B.J., Fifield, L.S., Jacobs, J.M., Addleman, S.R., Kaysen, G.A., Moudgil, B.M., Weber, T.J.: Adsorbed proteins influence the biological activity and molecular targeting of nanomaterials. Toxicol. Sci. **100**(1), 303–315 (2007)
89. Salvador-Morales, C., Flahaut, E., Sim, E., Sloan, J., Green, M.L., Sim, R.B.: Complement activation and protein adsorption by carbon nanotubes. Mol. Immunol. **43**(3), 193–201 (2006)
90. Lundqvist, M., Stigler, J., Elia, G., Lynch, I., Cedervall, T., Dawson, K.A.: Nanoparticle size and surface properties determine the protein corona with possible implications for biological impacts. Proc. Natl. Acad. Sci. U. S. A. **105**(38), 14265–14270 (2008)
91. Stolnik, S., Daudali, B., Arien, A., Whetstone, J., Heald, C.R., Garnett, M.C., Davis, S.S., Illum, L.: The effect of surface coverage and conformation of poly(ethylene oxide) (PEO) chains of poloxamer 407 on the biological fate of model colloidal drug carriers. Biochim. Biophys. Acta (BBA) Biomembr. 1514(2), 261–279 (2001)
92. Arora, P.S., Yamagiwa, H., Srivastava, A., Bolander, M.E., Sarkar, G.: Comparative evaluation of two two-dimensional gel electrophoresis image analysis software applications using synovial fluids from patients with joint disease. J. Orthop. Sci. **10**(2), 160–166 (2005)
93. Lai, Z.W., Yan, Y., Caruso, F., Nice, E.C.: Emerging techniques in proteomics for probing nano-bio interactions. ACS Nano **6**(12), 10438–10448 (2012)
94. Kim, H.R., Andrieux, K., Gil, S., Taverna, M., Chacun, H., Desmaële, D., Taran, F., Georgin, D., Couvreur, P.: Translocation of poly(ethylene glycol-co-hexadecyl)cyanoacrylate nanoparticles into rat brain endothelial cells: role of apolipoproteins in receptor-mediated endocytosis. Biomacromolecules **8**(3), 793–799 (2007)
95. Chang, S.Y., Zheng, N.-Y., Chen, C.-S., Chen, C.-D., Chen, Y.-Y., Wang, C.R.C.: Analysis of peptides and proteins affinity-bound to iron oxide nanoparticles by MALDI MS. J. Am. Soc. Mass Spectrom. **18**(5), 910–918 (2007)
96. Chittur, K.K.: FTIR/ATR for protein adsorption to biomaterial surfaces. Biomaterials **19**(4), 357–369 (1998)
97. Goormaghtigh, E., Gasper, R., Bénard, A., Goldsztein, A., Raussens, V.: Protein secondary structure content in solution, films and tissues: redundancy and complementarity of the information content in circular dichroism, transmission and ATR FTIR spectra. Biochim. Biophys. Acta (BBA) Proteins Proteomics 1794(9), 1332–1343 (2009)
98. Shao, M., Lu, L., Wang, H., Luo, S., Ma, D.D.D.: Microfabrication of a new sensor based on silver and silicon nanomaterials, and its application to the enrichment and detection of bovine serum albumin via surface-enhanced Raman scattering. Microchim. Acta **164**(1), 157–160 (2009)
99. Royer, C.A.: Probing protein folding and conformational transitions with fluorescence. Chem. Rev. **106**(5), 1769–1784 (2006)
100. Mátyus, L., Szöllősi, J., Jenei, A.: Steady-state fluorescence quenching applications for studying protein structure and dynamics. J. Photochem. Photobiol. B **83**(3), 223–236 (2006)
101. Vilanova, O., Mittag, J.J., Kelly, P.M., Milani, S., Dawson, K.A., Rädler, J.O., Franzese, G.: Understanding the kinetics of protein-nanoparticle corona formation. ACS Nano **10**(12), 10842–10850 (2016)

102. Kelly, S.M., Jess, T.J., Price, N.C.: How to study proteins by circular dichroism. Biochim. Biophys. Acta (BBA) Proteins Proteomics 1751(2), 119–139 (2005)
103. Shang, L., Wang, Y., Jiang, J., Dong, S.: pH-dependent protein conformational changes in albumin: gold nanoparticle bioconjugates: a spectroscopic study. Langmuir **23**(5), 2714–2721 (2007)
104. Deng, Z.J., Liang, M., Monteiro, M., Toth, I., Minchin, R.F.: Nanoparticle-induced unfolding of fibrinogen promotes Mac-1 receptor activation and inflammation. Nat. Nanotechnol. **6**, 39 (2010)
105. Ceccon, A., Lelli, M., D'Onofrio, M., Molinari, H., Assfalg, M.: Dynamics of a globular protein adsorbed to liposomal nanoparticles. JACS **136**(38), 13158–13161 (2014)
106. Stayton, P.S., Drobny, G.P., Shaw, W.J., Long, J.R., Gilbert, M.: Molecular recognition at the protein-hydroxyapatite interface. Crit. Rev. Oral Biol. Med. **14**(5), 370–376 (2003)
107. Carril, M., Padro, D., del Pino, P., Carrillo-Carrion, C., Gallego, M., Parak, W.J.: In situ detection of the protein corona in complex environments. Nat. Commun. **8**(1), 1542 (2017)
108. Baier, G., Costa, C., Zeller, A., Baumann, D., Sayer, C., Araujo, P.H.H., Mailänder, V., Musyanovych, A., Landfester, K.: BSA adsorption on differently charged polystyrene nanoparticles using isothermal titration calorimetry and the influence on cellular uptake. Macromol. Biosci. **11**(5), 628–638 (2011)
109. Lindman, S., Lynch, I., Thulin, E., Nilsson, H., Dawson, K.A., Linse, S.: Systematic investigation of the thermodynamics of HSA adsorption to N-iso-Propylacrylamide/N-tert-Butylacrylamide copolymer nanoparticles. Effects of particle size and hydrophobicity. Nano Lett. 7(4), 914–920 (2007)
110. Laera, S., Ceccone, G., Rossi, F., Gilliland, D., Hussain, R., Siligardi, G., Calzolai, L.: Measuring protein structure and stability of protein-nanoparticle systems with synchrotron radiation circular dichroism. Nano Lett. **11**(10), 4480–4484 (2011)
111. Bhogale, A., Patel, N., Mariam, J., Dongre, P.M., Miotello, A., Kothari, D.C.: Comprehensive studies on the interaction of copper nanoparticles with bovine serum albumin using various spectroscopies. Colloids Surf. B **113**, 276–284 (2014)
112. Astegno, A., Maresi, E., Marino, V., Dominici, P., Pedroni, M., Piccinelli, F., Dell'Orco, D.: Structural plasticity of calmodulin on the surface of CaF2 nanoparticles preserves its biological function. Nanoscale **6**(24), 15037–15047 (2014)
113. Huang, R., Carney, R.P., Ikuma, K., Stellacci, F., Lau, B.L.T.: Effects of surface compositional and structural heterogeneity on nanoparticle-protein interactions: different protein configurations. ACS Nano **8**(6), 5402–5412 (2014)
114. Michen, B., Geers, C., Vanhecke, D., Endes, C., Rothen-Rutishauser, B., Balog, S., Petri-Fink, A.: Avoiding drying-artifacts in transmission electron microscopy: characterizing the size and colloidal state of nanoparticles. Sci. Rep. **5**, 9793 (2015)
115. Balog, S., Rodriguez-Lorenzo, L., Monnier, C.A., Obiols-Rabasa, M., Rothen-Rutishauser, B., Schurtenberger, P., Petri-Fink, A.: Characterizing nanoparticles in complex biological media and physiological fluids with depolarized dynamic light scattering. Nanoscale **7**(14), 5991–5997 (2015)
116. Sharifi, S., Behzadi, S., Laurent, S., Laird Forrest, M., Stroeve, P., Mahmoudi, M.: Toxicity of nanomaterials. Chem. Soc. Rev. **41**(6), 2323–2343 (2012)
117. Lin, P.-C., Lin, S., Wang, P.C., Sridhar, R.: Techniques for physicochemical characterization of nanomaterials. Biotechnol. Adv. **32**(4), 711–726 (2014)
118. Treuel, L., Eslahian, K.A., Docter, D., Lang, T., Zellner, R., Nienhaus, K., Nienhaus, G.U., Stauber, R.H., Maskos, M.: Physicochemical characterization of nanoparticles and their behavior in the biological environment. Phys. Chem. Chem. Phys. **16**(29), 15053–15067 (2014)
119. Cho, E.C., Liu, Y., Xia, Y.: A simple spectroscopic method for differentiating cellular uptakes of gold nanospheres and nanorods from their mixtures. Angew. Chem. Int. Ed. **49**(11), 1976–1980 (2010)
120. Rischitor, G., Parracino, M., La Spina, R., Urbán, P., Ojea-Jiménez, I., Bellido, E., Valsesia, A., Gioria, S., Capomaccio, R., Kinsner-Ovaskainen, A., Gilliland, D., Rossi, F., Colpo, P.:

Quantification of the cellular dose and characterization of nanoparticle transport during in vitro testing. Part. Fibre Toxicol. **13**(1), 47 (2016)
121. Cho, E.C., Zhang, Q., Xia, Y.: The effect of sedimentation and diffusion on cellular uptake of gold nanoparticles. Nat. Nanotechnol. **6**, 385 (2011)
122. Mukherjee, D., Leo, B.F., Royce, S.G., Porter, A.E., Ryan, M.P., Schwander, S., Chung, K.F., Tetley, T.D., Zhang, J., Georgopoulos, P.G.: Modeling physicochemical interactions affecting in vitro cellular dosimetry of engineered nanomaterials: application to nanosilver. J. Nanopart. Res. **16**(10), 2616 (2014)
123. Hinderliter, P.M., Minard, K.R., Orr, G., Chrisler, W.B., Thrall, B.D., Pounds, J.G., Teeguarden, J.G.: ISDD: a computational model of particle sedimentation, diffusion and target cell dosimetry for in vitro toxicity studies. Part. Fibre Toxicol. **7**(1), 36 (2010)
124. DeLoid, G., Cohen, J.M., Darrah, T., Derk, R., Rojanasakul, L., Pyrgiotakis, G., Wohlleben, W., Demokritou, P.: Estimating the effective density of engineered nanomaterials for in vitro dosimetry. Nat. Commun. **5**, 3514 (2014)
125. DeLoid, G.M., Cohen, J.M., Pyrgiotakis, G., Pirela, S.V., Pal, A., Liu, J., Srebric, J., Demokritou, P.: Advanced computational modeling for in vitro nanomaterial dosimetry. Part. Fibre Toxicol. **12**, 32 (2015)
126. Rodriguez-Lorenzo, L., Rothen-Rutishauser, B., Petri-Fink, A., Balog, S.: Nanoparticle polydispersity can strongly affect in vitro dose. Part. Part. Syst. Charact. **32**(3), 321–333 (2015)
127. Thomas, D.G., Smith, J.N., Thrall, B.D., Baer, D.R., Jolley, H., Munusamy, P., Kodali, V., Demokritou, P., Cohen, J., Teeguarden, J.G.: ISD3: a particokinetic model for predicting the combined effects of particle sedimentation, diffusion and dissolution on cellular dosimetry for in vitro systems. Part. Fibre Toxicol. **15**(1), 6 (2018)
128. Zhang, S., Li, J., Lykotrafitis, G., Bao, G., Suresh, S.: Size-dependent endocytosis of nanoparticles. Adv. Mater. **21**(4), 419–424 (2009)
129. Abhishek, C., Giuseppe, B., Ramin, G.: The effect of interactions on the cellular uptake of nanoparticles. Phys. Biol. **8**(4), 046002 (2011)
130. Kinnear, C., Moore, T.L., Rodriguez-Lorenzo, L., Rothen-Rutishauser, B., Petri-Fink, A.: Form follows function: nanoparticle shape and its implications for nanomedicine. Chem. Rev. **117**(17), 11476–11521 (2017)
131. Sadik, O.A.: Anthropogenic nanoparticles in the environment. Environ. Sci. Process. Impacts **15**(1), 19–20 (2013)
132. Buzea, C., Pacheco, I.I., Robbie, K.: Nanomaterials and nanoparticles: sources and toxicity. Biointerphases 2(4), Mr17–Mr71 (2007)
133. Kuhlbusch, T., Asbach, C., Fissan, H., Gohler, D., Stintz, M.: Nanoparticle exposure at nanotechnology workplaces: a review. Part. Fibre Toxicol. **8**(1), 22 (2011)
134. Drasler, B., Sayre, P., Steinhauser, K.G., Petri-Fink, A., Rothen-Rutishauser, B.: In vitro approaches to assess the hazard of nanomaterials. Nanoimpact **8**, 99–116 (2017)
135. Mühlfeld, C., Rothen-Rutishauser, B., Blank, F., Vanhecke, D., Ochs, M., Gehr, P.: Interactions of nanoparticles with pulmonary structures and cellular responses. AJP-Lung **294**(5), L817–L829 (2008)
136. Conner, S.D., Schmid, S.L.: Regulated portals of entry into the cell. Nature **422**, 37 (2003)
137. Aderem, A., Underhill, D.M.: Mechanisms of phagocytosis in macrophages. Annu. Rev. Immunol. **17**(1), 593–623 (1999)
138. Spector, A.A., Yorek, M.A.: Membrane lipid composition and cellular function. J. Lipid Res. **26**(9), 1015–1035 (1985)
139. Kuhn, D.A., Vanhecke, D., Michen, B., Blank, F., Gehr, P., Petri-Fink, A., Rothen-Rutishauser, B.: Different endocytotic uptake mechanisms for nanoparticles in epithelial cells and macrophages. Beilstein J. Nanotech. **5**, 1625–1636 (2014)
140. Mahmoudi, M., Saeedi-Eslami, S.N., Shokrgozar, M.A., Azadmanesh, K., Hassanlou, M., Kalhor, H.R., Burtea, C., Rothen-Rutishauser, B., Laurent, S., Sheibani, S., Vali, H.: Cell "vision": complementary factor of protein corona in nanotoxicology. Nanoscale **4**(17), 5461–5468 (2012)

141. Feliu, N., Hühn, J., Zyuzin, M.V., Ashraf, S., Valdeperez, D., Masood, A., Said, A.H., Escudero, A., Pelaz, B., Gonzalez, E., Duarte, M.A.C., Roy, S., Chakraborty, I., Lim, M.L., Sjöqvist, S., Jungebluth, P., Parak, W.J.: Quantitative uptake of colloidal particles by cell cultures. Sci. Total Environ. **568**, 819–828 (2016)
142. Donaldson, K., Stone, V., Borm, P.J.A., Jimenez, L.A., Gilmour, P.S., Schins, R.P.F., Knaapen, A.M., Rahman, I., Faux, S.P., Brown, D.M., MacNee, W.: Oxidative stress and calcium signaling in the adverse effects of environmental particles (PM10). Free Radic. Biol. Med. **34**(11), 1369–1382 (2003)
143. Poland, C.A., Duffin, R., Kinloch, I., Maynard, A., Wallace, W.A.H., Seaton, A., Stone, V., Brown, S., MacNee, W., Donaldson, K.: Carbon nanotubes introduced into the abdominal cavity of mice show asbestos-like pathogenicity in a pilot study. Nat. Nanotechnol. **3**, 423 (2008)
144. Schins, R.P.F., Knaapen, A.M.: Genotoxicity of poorly soluble particles. Inhal. Toxicol. **19**(sup1), 189–198 (2007)
145. Krug, H.F., Wick, P.: Nanotoxicology: an interdisciplinary challenge. Angew. Chem. Int. Ed. **50**(6), 1260–1278 (2011)
146. Paur, H.-R., Cassee, F.R., Teeguarden, J., Fissan, H., Diabate, S., Aufderheide, M., Kreyling, W.G., Hänninen, O., Kasper, G., Riediker, M., Rothen-Rutishauser, B., Schmid, O.: In-vitro cell exposure studies for the assessment of nanoparticle toxicity in the lung—a dialog between aerosol science and biology. J. Aerosol Sci. **42**(10), 668–692 (2011)
147. Bourquin, J., Milosevic, A., Hauser, D., Lehner, R., Blank, F., Petri-Fink, A., Rothen-Rutishauser, B.: Biodistribution, clearance, and long-term fate of clinically relevant nanomaterials. Adv. Mater., 1704307 (2018)
148. Geers, C., Rodriguez-Lorenzo, L., Andreas Urban, D., Kinnear, C., Petri-Fink, A., Balog, S.: A new angle on dynamic depolarized light scattering: number-averaged size distribution of nanoparticles in focus. Nanoscale **8**(34), 15813–15821 (2016)
149. Mehan, S., Chinchalikar, A.J., Kumar, S., Aswal, V.K., Schweins, R.: Small-angle neutron scattering study of structure and interaction of nanoparticle, protein, and surfactant complexes. Langmuir **29**(36), 11290–11299 (2013)
150. Spinozzi, F., Ceccone, G., Moretti, P., Campanella, G., Ferrero, C., Combet, S., Ojea-Jimenez, I., Ghigna, P.: Structural and thermodynamic properties of nanoparticle-protein complexes: a combined SAXS and SANS study. Langmuir **33**(9), 2248–2256 (2017)
151. Diroll, B.T., Weigandt, K.M., Jishkariani, D., Cargnello, M., Murphy, R.J., Hough, L.A., Murray, C.B., Donnio, B.: Quantifying "Softness" of organic coatings on gold nanoparticles using correlated small-angle X-ray and neutron scattering. Nano Lett. **15**(12), 8008–8012 (2015)
152. Bhattacharjee, S.: DLS and zeta potential—what they are and what they are not? J. Contr. Release **235**, 337–351 (2016)
153. Huang, Y., Wang, X.B., Becker, F.F., Gascoyne, P.R.: Introducing dielectrophoresis as a new force field for field-flow fractionation. Biophys. J. **73**(2), 1118–1129 (1997)
154. Uma, B., Swaminathan, T.N., Radhakrishnan, R., Eckmann, D.M., Ayyaswamy, P.S.: Nanoparticle Brownian motion and hydrodynamic interactions in the presence of flow fields. Phys. Fluids **23**(7), 073602 (2011)
155. Das, S., Kundu, A., Hossain, S.M., Saha, H., Datta, S.K.: Effect of size on the scattering properties of silica nanoparticles. In: 2014 IEEE 2nd International Conference on Emerging Electronics (ICEE), 3–6 December 2014, pp. 1–4 (2014)
156. Horiba Instruments, I.: Zeta Potential of Bovine Serum Albumin (BSA) Protein. Irvine, CA, U.S.A (2009)
157. Vanhecke, D., Kuhn, D.A., Jimenez de Aberasturi, D., Balog, S., Milosevic, A., Urban, D., Peckys, D., de Jonge, N., Parak, W.J., Petri-Fink, A., Rothen-Rutishauser, B.: Involvement of two uptake mechanisms of gold and iron oxide nanoparticles in a co-exposure scenario using mouse macrophages. Beilstein J. Nanotechnol. 8, 2396–2409 (2017)
158. Nuhn, L., Gietzen, S., Mohr, K., Fischer, K., Toh, K., Miyata, K., Matsumoto, Y., Kataoka, K., Schmidt, M., Zentel, R.: Aggregation behavior of cationic nanohydrogel particles in human blood serum. Biomacromolecules **15**(4), 1526–1533 (2014)

159. Rausch, K., Reuter, A., Fischer, K., Schmidt, M.: Evaluation of nanoparticle aggregation in human blood serum. Biomacromolecules **11**(11), 2836–2839 (2010)
160. Hemmelmann, M., Mohr, K., Fischer, K., Zentel, R., Schmidt, M.: Interaction of pHPMA–pLMA copolymers with human blood serum and its components. Mol. Pharm. **10**(10), 3769–3775 (2013)
161. Barisik, M., Atalay, S., Beskok, A., Qian, S.: Size dependent surface charge properties of silica nanoparticles. J. Phys. Chem. C **118**(4), 1836–1842 (2014)
162. Durantie, E., Vanhecke, D., Rodriguez-Lorenzo, L., Delhaes, F., Balog, S., Septiadi, D., Bourquin, J., Petri-Fink, A., Rothen-Rutishauser, B.: Biodistribution of single and aggregated gold nanoparticles exposed to the human lung epithelial tissue barrier at the air-liquid interface. Part. Fibre Toxicol. **14**(1), 49 (2017)
163. Balog, S., Rodriguez-Lorenzo, L., Monnier, C.A., Michen, B., Obiols-Rabasa, M., Casal-Dujat, L., Rothen-Rutishauser, B., Petri-Fink, A., Schurtenberger, P.: Dynamic depolarized light scattering of small round plasmonic nanoparticles: when imperfection is only perfect. J. Phys. Chem. C **118**(31), 17968–17974 (2014)
164. Hirsch, V., Kinnear, C., Rodriguez-Lorenzo, L., Monnier, C.A., Rothen-Rutishauser, B., Balog, S., Petri-Fink, A.: In vitro dosimetry of agglomerates. Nanoscale **6**(13), 7325–7331 (2014)
165. Pal, N., Verma, S.D., Singh, M.K., Sen, S.: Fluorescence correlation spectroscopy: an efficient tool for measuring size, size-distribution and polydispersity of microemulsion droplets in solution. Anal. Chem. **83**(20), 7736–7744 (2011)
166. Shang, L., Nienhaus, G.U.: In situ characterization of protein adsorption onto nanoparticles by fluorescence correlation spectroscopy. Acc. Chem. Res. **50**(2), 387–395 (2017)
167. Milosevic, A.M., Rodriguez-Lorenzo, L., Balog, S., Monnier, C.A., Petri-Fink, A., Rothen-Rutishauser, B.: Assessing the stability of fluorescently encoded nanoparticles in lysosomes by using complementary methods. Angew. Chem. Int. Ed. Engl. **56**(43), 13382–13386 (2017)
168. Silvestri, A., Di Silvio, D., Llarena, I., Murray, R.A., Marelli, M., Lay, L., Polito, L., Moya, S.E.: Influence of surface coating on the intracellular behaviour of gold nanoparticles: a fluorescence correlation spectroscopy study. Nanoscale **9**(38), 14730–14739 (2017)
169. Yang, W., Lu, J., Gilbert, E.P., Knott, R., He, L., Cheng, W.: Probing soft corona structures of DNA-capped nanoparticles by small angle neutron scattering. J. Phys. Chem. C **119**(32), 18773–18778 (2015)
170. Camarero-Espinosa, S., Endes, C., Mueller, S., Petri-Fink, A., Rothen-Rutishauser, B., Weder, C., Clift, M.J.D., Foster, E.J.: Elucidating the potential biological impact of cellulose nanocrystals. Fibers 4(3) (2016)
171. Kinnear, C., Balog, S., Rothen-Rutishauser, B., Petri-Fink, A.: Thermally reversible self-assembly of nanoparticles via polymer crystallization. Macromol. Rapid Commun. **35**(23), 2012–2017 (2014)
172. Dorofeev, G.A., Streletskii, A.N., Povstugar, I.V., Protasov, A.V., Elsukov, E.P.: Determination of nanoparticle sizes by X-ray diffraction. Colloid J. **74**(6), 675–685 (2012)
173. Urban, D.A., Milosevic, A.M., Bossert, D., Crippa, F., Moore, T.L., Geers, C., Balog, S., Rothen-Rutishauser, B., Petri-Fink, A.: Taylor dispersion of inorganic nanoparticles and comparison to dynamic light scattering and transmission electron microscopy. Colloid Interface Sci. Commun. **22**, 29–33 (2018)
174. Balog, S., Urban, D.A., Milosevic, A.M., Crippa, F., Rothen-Rutishauser, B., Petri-Fink, A.: Taylor dispersion of nanoparticles. J. Nanopart. Res. 19(8) (2017)
175. Zhang, D., Neumann, O., Wang, H., Yuwono, V.M., Barhoumi, A., Perham, M., Hartgerink, J.D., Wittung-Stafshede, P., Halas, N.J.: Gold nanoparticles can induce the formation of protein-based aggregates at physiological pH. Nano Lett. **9**(2), 666–671 (2009)
176. Bekdemir, A., Stellacci, F.: A centrifugation-based physicochemical characterization method for the interaction between proteins and nanoparticles. Nat. Commun. **7**, 13121 (2016)
177. Walter, J., Löhr, K., Karabudak, E., Reis, W., Mikhael, J., Peukert, W., Wohlleben, W., Cölfen, H.: Multidimensional analysis of nanoparticles with highly disperse properties using multi-wavelength analytical ultracentrifugation. ACS Nano **8**(9), 8871–8886 (2014)

178. Ashby, J., Pan, S., Zhong, W.: Size and surface functionalisation of iron oxide nanoparticles influence the composition and dynamic nature of their protein corona. ACS Appl. Mater. Interfaces **6**(17), 15412–15419 (2014)
179. Zook, J.M., Rastogi, V., MacCuspie, R.I., Keene, A.M., Fagan, J.: Measuring agglomerate size distribution and dependence of localized surface plasmon resonance absorbance on gold nanoparticle agglomerate size using analytical ultracentrifugation. ACS Nano **5**(10), 8070–8079 (2011)
180. Planken, K.L., Colfen, H.: Analytical ultracentrifugation of colloids. Nanoscale **2**(10), 1849–1869 (2010)
181. Gigault, J., Pettibone, J.M., Schmitt, C., Hackley, V.A.: Rational strategy for characterization of nanoscale particles by asymmetric-flow field flow fractionation: a tutorial. Anal. Chim. Acta **809**, 9–24 (2014)
182. Kozak, D., Anderson, W., Vogel, R., Trau, M.: Advances in resistive pulse sensors: devices bridging the void between molecular and microscopic detection. Nano Today **6**(5), 531–545 (2011)
183. Blundell, E.L.C.J., Healey, M.J., Holton, E., Sivakumaran, M., Manstana, S., Platt, M.: Characterisation of the protein corona using tunable resistive pulse sensing: determining the change and distribution of a particle's surface charge. Anal. Bioanal. Chem. **408**(21), 5757–5768 (2016)
184. Sikora, A., Shard, A.G., Minelli, C.: Size and ζ-potential measurement of silica nanoparticles in serum using tunable resistive pulse sensing. Langmuir **32**(9), 2216–2224 (2016)
185. Cipelletti, L., Biron, J.-P., Martin, M., Cottet, H.: Polydispersity analysis of taylor dispersion data: the cumulant method. Anal. Chem. **86**(13), 6471–6478 (2014)
186. Balog, S.: Taylor dispersion of polydisperse nanoclusters and nanoparticles: modeling, simulation, and analysis. Anal. Chem. (2018)
187. Dominguez, D., Alhusain, M., Alharbi, N., Bernussi, A., Grave de Peralta, L.: Fourier plane imaging microscopy for detection of plasmonic crystals with periods beyond the optical diffraction limit, vol. 10 (2015)
188. Gustafsson, M.G.L.: Surpassing the lateral resolution limit by a factor of two using structured illumination microscopy. J. Microsc. **198**(2), 82–87 (2000)
189. Chang, B.-J., Lin, S.H., Chou, L.-J., Chiang, S.-Y.: Subdiffraction scattered light imaging of gold nanoparticles using structured illumination. Opt. Lett. **36**(24), 4773–4775 (2011)
190. Vainrub, A., Pustovyy, O., Vodyanoy, V.: Resolution of 90 nm (λ/5) in an optical transmission microscope with an annular condenser. Opt. Lett. **31**(19), 2855–2857 (2006)
191. Guttenberg, M., Bezerra, L., Neu-Baker, N.M., del Pilar Sosa Peña, M., Elder, A., Oberdörster, G., Brenner, S.A.: Biodistribution of inhaled metal oxide nanoparticles mimicking occupational exposure: a preliminary investigation using enhanced darkfield microscopy. J. Biophotonics 9(10), 987–993 (2016)
192. Peña, M.D.P.S., Gottipati, A., Tahiliani, S., Neu-Baker, N.M., Frame, M.D., Friedman, A.J., Brenner, S.A.: Hyperspectral imaging of nanoparticles in biological samples: simultaneous visualization and elemental identification. Microsc. Res. Tech. **79**(5), 349–358 (2016)
193. Monnier, C.A., Lattuada, M., Burnand, D., Crippa, F., Martinez-Garcia, J.C., Hirt, A.M., Rothen-Rutishauser, B., Bonmarin, M., Petri-Fink, A.: A lock-in-based method to examine the thermal signatures of magnetic nanoparticles in the liquid, solid and aggregated states. Nanoscale **8**(27), 13321–13332 (2016)
194. Drasler, B., Vanhecke, D., Rodriguez-Lorenzo, L., Petri-Fink, A., Rothen-Rutishauser, B.: Quantifying nanoparticle cellular uptake: which method is best? Nanomedicine **12**(10), 1095–1099 (2017)
195. Vanhecke, D., Rodriguez-Lorenzo, L., Clift, M.J.D., Blank, F., Petri-Fink, A., Rothen-Rutishauser, B.: Quantification of nanoparticles at the single-cell level: an overview about state-of-the-art techniques and their limitations. Nanomedicine **9**(12), 1885–1900 (2014)
196. Thieme, J., McNult, I., Vogt, S., Paterson, D.: X-ray spectromicroscopy—a tool for environmental sciences. Environ. Sci. Technol. **41**(20), 6885–6889 (2007)

197. Lawrence, J., Dynes, J., Korber, D., Swerhone, G., Leppard, G., Hitchcock, A.P.: Monitoring the fate of copper nanoparticles in river biofilms using scanning transmission X-ray microscopy (STXM), vol. 329, pp. 18–25 (2011)
198. Takechi-Haraya, Y., Goda, Y., Sakai-Kato, K.: Imaging and size measurement of nanoparticles in aqueous medium by use of atomic force microscopy. Anal. Bioanal. Chem. **410**(5), 1525–1531 (2018)
199. Cazaux, J.: Material contrast in SEM: fermi energy and work function effects. Ultramicroscopy **110**(3), 242–253 (2010)
200. Kisielowski, C., Freitag, B., Bischoff, M., van Lin, H., Lazar, S., Knippels, G., Tiemeijer, P., van der Stam, M., von Harrach, S., Stekelenburg, M., Haider, M., Uhlemann, S., Müller, H., Hartel, P., Kabius, B., Miller, D., Petrov, I., Olson, E.A., Donchev, T., Kenik, E.A., Lupini, A.R., Bentley, J., Pennycook, S.J., Anderson, I.M., Minor, A.M., Schmid, A.K., Duden, T., Radmilovic, V., Ramasse, Q.M., Watanabe, M., Erni, R., Stach, E.A., Denes, P., Dahmen, U.: Detection of single atoms and buried defects in three dimensions by aberration-corrected electron microscope with 0.5-Å information limit. Microsc. Microanal. 14(5), 469–477 (2008)
201. Liu, J.: Scanning transmission electron microscopy and its application to the study of nanoparticles and nanoparticle systems. J. Electron. Microsc. **54**(3), 251–278 (2005)
202. Michen, B., Geers, C., Vanhecke, D., Endes, C., Rothen-Rutishauser, B., Balog, S., Petri-Fink, A.: Avoiding drying-artifacts in transmission electron microscopy: characterizing the size and colloidal state of nanoparticles. Sci. Rep. 5 (2015)
203. Ahmad, N., Wang, G., Nelayah, J., Ricolleau, C., Alloyeau, D.: Exploring the formation of symmetric gold nanostars by liquid-cell transmission electron microscopy. Nano Lett. **17**(7), 4194–4201 (2017)
204. Milosevic, A.M., Rodriguez-Lorenzo, L., Balog, S., Monnier, C.A., Petri-Fink, A., Rothen-Rutishauser, B.: Assessing the stability of fluorescently encoded nanoparticles in lysosomes by using complementary methods. Angew. Chem. Int. Ed. **56**(43), 13382–13386 (2017)
205. Dillon, J.C.K., Bezerra, L., del Pilar Sosa Peña, M., Neu-Baker, N.M., Brenner, S.A.: Hyperspectral data influenced by sample matrix: the importance of building relevant reference spectral libraries to map materials of interest. Microsc. Res. Tech. 80(5), 462–470 (2017)
206. Mühlfeld, C., Rothen-Rutishauser, B., Vanhecke, D., Blank, F., Gehr, P., Ochs, M.: Visualization and quantitative analysis of nanoparticles in the respiratory tract by transmission electron microscopy. Part. Fibre Toxicol. **4**(1), 11 (2007)
207. Gundersen, H.J.G., Jensen, E.B.: The efficiency of systematic sampling in stereology and its prediction. J. Microsc. **147**(3), 229–263 (1987)
208. Slack, S.M., Horbett, T.A.: The Vroman effect. In: Proteins at Interfaces II, American Chemical Society, vol. 602, pp. 112–128 (1995)
209. Casals, E., Pfaller, T., Duschl, A., Oostingh, G.J., Puntes, V.: Time evolution of the nanoparticle protein corona. ACS Nano **4**(7), 3623–3632 (2010)
210. Vroman, L.: Effect of adsorbed proteins on the wettability of hydrophilic and hydrophobic solids. Nature **196**, 476 (1962)
211. Li, T., Senesi, A.J., Lee, B.: Small angle X-ray scattering for nanoparticle research. Chem. Rev. **116**(18), 11128–11180 (2016)
212. Fong, W.K., Salentinig, S., Prestidge, C.A., Mezzenga, R., Hawley, A., Boyd, B.J.: Generation of geometrically ordered lipid-based liquid-crystalline nanoparticles using biologically relevant enzymatic processing. Langmuir **30**(19), 5373–5377 (2014)
213. Warren, D.B., Anby, M.U., Hawley, A., Boyd, B.J.: Real time evolution of liquid crystalline nanostructure during the digestion of formulation lipids using synchrotron small-angle X-ray scattering. Langmuir **27**(15), 9528–9534 (2011)
214. Hummer, A.A., Rompel, A.: The use of X-ray absorption and synchrotron based micro-X-ray fluorescence spectroscopy to investigate anti-cancer metal compounds in vivo and in vitro. Metallomics **5**(6), 597–614 (2013)
215. Wang, B., Feng, W., Chai, Z., Zhao, Y.: Probing the interaction at nano-bio interface using synchrotron radiation-based analytical techniques. Sci. China Chem. **58**(5), 768–779 (2015)

216. Ilinski, P., Lai, B., Cai, Z., Yun, W., Legnini, D., Talarico, T., Cholewa, M., Webster, L.K., Deacon, G.B., Rainone, S., Phillips, D.R., Stampfl, A.P.J.: The direct mapping of the uptake of platinum anticancer agents in individual human ovarian adenocarcinoma cells using a hard X-ray microprobe. Cancer Res. **63**(8), 1776–1779 (2003)
217. Wang, B., Yin, J.-J., Zhou, X., Kurash, I., Chai, Z., Zhao, Y., Feng, W.: Physicochemical origin for free radical generation of iron oxide nanoparticles in biomicroenvironment: catalytic activities mediated by surface chemical states. J. Phys. Chem. C **117**(1), 383–392 (2013)
218. Wang, L., Li, J., Pan, J., Jiang, X., Ji, Y., Li, Y., Qu, Y., Zhao, Y., Wu, X., Chen, C.: Revealing the binding structure of the protein corona on gold nanorods using synchrotron radiation-based techniques: understanding the reduced damage in cell membranes. JACS **135**(46), 17359–17368 (2013)
219. Zhong, J., Song, L., Meng, J., Gao, B., Chu, W., Xu, H., Luo, Y., Guo, J., Marcelli, A., Xie, S., Wu, Z.: Bio-nano interaction of proteins adsorbed on single-walled carbon nanotubes. Carbon **47**(4), 967–973 (2009)
220. Robinson, I.: Nanoparticle structure by coherent X-ray diffraction. J. Phys. Soc. Jpn. **82**(2), 021012 (2012)
221. Li, X., Chiu, C.-Y., Wang, H.-J., Kassemeyer, S., Botha, S., Shoeman, R.L., Lawrence, R.M., Kupitz, C., Kirian, R., James, D., Wang, D., Nelson, G., Messerschmidt, M., Boutet, S., Williams, G.J., Hartmann, E., Jafarpour, A., Foucar, L.M., Barty, A., Chapman, H., Liang, M., Menzel, A., Wang, F., Basu, S., Fromme, R., Doak, R.B., Fromme, P., Weierstall, U., Huang, M.H., Spence, J.C.H., Schlichting, I., Hogue, B.G., Liu, H.: Diffraction data of core-shell nanoparticles from an X-ray free electron laser. Sci. Data **4**, 170048 (2017)
222. Whitesides, G.M.: The origins and the future of microfluidics. Nature **442**, 368 (2006)
223. Song, Y., Hormes, J., Kumar, C.S.S.R.: Microfluidic synthesis of nanomaterials. Small **4**(6), 698–711 (2008)
224. Salafi, T., Zeming, K.K., Zhang, Y.: Advancements in microfluidics for nanoparticle separation. Lab Chip **17**(1), 11–33 (2017)
225. Valencia, P.M., Farokhzad, O.C., Karnik, R., Langer, R.: Microfluidic technologies for accelerating the clinical translation of nanoparticles. Nat. Nanotechnol. **7**(10), 623–629 (2012)
226. Björnmalm, M., Yan, Y., Caruso, F.: Engineering and evaluating drug delivery particles in microfluidic devices. J. Contr. Release **190**, 139–149 (2014)
227. Lo Giudice, M.C., Herda, L.M., Polo, E., Dawson, K.A.: In situ characterization of nanoparticle biomolecular interactions in complex biological media by flow cytometry. Nat. Commun. **7**, 13475 (2016)
228. Sun, J., Xianyu, Y., Jiang, X.: Point-of-care biochemical assays using gold nanoparticle-implemented microfluidics. Chem. Soc. Rev. **43**(17), 6239–6253 (2014)
229. Fan, X., White, I.M.: Optofluidic microsystems for chemical and biological analysis. Nat. Photonics **5**, 591 (2011)
230. Varghese, S.S., Zhu, Y., Davis, T.J., Trowell, S.C.: FRET for lab-on-a-chip devices—current trends and future prospects. Lab Chip **10**(11), 1355–1364 (2010)
231. Dannhauser, D., Romeo, G., Causa, F., De Santo, I., Netti, P.A.: Multiplex single particle analysis in microfluidics. Analyst **139**(20), 5239–5246 (2014)
232. Stehle, R., Goerigk, G., Wallacher, D., Ballauff, M., Seiffert, S.: Small-angle X-ray scattering in droplet-based microfluidics. Lab Chip **13**(8), 1529–1537 (2013)

Part II
Membrane Transfer, Cellular Uptake and Intracellular Fate: Mechanisms and Detection Methods

Chapter 6
Nanoparticle-Cell Interactions: Overview of Uptake, Intracellular Fate and Induction of Cell Responses

Barbara Rothen-Rutishauser, Joël Bourquin and Alke Petri-Fink

Abstract The range of engineered nanoparticles (NPs) designed as specific carriers for biomedical applications, e.g. cell targeting and drug delivery, is still on the raise and the question on how NPs are interacting with single cells and sub-cellular structures remains important. The delivery to the cell surface as well as the interaction of NPs with cellular structures with possible subsequent response is highly influenced by various parameters such as (a) the physico-chemical properties of the NPs, (b) the cell and tissue type and (c) the intracellular fate of the NPs in the various organelles including biopersistence, exocytosis and/or transfer to other cells. The aim of this book chapter is to discuss, on the basis of existing literature, the interaction of NPs with single cells including the intracellular fate and their interference with signaling pathways.

6.1 Introduction

Over the past decades the increase in nanoparticle (NP) research has resulted in an increase of nanotechnology related products [1, 2] for numerous applications, including medicine, consumer products (such as food additives, cosmetics and sporting equipment), environmental remediation and information technology [2]. In order to realize these proposed benefits, heightened research has been performed to determine if the potential benefits of nanotechnology could be utilized without any adverse effects in human health or the environment.

B. Rothen-Rutishauser (✉) · J. Bourquin · A. Petri-Fink
BioNanomaterials, Adolphe Merkle Institute, Chemin des Verdiers 4,
1700 Fribourg, Switzerland
e-mail: barbara.rothen@unifr.ch

A. Petri-Fink
Department of Chemistry, University of Fribourg, Chemin du Museé 9,
1700 Fribourg, Switzerland

P. Gehr and R. Zellner (eds.), *Biological Responses to Nanoscale Particles*,
NanoScience and Technology, https://doi.org/10.1007/978-3-030-12461-8_6

The definition for a nanoparticle (NP); a nano-object (a material with one, two or three external dimensions in the nanoscale (1–100 nm)) with all three external dimensions in the nanoscale (ISO/TS: 27687:2008 [3]); will be used.

The number of new NPs with e.g. different materials, sizes, shapes, surface coatings (for reviews see [4–6]) is increasing and there is a need to apply reliable, cost and time effective, rapid and mechanistic based testing strategies enabling to understand interactions of engineered NPs at a cellular level; this all is imperative for their safe-by-design strategies and should also increase subsequent regulatory approvals [7]. It has been widely accepted that in vitro results can be useful for ranking NPs either by mechanistic studies enabling a deeper insight into mechanisms of NP-induced (potentially even nano-specific) effects or serving as a foundation for follow-up in vivo studies [8].

The interaction of NPs with cellular systems depends on the administration route to the human body and for biomedical applications the most commonly used administrations include, amongst others, injection, inhalation, oral or dermal administration (for a review see [9]). Independent of the administration route the NPs will encounter complex physiological fluids composed of various biomacromolecules such as e.g. proteins, lipids, and ions which then can result in the formation of a protein layer around the NPs, NP dissolution or NP aggregation [10, 11]. All these changes can strongly impact the interaction with cellular structures as well as the subsequent intracellular fate [12, 13]. The detailed description of the different administration routes and the behavior of NP in complex physiological fluids is, however, beyond the scope of this book chapter and have been thoroughly presented elsewhere (e.g. [14–16]).

Once the NPs have been administered they directly interact with cellular barriers, i.e. the primary barrier itself or, if translocated via the systemic circulation, at secondary barriers [9]. It is important to understand how NPs interact with cellular systems and the detection, localisation and quantification of NPs within cells is of central importance to understand how physico-chemical parameters might influence the possible interaction with a specific cell types and the cellular responses [17]. Once intracellular NPs are identified, their distribution in different cellular compartments, such as endosomes, lysosomes, mitochondria, the nucleus or cytosol may also provide some indications as to their potential biological impact [18, 19], as well as how to specifically design nanocarriers for cell targeting and drug delivery.

6.2 Cellular Barriers in Eukaryotic Cells

Once the NPs have reached their target cells, several other barriers remain, including the outer cell membrane and, only in eukaryotic cells, the intracellular membranes surrounding the different compartments to provide optimal microenvironmental con-

ditions for specialized metabolic pathways (for a review see [20]). The cell membrane consists of a lipid bilayer containing various phospholipids, glycolipids and sterols, carbohydrates and membrane proteins, which regulate the entry of small and large molecules into the cell and are held together mainly by non-covalent interactions [21]. The cell membrane also plays an important role in anchoring the cytoskeleton to the outer cell membrane providing the cell shape. Further the cell membrane enables to form tissues by attaching to other cells as well as to the extracellular matrix by the adhesion proteins e.g. integrins and cadherins [22]. The lipid molecules in cell membranes are arranged as a ca. 4–5 nm-thick, continuous double layer. This lipid bilayer is not rigid but rather dynamic in which lipids and proteins diffuse more or less easily and it was described as the fluid mosaic model by Singer and Nicolson ([23], for a review see [24]). Because of this fluidity of the phospholipid bilayer the components of the membranes can be arranged in a non-homogenous distribution and areas can differ in their lipid composition (for a review see [25]). Especially the clustering of sphingolipids and cholesterol into so-called lipid rafts has been associated with specific cellular and/or biological functions (for a review see [26]).

The cellular membrane is only selectively permeable, as it allows water to flow freely but provides a relatively impermeable barrier to the passage of most water-soluble molecules. Various routes exist for macromolecules or materials to enter a cell, such as passive diffusion through the membrane, transport-mediated uptake via transmembrane proteins serving as pumps or channels, or catalysing membrane-associated reactions and vesicular uptake mechanisms, including endocytotic processes such as pinocytosis and phagocytosis [27, 28]. The detailed mechanisms are also elaborated in more details in Sect. 6.3.2 Cellular uptake mechanisms and detection of nanoparticles by advanced imaging methods [29].

6.3 Nanoparticle-Cell Interactions

The principal interaction of NPs with a biological environment occurs at the cellular level through the interaction with structural and functional cell compartments (e.g. cell membranes, nucleus, organelles) [18] and the information about the localization of NPs is key in the assessment of the NP efficiency to perform a desired action [30]. It is also important to distinguish between NPs adhering to the outer cell membrane and intracellularly, as well as to quantify the internalized NPs; this is, however, covered thoroughly elsewhere [31–34]. There is convincing evidence that NPs are taken up by any cell, with most studies suggesting an endocytotic uptake route. NPs, however, might also be released, degraded and/or transferred to other cells which will then influence the efficacy of NPs and cellular reactions (Fig. 6.1) (for reviews see [7, 9, 35]). It also has been shown that NP endocytosis is not only particle but also cell type dependent [36] and for instance epithelial cells reveal different uptake mechanisms in comparison to phagocytotic cells, i.e. macrophages [37].

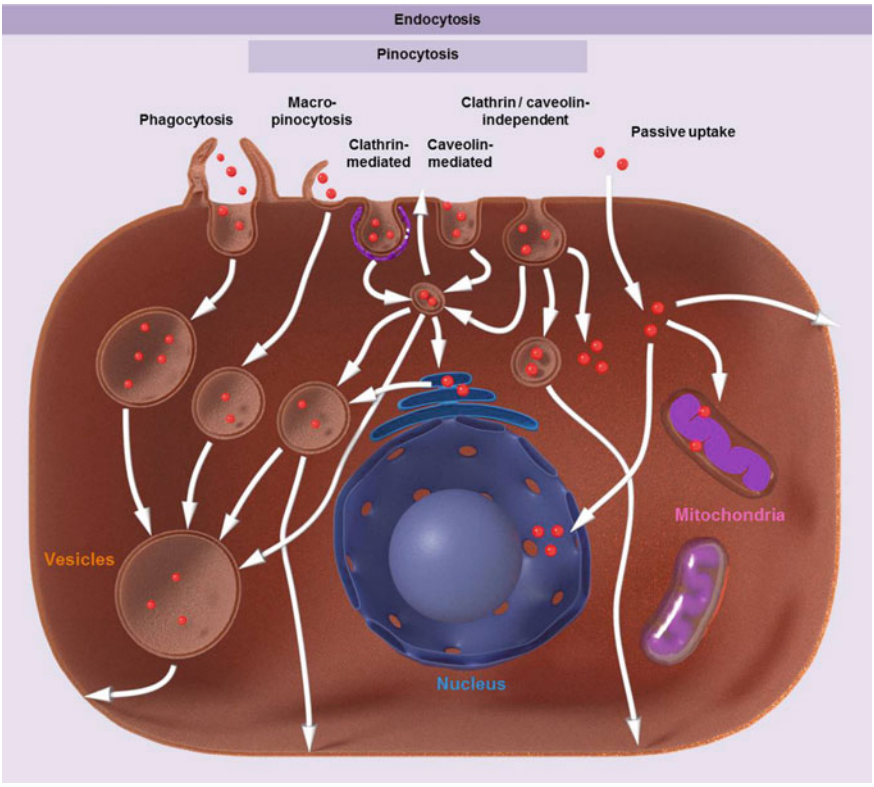

Fig. 6.1 Schematic representation for the different endocytotic mechanisms of particles. Large (micron-sized) particles may be actively incorporated via phagocytosis, whereas smaller particles can be internalized through multiple mechanisms, i.e. micropinocytosis (>1 μm), clathrin-mediated endocytosis (~120 nm), clathrin- and caveolae-independent endocytosis or caveolae-mediated endocytosis (~60 nm). Nanoparticles may also enter the cell passively via diffusion or passive uptake by van der Waals or steric interactions through the plasma membrane

6.3.1 Endocytotic Mechanisms

The uptake of NPs by eukaryotic cells occurs mainly via endocytotic pathways (Fig. 6.1) which includes pinocytosis ("cellular drinking"), i.e. the ingestion of fluid and molecules via small vesicles (<0.15 μm in diameter), and phagocytosis, i.e. the ingestion of large particles (generally >0.25 μm in diameter) (for reviews see [28, 38]).

Phagocytosis is mainly carried out by so-called professional phagocytes (i.e. monocytes/macrophages, neutrophils and dendritic cells), where particle internalization is regulated and initiated by the interaction with specific receptors on the surface of the cell (Fig. 6.2). This initiation then leads to the polymerization of actin filaments at the site of ingestion, i.e. membrane ruffling, and after internalization the

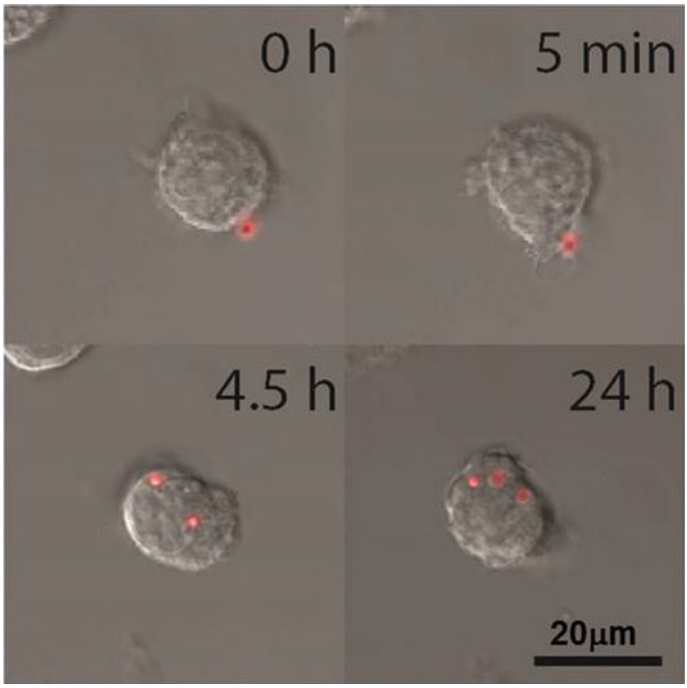

Fig. 6.2 Phagocytotic uptake of fluorescently labelled 1.2 µm silicon dioxide particles by a J774.A1 macrophage. The particles (red) were added at time point zero to the cultures and visualized up to 24 h using a Zeiss confocal microscope. After attachment to the outer cell membrane (0 h) the macrophage surrounds the particles by protrusion (5 min) and keep them engulfed (4.5 and 24 h)

phagosome matures by a series of fusion events with components of the endocytic pathway, culminating in the formation of the mature phagolysosome [39, 40].

The term pinocytosis includes macropinocytosis, clathrin- and caveolin-mediated endocytosis and clathrin- and caveolin-independent endocytosis [28]. Macropinocytosis triggers actin formation which then collapse onto and fuse with the plasma membrane to generate large endocytic vesicles called macropinosomes. Caveolin-mediated endocytosis is mostly used for the transport of serum proteins. Caveolae are static, flask-shaped invaginations of the plasma membrane that are slow in uptake and are observed in several cell types, including capillary endothelium, type I alveolar epithelial cells, smooth muscle cells and fibroblasts [28]. This mechanism is generally connected to cholesterol-rich microdomains, called rafts, with a diameter of 40–50 nm [41, 42]. Clathrin-mediated endocytosis is a form of receptor-mediated endocytosis, which is in general very fast. It occurs in all mammalian cells and carries out the continuous uptake of essential nutrients, such as the cholesterol-laden low-density lipoprotein particles that bind to the low-density lipoprotein receptor, and iron-laden transferrin that binds to transferrin receptors [43, 44].

After NP endocytosis the internalized particles are ultimately located in a vesicle. There are, however, studies that have shown not membrane-bound intracellular NPs [45–47], thus indicating endosomal/lysosomal escape as shown for sharp-shaped nanomaterials such as nanodiamonds, which could pierce the membranes of the endosomes and thus escaped to the cytoplasm [48] or alternative pathways such as passive diffusion through membrane pores and passive uptake by van der Waals or steric interactions (subsumed as adhesive interactions) [49]. In addition, highly positively charged particles such as polyethyleneimine coated NPs have been shown to escape the endo-lysosomal system by the so called proton sponge effect [50]. The localisation of free NPs in the cytosol is, however, only rarely observed and the majority of particles are found inside vesicular structures [51].

6.3.2 Intracellular Fate

After the cellular uptake the particles are mainly observed in vesicles (Fig. 6.3). As already stated upon phagocytosis of bigger sized particles (<0.5 mm) the phagosome matures by a series of fusion events with components of the endocytic pathway, i.e. the lysosomes, finally forming the mature phagolysosome [39]. The milieu in the phagolysosomes is acidic and hydrolytic, enabling the degradation of the engulfed particles [52], this, however, highly depends on the biopersistence (i.e. defined as the extent to which particles are able to resist chemical, physical, and other physiological clearance mechanisms in the body) and biodurability (i.e. defined as the ability to resist chemical/biochemical alteration and is a significant contributor to biopersistence) of the particles [53]. In addition, phagocytosis activity in human-derived macrophages and dendritic cells largely depends on particle size, surface charge as well as the surface coating [54, 55].

Many studies have shown receptor-mediated clathrin- and caveolae-dependent uptake to internalize nanoscale materials, i.e. NPs [35]. Once the NPs are inside endocytotic vesicles they fuse together to form early endosomes allowing for approximately 10 min. to fuse with other endocytic vesicles. Early endosomes are described to be the main sorting station in the endocytotic pathway. During this time the membrane and internal fluids such as transmembrane receptors are constantly recycled, while the cargo, e.g. NPs, is retained inside [40]. The maturation of early endosomes into late endosomes vesicles is accompanied with an acidification as well as with an extensive exchange with the trans-Golgi network sending proteins for the lysosomal digestion system, such as hydrolases or membrane-attached transport proteins, into the degradation pathway [56]. Late endosome are bigger than early endosomes, usually in the size of 250–400 nm, and are closer to the nucleus. Then the late endosomes mature into lysosome by fusion with pre-existing lysosomes to form the so-called endolysosomes. Finally the majority of the endosomal components are degraded with the preservation of the lysosomal parts. The maturation is associated with an additional drop of the pH which can finally be between 4.5 and 5. In the electron

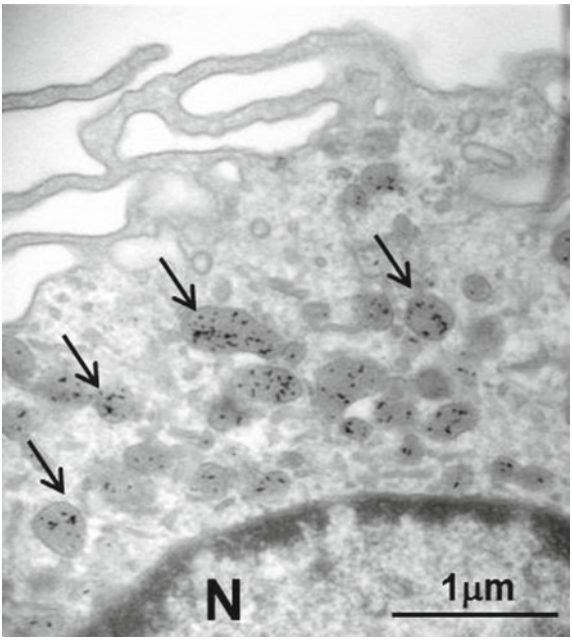

Fig. 6.3 Transmission electron micrograph of polymer coated gold NPs inside lysosomes in a dendritic cell (arrows). N refers to the nucleus Image courtesy of Kleanthis Fytianos

microscope the lysosomes appear as electron dense bodies and highly heterogeneous in terms of composition, density and morphology [40, 57].

Inside the lysosomal compartment the NPs are not only exposed to an acidic pH and high ionic strength but also up to 50 different and highly potent proteolytic enzymes have been described [58]. Such a harsh environment then can result in a possible degradation of NPs or change in colloidal stability. Enzymes in the lysosomes also can dissolve or detach the polymer coatings which stabilize the NPs and/or are used to add a specific functional surface. Kreyling et al. designed gold NPs coated with a radiolabelled indium polymer shell. They showed a localisation of the particles in endosomes and lysosomes in cells in vitro after endocytosis and a separation between the inorganic gold core and the organic polymer coating. In vivo the particles were found in liver cells where the polymer shell was exocytosed, then filtered by the renal system, and finally excreted via the urine [59]. We also have shown that in the case of fluorescently encoded carboxylated poly(vinyl alcohol) (COOH-PVA) gold NPs the intracellular environment (lysosomes) in J774A.1 monocyte/macrophage cells can cause the conformational changes within the polymer grafted on the NP surface, which then as a consequence has led to NP aggregation and quenching of the fluorescent dye present on the polymer surface [60]. Ma and colleagues prepared gold NPs with different coatings, i.e. human serum albumin (HSA), human γ-globulin (HGG) or human serum fibrinogen (HSF) and compared the cytotoxicity of the particles after exposure to HeLa cells. They showed that the degradation speed of the protein corona in the lysosomes is dependent on the corona

composition which then also impacts the aggregation of the NPs and the cellular cytotoxicity response [61]. In addition, the dissolution of metallic NPs in lysosomes has to be considered which can reduce the concentration of intracellular NPs as well as a release of (potentially toxic) ions [62]. The human neutrophil enzyme myeloperoxidase also can provoke a biodegradation of carbonaceous nanomaterials such as single-walled carbon nanotubes in neutrophils [63], again, the cell type is relevant regarding particle intracellular fate.

Organelle dysfunctions can contribute to many human diseases because their functions are intimately linked to cell growth, proliferation, differentiation and cell death. Therefore, the design of NPs for targeting the cellular sub-organelles for various therapies has recently emerged (for a review see [64]). For instance mitochondria which are pivotal for the production of energy can be used as a target in cancer or neurodegenerative disease therapy and concepts to produce mitochondriotropic particulate carriers to transport drugs to either rescue the cell or to promote cell death have been described [65, 66]. Another important target is the cell nucleus. The nuclear pores are in the size range of around 30 nm, but studies have shown that larger NPs tagged with specific nuclear localization sequence can enter the nucleus (for a review see [67]). In addition, larger NPs with a specific surface can access the nuclear content during mitosis when the nuclear membrane breaks down [68].

6.3.3 Exocytotic Mechanisms

While many studies exist about NP endocytosis, there are only a limited number of reports showing the exocytosis of particles. Two pathways of exocytosis have been described, one constitutive and one which is regulated [21, 69]. Constitutive exocytosis is observed in all cells where proteins are secreted by being packaged into transport vesicles in the Golgi apparatus and then carried to and incorporated into the plasma membrane. Then the regulated pathway is only found in cells that are specialized for secreting their products, such as hormones, neurotransmitters or digestive enzymes. This process is performed rapidly and on demand, which is often triggered by an influx of Ca^{2+}.

Endocytosis and exocytosis are coupled and can stimulate or compensate for one another [70]. Further, endocytotic processes occur much faster than exocytotic routes, where the excretion rate even decreases with increasing particle size as shown for 14, 50 and 74 nm gold NPs in HeLa cells [71]. It is also known that many parameters, such as the cell type [72], NP properties (i.e. size, surface and shape) as well as their applied concentration and exposure time can affect exocytosis thoroughly (for a review see [73]). Since the NP surface might alter during uptake and lysosomal processing, the exocytosed NPs might also exhibit a different surface and therefore recognize different targets or receptors on the cellular surface [14, 73]. Also time is important and it has been reported that only NPs not ended up in lysosomes can undergo exocytosis which indicates that exocytosis is mainly effective after a short NP exposure time [62].

Not only exocytosis of NPs has to be considered but there might be an eventual decrease of the total NP load per cell as a result of mitotic division, and/or NP transcytosis to another cell (for reviews see [35, 74, 75]).

6.4 Nanoparticle Induced Cell Responses

Once the NPs are inside the cells, or as already stated earlier attached to the outer cell membrane, several cellular responses have been described such as cytotoxicity [76], the generation of reactive oxygen species [77], the enhanced expression of pro-inflammatory cytokines [78], and genotoxicity [79]. However, the precise mechanism of possible NPs toxicology is still not fully understood [80] and it is also accepted that each in vitro test system has to be evaluated for each single NP [81].

Currently, the hypothesis for the mode of action of airborne particulate matter is the induction of oxidative stress, i.e. the oxidative stress paradigm, leading then to an inflammatory response and/or cytotoxicity [82, 83], this is also used as a basis for many NPs-based investigations. Other endpoints have been described such as the fibre paradigm [84] and the theory of genotoxicity [85]. In addition, some important aspects about the use of reliable methods and realistic test conditions to study possible risks of NPs have recently been reviewed in several publications. For instance the in-depth characterization of the NPs, the use of realistic doses, and the validity of the selected test methods have been highlighted [7, 86, 87].

6.4.1 Cytotoxicity

Usually one of the first endpoints assessed in NP-cell interaction studies is cytotoxicity [62, 76, 88]. Many different techniques to study cytotoxicity have been described, such as visualisation of cell morphology, the use of assays to determine the membrane integrity or the alteration of the metabolic activity. In addition, cell proliferation determination or evaluation of apoptic versus necrotic responses is regularly reported (for reviews see [7, 89]). It is important to mention that it is crucial to include interference tests of the NPs with the assays especially for cytotoxicity assays where usually also high NP concentrations are used [81]. Such interference tests, however, are not only relevant for cytotoxicity assay but for all assays including spectroscopic detections.

6.4.2 Oxidative Stress

Oxidative stress is the imbalance of reactive oxygen species (ROS) production and defense systems against them and the prevailing paradigm in the NP induced effects

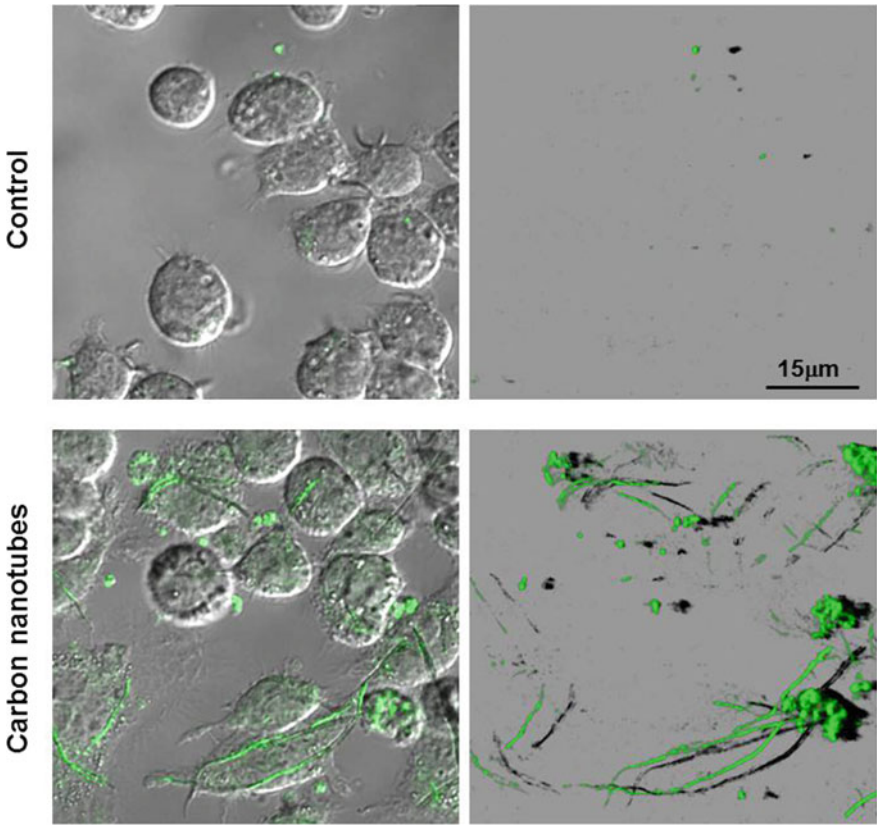

Fig. 6.4 Light microscopy images of J774.A1 macrophages without and treated with carbon nanotubes (left images). Intracellular reactive oxygen species were labelled using 2′, 7′ dichlorofluorescin diacetate assay and visualized by laser scanning microscopy (right images). Images represent 3D surface renderings showing the increased reactive oxygen species labels in the presence of the fibers as well as an unspecific signal from the carbon nanotubes

(Fig. 6.4). Cells generate ROS to maintain their normal homeostasis, however, its overproduction can provoke a hierarchical response; thus, ROS can interfere with a variety of signal transduction pathways, i.e. changing to an anti-oxidant defense, or eliciting oxidative damage to lipids and induction of DNA-strand breaks [90]. The anti-oxidant system consists of different enzyme systems such as the superoxide dismutase (SOD), the catalase (CAT) and the glutathione peroxidase (GPx) to neutralize ROS (for a review see [91]). Further associations between oxidative stress and various adverse outcomes such as (pro-)inflammation, general cytotoxicity and genotoxicity are described in the literature [82, 92, 93].

NP-induced oxidative stress can involve the oxidative properties of the NPs themselves as well as the oxidant generation upon interaction of NP with cellular components and many different NPs such as metals, metal oxides, fullerene or carbon

nanotubes have been shown to induce oxidative stress (for reviews see [94, 95]). The hypothesis postulated in 2003 by Donaldson and colleagues [82] that NPs induce adverse cellular effects via oxidative means (oxidative stress paradigm) is still used as a basis for many NP investigations.

6.4.3 Pro-inflammation Including Inflammasome Activation

The central role of oxidative stress for subsequent cellular responses such as inflammation was postulated by Nel and colleagues [96]. Indeed, ROS can activate the signalling pathway of mitogen-activated protein kinases (MAPKs) which then induce the transcription factors nuclear factor kappa B (NF-κB), activator protein-1 (AP-1) or Nrf2 followed by the transcription of pro-inflammatory genes (for a review see [97]). The cellular release of these pro-inflammatory mediators, i.e. cytokines which are signalling molecules or chemokines which are "chemo-attractant molecules" and play a key role in the activation of neutrophils and their recruitment to the site of inflammation, is then responsible for the inflammation.

Various key mediators have been described such as for example Interleukin (IL) −8, IL-6, IL-1 and tumor-necrosis factor alpha (TNFα), however, this short list is by far not complete. In addition, most of these mediators are secreted by typical cell types, i.e. IL-8 is a chemokine mainly produced by macrophages and epithelial cells [98, 99] and plays a key role in the inflammatory response, whereas the cytokine TNFα is primarily released from monocytes like dendritic cells or macrophages [98, 100] and functions as a regulator of inflammation reactions. The stimulated release of pro-inflammatory mediators by many NPs have been described in the literature and the physico-chemical properties of the NPs dictate the immune response (for a review see [101]).

The concept of inflammasome activation has been introduced by Tschopp and colleagues a decade ago [102] describing an important component of the innate immune response which is relevant for the clearance of pathogens, e.g. (nano)particles. The inflammasome complex comprises of a multimeric protein complex consisting of an inflammasome sensor molecule, the adaptor protein Apoptosis-associated Speck-like protein containing CARD(ASC) and caspase 1. Several sensor molecules have been described such as NOD-like receptors (NLR) 1, 3, 7, or 12. Once the protein complex has formed the enzyme caspase 1 is activated which then proteolytically activates the release of the pro-inflammatory cytokines, interleukin (IL)-1β and IL-18, which is leading to the induction of an inflammatory form of cell death called pyroptosis [103]. NLRP3 is the main sensor protein activated upon exposure to particles and is mainly expressed in macrophages. It has, however, been shown that the response cannot be directly triggered by the particles themselves but other mechanisms have been proposed such as lysosomal membrane damage resulting in lysosomal content being released, modification of intracellular ionic concentrations, intracellular redox unbalance and organelle damage (for a review see [104]). In addition to the activation of the caspase-1 enzyme the inactive pro-IL-1β cytokine has to be produced

by gene upregulation and this is typically triggered by microbial agents binding to membrane Toll-like receptors (TLR) receptors, such as the TLR4 agonist bacterial lipopolysaccharide (LPS) [105].

One of the first studies showing that NPs can activate the inflammasome was done with nano titanium dioxide [106]. Since then many other publications have revealed the underlying mechanisms of the inflammasome activation upon exposure to NPs. It is again important to mention that the physicochemical characteristics of the (nano)particles such as size, surface and shape are decisive for particle internalization, lysosomal alteration, and subsequent inflammasome/IL-1β processing [104]. The smallest and fiber- or needle-like particles are particularly active to induce inflammasome activation since the interaction of these particles/fibers with macrophages can led to frustrated phagocytosis and ROS production which then activates the cascade [107].

6.4.4 Genotoxicity

The potential damage of NPs to the genetic material in a cellular nucleus, i.e. DNA, is described as genotoxicity and can be classified as primary or secondary genotoxicity [85]. Primary genotoxicity is defined as genetic damage induced by NPs themselves via direct or indirect mechanisms. The direct genotoxicity results from physical interactions of the materials with the genomic DNA which can occur for smaller NPs capable of reaching the nucleus through the nuclear pore complexes [108], by penetration of the nuclear membrane as shown for multi-walled carbon nanotubes [109] and/or by interaction of the materials with the chromosomes/mitotic spindle during cell division [110]. Indirect, primary genotoxicity can occur via various pathways; for instance via formation of ROS by metals and organic constituents but not inducing inflammation [85]. Secondary genotoxicity implies the involvement of inflammatory cells resulting in the oxidative damage of DNA by ROS [108, 111].

The probably most established mechanism by which NPs can induce genetic damage is via their capacity to induce oxidative stress [112]. The biological mechanisms through which NPs can induce DNA damage have been thoroughly described in several recent reviews [113, 114].

6.5 Conclusions

The great potential of NPs for biomedical applications requires a thorough understanding on how these NPs interact with cells, how they are taken up, their subsequent localization within cells, but also if and how NPs can be cleared from cells. There is convincing evidence that NPs are taken up by any cell, with most studies suggesting an endocytotic uptake route determining the intracellular trafficking and fate. NPs also have been observed free in the cytoplasm resulted either by passive uptake via

adhesive interactions or endosomal escape, and depending on the NP properties the particles also can traffic to other cellular organelles, e.g. mitochondria or nucleus. It is important to consider that NPs can be released, degraded and/or transferred to other cells which will then influence the efficacy of NPs used for instance for contrast agents in imaging, or in drug delivery. The interaction of NPs with cells and the intracellular fate also determines the possible cellular response such as oxidative stress, pro-inflammatory responses including the activation of the inflammasome, and genotoxicity.

Acknowledgements We would like to acknowledge the Swiss National Science Foundation (310030_159847/1), the National Center of Competence in Research for Bio-Inspired Materials and the Adolphe Merkle Foundation for financial support. We kindly thank Dr. Miguel Spuch Calvar for the graphical design.

References

1. Gwinn, M.R., Vallyathan, V.: Nanoparticles: health effects—pros and cons. Env. Health Perspect. **114**, 1818–1825 (2006)
2. Maynard, A.D., Aitken, R.J., Butz, T., Colvin, V., Donaldson, K., Oberdorster, G., et al.: Safe handling of nanotechnology. Nature **444**, 267–269 (2006)
3. ISO/TS 27687 (2008)
4. Alex, S., Tiwari, A.: Functionalized gold nanoparticles: synthesis, properties and applications—a review. J. Nanosci. Nanotechnol. **15**, 1869–1894 (2015)
5. Pelaz, B., Alexiou, C., Alvarez-Puebla, R.A., Alves, F., Andrews, A.M., Ashraf, S., et al.: Diverse applications of nanomedicine. ACS Nano **11**, 2313–2381 (2017)
6. Dahoumane, S.A., Jeffryes, C., Mechouet, M., Agathos, S.N.: Biosynthesis of inorganic nanoparticles: a fresh look at the control of shape, size and composition. Bioengineering (Basel) **4** (2017)
7. Drasler, B., Sayre, P., Steinhäuser, K.G., Petri-Fink, A., Rothen-Rutishauser, B.: In vitro approaches to assess the hazard of nanomaterials. NanoImpact **8**, 99–116 (2017)
8. Vietti, G., Lison, D., van den Brule, S.: Mechanisms of lung fibrosis induced by carbon nanotubes: towards an Adverse Outcome Pathway (AOP). Part. Fibre Toxicol. **13**, 11 (2016)
9. Bourquin, J., Milosevic, A., Hauser, D., Lehner, R., Blank, F., Petri-Fink, A., et al.: Biodistribution, clearance, and long-term fate of clinically relevant nanomaterials. Adv. Mater. (2018)
10. Urban, D.A., Rodriguez-Lorenzo, L., Balog, S., Kinnear, C., Rothen-Rutishauser, B., Petri-Fink, A.: Plasmonic nanoparticles and their characterization in physiological fluids. Colloids Surf. B Biointerfaces **137**, 39–49 (2016)
11. Moore, T.L., Rodriguez-Lorenzo, L., Hirsch, V., Balog, S., Urban, D., Jud, C., et al.: Nanoparticle colloidal stability in cell culture media and impact on cellular interactions. Chem. Soc. Rev. **44**, 6287–6305 (2015)
12. Lynch, I., Cedervall, T., Lundqvist, M., Cabaleiro-Lago, C., Linse, S., Dawson, K.A.: The nanoparticle-protein complex as a biological entity; a complex fluids and surface science challenge for the 21st century. Adv. Colloid Interface Sci. **134–135**, 167–174 (2007)
13. Bertoli, F., Garry, D., Monopoli, M.P., Salvati, A., Dawson, K.A.: The intracellular destiny of the protein corona: a study on its cellular internalization and evolution. ACS Nano **10**, 10471–10479 (2016)
14. Mahon, E., Salvati, A., Baldelli, B.F., Lynch, I., Dawson, K.A.: Designing the nanoparticle-biomolecule interface for "targeting and therapeutic delivery". J. Control. Release **161**, 164–174 (2012)

15. Schottler, S., Landfester, K., Mailander, V.: Controlling the stealth effect of nanocarriers through understanding the protein corona. Angew. Chem. Int. Ed. Engl. **55**, 8806–8815 (2016)
16. Docter, D., Westmeier, D., Markiewicz, M., Stolte, S., Knauer, S.K., Stauber, R.H.: The nanoparticle biomolecule corona: lessons learned - challenge accepted? Chem. Soc. Rev. **44**, 6094–6121 (2015)
17. Frohlich, E.: The role of surface charge in cellular uptake and cytotoxicity of medical nanoparticles. Int. J. Nanomedicine **7**, 5577–5591 (2012)
18. Muhlfeld, C., Rothen-Rutishauser, B., Blank, F., Vanhecke, D., Ochs, M., Gehr, P.: Interactions of nanoparticles with pulmonary structures and cellular responses. Am. J. Physiol. Lung Cell. Mol. Physiol. **294**, L817–L829 (2008)
19. Unfried, K., Albrecht, C., Klotz, L.O., von Mikecz, A., Grether-Beck, S., Schins, R.P.: Cellular responses to nanoparticles: target structures and mechanisms. Nanotoxicology **1**, 1–20 (2007)
20. Trimble, W.S., Grinstein, S.: Barriers to the free diffusion of proteins and lipids in the plasma membrane. J. Cell. Biol. **208**, 259–271 (2015)
21. Alberts, B., Bray, D., Johnson, A, Lewis, J., Raff, M., Roberts, K., et al.: Essential Cell Biology: An Introduction to the Molecular Biology of the Cell. Garland Publishing, Inc (1998)
22. Warren, G., Wickner, W.: Organelle inheritance. Cell **84**, 395–400 (1996)
23. Singer, S.J., Nicolson, G.L.: The fluid mosaic model of the structure of cell membranes. Science (New York, N Y) **175**, 720–731 (1972)
24. Ritchie, K., Spector, J.: Single molecule studies of molecular diffusion in cellular membranes: determining membrane structure. Biopolymers **87**, 95–101 (2007)
25. Sonnino, S., Prinetti, A.: Membrane domains and the "lipid raft" concept. Curr. Med. Chem. **20**, 4–21 (2013)
26. Simons, K., Ikonen, E.: Functional rafts in cell membranes. Nature **387**, 569–572 (1997)
27. Hillaireau, H., Couvreur, P.: Nanocarriers' entry into the cell: relevance to drug delivery. Cell. Mol. Life Sci. **66**, 2873–2896 (2009)
28. Conner, S.D., Schmid, S.L.: Regulated portals of entry into the cell. Nature **422**, 37–44 (2003)
29. Fytianos, K., Blank, F., Müller, L.: Cellular uptake mechanisms and detection of nanoparticle uptake by advanced imaging methods. In: Zellner, R., Gehr, P. (eds.) Biological Responses to Nanoscale Particles. Springer (2018)
30. Drasler, B., Vanhecke, D., Rodriguez-Lorenzo, L., Petri-Fink, A., Rothen-Rutishauser, B.: Quantifying nanoparticle cellular uptake: which method is best? Nanomedicine (Lond) **12**, 1095–1099 (2017)
31. Elsaesser, A., Taylor, A., de Yanes, G.S., McKerr, G., Kim, E.M., O'Hare, E., et al.: Quantification of nanoparticle uptake by cells using microscopical and analytical techniques. Nanomedicine (Lond) **5**, 1447–1457 (2010)
32. Feliu, N., Huhn, J., Zyuzin, M.V., Ashraf, S., Valdeperez, D., Masood, A., et al.: Quantitative uptake of colloidal particles by cell cultures. Sci. Total Environ. **568**, 819–828 (2016)
33. Gottstein, C., Wu, G., Wong, B.J., Zasadzinski, J.A.: Precise quantification of nanoparticle internalization. ACS Nano **7**, 4933–4945 (2013)
34. Vanhecke, D., Rodriguez-Lorenzo, L., Clift, M.J.D., Blank, F., Petri-Fink, A., Rothen-Rutishauser, B.: Quantification of nanoparticles at the single cell level—an overview about state-of-the art techniques and their limitations. Nanomedicine (London, England) **9**, 1885–1900 (2014)
35. Oh, N., Park, J.H.: Endocytosis and exocytosis of nanoparticles in mammalian cells. Int. J. Nanomedicine **9**(Suppl 1), 51–63 (2014)
36. Mahmoudi, M., Saeedi-Eslami, S.N., Shokrgozar, M.A., Azadmanesh, K., Hassanlou, M., Kalhor, H.R., et al.: Cell "vision": complementary factor of protein corona in nanotoxicology. Nanoscale (2012)
37. Kuhn, D.A., Vanhecke, D., Michen, B., Blank, F., Gehr, P., Petri-Fink, A., et al.: Different endocytotic uptake mechanisms for nanoparticles in epithelial cells and macrophages. Beilstein J. Nanotechnol. **5**, 1625–1636 (2014)
38. Doherty, G.J., McMahon, H.T.: Mediation, modulation, and consequences of membrane-cytoskeleton interactions. Annu. Rev. Biophys. **37**, 65–95 (2008)

39. Aderem, A., Underhill, D.M.: Mechanisms of phagocytosis in macrophages. Annu. Rev. Immunol. **17**, 593–623 (1999)
40. Huotari, J., Helenius, A.: Endosome maturation. EMBO J. **30**, 3481–3500 (2011)
41. Anderson, R.G.: The caveolae membrane system. Annu. Rev. Biochem. **67**, 199–225 (1998)
42. Edidin, M.: Membrane cholesterol, protein phosphorylation, and lipid rafts. Sci. STKE **2001**, E1 (2001)
43. Brodsky, F.M., Chen, C.Y., Knuehl, C., Towler, M.C., Wakeham, D.E.: Biological basket weaving: formation and function of clathrin-coated vesicles. Annu. Rev. Cell. Dev. Biol. **17**, 517–568 (2001)
44. Schmid, S.L.: Clathrin-coated vesicle formation and protein sorting: an integrated process. Annu. Rev. Biochem. **66**, 511–548 (1997)
45. Geiser, M., Rothen-Rutishauser, B., Kapp, N., Schurch, S., Kreyling, W., Schulz, H., et al.: Ultrafine particles cross cellular membranes by nonphagocytic mechanisms in lungs and in cultured cells. Environ. Health Perspect. **113**, 1555–1560 (2005)
46. Lesniak, W., Bielinska, A.U., Sun, K., Janczak, K.W., Shi, X., Baker Jr., J.R., et al.: Silver/dendrimer nanocomposites as biomarkers: fabrication, characterization, in vitro toxicity, and intracellular detection. Nano Lett. **5**, 2123–2130 (2005)
47. Mu, Q., Hondow, N.S., Ski, L., Brown, A.P., Jeuken, L.J., Routledge, M.N.: Mechanism of cellular uptake of genotoxic silica nanoparticles. Part. Fibre Toxicol. **9**, 29 (2012)
48. Chu, Z., Zhang, S., Zhang, B., Zhang, C., Fang, C.Y., Rehor, I., et al.: Unambiguous observation of shape effects on cellular fate of nanoparticles. Sci. Rep. **4**, 4495 (2014)
49. Rimai, D.S., Quesnel, D.J., Busnaia, A.A.: The adhesion of dry particles in the nanometer to micrometer size range. Colloids Surf. A Physicochem. Eng. Asp. **165**, 3–10 (2000)
50. Benjaminsen, R.V., Mattebjerg, M.A., Henriksen, J.R., Moghimi, S.M., Andresen, T.L.: The possible "proton sponge" effect of polyethylenimine (PEI) does not include change in lysosomal pH. Mol. Ther. **21**, 149–157 (2013)
51. Brandenberger, C., Muhlfeld, C., Ali, Z., Lenz, A.G., Schmid, O., Parak, W.J., et al.: Quantitative evaluation of cellular uptake and trafficking of plain and polyethylene glycol-coated gold nanoparticles. Small **6**, 1669–1678 (2010)
52. Gray, M., Botelho, R.J.: Phagocytosis: hungry, hungry cells. Methods Mol. Biol. **1519**, 1–16 (2017)
53. Utembe, W., Potgieter, K., Stefaniak, A.B., Gulumian, M.: Dissolution and biodurability: important parameters needed for risk assessment of nanomaterials. Part. Fibre Toxicol. **12**, 11 (2015)
54. Thiele, L., Rothen-Rutishauser, B., Jilek, S., Wunderli-Allenspach, H., Merkle, H.P., Walter, E.: Evaluation of particle uptake in human blood monocyte-derived cells in vitro. does phagocytosis activity of dendritic cells measure up with macrophages? J. Control. Release **76**, 59–71 (2001)
55. Thiele, L., Diederichs, J.E., Reszka, R., Merkle, H.P., Walter, E.: Competitive adsorption of serum proteins at microparticles affects phagocytosis by dendritic cells. Biomaterials **24**, 1409–1418 (2003)
56. Bonifacino, J.S., Rojas, R.: Retrograde transport from endosomes to the trans-Golgi network. Nat. Rev. Mol. Cell. Biol. **7**, 568–579 (2006)
57. Wang, C., Zhao, T., Li, Y., Huang, G., White, M.A., Gao, J.: Investigation of endosome and lysosome biology by ultra pH-sensitive nanoprobes. Adv. Drug Deliv. Rev. **113**, 87–96 (2017)
58. Muller, S., Dennemarker, J., Reinheckel, T.: Specific functions of lysosomal proteases in endocytic and autophagic pathways. Biochim. Biophys. Acta **1824**, 34–43 (2012)
59. Kreyling, W.G., Abdelmonem, A.M., Ali, Z., Alves, F., Geiser, M., Haberl, N., et al.: In vivo integrity of polymer-coated gold nanoparticles. Nat. Nanotechnol. **10**, 619–623 (2015)
60. Milosevic, A.M., Rodriguez-Lorenzo, L., Balog, S., Monnier, C.A., Petri-Fink, A., Rothen-Rutishauser, B.: Assessing the stability of fluorescently encoded nanoparticles in lysosomes by using complementary methods. Angew. Chem. Int. Ed. Engl. **56**, 13382–13386 (2017)
61. Ma, Z., Bai, J., Jiang, X.: Monitoring of the enzymatic degradation of protein corona and evaluating the accompanying cytotoxicity of nanoparticles. ACS Appl. Mater. Interfaces. **7**, 17614–17622 (2015)

62. Frohlich, E.: Cellular targets and mechanisms in the cytotoxic action of non-biodegradable engineered nanoparticles. Curr. Drug Metab. **14**, 976–988 (2013)
63. Kagan, V.E., Konduru, N.V., Feng, W., Allen, B.L., Conroy, J., Volkov, Y., et al.: Carbon nanotubes degraded by neutrophil myeloperoxidase induce less pulmonary inflammation. Nat. Nanotechnol. **5**, 354–359 (2010)
64. Ma, X., Gong, N., Zhong, L., Sun, J., Liang, X.J.: Future of nanotherapeutics: targeting the cellular sub-organelles. Biomaterials **97**, 10–21 (2016)
65. Lu, P., Bruno, B.J., Rabenau, M., Lim, C.S.: Delivery of drugs and macromolecules to the mitochondria for cancer therapy. J. Control. Release **240**, 38–51 (2016)
66. Wongrakpanich, A., Geary, S.M., Joiner, M.L., Anderson, M.E., Salem, A.K.: Mitochondria-targeting particles. Nanomedicine (Lond) **9**, 2531–2543 (2014)
67. Tammam, S.N., Azzazy, H.M., Lamprecht, A.: How successful is nuclear targeting by nanocarriers? J. Control. Release **229**, 140–153 (2016)
68. Larsen, J., Ross, N., Sullivan, M.: Requirements for the nuclear entry of polyplexes and nanoparticles during mitosis. J. Gene Med. **14**, 580–589 (2011)
69. Burgess, T.L., Kelly, R.B.: Constitutive and regulated secretion of proteins. Annu. Rev. Cell. Biol. **3**, 243–293 (1987)
70. Dombu, C.Y., Kroubi, M., Zibouche, R., Matran, R., Betbeder, D.: Characterization of endocytosis and exocytosis of cationic nanoparticles in airway epithelium cells. Nanotechnology **21**, 355102 (2010)
71. Chithrani, B.D., Ghazani, A.A., Chan, W.C.: Determining the size and shape dependence of gold nanoparticle uptake into mammalian cells. Nano Lett. **6**, 662–668 (2006)
72. Chu, Z., Huang, Y., Tao, Q., Li, Q.: Cellular uptake, evolution, and excretion of silica nanoparticles in human cells. Nanoscale **3**, 3291–3299 (2011)
73. Sakhtianchi, R., Minchin, R.F., Lee, K.B., Alkilany, A.M., Serpooshan, V., Mahmoudi, M.: Exocytosis of nanoparticles from cells: role in cellular retention and toxicity. Adv. Colloid Interface Sci. **201–202**, 18–29 (2013)
74. Symens, N., Soenen, S.J., Rejman, J., Braeckmans, K., De Smedt, S.C., Remaut, K.: Intracellular partitioning of cell organelles and extraneous nanoparticles during mitosis. Adv. Drug Deliv. Rev. **64**, 78–94 (2012)
75. Iversen, T.G., Skotland, T., Sandvig, K.: Endocytosis and intracellular transport of nanoparticles: present knowledge and need for future studies. Nano Today **6**, 176–185 (2011)
76. Lujan, H., Sayes, C.: Cytotoxicological pathways induced after nanoparticle exposure: studies of oxidative stress at the 'nano-bio' interface. Toxicol. Res. **6**, 580 (2017)
77. Gonzalez-Flecha, B.: Oxidant mechanisms in response to ambient air particles. Mol. Asp. Med. **25**, 169–182 (2004)
78. Muller, J., Huaux, F., Moreau, N., Misson, P., Heilier, J.F., Delos, M., et al.: Respiratory toxicity of multi-wall carbon nanotubes. Toxicol. Appl. Pharmacol. **207**, 221–231 (2005)
79. Vinzents, P.S., Moller, P., Sorensen, M., Knudsen, L.E., Hertel, O., Jensen, F.P., et al.: Personal exposure to ultrafine particles and oxidative DNA damage. Environ. Health Perspect. **113**, 1485–1490 (2005)
80. Clift, M.J., Gehr, P., Rothen-Rutishauser, B.: Nanotoxicology: a perspective and discussion of whether or not in vitro testing is a valid alternative. Arch. Toxicol. **85**, 723–731 (2011)
81. Kroll, A., Pillukat, M.H., Hahn, D., Schnekenburger, J.: Interference of engineered nanoparticles with in vitro toxicity assays. Arch. Toxicol. **86**, 1123–1136 (2012)
82. Donaldson, K., Stone, V., Borm, P.J., Jimenez, L.A., Gilmour, P.S., Schins, R.P., et al.: Oxidative stress and calcium signaling in the adverse effects of environmental particles (PM10). Free Radic. Biol. Med. **34**, 1369–1382 (2003)
83. Kroll, A., Gietl, J.K., Wiesmuller, G.A., Gunsel, A., Wohlleben, W., Schnekenburger, J., et al.: In vitro toxicology of ambient particulate matter: correlation of cellular effects with particle size and components. Environ. Toxicol. **28**, 76–86 (2013)
84. Donaldson, K., Tran, C.L.: An introduction to the short-term toxicology of respirable industrial fibres. Mutat. Res. **553**, 5–9 (2004)

85. Schins, R.P., Knaapen, A.M.: Genotoxicity of poorly soluble particles. Inhal. Toxicol. **19**(Suppl 1), 189–198 (2007)
86. Krug, H.F., Wick, P.: Nanotoxicology: an interdisciplinary challenge. Angew. Chem. Int. Ed. Engl. (2011)
87. Paur, H.R., Cassee, F.R., Teeguarden, J.G., Fissan, H., Diabate, S., Aufderheide, M., et al.: In-vitro cell exposure studies for the assessment of nanoparticle toxicity in the lung—A dialog between aerosol science and biology. J. Aerosol Sci. **42**, 668–692 (2011)
88. Lewinski, N., Colvin, V., Drezek, R.: Cytotoxicity of nanoparticles. Small **4**, 26–49 (2008)
89. Khalili, F.J., Jafari, S., Eghbal, M.A.: A review of molecular mechanisms involved in toxicity of nanoparticles. Adv. Pharm. Bull. **5**, 447–454 (2015)
90. Moller, P., Jacobsen, N.R., Folkmann, J.K., Danielsen, P.H., Mikkelsen, L., Hemmingsen, J.G., et al.: Role of oxidative damage in toxicity of particulates. Free Radic. Res. **44**, 1–46 (2010)
91. He, L., He, T., Farrar, S., Ji, L., Liu, T., Ma, X.: Antioxidants maintain cellular redox homeostasis by elimination of reactive oxygen species. Cell. Physiol. Biochem. **44**, 532–553 (2017)
92. Brown, D.M., Donaldson, K., Borm, P.J., Schins, R.P., Dehnhardt, M., Gilmour, P., et al.: Calcium and ROS-mediated activation of transcription factors and TNF-alpha cytokine gene expression in macrophages exposed to ultrafine particles. Am. J. Physiol. Lung Cell. Mol. Physiol. **286**, 344–353 (2004)
93. Rahman, I., MacNee, W.: Oxidative stress and regulation of glutathione in lung inflammation. Eur. Respir. J. **16**, 534–554 (2000)
94. Manke, A., Wang, L., Rojanasakul, Y.: Mechanisms of nanoparticle-induced oxidative stress and toxicity. Biomed. Res. Int. **2013**, 942916 (2013)
95. Sarkar, A., Ghosh, M., Sil, P.C.: Nanotoxicity: oxidative stress mediated toxicity of metal and metal oxide nanoparticles. J. Nanosci. Nanotechnol. **14**, 730–743 (2014)
96. Nel, A., Xia, T., Madler, L., Li, N.: Toxic potential of materials at the nanolevel. Science (New York, N Y) **311**, 622–627 (2006)
97. Marano, F., Hussain, S., Rodrigues-Lima, F., Baeza-Squiban, A., Boland, S.: Nanoparticles: molecular targets and cell signalling. Arch. Toxicol. **85**, 733–741 (2011)
98. DeForge, L.E., Preston, A.M., Takeuchi, E., Kenney, J., Boxer, L.A., Remick, D.G.: Regulation of interleukin 8 gene expression by oxidant stress. J. Biol. Chem. **268**, 25568–25576 (1993)
99. Jimenez, L.A., Drost, E.M., Gilmour, P.S., Rahman, I., Antonicelli, F., Ritchie, H., et al.: PM(10)-exposed macrophages stimulate a proinflammatory response in lung epithelial cells via TNF-alpha. Am. J. Physiol. Lung Cell. Mol. Physiol. **282**, L237–L248 (2002)
100. Timmermann, M., Hogger, P.: Oxidative stress and 8-iso-prostaglandin F(2alpha) induce ectodomain shedding of CD163 and release of tumor necrosis factor-alpha from human monocytes. Free Radic. Biol. Med. **39**, 98–107 (2005)
101. Elsabahy, M., Wooley, K.L.: Cytokines as biomarkers of nanoparticle immunotoxicity. Chem. Soc. Rev. **42**, 5552–5576 (2013)
102. Dagenais, M., Skeldon, A., Saleh, M.: The inflammasome: in memory of Dr. Jurg Tschopp. Cell. Death Differ. **19**, 5–12 (2012)
103. Sharma, D., Kanneganti, T.D.: The cell biology of inflammasomes: mechanisms of inflammasome activation and regulation. J. Cell Biol. **213**, 617–629 (2016)
104. Rabolli, V., Lison, D., Huaux, F.: The complex cascade of cellular events governing inflammasome activation and IL-1beta processing in response to inhaled particles. Part. Fibre Toxicol. **13**, 40 (2016)
105. Boraschi, D., Italiani, P.: From antigen delivery system to adjuvanticy: the board application of nanoparticles in vaccinology. Vaccines (Basel) **3**, 930–939 (2015)
106. Yazdi, A.S., Guarda, G., Riteau, N., Drexler, S.K., Tardivel, A., Couillin, I., et al.: Nanoparticles activate the NLR pyrin domain containing 3 (Nlrp3) inflammasome and cause pulmonary inflammation through release of IL-1alpha and IL-1beta. Proc. Natl. Acad. Sci. U.S.A. **107**, 19449–19454 (2010)
107. Dostert, C., Petrilli, V., Van, B.R., Steele, C., Mossman, B.T., Tschopp, J.: Innate immune activation through Nalp3 inflammasome sensing of asbestos and silica. Science (New York, N Y) **320**, 674–677 (2008)

108. Nabiev, I., Mitchell, S., Davies, A., Williams, Y., Kelleher, D., Moore, R., et al.: Nonfunctionalized nanocrystals can exploit a cell's active transport machinery delivering them to specific nuclear and cytoplasmic compartments. Nano Lett. **7**, 3452–3461 (2007)
109. Cheng, C., Muller, K.H., Koziol, K.K., Skepper, J.N., Midgley, P.A., Welland, M.E., et al.: Toxicity and imaging of multi-walled carbon nanotubes in human macrophage cells. Biomaterials **30**, 4152–4160 (2009)
110. Sargent, L.M., Hubbs, A.F., Young, S.H., Kashon, M.L., Dinu, C.Z., Benkovic, S.A., et al.: Single-walled carbon nanotube-induced mitotic disruption. Mutat. Res. **745**, 28–37 (2012)
111. van Berol, D., Clift, M.J., Albrecht, C., Schins, R.P.: Carbon nanotubes: an insight into the mechanisms of their potential genotoxicity. Swiss Med. Wkly **142**, w13698 (2012)
112. Xia, T., Kovochich, M., Liong, M., Madler, L., Gilbert, B., Shi, H., et al.: Comparison of the mechanism of toxicity of zinc oxide and cerium oxide nanoparticles based on dissolution and oxidative stress properties. ACS Nano **2**, 2121–2134 (2008)
113. Singh, N., Manshian, B., Jenkins, G.J., Griffiths, S.M., Williams, P.M., Maffeis, T.G., et al.: NanoGenotoxicology: the DNA damaging potential of engineered nanomaterials. Biomaterials **30**, 3891–3914 (2009)
114. Magdolenova, Z., Collins, A., Kumar, A., Dhawan, A., Stone, V., Dusinska, M.: Mechanisms of genotoxicity. A review of in vitro and in vivo studies with engineered nanoparticles. Nanotoxicology **8**, 233–278 (2014)

Chapter 7
Cellular and Non-cellular Barriers to Particle Transport Across the Lungs

Nicole Schneider-Daum, Marius Hittinger, Xabier Murgia and Claus-Michael Lehr

Abstract Compared to the human body's other outer epithelia, like e.g. the skin and the GI tract, the lungs have the largest surface area. Moreover, the so called "air-blood-barrier" is extremely thin, but also very tight to fulfill its physiological function. This chapter discusses the lung as a biological barrier in the context of inhaled particles. This important function is provided by some specific cellular as well as non-cellular elements. How the lung copes with particles "after landing" is not only relevant regarding the risks of accidentally inhaled nanomaterials, but also for designing safe and efficient nanopharmaceuticals to be inhaled on purpose.

7.1 Introduction: What Distinguishes the Lung from Other Epithelia?

Along the Respiratory Tract the Epithelium Changes

The pulmonary epithelium holds multiple functions not only essential for tissue homeostasis. Various other requirements such as host defense or controlled transport are fulfilled by differences in the type and abundance of specialized cells at each location [1]. In general, similar types of pulmonary epithelial cells are found in all vertebrate lungs. In human lung, the airways are lined by a so-called pseudo-stratified

N. Schneider-Daum (✉) · M. Hittinger · X. Murgia · C.-M. Lehr
Helmholtz Institute for Pharmaceutical Research Saarland (HIPS), Campus E8 1, 66123 Saarbrücken, Germany
e-mail: Nicole.Daum@helmholtz-hips.de

M. Hittinger
e-mail: m.hittinger@pharmbiotec.de

X. Murgia
e-mail: Xabier.MurgiaEsteve@helmholtz-hips.de

C.-M. Lehr
e-mail: claus-michael.lehr@helmholtz-hips.de

M. Hittinger · C.-M. Lehr
PharmBioTec GmbH, Science Park 1, 66123 Saarbrücken, Germany

P. Gehr and R. Zellner (eds.), *Biological Responses to Nanoscale Particles*, NanoScience and Technology, https://doi.org/10.1007/978-3-030-12461-8_7

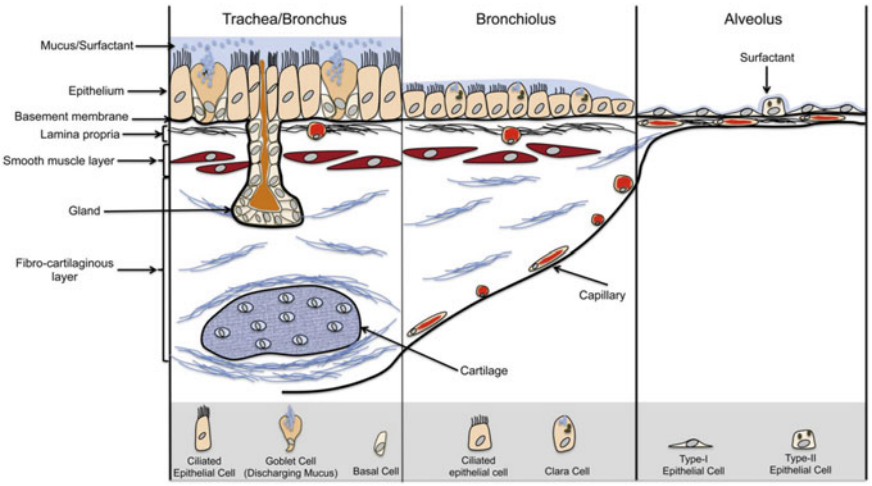

Fig. 7.1 Scheme of the 3 main parts of the respiratory tract, taken from [5]

columnar epithelium. It consists of a single layer of cells that give the appearance of multiple layers, due to the fact that the nuclei of these epithelial cells are at different levels leading to the illusion of being stratified. Predominant cell types are ciliated, basal, goblet and other secretory cells, including club cells (also known as Clara cells). While goblet cells secrete gel-forming mucins and are found in several epithelia, e.g. in the GI tract, the club cells produce glycosaminoglycans to protect the bronchiole lining. The alveolar region contains squamous alveolar type I (ATI) and cuboidal alveolar type II (ATII) cells (Fig. 7.1). The latter synthesize and secrete pulmonary surfactant, which lowers the surface tension in the alveoli relevant during inflation and play an important role as progenitors for ATI cells. These are found in close proximity to alveolar capillaries to allow for gas exchange. Their ability to form a thin but still very tight barrier is essential to avoid fluid accumulation in the alveolar space and to control transport processes of all kinds of substances and particles. Alveolar macrophages are the largest cell type and only loosely attach to the epithelium, as they move over the surface and phagocyte foreign materials [2–4].

Pulmonary Defense Mechanisms

An important function of the lungs is to keep itself clean of any foreign material in order to maintain gas exchange. Therefore, the lungs have developed sophisticated mechanisms to remove all kinds of particulate matter. This fact is also an ongoing challenge for inhalation therapies. From the trachea to the terminal air sacs the airway tubes are branched over 23 generations. The first 15 generations provide conducting airways, bronchi and bronchioles, whereas the last eight generations become transformed into the gas exchanging modules, the acini [4]. The repeated branching of the pulmonary tree allows the trapping of inhaled particles via impaction and sedimen-

tation, while inhaled gases are humidified and warmed to body temperature. Mucus on top of a ciliated epithelium is able to capture particles and to transport it via the mucociliary escalator to the oropharynx to be eventually swallowed. Furthermore, the pulmonary epithelium is a tight barrier accompanied by a variety of cells of the innate and adaptive immune system [6].

7.2 Barrier Properties and Transport Mechanisms at the Pulmonary Epithelia

The barrier properties of the pulmonary epithelia are an essential feature of the lungs and are formed as a consequence to the expression of intercellular tight junctions.

Particles and drugs that escape the pulmonary defense mechanisms reach the epithelial surface. By crossing such barrier, they then can be removed from the airspace following cellular internalization and subsequent translocation.

Depending on the substrate, tight polarized epithelia feature different transport mechanisms and pathways, e.g. (Fig. 7.2).

1. passive transcellular diffusion through the membrane (for small, sufficiently lipophilic molecules)
2. paracellular diffusion (for hydrophilic molecules), also depending on the integrity of intercellular junctions
3. transport-mediated uptake via transmembrane proteins serving as pumps or channels
4. catalyzing membrane-associated reactions and vesicular uptake mechanisms, including endocytotic processes
5. efflux systems or metabolism.

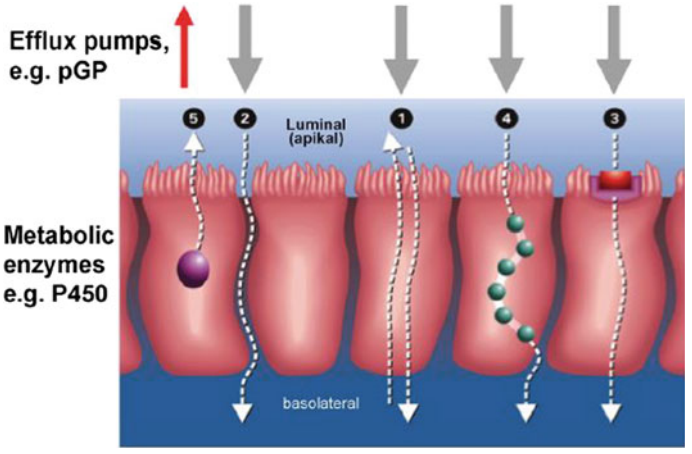

Fig. 7.2 Transport pathways for drugs across an epithelial barrier, taken from [6]

The uptake of nanomaterials by mammalian cells occurs mainly via endocytotic pathways such as pinocytosis and phagocytosis [7]. Besides, paracellular transport through cellular junctions cannot entirely be excluded and has already been proposed to explain the surprisingly high bioavailability of inhaled insulin [8].

However, due to the large diversity of nanomaterials and the limited availability of appropriate techniques to quantify their internalization in a systematic way, cellular uptake of nanomaterials is still poorly understood. The physical interaction of the material with the cell membrane, the material itself, and also the cell type play a significant role [7]. Furthermore, several publications point to the fact that alterations in characteristics of nanomaterials such as the radius of curvature, surface functionalization, size, geometry, and charge, can drastically affect uptake mechanisms and the intracellular fate of nanoparticles [9–13]. Endocytosis however, is not the only possible mechanism of internalization, as physical interactions of cells and nanoparticles may allow particle internalization, such as needle-like materials puncturing cellular membranes for internalization [14]. (See also Chap. 8 Cellular Uptake Mechanisms.)

Translocation from the respiratory tract to the body seems not to be limited to the alveolar part of the lung, but was also described for the upper part at the nasal level. Thereby, nanoparticles may reach the brain through the olfactory bulb. This pathway was reported by Oberdörster and co-workers having observed an accumulation of manganese oxide nanoparticles in the olfactory bulb [15].

The importance of drug transporters in the respiratory tract was underestimated for a long time, although the lungs express high levels of both efflux and uptake transporters. It has been reported, that different tissue and cell populations of the lung have distinct transporter expression patterns [16]. P-glycoprotein (P-gp) and organic cation transporters are among the most investigated ones, but also multi drug resistance proteins (MRP), peptide transporters, and several others have been intensively studied. Although, the recognition and trafficking of numerous small molecule chemotherapeutics or antibiotics by P-gp is nowadays well-described, the protein interaction with nanoparticulate drug carriers is still poorly understood. Recent findings suggest that nanoscale drug carriers incorporating P-gp substrates may benefit through minimization of surface presentation or the incorporation of P-gp inhibiting small molecules [17]. Furthermore, mucoadhesive, drug solubilizing nanoparticles were reported to enable the oral absorption of paclitaxel via the saturation of the P-gp pump by high local drug concentrations and by particle uptake and tight junction opening mechanisms [18]. Recently, Gupta et al. demonstrated that even the function of bacterial efflux pumps can be blocked by metallic nanoparticles which could help to increase the bactericidal effect of conventional antibiotics [19]. This could also be beneficial for the treatment of bacterial lung diseases.

Several cell- and tissue-based in vitro models of epithelial barriers have been developed to identify the mechanisms involved in cell-particle interaction and transport processes, not only from a toxicological point of view [20, 21], but also for the efficacy testing of drugs and nanomedicines [22–24]. Several reviews have already addressed this topic, describing models used either for drug delivery or toxicity of particulate matter [25, 26]. Independent whether safety or efficacy are the focus of

an in vitro study, such model systems allow for a better understanding of the aerosol-lung interactions by focusing on specified factors and endpoints while excluding others. Thereby, mimicking the human lung in the diseased state is challenging, but most helpful to identify novel therapeutic modalities and to evaluate not only their safety, but also efficacy [27]. The final goal would be human cell and tissue models with a validated in vitro–in vivo correlation (IVIVC) in order to predict the clinical performance of innovative formulations and novel drugs while replacing preclinical animal experiments, including all the inherent problems of ethical concerns and species differences. However, due to the complexity of the respiratory tract and the need to administer aerosols, such models appear not within short term reach, but their development is a matter of serious research per se.

7.3 Mucus as Non-cellular Barrier to Particle Transport

7.3.1 Role of Mucus in Health and Disease

A layer of mucus coats the conducting airways of the lungs. The main function of mucus is to condition the inhaled air before it undergoes gas exchange in the alveolar region. Thus, the mucus layer protects the lung epithelium by capturing away a large part of potentially harmful particulates contained in each and every breath. Mucus is synthesized and continuously secreted to the airway lumen by specialized epithelial secretory cells (goblet cells) and by submucosal glands [28]. The luminal mucus layer is in turn continuously propelled out of the lungs by the coordinated beating of the cilia located in the apical side of epithelial cells, featuring an extremely efficient clearance mechanism also termed mucociliary clearance [29, 30].

During the breathing process, the air-flow is highly turbulent in the trachea and main bronchi, and reduces its turbulence along the conducting airways, as the airway caliber is reduced, reaching the alveoli in a rather laminar flow regime [31]. Under the turbulent flow regime, the air movement occurs in all directions, both perpendicular and parallel to the airways, forcing the particles contained within the inhaled air to impact against the mucus-covered walls of the airways. Therefore, inhaled micro- and nanoparticles are somehow forced to interact with the mucus layer, increasing their chance to be adsorbed, entrapped and cleared out of the lungs.

Mucus entraps particles mainly by two mechanisms: on the one hand, mucus forms a complex interconnected 3D macromolecular network with a finite pore size, which acts as a physical barrier to inhaled particles (size filtering) [32]. On the other hand, mucus can establish different chemical interactions with foreign particles due to the wide variety of functional groups occurring in a mucous gel (interaction filtering) [33]. Both mechanisms are in any case governed by the complex chemical composition of mucus (Fig. 7.3).

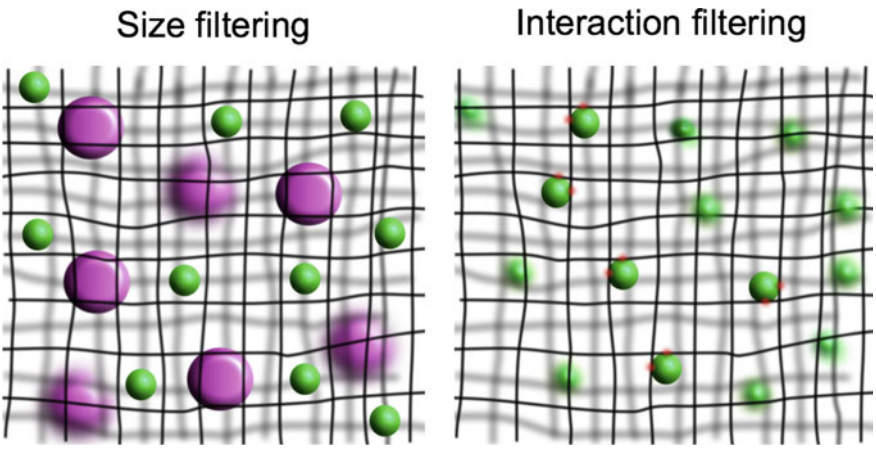

Fig. 7.3 Mucus can entrap nanoparticles mainly by two mechanisms: on the one hand, those particles with a bigger size than the mesh-spacing will be sterically hindered by the 3D network, size filtering (left). On the other hand, mucus can adsorb nanoparticles due to great array of functional groups contained in a mucus hydrogel, interaction filtering (right). Taken from [33]

Pulmonary mucus is a hydrogel composed mainly of water (95%), mucins (glycoproteins), salts, non-mucin proteins, lipids, DNA, and cell debris [34]. Among the organic constituents of mucus, mucins are the most relevant macromolecules, which are responsible for the formation of the interconnected molecular network that confers the mucus its characteristic viscoelastic properties [35]. The mucins are a class of glycoproteins present in all mucous gels across all human mucosal tissues (gastrointestinal and vaginal tract, airways and eyes) [33, 36, 37]. In the airways, the predominant gel-forming mucins are MUC5AC and MUC5B, which are synthesized and secreted by goblet cells and by submucosal glands, respectively [28, 38, 39].

Mucins are composed of a polypeptide backbone that displays highly glycosylated hydrophilic regions, hydrophobic globular structures, and cysteine rich regions [40–43]. The glycan component of mucin glycoproteins may account for up to 80% of the total mass of the macromolecules [44] and often display sialic acid and sulfated N-acetylgalactosamine or galactose as terminal residues of the oligosaccharide chains, conferring to mucus a net negative charge at physiological pH [45]. The non-glycosylated globular regions of the polypeptide backbone provide interaction sites for hydrophobic molecules. Both terminal flanks of mucins contain cysteine-rich regions, which serve to establish intermolecular disulfide bonds [43], creating a cross-linked macromolecular network that gives the airway mucus its characteristic viscoelastic trait [34, 46, 47]. A precise regulation of mucus viscoelasticity is of capital importance for the proper function of the unidirectional mucociliary clearance.

In disease states such as asthma, chronic obstructive pulmonary disease, or cystic fibrosis (CF), an imbalance of the mucus constituents can significantly compromise not only the mucus clearance but also the overall pulmonary function [48–50]. The

case of CF is paradigmatic to illustrate the life-threating consequences associated to the dysfunction of the mucociliary machinery. CF is a congenital disease derived from the mutation of the gene encoding for a chloride channel CF transmembrane conductance regulator (CFTR) [49]. The primary consequence of this mutation is a water imbalance of the mucus gel, which dramatically increases its viscosity, leading to the impairment of the mucociliary clearance. In the absence of an efficient clearance mechanism, mucus can be rapidly colonized by pathogens, which will in turn elicit the immune response of the host. The overall mucus viscosity is further increased (more stiff mucus) as a consequence of mucin hypersecretion [51], the establishment of additional inter- as well as intra-mucin disulfide bonds due to oxidative stress [52], and by the formation of parallel actin and DNA networks derived from the accumulation of apoptotic neutrophils [53].

7.3.2 Mucus-Particle Interactions are Primarily Governed by Particle Size and Surface Chemistry

The first consideration to be made when discussing the inhalation of particles (also including nanopartciles, NPs), both accidental (toxicology) or on purpose (pharmaceutical application), is that a great fraction will unavoidably deposit in the conducting airways. The fate of these particles will then mostly depend on their interaction with the mucus, which in turn will be governed by their size, shape, and surface chemistry.

The 3D network built by the mucins and other mucus components sets a size-dependent physical barrier to micro- and NPs. Mucous gels are rather inhomogeneous and riddled with pores ranging from few nanometers to larger voids in the micrometer size range [54]. Electron microscopy studies revealed a mean pore-size for CF sputum ranging between 100 and 400 nm [55]. The mesh-spacing of mucus has also been investigated by dispersing NPs in tracheal mucus and tracking their displacement over time [56]. Schuster et al. determined the mean squared displacement of 100, 200, and 500 nm stealth particles coated with a dense layer of polyethylene glycol (PEG) after dispersing them in human tracheal mucus [34]. They found that 500 nm particles were almost completely immobilized by the mucus mesh. Nevertheless, PEGylated (“muco-inert”) 100 and 200 nm particles could diffuse through undiluted human tracheal mucus, indicating that with the appropriate surface coating NPs with a diameter up to at least 200 nm could diffuse through airway mucus. Our investigations in this direction have taken into account not only the movement of NPs within mucus, after their mechanical dispersion, but also their penetration into mucus after aerosol deposition [54, 57, 58]. In this regard, we have observed a size-limited penetration into mucus of NPs deposited at the air-mucus interface after aerosol delivery, which is limited to NPs with a diameter below 100 nm, suggesting that pores at the air-mucus interface are either smaller or absent.

The small size of NPs alone, however, does not grant their effective diffusion through mucus. As previously mentioned, mucus also represents an interactive diffusion barrier featured by net negative charge, a wide array of functional groups (hydroxyl, carboxylic, sulfate, and amide groups, among others), as well as by the "naked" peptidic globular motifs that provide interaction sites for hydrophobic compounds [33]. For instance, hydrophobic polystyrene NPs with a diameter of 200 nm are avidly adsorbed and immobilized by mucins [34, 58, 59, 60], whereas the same NPs, modified with a dense PEG surface-coating that renders them hydrophilic, can diffuse unimpeded through the pores of mucus [34]. Bhattacharjee et al. have recently demonstrated that cationic NPs with a diameter of just 10 nm are almost completely immobilized by mucus [61], highlighting the fact that even at a relatively small NP size scales, the interaction with the mucus components will depend on the surface chemistry of the NPs.

7.3.3 Considerations for Drug Delivery to the Airways

Nanomedicine has a great potential to optimize the currently available treatments of a number of pulmonary diseases affecting the lungs. NP-mediated drug delivery may, in the near future, enable the efficient pulmonary delivery of poorly soluble drugs, including anti-infectives and anti-cancer drugs, nucleic acids, and other active pharmaceutical ingredients [62–64].

Besides the challenges in aerosol technology to efficiently deposit nanopharmaceuticals in the airways, it is important to achieve sufficient mucus penetration in order to elicit the intended therapeutic effect at the bronchial tissue. For instance, if nucleic acid-delivery is the pursued goal, the nanocarriers will need to overcome the mucus gel layer first, which has a height ranging between 10 and 100 μm [65–67], before crossing the cell membrane and reaching certain intracellular targets. On the other hand, if an antibiotic is encapsulated in a nanocarrier to treat an extracellular airway infection, a mild penetration of the mucus layer coupled with a controlled and sustained release mechanism may suffice to achieve the desired therapeutic effect.

Several strategies have been developed to deliver nanopharmaceuticals to mucus-coated epithelia. To achieve an efficient NP mucopenetration it is necessary to comply with the strict pore-size of the mucin network, yet displaying a stealth NP surface that will further reduce the chemical interaction between NPs and mucus. PEGylation was originally designed to increase the systemic circulation time of proteins and NPs [68], and has been successfully implemented for NP-mediated mucosal drug delivery [69, 70]. Generally, PEGylated NPs diffuse faster through mucus compared to their non-PEGylated equivalents. A shortcoming of NP PEGylation, however, is that it might as well reduce cell-NP interactions precluding their cellular uptake. Zwitterionic NPs, which alternate positive and negative charges on their surface, have shown good penetration of gastro-intestinal mucus, yet showing an acceptable cellular uptake [71].

Mucolytic agents can also be used to increase the mucus penetration of NP-based drug delivery systems, in particular in diseases where the viscoelasticity of mucus is dramatically altered. For instance, N-acetyl cysteine (NAC), which cleaves the inter-mucin disulfide bonds [72], and rhDNase (cleaves DNA), are routinely prescribed to CF patients in order to manage the viscous mucus secretions associated to the disease [73]. Suk et al. have demonstrated the feasibility of delivering highly compacted DNA NPs in combination with NAC. In this study a significantly higher NP diffusivity through mucus could be observed if the NPs were delivered in combination with the mucolytic agent [74]. Alternatively, the surface of the NPs can be decorated with mucolytic molecules in order to enhance their mucopenetration [75, 76].

The "sticky" nature of mucus has also been exploited for drug delivery purposes. Mucoadhesion intentionally seeks the chemical interaction between NPs and mucus in an attempt to prolong the residence time of NPs in the mucosa [77]. Mucoadhesion can be achieved by coating the NPs with cationic molecules [78, 79], with reactive thiol groups (-SH, thiomers) [80], or with polymers that will further enable physical chain entanglements with mucins [81].

As a last consideration for the therapeutic delivery of particles to the lungs, it is noteworthy to highlight that mucociliary clearance is a highly dynamic process which sets a limited time-window for drug delivery. The tracheal mucociliary clearance rates have been reported to range between 2 and 16 mm/min in humans and other animal species [82–86], which significantly limits the residence time of therapeutic NPs in the airways to just a few hours.

7.4 Surfactant as Outermost Element of the Pulmonary Air-Liquid Interface

7.4.1 Role of Surfactant in Health and Disease

The reduction of surface tension at the air-liquid interface by so-called "surfactants" is found in different species with inflating/deflating organs such as the swim bladder of gold fishes or the respiratory tract of reptiles and mammalians [87]. This chapter focuses on the composition and function of human pulmonary surfactant. Pulmonary surfactant is localized on top of the alveolar lining fluid at the air-liquid phase. In mammalians it is synthesized by ATII and has two important functions: reducing surface tension and supporting the immune system [88, 89].

The structure and composition of the pulmonary surfactant is pivotal to comply with the permanently changing alveolar radius and surface area during inhalation and exhalation, allowing to maintain near-zero minimal surface tension at the air-liquid interface [90]. The changing alveolar surface area challenges the surfactant with three important requirements: (i) a fast re-extension into the interface upon expansion, (ii) a change from a 2D layer to 3D structures during compression, and (iii) an interfacial adsorption from bilayers [91]. The approximately 90% lipids and 10%

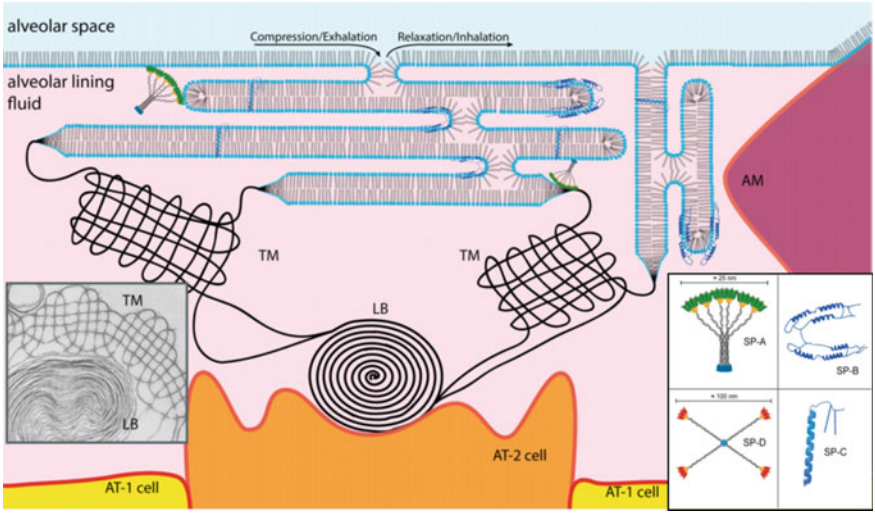

Fig. 7.4 Scheme of pulmonary surfactant and its organization. Lamellar bodies including surfactant are secreted by alveolar type II cells. The LBs form a tubular myelin network which acts as a reservoir for the surfactant film at the air-liquid interface. The surfactant needs to expand during inhalation and be compressed during exhalation. This process is possible due to a complex folding which is supported by the surfactant proteins (mainly the hydrophobic SP-B and SP-C). SP-A and SP-D are associated with an immune defense role. The figure was modified and adopted from [98]

proteins address this challenge by a 3D structured interplay of lipids and proteins. From the four lung associated surfactant proteins (SP) two are hydrophobic (SP-B, SP-C) and two are hydrophilic (SP-A, SP-D). SP-B and SP-C play an important role in "folding" and "de-folding" of the surfactant layer during compression and expansion [92, 93]. SP-A and SP-D are associated with the pulmonary immune defense and have a regulatory and opsonizing function [94]. All proteins contribute to alveolar surfactant homeostasis.

Alveolar surfactant homeostasis is of utmost importance as either a lack or an overproduction of surfactant will lead to respiratory distress. New pulmonary surfactant is synthesized in form of lamellar bodies (LB) which are secreted into the alveolar space. An intact transport-associated protein, the ATP binding cassette sub-family A member 3 (ABCA3), is required for this secretion. Once secreted, the LBs form an organized tubular myelin (TM) network which acts as a surfactant source for covering the air-liquid interface. SP-B is essential for the formation of LBs and the TM network [95] as illustrated in Fig. 7.4. The synthesis of new surfactant is relatively slow and consumes resources and energy, in consequence most of the surfactant (70–80%) is recycled by ATII cells and/or degraded by macrophages [96, 97].

Diseases caused by a lack or abundance of surfactant are usually associated with respiratory distress. Surfactant absence can occur, for example, in (preterm) neonates as consequence of a missing differentiation of ATII cells and is usually treated with exogenous, animal-derived surfactant [99]. Pulmonary alveolar proteinosis (PAP) is

a rare disease which is characterized by an abnormal presence of pulmonary surfactant (or its composition) and has different forms. These were currently reviewed by Lopez-Rodriguez et al. and Griese [95, 100]. The disease manifestation is age dependent and associated with a defect in surfactant synthesis or alveolar homeostasis. Genetic mutations of the gene encoding SP-B, SP-C or ABCA3 occur during the neonatal period and are life-threatening. Most adult patients with PAP suffer from an auto-immune response characterized by neutralizing antibodies against granulocyte/macrophage colony stimulating factor (GM-CSF). GM-CSF is required for the differentiation and function such as phagocytosis of alveolar macrophages. The consequence of this auto-immune disease is an enrichment of surfactant in the alveolar space [101].

7.4.2 Inhaled Particles—Interactions with Surfactant as a Defense Mechanisms and Transport Facilitator

Our environment contains airborne particles such as pathogens [102] or solid materials (e.g. dust). The human lung is designed to resist such foreign inhaled compounds. The interaction of particles and surfactant as "the first contact" in the alveoli depends on physical-chemical properties of the inhaled particle [103]. Thus, a hydrophilic particle might first interact with hydrophilic proteins while a hydrophobic particle first interacts with lipids before a multilayer of proteins and lipids forms the final corona. Raesch et al. investigated the corona of three different nanoparticles (PEG-, PLGA- and lipid nanoparticles) after incubating them in porcine alveolar surfactant and found similarly composed corona even for particles made of different materials (Fig. 7.5) [104]. The particle corona facilitates the uptake in immune cells such as alveolar macrophage phagocytosis and supports in consequence lung clearance [105, 106].

However, the surfactant corona may not always suffice to mask the differences between (nano-) particles, especially in case of diseases such as allergies. Wiemann et al. compared zirconium oxide (ZrO_2) nanoparticles coated with tetraoxidecanoic acid (TODS) or acrylic acid (Acryl) in rats. They found accumulation of both particles mainly in macrophages and in a small range in neutrophilic granulocytes, underscoring the assimilating function of the surfactant corona. Inflammation signs in rats were dose dependent, and only minor differences of both different coated particles were found. They further investigated the both mentioned particles and two additional coatings, polyethyleneglycol (PGA) and aminopropilsilane (APTS) in albumin-sensitized and non-sensitized mice. Interestingly, they found relevant differences for the sensitized allergic mouse model but not for the control group. They conclude that the surface functionalization has minor effects on the inflammatory lung response in healthy mice and rats, but the surface modification is relevant for individuals suffering from allergies [107]. This highlights the need for considering the individual biological (cellular) environment and the particle properties. This is get-

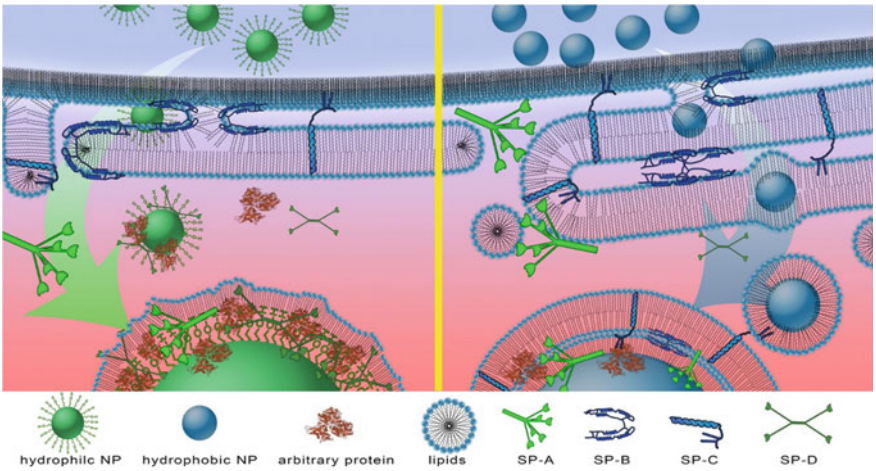

Fig. 7.5 The scheme illustrates the surfactant corona formation of hydrophobic and hydrophilic particles. Reprinted from [104]

ting even more complex when considering age-dependent changes in surfactant and alveolar homeostasis [108] or the influence of individual habits such as smoking [89].

Beside the view from the alveolar perspective on the entering particle, less is known about effects on stability of the pulmonary surfactant corona on (nano-) particles as the surface properties are crucial to prevent particle agglomeration. The OECD guideline "dispersion stability of nanomaterials in simulated environmental media" already addresses the importance of an aqueous environment (OECD 2017), but currently still neglects the potential role of surfactant. Adding surfactant towards such biosimilar dispersion media might allow for a more realistic particle characterization and thus to better predict their biological effects.

Interestingly enough, the presence of the surfactant proteins SP-A and SP-D is not limited to the lungs, but they have been reported also for other mucosal epithelia [109]. This may be particularly important for our immune system to cope with airborne biological particles such as fungi, bacteria and viruses which are regularly inhaled [102]. As part of the innate and adaptive immune system they opsonize particles/pathogens, inhibit their growth, facilitate phagocytosis and regulate cytokine levels. Details on these interactions are reviewed by Nayak et al. and Han et al. [110, 111].

7.5 Implications for Particle-Based Pulmonary Drug Delivery

Due to the excellent progress in aerosol science and technology, the efficient and reproducible deposition of oral inhalation drug products is nowadays well feasi-

ble. Since the introduction of the first pressurized metered dose inhaler (MDI) by Riker Laboratories, Inc. (now 3 M Drug Delivery Systems) in 1956 [112], inhalation aerosols have surged as an own branch of the pharmaceutical industry. While the classical three pillars of aerosol generation had been nebulizers, MDI's and dry powder inhalers, exciting innovations have been introduced, which span from rather simple low-cost solutions to advanced high-tech devices, which such as e.g. Boehringers Respimat® Soft Mist™ Inhaler [113]. As a pocket-size device that allows to generate a single-breath aerosol by nebulizing a metered dose of an aqueous drug solution, it may be considered as a hybrid of the classical device concepts. At the same time, quite some research had been invested in the design and manufacturing of particles with improved aerodynamic properties. As an example, the concept of large porous particles [114] may be mentioned here, which allows deep-lung deposition of particles much larger than 10 μm. This has interesting implications both for the biological (e.g. reduced macrophage clearance) as well as for the technological properties (e.g. less agglomeration) of such inhalable materials. By incorporating nanoparticles into microparticles or droplets with adequate aerodynamic properties, which disintegrate and release their cargo after deposition on the pulmonary lining fluid, effective delivery of nanocarriers to the alveolar epithelium is essentially well feasible [115].

In the light of this progress, pulmonary drug delivery is actually undergoing some shift of paradigm: While generating inhalable aerosols is still pivotal, current research efforts are now more addressing the question of what actually happens to an aerosol particle after it has landed in the lung. This means that questions of particle clearance, drug dissolution, epithelial permeability and eventually controlled drug release from a carrier particle meanwhile come into the picture. Pulmonary drug delivery is no longer dealing with "naked" molecules, to be aerosolized aqueous solution or as some rapidly dissolving lactose carrier.

Depending on the therapeutic needs of contemporary aerosol medicines, the following three scenarios may represent the goal of a given pharmaceutical development:

1. Rapid dissolution and release of the active compound in order to facilitate fast absorption and complete bioavailability; this holds for small molecules intended for local action in the lung such as e.g., betamimetics, corticosteroids
2. Facilitated transport of poorly permeable compounds across the rather tight alveolar epithelium. This applies for macromolecular biopharmaceuticals such as peptides (e.g. insulin), proteins (e.g. antibodies), and all kinds of future gene therapeutics (siRNA, mRNA, etc.)
3. Pulmonary controlled release systems aim to maintain higher drug concentrations in the pulmonary lining fluid over a longer period of time. This could be useful to reduce the dosing frequency of inhaled drugs for either local or systemic action which might be particularly attractive for inhaled anti-infectives. Due to the effective clearance mechanisms of the lungs for particles, however, developing such systems is challenging, but there are first examples that have reached the stage of clinical evaluation (e.g. ciprofloxacin: ORBIT-3 NCT01515007; and ORBIT-4 NCT02104245).

Like for other routes of drug delivery, the physicochemical and pharmacokinetic properties of the molecule to be delivered are quite decisive for the formulation. The typical divide between small organic molecules and macromolecular biopharmaceutical also applies for their pulmonary delivery. Besides, it is important to distinguish between local ("air-to-lung") or systemic ("air-to blood") delivery. While macromolecular biopharmaceuticals will probably require some nanotechnology-based carrier to enable their delivery at all, novel small molecules notoriously tend to suffer from poor solubility in physiological media. In consequence, there is a previously somewhat neglected need for adequate dissolution testing of aerosol powders [116]. In view of several parallels, but also distinct differences to oral drug delivery, the concept of a pulmonary biopharmaceutical classification system (pBSC) has emerged and its scope and relevance is subject of interesting ongoing discussions [6]. Overall, in vitro testing of orally inhaled products is becoming an increasingly important science-based regulatory issue [117], which must not only address the aerosol aspects, but also the biological barriers to be overcome in pulmonary drug delivery.

References

1. Rackley, C.R., Stripp, B.R.: Building and maintaining the epithelium of the lung. J. Clin. Investig. **122**, 2724–2730 (2012)
2. Besnard, V., Whitsett, J.A.: Chapter 73—Tissue engineering for the respiratory epithelium: cell-based therapies for treatment of lung disease A2—Lanza, Robert. In: Langer, R., Vacanti, J. (eds.) Principles of Tissue Engineering, 4th edn., pp. 1543–1560. Academic Press, Boston (2014)
3. Crapo, J.D., Barry, B.E., Gehr, P., et al.: Cell number and cell characteristics of the normal human lung. Am. Rev. Respir. Dis. **126**, 332–337 (1982)
4. Weibel, E.R.: Lung morphometry: the link between structure and function. Cell Tissue Res. **367**, 413–426 (2017)
5. Klein, S.G., Hennen, J., Serchi, T., et al.: Potential of coculture in vitro models to study inflammatory and sensitizing effects of particles on the lung. Toxicol. In Vitro **25** (2011)
6. Hastedt, J.E., Bäckman, P., Clark, A.R., et al.: Scope and relevance of a pulmonary biopharmaceutical classification system. In: AAPS/FDA/USP Workshop March 16–17th, 2015 in Baltimore, MD. AAPS Open 2:1 (2016)
7. Bourquin, J., Milosevic, A., Hauser, D., et al.: Biodistribution, clearance, and long-term fate of clinically relevant nanomaterials. Adv. Mater. (Deerfield Beach, Fla.) (2018)
8. Patton, J.S., Byron, P.R.: Inhaling medicines: delivering drugs to the body through the lungs. Nat. Rev. Drug Discov. **6**, 67–74 (2007)
9. Herd, H., Daum, N., Jones, A.T., et al.: Nanoparticle geometry and surface orientation influence mode of cellular uptake. ACS Nano **7**, 1961–1973 (2013)
10. Hillaireau, H., Couvreur, P.: Nanocarriers' entry into the cell: relevance to drug delivery. Cell. Mol. Life Sci. CMLS **66**, 2873–2896 (2009)
11. Puisney, C., Baeza-Squiban, A., Boland, S.: Mechanisms of uptake and translocation of nanomaterials in the lung. Adv. Exp. Med. Biol. **1048**, 21–36 (2018)
12. Rivera-Gil, P., Jimenez De Aberasturi, D., Wulf, V., et al.: The challenge to relate the physicochemical properties of colloidal nanoparticles to their cytotoxicity. Acc. Chem. Res. **46**, 743–749 (2013)

13. Vercauteren, D., Vandenbroucke, R.E., Jones, A.T., et al.: The use of inhibitors to study endocytic pathways of gene carriers: optimization and pitfalls. Mol. Ther. J. Am. Soc. Gene Ther. **18**, 561–569 (2010)
14. Doshi, N., Mitragotri, S.: Needle-shaped polymeric particles induce transient disruption of cell membranes. J. R. Soc. Interface **7**(Suppl 4), S403–410 (2010)
15. Elder, A., Gelein, R., Silva, V., et al.: Translocation of inhaled ultrafine manganese oxide particles to the central nervous system. Environ. Health Perspect. **114**, 1172–1178 (2006)
16. Nickel, S., Clerkin, C.G., Selo, M.A., et al.: Transport mechanisms at the pulmonary mucosa: implications for drug delivery. Expert Opin. Drug Deliv. **13**, 667–690 (2016)
17. Dreaden, E.C., Raji, I.O., Austin, L.A., et al.: P-glycoprotein-dependent trafficking of nanoparticle-drug conjugates. Small **10**, 1719–1723 (2014)
18. Soundararajan, R., Sasaki, K., Godfrey, L., et al.: Direct in vivo evidence on the mechanism by which nanoparticles facilitate the absorption of a water insoluble, P-gp substrate. Int. J. Pharm. **514**, 121–132 (2016)
19. Gupta, D., Singh, A., Khan, A.U.: Nanoparticles as efflux pump and biofilm inhibitor to rejuvenate bactericidal effect of conventional antibiotics. Nanoscale Res. Lett. **12**, 454 (2017)
20. Kasper, J.Y., Feiden, L., Hermanns, M.I., et al.: Pulmonary surfactant augments cytotoxicity of silica nanoparticles: studies on an in vitro air-blood barrier model. Beilstein J. Nanotechnol. **6**, 517–528 (2015)
21. Rothen-Rutishauser, B.M., Kiama, S.G., Gehr, P.: A three-dimensional cellular model of the human respiratory tract to study the interaction with particles. Am. J. Respir. Cell Mol. Biol. **32**, 281–289 (2005)
22. Hittinger, M., Mell, N.A., Huwer, H., et al.: Autologous co-culture of primary human alveolar macrophages and epithelial cells for investigating aerosol medicines. Part II: Evaluation of IL-10-loaded microparticles for the treatment of lung inflammation. ATLA Altern. Lab. Anim. **44**, 349–360 (2016)
23. Ong, H.X., Benaouda, F., Traini, D., et al.: In vitro and ex vivo methods predict the enhanced lung residence time of liposomal ciprofloxacin formulations for nebulisation. Eur. J. Pharm. Biopharm. Off. J. Arbeitsgemeinschaft fur Pharmazeutische Verfahrenstechnik e.V **86**, 83–89 (2014)
24. Salomon, J.J., Muchitsch, V.E., Gausterer, J.C., et al.: The cell line NCl-H441 is a useful in vitro model for transport studies of human distal lung epithelial barrier. Mol. Pharm. **11**, 995–1006 (2014)
25. De Souza Carvalho, C., Daum, N., Lehr, C.M.: Carrier interactions with the biological barriers of the lung: advanced in vitro models and challenges for pulmonary drug delivery. Adv. Drug Deliv. Rev. **75**, 129–140 (2014)
26. Muller, L., Riediker, M., Wick, P., et al.: Oxidative stress and inflammation response after nanoparticle exposure: differences between human lung cell monocultures and an advanced three-dimensional model of the human epithelial airways. J. R. Soc. Interface **7**(Suppl 1), S27–40 (2010)
27. Hittinger, M., Juntke, J., Kletting, S., et al.: Preclinical safety and efficacy models for pulmonary drug delivery of antimicrobials with focus on in vitro models. Adv. Drug Deliv. Rev. **85**, 44–56 (2015)
28. Zhu, Y., Chidekel, A., Shaffer, T.H.: Cultured human airway epithelial cells (Calu-3): a model of human respiratory function, structure, and inflammatory responses. Crit. Care Res. Pract. **2010**, 1–8 (2010)
29. Knowles, M.R., Boucher, R.C.: Mucus clearance as a primary innate defense mechanism for mammalian airways. J. Clin. Investig. **109**, 571–577 (2002)
30. Wanner, A., Salathé, M., O'riordan, T.G.: Mucociliary clearance in the airways. Am. J. Respir. Crit. Care Med. **154**, 1868–1902 (1996)
31. Leff, A.R., Schumacker, P.T.: Respiratory physiology: basics and applications (1993)
32. Lieleg, O., Ribbeck, K.: Biological hydrogels as selective diffusion barriers. Trends Cell Biol. **21**, 543–551 (2011)

33. Murgia, X., Loretz, B., Hartwig, O., et al.: The role of mucus on drug transport and its potential to affect therapeutic outcomes. Adv. Drug Deliv. Rev. **124**, 82–97 (2018)
34. Schuster, B.S., Suk, J.S., Woodworth, G.F., et al.: Nanoparticle diffusion in respiratory mucus from humans without lung disease. Biomaterials **34**, 3439–3446 (2013)
35. Lillehoj, E.P., Kim, K.C.: Airway mucus: its components and function. Arch. Pharmacal. Res. **25**, 770 (2002)
36. Lai, S.K., Wang, Y.-Y., Hida, K., et al.: Nanoparticles reveal that human cervicovaginal mucus is riddled with pores larger than viruses. Proc. Natl. Acad. Sci. U.S.A. **107**, 598–603 (2010)
37. Taylor, C., Allen, A., Dettmar, P.W., et al.: The gel matrix of gastric mucus is maintained by a complex interplay of transient and nontransient associations. Biomacromolecules **4**, 922–927 (2003)
38. Lillehoj, E.P., Kato, K., Lu, W., et al.: Cellular and molecular biology of airway mucins. Int. Rev. Cell Mol. Biol. **303**, 139–202 (2013)
39. Wickström, C., Davies, J.R., Eriksen, G.V., et al.: MUC5B is a major gel-forming, oligomeric mucin from human salivary gland, respiratory tract and endocervix: identification of glycoforms and C-terminal cleavage. Biochem. J. **334**(Pt 3), 685–693 (1998)
40. Bansil, R., Turner, B.S.: Mucin structure, aggregation, physiological functions and biomedical applications. Curr. Opin. Colloid Interface Sci. **11**, 164–170 (2006)
41. Perez-Vilar, J., Hill, R.L.: The structure and assembly of secreted mucins. J. Biol. Chem. **274**, 31751–31754 (1999)
42. Thornton, D.J., Sheehan, J.K.: From mucins to mucus. Proc. Am. Thorac. Soc. **1**, 54–61 (2004)
43. Turner, B.S., Bhaskar, K.R., Hadzopoulou-Cladaras, M., et al.: Cysteine-rich regions of pig gastric mucin contain von Willebrand factor and cystine knot domains at the carboxyl terminal1. The sequences described in this paper have been submitted to the GenBank Nucleotide Sequence Database, and have been assigned the Ge. Biochim. Biophys. Acta (BBA) Gene Struct. Expr. **1447**, 77–92 (1999)
44. Boegh, M., Nielsen, H.M.R.: Mucus as a barrier to drug delivery—understanding and mimicking the barrier properties. Basic Clin. Pharmacol. Toxicol. **116**, 179–186 (2015)
45. Murgia, X., De Souza Carvalho, C., Lehr, C.-M.: Overcoming the pulmonary barrier: new insights to improve the efficiency of inhaled therapeutics. Eur. J. Nanomed. **6**, 157–169 (2014)
46. Murgia, X., Yasar, H., Carvalho-Wodarz, C., et al.: Modelling the bronchial barrier in pulmonary drug delivery: a human bronchial epithelial cell line supplemented with human tracheal mucus. Eur. J. Pharm. Biopharm. **118**, 79–88 (2017)
47. Rubin, B.K., Ramirez, O., Zayas, J.G., et al.: Collection and analysis of respiratory mucus from subjects without lung disease. Am. Rev. Respir. Dis. **141**, 1040–1043 (1990)
48. Balsamo, R., Lanata, L., Egan, C.G.: Mucoactive drugs. Eur. Respir. Rev. **19**, 127–133 (2010)
49. Elborn, J.S.: Cystic fibrosis. The Lancet **388**, 2519–2531 (2017)
50. Ramos, F.L., Krahnke, J.S., Kim, V.: Clinical issues of mucus accumulation in COPD. Int. J. COPD 139–150 (2014)
51. Kreda, S.M., Davis, C.W., Rose, M.C.: CFTR, mucins, and mucus obstruction in cystic fibrosis. Cold Spring Harbor Perspect. Med. **2**, a009589 (2012)
52. Yuan, S., Hollinger, M., Lachowicz-Scroggins, M.E., et al.: Oxidation increases mucin polymer cross-links to stiffen airway mucus gels. Sci. Transl. Med. 7:276ra227–276ra227 (2015)
53. Perks, B., Shute, J.K.: DNA and actin bind and inhibit interleukin-8 function in cystic fibrosis sputa. Am. J. Respir. Crit. Care Med. **162**, 1767–1772 (2000)
54. Kirch, J., Schneider, A., Abou, B., et al.: Optical tweezers reveal relationship between microstructure and nanoparticle penetration of pulmonary mucus. Proc. Natl. Acad. Sci. U.S.A. **109**, 18355–18360 (2012)
55. Sanders, N.N., De Smedt, S.C., Van Rompaey, E., et al.: Cystic fibrosis sputum. Am. J. Respir. Crit. Care Med. **162**, 1905–1911 (2000)
56. Schuster, B.S., Ensign, L.M., Allan, D.B., et al.: Particle tracking in drug and gene delivery research: state-of-the-art applications and methods. Adv. Drug Deliv. Rev. **91**, 70–91 (2015)

57. Kirch, J., Guenther, M., Doshi, N., et al.: Mucociliary clearance of micro- and nanoparticles is independent of size, shape and charge—an ex vivo and in silico approach. J. Control. Release **159**, 128–134 (2012)
58. Murgia, X., Pawelzyk, P., Schaefer, U.F., et al.: Size-limited penetration of nanoparticles into porcine respiratory mucus after aerosol deposition. Biomacromolecules **17**, 1536–1542 (2016)
59. Nordgård, C.T., Nonstad, U., Olderøy, M.Ø., et al.: Alterations in mucus barrier function and matrix structure induced by guluronate oligomers. Biomacromol **15**, 2294–2300 (2014)
60. Suk, J.S., Xu, Q., Kim, N., et al.: PEGylation as a strategy for improving nanoparticle-based drug and gene delivery. Adv. Drug Deliv. Rev. **99**, 28–51 (2016)
61. Bhattacharjee, S., Mahon, E., Harrison, S.M., et al.: Nanoparticle passage through porcine jejunal mucus: microfluidics and rheology. Nanomed. Nanotechnol. Biol. Med. **13**, 863–873 (2017)
62. Beisner, J., Dong, M., Taetz, S., et al.: Nanoparticle mediated delivery of 2′-O-methyl-RNA leads to efficient telomerase inhibition and telomere shortening in human lung cancer cells. Lung Cancer **68**, 346–354 (2017)
63. Kuzmov, A., Minko, T.: Nanotechnology approaches for inhalation treatment of lung diseases. J. Control. Release **219**, 500–518 (2015)
64. Mahiny, A.J., Dewerth, A., Mays, L.E., et al.: In vivo genome editing using nuclease-encoding mRNA corrects SP-B deficiency. Nat. Biotech. **33**, 584–586 (2015)
65. Duneclift, S., Wells, U., Widdicombe, J.: Estimation of thickness of airway? Surface liquid in ferret trachea in vitro estimation of thickness of airway surface liquid in ferret trachea in vitro. 761–767 (2012)
66. Widdicombe, J.H.: Regulation of the depth and composition of airway surface liquid. J. Anat. **201** (2002)
67. Yoneda, K.: Mucous blanket of rat bronchus. Am. Rev. Respir. Dis. **114**, 837–842 (1976)
68. Abuchowski, A., Mccoy, J.R., Palczuk, N.C., et al.: Effect of covalent attachment of polyethylene glycol on immunogenicity and circulating life of bovine liver catalase. J. Biol. Chem. **252**, 3582–3586 (1977)
69. Huckaby, J.T., Lai, S.K.: PEGylation for enhancing nanoparticle diffusion in mucus. Adv. Drug Deliv. Rev. (2017)
70. Schneider, C.S., Xu, Q., Boylan, N.J., et al.: Nanoparticles that do not adhere to mucus provide uniform and long-lasting drug delivery to airways following inhalation. Sci. Adv. **3** (2017)
71. Shan, W., Zhu, X., Tao, W., et al.: Enhanced oral delivery of protein drugs using zwitterion-functionalized nanoparticles to overcome both the diffusion and absorption barriers. ACS Appl. Mater. Interfaces **8**, 25444–25453 (2016)
72. Vukosavljevic, B., Murgia, X., Schwarzkopf, K., et al.: Tracing molecular and structural changes upon mucolysis with N-acetyl cysteine in human airway mucus. Int. J. Pharm. **553**, 373–376 (2017)
73. Rubin, B.K.: Secretion properties, clearance, and therapy in airway disease. Transl. Respir. Med. **2**, 6 (2014)
74. Suk, J.S., Boylan, N.J., Trehan, K., et al.: N-acetylcysteine enhances cystic fibrosis sputum penetration and airway gene transfer by highly compacted DNA nanoparticles. Mol. Ther. **19**, 1981–1989 (2011)
75. Deacon, J., Abdelghany, S.M., Quinn, D.J., et al.: Antimicrobial efficacy of tobramycin polymeric nanoparticles for Pseudomonas aeruginosa infections in cystic fibrosis: formulation, characterisation and functionalisation with dornase alfa (DNase). J. Control. Release **198**, 55–61 (2015)
76. Dünnhaupt, S., Kammona, O., Waldner, C., et al.: Nano-carrier systems: strategies to overcome the mucus gel barrier. Eur. J. Pharm. Biopharm. **96**, 447–453 (2015)
77. Mathiowitz, E., Chickering III, D.E., Lehr, C.-M.: Bioadhesive drug delivery systems: fundamentals, novel approaches, and development. **696** (1999)
78. Bravo-Osuna, I., Vauthier, C., Farabollini, A., et al.: Mucoadhesion mechanism of chitosan and thiolated chitosan-poly(isobutyl cyanoacrylate) core-shell nanoparticles. Biomaterials **28**, 2233–2243 (2007)

79. Schipper, N.G.M., Vårum, K.M., Stenberg, P., et al.: Chitosans as absorption enhancers of poorly absorbable drugs. Eur. J. Pharm. Sci. **8**, 335–343 (1999)
80. Iqbal, J., Shahnaz, G., Dünnhaupt, S., et al.: Preactivated thiomers as mucoadhesive polymers for drug delivery. Biomaterials **33**, 1528–1535 (2012)
81. Cui, F., Qian, F., Yin, C.: Preparation and characterization of mucoadhesive polymer-coated nanoparticles. Int. J. Pharm. **316**, 154–161 (2006)
82. Cooper, J.L., Quinton, P.M., Ballard, S.T.: Mucociliary transport in porcine trachea: differential effects of inhibiting chloride and bicarbonate secretion. Am. J. Physiol. Lung Cell. Mol. Physiol. **304**, L184–L190 (2013)
83. Foster, W.M., Langenback, E., Bergofsky, E.H.: Measurement of tracheal and bronchial mucus velocities in man: relation to lung clearance. J. Appl. Physiol. **48**, 965–971 (1980)
84. Friedman, M., Dougherty, R., Nelson, S.R., et al.: Acute effects of an aerosol hair spray on tracheal mucociliary transport. Am. Rev. Respir. Dis. **116**, 281–286 (1977)
85. Henning, A., Schneider, M., Bur, M., et al.: Embryonic chicken trachea as a new in vitro model for the investigation of mucociliary particle clearance in the airways. AAPS PharmSciTech **9**, 521–527 (2008)
86. Hoegger, M.J., Awadalla, M., Namati, E., et al.: Assessing mucociliary transport of single particles in vivo shows variable speed and preference for the ventral trachea in newborn pigs. Proc. Natl. Acad. Sci. U.S.A. **111**, 2355–2360 (2014)
87. Veldhuizen, R., Nag, K., Orgeig, S., et al.: The role of lipids in pulmonary surfactant. Biochim. Biophys. Acta (BBA) Mol. Basis Dis. **1408**, 90–108 (1998)
88. Avery, M.E., Said, S.: Surface phenomena in lungs in health and disease. Medicine **44**, 503–526 (1965)
89. Papaioannou, A.I., Papiris, S., Papadaki, G., et al.: Surfactant proteins in smoking-related lung disease. Bentham Sci. 1574–1581 (2016)
90. Bernhard, W.: Lung surfactant: function and composition in the context of development and respiratory physiology. Ann. Anat. **208**, 146–150 (2016)
91. Serrano, A.G., Pérez-Gil, J.: Protein-lipid interactions and surface activity in the pulmonary surfactant system. Chem. Phys. Lipid. **141**, 105–118 (2006)
92. Baoukina, S., Tieleman, D.P.: Computer simulations of lung surfactant. Biochim. Biophys. Acta Biomembr. **1858**, 2431–2440 (2016)
93. Pérez-Gil, J.: Structure of pulmonary surfactant membranes and films: the role of proteins and lipid-protein interactions. Biochim. Biophys. Acta Biomembr. **1778**, 1676–1695 (2008)
94. Nathan, N., Taytard, J., Duquesnoy, P., et al.: Surfactant protein A: a key player in lung homeostasis. Int. J. Biochem. Cell Biol. **81**, 151–155 (2016)
95. Lopez-Rodriguez, E., Gay-Jordi, G., Mucci, A., et al.: Lung surfactant metabolism: early in life, early in disease and target in cell therapy. Cell Tissue Res. **367**, 721–735 (2017)
96. Brandsma, J., Postle, A.D.: Analysis of the regulation of surfactant phosphatidylcholine metabolism using stable isotopes. Ann. Anat. Anatomischer Anz. **211**, 176–183 (2017)
97. Khan, A., Agarwal, R.: Pulmonary alveolar proteinosis. Respir. Care **56**, 1016–1028 (2011)
98. Räsch, S.S.: The nanoparticle corona in the deep lung: pulmonary surfactant adsorption and its role in nano-bio interactions (2016)
99. Amigoni, A., Pettenazzo, A., Stritoni, V., et al.: Surfactants in acute respiratory distress syndrome in infants and children: past, present and future. Clin. Drug Investig. **37**, 1–8 (2017)
100. Griese, M.: Pulmonary alveolar proteinosis: a comprehensive clinical perspective. Pediatrics **140**, e20170610 (2017)
101. Carey, B., Trapnell, B.C.: The molecular basis of pulmonary alveolar proteinosis. Clin. Immunol. **135**, 223–235 (2011)
102. Ijaz, M.K., Zargar, B., Wright, K.E., et al.: Generic aspects of the airborne spread of human pathogens indoors and emerging air decontamination technologies. Am. J. Infect. Control **44**, S109–S120 (2016)
103. Hidalgo, A., Cruz, A., Pérez-Gil, J.: Pulmonary surfactant and nanocarriers: toxicity versus combined nanomedical applications. Biochim. Biophys. Acta Biomembr. **1859**, 1740–1748 (2017)

104. Raesch, S.S., Tenzer, S., Storck, W., et al.: Proteomic and lipidomic analysis of nanoparticle corona upon contact with lung surfactant reveals differences in protein, but not lipid composition. ACS Nano **9**, 11872–11885 (2015)
105. Kapralov, A.A., Feng, W.H., Amoscato, A.A., et al.: Adsorption of surfactant lipids by single-walled carbon nanotubes in mouse lung upon pharyngeal aspiration. ACS Nano **6**, 4147–4156 (2012)
106. Ruge, C.A., Schaefer, U.F., Herrmann, J., et al.: The interplay of lung surfactant proteins and lipids assimilates the macrophage clearance of nanoparticles. PLoS ONE **7**, e40775 (2012)
107. Vennemann, A., Alessandrini, F., Wiemann, M.: Differential effects of surface-functionalized zirconium oxide nanoparticles on alveolar macrophages, rat lung, and a mouse allergy model. Nanomaterials **7**, 280 (2017)
108. Moliva, J.I., Rajaram, M.V.S., Sidiki, S., et al.: Molecular composition of the alveolar lining fluid in the aging lung. Age (Dordrecht, Netherlands) **36**, 9633 (2014)
109. Ujma, S., Horsnell, W.G.C., Katz, A.A., et al.: Non-pulmonary immune functions of surfactant proteins A and D. J. Innate Immun. **9**, 3–11 (2017)
110. Han, S.H., Mallampalli, R.K.: The role of surfactant in lung disease and host defense against pulmonary infections. Ann. Am. Thorac. Soc. **12**, 765–774 (2015)
111. Nayak, A., Dodagatta-Marri, E., Tsolaki, A.G., et al.: An insight into the diverse roles of surfactant proteins, SP-A and SP-D in innate and adaptive immunity. Front. Immunol. **3**, 1–21 (2012)
112. Stein, S.W., Thiel, C.G.: The history of therapeutic aerosols: a chronological review. J. Aerosol. Med. Pulm. Drug. Deliv. **30**, 20–41 (2017)
113. Dalby, R.N., Eicher, J., Zierenberg, B.: Development of Respimat((R)) Soft Mist Inhaler and its clinical utility in respiratory disorders. Med. Devices (Auckland, N.Z.) **4**, 145–155 (2011)
114. Edwards, D.A., Hanes, J., Caponetti, G., et al.: Large porous particles for pulmonary drug delivery. Science (New York, N.Y.) **276**, 1868–1871 (1997)
115. Muralidharan, P., Malapit, M., Mallory, E., et al.: Inhalable nanoparticulate powders for respiratory delivery. Nanomed. Nanotechnol. Biol. Med. **11**, 1189–1199 (2015)
116. May, S., Jensen, B., Wolkenhauer, M., et al.: Dissolution techniques for in vitro testing of dry powders for inhalation. Pharm. Res. **29**, 2157–2166 (2012)
117. Forbes, B., Bäckman, P., Christopher, D., et al.: In vitro testing of orally inhaled products: development of science-based regulatory approaches. AAPSJ **17** (2015)

Chapter 8
Cellular Uptake Mechanisms and Detection of Nanoparticle Uptake by Advanced Imaging Methods

Kleanthis Fytianos, Fabian Blank and Loretta Müller

Abstract The specific mechanism, of uptake of a nanoparticle by a cell and the subcellular localisation are of great importance regarding the potential effect of the nanomaterial inside the cell. In order to study health risks and the potential of a nanoparticle to be used in biomedical applications, cellular internalization has to be investigated in great detail. This chapter highlights most relevant routes of nanoparticle uptake and includes current approaches for the visualization of particle uptake at the nano-level.

8.1 Introduction

The number of manufactured goods containing nanomaterials has been growing consistently over the last fifteen years [1]. The fundamental interactions of nanoparticles (NPs) with biological interfaces remain incompletely understood [2–6]. This is mainly due to a lack of mechanistic knowledge at the molecular level [2, 7] with regards to nanoparticle uptake by cells in particular. The mode of internalization of NPs into cells will determine intracellular fate and potential effects on the whole organism, including health effects. This is why even for intended therapeutic applications of NPs, possible health concerns need addressing [8–10]. In particular with regards to therapeutic applications, the entire field of nanomedicines has been greatly expanded by the development of a wide range of nanomaterials with a high degree of control over their physical (e.g., size, surface charge, shape, mechanical strength) and chemical attributes. Hence, a better understanding of the physiopathological nature of different diseases and insight into the interaction of nanomaterials with biolog-

K. Fytianos · F. Blank (✉)
Respiratory Medicine, Department of BioMedical Research (DBMR), University of Bern, Murtenstrasse 50, 3008 Bern, Switzerland
e-mail: fabian.blank@dbmr.unibe.ch

L. Müller
University Children's Hospital Basel, Spitalstrasse 33, 4056 Basel, Switzerland

Department of Pediatrics, Inselspital, Bern University Hospital, Freiburgstrasse 18, 3010 Bern, Switzerland

P. Gehr and R. Zellner (eds.), *Biological Responses to Nanoscale Particles*, NanoScience and Technology, https://doi.org/10.1007/978-3-030-12461-8_8

ical systems at various levels (i.e., systemic, organ, tissue, and cell) are of great importance for further progress towards bench-to-bedside translation [11]. A large number of studies in recent years has aimed at focusing on the molecular interactions involved in the biological actions of NPs [12]. NPs are of similar size to typical cellular organelles and are able to very efficiently enter living cells by exploiting the cellular endocytosis machinery, which may lead to adverse effects and even permanent cell damage [10, 13]. Only specialized cells are capable of phagocytosis, a form of endocytosis in which the cell engulfs larger particles. The most prominent type of phagocytes are macrophages, in general termed as professional phagocytes, since they are the main responsible cell type for clearance of cellular debris and foreign particles in most organs. Other phagocytic cell types of the innate and adaptive immune system include monocytes, neutrophils and dendritic cells. On the other hand, NPs can be internalized by almost all non-phagocytic cells via pinocytosis. It is one of the aims of this chapter to discuss the most important receptor mediated and receptor independent cellular uptake mechanisms for NPs which have been described up to now.

Different uptake mechanisms by cells are determined by the physico-chemical properties of NPs including size [14, 15], shape [14], surface charge [16–18] and surface chemistry [16, 19, 20], which strongly modulate the cellular uptake efficiency. Furthermore, by entering the organism, NPs interact with extracellular biomolecules dissolved in body fluids, including proteins, sugars and lipids forming a specific corona around the particle. The composition of the protein corona (which is discussed in detail in another chapter of this book) depends on diverse physical properties of the NPs like size, shape and surface chemistry and in turn determines the type of interaction with the cells during uptake. In the last two decades, there have been substantial activities to better understand the detailed molecular mechanisms involved in cellular uptake of NPs, often using fluorescence microscopy and other sophisticated biophysical techniques like flow cytometry. This chapter will discuss a number of approaches from recent studies, which were aiming to elucidate the molecular interactions promoting uptake of NPs. There is a number of novel emerging techniques to accurately visualize, monitor, characterize and quantify the uptake of NPs by different cell types. Accurate, well characterized and reliable techniques, to analyse and quantify cellular uptake of NPs is crucial for the design of novel nanocarriers for biomedical applications. A thorough understanding of the involved processes at the molecular level is important for example for the engineering of NPs that do not penetrate cells and evade the phagocytic cells responsible to clear particulates from the systemic circulation like the reticulo-endothelial system, as is the case for NP based contrast agents widely used in medical diagnosis. However, the opposite characteristics are needed for developing NPs designed for selective uptake by specific cells, for example, for targeted drug delivery [12]. The enhanced cellular uptake of NPs at the site of disease is of paramount importance, because targets for many theranostic agents against several disorders (including cancer) are localized in the subcellular compartments [21]. All these facts not only highlight the importance of a better understanding of cellular uptake mechanisms but also have fuelled recent

research into the development of nanocarriers capable of subcellular- and organelle-level targeting, referred to as a completely novel generation of nanomedicines [22].

8.2 Non-ligand Dependent Endocytic Uptake

There are a variety of different biological mechanisms enabling the active uptake of particles into cells. Mostly, it is the specific size of the particles, which defines the mechanisms that are involved. Among the non-ligand dependent endocytosis, we distinguish between the phagocytosis (also called "cell eating") and pinocytosis (also called "cell drinking") (see also Fig. 8.1).

Phagocytosis occurs with particles larger than 0.5 μm. Even tough, many cell types (e.g. epithelial cells, fibroblasts, immune cells) are able to perform phagocytosis, the uptake efficiency of phagocytic cells (macrophages, dendritic cells, neutrophils) is a lot higher and phagocytosis is predominately performed by those cells [24, 25]. Phagocytosis is performed to clean the organism from infectious microorganisms, senescent cells or disabled particles. This process is part of the immune response [26]. Particles, or more precisely, particular ligands on the particles, are either recognized by surface receptors of the phagocytes or by opsonins. Opsonins are small, soluble molecules, such as proteins from the complement system, antibodies, blood serum proteins (e.g. fibronectin, laminin). They recognize particles, bind to their surface and are then recognized by phagocytes [27]. Some of the most important receptors involved in phagocytosis are the following ones: Fc receptors family for immunoglobulins G, the complement receptors, and the α5β1 integrin [28]. The interaction of the particle with the cell surface receptors triggers a signal cascade with the result of particle engulfing: actin assemblies and cell surface extensions are formed to surround the particle. Once completely engulfed, the particle find itself in an intracellular vesicle of approximately 0.5–1 μm, so called phagosomes [25, 29]. Once inside of the cells, phagosomes undergo maturation due to several events of

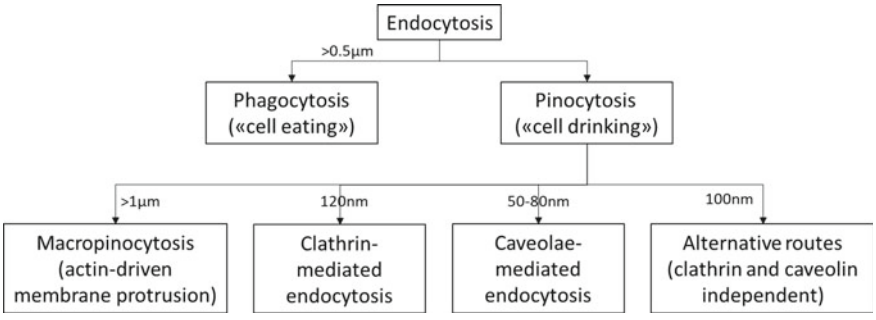

Fig. 8.1 Classification of uptake mechanisms based on size of the up taken particles. Adapted from [23]

fission and fusion with endosomes and lysosomes, resulting in so called phagolysosomes [23]. Particles in the phagolysosomes are degraded and receptors are recycled [23, 30].

Pinocytosis occurs in almost all cell types and is characterized by the uptake of fluid, which may—by coincidence—also contain particles. This process can be divided into four modes: Macropinocytosis, clathrin-mediated endocytosis, caveolae-mediated endocytosis, and alternative routes (see also Fig. 8.1) [31]. Macropinocytosis is the process of the nonspecific uptake of large amounts of external fluid via the uptake of large vesicles (0.5–10 μm) known as macropinosomes [32]. As particles may be localized close to the cell membrane, they may end up in one of those macropinosomes and thus, are taken up by the cells [23]. This mode of uptake is typical for the uptake of viruses [33], bacteria [34], and apoptotic cell fragments [35], and thus contributes to the antigen presentation in the major histocompatibility complex II [36, 37]. Macropinocytosis is an actin-driven process, which needs stimulation: growth factors (e.g. epidermal growth factor or platelet derived growth factor) interact with receptor tyrosine kinase [33], what activates the signal cascade to initiate actin polymerization to form membrane protrusions [38]. These protrusions fuse with the membrane generating uncoated endocytic vesicles of the size of about 1 μm. The shape of the macropinosomes is irregular. The uptake capacity by this mode is very high, but rather unspecific [39]. The clathrin-mediated endocytosis is the "classical" uptake mechanism, as it is known for a long time and very well characterized [40]. It is a complex pathway, which is initiated at the apical membrane of polarized cells (e.g. endothelial or epithelial cells) [31, 41, 42]. The whole process starts by the induction of a curvature in the membrane leading to the formation of vesicles [11]. Various proteins are involved in this induction, e.g. epsin [43], endophilin [44], clathrin assembly lymphoid myeloid leukemia protein [45]. The neck of a newly formed invagination is surrounded by a ring of the GTPase dynamin. The activity of the GTPase dynamin is responsible for the release of a vesicle from the plasma membrane [46, 47]. Once the vesicle is released, it can be targeted to more mature endosomes, lysosomes or multivesicular bodies, or it is recycled to the plasma membrane surface [23]. Usually, particles of sizes between 120 and 150 nm can be internalized by clathrin-mediated endocytosis [14, 48], however, also particles of 200 nm have been reported to enter the cells via this pathway [15]. The uptake route for non-targeted NPs depends on the particle characteristics (e.g. particle size, shape, surface charge) and also on the cell type supposed to take up the particle [23]. The detailed mechanism of the particle internalization is not completely understood. However, the efficient uptake of particles of about 100 nm in diameter via clathrin-mediated endocytosis, speaks for the main uptake route [23]. Particles of a diameter between 50 and 80 nm are predominantly uptaken via caveolin-mediated endocytosis. The uptake of particles via this process can be mostly observed on the basolateral side of endothelial cells [31, 49, 50]. The process starts with the building of caveolae (small, stable membrane-associated structures with flask-like shape) [51, 52], which are coated with caveolin-1 [53]. They have been shown to interact with pathogens, e.g. SV40 virus [54] cholera toxin subunit B or shiga toxin [55]. It is unclear what happens to NPs, once they are inside the caveolae, which have

been internalized by the cell. For a long time, it was thought that particles are localized inside so-called caveosomes (special type of caveolar endosomes), which are further transported to the Golgi apparatus. The pH inside the caveosomes is neutral and thus, there is no degradation as in lysosomes [11]. However, more recently, the caveosomes were shown to be artifacts of caveolin overexpression [23, 56], and routes of the intracellular trafficking of NPs are controversially discussed again [23]. This route is of importance for small NPs, as NPs between 20 and 40 nm are a lot faster taken up by this route than NPs of 100 nm [50, 57].

As discussed above, recent studies have highlighted a number of different non-ligand dependent mechanisms which are of great importance for the internalisation of NPs by cells. However, there are endocytic routes for NPs which do not fit the so far described categories. Most of them are clathrin- and caveolin-independent and are summarized as "alternative routes" [23]. Those routes have first been described for the entry of cell surface proteins and bacterial toxins. It has also been proposed to be involved in other cellular mechanisms, such as membrane repair, polarization, spreading and intracellular signaling [58]. Depending on the subtype of pathways, various proteins are involved, especially actin and actin-associated proteins [59]. Additionally, NPs can also enter a cell via passive diffusion [60, 61].

8.3 Receptor-Mediated Cellular Internalization and Nanoparticles for Targeted Uptake

The study and characterization of expression and overexpression of specific receptors on the surface of target disease cells has proven to be essential for the research and development of novel nanomedicines. This type of approach helps to improve cellular uptake of biomedical NPs in therapeutic and/or diagnostic procedures, while side-effects and off-side toxicity can be reduced as much as possible [11]. Well-characterized examples of receptors known for active disease cell targeting are folate receptor (FR), transferrin receptor (TfR), epidermal growth factor receptors (EGFR), G-protein coupled receptor (GPCR), low density lipoprotein receptor (LDLR) and lectins [62]. Receptor-mediated internalization of biomedical NPs has been investigated for various cargos such as vaccines, drugs, DNA, and RNA. For efficient cell targeting and internalization, different high affinity ligands have been conjugated to the surface of NPs. The major types of targeting ligands include peptides, high-affinity small molecules, aptamers (i.e. oligonucleotides or peptides) and antibodies. Recent developments using ligand-conjugated NPs for biomedical applications are described in this subchapter, with specific focus on FR, TfR, EGFR, prostate-specific membrane antigen (PSMA), integrin and neonatal Fc-receptor (FcRn). For a very comprehensive overview of targeted uptake, please consult the review written by Yameen et al. [11]. We have included a synthesis of this work in the following text.

8.3.1 Folate Receptor (FR) Targeting

FR is a glycoprotein of 38-44kDA molecular weight. There are two isoforms, FR-α and FR-β. While FR-α is expressed on some normal epithelial cells (e.g. kidney) [63] and on many epithelial cancer cells (e.g. ovarian, renal, brain) [64], FR-β has been shown to be present on activated macrophages [65] and on hematopoietic malignancies [66]. As folic acid binds with high affinity to the FR. This allows creating folate-conjugated nanocarriers which are selectively taken up by cells expressing FR [67]. This approach involving FR-β could be used to target chronic inflammatory diseases (e.g. diabetes type 2 or arteriosclerosis). The benefit of folate-conjugated NPs, liposomes, oligonucleotides, and chemotherapeutics has been shown in many in vivo and in vitro studies [68]. E.g. chemotherapeutic drugs loaded into folate-functionalized NPs showed higher antitumor activity compared to non-targeted NP therapeutics in an in vivo ovarian peritoneal metastasis model [69]. Folic acid is a small molecule, which has advantages compared to the use of peptides or antibodies as targeting ligands. It is highly stable in acidic or basic media and at high temperatures, there is no risk of toxicity or immune reaction as it is a vitamin, and the chemical modification and a potential scaling-up for clinical applications is easily doable [11].

8.3.2 Transferrin Receptor (TfR) Targeting

TfR is a cell membrane glycoprotein. It is present as a homodimer of two identical subunits located transmembranely. The main functions are the mediation of the cellular uptake of iron from plasma glycoproteins (e.g. transferrin) and the regulation of cell growth [70, 71]. While TfR is most probably expressed on all cells, the expression level varies: it is highly expressed in immature erythroid cells, placental tissue, and rapidly dividing cells. The fact that it is about 100 times higher expressed on cancer cells compared to normal cells [72], makes it to one of the most attractive targets for the cancer therapy with receptor-mediated endocytosis using drug NPs. Transferrin has been successfully used as ligand for TfR-mediated intracellular delivery of nanotherapeutics, as there are TfR-targeted nanomedicines in various stages of clinical trials [73].

8.3.3 Epidermal Growth Factor Receptor (EGFR) Targeting

EGFR is a member of the ErbB tyrosine kinase family and can stimulate tumor growth, invasion, and metastasis. It is overexpressed in various tumors, e.g. colorectal, brain, breast or ovarian [74–76]. Following the binding of ligands to EGFRs, the EGFRs homo- or heterodimerize with other members of the ErbB receptor

family and other cell-surface tyrosine kinases [73]. Monoclonal antibodies as well as small molecules have been used as EGFR-targeting ligands: epidermal growth factor, transforming growth factor-α, heparin binding EGF-like growth factor, epigen, betacelluin, and epiregulin [77]. Nanocarriers for drugs using EGFR to deliver drugs to specific cells are widely used and already reached clinical trial phase I [73]. One example for the use of EGFR for targeted anticancer therapy are cisplatin-encapsulated gelatin NPs with EGF. Those NPs improved the in vitro targeting ability and anticancer effects in A549 cells (high EGFR expression) compared to HFL1 cells (low EGFR expression). Additionally, the effect was shown in a tumor-bearing mouse model (with high EGFR expression) [78].

8.3.4 Prostate-Specific Membrane Antigen (PSMA) Targeting

PSMA is a type 2 integral membrane glycoprotein overexpressed on the surface of prostate carcinomas and of the neovasculature of many solid tumors [79, 80]. This makes PSMA a valid cancer target for therapies. One example is BIND-014, which has reached a Phase II clinical trial. It is a docetaxel-loaded, polymer-based nanomedicine with a small-molecule ligand (S,S-2-[3-[5-amino-1-carboxypentyl]-ureido]-pentanedioic acid, ACUPA) against PSMA [81].

8.3.5 Integrin Targeting

Integrins modulate interaction between endothelial cells and the extracellular matrix and are—via this interaction—involved in many vital cellular functions, such as adhesion, migration, invasion, stress responses, proliferation, differentiation, survival and apoptosis. They belong to a family of heterodimer transmembrane receptors [62]. The receptor αvβ3 is overexpressed in tumor-related endothelial cells during angiogenesis compared to endothelial cells in normal tissues [82–85]. Cyclic-RDG peptides were identified as promising targeting ligands for this receptor [62, 86, 87]. Recently, Pt(IV) prodrug-loaded PLGA-PEG NPs functionalized with cyclic-RGD were shown to be more efficacious compared to cisplatin in a non-particulate administration mode in a orthotopic human breast cancer xenocraft model. Additionally, it was better tolerated than the cisplatin [88].

8.3.6 Neonatal Fc-Receptor (FcRn) Targeting

FcRn is highly expressed in the neonatal intestine and in the apical region of epithelial cells in the small intestine of adults [11, 89]. This receptor has been used to test the uptake of nanomedicine delivered orally by Pridgen et al. [90]. PLA-PEG polymer

nanoparticle were functionalized on the surface with polyclonal IgG Fc fragments. Those NPs were shown to be transported transepithelially in vitro and in vivo. In mice, the particles were found in the lamina propria and also in other organs, showing the ability to enter the systemic circulation. The adsorption was 11.5 times higher for the targeted NPs compared to nontargeted ones. As it is a challenge for the nanomedical application to find ways to overcome the intestinal epithelial cell barrier [91], these findings using the FcRn receptor are of high interest for the future development. The oral administration route is of more convenience for patients, especially if frequent administration is required [92].

Recent studies have highlighted the importance of specific receptors for targeting by biomedical nanocarriers. A good knowledge of receptor mediated mechanisms of internalisation offers novel opportunities for treatments which are more efficient and show less side-effects due to precise targeting, in particular, for the treatment of cancer.

8.3.7 Methods of 3D Fluorescence Microscopy and Flow Cytometry to Determine and Characterize Cellular Uptake of Nanoparticles

Over the last decade, a wide range of different types of NPs have been developed, especially for the biomedical sector (i.e. nanomedicine and targeted drug delivery). Biomedical NPs can be suitably designed in order to reach the site of interest (i.e. lungs, tumours) and interact with specific cell types. Initially, NPs will interact with the cells of the specific site by either attaching to their membranes or be internalized. Cellular uptake is one of the most important factors to be investigated since it can determine the overall effect of the particles to the cells. Their effect could be drug release to a tumour site or immunogenic peptide delivery that can ultimately lead to effects like tumour size decrease or modulation of immune cells respectively. Fluorescently labelled NPs are widely used in pre-clinical applications at in vitro, in vivo and ex vivo settings. Imaging, bio-distribution and clearance can provide solid information for early development studies and thus dictate the direction of future experiments and strategies [93]. Alongside novel nanoparticle designs, technological advancements in the field of biomedical imaging (i.e. Stochastic Optical Reconstruction Microscopy—STORM) and scientific software (i.e. sophisticated image processing) can also help in the further development of the field, understanding of uptake mechanisms and ultimately lead to new scientific discoveries. Complementary to that, a portable device that can detect fluorescently labelled NPs as well as bacteria and viruses [94] has been reported. This device is compatible with smartphones, since it can be used as an extension that is attached to the camera of a smartphone. It utilizes an opto-mechanical system that contains a 450 nm diode. Such a device has potential to be used for quick quality control of NPs as well as for field applications [94]. The aim of this part of that chapter is to discuss about

some important nanoparticle types that are used in cellular uptake studies and some common and novel detection techniques (mainly based on fluorescence) that are used for their detection and cellular uptake measurements.

8.3.8 Quantum Dots and Inorganic Nanoparticles

Quantum dots have a size of 2–10 nm. Due to their very high surface to volume ratio, narrow excitation wavelengths (where according to their size they show a unique color) and electrical properties, they are widely used in semi-conductor and electronics industry and for fluorescence imaging. For the biomedical field they can be used for imaging and labelling purposes (i.e. cells or tissues). If used at concentrations of less than 100 μg/mL they do not interfere with cellular viability and cytotoxicity [95, 96]. Importantly, it has been shown that streptavidin-conjugated quantum dots can be used for cancer diagnosis. Since they can be utilized as contrast agents for biomedical imaging, they have been used in Magnetic Resonance Imaging (MRI), intra-vital in vivo imaging, flow cytometry and other bio-analytical assays. It is expected that in the future further developments will be established and their applications range will increase [97]. Bagalkot et al. [98] and Fontes et al. [99] highlight the importance of quantum dots in biomedical research, especially in the field of cancer imaging. They describe how quantum dots can specifically monitor drug release on target cancer cells, in real time. This is mainly attributed to their highly modifiable surface, electron density and photo-stability, which allows prolonged imaging times.

Gold NPs are one of the most studied types of inorganic nanomaterials. Due to their optical properties and evidence of low cytotoxicity and high affinity with biomolecules (i.e. peptides and nucleic acids) they are considered to be one of the most promising agents for imaging, drug delivery and diagnostic applications. Besides transmission electron microscopy, a novel and effective method to visualize uptake of gold NPs in cells and tissue is hyper-spectral imaging. The only system currently available for hyper-spectral imaging is the Cytoviva system (www.cytoviva.com). This instrument makes use of the unique spectrum of gold NPs, which enables accurate detection. Images are analyzed pixel-wise and the gold NPs can be mapped within the tissue or cells, due to their distinct UV-Vis spectrum. A recent example of the use of hyper-spectral imaging of gold NPs is given by England and colleagues [100]. However, the standard technique to measure gold and other inorganic NPs in cells remains transmission electron microscopy [101].

8.3.9 Fluorescently Labelled (Nano)Particles

Polymer based NPs and microparticles are generally regarded as safe for use for biological studies. Apart for very low records for cell viability and cytotoxicity, they

possess several competitive advantages compared to other NP types. For example, due to their chemical properties they can bind with many fluorescent molecules and thus become easier visible under fluorescent microscopes. Their chemical synthesis is also a straight-forward procedure. Additively, they are biodegradable and biocompatible, thus there are no concerns regarding bio-accumulation [102]. For all the above mentioned reasons, polymer based NPs have become a standard tool for cellular uptake, detection and imaging studies, mainly on a research scale [103]. In a recent review, Wolfbeis gives a very comprehensive overview of the nanomaterials that are mainly used in fluorescence-based imaging. For example, polymer-based particles, lipid-based particles and carbon nanomaterials among others. Bio-conjugation techniques like covalent and non-covalent binding of the fluorescent molecules to the nanomaterial surface are also reviewed.

8.3.10 Laser Scanning Confocal Microscopy and Live Cell Imaging

Understanding the interactions of internalized particles with endocytic vesicles is of crucial importance in order to determine mechanism of actions for therapeutic purposes. This can be done via Live Cell Imaging or Structured Illumination [104]. Widely used cell lines or primary cells can be used as cellular models to study such interactions with fluorescently labelled particles. These models allow concentration and time dependent studies in order to examine the uptake and accumulation of particles in cells [101, 12].

Complementary to that, working with realistic nanoparticle concentrations is important in terms of biomedical applications like vaccine development. For example, gold NPs were exposed to immune cells at concentrations ranging from 10 to 100 μg/mL in vitro, since different concentrations might result in different functional and immunological responses [105]. Especially for cellular internalization and co-localization studies, confocal microscopy is the most common and suitable technique to use since it allows: improved resolution compared to wide-field illumination techniques because the confocal aperture can be closed down to eliminate higher orders of the diffraction pattern. Furthermore, confocal systems allow z-stack projections with improved z-resolution that can prove if particles are internalized. Complementary to that, 3D rendering of the acquired images as well as further image processing (i.e. adjusting the transparency of specific channels) is possible with the use of scientific software (e.g. Fiji or IMARIS). A vivid example of what is currently possible in 3D rendering was recently shown by Lehmann et al. [106] who visualized fluorescent magnetic hybrid NPs after uptake by human blood monocyte derived macrophages in vitro with sub-cellular localization inside lysosomes and not entering mitochondria (Fig. 8.2). More specifically, Blom et al. [107] identified that virosome and liposome uptake by bone marrow derived dendritic cells is done via clathrin-mediated endocytosis as well as phagocytosis. Confocal microscopy was

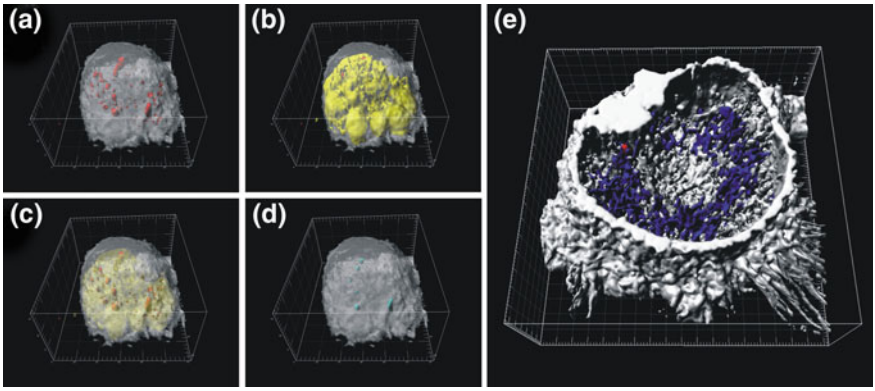

Fig. 8.2 Visualization of fluorescent magnetic hybrid NPs in macrophages with Laser scanning microscopy and 3D rendering. **a** Visualization of NPs (red) inside macrophages (light gray) shown in a 3D reconstruction. **a**–**d** Localization and co-localization (turquoise) of the particles with lysosomes (yellow) are shown. **c** By making the cell-body channel (light gray) transparent as well as the lysosome channels, the particles colocalized with the lysosomes become visible. **d** The colocalization of particles in lysosomes. **e** Mitochondria staining (blue) and particles (red) in a macrophage. Figure adapted from [106] with permission

used to identify that ingested particles co-localize in late endosomes. To further confirm the findings, uptake inhibitors were used as controls. In another study, Seydoux and colleagues [108] have examined the size effect of polystyrene NPs in terms of accumulation and co-localization in lysosomes. Results indicate that smaller particles are uptaken at larger numbers compared to their larger counterparts. Again, confocal microscopy was utilized.

A particular uptake mechanism of NPs in cells will most probably affect intracellular kinetics of NPs. Thus live cell imaging and time lapse experiments provide investigators with live information about cellular dynamics [109]. Other fluorescence-based microscopy techniques to monitor kinetics of NPs, which are used are:

Fluorescence Recovery After Photo-bleaching (FRAP)
Fluorescence Resonance Energy Transfer (FRET)
Fluorescence lifetime imaging microscopy (FLIM).

Those techniques are used to measure cellular dynamics and molecular interactions of living cells and will be briefly described hereunder [110]: For example, FRAP experiments can show rapidly interactions of the investigated fluorescently labelled NPs with cellular organelles like mitochondria and other cytoplasmic vesicles (i.e. intracellular fate of the NPs). For example, Hemmerich and von Mikecz examined the cellular uptake mechanisms as well as the deposition of the fluorescently labelled polystyrene NPs at cellular organelles like mitochondria and other cytoplasmic vesicles [109]. Basuki and colleagues have utilized FLIM to visualize polymer coated iron oxide NPs that contain doxorubicin. Nanoparticle uptake and

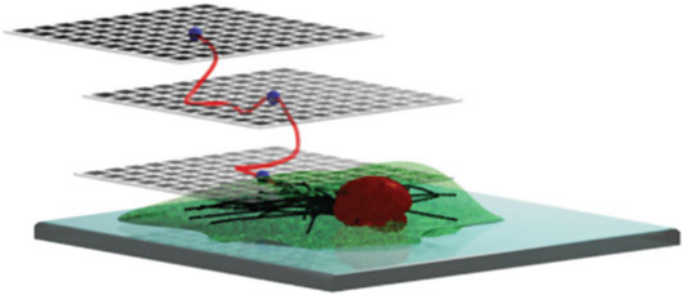

Fig. 8.3 Schematic representation of the 3D multi-resolution microscopy principle. The movement (trajectory) of the nano-probe (blue dot) is depicted in red lines. Then the nano-probe crosses different focal planes until it reaches cell surface (green). Picture adapted from [112]

controlled doxorubicin release was confirmed in cancer cell lines by FLIM [111]. Still, fluorescence microscopy techniques fail to sufficiently measure the early stages of internalization by cells, which would be a key analysis for drug delivery research. Welsher and Yang, proposed a method that peptide conjugated NPs can be visualized with 3D multi-resolution microscopy. Then, imaging software is used to draw the trajectories of the particles into the cells. Multi-resolution 3D visualization utilizes high-speed single-point detection of a nano-probe (i.e. fluorescently labelled NPs). The method allows real-time "target-locking" of the nano-probe, thus "following" the nano-probe at different focal-planes. The method also combines the principles of two-photon laser scanning microscopy. As the nano-probe moves to different focal planes the two-photon laser scanning microscope provides information about the movement of the nano-probe and thus images are built [112] (Fig. 8.3).

Complementary to that, van der Zwaag et al. (2016) have used Two-color Stochastic Optical Reconstruction Microscopy (STORM) and compared their findings with confocal microscopy and electron microscopy. The competitive advantage of STORM is that size and exact location of NPs can be identified inside cells. STORM is based on the principle that activated molecules emit photons. This allows precise localization of the specimen prior to photo-bleaching and beyond the optical resolution limit of 200 nm. Quantitative information can also be extracted via imaging software. The study concludes that STORM can provide additional information regarding cellular uptake of NPs that was missing with confocal and electron microscopy [113].

8.3.11 Super Resolution Microscopy

With the development of super resolution microscopy, imaging at the molecular level has become possible [114]. However, it remains a technically challenging technique, since non-proper stability of the instrument can introduce biasness to the analysis.

Due to their optical properties (i.e. surface plasmon resonance), metal NPs are mainly used in super resolution microscopy applications. Recently, Peuschel and colleagues have shown interactions of fluorescently labelled silica NPs with human alveolar epithelial type-II like cell line (A549). The authors used stimulated emission depletion (STED) super resolution microscopy [115]. The authors exposed in vitro A549 cells to various concentrations of fluorescently labelled polystyrene NPs of different sizes and used STED in order to quantify uptake. The principle of STED is based on a very narrow and focused excitation spot. STED uses both an excitation and a depletion laser, in order to first excite the fluorescent molecules and immediately after deplete them. Fluorescent molecules are depleted before they can emit light. This takes place only in the focused spot and thus the microscope can emit the fluorescence signals from the surrounding spots. This results in an enhanced signal, which allows super-resolution imaging. Such techniques can be used for quantitative approaches as well as to assure whether the NPs have been internalized or remain at the surface of the cells. Additively, co-localization studies can reveal new insights in terms of internalized particles and endocytic vesicles interactions.

8.3.12 Flow and Imaging Cytometry

Over the last years, we and others have published several articles highlighting the use of multi-color flow cytometry to measure cellular uptake in both in vitro and in vivo settings of various types of NP-related factors like material type, size, surface modification and concentration and associate their uptake with a wide range of functional cell type specific properties (i.e. apoptosis and surface marker expression) and immunological properties (immunophenotyping, antigen uptake, antigen processing and cytokine secretion patterns) [107, 108, 116–118]. Flow cytometry is a technique, which allows analysis of thousands of events within one second, thus high-throughput analysis can be designed. Many parameters could be measured simultaneously and in the data analysis phase, could be tested for correlation with cellular uptake. Complementary to that, imaging cytometry allows real-time bright-field images of single cells in suspension, apart from all the aforementioned capabilities of a conventional flow cytometer. For example, cell monocultures that are treated with fluorescently labelled NPs and labelled for some surface markers could be analyzed and thus the effect of particle uptake on cellular properties could be identified. Additively, extracellular vesicles have gained considerable attention in the field of diagnostics and imaging cytometry is also considered an appropriate method for imaging and quantification purposes [119]. Routine flow cytometry based measurements like cell cycle analysis, quantification of cancer cells, internalization and phagocytosis experiments, surface and intracellular localization can be further enhanced, since apart from the flow cytometry data, real time visual confirmation could be acquired. However, researchers must be cautious since if an experiment requires high resolution microscopy studies imaging cytometry might not be the most suitable option due to lack of high-resolution. Furthermore, since it is a rel-

atively new technique, further investigation and proper training might be needed [120].

Fluorescently labelled nano- and micro-particles have become a standard tool for cellular uptake measurements and pre-clinical studies. Established animal models and advanced in vitro co-culture systems, as well as primary and cell-line monocultures are widely used as model systems to study cellular uptake (i.e. qualitative/quantitative approaches and type of uptake). Laser scanning microscopy, flow cytometry and imaging flow cytometry combined with a suitable antibody panel one may provide a large amount of accurate and reliable data to study dynamics at the level of cell entry and intra-cellular trafficking. This information can be further fortified with the use of sophisticated imaging software and statistics. With the advancement of technology in the field of high-resolution imaging, more capabilities will become possible and accuracy will further increase. Taking together the large body of knowledge of cellular uptake related information with recent trends in computer science (i.e. big data management and computational biology) and 3D biomedical imaging, cellular uptake data can be collected from literature sources in order to develop electronic databases and precise prediction algorithms for cellular uptake. Such approaches may be beneficial for decision making in the drug delivery/nanotoxicology/nanomedicine fields as well as for regulatory and legislative purposes.

8.4 Conclusions and Outlook

With a huge number of new-emerging nanomaterials every year, toxicological risk assessment and the research for novel biomedical treatment approaches are of equal importance. Interaction with the biological interface in general and the involved mechanisms of particle uptake in particular, are of great importance to both fields and require advanced imaging techniques for improved investigation of potential risks and opportunities. In order to investigate how NPs are entering the cell and affect its interior, all of the specific characteristics an NP can show (i.e. size, surface, shape, charge, material, physico-chemical properties etc.), have to be considered. Advanced imaging techniques using fluorescently labelled NPs in combination with laser scanning microscopy have pushed into the super-resolution range already more than a decade ago and are constantly improved and refined. In combination with the long-time established techniques in the field of electron microscopy, super-resolution fluorescence imaging is complementing advanced imaging techniques for NPs by allowing visualization in living samples. Constantly improved imaging techniques at the nano-level will allow a better characterization of potential risks and opportunities of NPs by evaluating a larger number of different pathways of interaction with and uptake by cells and with the possibility to monitor more complex processes. For example, with the new goals of subcellular organelle-level targeting, the field of nanomedicine is now moving to a higher level of complexity [11]. Though the task is challenging, there are promising results highlighting the potential advances that

can be expected from organelle-level targeting. However, the concept of subcellular-targeted NPs is in its infancy, and few strategies have so far been reported organelles like for ER, mitochondria, and nucleus targeting. More detailed investigations are needed to assess the impact and relevance of NP uptake and subcellular targeting for future clinical applications.

References

1. Beddoes, C.M., Case, C.P., Briscoe, W.H.: Understanding nanoparticle cellular entry: a physicochemical perspective. Adv. Colloid Interface Sci. 48–68 (2015). https://doi.org/10.1016/j.cis.2015.01.007
2. Abbas, K., Cydzik, I., Del Torchio, R., Farina, M., Forti, E., Gibson, N., et al.: Radiolabelling of TiO2 nanoparticles for radiotracer studies. J Nanopart. Res. **12**, 2435–2443 (2010). https://doi.org/10.1007/s11051-009-9806-8
3. Maynard, A.D., Aitken, R.J., Butz, T., Colvin, V., Donaldson, K., Oberdörster, G., et al.: Safe handling of nanotechnology. Nature **444**, 267–269 (2006). https://doi.org/10.1038/444267a
4. Nel, A., Xia, T., Mädler, L., Li, N.: Toxic potential of materials at the nanolevel. Science 622–627 (2006). https://doi.org/10.1126/science.1114397
5. Service, R.F.: Priorities needed for nano-risk research and development. Science. **45** (2006). https://doi.org/10.1126/science.314.5796.45
6. Barnard, A.S.: Nanohazards: Knowledge is our first defence. Nat. Mater. **5**, 245–248 (2006). https://doi.org/10.1038/nmat1615
7. Handy, R.D., Von Der Kammer, F., Lead, J.R., Hassellöv, M., Owen, R., Crane, M.: The ecotoxicology and chemistry of manufactured nanoparticles. Ecotoxicology 287–314 (2008). https://doi.org/10.1007/s10646-008-0199-8
8. Linse, S., Cabaleiro-Lago, C., Xue, W.-F., Lynch, I., Lindman, S., Thulin, E., et al.: Nucleation of protein fibrillation by nanoparticles. Proc. Natl. Acad. Sci. **104**, 8691–8696 (2007). https://doi.org/10.1073/pnas.0701250104
9. Lunov, O., Zablotskii, V., Syrovets, T., Röcker, C., Tron, K., Nienhaus, G.U., et al.: Modeling receptor-mediated endocytosis of polymer-functionalized iron oxide nanoparticles by human macrophages. Biomaterials **32**, 547–555 (2011). https://doi.org/10.1016/j.biomaterials.2010.08.111
10. Lunov, O., Syrovets, T., Röcker, C., Tron, K., Ulrich Nienhaus, G., Rasche, V., et al.: Lysosomal degradation of the carboxydextran shell of coated superparamagnetic iron oxide nanoparticles and the fate of professional phagocytes. Biomaterials **31**, 9015–9022 (2010). https://doi.org/10.1016/j.biomaterials.2010.08.003
11. Yameen, B., Choi, W.I., Vilos, C., Swami, A., Shi, J., Farokhzad, O.C.: Insight into nanoparticle cellular uptake and intracellular targeting. J Control Release. **190**, 485–499 (2014). https://doi.org/10.1016/j.jconrel.2014.06.038
12. Treuel, L., Jiang, X., Nienhaus, G.U.: New views on cellular uptake and trafficking of manufactured nanoparticles. J. R. Soc. Interface **10**, 20120939–20120939 (2013). https://doi.org/10.1098/rsif.2012.0939
13. AshaRani, P.V., Mun, G.L.K., Hande, M.P., Valiyaveettil, S.: Cytotoxicity and genotoxicity of silver nanoparticles in human cells. ACS Nano **3**, 279–290 (2009). https://doi.org/10.1021/nn800596w
14. Chithrani, B.D., Ghazani, A.A., Chan, W.C.W.: Determining the size and shape dependence of gold nanoparticle uptake into mammalian cells. Nano Lett. **6**, 662–668 (2006). https://doi.org/10.1021/nl052396o
15. Rejman, J., Oberle, V., Zuhorn, I.S., Hoekstra, D.: Size-dependent internalization of particles via the pathways of clathrin- and caveolae-mediated endocytosis. Biochem J. **377**, 159–169 (2004). https://doi.org/10.1042/bj20031253

16. Labhasetwar, V., Song, C., Humphrey, W., Shebuski, R., Levy, R.J.: Arterial uptake of biodegradable nanoparticles: effect of surface modifications. J. Pharm. Sci. **87**, 1229–1234 (1998). https://doi.org/10.1021/js980021f
17. Arbab, A.S., Bashaw, L.A., Miller, B.R., Jordan, E.K., Lewis, B.K., Kalish, H., et al.: Characterization of biophysical and metabolic properties of cells labeled with superparamagnetic iron oxide nanoparticles and transfection agent for cellular MR imaging. Radiology **229**, 838–846 (2003). https://doi.org/10.1148/radiol.2293021215
18. Sun, X., Rossin, R., Turner, J.L., Becker, M.L., Joralemon, M.J., Welch, M.J., et al.: An assessment of the effects of shell cross-linked nanoparticle size, core composition, and surface PEGylation on in vivo biodistribution. Biomacromolecules **6**, 2541–2554 (2005). https://doi.org/10.1021/bm050260e
19. Nativo, P., Prior, I.A., Brust, M.: Uptake and intracellular fate of surface-modified gold nanoparticles. ACS Nano **2**, 1639–1644 (2008). https://doi.org/10.1021/nn800330a
20. Holzapfel, V., Lorenz, M., Weiss, C.K., Schrezenmeier, H., Landfester, K., Mailänder, V.: Synthesis and biomedical applications of functionalized fluorescent and magnetic dual reporter nanoparticles as obtained in the miniemulsion process. J. Phys. Condens. Matter. **18** (2006). https://doi.org/10.1088/0953-8984/18/38/s04
21. Rajendran, L., Knölker, H.-J., Simons, K.: Subcellular targeting strategies for drug design and delivery. Nat. Rev. Drug Discov. **9**, 29–42 (2010). https://doi.org/10.1038/nrd2897
22. Huang, J.G., Leshuk, T., Gu, F.X.: Emerging nanomaterials for targeting subcellular organelles. Nano Today 478–492 (2011). https://doi.org/10.1016/j.nantod.2011.08.002
23. Kettiger, H., Schipanski, A., Wick, P., Huwyler, J.: Engineered nanomaterial uptake and tissue distribution: from cell to organism. Int. J. Nanomed. 3255–3269 (2013). https://doi.org/10.2147/ijn.s49770
24. Aderem, A., Underhill, D.M.: Mechanisms of phagocytosis in macrophages. Annu. Rev. Immunol. **17**, 593–623 (1999). https://doi.org/10.1146/annurev.immunol.17.1.593
25. Hillaireau, H., Couvreur, P.: Nanocarriers' entry into the cell: relevance to drug delivery. Cell. Mol. Life Sci. **66**, 2873–2896 (2009). https://doi.org/10.1007/s00018-009-0053-z
26. Silverstein, S.C.: Phagocytosis of microbes: insights and prospects. Trends Cell Biol. **5**, 141–142 (1995). https://doi.org/10.1016/S0962-8924(00)88967-9
27. Owens, D.E., Peppas, N.A.: Opsonization, biodistribution, and pharmacokinetics of polymeric nanoparticles. Int. J. Pharm. 93–102 (2006). https://doi.org/10.1016/j.ijpharm.2005.10.010
28. Underhill, D.M., Goodridge, H.S.: Information processing during phagocytosis. Nat. Rev. Immunol. 492–502 (2012). https://doi.org/10.1038/nri3244
29. Rabinovitch, M.: Professional and non-professional phagocytes: an introduction. Trends Cell Biol. **5**, 85–87 (1995). https://doi.org/10.1016/S0962-8924(00)88955-2
30. Dobrovolskaia, M.A., Mcneil, S.E.: Immunological properties of engineered nanomaterials. Nat. Nanotechnol. **2**, 469–478 (2007)
31. Conner, S.D., Schmid, S.L.: Regulated portals of entry into the cell. Nature. **422**, 37–44 (2003). https://doi.org/10.1038/nature01451
32. Falcone, S., Cocucci, E., Podini, P., Kirchhausen, T., Clementi, E., Meldolesi, J.: Macropinocytosis: regulated coordination of endocytic and exocytic membrane traffic events. J. Cell Sci. **119**, 4758–4769 (2006). https://doi.org/10.1242/jcs.03238
33. Mercer, J., Helenius, A.: Virus entry by macropinocytosis. Nat. Cell Biol. 510–520 (2009). https://doi.org/10.1038/ncb0509-510
34. Kolb-Mäurer, A., Wilhelm, M., Weissinger, F., Bröcker, E.-B., Goebel, W.: Interaction of human hematopoietic stem cells with bacterial pathogens. Blood **100**, 3703–3709 (2002). https://doi.org/10.1182/blood-2002-03-0898
35. Fiorentini, C., Falzano, L., Fabbri, A., Stringaro, A., Logozzi, M., Travaglione, S., et al.: Activation of rho GTPases by cytotoxic necrotizing factor 1 induces macropinocytosis and scavenging activity in epithelial cells. Mol. Biol. Cell **12**, 2061–2073 (2001). https://doi.org/10.1091/mbc.12.7.2061
36. Steinman, R.M., Swanson, J.: The endocytic activity of dendritic cells. J Exp Med. United States **182**, 283–288 (1995)

37. Sallusto, F., Cella, M., Danieli, C., Lanzavecchia, A.: Dendritic cells use macropinocytosis and the mannose receptor to concentrate macromolecules in the major histocompatibility complex class II compartment: downregulation by cytokines and bacterial products. J. Exp. Med. **182**, 389–400 (1995). https://doi.org/10.1084/jem.182.2.389
38. Kerr, M.C., Teasdale, R.D.: Defining macropinocytosis. Traffic 364–371 (2009). https://doi.org/10.1111/j.1600-0854.2009.00878.x
39. Rima, W., Sancey, L., Aloy, M.T., Armandy, E., Alcantara, G.B., Epicier, T., et al.: Internalization pathways into cancer cells of gadolinium-based radiosensitizing nanoparticles. Biomaterials **34**, 181–195 (2013). https://doi.org/10.1016/j.biomaterials.2012.09.029
40. Kumari, S., Mg, S., Mayor, S.: Endocytosis unplugged: multiple ways to enter the cell. Cell Res. 256–275 (2010). https://doi.org/10.1038/cr.2010.19
41. Kirchhausen, T.: Clathrin. Annu. Rev. Biochem. **69**, 699–727 (2000). https://doi.org/10.1146/annurev.biochem.69.1.699
42. Sandvig, K., Pust, S., Skotland, T., van Deurs, B.: Clathrin-independent endocytosis: mechanisms and function. Curr. Opin. Cell Biol. 413–420 (2011). https://doi.org/10.1016/j.ceb.2011.03.007
43. Ford, M.G.J., Mills, I.G., Peter, B.J., Vallis, Y., Praefcke, G.J.K., Evans, P.R., et al.: Curvature of clathrin-coated pits driven by epsin. Nature **419**, 361–366 (2002). https://doi.org/10.1038/nature01020
44. Capraro, B.R., Shi, Z., Wu, T., Chen, Z., Dunn, J.M., Rhoades, E., et al.: Kinetics of endophilin N-BAR domain dimerization and membrane interactions. J. Biol. Chem. **288**, 12533–12543 (2013). https://doi.org/10.1074/jbc.M112.435511
45. Tebar, F., Bohlander, S.K., Sorkin, A.: Clathrin assembly lymphoid myeloid leukemia (CALM) protein: localization in endocytic-coated pits, interactions with clathrin, and the impact of overexpression on clathrin-mediated traffic. Mol. Biol. Cell **10**, 2687–2702 (1999). https://doi.org/10.1091/mbc.10.8.2687
46. Marsh, M., McMahon, H.T.: The structural era of endocytosis. Science 215–220 (1999). https://doi.org/10.1126/science.285.5425.215
47. Stowell, M.H., Marks, B., Wigge, P., McMahon, H.T.: Nucleotide-dependent conformational changes in dynamin: evidence for a mechanochemical molecular spring. Nat. Cell Biol. **1**, 27–32 (1999). https://doi.org/10.1038/8997
48. Harush-Frenkel, O., Rozentur, E., Benita, S., Altschuler, Y.: Surface charge of nanoparticles determines their endocytic and transcytotic pathway in polarized MDCK cells. Biomacromol **9**, 435–443 (2008). https://doi.org/10.1021/bm700535p
49. Oh, P., Borgström, P., Witkiewicz, H., Li, Y., Borgström, B.J., Chrastina, A., et al.: Live dynamic imaging of caveolae pumping targeted antibody rapidly and specifically across endothelium in the lung. Nat. Biotechnol. **25**, 327–337 (2007). https://doi.org/10.1038/nbt1292
50. Wang, Z., Tiruppathi, C., Minshall, R.D., Malik, A.B.: Size and dynamics of caveolae studied using nanoparticles in living endothelial cells. ACS Nano **3**, 4110–4116 (2009). https://doi.org/10.1021/nn9012274
51. Hommelgaard, A.M., Roepstorff, K., Vilhardt, F., Torgersen, M.L., Sandvig, K., van Deurs, B.: Caveolae: stable membrane domains with a potential for internalization. Traffic 720–724 (2005). https://doi.org/10.1111/j.1600-0854.2005.00314.x
52. Howes, M.T., Kirkham, M., Riches, J., Cortese, K., Walser, P.J., Simpson, F., et al.: Clathrin-independent carriers form a high capacity endocytic sorting system at the leading edge of migrating cells. J. Cell Biol. **190**, 675–691 (2010). https://doi.org/10.1083/jcb.201002119
53. Parton, R.G., Simons, K.: The multiple faces of caveolae. Nat. Rev. Mol. Cell Biol. 185–194 (2007). https://doi.org/10.1038/nrm2122
54. Pelkmans, L., Püntener, D., Helenius, A.: Local actin polymerization and dynamin recruitment in SV40-induced internalization of caveolae. Science (80-) **296**, 535–539 (2002). https://doi.org/10.1126/science.1069784
55. Hayer, A., Stoeber, M., Ritz, D., Engel, S., Meyer, H.H., Helenius, A.: Caveolin-1 is ubiquitinated and targeted to intralumenal vesicles in endolysosomes for degradation. J. Cell Biol. **191**, 615–629 (2010). https://doi.org/10.1083/jcb.201003086

56. Parton, R.G., Howes, M.T.: Revisiting caveolin trafficking: the end of the caveosome. J. Cell Biol. 439–441 (2010). https://doi.org/10.1083/jcb.201009093
57. Gratton, S.E.A., Ropp, P.A., Pohlhaus, P.D., Luft, J.C., Madden, V.J., Napier, M.E., et al.: The effect of particle design on cellular internalization pathways. Proc. Natl. Acad. Sci. **105**, 11613–11618 (2008). https://doi.org/10.1073/pnas.0801763105
58. Sandvig, K., Torgersen, M.L., Raa, H.A., Van Deurs, B.: Clathrin-independent endocytosis: from nonexisting to an extreme degree of complexity. Histochem. Cell Biol. 267–276 (2008). https://doi.org/10.1007/s00418-007-0376-5
59. Robertson, A.S., Smythe, E., Ayscough, K.R.: Functions of actin in endocytosis. Cellu. Mol. Life Sci. 2049–2065 (2009). https://doi.org/10.1007/s00018-009-0001-y
60. Rothen-Rutishauser, B., Mühlfeld, C., Blank, F., Musso, C., Gehr, P.: Translocation of particles and inflammatory responses after exposure to fine particles and nanoparticles in an epithelial airway model. Part Fibre Toxicol. **4** (2007). https://doi.org/10.1186/1743-8977-4-9
61. Rothen-Rutishauser, B., Schurch, S., Gehr, P.: Interaction of particles with membranes. In: Donaldson, K., Borm, P. (eds.) Particle Toxicology, pp. 139–160. CRC Press, Tyler & Francis Group, Boca Raton, FL (2007)
62. Xu, S., Olenyuk, B.Z., Okamoto, C.T., Hamm-Alvarez, S.F.: Targeting receptor-mediated endocytotic pathways with nanoparticles: rationale and advances. Adv. Drug Deliv. Rev. **65**, 121–138 (2013). https://doi.org/10.1016/j.addr.2012.09.041
63. Low, P.S., Kularatne, S.A.: Folate-targeted therapeutic and imaging agents for cancer. Curr. Opin. Chem. Biol. **13**, 256–262 (2009). https://doi.org/10.1016/j.cbpa.2009.03.022
64. Muller, C., Schibli, R.: Prospects in folate receptor-targeted radionuclide therapy. Front Oncol. **3**, 249 (2013). https://doi.org/10.3389/fonc.2013.00249
65. Xia, W., Hilgenbrink, A.R., Matteson, E.L., Lockwood, M.B., Cheng, J.X., Low, P.S.: A functional folate receptor is induced during macrophage activation and can be used to target drugs to activated macrophages. Blood **113**, 438–446 (2009). https://doi.org/10.1182/blood-2008-04-150789
66. Ross, J.F., Wang, H., Behm, F.G., Mathew, P., Wu, M., Booth, R., et al.: Folate receptor type beta is a neutrophilic lineage marker and is differentially expressed in myeloid leukemia. Cancer **85**, 348–357 (1999). http://www.ncbi.nlm.nih.gov/pubmed/10023702
67. Low, P.S., Henne, W.A., Doorneweerd, D.D.: Discovery and development of folic-acid-based receptor targeting for imaging and therapy of cancer and inflammatory diseases. Acc. Chem. Res. **41**, 120–129 (2008). https://doi.org/10.1021/ar7000815
68. Zhao, X., Li, H., Lee, R.J.: Targeted drug delivery via folate receptors. Expert Opin. Drug Deliv. **5**, 309–319 (2008). https://doi.org/10.1517/17425247.5.3.309
69. Werner, M.E., Karve, S., Sukumar, R., Cummings, N.D., Copp, J.A., Chen, R.C., et al.: Folate-targeted nanoparticle delivery of chemo- and radiotherapeutics for the treatment of ovarian cancer peritoneal metastasis. Biomaterials **32**, 8548–8554 (2011). https://doi.org/10.1016/j.biomaterials.2011.07.067
70. Ponka, P., Lok, C.N.: The transferrin receptor: role in health and disease. Int. J. Biochem. Cell. Biol. **31**, 1111–1137 (1999). http://www.ncbi.nlm.nih.gov/pubmed/10582342
71. Sadat Tabatabaei Mirakabad, F., Nejati-Koshki, K., Akbarzadeh, A., Yamchi, M.R., Milani, M., Zarghami, N., et al.: PLGA-based nanoparticles as cancer drug delivery systems. Asian Pac. J. Cancer Prev. **15**, 517–535 (2014)
72. Danhier, F., Feron, O., Preat, V.: To exploit the tumor microenvironment: passive and active tumor targeting of nanocarriers for anti-cancer drug delivery. J. Control Release **148**, 135–146 (2010). https://doi.org/10.1016/j.jconrel.2010.08.027
73. van der Meel, R., Vehmeijer, L.J., Kok, R.J., Storm, G., van Gaal, E.V.: Ligand-targeted particulate nanomedicines undergoing clinical evaluation: current status. Adv. Drug Deliv. Rev. **65**, 1284–1298 (2013). https://doi.org/10.1016/j.addr.2013.08.012
74. Mirghani, H., Amen, F., Moreau, F., Guigay, J., Hartl, D.M., Lacau St Guily, J.: Oropharyngeal cancers: relationship between epidermal growth factor receptor alterations and human papillomavirus status. Eur. J. Cancer **50**, 1100–1111 (2014). https://doi.org/10.1016/j.ejca.2013.12.018

75. Holbro, T., Civenni, G., Hynes, N.E.: The ErbB receptors and their role in cancer progression. Exp. Cell Res. **284**, 99–110 (2003). http://www.ncbi.nlm.nih.gov/pubmed/12648469
76. Lurje, G., Lenz, H.J.: EGFR signaling and drug discovery. Oncology **77**, 400–410 (2009). https://doi.org/10.1159/000279388
77. Harris, R.C., Chung, E., Coffey, R.J.: EGF receptor ligands. Exp. Cell Res. **284**, 2–13 (2003). http://www.ncbi.nlm.nih.gov/pubmed/12648462
78. Tseng, C.L., Su, W.Y., Yen, K.C., Yang, K.C., Lin, F.H.: The use of biotinylated-EGF-modified gelatin nanoparticle carrier to enhance cisplatin accumulation in cancerous lungs via inhalation. Biomaterials **30**, 3476–3485 (2009). https://doi.org/10.1016/j.biomaterials.2009.03.010
79. Rajasekaran, A.K., Anilkumar, G., Christiansen, J.J.: Is prostate-specific membrane antigen a multifunctional protein? Am. J. Physiol. Cell Physiol. **288**, C975–C981 (2005). https://doi.org/10.1152/ajpcell.00506.2004
80. Schulke, N., Varlamova, O.A., Donovan, G.P., Ma, D., Gardner, J.P., Morrissey, D.M., et al.: The homodimer of prostate-specific membrane antigen is a functional target for cancer therapy. Proc. Natl. Acad. Sci. U.S.A. **100**, 12590–12595 (2003). https://doi.org/10.1073/pnas.1735443100
81. Hrkach, J., Von Hoff, D., Mukkaram Ali, M., Andrianova, E., Auer, J., Campbell, T., et al.: Preclinical development and clinical translation of a PSMA-targeted docetaxel nanoparticle with a differentiated pharmacological profile. Sci. Trans. Med. **4**, 128ra39 (2012). https://doi.org/10.1126/scitranslmed.3003651
82. Tucker, G.C.: Integrins: molecular targets in cancer therapy. Curr. Oncol. Rep. **8**, 96–103 (2006). http://www.ncbi.nlm.nih.gov/pubmed/16507218
83. Gottschalk, K.E., Kessler, H.: The structures of integrins and integrin-ligand complexes: implications for drug design and signal transduction. Angew. Chem. Int. Ed. Engl. **41**, 3767–3774 (2002). https://doi.org/10.1002/1521-3773(20021018)41:20%3c3767:AID-ANIE3767%3e3.0.CO;2-T
84. Eliceiri, B.P., Cheresh, D.A.: Role of alpha v integrins during angiogenesis. Cancer J. **6**(Suppl 3), S245–9 (2000). http://www.ncbi.nlm.nih.gov/pubmed/10874494
85. Brooks, P.C., Stromblad, S., Sanders, L.C., von Schalscha, T.L., Aimes, R.T., Stetler-Stevenson, W.G., et al.: Localization of matrix metalloproteinase MMP-2 to the surface of invasive cells by interaction with integrin alphavbeta3. Cell **85**, 683–693 (1996). http://www.ncbi.nlm.nih.gov/pubmed/8646777
86. Liu, S.: Radiolabeled cyclic RGD peptides as integrin alpha(v)beta(3)-targeted radiotracers: maximizing binding affinity via bivalency. Bioconjug. Chem. **20**, 2199–2213 (2009). https://doi.org/10.1021/bc900167c
87. Auzzas, L., Zanardi, F., Battistini, L., Burreddu, P., Carta, P., Rassu, G., et al.: Targeting alphavbeta3 integrin: design and applications of mono- and multifunctional RGD-based peptides and semipeptides. Curr. Med. Chem. **17**, 1255–1299 (2010). http://www.ncbi.nlm.nih.gov/pubmed/20166941
88. Graf, N., Bielenberg, D.R., Kolishetti, N., Muus, C., Banyard, J., Farokhzad, O.C., et al.: alpha(V)beta(3) integrin-targeted PLGA-PEG nanoparticles for enhanced anti-tumor efficacy of a Pt(IV) prodrug. ACS Nano **6**, 4530–4539 (2012). https://doi.org/10.1021/nn301148e
89. Brambell, F.W.: The transmission of immune globulins from the mother to the foetal and newborn young. Proc. Nutr. Soc. **28**, 35–41 (1969). http://www.ncbi.nlm.nih.gov/pubmed/4182340
90. Pridgen, E.M., Alexis, F., Kuo, T.T., Levy-Nissenbaum, E., Karnik, R., Blumberg, R.S., et al.: Transepithelial transport of Fc-targeted nanoparticles by the neonatal fc receptor for oral delivery. Sci. Transl. Med. **5**, 213ra167 (2013). https://doi.org/10.1126/scitranslmed.3007049
91. Goldberg, M., Gomez-Orellana, I.: Challenges for the oral delivery of macromolecules. Nat. Rev. Drug Discov. **2**, 289–295 (2003). https://doi.org/10.1038/nrd1067
92. Borner, M.M., Schoffski, P., de Wit, R., Caponigro, F., Comella, G., Sulkes, A., et al.: Patient preference and pharmacokinetics of oral modulated UFT versus intravenous fluorouracil and leucovorin: a randomised crossover trial in advanced colorectal cancer. Eur. J. Cancer **38**, 349–358 (2002). http://www.ncbi.nlm.nih.gov/pubmed/11818199

93. Priem, B., Tian, C., Tang, J., Zhao, Y., Mulder, W.J.: Fluorescent nanoparticles for the accurate detection of drug delivery. Expert Opin. Drug Deliv. **12**, 1881–1894 (2015). https://doi.org/10.1517/17425247.2015.1074567
94. Wei, Q., Qi, H., Luo, W., Tseng, D., Ki, S.J., Wan, Z., et al.: Fluorescent imaging of single nanoparticles and viruses on a smart phone. ACS Nano **7**, 9147–9155 (2013). https://doi.org/10.1021/nn4037706
95. Jin, S., Hu, Y., Gu, Z., Liu, L., Wu, H.-C.: Application of quantum dots in biological imaging. J. Nanomater. **2011**, 1–13 (2011). https://doi.org/10.1155/2011/834139
96. He, X., Ma, N.: An overview of recent advances in quantum dots for biomedical applications. Coll. Surf. B Biointerfaces **124**, 118–131 (2014). https://doi.org/10.1016/j.colsurfb.2014.06.002
97. Michalet, X., Pinaud, F.F., Bentolila, L.A., Tsay, J.M., Doose, S., Li, J.J., et al.: Quantum dots for live cells, in vivo imaging, and diagnostics. Science **307**, 538–544 (2005). https://doi.org/10.1126/science.1104274
98. Bagalkot, V., Zhang, L., Levy-Nissenbaum, E., Jon, S., Kantoff, P.W., Langery, R., et al.: Quantum dot-aptamer conjugates for synchronous cancer imaging, therapy, and sensing of drug delivery based on Bi-fluorescence resonance energy transfer. Nano Lett. **7**, 3065–3070 (2007). https://doi.org/10.1021/nl071546n
99. Fontes, A., de Lira, R.B., Seabra, M.A.B.L., da Silva, T.G., Castro Neto, A.G., Santos, B.S.: Quantum dots in biomedical research, biomedical engineering—technical applications in medicine [Internet]. In: Hudak, R. (ed.) InTech. https://www.intechopen.com/books/biomedical-engineering-technical-applications-in-medicine/quantum-dots-in-biomedical-research (2012)
100. England, C.G., Huang, J.S., James, K.T., Zhang, G., Gobin, A., Frieboes, H.B.: Detection of phosphatidylcholine-coated gold nanoparticles in orthotopic pancreatic adenocarcinoma using hyperspectral imaging. PLoS One **10** (2015). https://doi.org/10.1371/journal.pone.0129172
101. Guggenheim, E.J., Khan, A., Pike, J., Chang, L., Lynch, I., Rappoport JZ. Comparison of confocal and super-resolution reflectance imaging of metal oxide nanoparticles. PLoS One **11** (2016). https://doi.org/10.1371/journal.pone.0159980
102. Repenko, T., Rix, A., Ludwanowski, S., Go, D., Kiessling, F., Lederle, W., et al.: Biodegradable highly fluorescent conjugated polymer nanoparticles for bio-medical imaging applications. Nat. Commun. **8** (2017). https://doi.org/10.1038/s41467-017-00545-0
103. Wolfbeis, O.S.: An overview of nanoparticles commonly used in fluorescent bioimaging. Chem. Soc. Rev. **44**, 4743–4768 (2015). https://doi.org/10.1039/C4CS00392F
104. Chen, X., Cui, J., Sun, H., Mullner, M., Yan, Y., Noi, K.F., et al.: Analysing intracellular deformation of polymer capsules using structured illumination microscopy. Nanoscale **8**, 11924–11931 (2016). https://doi.org/10.1039/c6nr02151d
105. Fytianos, K., Rodriguez-Lorenzo, L., Clift, M.J.D., Blank, F., Vanhecke, D., von Garnier, C., et al.: Uptake efficiency of surface modified gold nanoparticles does not correlate with functional changes and cytokine secretion in human dendritic cells in vitro. Nanomed. Nanotechnol. Biol. Med. **11** (2015). https://doi.org/10.1016/j.nano.2014.11.004
106. Lehmann, A.D., Parak, W.J., Zhang, F., Ali, Z., Röcker, C., Nienhaus, G.U., et al.: Fluorescent-magnetic hybrid nanoparticles induce a dose-dependent increase in proinflammatory response in lung cells in vitro correlated with intracellular localization. Small **6**, 753–762 (2010)
107. Blom, R.A.M., Amacker, M., Moser, C., van Dijk, R.M., Bonetti, R., Seydoux, E., et al.: Virosome-bound antigen enhances DC-dependent specific $CD4^{+}$T cell stimulation, inducing a Th1 and Treg profile in vitro. Nanomed. Nanotechnol. Biol. Med. **13** (2017). https://doi.org/10.1016/j.nano.2017.02.004
108. Seydoux, E., Rothen-Rutishauser, B., Nita, I.M., Balog, S., Gazdhar, A., Stumbles, P.A., et al.: Size-dependent accumulation of particles in lysosomes modulates dendritic cell function through impaired antigen degradation. Int. J. Nanomed. **9** (2014). https://doi.org/10.2147/ijn.s64353

109. Hemmerich, P.H., von Mikecz, A.H.: Defining the subcellular interface of nanoparticles by live-cell imaging. PLoS One **8** (2013). https://doi.org/10.1371/journal.pone.0062018
110. De Los, S.C., Chang, C.-W., Mycek, M.-A., Cardullo, R.A.: FRAP, FLIM, and FRET: detection and analysis of cellular dynamics on a molecular scale using fluorescence microscopy. Mol. Reprod. Dev. **82**, 587–604 (2015). https://doi.org/10.1002/mrd.22501
111. Basuki, J.S., Duong, H.T.T., Macmillan, A., Erlich, R.B., Esser, L., Akerfeldt, M.C., et al.: Using fluorescence lifetime imaging microscopy to monitor theranostic nanoparticle uptake and intracellular doxorubicin release. ACS Nano **7**, 10175–10189 (2013). https://doi.org/10.1021/nn404407g
112. Welsher, K., Yang, H.: Multi-resolution 3D visualization of the early stages of cellular uptake of peptide-coated nanoparticles. Nat. Nanotechnol. **9**, 198–203 (2014). https://doi.org/10.1038/nnano.2014.12
113. Van Der Zwaag, D., Vanparijs, N., Wijnands, S., De Rycke, R., De Geest, B.G., Albertazzi, L.: Super resolution imaging of nanoparticles cellular uptake and trafficking. ACS Appl. Mater. Interfaces **8**, 6391–6399 (2016). https://doi.org/10.1021/acsami.6b00811
114. Bon, P., Bourg, N., Lécart, S., Monneret, S., Fort, E., Wenger, J., et al.: Three-dimensional nanometre localization of nanoparticles to enhance super-resolution microscopy. Nat. Commun. **6** (2015). https://doi.org/10.1038/ncomms8764
115. Peuschel, H., Ruckelshausen, T., Cavelius, C., Kraegeloh, A.: Quantification of internalized silica nanoparticles via STED microscopy. Biomed. Res. Int. **2015** (2015). https://doi.org/10.1155/2015/961208
116. Rodriguez-Lorenzo, L., Fytianos, K., Blank, F., Von Garnier, C., Rothen-Rutishauser, B., Petri-Fink, A.: Fluorescence-encoded gold nanoparticles: library design and modulation of cellular uptake into dendritic cells. Small **10**, 1341–1350 (2014). https://doi.org/10.1002/smll.201302889
117. Clift, M.J.D., Fytianos, K., Vanhecke, D., Hočevar, S., Petri-Fink, A., Rothen-Rutishauser, B.: A novel technique to determine the cell type specific response within an in vitro co-culture model via multi-colour flow cytometry. Sci. Rep. **7**, 434 (2017). https://doi.org/10.1038/s41598-017-00369-4
118. Mills, N., Rnqvist, H.T., Gonzalez, M., Vink, E., Robinson, S., Soderberg, S., et al.: Ischaemic and thrombotic effects of dilute diesel exhaust inhalation in patients with coronary heart disease: mechanisms for the adverse cardiovascular effects of air pollution. Heart **93**, A9–A9 (2007)
119. Clark, R.T.: Imaging flow cytometry enhances particle detection sensitivity for extracellular vesicle analysis. Nat. Methods. Nature Publishing Group, a division of Macmillan Publishers Limited. All Rights Reserved; **12** (2015). http://dx.doi.org/10.1038/nmeth.f.380
120. Vanhecke, D., Rodriguez-Lorenzo, L., Clift, M.J.D., Blank, F., Petri-Fink, A., Rothen-Rutishauser, B.: Quantification of nanoparticles at the single-cell level: an overview about state-of-the-art techniques and their limitations. Nanomedicine **9** (2014). https://doi.org/10.2217/nnm.14.108

Chapter 9
Imaging Techniques for Probing Nanoparticles in Cells and Skin

Christina Graf and Eckart Rühl

Abstract Imaging techniques for probing the interactions of nanoparticles with cells and skin are essential for a qualitative and quantitative understanding of uptake and penetration processes. A variety of important visualization techniques is reviewed for providing an overview on established and recently developed techniques. This includes optical microscopy, fluorescence microscopy, electron microscopy, Raman microscopy, optical near-field microscopy, X-ray microscopy, as well as recent and emerging developments in the field of spectromicroscopy.

9.1 Introduction

Engineered nanomaterials, especially nanoparticles, have gained increasing importance in the last two decades. Nanoparticles are known to enter human cells and can penetrate human skin under certain conditions. The interactions between nanoparticles and living matter have been extensively studied in the last years particularly with regard to possible implications regarding biosafety and various biomedical applications of nanomaterials in diagnostics and therapy [1–6]. Since nanoparticles are in the same size range as biological molecules and their assemblies, such as proteins or viruses, they can be taken up by cells via the same endocytotic pathways. Nanoparticles in biological media typically adsorb biomolecules forming the so-called protein corona, which determines at least their initial encounter with cells [6–9]. Penetration of nanoparticles into the skin is primarily restricted by the barrier function of the *stratum corneum* [10]. Most nanoparticles do not cross this barrier if human skin is intact; exceptions are some soft nanoparticles, whereas, for other nanoparticles, such

C. Graf (✉)
Department of Chemistry and Biotechnology, University of Applied Sciences Darmstadt, Stephanstrasse 7, 64295 Darmstadt, Germany
e-mail: christina.graf@h-da.de

E. Rühl (✉)
Physical Chemistry, Institute of Chemistry and Biochemistry, Free University of Berlin, Takustrasse 3, 14195 Berlin, Germany
e-mail: ruehl@zedat.fu-berlin.de

P. Gehr and R. Zellner (eds.), *Biological Responses to Nanoscale Particles*, NanoScience and Technology, https://doi.org/10.1007/978-3-030-12461-8_9

penetration is only occasionally observed [11]. However, skin appendages, such as hair follicles, sebaceous glands, or sweat glands may enable such penetration processes as well as damage of the skin which might be due to pricking, injuries, or skin disorders [10]. Once the nanoparticles have overcome the *stratum corneum*, they can easily penetrate into deeper layers of the skin, i.e., the viable epidermis and dermis [12]. Various microscopic techniques have been applied for investigating the uptake of nanoparticles in skin and cells including electron microscopy [13–17], soft X-ray spectromicroscopy [18–20], Raman microscopy [21], infrared microscopies [22, 23], fluorescence microscopy [24–29], and single-molecule fluorescence microscopy [30–33], as well as optical microscopy including super-resolution microscopy [32–35]. These techniques vary in sensitivity, specificity, spatial resolution, the possibility to measure living or only fixed, embedded or frozen biological matter, and technical requirements [36, 37]. Ideally, an imaging technique has, on the one hand, high spatial resolution, allowing for imaging of single molecules or nanoparticles and possible temporal changes while enabling recognition of cellular structures and labeling of different biomolecules in the cell. On the other hand, it should be possible to observe cells or tissue in vivo to monitor intracellular processes of the nanoparticles, and the biological material should not be affected by preparation and processing for the respective imaging technique. Furthermore, the imaging method should be easy and fast to use as well as low-cost. None of the available methods fulfills all these conditions but combining and ideally, correlating different microscopy approaches with each other can solve many of these requirements. There are in the literature several reviews putting different emphasis on this subject, which includes intentionally made nanoparticles [38–40], and cosmetics [41].

In this review, the most important imaging techniques for probing nanoparticles in cells and skin are presented, and their advantages, challenges, and limitations are discussed and compared with each other. Also, several approaches combining or correlating different imaging approaches are discussed.

9.2 Optical Microscopy

Conventional fluorescence microscopy and classical bright-field light microscopy are standard techniques for imaging cells and tissue. They are non-invasive and allow for live imaging of biological specimens, require relative simple sample preparation, and yield a large amount of data in a relatively short period of time. However, in standard optical microscopes, the spatial resolution is limited by diffraction and does not allow the distinction between objects smaller than ~200 nm. Since nanoparticles have by definition diameters between 1 and 100 nm [42], they fall within this limit and consequently cannot be spatially resolved by optical microscopy, which makes their direct tracking and quantification impossible. Therefore, more sophisticated approaches in spectromicroscopy are required for this purpose.

9.3 Fluorescence Microscopy

Conventional fluorescence microscopy is an indispensable tool in biomedical research. Fluorescence intensities of emission wavelengths usually excited in the UV or visible spectral range are the observables of such studies [36]. Thereby, fluorophores which are endogenous to cells or skin (e.g., porphyrins, collagen, elastin, etc.), can be excited but usually, this approach requires fluorescent labeling to specifically visualize the cellular structures of interest as well as the nanoparticles under investigation [38, 43–47]. Labeling nanoparticles with a fluorescent marker, usually a fluorescent organic dye, can change the diffusive transport behavior as well as the bioreactivity of a nanoparticle if the dye is not fully embedded in the bulk interior of the nanoparticle [38, 48]. In addition, from dye-labeling may arise additional issues of photobleaching or phototoxicity to the cell, which may impede long-term studies [49]. Some engineered nanoparticles have inherent fluorescent properties, such as semiconductor nanoparticles (quantum dots) and lanthanoide doped upconversion nanoparticles [50]. Both have also been used for labeling colloidal particles in biomedical studies [6, 26, 51]. Quantum dots have an excellent photostability and enable from this point of view long-time studies. However, they consist of mostly cytotoxic semiconductors. Upconversion is an optical process comprising the sequential absorption of two or more photons which leads to the emission of light with a shorter wavelength than the exciting light [50]. Consequently, the emission of upconversion nanoparticles in the visible regime can be excited by near-infrared (NIR) radiation. This is in contrast to organic fluorescent dyes or quantum dots which are excited by UV radiation or visible light. In contrast to visible or ultraviolet (UV) light, NIR radiation is less absorbed or scattered by biological matter and, hence, it penetrates deeper into biological matter and does not induce autofluorescence of the surrounding tissue [26, 52]. Moreover, upconversion nanoparticles are known to have much lower cytotoxicity than semiconductor quantum dots. Song et al. investigated the transport of upconversion nanoparticles into excised intact and microneedle-treated human skin using wide-field epi-luminescence optical microscopy [26]. Due to the long excitation wavelength (980 nm), they achieved complete suppression of the background fluorescence and could show that 8 and 32 nm diameter upconversion nanoparticles stayed at the *stratum corneum* of the intact skin, whereas in case of the microneedle-treated skin, the 8 nm nanoparticles were found confined at the microneedle indentations and spread very slowly into the dermis [26]. Fluorescence detection of nanoparticles is often combined with immunofluorescent labeling of marker proteins, which allows for spatial co-localization of the nanoparticles and hence, an identification of the uptaking cell compartment and its activation status [38].

9.4 Single-Photon Confocal Microscopy

Single-photon confocal microscopy, especially laser scanning confocal microscopy (LSCM), is often used to image fluorescent nanoparticles in cells [24, 25] within tissues [53–55] and in vivo [56–58]. In LSCM, the excitation laser source scans point-by-point across the specimen to form a complete image of the focal plane. From a series of such sections, a three-dimensional image of the sample can be generated. LSCM is usually based on single photon processes, i.e. only one photon is absorbed and one photon of lower photon energy, corresponding to a longer wavelength than the exciting one, is emitted. Still, mostly fixed cells are investigated, which makes it difficult to investigate dynamic cellular processes. Time-lapse imaging of live cells is an effective tool for the observation of various cellular processes, such as cell proliferation and cell division [27]. Seynhaeve et al. followed in real-time the intercellular fate of doxorubicin and lipid-based nanoparticles containing doxorubicin in tumor cells [28]. Kang et al. studied the cellular association and internalization of liposomes as an effect of their surface charges using a laser scanning confocal microscope (LSCM) equipped with a live cell chamber system [59]. Wildt et al. combined live cell time-lapse microscopy and image analysis with fluorescence confocal microscopy detection of a classical dead-cell indicator dye using an LSCM. In this way, they could simultaneously investigate the kinetics of the uptake and cytotoxicity of unlabeled, i.e. non-fluorescent, silver nanoparticles in L-929 fibroblast cells [29].

The point by point laser excitation in LSCM often causes strong photobleaching. In a spinning disk confocal system, a rotating disk with a pattern of slits or holes is installed in the microscope plane that is conjugated with the specimen. This approach allows for faster imaging than LSCM and photobleaching and phototoxicity are strongly reduced [6, 60]. However, the confocality is slightly diminished. Spinning confocal disk microscopy is advantageous for studying nanoparticles of low photostability and for observing nanoparticle uptake processes in real time. Shan et al. used this technique for the systematic investigation of the time course of the in situ internalization process of nanoparticles of different materials in the size range from 3.3 to 100 nm by live cells [6]. In this way, they could show that quantum dots and gold nanoparticles with diameters <10 nm accumulate on the plasma membrane before their internalization by the cell, whereas polystyrene nanoparticles with diameters of ≈100 nm are directly internalized without prior accumulation, regardless of their surface charge [6].

In most studies applying LSCM to investigate nanoparticle penetration into skin either excised human [54, 61–63] or animal skin [64–67] is used. In clinical imaging reflectance confocal microscopy (RCM) is applied to skin, which also belongs to the group of single photon microscopy techniques. In RCM, low-energy laser light is focused on a specific area of the skin. Light is reflected from a small tissue spot at the focal point and enters the detector through a small pinhole so that only light from the focal point at the tissue is used for producing an image [68, 69]. Thereby, one exploits the fact that skin components, such as melanin, keratin, and collagen are

highly reflective. The resolution of reflectance confocal microscopy is lower than in LSCM (<1.25 μm in the horizontal plane and <5.0 μm in the vertical plane) in vivo. Lin et al. used RCM for the assessment of a topical nanoparticle penetration profile of <50 nm diameter silver nanoparticles in human volunteers [56].

9.5 Imaging Flow Cytometry Combined with Confocal Microscopy

In many cellular uptake studies, it is challenging to distinguish nanoparticle internalized into cells from the non-internalized ones. Vranic et al. used imaging flow cytometry to determine the cellular localization of fluorescently labeled SiO_2 nanoparticles, as well as light diffracting, non-fluorescent TiO_2 nanoparticles [70]. In this innovative technique, the inside of the cells is defined in data processing by eroding the cell borders. Thereby, Vranic et al. could determine the ratio of internalization of the nanoparticles and hence study nanoparticle uptake on a large number of cells. These functional studies were completed by LSCM observations also used for colocalization studies of nanoparticles with proteins, which are specific for different endocytic vesicles [71]. In this way, it could be shown that the uptake of SiO_2 nanoparticles by pulmonary epithelial NCI-H292 cells is a time and dose-dependent process which can be saturated. Based on these LSCM data, they could reveal that this a predominantly energy dependent internalization process and that 50 nm SiO_2 nanoparticles can also be taken up by passive diffusion [71].

9.6 Multi-photon Microscopy

Similar to confocal microscopy in two-photon or multi-photon microscopy, a laser is used to induce the emission of fluorescence from a sample, and the emitted light is detected. In contrast to the lasers used in LSCM, which provide single-photon excitation, the lasers used in two- or multiphoton photon microscopy excite by using near simultaneous absorption of two or more long wavelength (NIR) photons. The advantage is that such long wavelength radiation is less damaging for biological matter and penetrates more deeply into tissue than UV or visible (VIS) light, as used in confocal microscopy. Possible tissue damage is further minimized since nearly simultaneous absorption of two or more photons is only reached near the focal plane, where the intense radiation, leading to such processes, is mostly concentrated. Specifically, gold and silver nanoparticles exhibit two-photon photoluminescence, so that there is no need for secondary labeling of these particles [72–75].

Rane et al. used two-photon microscopy to systematically investigate the effect of different properties of gold nanoparticles on the penetration depth into three-dimensional cell spheroids formed from the HCT116 cells, which are a colorectal

carcinoma cell line [74]. They could demonstrate that two-photon microscopy enables quantitative localization of gold nanoparticles and that concentration data can be obtained from the single spheroid level. Labeling of the gold nanoparticles was not required due to their intrinsic two-photon emission. This study also revealed significant differences between the uptake profiles of gold nanoparticles in two-dimensional monolayers of cells as compared to three-dimensional cell spheroids [74]. In another study, a combined multiphoton imaging-UV-VIS spectroscopic analysis approach was applied to evaluate the uptake process of gold nanoparticles with diameters below the resolution of optical microscopy (size range: 15–80 nm) in A549 cells [76]. A quantitative analysis of the size effect on the cellular uptake behavior of gold nanoparticles was obtained from stacks of three-dimensional multiphoton laser scanning microscopy images. The authors were able to distinguish particles, which have entered into cells from those only adsorbed on the cell membrane. UV-VIS spectroscopy was complementarily utilized for determining the concentration and supported the results from multiphoton laser scanning microscopy [76].

Multiphoton microscopy is also well-suited for noninvasively imaging intact tissue, such as skin. Time-lapse volumetric multiphoton microscopy was successfully applied for in vivo imaging of immune cell dynamics in skin exposed to zinc oxide nanoparticles [77].

9.7 Fluorescence Lifetime Imaging Microscopy (FLIM)

In fluorescence lifetime imaging microscopy (FLIM), an image is produced based on the differences in the excited state decay rate from a fluorescent sample. Thus, in FLIM the contrast is based on differences in the lifetime of individual fluorophores rather than their emission spectra like in LSCM. Consequently, FLIM allows for the discrimination of fluorescent nanoparticles against the autofluorescence tissue or cellular background, since the fluorescence lifetime does not depend on concentration, sample thickness, absorption by the sample, photo-bleaching, or excitation intensity [36]. As a result, this technique is more robust than intensity-based methods. The fluorescence lifetime can be influenced by various environmental parameters, such as pH, ion or oxygen concentration, or molecular binding and is consequently an attractive approach for functional imaging in life sciences. This environmental sensitivity of the fluorescence lifetime also allows gaining insights into the local environment of the nanoparticle and its interactions with cellular substructures [36]. Basuki et al. applied FILM to monitor the intracellular controlled release mechanism of doxorubicin reversibly attached to iron oxide nanoparticles in H1299 lung cancer cells [78]. In this study, the authors exploited the fluorescence lifetime difference exhibited by native doxorubicin ($\tau \approx 1$ ns) compared to conjugated doxorubicin ($\tau \approx 4.6$ ns) and found a significant increase of native doxorubicin with time [78].

Most FLIM setups combine confocal laser scanning microscopy with time-correlated single photon counting (TCSPC). In this way, the fluorescence lifetime curves for each pixel are recorded [36, 79]. Besides this, multiphoton FLIM has

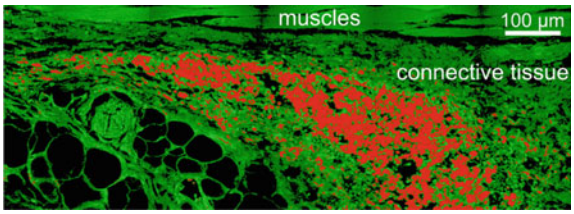

Fig. 9.1 Detection of amino-functionalized fluorescent silica nanoparticles (red color) in a mouse tissue sections (green color) using FLIM analysis. Reprinted from Ostrowski et al. [66], Copyright 2018, with permission from Elsevier

been employed for non-invasive imaging of skin penetration studies [80] and analysis of pH gradients in the *stratum corneum* [81]. FILM was successfully used for the localization of amino-functionalized fluorescent silica nanoparticles in mouse tissue sections after topical application, although the nanoparticles show a multiexponential fluorescence decay (see Fig. 9.1) [66]. For this purpose, multivariate data analysis was applied. Additionally, quantification of nanoparticle uptake was shown to be feasible. In this study a reference sample containing a defined concentration of silica nanoparticles allowed for the calibration of the fluorescence intensity to a defined nanoparticle [66].

To investigate the penetration of silver nanoparticles inside skin, Zhu et al. studied porcine ears treated with silver nanoparticles by two-photon tomography using the fluorescence lifetime imaging microscopy (TPT-FLIM) technique [75]. They could track the penetration depth of silver nanoparticles in porcine skin, which was due to different fluorescence lifetimes of skin components and silver nanoparticles and their resulting contribution to the multiexponential fluorescence decay. A maximum penetration depth of silver nanoparticles at ~14 µm was found, this value agreed well with results from surface-enhanced Raman scattering (SERS) and confocal Raman microscopy [75].

9.8 Super-Resolution Fluorescence Microscopy

According to their definition, the size range of nanoparticles (1–100 nm) is below the classical optical resolution limit [42]. Since the early 1990s, several techniques have been developed to improve the spatial resolution of optical microscopy. A variety of super-resolution microscopy techniques providing sub-50 nm spatial resolution have been developed, such as stimulated emission depletion (STED) [82], stochastic optical reconstruction microscopy (STORM) [83], photoactivation localization microscopy (PALM) [84], and structured illumination microscopy (SIM) [85]. These techniques open new opportunities to study nanoparticle-cell interactions and have already been successfully applied in life sciences to image cellular structures with sub-diffraction resolution [32].

In STED microscopy, fluorophores in the outer area of an excited spot are depleted while a center focal spot is left active to emit fluorescence light: in this way, the focus is sharpened and, therefore, the resolution in the lateral and/or axial plane is increased [33]. By the application of STED microscopy, it was shown that fluorescence-labeled silica nanoparticles with 30 nm diameter penetrated the nucleus of Caco-2 cells [86].

The quantification of absolute numbers of nanoparticles in cells is still a challenge, especially if the particles are below the classical optical resolution limit. Peuschel et al. used STED microscopy to produce three-dimensional image stacks to quantify internalized fluorescently labeled 25 and 85 nm sized silica nanoparticles in alveolar type II cells (A549) [33]. In this approach, the quantification of internalized nanoparticles is not based on a measurement of the mean fluorescence intensity of single particles or of cell-associated particles but on the analysis of segmented objects [33]. Van der Zwaag et al. combined STORM with single-molecule data analysis to investigate the uptake of polystyrene nanoparticles in dendritic cells [32]. They compared 300 nm Cy3-labeled particles with 80 nm Cy5-labeled particles and 300 nm ovalbumin-loaded particles also labeled with Cy5 and studied their interactions with the plasma membrane (see Fig. 9.2a). The authors achieved to image individual nanoparticles and tracked them during membrane binding and internalization (see Fig. 9.2b, c) and could quantify the number of particles inside dendritic cells. A comparison of different imaging techniques shows that transmission electron microscopy (TEM) (Fig. 9.2d) allows identifying small particles but does not yield any information on the nanoparticle color and thus their surface-functionalization. In contrast, STORM (Fig. 9.2e) and LCSM (Fig. 9.2f) can differentiate between nanoparticles with different labeling, which cannot be individually imaged by LCSM.

9.9 Photothermal Microscopy

Growing biomedical applications of non-fluorescent nanoparticles require novel tools for real-time detection of these materials in complex biological environments without additional labeling [87]. Photothermal microscopy (PTM) allows for the detection of nanometer-sized objects solely based on their absorption and hence, enables their efficient observation in scattering media notably gold nanoparticles in cells [88]. In PTM, small absorbers with minute luminescence yields convert upon resonant laser excitation all the absorbed energy into heat. This causes a rise in the temperature of their local environment inducing variations of the local refractive index. With an additional non-resonant laser beam, this photothermal effect can be efficiently probed [88]. PMT enables the spectroscopic identification and quantification of various non-fluorescent nanoparticles inside live cells and tissues without the need to use fluorescent labeling and with a minimal sensitivity toward the light scattering background [87]. Confocal PTM also allows three-dimensional (3D) mapping in live cells [87]. Multicolor PTM can be employed for spectral identification of nanoparticles in complex biological backgrounds. The spatial resolution of PTM (250–300 nm) is similar to those of other diffraction-limited optical microscopes. Zharov and coworkers applied confo-

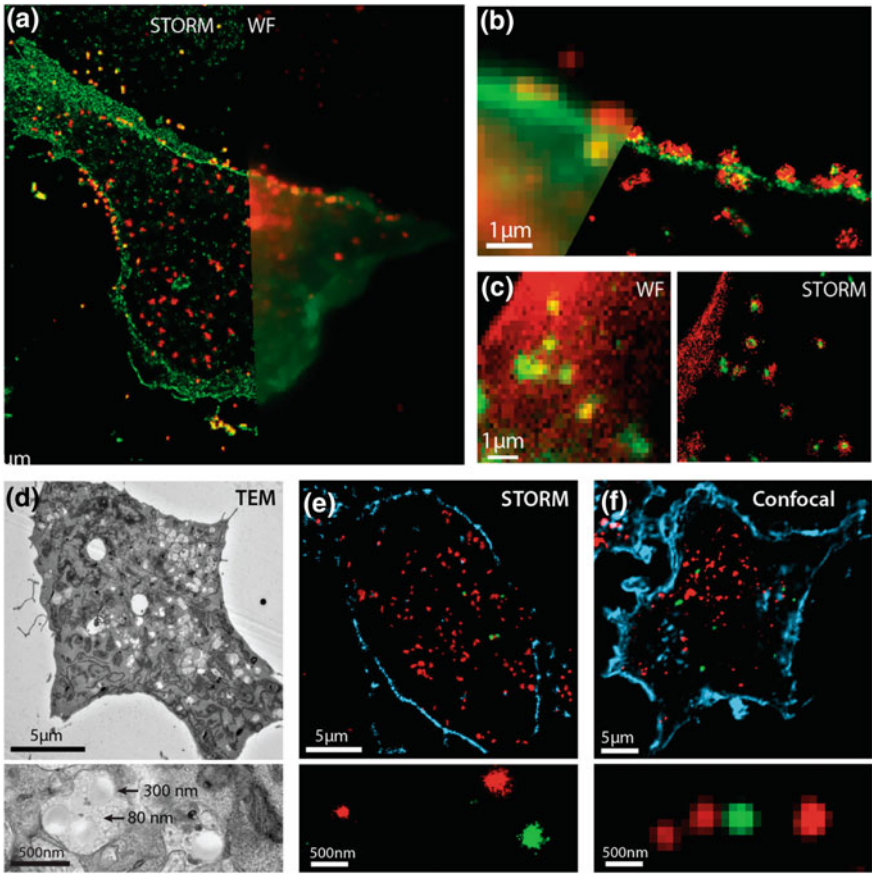

Fig. 9.2 **a** Two-color image of membrane-stained dendritic cells (green) and ovalbumin-labeled 300 nm polystyrene particles (red) in wide-field (WF) (right) and STORM (left); **b** magnified view of the membrane where individual nanoparticles bound to the plasma membrane and after internalization can be identified; **c** colocalization of ovalbumin-nanoparticles (cyan) with endosomal vesicles labeled by cholera toxin subunit (**b**); **d** TEM; **e** STORM; and **f** confocal imaging of the different nanoparticles inside dendritic cells. Bottom panels are enlarged views showing the ability of the different techniques to image nanoparticles of different size and color. Adapted with permission from van der Zwaag et al. [32]. Copyright 2018 American Chemical Society

cal PTM integrated with fluorescence microscopy to monitor molecular targeting of melanoma-associated chondroitin sulfate proteoglycan (MCSP) receptors of human melanoma cells (SK-mel-1 cell line) [87, 89]. For this purpose, melanoma cells were labeled with 50 nm anti-MCSP magnetic nanoparticles. An analysis of a stack of two-dimensional PT images confirmed that the nanoparticulate MCSP markers are distributed on the cell surface and indicate an intracellular accumulation of melanin (Fig. 9.3a). These two-dimensional stacks were then used to reconstruct a 3D distribution of cell absorption profiles (Fig. 9.3b). An analysis of nanoparticle-associated PT

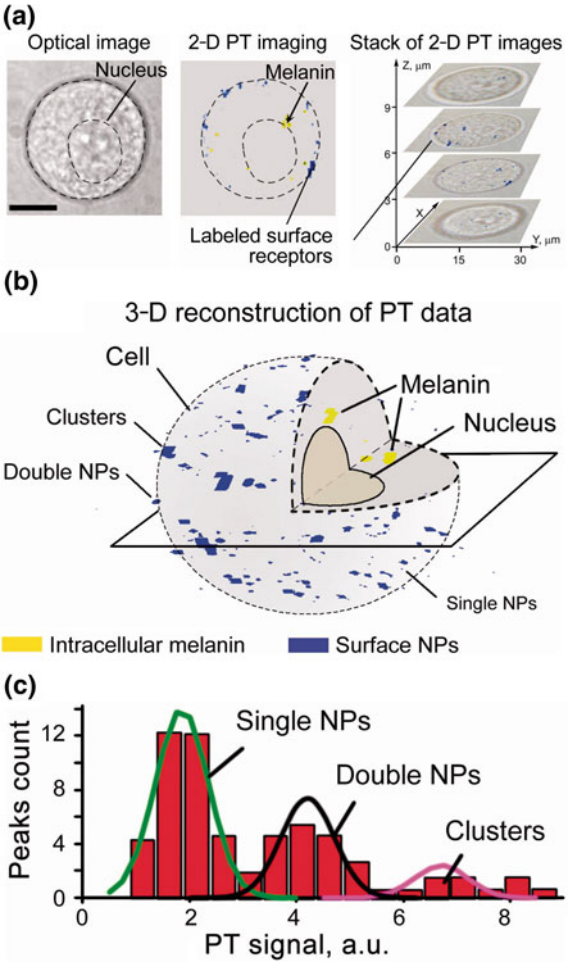

Fig. 9.3 **a** Sequent two-dimensional PTM images of different cross-sections of a cell targeted by anti-MCSP labeled, 50 nm diameter magnetic nanoparticles and a corresponding stack of two-dimensional PTM images; **b** Three-dimensional spatial reconstruction of surface MCSP receptors (blue) and intracellular melanin (yellow) distribution; **c** Histogram of the photothermal signal amplitudes of single and clustered magnetic nanoparticles on the cell surface Figure (**a**) was reprinted with permission from Nedosekin et al. [87]. www.tandfonline.com Figure (**b**) and (**c**) were adapted from [89]

signal amplitudes enabled the authors to distinguish single NPs from clustered NPs around single and clustered markers (Fig. 9.3c). These findings indicate that PTM is a promising approach for studying nanoparticle aggregation upon cellular uptake.

9.10 Photothermal Raster Image Correlation Spectroscopy

In raster image correlation spectroscopy (RICS) the diffusion of fluorescently labeled molecules or nanoparticles is obtained from stacks of confocal microscopy images by analyzing correlations within the image. Based on RICS, Nieves et al. implemented a novel photothermal imaging technique for probing the diffusion dynamics of gold

nanoparticles, photothermal raster image correlation spectroscopy (PhRICS) [90]. In this approach, single gold nanoparticles are imaged at short pixel dwell times (60 μs) with a piezo-scanning photothermal heterodyne imaging microscope. The method was then applied for diffusion measurements of gold nanoparticle-labeled FGF2 protein in a live cell [90].

9.11 Electron Microscopy

The tremendous progress of nanoparticle development and their applications in biomedicine would not have been possible without the rapid advancement of electron microscopy techniques. With high-resolution transmission electron microscopy (HRTEM) and scanning transmission microscopy (STEM), a spatial resolution <0.05 nm can be reached [91]. Transmission electron microscopy (TEM) and scanning electron microscopy (SEM) are standard methods for the characterization of size, morphology, and crystalline structure of nanoparticles. In combination with spectroscopic techniques, such as energy dispersive X-ray spectroscopy (EDX) and electron energy loss spectroscopy (EELS), SEM, and TEM yield spatially resolved information on the elemental composition of nanomaterials. Due to the high spatial resolution TEM and SEM are highly suited for tracking nanoparticles in skin and tissue. TEM provides detailed information on subcellular structures so that potentially toxicological changes due to interactions with nanoparticles become visible [92]. TEM usually operates in high vacuum to increase the mean free path of the electron gas—interactions, which requires a specific sample preparation. Current nanoscale methods for the investigation of cells mostly involve TEM of thin polymer embedded sections [93], frozen sections [93–96], edges of frozen cells [97], or fractures [98] of cellular samples [17]. Usually, the cells are stained by heavy metal salts for obtaining sufficient contrast. For tomographic information, cells are sectioned and imaged in a serial process [17, 99]. In Fig. 9.4 TEM images from resin-embedded, stained sections of HaCaT cells (immortalized human keratinocytes) after the uptake of silver nanoprisms (Fig. 9.4a–c) and silver nanospheres (Fig. 9.4d–f) are shown. The silver particles partially dissolve during this uptake process, which can be well observed when the particles before and after cellular uptake are compared to each other (Fig. 9.4c, f) [13].

However, TEM imaging has the disadvantage that the sample preparation is more laborious and prone to artifacts compared to other microscopy techniques [92, 100]. Furthermore, only a tiny volume of 1–10 μm^3 is usually analyzed [100–104]. The volume of cells and tissue strongly shrinks during the standard preparation of electron microscopy samples, mostly as a consequence of chemical fixation [105, 106]. Dehydration effects can also change the ultrastructure of tissues [107].

In cryogenic approaches, chemical fixation is avoided, and the normal hydration state of cells and tissue is maintained [108]. The state-of-the-art approach for TEM sample preparation for whole cells comprises high-pressure freezing and cryosec-

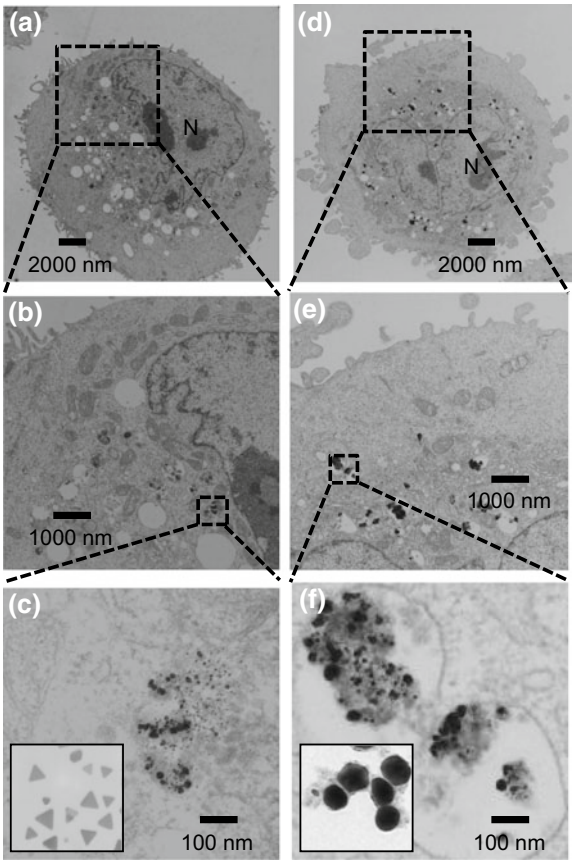

Fig. 9.4 Uptake of HaCaT cells observed by TEM after (**a**–**c**) 24 h of incubation with silver nanoprisms and (**d**–**f**) 24 h of incubation with silver nanospheres. The insets show particles of the same batches before their incubation with cells at the same magnification. Reprinted with permission from Graf et al. [13]. Copyright 2018 American Chemical Society

tioning [96, 109, 110]. Cryo-TEM has also been applied for the investigation of skin samples on the ultrastructural level [111].

9.12 Scanning Electron Microscopy (SEM)

In scanning electron microscopy (SEM), an electron beam is raster-scanned over the surface of a sample. The image is produced by the detection of the emitted electrons, known as secondary electrons (with energies smaller than 50 eV) and backscattered electrons (with energies above 50 eV) [39]. In modern SEM based on the use of field emission guns at low voltages, a spatial resolution of around 1 nm is achieved, which satisfies for many applications the spatial resolution requirements for investigating nanoparticle-cell systems [38, 112]. Conventional SEM operates as TEM in high vacuum. As for TEM; cryo-techniques can be applied to study biological systems in

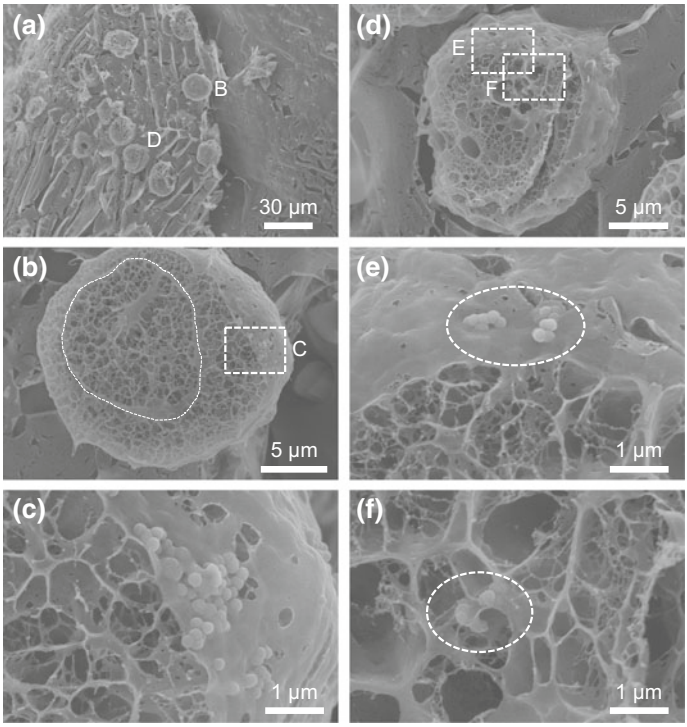

Fig. 9.5 Cryo-SEM images of HaCat cells after 19 h incubation with silica particles (170 nm diameter); **a** overview image; **b** incised cell B, the nuclear membrane is labeled by a dashed line; **c** enlarged view of partially aggregated silica particles on the cell membrane of cell B; **d** incised cell D; **e** enlarged view of silica particles on the cell membrane of cell D; **f** enlarged view of silica particles which where taken up by cell D

a near-native, hydrated environment. Typically, biological samples are plunged into a cryogen to trap the sample in a thin film of vitreous ice [113]. Before imaging, the specimens are usually sputter-coated, i.e., covered with a few nanometers thin layer of conductive material, such as Pt. This impedes the imaging of small metallic nanoparticles on the surface of the biological sample. In Fig. 9.5 cryo-SEM images of plunge-frozen, Pt-sputtered HaCaT cells incubated with 170 nm silica nanoparticles are presented. The cells are fractured by a cold knife. Nanoparticle on the surface of the cell membrane (Fig. 9.5c, e) as well as taken up particles (Fig. 9.5f) are visible. Figure 9.5c, e reveal that the initially well-dispersed particles cluster on the cell membrane and are covered by their protein corona. The porous structure of the cells is partially an artifact due to frost damages. With improved but also more elaborate freezing techniques, such as high-pressure freezing, such effects can be prevented, as shown for example for the ultrastructural examination of skin [73].

9.13 High-Angle Annular Dark-Field Scanning Transmission Electron Microscopy (HAADF STEM)

For the visualization of cellular structures, thin sections usually have to be stained with heavy-metal salts before TEM imaging. Staining may induce artifacts because of metals which precipitate from stains and cannot be distinguished from small nanoparticles, if not additional analytical methods, such as EDX are applied [15]. In annular dark-field scanning transmission electron microscopy (ADF STEM) images are formed by collecting scattered electrons with an annular dark-field detector. Since an annular dark field image is only formed by incoherently scattered electrons, ADF-STEM is sensitive to variations in the atomic number and allows for imaging of biological samples without staining [15, 114–116]. The sensitivity of this technique was improved by using electrons which are scattered in large angles, introducing a novel technique called high-angle annular darkfield (HAADF) STEM. HAADF-STEM has been employed to image thin cell sections and nanoscale objects therein at high electron energies [15, 117, 118]. Due to its high sensitivity, HAADF-STEM allows imaging of biological samples also at low energies. Hondow et al. applied low-energy HAADF STEM in a scanning electron microscope to analyze the uptake of platinum nanoparticles with a broad size distribution between 2 nm and 4 μm in HT29 colon carcinoma cells [14]. The authors achieved to obtain high contrast images of the ultrastructure of cells without post-staining and to distinguish the differently sized particles which provide valuable information on the effect of particle size on cellular uptake processes [15].

9.14 Environmental Scanning Electron Microscopy (ESEM)

Since conventional TEM and SEM operate in high vacuum only completely dried, embedded, or frozen samples can be imaged. The required sample preparation can change the sample (see above) and evidently, studies on live cells are impossible. About 15 years ago, environmental scanning electron microscope (ESEM) was introduced, which permits wet and insulating samples to be imaged without prior preparation. A low pressure (up to around 1000 Pa) of a gas, in case of biological samples water, can be accommodated around the sample. Consequently, hydrated biological samples can be kept in their native state. For details of detection and operation of this method see [119]. ESEM has been applied for imaging the surfaces of cells in a wet environment [120–122]. However, for ESEM cells must first be transferred to a cooled pure water environment. While various microorganisms and plant cells withstand this transfer process and ESEM imaging of their pristine surfaces is feasible, for eukaryotic cells this transfer process causes significant changes in the cellular morphology and can induce cell death [17]. However, fixed but still hydrated samples can be imaged instead [122]. Coupling ESEM with STEM detection enables imag-

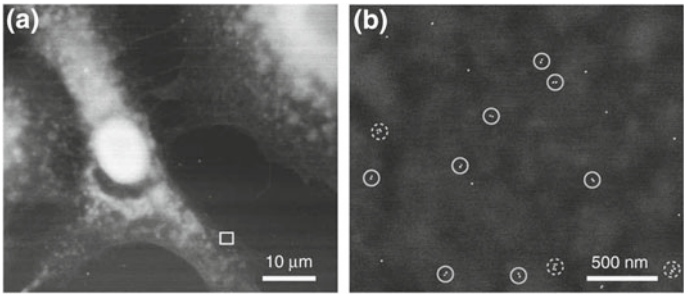

Fig. 9.6 Environmental scanning electron microscopy-scanning transmission electron microscopy (ESEM-STEM) of a whole fixed A549 cell in hydrated state. **a** Overview dark-field ESEM-STEM image of the contours of three cells (gray color) and thicker cellular regions (white color); **b** Enlarged view of the white rectangle in (**a**) showing individual gold nanoparticles, gold nanoparticle dimers (circles), and larger clusters (dashed circles). Image (**a**) is reprinted from [16], image (**b**) is reprinted with permission from Peckys and de Jonge [17]. Copyright 2018 Cambridge University Press

ing of unstained intracellular structures [17, 123]. Peckys et al. imaged individual gold nanoparticles, gold nanoparticle dimers, and larger clusters of these particles in whole fixed A549 cells in hydrated state using ESEM-STEM (see Fig. 9.6) [16, 17].

9.15 Liquid Scanning Transmission Electron Microscopy (Liquid STEM)

The development of Si_3N_4 membranes for use as TEM windows in a liquid compartment [124] enables the concept to reach nanometer resolution on fully hydrated cells [125, 126]. Eukaryotic cells in liquids were placed in a microfluidic chamber providing a ~6 µm space through which buffered liquids continuously flow. Then, STEM can image nanoparticles with a high *Z*-contrast, such as gold nanoparticles, that can be well observed [17]. Brownian motion of the nanoparticles did not hinder to reach nanoscale resolution since their diffusion near the membrane strongly slowed down [126, 127]. TEM micrographs obtained from this liquid STEM approach of complete samples significantly differ from those making use of thin sections, usually taken to image cellular ultrastructure, since a significantly thicker sample leads to reduced contrast [17].

9.16 Multimodal Imaging and Correlative Microscopy

Since each imaging method has its limitations, in many studies on the interactions of nanoparticles with cells and tissue the capabilities of different powerful microscopy and analytical platforms are coupled. Such combinations are especially valuable if the images of different techniques are correlated with each other. Several

authors reported on correlative microscopy approaches where conventional optical microscopy, high-resolution confocal microscopy, and TEM or SEM were combined [128–130]. Optical microscopy provides functional information based on fluorescent labeling in both living and fixed samples, while electron microscopy provides significantly higher spatial resolution, extending this information by detailed images of precisely the same region [131]. Le Trequesser et al. developed a triple correlative microscopy approach exploiting the complementarity of fluorescence microscopy, SEM, and ion beam analysis to in situ detect, track, and quantify fluorescently-labeled TiO_2 nanoparticles in a single human keratinocyte [128]. In ion beam analysis a MeV ion beam probes the composition and yields elemental depth profiles of the sample. SEM and ion beam analysis are complementary to each other since SEM provides the surface composition and the ion beam analysis yields bulk information on the morphology of the cell as well as on the exact localization of the nanoparticles. Peckys et al. applied correlated fluorescence microscopy with liquid STEM to study quantum dots labeled by epidermal growth factor receptor in COS7 cells fully immersed in a liquid. Also, they imaged thin edges of the cells in a cooled wet environment by ESEM-STEM and correlated these micrographs to fluorescence images [129]. In this way, they could analyze spatial and stoichiometric distributions of the labeled quantum dots on a multiple of whole cells in the liquid by a method, which is not much more time consuming than standard fluorescence microscopy approaches. Liu et al. used correlative fluorescence microscopy and plasmonics-based dark-field microscopy to gain a mechanistic understanding of the endocytosis and intracellular trafficking of DNA-labeled gold nanoparticles in HeLa cells [130]. In plasmonics-based dark-field microscopy, the fact that metallic nanostructures provide upon excitation by light sub-wavelength localization of surface plasmon-polaritons is employed for imaging sub-diffraction limited structures [132]. Since clustering of metallic nanoparticles causes a significant spectral wavelength shift due to plasmon coupling of nanoparticles, this method allowed to monitor the clustering state of nanoparticles [14]. As the cells were labeled by fluorescent protein markers, co-localization of gold nanoparticles in different aggregation states with cellular substructures became possible (see Fig. 9.7a, b). Consequently, the direct observation of the relationship between the clustering states of nanoparticles and their real-time intracellular transport at the single-cell level was enabled. The results were additionally confirmed by TEM imaging and inductively coupled plasma atomic emission spectrometry (ICP-AES) analysis of elemental gold in cells as a function of time (see Fig. 9.7c) [130].

9.17 Raman Microscopy

Vibrational properties of target molecules are suitably investigated by Raman-based techniques. These rely in the most simple approach on a continuous wave laser source operating in the visible regime while gathering the inelastically scattered radiation. Scanning the sample in an optical microscope provides spatially resolved

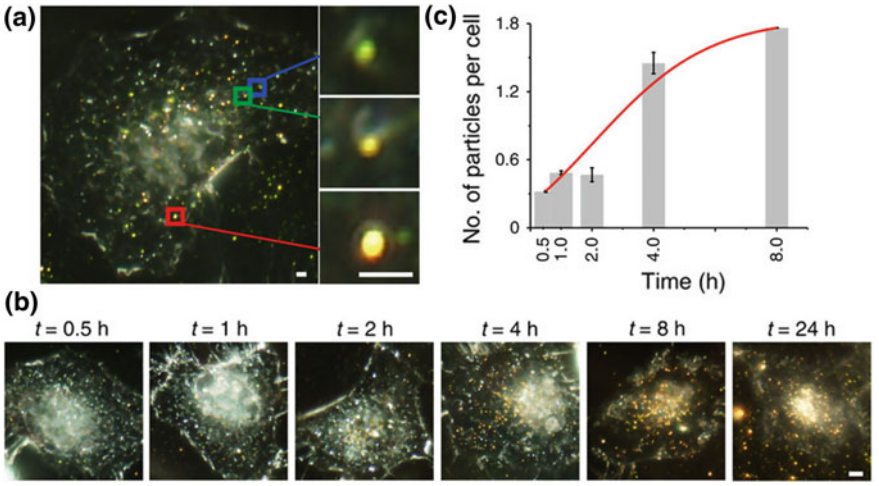

Fig. 9.7 **a** Representative correlative fluorescence microscopy and plasmonics-based dark-field microscopy (DFM) image of HeLa cells depicting the presence of single DNA-labeled gold nanoparticles (green spots in blue rectangle) and small clusters (yellow spots in green rectangle) and large clusters (bright yellow spots in red rectangle) of them. Scale bar, 2 μm; **b** DFM images for the time evolution of gold incubated with HeLa cells. Scale bar, 5 μm; **c** ICP-AES analysis of elemental gold in cells as a function of time (adapted from [130])

maps of chemical selectivity. The spatial resolution is significantly higher as compared to the spatially resolved absorption of infrared radiation gathered in an infrared microscope. This is mostly due to the shorter wavelengths that are used in Raman microscopy, which is related to the diffraction limit outlined above. Raman studies have been applied to biological matter including skin samples providing detailed information on processes occurring there, including chemical transformations [133, 134]. Further advantages of this technique are that much thicker samples than in electron microscopy can be investigated in three dimensions without slicing, where the sample thickness is typically of the order of 10 μm. Three-dimensional scanning is simply done by moving the focus of the laser radiation through the sample while scanning it layer by layer.

Even though Raman microscopy studies have provided substantial knowledge to the field of life sciences, it cannot be fully ignored that conventional Raman-based spectroscopy relying on spontaneous emission is not quite sensitive due to low scattering cross sections. This lack of sensitivity is efficiently overcome by more advanced Raman techniques. This includes stimulated Raman microscopy (SRS), which requires two pulsed laser beams that are spatially and temporally superimposed to each other [135]. If the difference in photon energy corresponds to a vibrational transition of the target, then the Raman gain or loss can be significantly more sensitively measured than by spontaneous Raman microscopy [136]. This background-free approach allows, for example, to measure depth profiles of typical species occurring in skin as well as penetrating drugs or solvents [137, 138]. Furthermore, the impact

of polymeric nanogels on changes in the protein and lipid distribution has been recently evaluated by stimulated Raman microscopy [139]. In addition, there are other variants of advanced Raman techniques, such as Coherent Anti-Stokes Raman Scattering (CARS), a four-wave mixing process, which has also been applied for studies on biological samples [140]. Furthermore, surface-enhanced Raman scattering is another suitable way to increase the intensity of the Raman signal, provided the sample is deposited on a suitable noble metal substrate, such as rough surfaces of gold or gold nanostructures [141]. Biomedical applications as well as in vivo studies have been reported before. The use of radiation in the optical regime at wavelengths >650 nm allows for deep penetration and suppresses efficiently the autofluorescence background from tissue.

9.18 Atomic-Force Microscopy-Based Techniques

Recent advances of atomic force microscopy (AFM) in combination with spectroscopic techniques provides novel and unique ways to enhance the spatial resolution along with spectroscopic specificity [142]. There are several variants how an AFM can be exploited for spectromicroscopy investigations, especially for studies in life sciences. Apertureless optical-near field microscopy is one suitable approach, requiring a tunable infrared source along with an AFM, which might be a tunable laser [143] or even synchrotron radiation [144]. Another technique is tip-enhanced Raman spectroscopy (TERS), which combines scattering scanning optical near-field microscopy (s-SNOM) with Raman spectroscopy [145]. This yields spatially resolved Raman spectra with a resolution of the order of 20–30 nm. This technique has been applied to biological targets, as has been reviewed recently [145]. A variant relying on pulsed lasers is photothermal expansion, where changes in sample height due to resonant excitation by tunable infrared radiation are sensitively probed by AFM [146]. These techniques have in common that they have a great potential for being exploited for biological applications since the spatial resolution has the potential to reach below 10 nm, so that with high chemical specificity due to spectroscopic properties a novel understanding far below the diffraction limit can be gained.

9.19 X-ray Microscopy

Tunable and tightly focused X-rays represent a unique way to probe spatially resolved biological samples including nanoparticles, which is commonly called X-ray microscopy [147]. Most suitably tunable synchrotron radiation is used as an X-ray source. The scientific importance of X-ray microscopy has increased during the last decades since the number of accessible instruments is constantly growing. Soft X-rays (100–2000 eV photon energy) probe element-selectively by resonant excitation light elements contained in cells and tissue, such as carbon ($E \approx 290$ eV),

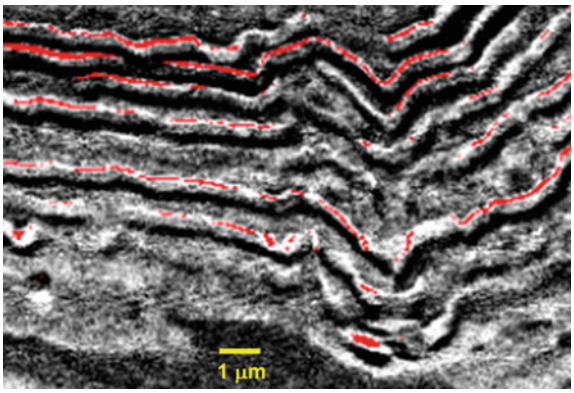

Fig. 9.8 Section of the lower part of the human stratum corneum investigated by X-ray microscopy at 530.5 eV for highlighting the spatial distribution of topically applied dexamethasone, as indicated by red color. The stratified structure of stratum corneum is visible due to corneocytes, where no drug is observed (cf. [20]). The skin surface is found near the top of the figure, the scale bar corresponds to 1 µm

nitrogen ($E \approx 400$ eV), and oxygen ($E \approx 530$ eV) [148, 149]. Tunable hard X-rays with photon energies >2 keV are used for probing heavy elements, such as metals, as is also provided by synchrotron radiation. In addition to element selectivity comes the chemical shift that probes the local electronic environment of the absorbing element, so that differently bound elements of the same kind can be distinguished [149]. X-ray microscopy relies on the absorption of the X-rays yielding, according to the Beer-Lambert-Law, absolute concentrations of the probed species of interest [18]. This is of central interest for quantitative studies, where, e.g., the amount of topically applied drugs is determined in ex vivo skin samples as a function of penetration time, yielding a detailed understanding on the driving forces of drug penetration [150]. Crucial factors that were identified include the free energy and the diffusion coefficient. A drop in free energy leads to the uptake of a drug into skin. For example, the lipophilic drug dexamethasone is readily taken up by the lipophilic lamellae between the corneocytes, as indicated in Fig. 9.8 by red color. This corresponds to about 100 nm wide regions, as discussed in greater detail in [20].

X-ray microscopy has several advantages compared to transmission electron microscopy, that is reviewed above, with regard to the following properties: (i) significantly thicker samples can be investigated, even permitting to study entire cells. Especially in the hard X-ray regime samples of >10 mm thickness can be studied, whereas by soft X-rays the sample must be thinner, typically <500 nm [18]. This also includes tomography studies for deriving 3-dimensional information [151]; (ii) wet samples can be studied, so that no drying is needed. Furthermore, the samples can be studied at a much higher pressure, reaching even ambient pressure in the hard X-ray regime, which is not possible for electron microscopy; (iii) no staining of the samples is required, but also samples prepared for electron microscopy can be studied by X-ray microscopy, if the sample thickness is properly increased to have

sufficient attenuation of the incident X-rays due to absorption by the sample; (iv) quantitative results are derived as outlined above at a spatial resolution of 10–20 nm. At the same time also large areas can be scanned. This spatial resolution is clearly inferior compared to electron microscopy but is for biological samples by far superior compared to optical microscopy. As a result, the depth of information emerging from X-ray microscopy is enormous and may even reach the molecular level.

X-ray microscopy has been used in the past for probing skin penetration of inorganic nanoparticles above 50 nm [152]. Clearly, intact skin samples show that the particles only penetrate the top layers of stratum corneum. Even small and flexible polymer particles with a size of ~10 nm cannot penetrate into deeper skin layers [19], that are only reached by low molecular weight drugs underscoring the 500 Da rule for skin penetration [153].

9.20 Conclusions

A variety of imaging techniques is reviewed for investigating nanoparticles in cells and skin as well as related subjects. Standard techniques are included forming the foundation for more advanced studies involving tunable radiation sources along with detection schemes reaching far below the diffraction limit of optical microscopy. The potential of these approaches is that even single nanoscopic objects can be identified and quantified in their biological surroundings. Structural details can be identified in the biological surroundings facilitating to understand in the future further details of the molecular processes of transport and penetration of nanoscopic matter in cells and skin.

Acknowledgements We are grateful for the contributions of our collaborators contributing to some of the results shown. Specifically, we are indebted to Dr. F. Rancan, Dr. A. Klossek, K. Yamamoto, and Dr. R. Flesch. We thankfully acknowledge the Deutsche Forschungsgemeinschaft for the support of the Priority Program SPP 1313 “Biological Responses to Nanoscale Particles”, project RU420/12-1, and SFB 1112.

References

1. Stark, W.J.: Nanoparticles in biological systems. Angew. Chem. Int. Ed. **50**(6), 1242–1258 (2011)
2. Shang, L., Nienhaus, G.U.: Small fluorescent nanoparticles at the nano-bio interface. Mater. Today **16**(3), 58–66 (2013)
3. Treuel, L., Jiang, X.E., Nienhaus, G.U.: New views on cellular uptake and trafficking of manufactured nanoparticles. J. R. Soc. Interface **10**(82), 20120939 (2013)
4. Pelaz, B., et al.: Interfacing Engineered nanoparticles with biological systems: anticipating adverse nano-bio interactions. Small **9**(9–10), 1573–1584 (2013)
5. Geiser, M., Kreyling, W.G.: Deposition and biokinetics of inhaled nanoparticles. Part. Fibre Toxicol. **7**(2), 17 (2010)

6. Shang, L., et al.: Nanoparticle interactions with live cells: quantitative fluorescence microscopy of nanoparticle size effects. Beilstein J. Nanotechnol. **5**, 2388–2397 (2014)
7. Lundqvist, M., et al.: Nanoparticle size and surface properties determine the protein corona with possible implications for biological impacts. Proc. Nat. Acad. Sci. **105**(38), 14265–14270 (2008)
8. Treuel, L., Nienhaus, G.U.: Toward a molecular understanding of nanoparticle–protein interactions. Biophys. Rev. **4**(2), 137–147 (2012)
9. Monopoli, M.P., et al.: Biomolecular coronas provide the biological identity of nanosized materials. Nat. Nanotechnol. **7**(12), 779–786 (2012)
10. Xiao Wen, L., et al.: Penetration of Nanoparticles into Human Skin. Curr. Pharm. Des. **19**(35), 6353–6366 (2013)
11. Döge, N., et al.: Identification of polystyrene nanoparticle penetration across intact skin barrier as rare event at sites of focal particle aggregations. J. Biophotonics **11**(4), e201700169 (2018)
12. Graf, C., et al.: Penetration of spherical and rod-like gold nanoparticles into intact and barrier-disrupted human skin. In: SPIE BiOS, vol. 9338, pp. 93381L–933811. SPIE 9338 (2015)
13. Graf, C., et al.: Shape-dependent dissolution and cellular uptake of silver nanoparticles. Langmuir **34**(4), 1506–1519 (2018)
14. Wang, H., et al.: Optical sizing of immunolabel clusters through multispectral plasmon coupling microscopy. Nano Lett. **11**(2), 498–504 (2011)
15. Blank, H., et al.: Application of low-energy scanning transmission electron microscopy for the study of Pt-nanoparticle uptake in human colon carcinoma cells. Nanotoxicology **8**(4), 433–446 (2014)
16. Peckys, D.B., et al.: Epidermal growth factor receptor subunit locations determined in hydrated cells with environmental scanning electron microscopy. Sci. Rep. **3**, 2626 (2013)
17. Peckys, D.B., de Jonge, N.: Liquid scanning transmission electron microscopy: imaging protein complexes in their native environment in whole eukaryotic cells. Microsc. Microanal. **20**(2), 346–365 (2014)
18. Yamamoto, K., et al.: Selective probing of the penetration of dexamethasone into human skin by soft X-ray spectromicroscopy. Anal. Chem. **87**(12), 6173–6179 (2015)
19. Yamamoto, K., et al.: Core-multishell nanocarriers: transport and release of dexamethasone probed by soft X-ray spectromicroscopy. J. Control. Release **242**, 64–70 (2016)
20. Yamamoto, K., et al.: Influence of the skin barrier on the penetration of topically-applied dexamethasone probed by soft X-ray spectromicroscopy. Eur. J. Pharm. Biopharm. **118**(SI), 30–37 (2017)
21. Meinke, M.C., et al.: Evaluation of carotenoids and reactive oxygen species in human skin after UV irradiation: a critical comparison between in vivo and ex vivo investigations. Exp. Dermatol. **24**(3), 194–197 (2015)
22. Honeywell-Nguyen, P.L., Gooris, G.S., Bouwstra, J.A.: Quantitative assessment of the transport of elastic and rigid vesicle components and a model drug from these vesicle formulations into human skin in vivo. J. Invest. Dermatol. **123**(5), 902–910 (2004)
23. Witting, M., et al.: Interactions of hyaluronic acid with the skin and implications for the dermal delivery of biomacromolecules. Mol. Pharm. **12**(5), 1391–1401 (2015)
24. Lewin, M., et al.: Tat peptide-derivatized magnetic nanoparticles allow in vivo tracking and recovery of progenitor cells. Nat. Biotechnol. **18**(4), 410–414 (2000)
25. Selvi, B.R., et al.: Intrinsically fluorescent carbon nanospheres as a nuclear targeting vector: delivery of membrane-impermeable molecule to modulate gene expression in vivo. Nano Lett. **8**(10), 3182–3188 (2008)
26. Song, Z., et al.: Background free imaging of upconversion nanoparticle distribution in human skin. J. Biomed. Opt. **18**(6), 061215 (2013)
27. Huang, Y., Fenech, M., Shi, Q.H.: Micronucleus formation detected by live-cell imaging. Mutagenesis **26**(1), 133–138 (2011)
28. Seynhaeve, A.L.B., ten Hagen, T.L.M.: Using in vitro live-cell imaging to explore chemotherapeutics delivered by lipid-based nanoparticles. J. Vis. Exp. **129**, e55405 (2017)

29. Wildt, B.E., et al.: Intracellular accumulation and dissolution of silver nanoparticles in L-929 fibroblast cells using live cell time-lapse microscopy. Nanotoxicology **10**(6), 710–719 (2016)
30. Boreham, A., et al.: Determination of nanostructures and drug distribution in lipid nanoparticles by single molecule microscopy. Eur. J. Pharm. Biopharm. **110**, 31–38 (2017)
31. Volz, P., et al.: Application of single molecule fluorescence microscopy to characterize the penetration of a large amphiphilic molecule in the stratum corneum of human skin. Int. J. Mol. Sci. **16**(4), 6960–6977 (2015)
32. van der Zwaag, D., et al.: Super resolution imaging of nanoparticles cellular uptake and trafficking. ACS Appl. Mater. Inter. **8**(10), 6391–6399 (2016)
33. Peuschel, H., et al.: Quantification of internalized silica nanoparticles via STED microscopy. Biomed. Res. Int. **2015**, 961208 (2015)
34. Wang, S.H., et al.: Evolution of gold nanoparticle clusters in living cells studied by sectional dark-field optical microscopy and chromatic analysis. J. Biophotonics **9**(7), 738–749 (2016)
35. Deka, G., et al.: Nonlinear plasmonic imaging techniques and their biological applications. Nanophotonics **6**(1), 31–49 (2017)
36. Alexiev, U., et al.: Time-resolved fluorescence microscopy (FLIM) as an analytical tool in skin nanomedicine. Eur. J. Pharm. Biopharm. **116**(SI), 111–124 (2017)
37. Vogt, A., et al.: Nanocarriers for drug delivery into and through the skin—do existing technologies match clinical challenges? J. Control. Release **242**, 3–15 (2016)
38. Ostrowski, A., et al.: Overview about the localization of nanoparticles in tissue and cellular context by different imaging techniques. Beilstein J. Nanotechnol. **6**, 263–280 (2015)
39. Baeza, A., et al.: Electron microscopy for inorganic-type drug delivery nanocarriers for antitumoral applications: what does it reveal? J. Mater. Chem. B **5**(15), 2714–2725 (2017)
40. Chen, D.D., Monteiro-Riviere, N.A., Zhang, L.S.W.: Intracellular imaging of quantum dots, gold, and iron oxide nanoparticles with associated endocytic pathways. Wiley Interdiscip. Rev. Nanomed. Nanobiotechnol. **9**(2), e1419 (2017)
41. Lin, L.L., et al.: Non-invasive nanoparticle imaging technologies for cosmetic and skin care products. Cosmetics **2**, 196–210 (2015)
42. Potocnik, J.: Commission recommendation of 18 October 2011 on the defnition of nanomaterals. Official J. Europ. Union L275/38 (2011)
43. Panyam, J., Labhasetwar, V.: Dynamics of endocytosis and exocytosis of poly(D, L-Lactide-co-Glycolide) nanoparticles in vascular smooth muscle cells. Pharm. Res. **20**(2), 212–220 (2003)
44. Jiang, X., et al.: Endo- and exocytosis of zwitterionic quantum dot nanoparticles by live HeLa cells. ACS Nano **4**(11), 6787–6797 (2010)
45. Clift, M.J.D., et al.: The impact of different nanoparticle surface chemistry and size on uptake and toxicity in a murine macrophage cell line. Toxicol. Appl. Pharmacol. **232**(3), 418–427 (2008)
46. dos Santos, T., et al.: Quantitative assessment of the comparative nanoparticle-uptake efficiency of a range of cell lines. Small **7**(23), 3341–3349 (2011)
47. Byrne, G.D., et al.: Live imaging of cellular internalization of single colloidal particle by combined label-free and fluorescence total internal reflection microscopy. Mol. Pharm. **12**(11), 3862–3870 (2015)
48. Ann, F.H., et al.: Nanotechnology: toxicologic pathology. Toxicol. Pathol. **41**(2), 395–409 (2013)
49. Song, C.X., et al.: Formulation and characterization of biodegradable nanoparticles for intravascular local drug delivery. J. Control. Release **43**(2), 197–212 (1997)
50. Haase, M., Schaefer, H.: Upconverting Nanoparticles. Ang. Chem. Int. Ed. **50**(26), 5808–5829 (2011)
51. Song, C.X., et al.: Bifunctional cationic solid lipid nanoparticles of β-$NaYF_4$: Yb, Er upconversion nanoparticles coated with a lipid for bioimaging and gene delivery. RSC Adv. **7**(43), 26633–26639 (2017)
52. Kuo, T.-R., et al.: Chemical enhancer induced changes in the mechanisms of transdermal delivery of zinc oxide nanoparticles. Biomaterials **30**(16), 3002–3008 (2009)

53. Prow, T.W., et al.: Quantum dot penetration into viable human skin. Nanotoxicology **6**(2), 173–185 (2012)
54. Labouta, H.I., et al.: Gold nanoparticle penetration and reduced metabolism in human skin by toluene. Pharm. Res. **28**(11), 2931–2944 (2011)
55. Prow, T., et al.: Nanoparticle tethered antioxidant response element as a biosensor for oxygen induced toxicity in retinal endothelial cells. Mol. Vis. **12**(67–69), 616–625 (2006)
56. Prow, T.W., et al.: Nanoparticles and microparticles for skin drug delivery. Adv. Drug. Del. Rev. **63**(6), 470–491 (2011)
57. de Campos, A.M., et al.: Chitosan nanoparticles as new ocular drug delivery systems: in vitro stability, in vivo fate, and cellular toxicity. Pharm. Res. **21**(5), 803–810 (2004)
58. Prow, T.W., et al.: Ocular nanoparticle toxicity and transfection of the retina and retinal pigment epithelium. Nanomedicine **4**(4), 340–349 (2008)
59. Kang, J.H., Jang, W.Y., Ko, Y.T.: The effect of surface charges on the cellular uptake of liposomes investigated by live cell imaging. Pharm. Res. **34**(4), 704–717 (2017)
60. Oreopoulos, J., Berman, R., Browne, M.: Spinning-disk confocal microscopy: present technology and future trends. In: Waters, Wittmann, T. (eds.) Quantitative Imaging in Cell Biology, pp. 153–175. Elsevier Academic Press Inc, San Diego (2014)
61. Baroli, B., et al.: Penetration of metallic nanoparticles in human full-thickness skin. J. Invest. Dermatol. **127**(7), 1701–1712 (2007)
62. Cross, S.E., et al.: Human skin penetration of sunscreen nanoparticles: in-vitro assessment of a novel micronized zinc oxide formulation. Skin Pharmacol. Physiol. **20**(3), 148–154 (2007)
63. Gratieri, T., et al.: Penetration of quantum dot particles through human skin. J. Biomed. Nanotechnol. **6**(5), 586–595 (2010)
64. Alvarez-Roman, R., et al.: Skin penetration and distribution of polymeric nanoparticles. J. Control. Release **99**(1), 53–62 (2004)
65. Mortensen, L.J., et al.: In vivo skin penetration of quantum dot nanoparticles in the murine model: the effect of UVR. Nano Lett. **8**(9), 2779–2787 (2008)
66. Ostrowski, A., et al.: Skin barrier disruptions in tape stripped and allergic dermatitis models have no effect on dermal penetration and systemic distribution of AHAPS-functionalized silica nanoparticles. Nanomedicine **10**(7), 1571–1581 (2014)
67. Rouse, J.G., et al.: Effects of mechanical flexion on the penetration of fullerene amino acid-derivatized peptide nanoparticles through skin. Nano Lett. **7**(1), 155–160 (2007)
68. Gonzalez, S., et al.: Changing paradigms in dermatology: Confocal microscopy in clinical and surgical dermatology. Clin. Dermatol. **21**(5), 359–369 (2003)
69. Shahriari, N., et al.: In vivo reflectance confocal microscopy image interpretation for the dermatopathologist. J. Cutan. Pathol. **45**(3), 187–197 (2018)
70. Summers, H.D., et al.: Statistical analysis of nanoparticle dosing in a dynamic cellular system. Nat. Nanotechnol. **6**(3), 170–174 (2011)
71. Vranic, S., et al.: Deciphering the mechanisms of cellular uptake of engineered nanoparticles by accurate evaluation of internalization using imaging flow cytometry. Part. Fibre Toxicol. **10**, 2 (2013)
72. Gao, N.Y., et al.: Shape-dependent two-photon photoluminescence of single gold nanoparticles. J. Phys. Chem. B **118**(25), 13904–13911 (2014)
73. Richter, T., et al.: Dead but highly dynamic—the stratum corneum is divided into three hydration zones. Skin Pharmacol. Physiol. **17**(5), 246–257 (2004)
74. Rane, T.D., Armani, A.M.: Two-photon microscopy analysis of gold nanoparticle uptake in 3D cell spheroids. PLoS ONE **11**(12), e0167548 (2016)
75. Zhu, Y.J., et al.: Penetration of silver nanoparticles into porcine skin ex vivo using fluorescence lifetime imaging microscopy, Raman microscopy, and surface-enhanced Raman scattering microscopy. J. Biomed. Opt. **20**(5), 051006 (2015)
76. Li, K., Schneider, M.: Quantitative evaluation and visualization of size effect on cellular uptake of gold nanoparticles by multiphoton imaging-UV/Vis spectroscopic analysis. J. Biomed. Opt. **19**(10), 101505 (2014)

77. Graf, B.W., et al.: In vivo imaging of immune cell dynamics in skin in response to zinc-oxide nanoparticle exposure. Biomed. Opt. Exp. **4**(10), 1817–1828 (2013)
78. Basuki, J.S., et al.: Using fluorescence lifetime imaging microscopy to monitor theranostic nanoparticle uptake and intracellular doxorubicin release. ACS Nano **7**(11), 10175–10189 (2013)
79. Boreham, A., et al.: Exploiting fluorescence lifetime plasticity in FLIM: target molecule localization in cells and tissues. ACS Med. Chem. Lett. **2**(10), 724–728 (2011)
80. Roberts, M.S., et al.: Non-invasive imaging of skin physiology and percutaneous penetration using fluorescence spectral and lifetime imaging with multiphoton and confocal microscopy. Eur. J. Pharm. Biopharm. **77**(3), 469–488 (2011)
81. Hanson, K.M., et al.: Two-photon fluorescence lifetime imaging of the skin stratum corneum pH gradient. Biophys. J. **83**(3), 1682–1690 (2002)
82. Hell, S.W.: Nanoscopy with focused light (Nobel Lecture). Angew. Chem. Int. Ed. **54**(28), 8054–8066 (2015)
83. Kamiyama, D., Huang, B.: Development in the STORM. Dev. Cell **23**(6), 1103–1110 (2012)
84. Betzig, E.: Single molecules, cells, and super-resolution optics (Nobel Lecture). Ang. Chem. Int. Ed. **54**(28), 8034–8053 (2015)
85. Gustafsson, M.G.L.: Nonlinear structured-illumination microscopy: wide-field fluorescence imaging with theoretically unlimited resolution. Proc. Natl. Acad. Sci. U.S.A. **102**(37), 13081–13086 (2005)
86. Schübbe, S., et al.: Size-dependent localization and quantitative evaluation of the intracellular migration of silica nanoparticles in Caco-2 cells. Chem. Mater. **24**(5), 914–923 (2012)
87. Nedosekin, D.A., et al.: Photothermal confocal multicolor microscopy of nanoparticles and nanodrugs in live cells. Drug Metab. Rev. **47**(3), 346–355 (2015)
88. Vermeulen, P., Cognet, L., Lounis, B.: Photothermal microscopy: optical detection of small absorbers in scattering environments. J. Microsc. **254**(3), 115–121 (2014)
89. Galanzha, E., Zharov, V.P.: Circulating tumor cell detection and capture by photoacoustic flow cytometry in vivo and ex vivo. Cancers **5**(4), 1691–1738 (2013)
90. Nieves, D.J., et al.: Photothermal raster image correlation spectroscopy of gold nanoparticles in solution and on live cells. R. Soc. Open Sci. **2**(6), 140454 (2015)
91. Erni, R., et al.: Atomic-resolution imaging with a sub-50-pm electron probe. Phys. Rev. Lett. **102**(9), 096101 (2009)
92. Jane, A.F., et al.: Ultrastructural analysis in preclinical safety evaluation. Toxicol. Pathol. **40**(2), 391–402 (2012)
93. Hoenger, A., McIntosh, J.R.: Probing the macromolecular organization of cells by electron tomography. Curr. Opin. Cell Biol. **21**(1), 89–96 (2009)
94. Leis, A., et al.: Visualizing cells at the nanoscale. Trends Biochem. Sci. **34**(2), 60–70 (2009)
95. Kourkoutis, L.F., Plitzko, J.M., Baumeister, W.: Electron microscopy of biological materials at the nanometer scale. Annu. Rev. Mater. Res. **42**(1), 33–58 (2012)
96. Pierson, J., et al.: Toward visualization of nanomachines in their native cellular environment. Histochem. Cell Biol. **132**(3), 253–262 (2009)
97. Medalia, O., et al.: Macromolecular architecture in eukaryotic cells visualized by cryoelectron tomography. Science **298**(5596), 1209–1213 (2002)
98. Fujimoto, K.: Freeze-fracture replica electron microscopy combined with SDS digestion for cytochemical labeling of integral membrane proteins. Application to the immunogold labeling of intercellular junctional complexes. J. Cell. Sci. **108**(11), 3443–3449 (1995)
99. Bushby, A.J., et al.: Imaging three-dimensional tissue architectures by focused ion beam scanning electron microscopy. Nat. Protoc. **6**(6), 845–858 (2011)
100. Gontier, E., et al.: Is there penetration of titania nanoparticles in sunscreens through skin? A comparative electron and ion microscopy study. Nanotoxicology **2**(4), 218–231 (2008)
101. Hubbs, A.F., et al.: Nanotoxicology-a pathologist's perspective. Toxicol. Pathol. **39**(2), 301–324 (2011)
102. Adachi, K., et al.: In vivo effect of industrial titanium dioxide nanoparticles experimentally exposed to hairless rat skin. Nanotoxicology **4**(3), 296–306 (2010)

103. Marquis, B.J., et al.: Analytical methods to assess nanoparticle toxicity. Analyst **134**(3), 425–439 (2009)
104. Kempen, P.J., et al.: A scanning transmission electron microscopy approach to analyzing large volumes of tissue to detect nanoparticles. Microsc. Microanal. **19**(5), 1290–1297 (2013)
105. Droste, M.S., et al.: Noninvasive measurement of cell volume changes by negative staining. J. Biomed. Opt. **10**(6), 064017 (2005)
106. Richter, T., et al.: Pros and cons: cryo-electron microscopic evaluation of block faces versus cryo-sections from frozen-hydrated skin specimens prepared by different techniques. J. Microsc. Oxford **225**(2), 201–207 (2007)
107. Echlin, P.: Low-Temperature Microscopy and Analysis. Springer, Berlin (1992)
108. Lucas, M.S., Günthert, M., Gasser, P., Lucas, F., Wepf, R.: Bridging microscopes: 3D correlative light and scanning electron microscopy of complex biological structures. In: Müller-Reichert, T., Verkade, P. (eds.) Correlative Light and Electron Microscopy, pp. 325–356. Academic Press, Cambridge (2012)
109. McDonald, K.L.: A review of high-pressure freezing preparation techniques for correlative light and electron microscopy of the same cells and tissues. J. Microsc. **235**(3), 273–281 (2009)
110. Webster, P., Schwarz, H., Griffiths, G.: Preparation of cells and tissues for immuno EM, Chap. 3. In: Methods Cell Biology, pp. 45–58. Academic Press, Amsterdam (2008)
111. Norlén, L.: Nanostructure of the stratum corneum extracellular lipid matrix as observed by cryo-electron microscopy of vitreous skin sections. Int. J. Cosmet. Sci. **29**(5), 335–352 (2007)
112. Asahina, S., Togashi, T., Terasaki, O., Takami, S., Adschiri, T., Shibata, M., Erdman, N.: High-resolution low-voltage scanning electron microscope study of nanostructured materials. Microsc. Anal. **26**, S12–S14 (2012)
113. Callaway, E.: The revolution will not be crystallized: a new method sweeps through structural biology. Nature **525**(7568), 172–174 (2015)
114. Engel, A., Dubochet, J., Kellenberger, E.: Some progress in the use of a scanning transmission electron microscope for the observation of biomacromolecules. J. Ultrastruct. Res. **57**(3), 322–330 (1976)
115. Ohtsuki, M.: Observation of unstained biological macromolecules with STEM. Ultramicroscopy **5**(3), 317–323 (1980)
116. Colliex, C., Mory, C.: Scanning transmission electron microscopy of biological structures. Biol. Cell **80**(2–3), 175–180 (1994)
117. Porter, A.E., et al.: Direct imaging of single-walled carbon nanotubes in cells. Nat. Nanotechnol. **2**(11), 713–717 (2007)
118. Uchida, M., et al.: Intracellular distribution of macrophage targeting ferritin-iron oxide nanocomposite. Adv. Mater. **21**(4), 458–462 (2009)
119. Donald, A.M.: The use of environmental scanning electron microscopy for imaging wet and insulating materials. Nat. Mater. **2**, 511–516 (2003)
120. de Jonge, N., Ross, F.M.: Electron microscopy of specimens in liquid. Nat. Nanotechnol. **6**, 695–704 (2011)
121. Stokes, D.J.: Principles and practice of variable pressure/environmental scanning electron microscopy (VP-ESEM). Wiley, Chichester, West-Sussex (2008)
122. Kirk, S.E., Skepper, J.N., Donald, A.M.: Application of environmental scanning electron microscopy to determine biological surface structure. J. Microsc. **233**(2), 205–224 (2009)
123. Bogner, A., et al.: Wet STEM: a new development in environmental SEM for imaging nano-objects included in a liquid phase. Ultramicroscopy **104**(3), 290–301 (2005)
124. Williamson, M.J., et al.: Dynamic microscopy of nanoscale cluster growth at the solid–liquid interface. Nat. Mater. **2**(8), 532–536 (2003)
125. de Jonge, N., et al.: Scanning transmission electron microscopy of biological specimens in water. Microsc. Microanal. **13**(S02), 242–243 (2007)
126. de Jonge, N., et al.: Electron microscopy of whole cells in liquid with nanometer resolution. Proc. Natl. Acad. Sci. **106**(7), 2159–2164 (2009)

127. Peckys, D.B., et al.: Nanoscale imaging of whole cells using a liquid enclosure and a scanning transmission electron microscope. PLoS ONE **4**(12), e8214 (2009)
128. Le Trequesser, Q., et al.: Single cell in situ detection and quantification of metal oxide nanoparticles using multimodal correlative microscopy. Anal. Chem. **86**(15), 7311–7319 (2014)
129. Peckys, D.B., Bandmann, V., de Jonge, N.: Correlative fluorescence and scanning transmission electron microscopy of quantum dot-labeled proteins on whole cells in liquid. In: Müller-Reichert, T., Verkade, P. (eds.) Methods in Cell Biology, vol. 124, pp. 305–322. Academic Press, Cambridge (2014)
130. Liu, M.M., et al.: Real-time visualization of clustering and intracellular transport of gold nanoparticles by correlative imaging. Nat. Commun. **8**, 15646 (2017)
131. Jahn, K.A., et al.: Correlative microscopy: providing new understanding in the biomedical and plant sciences. Micron **43**(5), 565–582 (2012)
132. Lal, S., Link, S., Halas, N.J.: Nano-optics from sensing to waveguiding. Nat. Photon. **1**(11), 641–648 (2007)
133. Krafft, C., et al.: Label-free molecular imaging of biological cells and tissues by linear and nonlinear Raman spectroscopic approaches. Ang. Chem. Int. Ed. **56**, 4392–4430 (2017)
134. Zhang, G.J., et al.: Imaging the prodrug-to-drug transformation of a 5-fluorouracil derivative in skin by confocal Raman microscopy. J. Invest. Dermatol. **127**(5), 1205–1209 (2007)
135. Freudiger, C.W., et al.: Label-free biomedical imaging with high sensitivity by stimulated raman scattering microscopy. Science **322**(5909), 1857–1861 (2008)
136. Klossek, A., et al.: Studies for improved understanding of lipid distributions in human skin by combining stimulated and spontaneous Raman microscopy. Eur. J. Pharm. Biopharm. **116**(SI), 76–84 (2017)
137. Belsey, N.A., et al.: Evaluation of drug delivery to intact and porated skin by coherent Raman scattering and fluorescence microscopies. J. Control. Release, **174**, 37–42 (2014)
138. Saar, B.G., et al.: Imaging drug delivery to skin with stimulated Raman scattering microscopy. Mol. Pharm. **8**(3), 969–975 (2011)
139. Giulbudagian, M., et al.: Correlation between the chemical composition of thermoresponsive nanogels and their interaction with the skin barrier. J. Control. Release **243**, 323–332 (2016)
140. Zhang, C., Zhang, D.L., Cheng, J.X.: Coherent Raman scattering microscopy in biology and medicine. In: Yarmush, M.L. (ed.) Annual Review of Biomedical Engineering, vol. 17, pp. 415–445 (2015)
141. Vo-Dinh, T., et al.: SERS nanosensors and nanoreporters: golden opportunities in biomedical applications. Wiley Interdiscip. Rev.-Nanomedicine Nanobiotechnology **7**, 17–33 (2015)
142. Li, Q., et al.: AFM-based force spectroscopy for bioimaging and biosensing. RSC Adv. **6**(16), 12893–12912 (2016)
143. Berweger, S., et al.: Nano-chemical infrared imaging of membrane proteins in lipid bilayers. J. Am. Chem. Soc. **135**(49), 18292–18295 (2013)
144. Hermann, P., et al.: Enhancing the sensitivity of nano-FTIR spectroscopy. Opt. Express **25**(14), 16574–16588 (2017)
145. Verma, P.: Tip-enhanced Raman spectroscopy: technique and recent advances. Chem. Rev. **117**(9), 6447–6466 (2017)
146. Dazzi, A., Prater, C.B.: AFM-IR: technology and applications in nanoscale infrared spectroscopy and chemical imaging. Chem. Rev. **117**, 5146–5173 (2017)
147. Lawrence, J.R., et al.: Soft X-ray spectromicroscopy for speciation, quantitation and nano-eco-toxicology of nanomaterials. J. Microsc. **261**, 130–147 (2016)
148. Karunakaran, C., et al.: Introduction of soft X-ray spectromicroscopy as an advanced technique for plant biopolymers research. PLoS ONE **10**, e0122959 (2015)
149. Stöhr, J.: NEXAFS spectroscopy. In: Gomer, R. (ed.) Springer Series in Surface Science, vol. 25. Springer, Berlin (1992)
150. Schulz, R., et al.: Data-based modeling of drug penetration relates human skin barrier function to the interplay of diffusivity and free-energy profiles. Proc. Natl. Acad. Sci. U.S.A. **114**(14), 3631–3636 (2017)

151. Schneider, G., et al.: Three-dimensional cellular ultrastructure resolved by X-ray microscopy. Nat. Methods **7**(12), 985–987 (2010)
152. Graf, C., et al.: Qualitative detection of single submicron and nanoparticles in human skin by scanning transmission X-ray microscopy. J. Biomed. Opt. **14**(2), 021015 (2009)
153. Bos, J.D., Meinardi, M.: The 500 Dalton rule for the skin penetration of chemical compounds and drugs. Exp. Dermatol. **9**(3), 165–169 (2000)

Part III
Cellular Responses and Health Effects

Chapter 10
Cellular Defense Mechanisms Following Nanomaterial Exposure: A Focus on Oxidative Stress and Cytotoxicity

Stephen J. Evans, Gareth J. Jenkins, Shareen H. Doak and Martin J. D. Clift

Abstract In response to the significant increase in nanotechnology over the last three decades, and the plethora of engineered nanomaterials (ENMs) now becoming available, understanding as to how nano-sized particles may impact upon human health has become a dominating area of research worldwide since the late 1990's (Stone et al. in Environmental Health Perspectives, 2017) [1]. Whilst approaches constantly adapt to the increasing number and variety of ENMs produced for a plethora of different applications, the quantity of alternative physico-chemical characteristics, a key factor in the potential hazard of ENMs (Bouwmeester et al. in Nanotoxicology 5:1–11, 2011) [2], is further increasing in number and type.

10.1 Introduction

In response to the significant increase in nanotechnology over the last three decades, and the plethora of engineered nanomaterials (ENMs) now becoming available, understanding as to how nano-sized particles may impact upon human health has become a dominating area of research worldwide since the late 1990s [1]. Whilst approaches constantly adapt to the increasing number and variety of ENMs produced for a plethora of different applications, the quantity of alternative physico-chemical characteristics, a key factor in the potential hazard of ENMs [2], is further increasing in number and type. Although it is well documented which characteristics influence ENM toxicity, the precise mechanism by which this observed toxicity occurs is not fully understood [3]. Despite this, as a result of increased laboratory-based investigations that have been conducted over the last three decades [1], a number of specific paradigms have been formulated in order to deduce and define the potential (human health) hazard posed by ENMs.

S. J. Evans · G. J. Jenkins · S. H. Doak · M. J. D. Clift (✉)
In Vitro Toxicology Group, Swansea University Medical School, Institute of Life Sciences, Singleton Park Campus, Swansea, Wales SA2 8PP, UK
e-mail: m.j.d.clift@swansea.ac.uk

P. Gehr and R. Zellner (eds.), *Biological Responses to Nanoscale Particles*, NanoScience and Technology, https://doi.org/10.1007/978-3-030-12461-8_10

10.2 Paradigms in Particle Toxicology

Of the three specific paradigms, also known as theory's, the main one is the 'oxidative stress paradigm', which is discussed in the latter paragraphs. However, while the potential for ENMs to cause oxidative stress has been the basis for increased research since the advent of nanoparticle toxicology in the early 1990s [4], two further paradigm's/theory's also exist; the fibre paradigm [5, 6], and the theory of genotoxicity [7, 8]. The latter is predominantly based upon the oxidative stress paradigm; however, it moves on from determining an inflammatory response to assess what the stimulation of oxidative and inflammatory mediators could induce to the biological system in regard to human health. The theory describes a two-tiered approach: (i) primary genotoxicity and (ii) secondary toxicity. In regard to primary genotoxicity, it is suggested that NPs can cause genotoxicity following direct exposure to the biological system. Secondary genotoxicity however describes, initially, the oxidative stress paradigm (in theory: NP exposure = ROS/reactive nitrogen species (RNS) production [also oxidative stress (oxidant/antioxidant imbalance)] = chronic inflammatory response), which causes genotoxicity and (possibly) subsequent tumour formation. Secondary genotoxicity, however, may not be caused by the NPs alone; it may also be caused via interaction of the biological system and the chemicals contained within the NPs. It is suggested that the NPs might be completely inert but are able to penetrate the cellular membrane, possibly locating within the nucleus. At this stage, due to the highly acidic pH, the chemicals present within the NPs could be released (such as Fe within Fe platinum NPs), causing a toxic response. This form of secondary toxicity has also been referred to as the "Trojan horse" effect [9]. It is also possible, however, in relation to this theory that the cells might undergo cell death and thus not induce genotoxicity and tumor formation.

As previously discussed in Clift and Rothen-Rutishauser [10], although both the oxidative stress paradigm and theory of genotoxicity can fit to any form or NP, they have predominantly been focused upon through the assessment of the biological response to spherical, crystalline, and non-fibrous NPs. However, since the portrayal that CNTs may cause "asbestos-like" effects in the lung [11], increased research has been performed using the theory of genotoxicity with fibrous NPs. While this is apt, specific, well-studied, and proposed paradigms already exist in regard to the biological effects following fibrous stimuli [6], including asbestos and glass wool; otherwise known as the fibre paradigm, with a specific set of rules, as detailed in Donaldson et al. [6]. Although there has been increased focus upon the fibre paradigm in regards to high aspect ratio nanomaterials (HARN), since the seminal paper of Poland and colleagues [11], and further intensity is being given towards the potential for ENMs to cause genotoxicity when considering a chronic, repeated and low-dose/concentration exposure to humans, the key toxicological paradigm associated with ENMs remains the 'oxidative stress paradigm' (Fig. 10.1).

Oxidative stress occurs when a greater number of oxidants than antioxidants are present within the cell, causing an oxidant/antioxidant imbalance. Increased oxidation can occur within cells, such as macrophages following activation. The activation

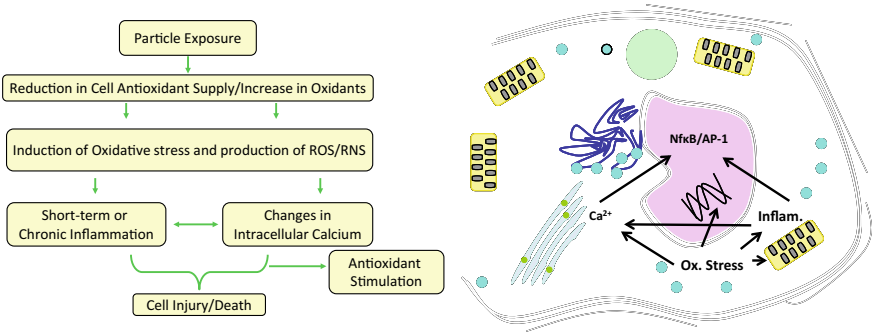

Fig. 10.1 Overview of the oxidative stress paradigm, as both a flow diagram (right) [10], and indicative within any mammalian cell (left). Both aspects highlight the foundation of the oxidative stress paradigm, where a ENM may induce an oxidative attack upon cells either independently, or cause inflammatory response which, both, can then impede cellular signaling pathways. This mechanistic toxic effect has then been known to initiate long-term detrimental effects upon cellular homeostasis (noted by the impact upon intracellular Ca^{2+} levels)

of macrophage cells can cause the generation of the superoxide anion, which is readily converted into the hydroxyl radical (•OH) via the influence of superoxide dismutase. The presence of the •OH, as well as the superoxide anion, which are examples of reactive oxygen species (ROS), can thus cause increased oxidation within the cell because these molecules possess unpaired electrons and are highly unstable. Additionally, ROS can be produced via—nicotinamide adenine dinucleotide phosphate (NADPH) oxidase, which is the most common form of ROS found in cells, and is—usually produced when cells are performing the phagocytosis of xenobiotics. Therefore, this suggests that although cells purposefully clear hazardous particles from the tissue, the phagocytosing cells can unintentionally or intentionally produce ROS. In addition, the potential production of ROS following encapsulation of particles via phagocytosis further emphasizes the necessity to understand the specific uptake mechanism of NPs, in order to determine their potential route within the cell, and how their uptake may relate to their toxicity. As it is not possible to explore in detail the entry mechanisms of NPs into cells, the reader is referred to the comprehensive review of Unfried et al. [12].

The production of ROS and subsequent oxidative stress in cells can be extremely deleterious, causing a reduction in cell metabolic competence via a reduction in mitochondrial respiration as well as an increase in the production of (pro)inflammatory—mediators (i.e., cytokines and chemokines). The effects of ROS production and subsequent oxidative stress/inflammatory response can further be associated with diseases and illnesses such as pulmonary and cardiovascular diseases, including asthma, chronic obstructive pulmonary disease, as well as atherosclerosis and even tumor formation.

In a study by Stone et al. [1], the potential for NPs, specifically ufCB, to cause oxidative stress was assessed in A549 epithelial cells. Cells were measured for their

glutathione content to determine the level of oxidative stress present. Glutathione is the most abundant nonprotein thiol present inside most cells, and it is essential for maintaining cell viability by detoxification of pathogens as well as by regulating cell cycle and gene expression. A reduction in the glutathione content of cells, therefore, is known to indicate an oxidative stress environment. It is also known that glutathione can have a protective role following the onset of oxidative stress, due to its antioxidant gene characteristics. Antioxidant genes are common throughout cells, such as the c-*fos* gene. This gene is part of a series of growth- and differentiation–related genes that are expressed by cells in response to foreign materials. It is thought that antioxidant genes are "switched on" following NP stimulus, which can thus overwhelm the NP effect. Research into these effects, however, is limited and requires further investigation. In relation to the potential for NPs to induce oxidative stress, it was observed by Stone et al. [1] that following treatment of A549 epithelial cells with up to 0.78 $\mu g\ mm^2$ of ufCB and CB, the glutathione levels, as measured specifically in its reduced form (GSH), decreased after 2 h, with a significant decrease also found after 6-h exposure to ufCB, but not to CB. It was subsequently concluded by Stone et al. that ufCB is more potent at inducing oxidative stress than its larger counterpart, CB. Li et al. further studied the potential for NPs to induce oxidative stress in cells. In the study by Li et al., the effects of ambient (25–10 μm), fine (<2.5 μm), and uf (<0.1 μm) particles on RAW 264.7 macrophage cells and BEAS-2B epithelial cells were assessed. It was observed that NPs, in comparison to both ambient and fine particles, induced an increased cellular expression of heme-oxygenase–1 (HO-1) expression in each cell line, indicative of oxidative stress, as well as a decrease in intracellular glutathione levels. High levels of ROS production were also demonstrated following dithiothreitol (DTT) analysis. Further examination of the different particle types by transmission electron microscopy (TEM) showed the NPs, as well as a small amount of larger particles, to predominantly locate within mitochondria, causing subsequent major structural damage thought to contribute to increased oxidative stress (decrease in GSH) and toxicity previously observed. It was therefore concluded that the increased biological potency of NPs can be associated with the redox cycling of organic chemicals due to their increased ability to damage the mitochondria, causing ROS and oxidative stress. Recently, Xia et al. also showed ufCB, in comparison to TiO_2 and CB, to cause an increased production of ROS, as measured via the ROS quencher, furfuryl alcohol, as well as by assessment of the level of NADPH peroxidase with RAW 264.7 macrophage cells over a 4- and 16-h period. Subsequent analysis of the oxidative stress levels in these macrophage cells found depletion in GSH levels, as well as toxic oxidative stress after similar exposure periods. It was further illustrated that the toxic oxidative stress observed was specific to an injury to mitochondria due to increased cytosolic calcium (Ca^{2+}) production and uptake, causing structural damage to the organelle. Ca^{2+} is an essential and the most abundant mineral in the body. Maintaining normal Ca^{2+} levels (~155 ± 9 nM) within the cell, also known as Ca^{2+} homeostasis, is essential for cell viability. The finding by Xia et al. that an increased Ca^{2+} production (signaling) can occur in cells following exposure to NPs supports previous studies that have suggested the increase of cytosolic Ca^{2+} to be associated with the onset of increased ROS

production and subsequent oxidative stress. Stone et al. initially showed that ufCB exposure for 30 min to Mono Mac 6 (MM6) human macrophage cells induced a 1.6-fold increase in the resting cytosolic Ca^{2+}concentration, measured using the Ca^{2+} chelator Fura 2-AM in MM6 cells at a concentration of 66 μg/m, while no changes were observed following treatment of MM6 cells with CB. Subsequent investigation by Stone et al. examined the effects of CB, both fine and uf (33 μg/ml), and latex beads (64, 202, and 535 nm in diameter) (1 mg/ml) on MM6 cells and primary rat macrophages. Analysis of the latex beads showed a 2.3-fold increase in cytosolic Ca^{2+}concentration (as determined by using the Fura 2-AM molecule) in response to thapsigargin stimulation following treatment with the 64-nm latex beads; however, no effects on MM6 cell Ca^{2+} concentration were observed following treatment with either the 202- or 535-nm latex beads. In this study, thapsigargin was used to assess the viability of the cells via Ca^{2+} signaling. This chemical stimulant causes release of Ca^{2+} from the endoplasmic reticulum (ER); a loss of cell viability, via apoptosis, can be related to a loss of Ca^{2+} in the ER store and therefore a reduced Ca^{2+} response to thapsigargin stimulation. Similarly, Stone et al. showed a 2.6-fold increase in Ca^{2+} in BAL cells (>80% macrophages) following stimulation with thapsigargin and after exposure to ufCB, but not to CB. These latter findings support those previously reported by Stone et al. that ufCB can cause an increase in cytosolic Ca^{2+} concentration and further demonstrate that different macrophage types (MM6 and primary rat macrophages) can elicit similar responses following NP exposure. Further analysis by Stone et al. demonstrated that these effects were attenuated when the MM6 cells were pretreated with either the antioxidant mannitol or nacystelyn, suggesting that the increased cytosolic Ca^{2+} concentrations observed following NP exposure could be mediated via ROS and oxidative stress. Stone et al. performed further examination of the potential of all sizes of the latex beads to produce ROS, using the dye 2′,7′-dichlorofluorescin diacetate (DCFH-DA), which when oxidized converts into 2′,7′-dichlorofluorescin (DCFH) and shows an increasing fluorescence intensity relative to an increase in ROS production. It was found that the NP latex beads (64 nm) were more potent in causing ROS, with the 202- and 535-nm latex beads showing no oxidative effects after 10 min. These findings were subsequently supported by Brown et al., who also measured cytosolic Ca^{2+} via the use of the fluorescent marker Fura 2-AM. It was reported that ufCB elicited a heightened cytosolic Ca^{2+} concentration in MM6 cells following treatment for 30 min. Subsequent analysis by Brown et al., which examined the effects of transition metals, specifically Fe in the form of Fe chloride ($FeCl_2$), using the transition metal chelator, Desferal, found that these metals had no effect on cytosolic Ca^{2+} concentration after 30 min of exposure. In addition, Brown et al. also investigated the inflammatory potential of the ufCB and CB particles as well as of the transition metals in vivo. It was observed that the ufCB particles, but not the CB particles, induced an increase in the number of PMNs present within the lungs of rats, with a significant increase in the number of neutrophils found within the BAL fluid after 24-h exposure. No inflammatory effects were found with $FeCl_2$. Following inductively coupled plasma–mass spectrometry, it was observed that the $FeCl_2$ particles were detectable in ng mg^{-1} concentrations within ufCB particles. It was subsequently concluded that

ufCB does elicit an increase in cytosolic Ca^{2+} concentration, in support of Stone et al., and that ufCB particles induce an inflammatory response from cells, which was suggested to be independent of the transitional metal content of these NPs. The observation by Brown et al. that ufCB can cause increased inflammation supports the suggestion that ROS production, oxidative stress, and altered Ca^{2+} signaling caused by these NPs can cause an activation of transcription pathways, via a cascade of events within the cell, including both the nuclear factor–kappa B (NF-κB) and activator protein-1 (AP-1) pathways. Activation of these pathways was subsequently proposed to result in an escalated inflammatory response, with an increase in proinflammatory gene expression and proinflammatory mediator production, such as the cytokines IL-8 and TNF-α. Subsequent analysis by Brown et al. further supported this hypothesis, demonstrating that ufCB particles, and not CB particles, cause an increase in resting cytosolic Ca^{2+} concentration (as assessed by using Fura 2-AM) in rat alveolar macrophages. Similar effects were also found on treatment of rat alveolar macrophages in a dose–response relationship (12.5–50 μg/ml) following thapsigargin stimulation. It is also worth noting that these effects are similar to the findings of Stone et al. and Brown et al., further demonstrating the consistency between different forms of macrophage cells in assessing the toxicity associated with NP exposure. Additional study by Brown et al. also showed that these effects were decreased following addition of antioxidants (Trolox and nacystelyn), further supporting the findings of Stone et al., who concluded that the increased Ca^{2+} signaling observed in macrophage cells after NP exposure was mediated via ROS. As it was suggested, by Donaldson et al., that subsequent inflammation could occur due to the activation of specific transcription pathways (such as NF-κB and AP-1) following the altered Ca^{2+} signaling caused by ROS and oxidative stress of NP-treated cells, Brown et al. further studied the effects of ufCB on both NF-κB and AP-1 transcription pathways. Investigation of the NF-κB pathway showed ufCB (100 μg/ml) treated human monocyte cells to show increased fluorescence of the sub-units of NF-κB, p50, and p65 over a 4-h period compared with untreated monocyte cells. Additional analysis of the AP-1 pathway showed no significant increase in the intensity of the AP-1 protein following treatment with ufCB at 200 μg/ml, after 4 h in rat alveolar macrophages. The findings relative to both these pathways were found to be attenuated following the addition of antioxidants, further supporting the suggestion that these events are mediated via ROS production. Subsequent analysis of the inflammatory potential of ufCB in rat alveolar macrophages found the production of the proinflammatory cytokine TNF-α to be dose dependent (25–200 μg/ml) after 4-h exposure. It was subsequently concluded by Brown et al. that uf particles can exert proinflammatory effects by altering Ca^{2+} signaling, activating transcription factors and causing the production of proinflammatory cytokines via ROS-mediated mechanism, thus supporting the proposed oxidative stress paradigm. Although the findings of these studies suggest that the toxicity observed following exposure to NPs is relative to increases in the production of ROS and subsequent oxidative stress, as well as an escalation in Ca^{2+} signaling and inflammation within cells, the oxidative paradigm is only a hypothesis, and further research is required to fully understand the mechanisms of NP toxicity and how they may relate to the many new and different types of NPs being manufactured.

It is prudent to note that the oxidative stress paradigm is flexible. In the previously discussed literature, it is evident that oxidative stress induces an inflammatory response which affects cell signaling. This sequence, while correct, is not always true for NPs. Any resultant effects can be initiated following the onset of oxidative stress following NP exposure occur either in the presence or absence of a state of oxidative stress.

10.3 Cellular Defense Mechanisms in Mammalian Cells

Whilst oxidative stress has been well studied in terms of the mechanics of the toxicological response to ENMs, it is a common misconception that it is a negative aspect within mammalian cells, and only associated with a hazard effect response. Yet, in terms of the cellular defence of any cell type within the human body, there are a number of able defense mechanisms, of which oxidative stress is one. Such defense mechanisms include specific active (and passive) uptake mechanisms (please refer to Conner and Schmid [13] since it is not the absolute intention of this chapter is not to provide an overview of the different uptake mechanisms possible by any mammalian cell type). Yet, a side-effect of this the two major forms of 'cell-eating', or scenario is also the inflammatory response, which is another defense mechanism of the human body to any foreign body invasion (including ENMs). Yet, of all the defense mechanisms that mammalian cells have, it is their ability to engage the redox action that creates an imbalance between the cells antioxidant defence system, and the oxidants present in the cell/tissue.

10.4 Oxidative Stress, Antioxidants and Reactive Oxygen Species

As noted above, the major mechanism by which nanomaterials (NMs) are considered to induce cellular toxicity is via oxidative stress, which refers to a cellular redox imbalance as a result of increased intracellular highly Reactive Oxygen Species (ROS). The term ROS encompasses a number of molecules and free radicals derived from oxygen including primary ROS–H_2O_2, $O2^-$ and secondary ROS–OH• [14]. During normal cellular function ROS are produced as by-products of metabolism. For example, a one electron gain by the oxygen molecule (O_2) results in the formation of the superoxide free ion $O_2^{\bullet}$. This reduction happens frequently during numerous biological processes such as the electron transfer chain within the mitochondria; as several components of complexes I, II and III express thermodynamic properties required for the reduction of O_2 to O_2^- [15]. Other cellular source of O_2^- include the microsomal transfer chain via NADPH-cytochrome P_{450} and NADH-cytochrome b_5 reductase activities, the respiratory burst action of phagocytic cells, peroxisomal

beta-oxidation and Fenton reactions [16]. At low levels ROS may act as 'redox messengers' in intracellular signalling [17]. This is achieved by the activation of Redox sensitive transcription factors include AP-1, p53 and NF-κB which regulate pro-inflammatory cytokine expression, cell differentiation and apoptosis [18]. This signalling maybe utilised during the initiation of an inflammatory response with in a tissue for example.

Due the fact that ROS are a natural cellular occurrence due to normal processes, a homeostasis is maintained by a series of antioxidant proteins. The main class of this antioxidants is superoxide dismutases (SOD) including Cu–Zn–SOD (SOD1) and Mn–SOD (SOD2). Both SOD1 and SOD2 catalyse the conversion of O_2• to the less reactive H_2O_2 which can subsequently be converted to H_2O by catalyse and glutathione (GSH) [19]:

$$2O_2^{\bullet -} + 2H^+ \rightarrow H_2O_2 + O_2$$

$$2H_2O_2 \rightarrow O_2 + 2H_2O$$

The role of antioxidants is critical to maintaining cellular health, if an imbalance occurs between the levels of ROS and antioxidants, indiscriminate damage may be inflicted on a range of biological molecules. This include lipid peroxidation where ROS attack polyunsaturated fatty acids within the cell membrane, this results in the formation of a peroxyl-fatty acid radical and a subsequent chain reaction of membrane damage [20]. Lipid peroxidation can ultimately lead to impaired cellular functioning and cell rupture. Furthermore oxidative damage to the mitochondrial membrane can result in electron chain dysfunction and subsequently cell death [21]. ROS can also promote protein oxidation resulting in fragmentation at amino acid residues, protein cross links and oxidation of the amino acid chains resulting in loss of function [22]. The ability of ROS to cause protein damage has the potential to impact a multitude of cellular functions in addition to the risk of a build-up of malformed protein within the cell. In addition to protein oxidation and lipid peroxidation a key risk is ROS-induced DNA damage which is typified by single and double stranded DNA breaks, base modification (e.g. DNA adducted formation and DNA cross linkage) [23].

10.5 NMs and Oxidative Stress

A number of NMs have been shown to be inducers of oxidative stress, in particular metal oxide nanoparticles which may release ions capable of inducing the formation of the highly reactive hydroxyl radical (•OH) by conversion of H_2O_2 by Fenton chemistry.

H_2O_2 is not reactive as it has no unpaired electrons but it is however a mediator in the formation of secondary ROS in the form of hydroxyl radicals (•OH). This •OH formation can be initiated via transition metal ion promoted Fenton chemistry [24, 25]

$$M^{n+} + H_2O_2 \rightarrow M^{(n+1)} + {}^{\bullet}OH + OH^{-}$$

M represents transition metal.

Transition metal based NM's such as iron, copper, nickel, cobalt, and zinc may therefore release ions that can take part in the Fenton reaction promoting an increase in intracellular •OH formation. This free radical presents a significant risk for DNA damage as •OH is capable of attacking the DNA backbone and nucleotide bases promoting the formation of DNA lesions. More than 20 oxidative base lesions have been identified, the most notable being 8-hydroxygyanine (8-OH-dG) which frequently miss-pairs with thymine resulting double stranded breaks and point mutations [26].

A number of studies have identified transition metal based NM's as inducers of oxidative stress. For example, copper oxide promoted increased micronucleus formation in the Neuro-2A cell line as a resulted of oxidative damage measured by the formation of malondialedhyde (MDA) [27]. Moreover, significant MDA formation has been exhibited in the brains of Wister rats following treatment with gold (Au) nanoparticles (NPs) [28]. Perhaps the mostly widely studied transition metal NM is silver (Ag) due to it antimicrobial properties. Indeed, Ag NPs have been shown to induce ROS formation in lung epithelial cells (A549) as measured by the 2′-7′-Dichlorodihydrofluorescein diacetate (DCFDA) assay [29]. Similarly, when tested in HepG2 cells Ag NPs promoted increased ROS production (quantified by DCFDA) promoting downstream double stranded DNA breaks [30].

NM oxidative stress potential not limited to those comprised of transition metals, a number of NMs have been shown to catalyse ROS production at their surface in aqueous suspension including silica and carbon nanotubes [31]. This is likely due to immobilised free bonds of the atoms located on the NM surface. Quartz NPs for instance have been associated with the generation of ROS due to the presence of surface bound SiO• and SiO_2• [32]. Furthermore, the quantum confinement effect of quantum dots modulates their ability to accept and donate electric charge and potentially enable them to catalyse ROS formation [33].

10.6 NM Induced Immune Response and Oxidative Stress

If a NM is capable of promoting an immune response in vivo this may result in the formation of ROS by the cellular components of the immune system. NMs have indeed been shown to be capable of triggering ROS production in activated phagocytes (macrophages and neutrophils) in the form of a NADPH mediated respiratory burst [34–36]. If this respiratory burst is maintained downstream oxidative damage may be promoted in other cell types within the NM exposed tissue. ROS themselves are in fact mediators in the activation and recruitment of other immune cells, by promoting inflammatory cytokine production via activation of the transcriptional regulatory factor NF-κB. A vicious circle of chronic inflammation inducing downstream genotoxicity is therefore a possible scenario upon NM exposure [7].

10.7 ROS and Cytotoxicity

Due to the ability of ROS to mediate redox sensitive transcription factors its excessive presence in with in the cell can cause activation of apoptosis. This can be initiated by the upregulation of the tumour suppressor protein p53 which one cell stress is low can induce cell cycle arrest and DNA repair [37]. At high levels of cell stress however p53 can down regulate pro-survival factors, upregulate apoptotic factors and induction of the caspase cascade [38]. Due to the association of the upregulation of TNFα and ROS there is also evidence of linkage between ROS and apoptosis initiated by the extrinsic pathway [39].

10.8 Summary

The field of nanoparticle toxicology is a complex discipline that incorporates a plethora of different disciplines. It allows for the gaining of novel understanding towards an aspect that is vital regarding human long-term health effects. To date, there has been limited indication that nanomaterials are able to affect long-term human health, but this is due to a lack of research into this area and also the model systems to study it. Instead acute effects have been focussed upon, that have shown that commonly, realistic exposure concentrations/doses used in studies indicate that cellular machinery is often impeded, most notably by mechanisms associated with an oxidative stress response. Whilst oxidative stress is normal, it occurs within every organ/tissue/cell routinely, excess oxidative stress (commonly caused through reactive oxygen/nitrogen species) is a negative cellular response that can have both hazardous acute and chronic effects (e.g. inflammatory response), and so is essential to maintain in regards to the ENM-cell interaction.

Acknowledgements The authors would like to acknowledge all members of the In Vitro Toxicology group who contribute to the exhaustive scientific discussions.

References

1. Stone, V., Miller, M.R., Clift, M.J D., Elder, A., Mills, N.L., Moller, P., Schins, R.P.F., Vogel, U., Kreyling, W.G., Jensen, K.A., Kuhlbusch, T.A.J., Schwarze, P.E., Hoet, P., Pietroiusti, A., De Vizcaya-Ruiz, A., Baeza-Squiban, A., Tran, L., Cassee, F.R.: Nanomaterials vs ambient ultrafine particles: an opportunity to exchange toxicology knowledge. Environ. Health Perspect. (2017) http://dx.doi.org/10.1289/EHP424
2. Bouwmeester, H., Lynch, I., Marvin, H.J.P., Dawson, K.A., Berges, M., Braguer, D., Byrne, H.J., Casey, A., Chambers, G., Clift, M.J.D., Elia, G., Fernandes, T.F., Fjellsbø, L.B., Hatto, P., Juillerat, L., Klein, C., Kreyling, W.G., Nickel, C., Riediker, M., Stone, V.: Minimal analytical characterisation of engineered nanomaterials needed for hazard assessment in biological matrices. Nanotoxicology **5**, 1–11 (2011)

3. Clift, M.J.D., Gehr, P. Rothen-Rutishauser, B.: In vitro testing for Nanotoxicology: a valid alternative? Arch. Toxicol. **85**, 723–731 (2011)
4. Ferin, J., Oberdorster, G., Penney, D.P.: Pulmonary retention of ultrafine and fine particles in rats. Am. J. Respir. Cell Mol. Biol. **6**, 535–542 (1992)
5. Donaldson, K., Tran, C.L.: An introduction to the short-term toxicology of respirable industrial fibres. Mutat. Res./Fundamen. Mol. Mechan. Mutagen. **553**, 5–9 (2004)
6. Donaldson, K., Murphy, F.A., Duffin, R., Poland, C.A.: Asbestos, carbon nanotubes and the pleural mesothelium: a review of the hypothesis regarding the role of long fibre retention in the parietal pleura, inflammation and mesothelioma. Part Fibre Toxicol. **7**, 5 (2010)
7. Evans, S.J., Clift, M.J., Singh, N., de Oliveira Mallia, J., Burgum, M., Wills, J.W., Wilkinson, T.S., Jenkins, G.J., Doak, S.H.: Critical review of the current and future challenges associated with advanced in vitro systems towards the study of nanoparticle (secondary) genotoxicity. Mutagenesis **4** (2017)
8. Schins, R.P., Knaapen, A.M.: Genotoxicity of poorly soluble particles. Inhal. Toxicol. **19**, 189–198 (2007)
9. Limbach, L.K., Li, Y., Grass, R.N., Brunner, T.J., Hintermann, M.A., Muller, M., Gunther, D., Stark, W.J.: Oxide nanoparticle uptake in human lung fibroblasts: effects of particle size, agglomeration, and diffusion at low concentrations. Environ. Sci. Technol. **39**, 9370–9376 (2005)
10. Clift, M.J.D., Rothen-Rutishauser, B.: Studying the oxidative stress paradigm in vitro: a theoretical and practical perspective. In: Armstrong D., Bharali, D. (eds.) Oxidative Stress and Nanotechnology vol. 1082, pp. 115–133 (2013)
11. Poland, C.A., Duffin, R., Kinloch, I., Maynard, A., Wallace, W.A.H., Seaton, A., Stone, V., Brown, S., MacNee, W., Donaldson, K.: Carbon nanotubes introduced into the abdominal cavity of mice show asbestos-like pathogenicity in a pilot study. Nat Nanotech **3**, 423–428 (2008)
12. Unfried, K., Albrecht, C., Klotz, L.O., von Mikecz, A., Grether-Beck, S., Schins, R.P.F.: Cellular responses to nanoparticles: target structures and mechanisms. Nanotox **1**, 1–20 (2007)
13. Conner, S.D., Schmid, S.L.: Regulated portals of entry into the cell. Nature **422**, 37–44 (2003)
14. Gamaley, I.A., Klyubin, I.V.: Roles of reactive oxygen species: signaling and regulation of cellular functions. Int. Rev. Cytol. **188**, 203–255 (1999)
15. Cadenas, E., Boveris, A., Ragan, C.I., Stoppani, A.O.M.: Production of superoxide radicals and hydrogen peroxide by NADH-ubiquinone reductase and ubiquinol-cytochrome c reductase from beef-heart mitochondria. Arch. Biochem. Biophys. **180**, 248–257 (1977)
16. Poljsak, B., Šuput, D., Milisav, I.: Achieving the balance between ROS and antioxidants: when to use the synthetic antioxidants. Oxid. Med. Cell. Longev **11** (2013)
17. Circu, M.L., Aw, T.Y.: Reactive oxygen species, cellular redox systems and apoptosis. Free Radic. Biol. Med. **48**, 749–762 (2010)
18. Burton, G.J., Jauniaux, E.: Oxidative stress. Best Pract. Res. Clin. Obstet. Gynaecol. **25**, 287–299 (2011)
19. Zhang, J., Wang, X., Vikash, V., Ye, Q., Wu, D., Liu, Y., Dong, W.: ROS and ROS-mediated cellular signaling. Oxid. Med. Cell. Longev. **2016**, 18 (2016)
20. Vasilaki, A.T., McMillan, D.C.: Lipid peroxidation. In: Schwab, M. (ed.) Encyclopedia of Cancer. Springer, Berlin, Heidelberg (2011)
21. Manke, A., Wang, L., Rojanasakul, Y.: Mechanisms of nanoparticle-induced oxidative stress and toxicity. Biomed. Res. Int. **2013**, 15 (2013)
22. Dalle-Donne, I., Rossi, R., Giustarini, D., Milzani, A., Colombo, R.: Protein carbonyl groups as biomarkers of oxidative stress. Clin. Chim. Acta **329**, 23–38 (2003)
23. Singh, N., Manshian, B., Jenkins, G.J., Griffiths, S.M., Williams, P.M., Maffeis, T.G., Wright, C.J., Doak, S.H.: NanoGenotoxicology: the DNA damaging potential of engineered nanomaterials. Biomaterials **30**, 3891–3914 (2009)
24. Valko, M., Izakovic, M., Mazur, M., Rhodes, C., Telser, J.: Role of oxygen radicals in DNA damage and cancer incidence. Mol. Cell Biochem. **266** (2004)

25. Valko, M., Rhodes, C.J., Moncol, J., Izakovic, M., Mazur, M.: Free radicals, metals and antioxidants in oxidative stress-induced cancer. Chem. Biol. Interact. **160**, 1–40 (2006)
26. Cooke, M., Evans, M., Dizdrogla, M., Lunec, J.: Oxidative DNA damage: mechanisms, mutation, and disease. FASEB J. **17** (2003)
27. Perreault, F., Pedroso Melegari, S., Henning da Costa, C., de Oliveira Franco Rossetto, A.L., Popovic, R., Gerson Matias, W.: Genotoxic effects of copper oxide nanoparticles in Neuro 2A cell cultures. Sci. Total Environ. **441,** 117–124 (2012)
28. Siddiqi, N.J., Abdelhalim, M.A.K., El-Ansary, A.K., Alhomida, A.S., Ong, W.: Identification of potential biomarkers of gold nanoparticle toxicity in rat brains. J. Neuroinflamm. **9**, 1 (2012)
29. Foldbjerg, R., Dang, D.A., Autrup, H.: Cytotoxicity and genotoxicity of silver nanoparticles in the human lung cancer cell line, A549. Arch. Toxicol. **85**, 743–750 (2011)
30. Kim, S., Choi, J.E., Choi, J., Chung, K.H., Park, K., Yi, J., Ryu, D.Y.: Oxidative stress-dependent toxicity of silver nanoparticles in human hepatoma cells. Toxicol. In Vitro **23**, 1076–1084 (2009)
31. Magdolenova, Z., Collins, A., Kumar, A., Dhawan, A., Stone, V., Dusinska, M.: Mechanisms of genotoxicity. A review of in vitro and in vivo studies with engineered nanoparticles. Nanotoxicology **8**, 233–278 (2014)
32. Huang, Y.-W., Wu, C.-H., Aronstam, R.S.: Toxicity of transition metal oxide nanoparticles: recent insights from in vitro studies. Materials **3**, 4842 (2010)
33. Abdal dayem, A., Hossain, M.K., Lee, S.B., Kim, K., Saha, S.K., Yang, G.-M., Choi, H.Y., Cho, S.-G.: The role of reactive oxygen species (ros) in the biological activities of metallic nanoparticles. Int. J. Mol. Sci. **18**, 120 (2017)
34. Sun, S., Wang, Q., Giang, A., Cheng, C., Soo, C., Wang, C.-Y., Liau, L., Chiu, R.: Knockdown of CypA inhibits interleukin-8 (IL-8) and IL-8-mediated proliferation and tumor growth of glioblastoma cells through down-regulated NF-kB. J. Neurooncol. **101** (2011)
35. Trouiller, B., Reliene, R., Westbrook, A., Solaimani, P., Schiestl, R.H.: Titanium dioxide nanoparticles induce DNA damage and genetic instability in vivo in mice. Can. Res. **69**, 8784–8789 (2009)
36. Tulinska, J., Kazimirova, A., Kuricova, M., Barancokova, M., Liskova, A., Neubauerova, E., Drlickova, M., Ciampor, F., Vavra, I., Bilanicova, D., Pojana, G., Staruchova, M., Horvathova, M., Jahnova, E., Volkovova, K., Bartusova, M., Cagalinec, M., Dusinska, M.: Immunotoxicity and genotoxicity testing of PLGA-PEO nanoparticles in human blood cell model. Nanotoxicology **1**, 33–43 (2015)
37. Kaminskyy, V.O., Zhivotovsky, B.: Free radicals in cross talk between autophagy and apoptosis. Antioxid. Redox. Signal. **21**, 86–102 (2014)
38. Redza-Dutordoir, M., Averill-Bates, D.A.: Activation of apoptosis signalling pathways by reactive oxygen species. Biochimica et Biophysica Acta (BBA)—Mol. Cell Res. **1863**, 2977–2992 (2016)
39. Vandenabeele, P., Galluzzi, L., Berghe, T.V., Kroemer, G.: Molecular mechanisms of necroptosis: an ordered cellular explosion. Nat. Rev. Mol. Cell Biol. **11**, 700 (2010)

Chapter 11
Nanocarriers and Immune Cells

Lorna Moll and Volker Mailänder

Abstract Nanocarriers (NCs) have a high potential as target-specific drug-delivery system. Especially immune cells are a prime target in the nanoparticle-cell interaction. Uptake into the correct subtype of immune cells is crucial. Therefore uptake processes as well as intracellular processing is of utmost importance. The so-called protein corona heavily affects the interaction with immune cells which can decide the fate of the NC for degradation. On a wider perspective also nanoparticles which were not intentionally made for the transport of drugs get in contact with immune cells e.g. in the lungs. These immune cells are then trying to degrade these foreign materials.

11.1 Introduction

The field of nanomedicine is a fast growing research topic in cancer therapy or immunotherapy as target-specific drug-delivery system. Nanocarriers (NC) belong to the group of nanoparticles (NP). Nanocarriers are classified by their intended use: to transport drugs or specific signal molecules to a certain set of cells within the patient's body.

The interaction of NCs with immune cells is an important aspect of the development of NC based therapies, either as an obstacle to a non-immune cell target or a great opportunity when the immune cell is itself the intended target cell.

The immune system's main function is to identify and neutralize foreign materials which can cause harm to the body and physiological functions. The immune system is continuously challenged by such non-body own objects. These objects are composed to a large extent from the same basic components like DNA, RNA, peptides, proteins, sugars and lipids, but their specific composition e.g. of lipids or sugar motifs or the

L. Moll · V. Mailänder (✉)
Department of Dermatology, University Medical Center of the Johannes Gutenberg-University Mainz, Langenbeckstrasse 1, 55131 Mainz, Germany
e-mail: Volker.mailaender@unimedizin-mainz.de

L. Moll · V. Mailänder
Max-Planck-Institute for Polymer Research, Ackermannweg 10, 55128 Mainz, Germany

P. Gehr and R. Zellner (eds.), *Biological Responses to Nanoscale Particles*,
NanoScience and Technology, https://doi.org/10.1007/978-3-030-12461-8_11

appearance of DNA in the cytoplasm of mammalian cells is a non-physiological condition and therefore these are then detected as danger signals. Danger signals can be also caused by toxins, microorganisms, xenobiotics, mechanical stresses, or by contaminants [1]. NCs can induce an immune response due to these danger signals and hereby being recognized as harmful to the body and therefore being destroyed. Another option is that the immune system does not recognize the NC as harmful. This can be achieved by changes in the NC's properties which result in immunological tolerance, i.e. the NC is being ignored. Such properties of the NCs are the shape, surface charge, size, chemical composition as well as the type of administration. These properties have a major impact on the endurance of the NC in the body and not to be degraded which affects its effectiveness [1].

While material properties have been investigated for their immunological consequences, the field has learned in the last years that proteins readily adsorb on these nanocarriers. NCs as other NPs adsorb proteins from the surroundings and form the "protein corona". This corona has a major impact even on physical parameters like the size, surface charge, and aggregation behavior of the NCs. Most importantly, the corona affects the interaction with different types of cells. Cytotoxicity, endocytosis by certain cell types, and distribution in the patient's body is heavily influenced by the corona [2, 3]. Therefore, the protein corona of NCs plays an important role for the development and application of NCs as drug-delivery system.

The corona is divided into the "hard" and the "soft" corona which correlates to the strength of binding of the corona protein to the NC [4–6]. The composition of the corona is very dependent on the environment of the NC. When applied intravenously, then the corona undergoes constant changes. The stability of the NC as well as the surface properties, but also the body temperature of the patient and the composition of the blood resulting from different gender or age, cause changes to the corona [1, 6]. In cultured cells, the composition of the corona depends on experimental parameters like the culture medium, temperature, protein source, and concentration [7–9].

The formation of the protein corona as well as the composition are the focus of several studies in order to better understand the interaction of NC with immune cells and to unravel the mechanisms that lead to the degradation of NCs.

The modulation of the recognition of NCs by the immune system is a major challenge of the nanomedicine research field. The "Trojan horse" concept of nanomedicine described by Limbach and coworkers represents the need to avoid an immune response after application of NCs [10]. Possibilities to avoid this response can be achieved by negatively charged polysialic acids, a component of pathogenic bacteria such as *Neisseria meningitides* that is identical to host polysaccharides [11]. Most commonly used in nanomedicine is the coating of the NCs with block copolymers such as polyethylene glycol (PEG). This coating of the NC reduces the formation of the protein corona and therefore lowers its potential to activate an immune response in vitro as well as in vivo. Furthermore, the size and shape of the NC can be modified in order to reduce the recognition by immune cells [12, 13].

Nanomedicine is a challenging field of research which may result in the development of highly innovative tools for the therapy of tumors or immune diseases. Herefore, we need to understand the composition of the immune system and the interaction of nanocarriers with these different cell types.

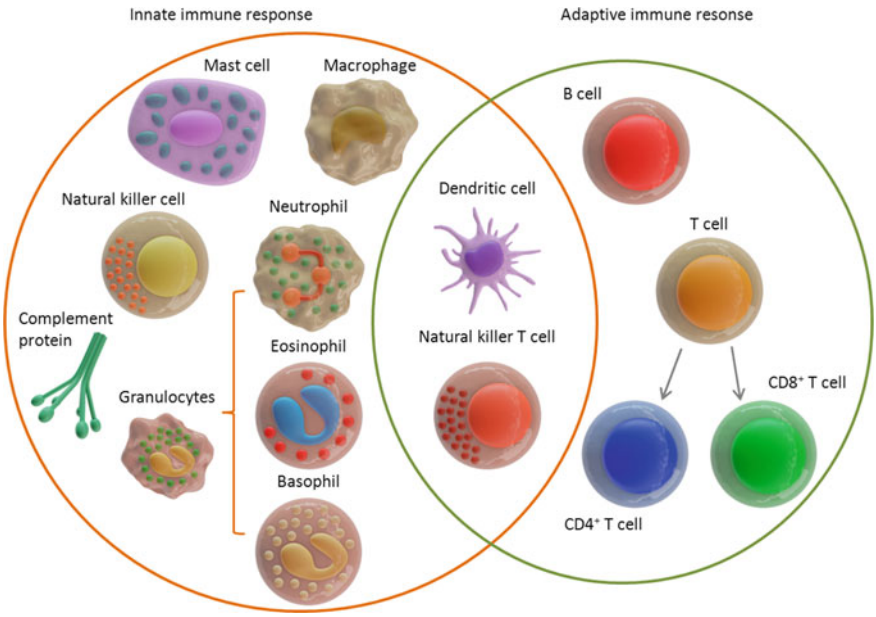

Fig. 11.1 Components of the innate and adaptive immune response. The innate immune response is the first line of defense against pathogens or other harmful threats from outside. Macrophages, mast cells, natural killer cells, granulocytes (neutrophils, eosinophils, basophils), and complement proteins mediate the innate immune response. Dendritic cells and natural killer T cells belong to both innate and adaptive immune response. The adaptive immune response develops slower and can memorize antigens. B cells together with antibodies as well as $CD4^+$ T cells, and $CD8^+$ T cells mediate the adaptive immune response [17] (The figure was modified from [17].)

11.2 Cell Types Comprising the Immune System and Their In Vivo Distribution

The immune responses are divided into the innate and the adaptive immune response (Fig. 11.1). The innate immune response reacts in a fast manner to various infections or other harmful threats [14]. These cells act without having been exposed to the harmful threat before. In contrast, the adaptive immune response needs first a phase of recognition and therefore evolves slower but memorizes antigens and is able to arm the defense mechanisms against formerly exposed antigens by enabling a highly specific attack. The adaptive immune response can result in immunogenicity and resistance towards infections or cancer. This can also induce tolerance or overreactions in cases such as autoimmunity, allergy, or transplantation [15].

The innate immune response consists of a variety of cell types. Here granulocytes, macrophages, dendritic cells (DCs), and natural killer cells (NK) are the most important ones, but not all main players. Granulocytes are subdivided into neutrophils, eosinophils, and basophils. Furthermore, it comprises soluble factors like

the complement proteins. The innate immune response regulates inflammation [16, 17]. The major players of the adaptive immune response are $CD4^+$ and $CD8^+$ T cells as well as antibodies which are produced by B cells [17, 18] (Fig. 11.1).

Neutrophils react to infections or injuries. They are recruited to the site of infection by migration through the bloodstream. Afterwards neutrophils cross the endothelium and enter the tissue interstitium [19]. Neutrophils consist of granules that contain proteases and antimicrobial peptides which can fuse to the cell membrane. This process is described as "degranulation". Otherwise these can also fuse intracellularly with materials taken up from the outside. Activated neutrophils phagocyte and destroy pathogens by the generation of reactive oxygen species (ROS), degranulation, and by bearing neutrophil extracellular traps (NETs) [20]. In vitro studies using neutrophils are of particular difficulty due to their short life span and easy, unspecific and unwanted activation. These characteristics prevent largely the possibility of genetic manipulation for in vitro studies [20].

Another group of granula-containing cells are the eosinophils. They play a role in parasitic infections and allergies [21].

The last and least abundant granula-containing cell type comprises of the basophilic cells (Fig. 11.1). They are involved in allergies as well as in parasitic infections [21]. They are involved in allergic reactions by releasing histamine as the most widely known allergic mechanism. Furthermore, basophils are known to be involved in chronic myelogenous leukemia, Crohn's disease, and contact dermatitis [22].

Macrophages belong to the innate immune response (Fig. 11.1). Their function is the uptake and digestion of pathogens and cellular debris as well as the secretion of cytokines [23]. Macrophages develop from circulating blood monocytes. Macrophages are located at potential entry sites for pathogens or other foreign and potentially harmful material. Macrophages are subdivided into microglia that are located in the central nervous system, Kupffer cells of the liver that degrade toxins, and alveolar macrophages that can be found in pulmonary alveoli [24, 25]. Monocytes—which are the precursors located in the blood stream—differentiate to macrophages upon activation by cytokines such as macrophage colony-stimulating factor (CSF1) or granulocyte-macrophage colony-stimulating factor (CSF2). Additional stimuli result in polarization of macrophages. This leads to the development of "classically activated" macrophages (M1) or "alternatively activated" macrophages (M2). M1 are activated by lipopolysaccharides derived from bacteria or by IFN-γ which is produced by T_{H1} cells. M2 are stimulated by IL-4 and IL-13. These cytokines are generated by T_{H2} cells. In addition, the polarization of macrophages into M1 or M2 is also directed by the differentiation signal of CSF2 or CSF1, respectively [26, 27].

M1 are involved in pro-inflammatory processes including the activation of an intracellular key protein NF-κB. This is followed by induction of pro-inflammatory cytokines like tumor necrosis factor alpha (TNF-α), IL-1β, IL-12. These then can activate T cells, and IL-23 that promotes inflammation and is involved in polarization of T_{H1} and T_{H17} cells [28].

M2 on the contrary can be found in tumors and are therefore also described as tumor-associated macrophages (TAM). TAM play a role in angiogenesis and progression of the tumor [28].

While macrophages to some degree are mediators between the innate and the adaptive immune system by taking up antigens, so much more dendritic cells have this role. They belong to the group of antigen-presenting cells (APCs). DCs engulf soluble proteins and aggregates from the extracellular surrounding. DCs are subdivided into myeloid and plasmacytoid DCs with different abilities to take up antigens. These objects are in the range of several nanometers up to several hundred nanometers. After uptake, the material is digested, processed, and afterwards presented on the membrane to T cells [29]. Therefore, DCs mediate adaptive immunity and tolerance against foreign antigens. DCs represent the major link between the innate and the adaptive immune response. DCs are the most compelling type of cells that engulf, degrade, and present the antigen on their membranes [15, 30, 31]. DCs are located at body surfaces such as skin, upper esophagus as well as at the mucosa of the respiratory and gastrointestinal system [15, 32]. DCs also migrate within the body. After antigens are presented on their major histocompatibility complex (MHC), DCs migrate to the lymphoid organs where T cells are located. Then the antigens that are presented by the DCs are recognized by T cells. A danger signal (see above) is needed to start proliferation and clonal selection of T cells [33–35]. These danger signals are recognized by a group of proteins. The most prominent ones are toll-like receptors (TLR). Additional receptors are NOD-like receptors and scavenger receptors [36]. TLRs of DCs recognize different components of microbial pathogens and result in the activation of DCs. TLR4 promotes IFN-β production while TLR2 cannot induce IFN-α or -β production. TLR3, TLR7, and TLR9 are able to promote the generation of IFN-α and IFN-β [37]. CpG motifs that are not methylated can be frequently found as a component of bacterial DNA [38]. CpG-containing oligodesoxynucleotides activate TLR9 of DCs to induce an immune response [39].

CD80 and CD86 are stimulatory molecules generated by APCs. CD80 and CD86 are important for subsequent T cell proliferation and production of cytokines. CD80 binds to CD28, which promotes T cell proliferation. In contrast, when CD80 binds to cytotoxic T lymphocyte antigen-4 (CTLA-4), T cell response is suppressed [40]. CD80 and CD86 bind to the same receptors but show functional differences in the outcome of the binding [41–43]. Therefore, DCs control the ability to recognize a variety of antigens by T cells. These T cells consist of different lymphocytes containing a near random variety set of antigen receptors [15].

DCs can also have the opposite effect: "tolerogenic DCs" induce silencing or tolerance of lymphocytes towards a potential antigen [44]. These DCs cause elimination (deletion) or blockage (suppression) of T cells recognizing the specific antigen [15, 44–46]. When the T cells are not eliminated, they differentiate into helper or killer cells. DCs promote the ability of T helper cells (T_{H1} cells) to generate cytokines such as interferon gamma (IFN-γ) in order to activate macrophages in case of microbial infection [47–49]. Additionally, DCs regulate the production of interleukin-4 (IL-4), -5, and -13 by T_{H2} cells which mobilize white cells for defense against helminths as well as the synthesis of IL-17 by T_{H17} cells to recruit phagocytes [50, 51]. DCs

can also inhibit immunity by promoting the development of regulatory T cells (T_{reg} 1 cells) or $FOXP3^+$ cells [46, 52]. Furthermore, DCs play an important role in the development of killer T cells (T_{h1}) or the T cell memory towards certain antigens [53, 54]. This is important for a prolonged success of vaccinations. DCs are subdivided into myeloid and plasmacytoid DCs with different abilities to take up antigens.

11.3 Danger-Associated Molecular Patterns

Danger-associated molecular patterns (DAMPs) are endogenous molecules that are generated upon different processes such as oxidative or cellular stress [55]. An additional trigger is the damage of tissues [56]. These stresses lead to the production of molecules that stimulate innate immunity and sterile inflammation [57]. Sterile inflammation is a stress-induced cytokine/chemokine response. It is detected in tissues as well as in the blood. The outcome of this inflammation can be beneficial or harmful of the host depending on the context and play a major role in processes such as wound healing [58–64]. DAMP-activated sterile inflammation is of great importance for diseases such as autoimmune diseases, cancer, atherosclerosis, and myocardial infarction [65].

DAMPs have to be located in the extracellular space in order to function as such. They are released upon stimuli or necrotic cell death. Extracellular heat shock proteins (eHsp72), mitochondrial DNA, ATP, uric acid crystals, and high mobility group box 1 (HMGB1) belong to the group of DAMPs [57]. These components are usually located inside the cell. They are released upon cell death or as a response toward a certain stress [66] (Fig. 11.2).

Cell death and immune responses to pathogens result in the activation of specific pattern recognition receptors (PRPs) as well as the presence of neutrophils and inflammation. These two signaling pathways belong to the common danger response system, which are activated by DAMPs or by pathogen-associated molecular patterns (PAMPs). These pathways aim to defend the organism against the threat caused by a pathogen or to restore the wounded tissue [66] (Fig. 11.2).

11.4 Receptors for DAMPs and Uptake of Nanoobjects

Professional phagocytes such as monocytes, macrophages, and neutrophils perform receptor-dependent endocytosis. Macrophages recognize and bind foreign antigens with their pattern recognition receptors, namely toll-like receptors (TLRs). Upon binding of the TLR to the corresponding antigen, a signal pathway and immune response is activated [68]. It was previously shown that it is more likely that positively charged or neutral NCs promote an inflammatory response compared to negatively charged carriers [69]. A possible explanation for this is that macrophages exhibit a negatively charged sialic acid on their surface. The interaction with positively charged

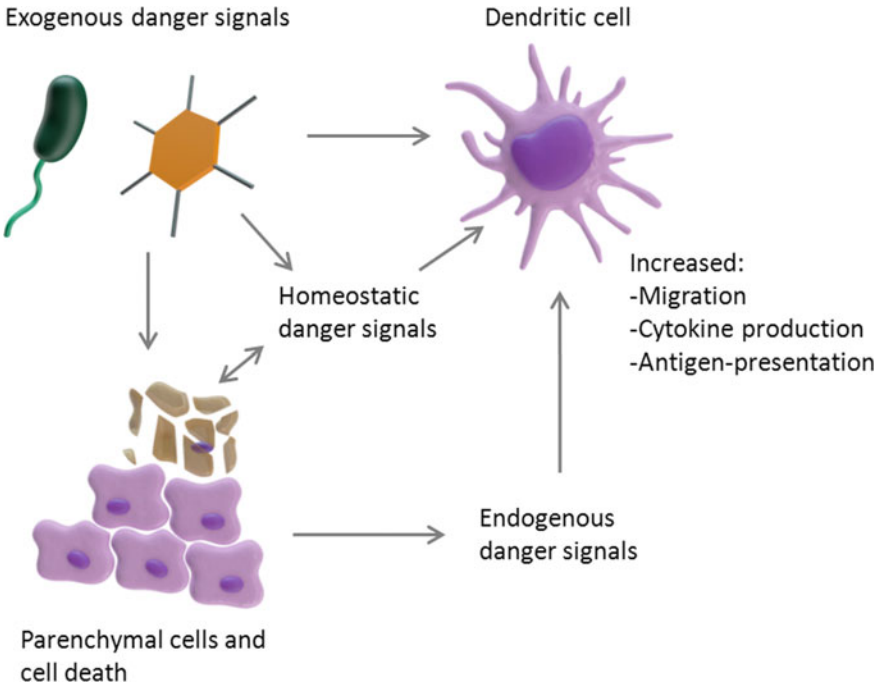

Fig. 11.2 Dendritic cells respond to danger signals. Exogenous danger signals such as pathogen-associated molecular patterns activate DCs through pattern recognition receptors. These exogenous danger signals can cause inflammatory cell death and subsequent release of endogenous danger signals which in turn activate DCs. Homeostatic danger signals such as a decreased pH in the tissue suffering from inflammation, can also activate DCs. Activated DCs migrate to the location of inflammation, exhibit antigen-presentation, and induce the production of cytokines [67]. (The figure was modified from [67].)

NCs is therefore more likely to occur [68]. In addition, NCs engulfment may occur by the reticuloendothelial system (RES) on the organ level. This system consists of leukocytes, endothelial as well as epithelial cells, macrophages, and dendritic cells. Cells of the RES are mostly found in organs such as the liver and the spleen. Also for this system, studies showed that the uptake of positively charged NCs is of high prevalence and results in the internalization of the NCs [70–72].

NCs can be opsonized with either C3ib that displays one of the activated components of the complement cascade or IgG. These opsonins can interact with the receptors for C3ib and Fcγ localized on the membrane of the phagocyte. This recognition is followed by the uptake of the NC by the phagocyte. The uptake can be hampered by the presence of serum albumin but is not completely diminished mostly [70, 73].

Furthermore, NCs can be modified to directly target diseased cells. The folate receptor (FR) is overexpressed in different types of tumor cells [74]. FR consists of two isoforms, FR-α which is mainly expressed in epithelial cancers and FR-β which is localized on activated macrophages and expressed in myeloid leukemia [75–78].

Folate-conjugated NCs can therefore be specifically directed to diseased cells [79]. A previous study could demonstrate that a folate-conjugated hapten treatment lead to an increase of immunogenic tumor cells and subsequently promoted the anticancer immune reaction against these tumor cells [80]. Another receptor to target certain cell types is the transferrin receptor (TfR). This receptor is thought to be expressed in all cell types. However, it is known to be highly expressed in rapidly dividing cells and therefore it is a very suitable target for cancer therapy using NCs [75, 81]. NCs conjugated to transferrin or TfR binding single chain antibody fragment (TfRscFv) were utilized for target-specific drug delivery in cancer therapy [82].The epidermal growth factor receptor (EGFR) is expressed in solid tumors such as brain or breast tumors and can also be used as a target for NC [82, 83].

These studies show a variety of approaches for nanomedicine. NCs can directly interact with immune cells or target disease cells for subsequent treatment such as immunotherapy.

11.5 Immune Cells in Cell Culture

The study of the interaction and uptake of NCs by immune cells is often performed using cultured cells. Especially in the field of nanocarriers this is a common approach. Phagocytosis of debris by phagocytes such as macrophages results in the formation of phagosomes. These phagosomes then fuse with lysosomes to generate phagolysosomes. In these phagolysosomes the presence of a low pH, lysosomal enzymes, and an increased production of ROS leads to the degradation of the debris or the NCs taken up [84]. This increased ROS production explains the need for toxicological studies of NCs using macrophages [85].

Cell lines from leukemia and lymphoma patients are commonly used to study NC interaction with immune cells as well as the engulfment of NCs. Toxicity studies were mainly performed using human or murine leukemia cancer cell lines at different stages of differentiation [85–87]. One of such cell lines is THP-1 which was generated from the blood of a boy who suffered from acute monocytic leukemia. Childhood myelomonocytic leukemia displays a disease that affects pluripotent stem cells. They overproduce monocytic cells that infiltrate organs like the liver or the lungs [88]. For in vitro studies, the monocytic cells can be differentiated using phorbol-12-myristate-13-acetate (PMA) to reach the differentiated stage of macrophages [89, 90].

Macrophages are of particular interest because these cells display an important part of the immune response and engulf as well as degrade foreign material in the blood. A prominent cell line is RAW264.7, a murine macrophage-like cell line. A major challenge of nanomedicine is for the NCs to escape from macrophages in order to be able to reach the target destination [91]. Here in these cell cultures the analysis of the protein corona of NCs and its interaction with immune cells has been studied. The influence of the protein corona showed dependence on the protein source and anticoagulant in the media of the cells as it affects the uptake behavior of tissue cultured cells [92].

A commonly used model for T cells are Jurkat cells. Upon stimulation with phytohaemagglutinin, Jurkat cells produce IL-2 [93]. Jurkat cells were previously used to investigate the T cell receptor signaling pathway and by now several T cell receptor signaling mutant Jurkat cell-lines have been generated [94]. A problem of the Jurkat cell line are the defective phosphatase and tensin homologue (PTEN) and SH2-domain-containing inositol polyphosphate 5′ phosphatase [95–97]. Especially defective PTEN might influence T cell receptor signaling through constitutive activation of the phosphatidylinositol 3-kinase (PI3 K)–signaling pathway. Components of this pathway are the serine-threonine kinase AKT and the protein tyrosine kinase IL-2-inducible T cell kinase (ITK) [98].

B cells—the cells producing antibodies after contact with the antigen and proliferation—are a widely neglected cell type in the field of nanomedicine. Here further studies are highly needed.

11.6 Immune Cells In Vivo

NCs are intended to be used as target-specific drug delivery system. Therefore, the in vivo application of NCs needs to be thoroughly investigated. After intravenous (IV) administration, the NCs are engulfed by the mononuclear phagocytic system (MPS) and are stored in the liver or spleen [99]. A previous study analyzed the distribution of fluorescently labelled Polystyrene NCs in NOD-SCID IL2Rγnull; NSG mice. The analysis of the aggregation behavior of the NCs caused by bound serum-proteins and the composition of the protein corona can be a tool for the prediction of the in vivo distribution of the NCs. Mohr and coworkers were able to show that NCs which tend to aggregate mainly locate to the liver while NC that do not aggregate scatter to all organs [99].

In a recent study, researchers used NCs that target T cells in vivo for immunotherapy of tumors. These poly(lactic-co-glycolic acid) (PLGA) and PEG based NCs coated with antibodies that specifically bind $CD8^+$ T cells in the lymphoid tissues, blood, and tumors of mice. The NCs were administered intravenously into a subcutaneous model of B16 melanoma. In addition, the researchers developed similar NCs to target programmed cell death protein 1 ($PD\text{-}1^+$) T cells [100]. PD-1 is a marker to identify the tumor-reactive $CD8^+$ cells that infiltrate tumors of humans and $CD8^+$ T cells in the blood of patients suffering from melanoma [101, 102].

These results present a promising use of NCs to target certain cell types in a multicellular organism for subsequent treatment approaches.

11.7 Interaction of Nanocarriers with Immune Cells in Cell Culture

The physicochemical properties of NCs play a major role for their immunomodulatory effects which can result in suppression or activation of the immune response [103].

In vitro studies of the protein corona that affects the interaction of NCs with immune cells showed that its formation is highly dependent on the environment [1–7]. Among others, the choice of protein source for in vitro studies is very important and heavily affects the interaction with the immune cells. A recent study showed that the uptake of NCs by cultured cells is reduced when serum and plasma concentration added to the cells is as low as 0.5%. Furthermore, an increased uptake of fetal bovine serum (FBS) coated NCs by HeLa cells and macrophages was observed. In contrast, human serum and human citrate plasma reduced the NC uptake. Interestingly, NCs that were incubated in the human anticoagulant heparin plasma were internalized by macrophages but not by HeLa cells. These results indicate that the environment affects the formation of the protein corona as well as the interaction with different cell types [92].

Another study generated a tailor-made artificial protein corona using human plasma. This study identified proteins from protein fractions of human plasma such as human serum albumin which resulted in an increased uptake by macrophages while other low abundant protein fractions caused a decreased uptake [104].

Schöttler and coworkers demonstrated that polystyrene NCs modified with polyethylene glycol (PEG) or with poly(ethyl ethylene phosphate) (PEEP) and incubated with plasma proteins present a low uptake by RAW264.7 cells. When these NCs were not exposed to plasma proteins, then a high non-specific uptake occurred. The researchers identified the protein clusterin which is also known as apolipoprotein J, to be a major component of the protein corona of PEGylated NCs. Interestingly, the incubation of the NCs with clusterin reduced the non-specific cellular uptake. These results show that PEG and PEEP not only reduce the formation of the protein corona but also affect the composition of the corona. Certain proteins as part of the corona can prevent non-specific cellular uptake [91].

On the other hand some proteins promote uptake, like immunoglobulin G (IgG). IgG acts as defense molecule (an opsonin) against microorganisms that might cause an infection. NCs which are covered with opsonins can be recognized and degraded by phagocytes [1]. The coating of the NCs using PEG (PEGylation) can reduce opsonization and thereby prevents the recognition of the NC by the RES and especially DCs as well as increasing the blood circulation time of the NC [105, 106].

Myeloid DCs were shown to be able to engulf zeolite particles bound to IgG. The amount of adsorbed IgG affected this uptake. This engulfment was dependent on the amount of adsorbed IgG and could not be detected for plasmacytoid DCs [107].

Analyzing the uptake of NCs in tissue cultured cells helps to understand the mechanism of action but for further knowledge, in vivo experiments are needed to

evaluate the uptake of the NCs as well as the interplay of different cell types as a reaction to NCs in a multicellular organism.

11.8 Routes of Applications for Nanoparticles

NCs can be applied to patients by different methods. Common parenteral administrations are: intradermal (ID), subcutaneous (SC), intramuscular (IM), intravenous (IV), and intra-arterial [105]. The properties of the applied particles such as surface charge, size as well as hydrophobicity or hydrophilicity affect IV administration and subsequent distribution [108]. This determines their potential to interact with different immune cell types. NCs can be administered by IV because they can also enter microvessels in the body which feature a diameter of 5–10 μm. After injection, NCs with a size of more than 100 nm are more prone to be caught by the reticuloendothelial system (RES) in the spleen, liver, lung, and bone marrow than NCs with a smaller size. These can circulate for a longer time in the body [105]. As already mentioned, also other properties of the NC affect the application. Hydrophobic NCs are efficiently taken up by different tissues. In contrast, hydrophilic NCs coated with PEG and a size smaller than 100 nm circumvent better to be engulfed by macrophages [105, 109].

The intravenous injection of NCs causes them to interact with the membranes of red blood cells. More specifically, the NCs interact with the membrane glycocalix components and receptors such as integrins or as an example the Duffy antigen/chemokine receptor. In addition, NCs absorb a variety of blood components such as proteins. These components locate on the surface of the NC and form the "protein corona" [6] as detailed above.

Other routes besides IV are rarely investigated. Although also in clinic other routes of applications are rare, it may still be worthwhile to investigate these and demonstrate how they can benefit for shaping the biodistribution. This is clearly a blind spot of the nanomedicine community.

Nonparenteral routes of administration are the oral, nasal, ocular, and the pulmonary way to apply NCs. Chitosan microcarriers were previously shown to be able to protect their cargo from the gastrointestinal tract [110]. Nasal application of chitosan NCs coated with ovalbumin and cholera toxins promote immune responses in rats. Furthermore, these NCs were shown to specifically target nasal-associated lymphoid tissues to obtain nasal vaccine delivery [105, 111]. Immunization of mice using chitosan microspheres containing *Bordetella bronchiseptica* antigens results in an increase of *B. bronchiseptica*-specific IgA antibody levels correlated with an enhanced survival rate of the mice [105, 112, 113].

Nanoparticles can enter the lung by diffusion and be cleared by alveolar macrophages [114]. This field is mostly studied for its toxicity but holds great promises for drug delivery. Due to their deposition properties microparticles are more suitable than nanoparticles for this route of application [115]. Studies using

chitosan NCs and microparticles show a promising use for the application of drugs by NCs through inhalation [105].

11.9 Interaction of Nanocarriers with Immune Cells In Vivo

The design of NCs such as the size can affect the reactivity with immune cells as well as the penetration into tissues and cells [116]. Depending on the concentration of the NCs, a high dosage can induce cytotoxicity while a low dosage can lead to sub-lethal and long-term effect of the cells [117–120]. NCs can be identified by the immune system as foreign and induce an immune response or the carriers can interfere with the immune system [121]. Such immunomodulatory effects in an organism have to be considered while developing NCs for medical approaches. The study of such effects is of particular importance due to the use of NCs as drug delivery system [103]. On the other hand, it is most likely that NCs get into contact and interact with immune cells [103, 121]. This should also be viewed as an opportunity: this interaction can be directed in order to develop NCs for immunotherapies [69, 121].

The physicochemical properties of NCs have a major impact on the immunomodulatory effects. They can result in suppression or activation of the immune response [103].

As a preporatory exploration ex vivo whole blood can be used for screening NCs. A previous study by Baumann and coworkers showed NC interaction using whole blood samples. In this study an ex vivo assay was performed in order to investigate NC interaction with primary cells of the bloodstream instead of malignant or immortalized cells that are commonly used for in vitro experiments [122, 123]. Such an ex vivo approach can connect in vitro and in vivo experiments [124]. Negatively charged NCs prepared with acrylic acid (AA) and sodium dodecyl sulfate (SDS) or positively charged and prepared with 2-aminoethyl methacrylate (AEMH) and cetyltrimethylammonium chloride (CTMA-Cl) AA introduced amino groups to the NCs and AEMH introduced amino groups. The addition of SDS or CTMA-Cl resulted in a uniform charge of the NCs [122]. The human blood samples were treated with heparin. The uptake of these NCs by different cells in the blood varied highly. The majority of carboxy-functionalized NCs were engulfed by $CD14^+$ monocytes followed by amino-functionalized NCs. T and B cells showed a low uptake rate [122]. This effect can be due to the fact that these cells do not have phagocytosis activity [123].

11.10 Uptake and Intracellular Processing of Nanocarriers in Immune Cells

NCs that enter the body can induce an immune response by interacting with immune cells. Phagocytes can take up NCs via endocytosis. This process depends on the size, the surface, and the shape of the NC. The uptake of NCs can be receptor-dependent or receptor–independent. The way of uptake is determined by size and the proteins that are adsorbed to the surface of the NC. Larger particles of <5 μm are engulfed by phagocytosis or micropinocytosis. Smaller particles are taken up by receptor-dependent endocytosis. The uptake is again dependent on clathrin, lipid rafts, or caveolae. The endocytosis of <150 nm particles is mediated by clathrin and the engulfment of particles with a size of 50–80 nm is favored by caveolae mediated endocytosis. The size of the particles that are taken up by lipid raft-mediated endocytosis is not yet fully understood [1].

11.10.1 Pinocytosis

Clathrin-mediated endocytosis (CME) involves the formation of a clathrin-coated pit at the plasma membrane followed by the generation of a vesicle by the activity of the GTPase dynamic (Fig. 11.3). The vesicle fuses with early endosomes or with lysosomes. Most receptor-mediated engulfment of nanoparticles occurs via CME [75]. Cationic particles (100 nm) made of polylactide-co-polyethylene glycol (PLA-PEG) are internalized just via CME [126]. poly(D,L-lactide-co-glycolide) NPs exhibiting poly(L-Lysine), a cationic polymer, at their surface, increase the uptake by CME [127].

Another endocytosis pathway is clathrin-independent. Compared to CME, clathrin-independent endocytosis (CIE) does not require a coating protein at the site of vesicle formation. The loaded material in the vesicle is transported for degradation to late endosomes and lysosomes [75]. A previous study showed that the trisaccharide-substituted chitosan oligomers (SBTCO) resulted in an increased uptake compared to linear chitosan (LCO). The uptake of SBTCO mainly occurred via CIE [128].

Caveolae are invaginations that are present in the plasma membrane and play an important role for processes such as signal transduction and endocytosis [75, 129]. Caveolae-mediated endocytosis (CavME) results in the accumulation of material in caveosomes with neutral pH [130]. A study by Liu and coworkers identified the uptake of a DNA conjugated poly(amido amine) dendrimer conjugated to the rabies virus glycoprotein RVG29 (29-amino-acid peptide) in brain capillary endothelial cells by clathrin- and caveolae-dependent endocytosis [131].

Macropinocytosis is a type of endocytosis that is dependent on actin. During macropinocytosis cells engulf extracellular fluid in vesicles with a diameter of 0.5–10 μm into vesicles (Fig. 11.3). These vesicles are also known as macropinosomes [132]. In addition to extracellular fluid, viruses, bacteria, and apop-

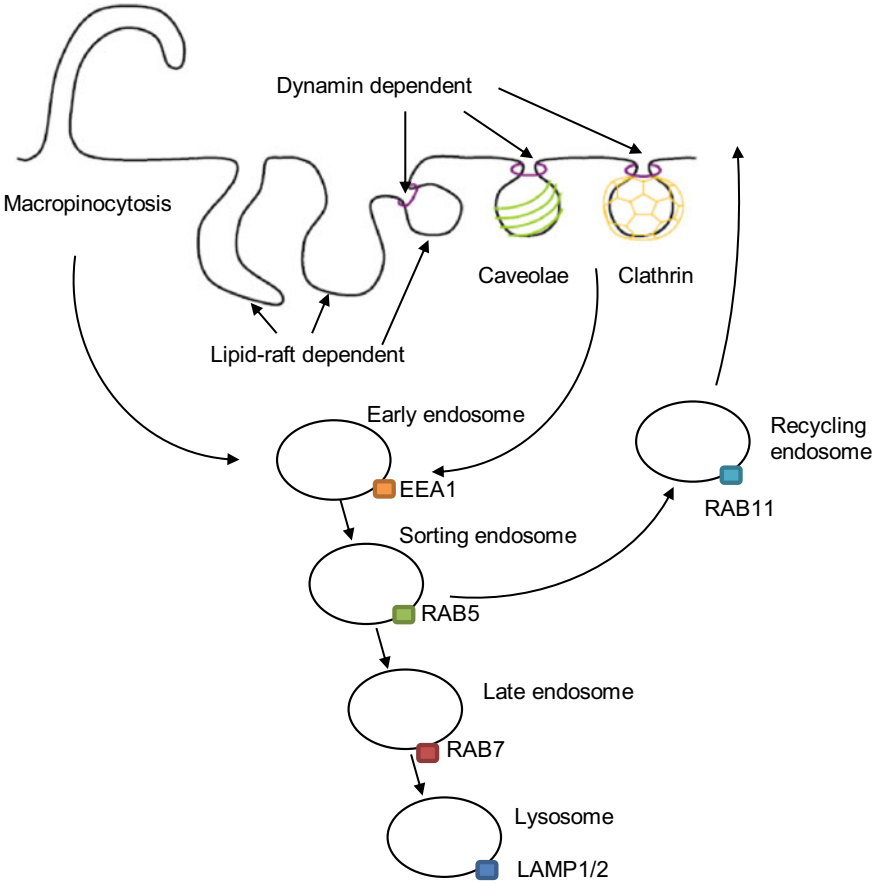

Fig. 11.3 Endocytosis mechanisms of Nanocarriers. Endocytosis of Nanocarriers can occur via Macropinocytosis, Pinocytosis, or Phagocytosis. EEA1: Early endosomal antigen; LAMP: Lysosomal-associated membrane protein, RAB: Ras-related protein [125]. Reproduced with permission from Nanomedicine as agreed by Future Medicine Ltd. [125]

totic cell fragments are internalized by macropinocytosis [75, 133–135]. This process is involved in antigen-presentation by MHC class II [136, 137]. A previous study showed that lapatinib conjugated NCs including a lipid corona made of egg yolk lecithin and a core from albumin with a size of 62 nm were internalized by a human mammary gland carcinoma cell line by clathrin-dependent pinocytosis as well as by micropinocytosis [138]. While there are a variety of publications on how different nanoparticles enter macrophages and more interestingly DCs, little is known about the consequences.

A major concern is the possible cellular toxicity mediated by the uptake of NCs. A few studies investigated changes of cellular behavior after NC uptake. It was found that several cell lines generate formazan deposits independent of the NC concentra-

tion [139–142]. Formazan is considered to be a marker for mitochondrial stress due to a change of mitochondrial activity which leads to an increase of reactive oxygen species (ROS) [142, 143]. This production of ROS results in cell damages such as cytoskeleton disorganization and cell death [142, 144, 145]. Some studies showed further that different NCs cause an increase of intracellular calcium concentration [142, 146–148]. Calcium is known to be a major second messenger involved in a variety of signaling pathways [142, 146]. Furthermore, NCs may change the ionic currents across the plasma membrane. A study showed that polystyrene NC can change the function of ion-channels in human airway epithelial cells [142, 149].

These results show that it is of crucial importance to investigate the consequences of NC uptake on cells and tissues in order for the intended therapy to be successful.

11.10.2 Phagocytosis and Cross-Presentation After NC Uptake

DCs belong to the group of phagocytes. Immature DCs (iDC) present a high endocytic activity and continuous micropinocytosis while mature DCs (mDC) show a decreased activity [150, 151]. In addition, both DC subtypes can take up antigens by receptor-mediated endocytosis and present the peptides bound to a specific class or proteins, termed major histocompatibility complex (MHC) [152, 153]. In general, peptides from endogenous antigens are presented on MHC class I and peptides from exogenous antigens are exhibited on MHC class II molecules of antigen-presenting cells [154, 155]. Antigen-presentation by MHC class I molecules is needed to develop and activate $CD8^+$ T cells. These cells can promote cytotoxicity as a response [26]. DCs are able to perform cross-presentation in order to present exogenous antigens via MHC class I molecules as well as class II [156]. After uptake, the antigens can either escape from the phagosome and be released into the cytoplasm followed by MHC class I presentation or the antigen is degraded inside the phagosome resulting in presentation on MHC class II molecules [156]. Specialized endoplasmatic reticulum(ER)-phagosomes function during cross-presentation to promote antigen presentation by MHC class I [125, 156, 157].

A previous study showed that 350 nm particles loaded with ovalbumin were engulfed by DCs and resulted in cross-presentation in vitro as well as in subsequent T cell activation when administered in vivo. Larger PLGA particles of 112 μm failed to have such an effect [158]. In contrast, polystyrene beads of small and large sizes (<0.2 μm and >1 μm, respectively) were able to induce cross-presentation, but the larger beads showed a lower rate of uptake. At a concentration of the beads resulting in a similar uptake, the larger beads caused an increased presentation by MHC class I. This result is due to the lysosomal degradation of small particles compared to the uptake of larger particles into other compartments of the cell exhibiting a neutral pH and therefore supposedly degraded more slowly [156]. Another study showed that latex beads were engulfed by DCs and transferred into early phagosomes which then

fused to the endoplasmatic reticulum. Such early phagosomes are characterized by calnexin [157]. Fewer beads were encapsulated into LAMP2-positive phagosomes. In addition, an enhanced cross-presentation could be observed when applying PLGA particles loaded with ovalbumin compared to latex beads that were coated with albumin. PLGA particles did not end up in the phagosome and therefore showed reduced proteasomal degradation [159]. Intracellular trafficking of NCs can also be affected by modifications of the particle itself. PLGA particles coated with KKXX signals of the ER did not affect the cross-presentation mediated by ER-phagosomes [160]. Most importantly, it was shown that micro- and nanoparticles promote cross-presentation more efficiently than soluble antigens [125, 158].

This field of research is still developing in order to understand what modifications and other characteristics are needed for the NCs to be processed in a desirable way.

11.11 Immune Cell Responses to Nanocarrier Interactions

NCs can be identified as foreign by interaction with cells of the immune system. This can result in immune responses such as complement activation, inflammation as well as the production of antibodies. These actions can lead to pathological conditions like hemolysis, thrombosis, or hypersensitivity. Furthermore, the interaction of NCs with immune cells can cause their degradation [161]. A fast degradation of the NCs is a major problem for the use of targeted nanomedicines.

NCs may not only affect the uptake and intracellular processing by immune cells such as macrophages, but they may also influence the activity or function of the cell that internalizes the NC. A recent study investigated the effect of carboxyl- (PS-COOH) and amino-functionalized (PS-NH_2) polystyrene NCs on M1/M2 polarization. Fuchs and co-workers were able to show that these NCs had no effect on the viability of the macrophages and did not influence the expression of the M1 markers CD86, NOS2, IL-1β, and TNF-α [162]. In M2, both types of NCs reduced the expression of the scavenger receptors CD163 and CD200R. In addition, the release of IL-10 was decreased. Furthermore, PS-NH2 inhibited the ability to phagocyte *Escherichia coli* by M1 and M2. In contrast, PS-COOH increased the protein mass of M1 and M2 by promoting protein synthesis as well as the release of TGF-β1 by M1 and the generated ATP levels in M2. Taken together, these results showed that cationic and anionic surfaces of NCs inhibited the M2 polarization. These findings may provide a tool to reprogram M1/M2 polarization in patients suffering from chronic inflammation or cancer [162]. For this clearly polystyrene should be substituted with a biodegradable polymer.

While not directly a part of the immune system, platelets have been shown to modify immune cell interactions. Platelet activation is characterized by an increased expression of P-selectin, release of serotonin, procoagulant activity as well as an increased release of calcium, exposure to phosphatidylserine, and production of thrombin. This event is triggered by complement activation or by direct interaction with NCs [1, 163]. Here is a strong link between immune activation and clotting, both

finely tuned and regulated by multiple instances in a complex network of proteins and cells and fragments of cells.

11.12 Summary

NCs display a new and innovative therapeutic tool as target-specific drug-delivery system. In addition, NCs can transport signaling molecules, DNA or other components to a certain set of cells. A major challenge for nanomedicine is the detection of the NCs by the immune system. For many applications a rapid degradation of NCs by cells of the immune system such as macrophages needs to be avoided to prolong the circulation of the NCs in the blood of the patients as well as for the NCs to reach their target destination of action. But this strong interaction and unspecific uptake can also be used for new and potentially more effective vaccines. Investigations of different types of NCs using a variety of modifications help to understand which NCs need to be used for a certain approach. The protein corona that is formed and surrounds the NCs as soon as they are administered to the blood stream plays an important role for the interaction of the NCs with immune cells. The composition of the protein corona affects the uptake of the NCs especially into immune cells. NCs can further be used to modulate the immune response to treat diseases such as cancer or immune diseases. The immune response may be activated and directed to treat certain tumors or it may be inactivated to treat autoimmune diseases or chronic inflammation.

Major progresses have been made during the past years in the field of nanomedicine. Still questions remain to be answered such as: What are the long-term effects of NC treatments for the patient? Do degraded NCs remain in the body or are they released? What are the routes of NC remaining in the body? How do we best use the preferred uptake of nanocarriers into phagocytic cells?

Overall, NCs have a very high potential for solving many pharmaceutical obstacles of standard procedures such as delivering a drug directly to desired destination.

References

1. Boraschi, D., Costantino, L., Italiani, P.: Interaction of nanoparticles with immunocompetent cells: nanosafety considerations. Nanomedicine (Lond.) **7**(1), 121–131 (2012)
2. Walkey, C.D., Chan, W.C.: Understanding and controlling the interaction of nanomaterials with proteins in a physiological environment. Chem. Soc. Rev. **41**(7), 2780–2799 (2012)
3. Hellstrand, E., Lynch, I., Andersson, A., Drakenberg, T., Dahlback, B., Dawson, K.A., et al.: Complete high-density lipoproteins in nanoparticle corona. FEBS J. **276**(12), 3372–3381 (2009)
4. Milani, S., Bombelli, F.B., Pitek, A.S., Dawson, K.A., Radler, J.: Reversible versus irreversible binding of transferrin to polystyrene nanoparticles: soft and hard corona. ACS Nano **6**(3), 2532–2541 (2012)

5. Cedervall, T., Lynch, I., Lindman, S., Berggard, T., Thulin, E., Nilsson, H., et al.: Understanding the nanoparticle-protein corona using methods to quantify exchange rates and affinities of proteins for nanoparticles. Proc. Natl. Acad. Sci. U.S.A. **104**(7), 2050–2055 (2007)
6. Lundqvist, M., Stigler, J., Elia, G., Lynch, I., Cedervall, T., Dawson, K.A.: Nanoparticle size and surface properties determine the protein corona with possible implications for biological impacts. Proc. Natl. Acad. Sci. U.S.A. **105**(38), 14265–14270 (2008)
7. Maiorano, G., Sabella, S., Sorce, B., Brunetti, V., Malvindi, M.A., Cingolani, R., et al.: Effects of cell culture media on the dynamic formation of protein-nanoparticle complexes and influence on the cellular response. ACS Nano **4**(12), 7481–7491 (2010)
8. Ghavami, M., Rezaei, M., Ejtehadi, R., Lotfi, M., Shokrgozar, M.A., Abd Emamy, B., et al.: Physiological temperature has a crucial role in amyloid beta in the absence and presence of hydrophobic and hydrophilic nanoparticles. ACS Chem. Neurosci. **4**(3), 375–378 (2013)
9. Mahmoudi, M., Abdelmonem, A.M., Behzadi, S., Clement, J.H., Dutz, S., Ejtehadi, M.R., et al.: Temperature: the "ignored" factor at the NanoBio interface. ACS Nano **7**(8), 6555–6562 (2013)
10. Limbach, L.K., Wick, P., Manser, P., Grass, R.N., Bruinink, A., Stark, W.J.: Exposure of engineered nanoparticles to human lung epithelial cells: influence of chemical composition and catalytic activity on oxidative stress. Environ. Sci. Technol. **41**(11), 4158–4163 (2007)
11. Byrne, B., Donohoe, G.G., O'Kennedy, R.: Sialic acids: carbohydrate moieties that influence the biological and physical properties of biopharmaceutical proteins and living cells. Drug Discov. Today. **12**(7–8), 319–326 (2007)
12. Kah, J.C., Wong, K.Y., Neoh, K.G., Song, J.H., Fu, J.W., Mhaisalkar, S., et al.: Critical parameters in the pegylation of gold nanoshells for biomedical applications: an in vitro macrophage study. J. Drug Target. **17**(3), 181–193 (2009)
13. Lin, S.Y., Hsu, W.H., Lo, J.M., Tsai, H.C., Hsiue, G.H.: Novel geometry type of nanocarriers mitigated the phagocytosis for drug delivery. J. Control. Release **154**(1), 84–92 (2011)
14. Janeway Jr., C.A., Medzhitov, R.: Innate immune recognition. Annu. Rev. Immunol. **20**, 197–216 (2002)
15. Steinman, R.M., Banchereau, J.: Taking dendritic cells into medicine. Nature **449**(7161), 419–426 (2007)
16. Janeway, C.A.: How the immune system works to protect the host from infection: a personal view. Proc. Natl. Acad. Sci. U.S.A. **98**(13), 7461–7468 (2001)
17. Dranoff, G.: Cytokines in cancer pathogenesis and cancer therapy. Nat. Rev. Cancer **4**(1), 11–22 (2004)
18. Zinkernagel, R.M.: On natural and artificial vaccinations. Annu. Rev. Immunol. **21**, 515–546 (2003)
19. Jenne, C.N., Liao, S., Singh, B.: Neutrophils: multitasking first responders of immunity and tissue homeostasis. Cell Tissue Res. (2018)
20. Mayadas, T.N., Cullere, X., Lowell, C.A.: The multifaceted functions of neutrophils. Annu. Rev. Pathol. **9**, 181–218 (2014)
21. Lin, A., Lore, K.: Granulocytes: new members of the antigen-presenting cell family. Front. Immunol. **8**, 1781 (2017)
22. Siracusa, M.C., Kim, B.S., Spergel, J.M., Artis, D.: Basophils and allergic inflammation. J. Allergy Clin. Immunol. **132**(4), 789–801; quiz 788 (2013)
23. Guilliams, M., Ginhoux, F., Jakubzick, C., Naik, S.H., Onai, N., Schraml, B.U., et al.: Dendritic cells, monocytes and macrophages: a unified nomenclature based on ontogeny. Nat. Rev. Immunol. **14**(8), 571–578 (2014)
24. Geissmann, F., Manz, M.G., Jung, S., Sieweke, M.H., Merad, M., Ley, K.: Development of monocytes, macrophages, and dendritic cells. Science **327**(5966), 656–661 (2010)
25. Mosser, D.M., Edwards, J.P.: Exploring the full spectrum of macrophage activation. Nat. Rev. Immunol. **8**(12), 958–969 (2008)
26. Verreck, F.A., de Boer, T., Langenberg, D.M., Hoeve, M.A., Kramer, M., Vaisberg, E., et al.: Human IL-23-producing type 1 macrophages promote but IL-10-producing type 2 macrophages subvert immunity to (myco)bacteria. Proc. Natl. Acad. Sci. U.S.A. **101**(13), 4560–4565 (2004)

27. Murray, P.J., Allen, J.E., Biswas, S.K., Fisher, E.A., Gilroy, D.W., Goerdt, S., et al.: Macrophage activation and polarization: nomenclature and experimental guidelines. Immunity **41**(1), 14–20 (2014)
28. Murray, P.J., Wynn, T.A.: Protective and pathogenic functions of macrophage subsets. Nat. Rev. Immunol. **11**(11), 723–737 (2011)
29. Buckwalter, M.R., Albert, M.L.: Orchestration of the immune response by dendritic cells. Curr. Biol. **19**(9), R355–R361 (2009)
30. Villadangos, J.A., Schnorrer, P.: Intrinsic and cooperative antigen-presenting functions of dendritic-cell subsets in vivo. Nat. Rev. Immunol. **7**(7), 543–555 (2007)
31. Heath, W.R., Belz, G.T., Behrens, G.M., Smith, C.M., Forehan, S.P., Parish, I.A., et al.: Cross-presentation, dendritic cell subsets, and the generation of immunity to cellular antigens. Immunol. Rev. **199**, 9–26 (2004)
32. Niess, J.H., Brand, S., Gu, X., Landsman, L., Jung, S., McCormick, B.A., et al.: CX3CR1-mediated dendritic cell access to the intestinal lumen and bacterial clearance. Science **307**(5707), 254–258 (2005)
33. Cyster, J.G.: Chemokines and the homing of dendritic cells to the T cell areas of lymphoid organs. J. Exp. Med. **189**(3), 447–450 (1999)
34. Itano, A.A., Jenkins, M.K.: Antigen presentation to naive CD4 T cells in the lymph node. Nat. Immunol. **4**(8), 733–739 (2003)
35. Randolph, G.J., Angeli, V., Swartz, M.A.: Dendritic-cell trafficking to lymph nodes through lymphatic vessels. Nat. Rev. Immunol. **5**(8), 617–628 (2005)
36. Gordon, J.R., Ma, Y., Churchman, L., Gordon, S.A., Dawicki, W.: Regulatory dendritic cells for immunotherapy in immunologic diseases. Front. Immunol. **5**, 7 (2014)
37. Kaisho, T., Akira, S.: Regulation of dendritic cell function through Toll-like receptors. Curr. Mol. Med. **3**(4), 373–385 (2003)
38. Krieg, A.M.: CpG motifs in bacterial DNA and their immune effects. Annu. Rev. Immunol. **20**, 709–760 (2002)
39. Verthelyi, D., Zeuner, R.A.: Differential signaling by CpG DNA in DCs and B cells: not just TLR9. Trends Immunol. **24**(10), 519–522 (2003)
40. Manzotti, C.N., Liu, M.K., Burke, F., Dussably, L., Zheng, Y., Sansom, D.M.: Integration of CD28 and CTLA-4 function results in differential responses of T cells to CD80 and CD86. Eur. J. Immunol. **36**(6), 1413–1422 (2006)
41. Odobasic, D., Kitching, A.R., Tipping, P.G., Holdsworth, S.R.: CD80 and CD86 costimulatory molecules regulate crescentic glomerulonephritis by different mechanisms. Kidney Int. **68**(2), 584–594 (2005)
42. Lenschow, D.J., Ho, S.C., Sattar, H., Rhee, L., Gray, G., Nabavi, N., et al.: Differential effects of anti-B7-1 and anti-B7-2 monoclonal antibody treatment on the development of diabetes in the nonobese diabetic mouse. J. Exp. Med. **181**(3), 1145–1155 (1995)
43. Xiang, J., Gu, X., Qian, S., Chen, Z.: Graded function of CD80 and CD86 in initiation of T-cell immune response and cardiac allograft survival. Transpl. Int. **21**(2), 163–168 (2008)
44. Probst, H.C., McCoy, K., Okazaki, T., Honjo, T., van den Broek, M.: Resting dendritic cells induce peripheral CD8 + T cell tolerance through PD-1 and CTLA-4. Nat. Immunol. **6**(3), 280–286 (2005)
45. Hawiger, D., Inaba, K., Dorsett, Y., Guo, M., Mahnke, K., Rivera, M., et al.: Dendritic cells induce peripheral T cell unresponsiveness under steady state conditions in vivo. J. Exp. Med. **194**(6), 769–779 (2001)
46. Luo, X., Tarbell, K.V., Yang, H., Pothoven, K., Bailey, S.L., Ding, R., et al.: Dendritic cells with TGF-beta1 differentiate naive $CD4^+$ $CD25^-$ T cells into islet-protective $Foxp3^+$ regulatory T cells. Proc Natl Acad Sci U S A. **104**(8), 2821–2826 (2007)
47. Pulendran, B., Smith, J.L., Caspary, G., Brasel, K., Pettit, D., Maraskovsky, E., et al.: Distinct dendritic cell subsets differentially regulate the class of immune response in vivo. Proc. Natl. Acad. Sci. U.S.A. **96**(3), 1036–1041 (1999)
48. Maldonado-Lopez, R., De Smedt, T., Michel, P., Godfroid, J., Pajak, B., Heirman, C., et al.: CD8 alpha(+) and CD8 alpha(−) subclasses of dendritic cells direct the development of distinct T helper cells in vivo. J. Exp. Med. **189**(3), 587–592 (1999)

49. Napolitani, G., Rinaldi, A., Bertoni, F., Sallusto, F., Lanzavecchia, A.: Selected Toll-like receptor agonist combinations synergistically trigger a T helper type 1-polarizing program in dendritic cells. Nat. Immunol. **6**(8), 769–776 (2005)
50. Seder, R.A., Paul, W.E., Davis, M.M., Fazekas de St Groth, B.: The presence of interleukin 4 during in vitro priming determines the lymphokine-producing potential of $CD4^+$ T cells from T cell receptor transgenic mice. J. Exp. Med. **176**(4), 1091–1098 (1992)
51. LeibundGut-Landmann, S., Gross, O., Robinson, M.J., Osorio, F., Slack, E.C., Tsoni, S.V., et al.: Syk- and CARD9-dependent coupling of innate immunity to the induction of T helper cells that produce interleukin 17. Nat. Immunol. **8**(6), 630–638 (2007)
52. Jonuleit, H., Schmitt, E., Schuler, G., Knop, J., Enk, A.H.: Induction of interleukin 10-producing, nonproliferating CD4(+) T cells with regulatory properties by repetitive stimulation with allogeneic immature human dendritic cells. J. Exp. Med. **192**(9), 1213–1222 (2000)
53. Badovinac, V.P., Messingham, K.A.N., Jabbari, A., Haring, J.S., Harty, J.T.: Accelerated CD8(+) T-cell memory and prime-boost response after dendritic-cell vaccination. Nat. Med. **11**(7), 748–756 (2005)
54. Trumpfheller, C., Finke, J.S., Lopez, C.B., Moran, T.M., Moltedo, B., Soares, H., et al.: Intensified and protective $CD4^+$ T cell immunity in mice with anti-dendritic cell HIV gag fusion antibody vaccine. J. Exp. Med. **203**(3), 607–617 (2006)
55. Amer, M.G., Mazen, N.F., Mohamed, A.M.: Caffeine intake decreases oxidative stress and inflammatory biomarkers in experimental liver diseases induced by thioacetamide: biochemical and histological study. Int. J. Immunopathol. Pharmacol. **30**(1), 13–24 (2017)
56. Lunin, S.M., Khrenov, M.O., Glushkova, O.V., Vinogradova, E.V., Yashin, V.A., Fesenko, E.E., et al.: Extrathymic production of thymulin induced by oxidative stress, heat shock, apoptosis, or necrosis. Int. J. Immunopathol. Pharmacol. **30**(1), 58–69 (2017)
57. Fleshner, M., Crane, C.R.: Exosomes, DAMPs and miRNA: features of stress physiology and immune homeostasis. Trends Immunol. **38**(10), 768–776 (2017)
58. Fleshner, M.: Stress-evoked sterile inflammation, danger associated molecular patterns (DAMPs), microbial associated molecular patterns (MAMPs) and the inflammasome. Brain Behav. Immun. **27**, 1–7 (2013)
59. Rock, K.L., Latz, E., Ontiveros, F., Kono, H.: The sterile inflammatory response. Annu. Rev. Immunol. **28**, 321–342 (2010)
60. Fleshner, M., Nguyen, K.T., Cotter, C.S., Watkins, L.R., Maier, S.F.: Acute stressor exposure both suppresses acquired immunity and potentiates innate immunity. Am. J. Physiol. **275**(3 Pt 2), R870–R878 (1998)
61. Campisi, J., Fleshner, M.: Role of extracellular HSP72 in acute stress-induced potentiation of innate immunity in active rats. J. Appl. Physiol. (1985) **94**(1):43–52 (2003)
62. Maslanik, T., Mahaffey, L., Tannura, K., Beninson, L., Greenwood, B.N., Fleshner, M.: The inflammasome and danger associated molecular patterns (DAMPs) are implicated in cytokine and chemokine responses following stressor exposure. Brain Behav. Immun. **28**, 54–62 (2013)
63. Beninson, L.A., Brown, P.N., Loughridge, A.B., Saludes, J.P., Maslanik, T., Hills, A.K., et al.: Acute stressor exposure modifies plasma exosome-associated heat shock protein 72 (Hsp72) and microRNA (miR-142-5p and miR-203). PLoS ONE **9**(9), e108748 (2014)
64. Rock, K.L., Lai, J.J., Kono, H.: Innate and adaptive immune responses to cell death. Immunol. Rev. **243**(1), 191–205 (2011)
65. Chen, G.Y., Nunez, G.: Sterile inflammation: sensing and reacting to damage. Nat. Rev. Immunol. **10**(12), 826–837 (2010)
66. Hernandez, C., Huebener, P., Schwabe, R.F.: Damage-associated molecular patterns in cancer: a double-edged sword. Oncogene **35**(46), 5931–5941 (2016)
67. Gallo, P.M., Gallucci, S.: The dendritic cell response to classic, emerging, and homeostatic danger signals. Implications for autoimmunity. Front Immunol. **4**, 138 (2013)
68. Dwivedi, P.D., Misra, A., Shanker, R., Das, M.: Are nanomaterials a threat to the immune system? Nanotoxicology **3**(1), 19–26 (2009)

69. Dobrovolskaia, M.A., McNeil, S.E.: Immunological properties of engineered nanomaterials. Nat. Nanotechnol. **2**(8), 469–478 (2007)
70. Thiele, L., Rothen-Rutishauser, B., Jilek, S., Wunderli-Allenspach, H., Merkle, H.P., Walter, E.: Evaluation of particle uptake in human blood monocyte-derived cells in vitro. Does phagocytosis activity of dendritic cells measure up with macrophages? J. Control. Release **76**(1–2), 59–71 (2001)
71. Foged, C., Brodin, B., Frokjaer, S., Sundblad, A.: Particle size and surface charge affect particle uptake by human dendritic cells in an in vitro model. Int. J. Pharm. **298**(2), 315–322 (2005)
72. Thiele, L., Merkle, H.P., Walter, E.: Phagocytosis and phagosomal fate of surface-modified microparticles in dendritic cells and macrophages. Pharm. Res. **20**(2), 221–228 (2003)
73. Thiele, L., Diederichs, J.E., Reszka, R., Merkle, H.P., Walter, E.: Competitive adsorption of serum proteins at microparticles affects phagocytosis by dendritic cells. Biomaterials **24**(8), 1409–1418 (2003)
74. Muller, C., Schibli, R.: Prospects in folate receptor-targeted radionuclide therapy. Front Oncol. **3**, 249 (2013)
75. Yameen, B., Choi, W.I., Vilos, C., Swami, A., Shi, J.J., Farokhzad, O.C.: Insight into nanoparticle cellular uptake and intracellular targeting. J. Control. Release **190**, 485–499 (2014)
76. Low, P.S., Kularatne, S.A.: Folate-targeted therapeutic and imaging agents for cancer. Curr. Opin. Chem. Biol. **13**(3), 256–262 (2009)
77. Xia, W., Hilgenbrink, A.R., Matteson, E.L., Lockwood, M.B., Cheng, J.X., Low, P.S.: A functional folate receptor is induced during macrophage activation and can be used to target drugs to activated macrophages. Blood **113**(2), 438–446 (2009)
78. Ross, J.F., Wang, H., Behm, F.G., Mathew, P., Wu, M., Booth, R., et al.: Folate receptor type beta is a neutrophilic lineage marker and is differentially expressed in myeloid leukemia. Cancer **85**(2), 348–357 (1999)
79. Low, P.S., Henne, W.A., Doorneweerd, D.D.: Discovery and development of folic-acid-based receptor targeting for imaging and therapy of cancer and inflammatory diseases. Acc. Chem. Res. **41**(1), 120–129 (2008)
80. Lu, Y., Sega, E., Leamon, C.P., Low, P.S.: Folate receptor-targeted immunotherapy of cancer: mechanism and therapeutic potential. Adv. Drug Deliv. Rev. **56**(8), 1161–1176 (2004)
81. Danhier, F., Feron, O., Preat, V.: To exploit the tumor microenvironment: Passive and active tumor targeting of nanocarriers for anti-cancer drug delivery. J. Control. Release. **148**(2), 135–146 (2010)
82. van der Meel, R., Vehmeijer, L.J., Kok, R.J., Storm, G., van Gaal, E.V.: Ligand-targeted particulate nanomedicines undergoing clinical evaluation: current status. Adv. Drug Deliv. Rev. **65**(10), 1284–1298 (2013)
83. Lurje, G., Lenz, H.J.: EGFR signaling and drug discovery. Oncology **77**(6), 400–410 (2009)
84. Xia, T., Kovochich, M., Liong, M., Zink, J.I., Nel, A.E.: Cationic polystyrene nanosphere toxicity depends on cell-specific endocytic and mitochondrial injury pathways. ACS Nano **2**(1), 85–96 (2008)
85. Loos, C., Syrovets, T., Musyanovych, A., Mailander, V., Landfester, K., Nienhaus, G.U., et al.: Functionalized polystyrene nanoparticles as a platform for studying bio-nano interactions. Beilstein J. Nanotechnol. **5**, 2403–2412 (2014)
86. Sohaebuddin, S.K., Thevenot, P.T., Baker, D., Eaton, J.W., Tang, L.: Nanomaterial cytotoxicity is composition, size, and cell type dependent. Part Fibre Toxicol. **7**, 22 (2010)
87. Lanone, S., Rogerieux, F., Geys, J., Dupont, A., Maillot-Marechal, E., Boczkowski, J., et al.: Comparative toxicity of 24 manufactured nanoparticles in human alveolar epithelial and macrophage cell lines. Part Fibre Toxicol. **6**, 14 (2009)
88. Loh, M.L.: Recent advances in the pathogenesis and treatment of juvenile myelomonocytic leukaemia. Br. J. Haematol. **152**(6), 677–687 (2011)
89. Kohro, T., Tanaka, T., Murakami, T., Wada, Y., Aburatani, H., Hamakubo, T., et al.: A comparison of differences in the gene expression profiles of phorbol 12-myristate 13-acetate differentiated THP-1 cells and human monocyte-derived macrophage. J. Atheroscler. Thromb. **11**(2), 88–97 (2004)

90. Park, E.K., Jung, H.S., Yang, H.I., Yoo, M.C., Kim, C., Kim, K.S.: Optimized THP-1 differentiation is required for the detection of responses to weak stimuli. Inflamm. Res. **56**(1), 45–50 (2007)
91. Schottler, S., Becker, G., Winzen, S., Steinbach, T., Mohr, K., Landfester, K., et al.: Protein adsorption is required for stealth effect of poly(ethylene glycol)- and poly(phosphoester)-coated nanocarriers. Nat. Nanotechnol. **11**(4), 372–377 (2016)
92. Schottler, S., Klein, K., Landfester, K., Mailander, V.: Protein source and choice of anticoagulant decisively affect nanoparticle protein corona and cellular uptake. Nanoscale **8**(10), 5526–5536 (2016)
93. Gillis, S., Watson, J.: Biochemical and biological characterization of lymphocyte regulatory molecules. V. Identification of an interleukin 2-producing human leukemia T cell line. J. Exp. Med. **152**(6), 1709–1719 (1980)
94. Abraham, R.T., Weiss, A.: Jurkat T cells and development of the T-cell receptor signalling paradigm. Nat. Rev. Immunol. **4**(4), 301–308 (2004)
95. Astoul, E., Edmunds, C., Cantrell, D.A., Ward, S.G.: PI 3-K and T-cell activation: limitations of T-leukemic cell lines as signaling models. Trends Immunol. **22**(9), 490–496 (2001)
96. Shan, X., Czar, M.J., Bunnell, S.C., Liu, P., Liu, Y., Schwartzberg, P.L., et al.: Deficiency of PTEN in Jurkat T cells causes constitutive localization of Itk to the plasma membrane and hyperresponsiveness to CD3 stimulation. Mol. Cell. Biol. **20**(18), 6945–6957 (2000)
97. Wang, X., Gjorloff-Wingren, A., Saxena, M., Pathan, N., Reed, J.C., Mustelin, T.: The tumor suppressor PTEN regulates T cell survival and antigen receptor signaling by acting as a phosphatidylinositol 3-phosphatase. J. Immunol. **164**(4), 1934–1939 (2000)
98. Seminario, M.C., Wange, R.L.: Signaling pathways of D3-phosphoinositide-binding kinases in T cells and their regulation by PTEN. Semin. Immunol. **14**(1), 27–36 (2002)
99. Mohr, K., Sommer, M., Baier, G., Schöttler, S., Okwieka, P., Tenzer, S., et al.: Aggregation behavior of polystyrene-nanoparticles in human blood serum and its impact on the in vivo distribution in mice. J. Nanomed. Nanotech. **5**, 193 (2014)
100. Schmid, D., Park, C.G., Hartl, C.A., Subedi, N., Cartwright, A.N., Puerto, R.B., et al.: T cell-targeting nanoparticles focus delivery of immunotherapy to improve antitumor immunity. Nat. Commun. **8**(1), 1747 (2017)
101. Gros, A., Robbins, P.F., Yao, X., Li, Y.F., Turcotte, S., Tran, E., et al.: PD-1 identifies the patient-specific CD8(+) tumor-reactive repertoire infiltrating human tumors. J. Clin. Invest. **124**(5), 2246–2259 (2014)
102. Gros, A., Parkhurst, M.R., Tran, E., Pasetto, A., Robbins, P.F., Ilyas, S., et al.: Prospective identification of neoantigen-specific lymphocytes in the peripheral blood of melanoma patients. Nat. Med. **22**(4), 433–438 (2016)
103. Zolnik, B.S., Gonzalez-Fernandez, A., Sadrieh, N., Dobrovolskaia, M.A.: Nanoparticles and the immune system. Endocrinology **151**(2), 458–465 (2010)
104. Muller, L.K., Simon, J., Schottler, S., Landfester, K., Mailander, V., Mohr, K.: Pre-coating with protein fractions inhibits nano-carrier aggregation in human blood plasma. RSC Adv. **6**(99), 96495–96509 (2016)
105. Ahmed, T.A., Aljaeid, B.M.: Preparation, characterization, and potential application of chitosan, chitosan derivatives, and chitosan metal nanoparticles in pharmaceutical drug delivery. Drug Des. Dev. Ther. **10**, 483–507 (2016)
106. Owens, D.E., Peppas, N.A.: Opsonization, biodistribution, and pharmacokinetics of polymeric nanoparticles. Int. J. Pharm. **307**(1), 93–102 (2006)
107. Andersson, L.I., Hellman, P., Eriksson, H.: Receptor-mediated endocytosis of particles by peripheral dendritic cells. Hum. Immunol. **69**(10), 625–633 (2008)
108. Tabata, Y., Ikada, Y.: Macrophage phagocytosis of biodegradable microspheres composed of L-lactic acid/glycolic acid homo- and copolymers. J. Biomed. Mater. Res. **22**(10), 837–858 (1988)
109. Guo, S.T., Huang, L.: Nanoparticles escaping RES and endosome: challenges for siRNA delivery for cancer therapy. J. Nanomater. (2011)

110. Wei, W., Ma, G.H., Wang, L.Y., Wu, J., Su, Z.G.: Hollow quaternized chitosan microspheres increase the therapeutic effect of orally administered insulin. Acta Biomater. **6**(1), 205–209 (2010)
111. Nagamoto, T., Hattori, Y., Takayama, K., Maitani, Y.: Novel chitosan particles and chitosan-coated emulsions inducing immune response via intranasal vaccine delivery. Pharm. Res. **21**(4), 671–674 (2004)
112. Jiang, H.L., Kang, M.L., Quan, J.S., Kang, S.G., Akaike, T., Yoo, H.S., et al.: The potential of mannosylated chitosan microspheres to target macrophage mannose receptors in an adjuvant-delivery system for intranasal immunization. Biomaterials **29**(12), 1931–1939 (2008)
113. Kang, M.L., Jiang, H.L., Kang, S.G., Guo, D.D., Lee, D.Y., Cho, C.S., et al.: Pluronic F127 enhances the effect as an adjuvant of chitosan microspheres in the intranasal delivery of Bordetella bronchiseptica antigens containing dermonecrotoxin. Vaccine **25**(23), 4602–4610 (2007)
114. Ferin, J., Oberdorster, G., Soderholm, S.C., Gelein, R.: Pulmonary tissue access of ultrafine particles. J. Aerosol. Med. **4**(1), 57–68 (1991)
115. Huang, Y.C., Vieira, A., Huang, K.L., Yeh, M.K., Chiang, C.H.: Pulmonary inflammation caused by chitosan microparticles. J. Biomed. Mater. Res. A **75**(2), 283–287 (2005)
116. Donaldson, K., Poland, C.A., Schins, R.P.: Possible genotoxic mechanisms of nanoparticles: criteria for improved test strategies. Nanotoxicology **4**, 414–420 (2010)
117. Przybytkowski, E., Behrendt, M., Dubois, D., Maysinger, D.: Nanoparticles can induce changes in the intracellular metabolism of lipids without compromising cellular viability. FEBS J. **276**(21), 6204–6217 (2009)
118. Saptarshi, S.R., Feltis, B.N., Wright, P.F.A., Lopata, A.L.: Investigating the immunomodulatory nature of zinc oxide nanoparticles at sub-cytotoxic levels in vitro and after intranasal instillation in vivo. J. Nanobiotechnol. **13** (2015)
119. Kawata, K., Osawa, M., Okabe, S.: In vitro toxicity of silver nanoparticles at noncytotoxic doses to HepG2 human hepatoma cells. Environ. Sci. Technol. **43**(15), 6046–6051 (2009)
120. Dworak, N., Wnuk, M., Zebrowski, J., Bartosz, G., Lewinska, A.: Genotoxic and mutagenic activity of diamond nanoparticles in human peripheral lymphocytes in vitro. Carbon **68**, 763–776 (2014)
121. Smith, M.J., Brown, J.M., Zamboni, W.C., Walker, N.J.: From immunotoxicity to nanotherapy: the effects of nanomaterials on the immune system. Toxicol. Sci. **138**(2), 249–255 (2014)
122. Baumann, D., Hofmann, D., Nullmeier, S., Panther, P., Dietze, C., Musyanovych, A., et al.: Complex encounters: nanoparticles in whole blood and their uptake into different types of white blood cells. Nanomedicine (Lond.) **8**(5), 699–713 (2013)
123. Lunov, O., Syrovets, T., Loos, C., Beil, J., Delacher, M., Tron, K., et al.: Differential uptake of functionalized polystyrene nanoparticles by human macrophages and a monocytic cell line. ACS Nano **5**(3), 1657–1669 (2011)
124. Clift, M.J., Gehr, P., Rothen-Rutishauser, B.: Nanotoxicology: a perspective and discussion of whether or not in vitro testing is a valid alternative. Arch. Toxicol. **85**(7), 723–731 (2011)
125. Tonigold, M., Mailander, V.: Endocytosis and intracellular processing of nanoparticles in dendritic cells: routes to effective immunonanomedicines. Nanomedicine (Lond.) **11**(20), 2625–2630 (2016)
126. Harush-Frenkel, O., Debotton, N., Benita, S., Altschuler, Y.: Targeting of nanoparticles to the clathrin-mediated endocytic pathway. Biochem. Biophys. Res. Commun. **353**(1), 26–32 (2007)
127. Vasir, J.K., Labhasetwar, V.: Quantification of the force of nanoparticle-cell membrane interactions and its influence on intracellular trafficking of nanoparticles. Biomaterials **29**(31), 4244–4252 (2008)
128. Garaiova, Z., Strand, S.P., Reitan, N.K., Lelu, S., Storset, S.O., Berg, K., et al.: Cellular uptake of DNA-chitosan nanoparticles: the role of clathrin- and caveolae-mediated pathways. Int. J. Biol. Macromol. **51**(5), 1043–1051 (2012)
129. Parton, R.G., Simons, K.: The multiple faces of caveolae. Nat. Rev. Mol. Cell Biol. **8**(3), 185–194 (2007)

130. Sahay, G., Alakhova, D.Y., Kabanov, A.V.: Endocytosis of nanomedicines. J. Control. Release. **145**(3), 182–195 (2010)
131. Liu, Y., Huang, R., Han, L., Ke, W., Shao, K., Ye, L., et al.: Brain-targeting gene delivery and cellular internalization mechanisms for modified rabies virus glycoprotein RVG29 nanoparticles. Biomaterials **30**(25), 4195–4202 (2009)
132. Falcone, S., Cocucci, E., Podini, P., Kirchhausen, T., Clementi, E., Meldolesi, J.: Macropinocytosis: regulated coordination of endocytic and exocytic membrane traffic events. J. Cell Sci. **119**(Pt 22), 4758–4769 (2006)
133. Mercer, J., Helenius, A.: Virus entry by macropinocytosis. Nat. Cell Biol. **11**(5), 510–520 (2009)
134. Kolb-Maurer, A., Wilhelm, M., Weissinger, F., Brocker, E.B., Goebel, W.: Interaction of human hematopoietic stem cells with bacterial pathogens. Blood **100**(10), 3703–3709 (2002)
135. Fiorentini, C., Falzano, L., Fabbri, A., Stringaro, A., Logozzi, M., Travaglione, S., et al.: Activation of rho GTPases by cytotoxic necrotizing factor 1 induces macropinocytosis and scavenging activity in epithelial cells. Mol. Biol. Cell **12**(7), 2061–2073 (2001)
136. Steinman, R.M., Swanson, J.: The endocytic activity of dendritic cells. J. Exp. Med. **182**(2), 283–288 (1995)
137. Sallusto, F., Cella, M., Danieli, C., Lanzavecchia, A.: Dendritic cells use macropinocytosis and the mannose receptor to concentrate macromolecules in the major histocompatibility complex class II compartment: downregulation by cytokines and bacterial products. J. Exp. Med. **182**(2), 389–400 (1995)
138. Zhang, L., Zhang, S., Ruan, S.B., Zhang, Q.Y., He, Q., Gao, H.L.: Lapatinib-incorporated lipoprotein-like nanoparticles: preparation and a proposed breast cancer-targeting mechanism. Acta Pharmacol. Sin. **35**(6), 846–852 (2014)
139. Gupta, A.K., Gupta, M.: Cytotoxicity suppression and cellular uptake enhancement of surface modified magnetic nanoparticles. Biomaterials **26**(13), 1565–1573 (2005)
140. Zhang, J., Chen, X.G., Huang, L., Han, J.T., Zhang, X.F.: Self-assembled polymeric nanoparticles based on oleic acid-grafted chitosan oligosaccharide: biocompatibility, protein adsorption and cellular uptake. J. Mater. Sci. Mater. Med. **23**(7), 1775–1783 (2012)
141. Wadhwa, S., Rea, C., O'Hare, P., Mathur, A., Roy, S.S., Dunlop, P.S., et al.: Comparative in vitro cytotoxicity study of carbon nanotubes and titania nanostructures on human lung epithelial cells. J. Hazard. Mater. **191**(1–3), 56–61 (2011)
142. Panariti, A., Miserocchi, G., Rivolta, I.: The effect of nanoparticle uptake on cellular behavior: disrupting or enabling functions? Nanotechnol. Sci Appl. **5**, 87–100 (2012)
143. Ahamed, M.: Toxic response of nickel nanoparticles in human lung epithelial A549 cells. Toxicol. In Vitro **25**(4), 930–936 (2011)
144. Gourlay, C.W., Ayscough, K.R.: The actin cytoskeleton: a key regulator of apoptosis and ageing? Nat. Rev. Mol. Cell Biol. **6**(7), 583–589 (2005)
145. Buyukhatipoglu, K., Clyne, A.M.: Superparamagnetic iron oxide nanoparticles change endothelial cell morphology and mechanics via reactive oxygen species formation. J. Biomed. Mater. Res. A **96**(1), 186–195 (2011)
146. Scherbart, A.M., Langer, J., Bushmelev, A., van Berlo, D., Haberzettl, P., van Schooten, F.J., et al.: Contrasting macrophage activation by fine and ultrafine titanium dioxide particles is associated with different uptake mechanisms. Part Fibre Toxicol. **8**, 31 (2011)
147. Wang, H.J., Growcock, A.C., Tang, T.H., O'Hara, J., Huang, Y.W., Aronstam, R.S.: Zinc oxide nanoparticle disruption of store-operated calcium entry in a muscarinic receptor signaling pathway. Toxicol. In Vitro **24**(7), 1953–1961 (2010)
148. Horie, M., Nishio, K., Kato, H., Fujita, K., Endoh, S., Nakamura, A., et al.: Cellular responses induced by cerium oxide nanoparticles: induction of intracellular calcium level and oxidative stress on culture cells. J. Biochem. **150**(4), 461–471 (2011)
149. McCarthy, J., Gong, X., Nahirney, D., Duszyk, M., Radomski, M.: Polystyrene nanoparticles activate ion transport in human airway epithelial cells. Int. J. Nanomed. **6**, 1343–1356 (2011)
150. Garrett, W.S., Chen, L.M., Kroschewski, R., Ebersold, M., Turley, S., Trombetta, S., et al.: Developmental control of endocytosis in dendritic cells by Cdc42. Cell **102**(3), 325–334 (2000)

151. Zhang, L.W., Baumer, W., Monteiro-Riviere, N.A.: Cellular uptake mechanisms and toxicity of quantum dots in dendritic cells. Nanomedicine (Lond.) **6**(5), 777–791 (2011)
152. Le Roux, D., Le Bon, A., Dumas, A., Taleb, K., Sachse, M., Sikora, R., et al.: Antigen stored in dendritic cells after macropinocytosis is released unprocessed from late endosomes to target B cells. Blood **119**(1), 95–105 (2012)
153. Platt, C.D., Ma, J.K., Chalouni, C., Ebersold, M., Bou-Reslan, H., Carano, R.A., et al.: Mature dendritic cells use endocytic receptors to capture and present antigens. Proc. Natl. Acad. Sci. U.S.A. **107**(9), 4287–4292 (2010)
154. Rodriguez, A., Regnault, A., Kleijmeer, M., Ricciardi-Castagnoli, P., Amigorena, S.: Selective transport of internalized antigens to the cytosol for MHC class I presentation in dendritic cells. Nat. Cell Biol. **1**(6), 362–368 (1999)
155. Harding, C.V., Song, R.: Phagocytic processing of exogenous particulate antigens by macrophages for presentation by class I MHC molecules. J. Immunol. **153**(11), 4925–4933 (1994)
156. Joffre, O.P., Segura, E., Savina, A., Amigorena, S.: Cross-presentation by dendritic cells. Nat. Rev. Immunol. **12**(8), 557–569 (2012)
157. Guermonprez, P., Saveanu, L., Kleijmeer, M., Davoust, J., Van Endert, P., Amigorena, S.: ER-phagosome fusion defines an MHC class I cross-presentation compartment in dendritic cells. Nature **425**(6956), 397–402 (2003)
158. Silva, A.L., Rosalia, R.A., Varypataki, E., Sibuea, S., Ossendorp, F., Jiskoot, W.: Poly-(lactic-co-glycolic-acid)-based particulate vaccines: particle uptake by dendritic cells is a key parameter for immune activation. Vaccine **33**(7), 847–854 (2015)
159. Shen, H., Ackerman, A.L., Cody, V., Giodini, A., Hinson, E.R., Cresswell, P., et al.: Enhanced and prolonged cross-presentation following endosomal escape of exogenous antigens encapsulated in biodegradable nanoparticles. Immunology **117**(1), 78–88 (2006)
160. Sneh-Edri, H., Likhtenshtein, D., Stepensky, D.: Intracellular targeting of PLGA nanoparticles encapsulating antigenic peptide to the endoplasmic reticulum of dendritic cells and its effect on antigen cross-presentation in vitro. Mol. Pharm. **8**(4), 1266–1275 (2011)
161. Jiskoot, W., van Schie, R.M., Carstens, M.G., Schellekens, H.: Immunological risk of injectable drug delivery systems. Pharm. Res. **26**(6), 1303–1314 (2009)
162. Fuchs, A.K., Syrovets, T., Haas, K.A., Loos, C., Musyanovych, A., Mailander, V., et al.: Carboxyl- and amino-functionalized polystyrene nanoparticles differentially affect the polarization profile of M1 and M2 macrophage subsets. Biomaterials **85**, 78–87 (2016)
163. Andersen, A.J., Hashemi, S.H., Andresen, T.L., Hunter, A.C., Moghimi, S.M.: Complement: alive and kicking nanomedicines. J. Biomed. Nanotechnol. **5**(4), 364–372 (2009)

Chapter 12
Fate and Translocation of (Nano)Particulate Matter in the Gastrointestinal Tract

Andreas Frey, Katrin Ramaker, Niels Röckendorf, Barbara Wollenberg, Ingmar Lautenschläger, Gabriella Gébel, Artur Giemsa, Markus Heine, Denise Bargheer and Peter Nielsen

Abstract Nanoscience has flourished with increasing use of nanoparticles in many products. The particles enter the environment and affect both biotic and abiotic components of the ecosystem. Via the water supply and the food chain, humans could be affected by ingesting those particles. In this chapter, we will discuss mechanisms by which nanoparticles or their constituents can be translocated from the gastrointestinal tract, what their fate may be and how relevant this is for human health.

12.1 Introduction

In the usual sense, the term "nanoparticle" stands for manufactured or engineered nanoparticulate matter. Several thousand tons of engineered nanoparticles per year are produced worldwide [1]. Many different classes of nanoparticles are designed that offer tuneable properties to cover many applications in materials science, electronics, dyes, pigments and paint technology, catalysis, antibiotics, as well as in nanomedicine and many others [2] (Fig. 12.1).

What is less well known is the fact that nature itself is a skilled nanotechnologist and naturally formed nanoparticles occur in volcanic ash clouds, wood soot, spring

A. Frey (✉) · K. Ramaker · N. Röckendorf
Division of Mucosal Immunology and Diagnostics, Research Center Borstel, Parkallee 1-40, 23845 Borstel, Germany
e-mail: afrey@fz-borstel.de

B. Wollenberg
Department of Ear, Nose and Throat, University Hospital Schleswig-Holstein, Ratzeburger Allee 160, 23538 Lübeck, Germany

I. Lautenschläger
Clinic for Anesthesiology and Operative Intensive Care Medicine, University Hospital Schleswig-Holstein, Arnold-Heller-Strasse 3, 24105 Kiel, Germany

G. Gébel · A. Giemsa · M. Heine · D. Bargheer · P. Nielsen
Institute of Biochemisty and Molecular Cell Biology, University Medical Center Eppendorf, Martinistrasse 52, 20246 Hamburg, Germany
e-mail: nielsen@uke.de

P. Gehr and R. Zellner (eds.), *Biological Responses to Nanoscale Particles*, NanoScience and Technology, https://doi.org/10.1007/978-3-030-12461-8_12

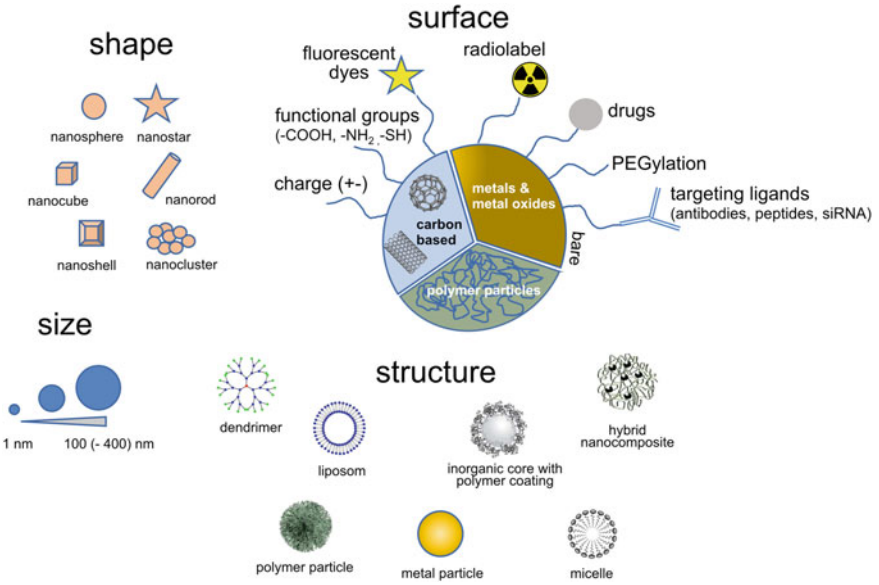

Fig. 12.1 Different classes of engineered nanoparticles. Many properties such as size, shape, surface charge, surface coating can be designed in synthesis what determines their specific physiochemical properties and may strongly influence their translocation and fate in the gastrointestinal tract when ingested

water, fine sand, and in biological materials as well [3]. These natural nanomaterials exist since millions of years on Earth.

Nanoparticles can be swallowed directly via food, beverages and drugs. Ingestion can also result from hand to mouth contact in the workplace [4], as well as from airway secretions which are contaminated with particles that have been cleared from the respiratory tract by the mucociliary escalator [5]. A new approach in nanotechnology is the field of nano-food [6, 7]. This includes the use of nanotechnology in packaging materials, farming practices, food processing, and also in the foods themselves.

Thus, nanoparticles are already in the food chain and may ever have been. The questions are: what happens to them in the gastrointestinal tract, and is there a significant health risk from ingested nanoparticles?

The uptake of particles in the gastrointestinal tract was first described by the German physiologist Gustav Herbst in 1844 when he found ingested starch bodies in the sub-millimeter range showing up in the circulation [8]. The finding was confirmed by others, forgotten, rediscovered in 1906 [9] and confirmed again [10] but always remained subject of critical debate [11].

Decades before the onset of nanotechnology, in the second half of the twentieth century, another round of studies begun, this time with better defined particulate chemical matter (asbestos, resin particles, latex particles) [12–15] but the controversy persisted. Again incorporation was detected, but the rates of uptake that were

reported varied significantly. Main reason for these conflicting results seems to be the methodology with which particle uptake was detected [16]. Bulk tissue analyses were performed often without discriminating between taken up and adherent particulate matter [17] which was later found to have a tremendous impact on detection rates [18]. Histological analyses may overcome this problem to some extent but are not quantitative [16] and one runs the risk of smearing luminal particles across the sectioned tissue during workup (own observation). Although the initial finding concerning the sub-millimeter starch particles was rejected, there was consent at that point in time that particles in the micrometer range can readily be taken up by the gastrointestinal mucosa and carried onwards within the body.

However, again it must be stated that this picture becomes less clear today, even when we apply present-day highly advanced methodology for detecting and quantifying translocation of even smaller particles into the body [19]. The reasons for this are (i) the diverse character and the limited colloidal stability of the ingested nanoparticles, (ii) the problem that the gastrointestinal tract is a site of very complex processes where even symbiotic interactions between host cells and the resident microbiome must be taken into account, (iii) the fact that the majority of literature addressing biological effects of nanoparticles in human-relevant systems concerns isolated cell systems or lung biology and less in vivo studies of processes in the gastrointestinal tract.

In the following sections we will look into detail into the anatomy and physiology of the gut, into reactions that modify or degrade nanoparticles after ingestion, into the types and features of nanoparticles that should predispose for interaction, into model systems to investigate those interactions, into the medical exploitation of nanoparticles in the alimentary tract and into the ultimate fate and the risk ingested nanoparticles may pose.

12.2 Architecture of the Gastrointestinal Tract

As part of the terrestrial ecosystem humans are in constant physical and chemical interaction with their environment. Per day an adult human being breathes more than 10 m^3 air thereby resorbing about 500 l or 700 g of oxygen, ingests 1–3 l of water and consumes pounds of food of which about 300–500 g of nutrients actually are incorporated. In order to manage assimilation of such an extent in a timely manner the cellular interface where the actual transport events occur must cover a substantial surface area. In the airways, the site of gas exchange, the interface encompasses about 75 m^2, in the alimentary tract where water and solutes are taken up this area is approximately 35 m^2 [20]. The large mucosal surface area of the alimentary tract is not tailored evenly along the oro-rectal axis of the digestive system. At the site of food and water ingestion—oral cavity, oropharynx and oesophagus—the mucosal lining is plain and consists of multi-layered, partially keratinized squamous epithelia which provide a robust barrier against mechanical stress as it may be caused by movement of solid, undigested food constituents. The architecture of these epithelia

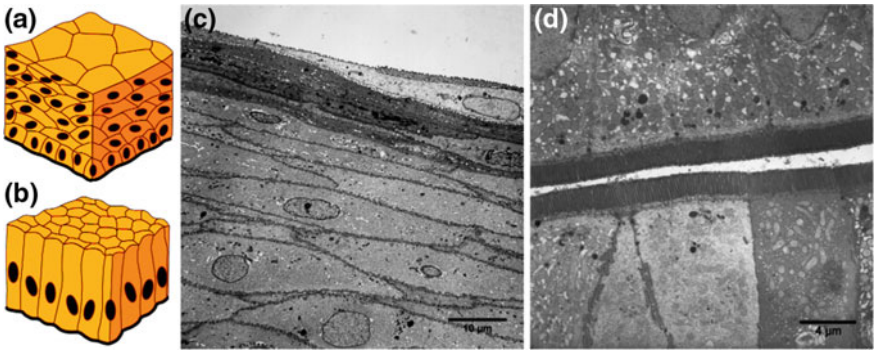

Fig. 12.2 Predominant cell types in the mucosal lining of the alimentary tract. Left: Schematic drawing of **a** stratified squamous epithelia lining the oral cavity, the oropharynx and the esophagus; **b** columnar epithelium lining the assimilation-active mucosae from the stomach downwards. Right: Electron micrographs of human tissue sections: **c** squamous epithelium of human tonsil, displaying the typical cell multilayer with masonry bond-type organization; **d** columnar epithelium of human small intestine (ileum) displaying tight cell-to-cell contacts. The images were acquired in the context of an extensive electron microscopic cell surface analysis study performed by some of the authors [24]

resembles that of a brick wall where the bricks are staggered such that each brick covers the gap beneath the rows above and below (Fig. 12.2a, c) [21]. In addition to this masonry bond some kind of "molecular grout" or "mortar" between cells exists which is hydrophobic in nature and seems to derive from membrane granules of the epithelia and which seals the gaps [21–23]. Although such an architecture is perfectly suited to withstand mechanical stress, it is inappropriate for translocation of nutrients and water. For that reason the mucosae follow a different concept to fit the needs of rapid substance exchange further down the alimentary tract. These are the sites where large amounts of digestive fluids have to be secreted and where nutrients and water have to be taken up. Thus, from the stomach downwards the mucosal lining no longer consists of stratified squamous epithelia but of columnar epithelia of various types whose hallmark is a monolayer of column-like cells that are sealed together by tight junctions or *zonulae occludens* (Fig. 12.2b, d).

Tight junctions are gasket-like ribbons of membrane proteins that are linked internally to the cellular cytoskeleton and externally to their protein counterparts in neighbouring cells, so tightly that even ions and water cannot pass through.

Although an elaborate tight stratum, the epithelium of the alimentary tract is not designed to endure over the entire life span of an individual. On the contrary, it renews rather rapidly. While the stratified squamous epithelia of the upper alimentary tract replenish themselves within about 3 weeks, the columnar epithelium of the lower gastrointestinal tract renews even faster, within less than a week [21]. In order to prevent the building of an unguarded portal of entry at the site of a dying cell, neighbouring vital columnar epithelial cells contact each other underneath a

moribund cell and form tight junctions before the cell cadaver is sloughed off into the lumen [25–28].

Tight junctions not only seal neighbouring cells together. Due to the fact that they surround the entire cell like a waistband they separate the upper membrane hemisphere from the lower one and do not allow membrane molecule diffusion from one hemisphere to the other. As a consequence of this so-called cell polarisation a structural specialization of the cell membrane in the "upper" and "lower" half and a vectorial organization of transport systems exists. With its lower/inner hemisphere the cell is anchored onto a fabric mesh of elastic extracellullar matrix proteins, the basal membrane. With its upper/outer hemisphere the cell communicates with luminal content. In order to provide more surface area for substance exchange, the luminal outer membrane of each cell is stretched over a dense array of cytoskeletal spikes thereby forming a brush-like structure, the so-called brush border or microvilli. In analogy to the cellular level, the surface area is further increased macroscopically by organizing the whole intestinal surface tissue in extensions—or villi—reaching into the luminal pipe.

Anchored in the cell membrane of the epithelial lining cells, a fluffy layer of interwoven glycoproteins, the glycocalyx, resides on top of the microvilli [24, 29]. The role of this glycocalyx is to protect the fragile membrane lipid bilayer against luminal content and to provide an unstirred fluid layer into which nutrients can diffuse and be taken up perpendicular to the bowel movement by the enterocytes, the major assimilating cells. The glycocalyx produced by each cell is able to interlace with that of neighbouring cells thereby creating a gap-less molecular fleece. Main constituents of the glycocalyx are the membrane-anchored glycoproteins MUC3, MUC12 and MUC17 [30], members of the mucin family of proteins which is named after mucus, the slippery surface coat present on mucosal surfaces. Mucus represents the outermost layer of defense on the epithelial lining. In contrast to the glycocalyx it is neither produced by regular epithelial lining cells nor firmly attached to them [31, 32]. Mucus is generated by goblet cells which mainly reside in the valleys ("crypts") between neighbouring villi. From these crypts the mucus is expelled like from a nozzle and squeezed onto the glycocalyx by the moving luminal constituents. Depending on the segment of the lower alimentary tract, the mucus blanket either consists of a single layer of low density or of a double layer with dense inner and light outer stratum [30]. The double layer is present on sites of little assimilation and aggressive luminal matter, i.e. the stomach and the large intestine, whereas the monolayer is found in the small intestine where nutrient uptake takes place, the pH is near neutral and microbial colonization is low. The double layer design may thus represent a barrier in the barrier where the outer film is offered for breakdown by stomach fluid and colorectal flora [33] and the inner one acts as protective coating, lubricant and trap for hazardous particulate luminal contents.

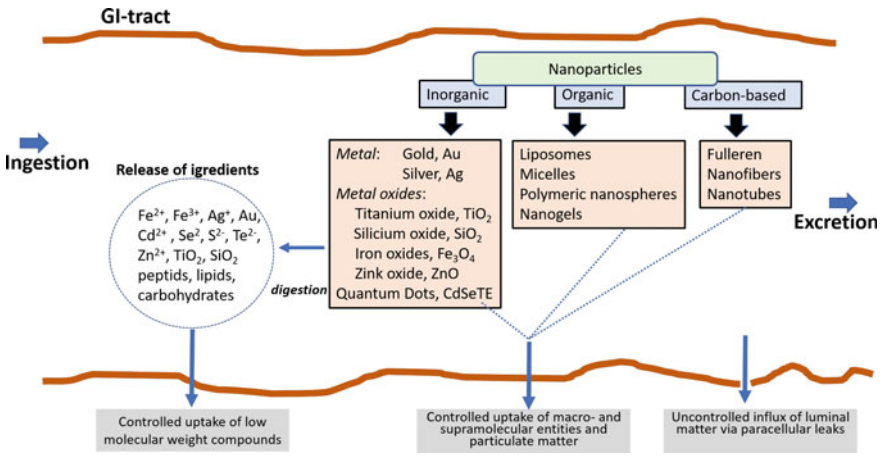

Fig. 12.3 Potential fates of nanoparticles in the gastrointestinal tract. Ingested nanoparticles are confronted first with the acidic milieu of the stomach and then with the highly active hydrolytic enzymes in the intestinal tract. It can be expected that acid- or chelator-susceptible inorganic nanoparticles will partly dissolve and small molecules, atoms or ions contained therein will be released. Organic nanoparticles consisting of carbohydrate polymers or lipids could in part be enzymatically degraded. Finally, absorption of low molecular weight components by physiological uptake mechanisms may occur, and unchanged particles or shrunken remnants may also pass across the barrier

12.3 Nanoparticulate Matter Confronting the Gastrointestinal Tract

Whether or not ingested particulate matter poses a risk to an individual is difficult to assess. In size, particulate matter may range from the macroscopic scale down to the nanometer range. It may vary in shape and surface texture, and its resistance to the luminal environment may differ considerably. In terms of its impact on the host, size has an enormous influence: the bigger the particle the higher the physical but the lower the physiological impact, and vice versa. A swallowed glass marble or bead may traumatize the esophagus but will remain inert towards the molecular and cellular processes in the gut. Ingested cake frosting will smoothly pass the upper alimentary tract but its nanoparticulate color pigments may interact with luminal content and the epithelial lining. For that reason ingestion of objects invisibly small such as the pigment particles in the frosting have raised considerable safety concerns in recent years. Small size, in particular in the nanometer range, enables the matter to undergo interactions on the cellular and molecular level which are difficult to predict. A lot of interactions and crossroads are possible for a nanoparticle in the GI tract. Nanoparticles can be broken down, taken up, adsorbed to luminal matter, become modified or be excreted or any of these processes may happen in combination (Fig. 12.3).

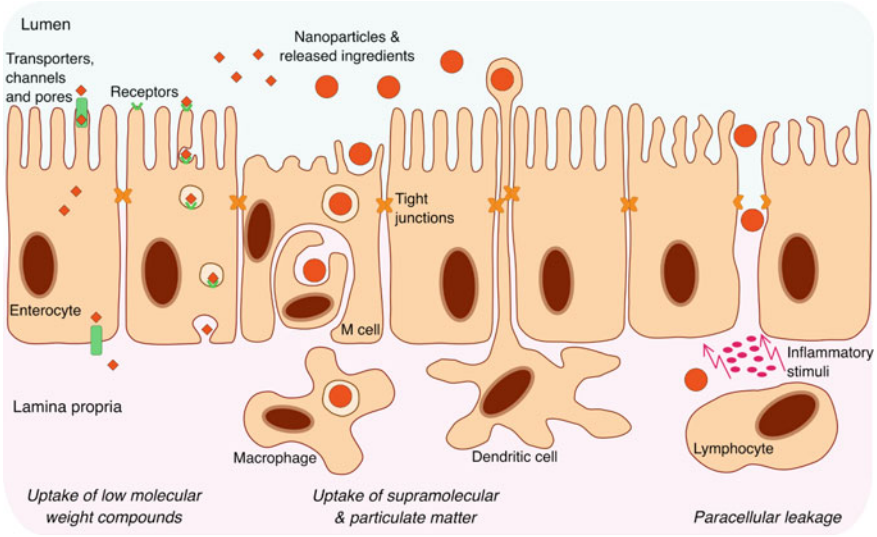

Fig. 12.4 Potential routes for nanoparticles and released ingredients across the intestinal epithelium. Enterocytes can actively or passively take up low molecular weight compounds via transporters, channels or pores, or via receptor-mediated or bulk endocytosis. Particulate matter is taken up by specialized endocytotic cells (M cells) and handed over to macrophages, or sampled from the lumen by dendritic cells. Break-up of tight junctions e.g. in a state of inflammation allows nonspecific paracellular diffusion

The mucosal lining contains gateways via which the body can sample content of the alimentary tract and can assimilate substances necessary for subsistence. These gateways in principle also constitute the entrance way for nanoparticles or their ingredients and break-down products. In a healthy individual, uptake generally occurs at designated sites which in turn results in specific uptake mechanisms. These include active or passive transport via distinct transporters or channels, receptor-mediated or bulk endocytosis/pinocytosis and uptake via specialized cells. A main determinator for uptake selectivity appears to be the size of the respective freight. In contrast, paracellular leakage is usually a consequence of some pathologic barrier disturbance and is rather non-specific regarding the transported goods (Fig. 12.4).

12.3.1 Controlled Uptake of Low Molecular Weight Compounds

For the low molecular weight level one usually discriminates between nutrients, essential salts and water, and low molecular weight xenobiotics. The former are indispensable for growth and survival of the host and thus are translocated by dedicated transport systems which reside in the apical membrane of the intestinal epithelial

cells. Specific examples for this are summarized in Table 12.1. Xenobiotics usually have no natural function inside the body, on the contrary, they even can be highly toxic for an individual. While natural/environmental origin of xenobiotics is prevalent, anthropogenic materials become increasingly relevant as a source for these substances. Uptake of such small xenobiotic molecules typically occurs by making use of existing molecular transport systems (Table 12.1).

With regard to the incorporation of (nano)particulate matter, these systems are not of relevance for the particles themselves, as even very small nanoparticles will not fit into such transporters. Yet, a particle, as any ingested matter, usually will be subject to strong physiological "attacks" in the alimentary tract. Susceptible nanoparticles may be partially or completely degraded by digestive juices and release their constituents. Of those, any metabolite of nutritional or physiological value, like e.g. carbohydrates, lipids, amino acids, or inorganic ions, will be accepted by the dedicated molecular transporters listed in Table 12.1. But nanoparticles can also harbour non-physiological and/or toxic materials or they contain an excess of an otherwise beneficial compound. Such luminally liberated substances may be viewed as a collapsed (nano)particle shrunk to fit into an otherwise irrelevant gateway. Since (nano)particulate heavy metal chalcogenids fall into this category and are abundant nanomaterials, we will examplify the "shrink-to-fit" route with two types of nanoparticles, iron oxide/sulfide nanoparticles and cadmium oxide/selenide nanoparticles. Both may stem from abrasive and melding dusts or from biomedical labelling and contrast agents.

Imaging-grade superparamagnetic iron oxide nanoparticles (SPIONs) consist of an iron oxide core (usually magnetite $Fe^{2+}(Fe^{3+})_2O_4$) and a designed shell to render them water soluble and to give them a desired function. Under the acidic pH conditions prevalent in the stomach, the core is sensitive for dissolution releasing Fe^{3+} and Fe^{2+} ions. Intestinal iron absorption in humans is specific for Fe^{2+} which is better soluble at neutral pH in the duodenum and can be absorbed by the divalent metal transporter 1 (DMT1; SLC11A2). Taken up into the assimilation-active enterocytes it is then under the control of whole body iron regulation and released via ferroportin exporter from the basolateral membrane into the blood stream, bound to apotransferrin, transported to cells in need for iron, or when in excess stored in ferritin molecules in cells of the liver, muscle, and bone marrow.

Using a radiolabelled-SPION as a model system for metal oxide nanoparticles, the fate of these particles in the gastrointestinal tract was studied in mice. The uptake of ^{59}Fe into the body from two different preparations was measured by whole-body-counting after 7–14 days, when the non-absorbed part was completely excreted in the faeces (Fig. 12.5) [58]. It should be noted that this technique is the most sensitive and reliable method for detecting the iron absorption in vivo [59]. In one preparation, the oleic acid-stabilized lipophilic iron oxide cores (11 nm) were coated with a polymer containing COOH-groups at the surface to make the particles water soluble (polym.-SPION). In the other form, the lipophilic cores were embedded into lipoprotein—micelles that transport lipids and other hydrophobic substances in human blood ("nanosomes") [60]. It was found that from both forms about 5–7% of the ^{59}Fe-label were absorbed into the body and used for haemoglobin synthesis, clearly indicating

Table 12.1 Selection of molecular transporters residing in the apical membrane of intestinal epithelial cells

Nutrient type	Freight	Foreign cargo	Transport/coupling ions	Name of apical intestinal transporter (Abbreviation)	SLC-Classification	References
Amino acids	Basic, neutral and aromatic amino acids		No coupling	Neutral and Basic amino-acid transporter (NBAT, rBAT)	SLC3A1	[34, 35]
	Glycine	Nothing known	Coupled/$Na^+ + Cl^-$	Glycine transporter 1 (GLYT1)	SLC6A9	[36, 37]
	Large neutral amino acids		Coupled: Na^+	Sodium-dependent neutral amino acid transporter (B^0AT1)	SLC6A19	[37, 38]
	Imino acids, sarcosine pipecolate		Coupled: Na^+	Sodium/imino-acid transporter/imino transporter (SIT1, IMINO, NTT4/XT1)	SLC6A20	[37, 39]
	Small, unbranched, zwitterionic α-, β-, and γ-amino and imino acids, short chain fatty acids	D-amino acids, β-alanine, 5-amino-levulinic acid, N-methylated amino acids, 3-amino-1-propanesulphonic acid, 1-aminocyclopropane-carboxylic acid, etc.	Coupled: H^+	Proton-coupled amino acid transporter (hPAT1)	SLC36A1	[40]

(continued)

Table 12.1 (continued)

Nutrient type	Freight	Foreign cargo	Transport/coupling ions	Name of apical intestinal transporter (Abbreviation)	SLC-Classification	References
Carbo-hydrates	Fructose		No coupling	Fructose transporter (GLUT5)	SLC2A5	[41]
	Glucose, galactose	C-linked glycosides of polyphenols	Coupled: Na^+	Sodium-glucose cotransporter (SGLT1)	SLC5A1	[42, 43]
Non-alkali metal ions	Ca^{2+}	Ba^{2+}, Sr^{2+}	No coupling, but GSH- and vitamin D-dependent	Apical calcium channel CaT1 or ECAC2 (TRPV6)	–	[44, 45]
	Fe^{2+}, Co^{2+}, Mn^{2+}, Zn^{2+}	Cd^{2+}, Pb^{2+}, Cu^+ (not Cu^{2+})	Coupled: H^+	Divalent metal ion transporter-1 (DMT1)	SLC11A2	[45, 46]
	Zn^{2+}	(Cu^{2+})	Not known	Zip4	SLC39A4	[45, 47]
	Mg^{2+}	Ba^{2+}, Ni^{2+}	No coupling	TRPM6	–	[47, 48]
	Cu^{2+}			CTR1	SLC31A1	[47]
Cholesterol	Cholesterol, vitamins D, E and K, carotenoid			Scavenger receptor class B-I (SR-BI)		[49, 50]
	Cholesterol, vitamins D, E and K, phytosterols		Clathrin-mediated endocytosis	NPC1-like cholesterol transpoter 1 NPC1L1		[49, 50]

(continued)

Table 12.1 (continued)

Nutrient type	Freight	Foreign cargo	Transport/coupling ions	Name of apical intestinal transporter (Abbreviation)	SLC-Classification	References
Fatty acids	Fatty acids			FATP4	SLC27A4	[51]
Peptides	Di- and tripeptides	Various drugs: beta-lactam antibiotics, ACE-inhibitors, 5-amino-levulinic acid	Coupled: H^+	Oligopeptide transporter 1 PEPT1	SLC15A1	[52]
Vitamins	Vitamin C (ascorbate)	Various ascorbate-derivatives (used for drug delivery)	Coupled/Na^+	SVCT1	SLC23A1	[53]
	Vitamin B2 (riboflavin)		Coupled: H^+	Riboflavin transporter RFVT3	SLC52A3	[54]
	Folate		Coupled: H^+	Proton-coupled folate transporter PCFT	SLC46A1	[55]
	Thiamin		Coupled: H^+	Thiamin Transporter ThTr 2	SLC19A3	[55, 56]
Organic compounds	L-carnitine/organic cations		Coupled/Na^+/No coupling	OCTN2	SLC22A5	[57]
	Organic anions: cholate, bile acids, steroids, thyroxine,	Various toxins (microcys-tins), drugs (statins, quino-lines, antibiotics, metho-trexate)	No coupling	Organic anion transporting polypeptides OATP1A2	SLCO1A2	[57]

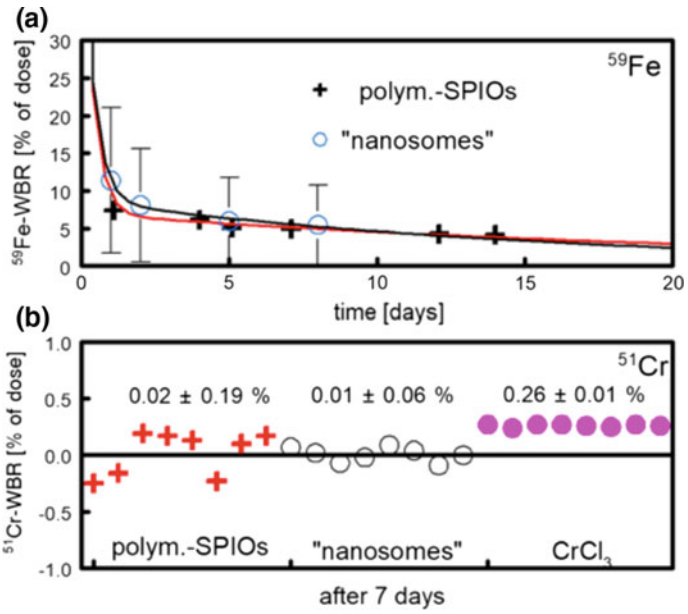

Fig. 12.5 Absorption of ^{59}Fe- or ^{51}Cr-labeled SPIONs in mice [58]. **a** ^{59}Fe-labeled polymer-coated SPIONs or so-called "nanosomes" (oleic acid stabilized, hydrophobic SPIONs embedded in chylomicron-like lipid micelles were administered by gavage to groups of mice (n = 4–5) and the ^{59}Fe-whole-body-retention (WBR) was measured after 1-14 days. **b** Same procedure with ^{51}Cr-labelled SPIONs, nanosomes, or $CrCl_3$ (n = 8). Individual values of ^{51}Cr-whole-body-retention (WBR) after 7 days (=apparent gastrointestinal absorption) are given (figure taken from [58] under Beilstein-Institut Open Access License 1.1; https://www.beilstein-journals.org/bjnano/terms#lic11)

a significant absorption from the gut (Fig. 12.5a). However, it remained questionable if this numbers truly represented intact particle uptake. To test this, the iron oxide cores were exchange-labelled with $^{51}CrCl_3$ in a stable and homogenous form [58].

It is well known that the intestinal absorption of ionic Cr^{3+} in contrast to Fe^{2+} is extremely low in rodents [61]. The results from analogous experiments in mice using the two forms of $^{51}Cr^{3+}$-spiked SPION showed that the absorption of Cr^{3+} was extremely low as expected (0.01–0.02% absorption rate) (Fig. 12.5b). Thus, the in vivo experiments virtually excluded the uptake of the two different forms of intact nanoparticles, namely a typical polymer-coated iron oxide as well as a micelle-type nanoparticle in mice. Therefore, the ^{59}Fe-results in Fig. 12.5a must be interpreted as a partial digestion of SPIONs in the stomach followed by absorption of released ionic Fe^{2+}.

Cadmium selenide is present in certain nanoparticulate semiconductors—so called quantum dots (Qdots)—which are used as replacement for classical fluorescent dyes in biomedical imaging due to their extreme photostability. Being a heavy metal chalcogenide like iron oxide, CdSe is also susceptible to digestive fluids and

the potential release of Cd^{2+} from ingested Qdots is a major concern with respect to biosafety. Many studies have demonstrated the toxicity of various Qdots in cell culture [62–67]. And as CdSe crystals are sensitive to acidic or oxidizing environments, Qdots survive a gastrointestinal transit only when coated with special shells [68, 69]. Otherwise they rapidly lose their fluorescent properties, due to etching processes (own observation; [70, 71]). In the latter case, the Cd^{2+} is liberated and it is assumed that cadmium ions misuse molecular transporters for divalent metals such as those for Fe^{2+}, Zn^{2+}, Mn^{2+} or Ca^{2+} thereby entering the body. For example, Cd accumulation is enhanced in animals fed a diet deficient in zinc (Zn), iron (Fe), and calcium (Ca). Obviously, Cd can be absorbed through two main transporters: the divalent metal transporter (DMT) 1, a preferential Fe-transporter, and calcium transporter (CaT) 1 [72]. However, when realistic dosing was applied in mice and rats no abnormal behaviour or tissue damage was observed over the several months' time span even after systemic administration of Qdots [73–75].

Unlike with SPIONs, where the released but not absorbed iron is simply integrated into the much larger pool on nonabsorbed food iron, the Cd^{2+} release from unprotected Qdots may cause an intoxication of the host not only from ingested Qdots. Released Cd^{2+} could also affects the luminal flora. It was shown in animal studies that chronic oral Cd^{2+} intake reduced the total number of intestinal bacteria among which the growth of *Bacteroidetes* spp. was significantly suppressed whereas the growth of *Lactobacillaceae* spp. was not inhibited [76] or even increased [77]. This is in line with another observation where certain lactobacillus species not only showed a high tolerance against Cd^{2+} but also bound this heavy metal ion and thus may act as detoxifying "enterosorbent" if present [78]. Moreover, the complete lack of an intestinal flora and thus the lack of any microbial Cd^{2+} binders obviously increases cadmium uptake and induces the expression of metallothioneins—heavy metal scavenger proteins—by the host [79]. The widely used nanosilver when ingested could also work in this direction. A chronic feeding of AgNP (50 and 200 ppm) over 60 days showed nephrotoxic effects in Wistar rats [80]. These concentrations are below previously reported lowest observed adverse effect level for bulk silver. The high surface of the particle could release oxidised Ag^{+} with the know high reactivity towards bacterial proteins. All in all, heavy metal metabolism in the alimentary tract is a complex process, and the intake of such substances may have far reaching physiological consequences. This holds also true if those heavy metals are contained in nanoparticulate matter because they may become luminally released.

However, regarding the release of toxic metal ions and chalcogenides such as Cd^{2+}, Ag^{+}, Se^{2-}, Te^{2-} etc., noble metal atoms such as Au, Ag, Pt, or any other ingredient of nanoparticles in the gastrointestinal tract, it should be noted that this represents not an entirely new situation for human health because these substances are present already in the environment and in the food chain [81]. Especially the heavy metals burden (Cd, Pd, Hg, Ag) follows the industrial development in many countries and the impact to human health mainly from uncontrolled working processes in the past are quite well investigated and are the basis of non-occupational or occupational exposure limits. That does not mean that no effects are awaited. In the lack of conclusive study data on effects and mechanism in the gut, it can only be estimated that the amount

of toxic materials released from ingested natural or engineered nanoparticles in the gut should be below harmful levels of environmental, health and safety protection.

12.3.2 Controlled Uptake of Macro- and Supramolecular Entities and Particulate Matter

As the digestive system usually breaks down biopolymers into their monomeric building blocks, the advance of polymers that survived digestion ("too-fit-to-shrink") is suspicious. At best the polymer is an innocuous food constituent such as cellulose or chitin. Being digestion-resistant it would be useless for the body but difficult to excrete. At worst the polymer evolved to withstand the lumen of the gastrointestinal tract for a particular purpose. Toxins of diarrhoea-inducing bacteria, such as cholera toxin, are one example of the latter. They are secreted by pathogenic bacteria in order to manipulate the host in favour of their own survival and dissemination. Cholera toxin possesses a hydrodynamic diameter of about 6 nm [29]. If structures this small can already pose a risk to the body and are metabolically worthless, incorporation of even larger structures such as microbes is even less desirable. Nevertheless, for the healthy organism it is indispensable to sample flora from the gut lumen in order to monitor and re-adjust microbial homeostasis within the alimentary pipe. Thus, several different, but always well-guarded doors along the gastrointestinal tract wall exist in case of a vital, healthy mucosal epithelium (Fig. 12.4). At such sites, the epithelium actively or passively samples macromolecules or larger entities and forwards them to the underlying mucosal immune system for further inspection. Due to the inherent danger of those substances, their presence may even trigger de novo formation of uptake/monitoring sites as is the case e.g. for cholera toxin which induces formation of an epithelial cell type specialized in uptake and translocation of macromolecular and particulate matter—the so-called M cells [82]. M cells are a unique variant of columnar intestinal epithelial cells. They lack a prominent glycocalyx, and it could be shown that M cells are able to pick up digestion resistant matter that adheres to their luminal cell membrane, such as choleratoxin B subunit-coated gold or polystyrene nanoparticles [29, 83] (Fig. 12.6). The cargo is translocated into a pocket which each M cell forms on the basolateral side and handed over to residing phagocytic cells for immunological survey [84, 85]. Due to the local abundance of specific differentiation inducing molecules M cells are most prominent above nodes of organized mucosa-associated lymphoid tissue (O-MALT), the so-called Peyer's patches, which usually reside opposite the vascularization and abdominal suspension of the gut pipe (mesenterium) [82, 86–89], but M cells can also be found within the epithelial lining outside Peyer' patches [90] and possibly be induced by proinflammatory stimuli [82]. While M cells are mere transporters for attached matter, dendritic cells (DCs) actively gather luminal content along the alimentary tract. In order to gain access to the lumen, DCs either cooperate with M cells sending their protrusions through a pore which the M cell forms through its cytoplasm [91], or they push their

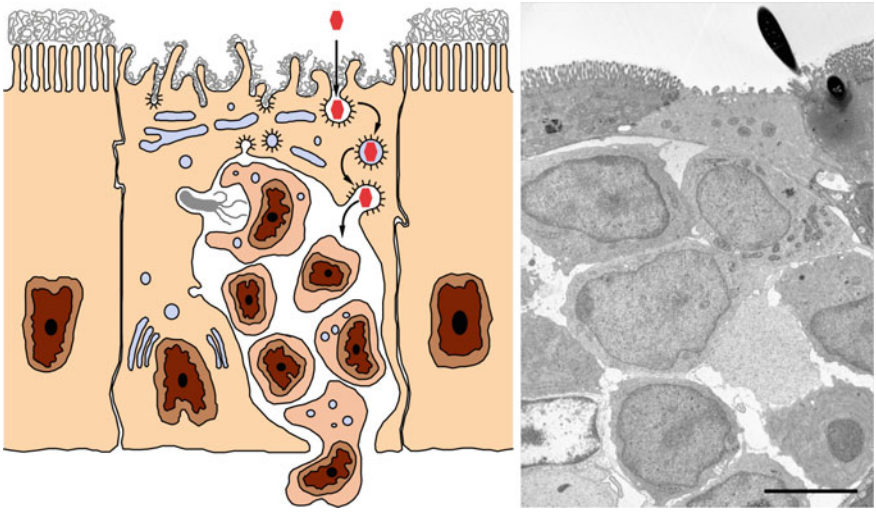

Fig. 12.6 Transcytosis via Peyer's patch M cells. Left: Schematic depiction of an M cell: the apical membrane is covered only by a rudimentary glycocalyx. Pathogens and other particulate matter are picked up from the lumen by endocytosis and transported to the basolateral side. Here they are released to be taken up by macrophages which reside in a pocket formed by the M cell. Right: Electron micrograph of an M cell from mouse ileal Peyer's patch. Macrophages in the M cell pocket await the delivery of microbes endocytosed by the M cell from the gut lumen. Bar: 5 μm

protrusions between regular columnar epithelial cells. As the respective type of DC also expresses tight junction proteins the generated hole via which the DCs pick up luminal material can be sealed on the fly [86]. More recent findings even suggest an active role of the glycocalyx for sensing of gut content. The mucin MUC17 which is a major constituent of the intestinal glycocalyx was shown to relocate from the apical surface to an intracellular vesicular pool distinct from classical endosomes upon parasympathetic stimulation (carbachol) [92]. Gut content adherent to MUC17 may be ferried into the epithelium under those conditions and offered to underlying immune cells for further examination.

A very special digestion-resistant polymer type which may be encountered in the intestine are prions. Infectious prions are extremely stable ("too-fit-to-shrink"), misfolded protein aggregates of 17–27 nm diameter [93] which—upon incorporation—catalyze misfolding of the respective counterpart in the host. Accumulation of prion aggregates will eventually result in a dementia-like disorder, the so-called spongiform encephalopathy, e.g. Creutzfeldt-Jakob disease in humans [94]. The disease is highly contagious and believed to be transmitted via the alimentary tract, simply by ingestion of prion-contaminated foodstuff. Transmission apparently occurs via M cells as it was demonstrated that mice which do not develop M cells due to a genetic defect are largely resistant to oral prion transmission [95], whereas mice being triggered to form more M cells are highly susceptible to oral prion infection [96].

As mentioned above, sampling of potential microbial dwellers or intruders from the glacis of the mucosal barrier is a controlled process exerted by M cells and dendritic cells. Hence, both cell types are capable to pick up particles of microbial size and above. M cells were reported to translocate particles of up to 10 μm in diameter [97]; dendritic cells (DCs) are able to engulf particles of up to 15 μm in vitro [98]. Yet, uptake appears to be most efficient with particles in the mid-to-high-nanometer range (500 ± 250 nm) [97–102].

This is in strong contrast to early studies which reported incorporation of orally administered particles in the size range of several hundred micrometers. In light of the more recent findings on gastrointestinal barrier function and cellular transport capacity—as described before in this chapter—it still remains an enigma how particles this big are able to traverse the mucosal lining. Passage due to paracellular leakage seems to be the most plausible explanation at this point in time.

12.3.3 Uncontrolled Influx of Luminal Matter via Paracellular Leaks

Ingress of particles considerably bigger than any of the gateways described above and the occurrence of luminal bacteria in the peritoneal cavity [103] indicates that even the staggered defences of the epithelial layer can be overcome by luminal matter. Such events seem to occur rather frequently, and the mammalian gut appears to have adjusted to such recurring epithelial leakages. For example, the polarized goblet cells of the gastrointestinal tract express toll-like receptor 5 (TLR5), an innate immune sensor for bacterial flagella, on their basolateral instead of their apical side [104] such that it can act as a "leakage detector" underneath the epithelial tight junctions. There are believed to be three main reasons for transmural flux of luminal matter: (i) bacterial overgrowth in the lower small intestines due to a defect in the gastric barrier and/or delayed intestinal clearance [103, 105]; (ii) deficiencies in the host gastrointestinal immune defense [103]; and (iii) increased permeability and damage of the intestinal barrier [103]. Barrier damage may either occur spontaneously or be caused by trauma. The latter cause is the most frequent one; physical impacts onto the abdomen, ingestion of rigid foreign objects or consumption of foods that contain bone or wood splinter may be traumatic to the gastrointestinal lining. Spontaneous perforation is less common and in most cases due to an underlying gastrointestinal affliction. Luminal bacterial pathogens may contribute by secreting specific tight junction-altering proteins or toxins [106–108]. Chronic inflammatory disorders such as Crohn's disease, colitis or celiac disease as well as intestinal infections are known triggers for spontaneous fissures, too [109–111]. The inflammatory events predispose for that by weakening tight junction integrity [112]. In an experimental set-up with intestinal biopsies from patients suffering from inflammatory bowel disease it was shown that the translocation of different nanoparticle types across the epithelium was higher in inflamed tissue than in healthy mucosa [113].

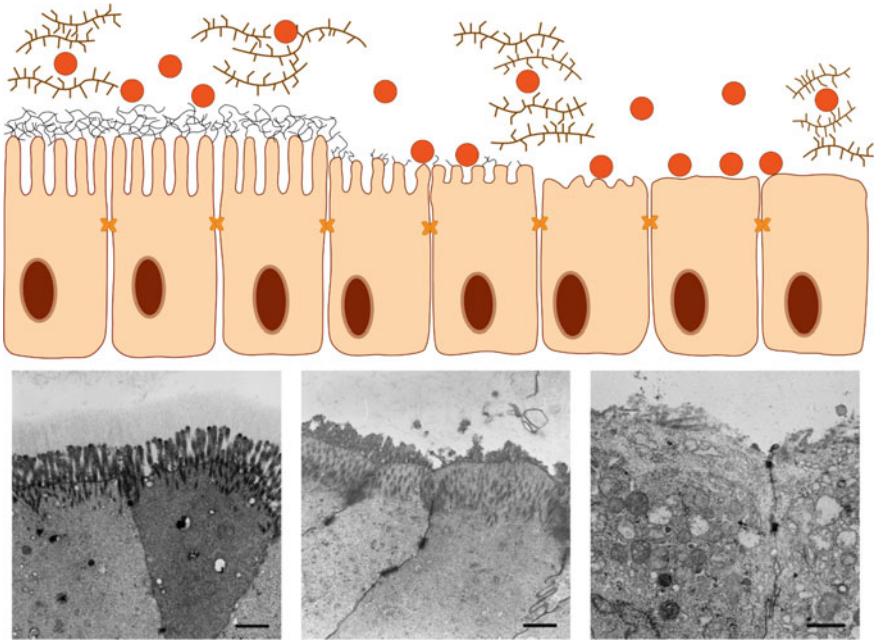

Fig. 12.7 Lack of an epithelial glycocalyx at cancerous lesions in the human intestine. The schematic drawing illustrates how the presence of a glycocalyx on fully differentiated enterocytes (left part) prevents access of nanoparticles to the epithelial surface. Lack of a glycocalyx on precancerous or adenoma regions (middle part) or on cancer cells (right part) allows attachment of particles to the unprotected apical cell membrane. Electron micrographs beneath the scheme depict typical examples of healthy epithelium (left), adenoma (middle) and cancer cells (right) in human colon. A glycocalyx is only visible on the healthy epithelial cells. Bar: 1 μm

Cancerous or precancerous lesions also foster spontaneous damage of the gastrointestinal barrier [109]. Although barrier perforation was reported mostly in the context of metastatic tumors, primary tumors of the large intestines may also promote access of luminal particulate matter to the epithelial lining. It was shown that both, intestinal polyps and epithelial cancers lack a mature glycocalyx and thus allow advance of particulate matter up to the cell membranes [24] (Fig. 12.7). Since polyps and manifest cancers are not subject to epithelial renewal luminal particles may accumulate at such sites. In light of this the hypothesis that the presence of (nano)particulate luminal matter indicates tumorigenesis by these particles seems questionable. The particles may simply accumulate at this site due to the lack of epithelial renewal in combination with the lack of a glycocalyx.

Nevertheless, the possibility of luminal nanoparticles to accumulate specifically at cancerous and precancerous intestinal lesions may provide a means to detect these malignancies early on.

12.3.4 Features Qualifying (Nano)Particulate Matter for Gastrointestinal Uptake

Whether or not a nanoparticle adheres to an intestinal translocation site or is broken down on route through the alimentary tract will depend on the properties of the particle itself and on the luminal environment. Particles have a certain size, shape and special surface properties. In the initial studies presented at the beginning of this chapter particle size was the most important parameter correlated with fate. Numerous studies investigate this relationship using spherical micro- and nanoparticulate objects. However, particles are not always isotropic. Rod-, disk- or ellipsoid-like particles can also be manufactured or be generated by nature (Fig. 12.1). If their long axis exceeds the size of the cellular gateways uptake may occur only if the particle approaches in a certain orientation. This influence of orientation was impressively demonstrated for particle phagocytosis by macrophages [114] but no information exists on how intestinal dendritic cells or M cells may cope with anisotropic nanoparticles, in particular when the aspect ratio is high. Beyond size and shape the particle surface properties are an important criterion for particle handling by the host. Nanotechnologists have methodologies at hand to customize the surface of nanoparticulate matter to their needs or liking and there are also numerous analytical tools to confirm the desired surface design. Yet, most of these efforts may be futile attempts because it is naive to assume that an ingested particle will not interact with luminal matter on its way through the gut. Especially particles with hydrophobic and charged surfaces may eagerly adsorb hydrophobic or counterionic intestinal constituents (e.g. lipids, nucleic acids, proteins, solute ions) and cover themselves with a so-called corona (e.g. [115–117]). For systemically administered nanoparticulate preparations the formation, composition and consequences of a corona became subject of intense investigation in the last decade. Unfortunately, no information about a gastrointestinal nanoparticle corona exists as yet. Only a few studies with bacteria have been conducted. They show that the presence of soluble non-starch plantain-fibers suppresses intestinal infection of chicken by *Salmonella* spp. [118, 119] and blocks adhesion of intestinal pathogens and commensals to M cells [120, 121] whereas the presence of emulsifier in the diet such as polysorbate-80 increases M cell translocation of bacteria [120]. As the cells were preincubated without washing it remains unclear at this point whether the epithelial surface was passivated/activated by the soluble non-starch plantain-fibres or the detergent or whether the bacteria adopted a detergent or non-starch plantain-fibre corona that supported or prevented uptake.

In light of the latter it seems clear that luminal content can have a substantial influence on particle uptake and translocation by the intestinal epithelium. The observation in the chicken-infection-study that only broccoli- and banana- but not apple- and leek-plantain fibres excerted a protective effect again demonstrates how complex the various influences on nanoparticle-host-interactions in the gut must be.

Table 12.2 Examples of nanoparticles from natural source as well as engineered nanoparticles

Naturally occurring nanoparticles			Anthropogenic nanoparticles		
Source	Chemical structure	References	Type/Class	Constituent(s)	References
Surface water	$CaCO_3$, Al_2O_3, SiO_4^{4-}	[123–125]	Inorganic	Metals (nAu, nAg, nCu, nPt) Metal oxides (FexOy, ZnO, TiO_2) Quantum Dots (CdS, CdSe, and InAs)	[126, 127]
Volcano ashes	SiO_2				[128]
Iceberg sediments	Fe_3O_4				[129]
Soot from pyrolysis	C, nanotubes, Fullerene		Organic	Non-biogenic polymers	
Mineral wells	S				
Umbra	MnO, Fe_3O_4			Biogenic polymers, lipids	[130]
Bacteria and fungi	Se-Protein		Carbon-based	Fullerene, carbon tubes, carbon fibres	[131, 132]
Meteorites	Fulleren				
Plants and atmosphere	Adducts of oxidized terpens	[133–135]		Carbon black	[136]

12.4 Types of Nanoparticles Unintentionally Occuring in the Alimentary Tract

A basic distinction is drawn between natural and engineered nanoparticles. The mounting concern about a possible impact of nanoparticle exposure on human health is based on the tacit assumption that nanotechnology with its increasing market of engineered nanoparticles is exclusively responsible for this. However, what is disregarded in this context is the fact that nature itself is a large producer of nanoparticulate matter which presents in manifold sizes, shapes and compositions and stems from various sources (Table 12.2). It is estimated that those "natural" nanoparticles formed by biogeochemical processes amount to several billon metric tons per year which is orders of magnitude more than the current annual production of engineered nanoparticles [122, 123].

One of the main sources are eroded minerals which are carried into the atmosphere by storms over arid areas (e.g. asian dust). Estimates are that the atmosphere contains about 0.3 billion tons of submicron particles of which about a quarter precipitates in wet state [137]. Among the biggest biological sources encompassing 10–30 million metric tons per year are so-called secondary organic aerosols (SOAs) which are formed continuously in the atmosphere from terpens (e.g. α-pinene) released by plants [138]. Little is known whether and to what extent such natural nanoparticles affect the environment but it seems reasonable to assume that nature can cope with its own products. Consequently, there is a rapidly growing interest in mimicing those natural production processes by so-called phyto- and phyco-nanotechnology. With this it is already possible to generate natural-identical nanoparticles by bioreduction or abrasion in bacterial or fungal processes [139].

In the usual sense, however, the term "nanoparticle" stands for manufactured or engineered nanoparticles. Based on their composition, engineered nanoparticles (ENPs) can be classified in three main groups (Table 12.2): inorganic, organic and carbon-based nanoparticles [2].

The family of inorganic nanoparticles usually consist of elemental metal or of metal chalkogenids. Of noble metals such as Ag, Au, Pt etc. rather stable nanoparticles can be formed with physicochemical properties different to bulk material. Nanosilver (nAg) particles typically measure 25 nm. They have an extremely large relative surface area and release Ag^+ ions when placed in distilled water as solvent. These ions vastly improve the bactericidal and fungicidal effectiveness of nAg by denaturation or oxidation of respective microbiotic proteins. Based on these properties, nanosilver is widely used in cosmetics (creams, shampoos, deodorants, and body lotions) as well as in textiles (socks, shirts, trousers, and active underwear). A growing number of textiles are even fabricated with metal NPs in the structure (for example 31–2,600 ppm of nAg in T-shirts). This additive offers biocidal properties and prevents excessive sweating [127, 140].

Nanogold (nAu) particles are manufacturable in a wide size range between 1 and 100 nm and exhibit photothermal stability. Most valuable, however, are the special optical properties of nAu which make them interesting for all kind of medical diagnostics, e.g. liquid-phase assays electron microscopy, predominantly, transmission electron microscopy (TEM) or the so-called surface plasmon resonance spectroscopy [126].

Among the metal chalkogenids, oxides are the most versatile nanostructures because of their either metallic, semiconductor, or insulator characteristics. They offer diverse and tunable structural, physical and chemical properties and functionalities which make them widely usable as optical, optoelectronic, magnetic, electrical, mechanical, thermal, catalytic, photochemical tools. One prominent example already presented above are superparamagnetic iron-oxide nanoparticles (SPION) consisting of a γ-Fe_3O_4-core that is made water-soluble by a variety of different coating materials which easily can be functionalized by any kind of bioorganic molecules including antibodies, aptamers, and the like [128].

For nanoparticulate heavy metal sulfides, selenides and tellurides their unique optical properties are the most interesting physical feature. Upon excitation those

Quantum dots (Qdots), of which the already discussed cadmium selenide is an archetype, emit fluorescent light whose wavelength can be adjusted with particle size (2–10 nm). They are used in TV-screens and have been proposed as fluorescent labels for biomedical assays and imaging applications when fortified with a protective organic shell [129].

Organic nanoparticles make up the most diverse group of nanoparticulate materials as almost all biogenic and non-biogenic organic polymers can be formulated as nanoparticles with the right technology at hand. Family members range from spherical solid nanoparticles, dendrimers, over micelles and liposomes to drug conjugates. Organic nanoparticles are the system of choice for drug delivery as discussed below.

Carbon based nanoparticles represent the third major class of anthropogenic nanoparticles. To this class belong abundant products like amorphous carbon particles and carbon black (CB) but also more sophisticated materials such as C60 fullerenes, graphenes, carbon nanodots and single-walled carbon nanotubes (SWCNT) [131, 132]. Amorphous carbon particles, in particular carbon black, is produced in huge amounts but not all carbon black comes in the nanometer scale. While carbon black seed nanoparticles (nodules) are about 15–400 nm in diameter, also particulates in the high micrometer size can be manufactured [141, 142]. Amorphous carbon and carbon black nanoparticles (CBNP) are made use of as pigments in cosmetics [143], as catalysts [144] and possibly in future supercapacitor and flat screen designs [145, 146] as well as in bioassays [147]. Fullerenes and the other graphene-related carbon nanomaterials listed above will have an even broader field of application in the years to come ranging from sun glasses [148] over energy storage (solar cells [149], supercapacitors [150, 151], hydrogen stores [152–154]) to biomedical uses (antimicrobials [155], imaging, biosensors [156]) and possibly a lot of other applications we do not even imagine by now.

12.5 Intentional Administration: Drug Delivery and Contrast Agents

Peroral administration of drugs is the preferred route for self-medication. Unfortunately, the gastrointestinal tract is also a hostile environment in which present-day biological drugs (e.g. therapeutic antibodies, insulin, peptides, siRNA, aptamers, etc.) barely survive. For that reason pharmaceutical scientists develop micro- and nanoencapsulation systems that fortify susceptible drugs against gastrointestinal breakdown. Research in this area literally exploded within the last decade with a continuously increasing number of encapsulation techniques, matrix variants, particle surface functionalizations and drug loads. As a comprehensive presentation of this field would be beyond the scope of this chapter, we will focus here only on the basic principles of nanoparticulate gastrointestinal drug delivery systems.

12.5.1 Nanoparticulate Drug Delivery Systems

The field of nanoparticulate drug delivery emerged in the last decade of the last century, mainly driven by mucosal immunologists who realized the need for oral delivery systems in order to induce protective immunity at mucosal surfaces. Mucosal immunity mainly relies on the formation and secretion of secretory antibodies of the immunoglobulin A class which is induced if the respective antigen is taken up by the mucosal antigen gatherers, M cells and dendritic cells. As those gatherers prefer particulate matter in analogy to the bacteria they usually pick, a micro-to-nanoparticulate vaccine formulation is considered a logical solution [157–159]. Experimental mucosal immunization with particulate vaccines worked because the amount of antigen required to induce an immune reaction is low, a "catalytic" amount to use chemical terms. Nevertheless, particulate mucosal vaccines have not entered the market as yet. Excited by the pioneering work in the vaccine field pharmaceutical scientists envisioned the possibility to deliver degradation-sensitive drugs via the per-oral route by protecting them in a micro/nanocapsule. In retrospective, the delivery of encapsulated drugs across the gastrointestinal barrier "into the house" was not a success story. However, dropping the parcel "right at the doorstep" turned out to be a more favorable, yet still experimental approach. When the particles are able to reach the epithelial glycocalyx or the covering mucus layer they are as close as it gets to the recipient. In case of glycocalyx adhesion only a couple of hundred micrometers have to be passed by a drug that is released by the adhering nanoparticle. In contrast to the maze of obstacles and traps set by the luminal content the odds are considerably higher for the drug to become incorporated as long as the underlying cell has the right machinery for uptake. Using this approach, various drugs have experimentally been delivered to the desired site of uptake [158, 160–162]. To meet that goal the nanoparticulate drug formulation must be stable enough to reach their target cell environment but at the same time be so fragile that the matrix desintegrates slowly at the particle attachment site. Lipidic formulations meet that requirement [163] but also poly-lactide-coglycolide and other hydrolysis susceptible polymers [162, 164]. In order to enable nanoparticle adherence lectins are often used as particle coating because they mediate binding to the glycocalyx or the mucus [164, 165]. If the particles are to penetrate the mucus layer or have to "hide" in the mucus desintegrating enzymes or reducing compounds (thiols) are employed [166]. A disadvantage of micro- or nanoencapsulation is the slower Brownian motion of the particle as compared to the free drug and the fact that an excreted particle that did not reach its destination dumps at one push billions of drug molecules which thereby did not have a chance to enter the body. Those disadvantages are a double-edged sword. While low epithelial contact and rapid excretion of undesired nanoparticles is welcome, the same processes make life miserable for parmaceutical scientists involved in the development of nanoparticulate drug delivery systems.

12.5.2 Particulate Matter for Contrasting the Gastrointestinal Tract for Medical Imaging

The classical diagnostics of gastrointestinal diseases is based on endoscopic investigations and x-ray exams with a barium sulphate swallow. Advances in non-invasive imaging modalities including contrast enhanced ultrasound (CEUS), computed tomography (CT), positron emission tomography (PET) and magnetic resonance imaging (MRI) have in the last decades revolutionised the way in which the gastrointestinal tract can be studied. Avoiding radiation exposure, MRI is, besides CEUS, the most favourable technique combining excellent soft tissue contrast, spatial resolution, and depth of penetration [167]. A variety of contrast agents has been evaluated for MRI enterography including paramagnetic gadolinium chelates which reduce the longitudinal T1-relaxation property and result in a brighter signal, and superparamagnetic iron oxide based nanoparticles (SPION) which show size dependent T1- or T2-effects. SPION have been used in clinical MRI for more than 20 years [168], and over time, the FDA approved several SPION formulations, mainly for

Table 12.3 Characteristics of widely used clinical iron oxide nanoparticles

Generic name/product number	Trade name	Coating	Hydrodynamic diameter	Blood half-life	References
Intravenous (i.v.)					
Ferumoxides AMI-25	Endorem Feridex	Dextran	SPIO: 50–100	10 min	[168–170]
Ferucarbotran SHU555A	Resovist# (Japan)	Carboxy-dextran	SPIO: 60–80 nm	12 min	
	Resovist S Supravist	Carboxy-dextran	USPIO: 20–25 nm	6–8 h	
Ferumoxtran-10 AMI-227	Sinerem# (Europe)	Dextran	USPIO: 20–50 nm	24 h	
Feruglose NC100150	Clariscan	Carbohydrate-polyethylene glycol	USPIO: 11–15 nm	2 h	
Ferumoxytol AMI-7228	Feraheme# (USA)	Carboxy-methyldextran	USPIO: 20–30 nm	10–14 h	
oral (p.o.)					
Ferumoxsil AMI-121	GastroMARK# (USA) Lumirem# (Europe)	Siloxane	SPIO: 10–300 nm		[171, 172]

Contrast media that are currently available for use in patients in countries listed. Other media have already been withdrawn from the market in certain countries

intravenous administration for indications including MR angiography, tissue perfusion studies, and atherosclerotic plaque and tumor imaging (Table 12.3) [169].

The FDA approval of *Ferumoxytol* as an intravenous iron drug in 2009 and 2017 has led to a renaissance of "off-label" use of SPION also for a variety of MRI imaging applications, in particular because these nanoparticles are regarded as safer contrast agents compared to the frequently used gadolinium chelates, especially in patients with renal insufficiency [170].

To date, *Ferumoxsil* is the only FDA-approved SPION for oral administration. This contrast agent is composed of iron particles of about 10 nm, coated with a non-biodegradable and insoluble matrix (siloxane) and suspended in viscosity-increasing agents such as starch and cellulose. After oral administration, *Ferumoxsil* fills the stomach and intestines and the T2 relaxation is enhanced, thereby darkening the contrast agent-containing portion of the gastrointestinal tract, distinguishing bowel from organs and tissues adjacent to the upper regions of the gastrointestinal tract. Routine indication for *Ferumoxsil* is the Magnetic Resonance Cholangiopancreatography (MRCP), the non-invasive imaging technique of choice to evaluate the pancreatobiliary system, where the fluid in the biliary and pancreatic ducts is visualized with heavily T2-weighted sequences [171]. In T2-weighted bowel MR imaging, *Ferumoxil* is also routinely used to highlight Crohn's disease lesions, and can detect mural and transmural inflammation with the same accuracy as gadolinium-enhanced T1-weighted MR [172].

Magnetic particle imaging (MPI) is a new imaging modality with extraordinary contrast and sensitivity using superparamagnetic iron nanoparticles [173, 174]. Recently, first gastrointestinal applications for this method using a designed nanodevice have been published [175]. MPI-tailored, long-circulating SPIONs were injected through the tail vein in a mouse model of induced acute gastrointestinal bleeding. The captured tracer accumulation in the lower GI tract was monitored with excellent contrast showing a bleed rate between 1 and 5 μL/min in this model. This could be an important clinical translation in the future, because unclear gastrointestinal bleeding is a major concern in internal medicine.

However, with all the described applications of nanoparticles as oral contrast media for MRI, a possible uptake of intact or partly digested particles or particles materials was not addressed so far, always relying on the expected low toxicity of iron as essential trace element.

12.6 Fate of Ingested Particulate Matter: Beeline or Detour

Cells interact with their surroundings and will, upon contact, also try to incorporate nanoparticles. It is well known from cell-culture studies that almost all mammalian cells take up nanoparticles to some extent using a variety of uptake mechanisms which are mostly nonspecific. Extensive in vitro studies have explored the features of nanoparticles (size and physical properties) that influence their cellular uptake

and intracellular processing resulting in elimination, degradation or storage of the particles in the respective cell.

However, it should be asked at this point, how relevant these results are for the in vivo situation. Despite their general capability to take up larger molecules and particles, normal cells in the body will routinely not be involved in this process because, in a close interaction between tissues, incorporated nanoparticles are recognized as exogenous materials and sequestered by mononuclear phagocytic system (MPS) cells mainly in liver or spleen. When dealing with particles that are taken up via the digestive tract, the central question is certainly how many of them are capable of crossing the epithelial barrier at all before they can encounter any other cells inside the body.

12.6.1 Measuring Gastrointestinal Particle Uptake in Model Systems

The question of particle uptake/translocation at mucosal surfaces has incented numerous investigations using different model systems which reflect the in vivo situation and the compartments involved in particle-host-interaction to various degrees. In vitro, ex vivo and in vivo systems for particle uptake studies have been developed which shall address different aspects of the process [176].

In vitro cell culture systems use intestinal epithelial cells of various origin, with the human colon carcinoma-derived cell line Caco-2 being the favourite tool. In culture, Caco-2 cells differentiate into a columnar epithelial cell type upon reaching confluence, with several biochemical and morphological characteristics of small intestinal enterocytes, e.g. microvilli and tight junctions [177–179]. Co-culture models, where Caco-2 cells are mixed with other cell types, try to more closely imitate the in vivo situation: Co-culture with the human adenocarcinoma cell line HT29 will introduce a goblet-cell-type into the cell layer and lead to the formation of a mucus layer on the apical cell surface [180, 181], induction of M cell formation is attempted by co-culturing Caco-2 cells with lymphocytes isolated from murine intestinal Peyer's patches [182] or human Burkitt's lymphoma B cells [183–185], and triple cultures attempt to combine all these features [186]. Studies on particle uptake and translocation are usually performed using a so-called transwell-system where the intestinal epithelial cells are grown on permeable filter supports inserted into the wells of culture dishes. This way, both sides of a polarized cell monolayer are in contact with a separate fluid compartment which shall render the system particularly versatile for transport studies [178, 187]. In the different experimental set-ups, particle uptake and/or translocation was observed to various degrees, obviously depending on factors such as particle type, size, and surface modification. In most cases, particle acquisition by the Caco-2 layer appears to follow an endocytosis/transcytosis mechanism, with clathrin- or receptor-mediated endocytosis, macropinocytosis and lipid raft/caveolae all contributing to the process [188–191]. Only rarely, opening of tight junctions

and paracellular transport have been described [191]. With lipidic nanoparticulate formulations which may desintegrate in the cells substantial uptake of a hydrophilic fluorescent dye encapsulated in the particles could be observed [192] but in studies where actual translocation in a transwell system was tested free cargo was transported at least as good or even better than cargo formulated in lipidic nanoparticles [193]. In the few examples were stable particles were used and quantification was given at all, translocation rate of particles was almost always well below 1% of all particles offered [189, 190, 194]. The presence of M-like cells in the Caco-2 co-culture models greatly increased translocation of plain latex or polystyrene particles between 100 and 1000 nm in size [183–185, 194]. However, the significance of these findings for the in vivo situation must be regarded with caution, since the M cell concentration in the human intestine (<5% in the FAE and <1‰ in the total intestine) is far below the value described in these studies (up to 30%). Also, co-culture with M-like cells did not enhance transport of polyacrylic acid-coated iron oxide or silver nanoparticles of <10 nm core size [194]. Thus, for in vitro systems uptake was reported quite often but the taken-up particles seem to become trapped inside the cultured cells. This is bad news with regard to drug delivery and good news in terms of nanoparticle safety since the particle-laden cells would be sloughed off into the gastrointestinal lumen within a few days. What still remains entirely unconsidered in those systems is the question whether nanoparticles would actually gain access to the epithelial cell membrane where they can be taken up. The apical cell membrane of Caco-2 cells is far better accessible for particles than that of enterocytes in vivo because Caco-2 cell layers display only a rudimentary often gappy glycocalyx of max. 30–50 nm hight [29, 193, 195, 196] as compared to the continuous enterocyte glycocalyx in vivo which is several hundred nanometers thick [24]. In co-culture studies with mucus producing cells the important filter- and sink-like effect of an apical surface coat, in this case mucus, was reported [160, 191, 197, 198]. Considering all of the above, it seems questionable whether in vitro cell culture systems are able to yield robust and valid data concerning nanoparticle translocation at the gastrointestinal mucosa.

In an attempt to more closely reflect the in vivo situation, some work has been performed using ex vivo animal experiments. In the everted sac model, a segment of the rat small intestine is dissected, flushed, turned inside-out, and the ends are ligated. Uptake from the—former luminal—outside into the serosal compartment is analyzed after incubation of the sac in the medium of interest. Using this method, uncoated silica particles between 70 and 1000 nm were not absorbed through the intestine in a measurable extent, but after surface modification with amine- or carboxyl groups, uptake of 70-nm particles was demonstrated [199]. In the same system, polyamidoamine dendrimers of approximately 3–7 nm diameter were clearly crossing into the serosal compartment, whereby anionic nanoparticles displayed a higher transfer rate than cationic ones [200].

Still more close to the in vivo situation is the isolated perfused rat intestine model. Here, the complete small intestine of a rat including mesenteric artery and portal vein is explanted. The organ is placed in a perfusion chamber where a constant supply of nutrients and oxygen can be provided via the cannulated vessels (Fig. 12.8). In this system, import into as well as efflux out of the gut lumen can be investigated

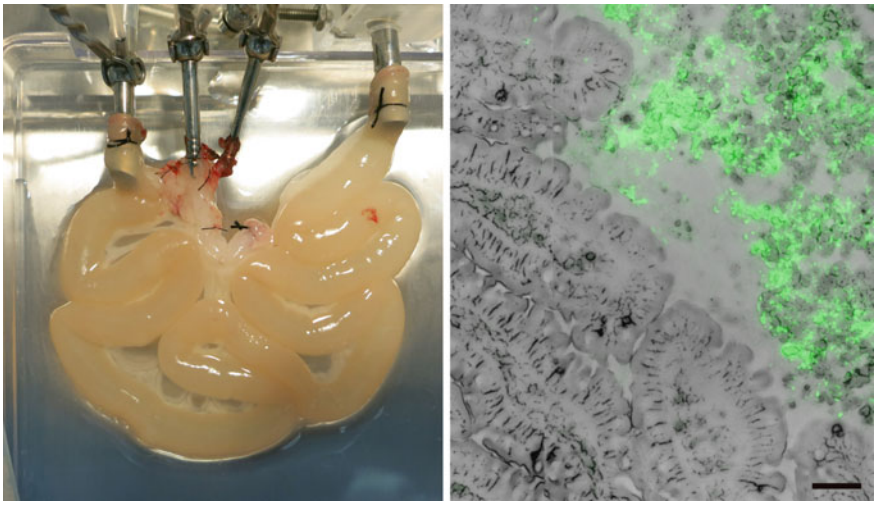

Fig. 12.8 Nanoparticle uptake studies in an ex vivo model. Left: Isolated rat intestinal explant in the perfusion chamber. Via the cannulated artery, the explant is supplied with artificial blood plasma; particle samples can be applied luminally, and their final location in different compartments (luminal, lymph, tissue) can be analyzed. Right: Entrapment of NPs in intestinal mucus. Cryostat section of gut tissue after luminal application of fluorescent 20 nm particles into the lumen of the isolated rat intestine. Bar: 50 μm

by separately collecting and analyzing the fluid from lumen, vascular perfusate and lymph [201]. In particle uptake studies using the isolated perfused rat intestine and luminally applied fluorescent polystyrene particles of 20, 40 and 200 nm in size, no particles could be found in either vascular or lymphatic effluate samples, nor were any particles detected by histological examination in the gut tissue. Instead, a large fraction of the NPs was trapped in the mucus layer lining the intestinal wall (Fig. 12.8) [202].

The few data obtained from the organ explant/ex vivo studies indicate only very sparse, if any, uptake of nanoparticles in the size range between 20 nm and 100 nm in the intestine, but particulate matter below 10 nm in size can cross the epithelial barrier to a certain extent.

No matter how well an in vitro/ex vivo model performs, the most reliable answers will be obtained by in vivo evaluations. With regard to the fate of ingested nanoparticles, several animal models have been established and used in uptake and toxicity experiments [203, 204]. Application of particles is usually done via feeding or intragastric delivery, but the different experimental set-ups vary in their methodology to detect and quantify uptake of nanoparticles into the body. An in vivo study can be performed in two ways: “in situ”, i.e. by continuous or time-lapsed recording of the consequences of a set trigger, or “ex situ”, i.e. by analyzing the outcome of a set trigger once after a defined period of time.

In situ analyses of nanoparticle-host-interaction require cutting-edge technologies which allow detection of the particles inside the body in a time- and spatially-resolved manner, ideally on microscopic scale [205]. Due to this demanding instrumental requirements few studies have been conducted as yet on the in situ level, either via intravital optical imaging after application of fluorescent probes, or by whole body scintigraphy if radioactive particles were used. In general, the in situ acquired data could only give a very limited overview of particle distribution; to date, this approach is neither sensitive nor accurate enough for quantitative interpretations. For example, when silica-based rhodamine-derivatized nanoparticles (20 and 100 nm) or polymer-coated quantum dots (33–36 nm) were applied orally to mice and tissue distribution was monitored at different time points with intravital imaging systems, fluorescence signals were mainly visualized in the gastrointestinal region [68, 206]. Only subsequent ex situ imaging of dissected organs allowed some quantification of the fluorescence signals in one study and proved dissemination of particles over the body, with accumulation in lung, liver and kidney [206]. At the starting point of the particle uptake process, intravital confocal microscopy revealed uptake of 20- and 40-nm particles by intestinal epithelial cells and transport into the serosa and the lymphatics of the intestine, but larger particles (100–2000 nm) were scarcely internalized [207]. Here again, quantification of results was only relative, and no absolute uptake rates could be deduced.

Ex situ analysis is the methodology of choice in most particle uptake studies, simply because one needs less sophisticated instrumentation to analyse a faeces or urine sample or post mortem resected tissue. In case of intestinal tissue which ought to be most informative about the sites and degrees of particle entry the specimen is either fixed, cut and investigated by classical microscopy (light or electron microscopically). Alternatively, bulk analyses are performed where the whole tissue, blood or excretion is digested selectively in solutions that either leave particles intact or disintegrate them, too, with particle constituents becoming solutes. Intact particles are then counted on filters or in Neubauer chambers, constituents from dissolved particles are determined radiologically or spectroscopically, e.g. by fluorescence or inductively-coupled plasma mass spectroscopy (ICP-MS) [203]. Each of these ex situ techniques has its strengths and weaknesses. Only a careful combination of histological and bulk analysis will provide the desired information about site and degree of particle uptake [16]. Looking histologically, numerous studies report uptake of particulate matter in the Peyer's patches/follicle associated epithelium, presumably via M cells, though most of those studies use particles above 1 μm in size [97, 99], but location in/transport via villus regions was also observed with particles below 100 nm [207, 208]. Performing bulk analyses of tissues, organs and excretions after oral nanoparticle exposure still reveals conflicting results. While in several studies nanoparticles up to 100 nm in size were found—to various extents—in spleen, liver, kidney, blood and urine [203, 204, 209], others describe that no measurable amounts of nanoparticle material could be detected in any of these tissues [210, 211].

Ex situ bulk analyses is also the method of choice for the archetype food-borne nanoparticle, titanium dioxide (titania), because the oxide is believed to be sufficiently resistant to luminal content of the gut. Numerous studies have been con-

ducted in rodents with adverse effects to inner organs been detected [212]. In these studies titania doses ranging from 1.5 to 5000 mg/kg body weight were used, with a mean dosage of 453 mg/kg and a median dosage of 27.5 mg/kg. Even studies on human volunteers were performed with the titanium content of blood samples being determined [213–215]. In two of the three human studies elevated serum titanium levels were found; whether or not those elevated levels caused any pathology was not checked. In these three studies titania doses ranging from 0.31–5 mg/kg body weight were used with a mean dosage of 2.26 mg/kg and a median dosage of 1.34 mg/kg. The latter doses were 200-fold (mean) or 20-fold (median) lower than those used in rodents where pathology was observed. Yet, dosing in human beings was still about 4100-fold (mean) or 2400-fold (median) higher than the estimated daily titania nanoparticle intake of 7–69 year old humans (0.55 μg/kg body weight) in the Netherlands [216]. The daily Dutch titanium dioxide nanoparticle intake differs considerably from calculations for North-American citizens who are believed to ingest about 1 mg titania nanoparticles per kg body weight and day [217]. Why a North-American may ingest about 180-times more titania nanoparticles than the average European cannot be clarified at this point. Even then is the dosing in the rodent studies in which adverse effects of titania on inner organs were observed on average 27-fold (median) to 450-fold (mean) higher than the food-borne titania nanoparticle intake of North-Americans. For Europeans the animal models are overloaded by a factor of about 5000 (median) to 800,000 (mean). In light of this, it seems questionable whether those models can faithfully predict possible risks for human beings. In some of the (overloaded) rodent studies deposition rates in certain inner organs were reported. In most cases the amount of titanium found was less than 1% of the administered dose. Only in one study [218] a comprehensive analysis of 11 tissues was conducted. Here a cumulative TiO_2 deposition of about 5% of the administered amount was reported. Deposition was highest in Peyer's patches and the mesentery network which is in line with the particle uptake mechanisms presented above. Exogenous pigment was also found consistently in Peyer's patches of human beings beyond preschool age [219, 220]. The amount of those aluminium, silicon and titania-containing deposits seems to increase with age.

Taken together, the majority of ex vivo and in vivo studies which most closely reflect the situation in the human gastrointestinal tract show that incorporation of digestion-resistant nanoparticles occurs in the alimentary tract but at a low rate and preferentially at sites dedicated for collection of luminal matter. Nanoparticles may be an inevitable by-catch and may ever have been. Whether or not the deposition rate is higher nowadays than it used to be in the preindustrial age is open to debate.

12.6.2 Deposition, Breakdown and Excretion of Incorporated Matter

The biological and toxical effects of nanoparticles depend on their ability to reach and to interact with cells and organs in the body. The first step is uptake into the body, which usually implies nanoparticle contact with and penetration of either of the

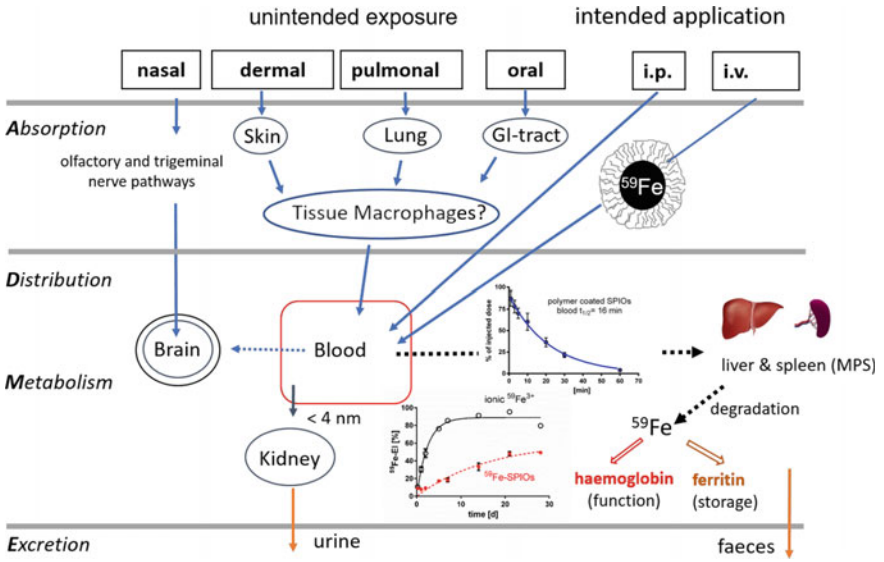

Fig. 12.9 Uptake into and fate of nanoparticles in the body. The acronym ADME stands for the pharmacokinetic processes involved: absorption, distribution, metabolism and elimination. The fate of an iron-based nanoparticle (polymer-coated ^{59}Fe-labelled-SPION, 25 nm hydrodynamic diameter) is depicted as an example showing the fast clearance from the blood (half-life 16 min), degradation in the liver and use of iron in newly formed haemoglobin or storage in form of ferritin. MPS, mononuclear phagocytic system (figure adapted from [221])

three main body barriers, namely the skin, the lung, and the mucous membrane of the gastrointestinal tract (Fig. 12.9). The evaluation of the respective uptake mechanisms is of great importance for basic science but also for developing effective and safe nanomedical applications.

Different exposure conditions are not only of considerable impact on how much nanoparticles are incorporated into the body, but also on how they may be distributed, excreted or metabolised. In most currently used or planned nanomedical applications, the respective nanodevice is administered by intravenous injection. Here, the complete bolus dose is given into a peripheral vein. The particles are swirled around with thousands of plasma proteins throughout the venous systems, are facing billions of moving cells and the large surface area of vascular endothelial cells.

The intravenous application of nanoparticles can be regarded as a model of how natural defense mechanisms cope with natural or xenobiotic particles larger than the normal molecules [221]. Such particles are almost immediately covered by a protein corona including specialized plasma proteins, so-called opsonins. Opsonins serve as a signal for a fast clearance of these particles from the blood by uptake into cells of the so-called Mononuclear-Phagocyte-System (MPS) mainly based in the liver and spleen. Again, using a radiolabelled polymer-coated SPION (compare also Fig. 12.5), it was shown that these particles upon injection in mice were rapidly taken up into

the liver mainly by macrophages (Kupffer cell), but surprisingly also by sinus-lining endothelial cells [222]. After some days, the ^{59}Fe-label was incorporated into newly formed erythrocytes, indicating a complete degradation of the iron oxide cores and use of the iron in the iron metabolism of the mice.

The intraperitoneal injection (i.p.) could also be an application modus for future nanodevices in nanomedicine. In this context, it was shown that ^{59}Fe-labeled SPION, which were embedded into the lipid core of triglyceride-rich lipoproteins (TRL-^{59}Fe-SPION) (nanosomes, similar to shown in Fig. 12.5) and injected i.p. into mice did appear in the blood to a substantial extent ($10.1 \pm 0.91\%$ of the injected doses after 24 h), whereas polymer-coated SPION were not able to escape the abdominal cavity barrier [223].

However, the situation after intravenous or intraperitoneal injection is different from dermal, pulmonal, or oral exposure which can deliver at most only the minor fraction of particles that is able to cross the barrier by different mechanisms and reaches specific cells in deeper layers of the skin, lung, or gastrointestinal tract before these particles can enter small capillary blood vessels.

To detect and—even better—to quantify these small amounts of nanoparticles in the body is a very tough experimental challenge. To quantify nanoparticles in biological surroundings, a number of methods have been used which attempt to exploit specific chemical properties of the respective class of matter. Quantum dots, for example, show a very strong and stable fluorescence which renders these particles identifiable even in living tissue by confocal microscopy. In order to better separate the signals from nonspecific noise, the wavelength of the fluorescence maxima can even be tuned by simply changing the size of the particles. A number of drug delivery nanodevices have been used to document an apparent successful overcoming of multiple gastrointestinal barriers using Quantum dots composite particles [224]. However, as discussed before, a true and sensitive quantification by fluorescence alone is almost impossible, especially when only a small uptake of particles can be expected.

As shown already in Fig. 12.5, radiolabelling of nanoparticles is a sensitive and reliable technique and represents so far the methodological gold standard to investigate the translocation of nanoparticles into the body. But also with radiolabelled probes, the detection of minor translocation processes requires special techniques and equipment. ^{59}Fe is an isotope radiating hard γ-rays which makes it easy to measure small amounts of incorporated ^{59}Fe in living mice by whole-body-counting. This technique has been used successfully to measure particokinetics and biodistribution in nanoscience. Consequently, much is known about iron-oxide based nanoparticles including the uptake from the intestinal tract [58, 222, 225, 226].

The group of Wolfgang Kreyling has studied the translocation of radiolabelled gold nanoparticles. The advantage of AuNP is the availability of a wide range of possible core diameters and Au can easily be neutron-activated to form ^{198}Au, a weak γ-radiating isotope with rather short half-life (2.7 d). These characteristics make, however, the analysis of low activities of ^{198}Au in tissue samples less sensitive compared to ^{59}Fe, especially when no whole body counter is available. When the translocation of intratracheally instilled ^{198}Au-particles with different size (1.4–200 nm)

was analysed in rats, low ^{198}Au activities were measured in different tissues such as liver and spleen, with a significant translocation into organs only for the small particles (1.4 and 2.8 nm) [227]. It appears likely that the small particles can cross the very thin air-blood-barrier to the circulation. A similar approach was performed with intra-esophagal installation of ^{198}AuNP. Again, only small amounts of ^{198}AuNP reached the circulation (after 24 h, $0.37 \pm 0.10\%$ for 1.4 nm particles; $0.12 \pm 0.02\%$ for 18 nm particles) with some methodological problems to properly define a reliable 100%-reference value for the short investigation time span of 24 h. The highest amount of the applied particles was detected in the remaining carcass, which encompassed adipose tissue, bones, muscles and skin [228]. Thus, from the studies with radiolabelled iron- or gold particles it can be concluded that nanoparticles with a typical size of 10–20 nm are almost not absorbed from the normal intestinal tract of rodents. The very small ^{198}Au-particles (1.4 nm) may be different, but also here is the absorption very limited.

What remains unclear is the biodistribution of particles that can cross the epithelial layer in the gastrointestinal tract. A true translocation of a particle through a cell has so far not been unequivocally established. As mentioned above, many cells can engulf particulate matter to a certain extent, and they will always try to degrade xenobiotic particles with different success, macrophages being most potent for this. As for the epithelial cells in the intestinal lining, intracellularly located particles may face another fate altogether: Considering that the cells in the gastrointestinal tract have a short half-life of several days only, a major fraction of particles taken up directly by epithelial cells in the gut will not reach the circulation, but be expelled by exfoliation. Another fraction may be taken up by tissue-based macrophages via phagocytosis and will be metabolised within these cells, and components (including e.g. radiolabels) will then reach the circulation. Some cells which have taken up highly toxic nanoparticles could also die of apoptosis and remnant particles, located in siderosomes may be taken up by other cells. Thus, the biodistribution will be very much different from experiments with intravenous application with a more local distribution apart from the MPS system.

12.7 Conclusions

Nanoparticles, most abundant from natural sources, but increasingly also as engineered substances, are perpetually present in the environment and in the food chain. Ingestion and uptake from the gastrointestinal tract represents one of the most relevant routes for unintended exposure to nanoparticles.

A main process that nanoparticles have to face in stomach and intestine is digestion mediated by hydrochloric acid as well as hydrolytic enzymes. Many nanoparticles with limited colloidal stability will thereby shrink and liberate all kinds of ingredients. Released low molecular weight components may then be taken up by the intestinal epithelial cells utilizing transport mechanisms originally intended for uptake of nutrients. As far as dietary useful components are concerned, their release

from nanoparticles would simply contribute to nutrition. With any toxic ingredient such as Cd^{2+} from Quantum dots, or Ag^{+} from AgNP, release from nanoparticles would fall into the field of toxicology of bulk materials. Yet, within all logical considerations, the expected concentration should be well below any permissive limit values.

It may be that very small sized nanoparticles can directly cross the intestinal barriers to a small but significant degree, reach the circulation, but then are mostly excreted by the kidneys due to their small size (<4–5 nm). A controlled uptake of rather large particles in the micrometer size range can be mediated by M cells and dendritic cells. However, due to the low number of these cells, this represents only a limited uptake possibility for nanoparticles. Another uptake route for nanoparticles could be the consequence of recurring epithelial leakages resulting in paracellular influx. Inflammatory bowel diseases may trigger the formation of spontaneous fissures, and—discussed at the moment—the gut epithelium may partly lose its barrier function towards nanoparticles in diseases such as Crohn's disease.

A matter of high relevance when looking at the fate of nanoparticles in the gastrointestinal tract is the issue of drug delivery since the oral application route is highly attractive for the administration of drugs and mucosal vaccines. In this field, many studies using larger drug-delivery nanoconstructs have been published. However, successful achievement on the oral route was more often proclaimed than conclusive experimental data was given. Clearly more in vivo studies in health and disease using better quantification techniques are needed, because the relevance of cell culture studies for this purpose is more than questionable.

So far, the experimental evidence shows that the uptake of nanoparticles from the intestine in vivo is very limited. It appears that the gastrointestinal tract is a very complex organ that can quite well discriminate between valuable dietary ingredients, which are taken up by a battery of specific uptake mechanisms, and worthless particles, which hardly can overcome effective barriers in the healthy gut.

Therefore, despite the risk of increasing amounts of engineered nanomaterial in the food chain, a harmful acute or chronic poisoning with ingested nanoparticles seems to be highly unlikely at this point in time.

References

1. Piccinno, F., Gottschalk, F., Seeger, S., Nowack, B.: Industrial production quantities and uses of ten engineered nanomaterials in Europe and the world. J. Nanopart. Res. **14**, 1109 (2012). https://doi.org/10.1007/s11051-012-1109-9
2. Ostiguy, C., Roberge, B., Woods, C., Soucy, B.: Engineered Nanoparticles: Current Knowledge about OHS Risks and Prevention Measures, 2nd edn. Institut de recherche Robert-Sauvé en santé et en sécurité du travail (2010). ISBN 2896314792, 9782896314799. https://www.irsst.qc.ca/en/publications-tools/publication/i/100529/n/engineered-nanoparticles-current-knowledge-about-occupational-health-and-safety-risks-and-prevention-measures-second-edition-r-656/redirected/1

3. Griffin, S., Masood, M.I., Nasim, M.J., Sarfraz, M., Ebokaiwe, A.P., Schäfer, K.-H., Keck, C.M., Jacob, C.: Natural nanoparticles: a particular matter inspired by Nature. Antioxidants **7**, 3 (2018). https://doi.org/10.3390/antiox7010003
4. Boccuni, F., Ferrante, R., Tombolini, F., Lega, D., Antonini, A., Alvino, A., Pingue, P., Beltram, F., Sorba, L., Piazza, V., Gemmi, M., Porcari, A., Iavicoli, S.: Workers' exposure to nano-objects with different dimensionalities in R&D laboratories: measurement strategy and field studies. Int. J. Mol. Sci. **19**, 349–377 (2018). https://doi.org/10.3390/ijms19020349
5. Kirch, J., Guenther, M., Doshi, N., Schaefer, U.F., Schneider, M., Mitragotri, S., Lehr, C.-M.: Mucociliary clearance of micro- and nanoparticles is independent of size, shape and charge—an ex vivo and in silico approach. J. Control Rel. **159**, 128–134 (2012). https://doi.org/10.1016/j.jconrel.2011.12.015
6. Pan, K., Zhong, Q.: Organic nanoparticles in foods: fabrication, characterization and utilization. Annu. Rev. Food Sci. Technol. **7**, 245–266 (2016). https://doi.org/10.1146/annurev-food-041715-033215
7. Sekhon, B.S.: Food nanotechnology—an overview. Nanotechnol. Sci. Appl. **3**, 1–15 (2010). https://doi.org/10.2147/NSA.S8677
8. Herbst, E.F.G.: Das Lymphgefäßsystem und seine Verrichtungen, pp. 333–337, Göttingen (1844)
9. Hirsch, R.: Über das Vorkommen von Stärkekörnern im Blut und im Urin. Z. Exp. Path. Ther. **3**, 390 (1906)
10. Volkheimer, G.: Detection of starch in tissue and urine after oral starch intake. Dtsch Gesundheitsw **15**, 1298–1302 (1960)
11. Jani, P.U., Florence, A.T., McCarthy, D.E.: Further histological evidence of the gastrointestinal absorption of polystyrene nanospheres in the rat. Int. J. Pharm. **84**, 245–252 (1992). https://doi.org/10.1016/0378-5173(92)90162-U
12. Alpar, H.O., Field, W.N., Hyde, R., Lewis, D.A.: The transport of microspheres from the gastro-intestinal tract to inflammatory air pouches in the rat. J. Pharm. Pharmacol. **41**, 194–196 (1989). https://doi.org/10.1111/j.2042-7158.1989.tb06429.x
13. Payne, J.M., Sansom, B.F., Garner, R.J., Thomson, A.R., Miles, B.J.: Uptake of small resin particles (1-5 μ diameter) by the alimentary canal of the calf. Nature **188**, 586–587 (1960). https://doi.org/10.1038/188586a0
14. Pontefract, R.D., Cunningham, H.M.: Penetration of asbestos through the digestive tract of rats. Nature **243**, 352–353 (1973). https://doi.org/10.1038/243352a0
15. Sanders, E., Ashworth, C.T.: A study of particulate intestinal absorption and hepatocellular uptake: Use of polystyrene latex particle. Exp. Cell Res. **22**, 137–145 (1961). https://doi.org/10.1016/0014-4827(61)90092-1
16. Hodges, G.M., Carr, E.A., Hazzard, R.A., O'Reilly, C., Carr, K.E.: A commentary on morphological and quantitative aspects of microparticle translocation across the gastrointestinal mucosa. J. Drug Target. **3**, 57–60 (1995). https://doi.org/10.3109/10611869509015934
17. Ebel, J.P.: A method for quantifying particle absorption from the small intestine of the mouse. Pharm. Res. **7**, 848–851 (1990). https://doi.org/10.1023/A:1015964916486
18. Limpanussorn, J., Simon, L., Dayan, A.D.D.: Transepithelial transport of large particles in rat: a new model for the quantitative study of particle uptake. J. Pharm. Pharmacol. **50**, 753–760 (1998). https://doi.org/10.1111/j.2042-7158.1998.tb07136.x
19. Powell, J.J., Faria, N., Thomas-McKay, E., Pele, L.C.: Origin and fate of dietary nanoparticles and microparticles in the gastrointestinal tract. J. Autoimmun. **34**, J226–J233 (2010). https://doi.org/10.1016/j.jaut.2009.11.006
20. Fröhlich, E., Mercuri, A., Wu, S., Salar-Behzadi, S.: Measurements of deposition, lung surface area and lung fluid for simulation of inhaled compounds. Front. Pharmacol. **7**, 181 (2016). https://doi.org/10.3389/fphar.2016.00181
21. Squier, C.A., Kremer, M.J.: Biology of oral mucosa and esophagus. J. Natl. Cancer Inst. Monogr. **29**, 7–15 (2001). https://doi.org/10.1093/oxfordjournals.jncimonographs.a003443
22. Squier, C.A.: The permeability of keratinized and nonkeratinized oral epithelium to horseradish peroxidase. J. Ultrastruct. Res. **43**, 160–177 (1973). https://doi.org/10.1016/S0022-5320(73)90076-2

23. Squier, C.A.: The permeability of oral mucosa. Crit. Rev. Oral Biol. Med. **2**, 13–32 (1991)
24. Ramaker, K., Bade, S., Röckendorf, N., Meckelein, B., Vollmer, E., Schulz, H., Fröschle, G.-W., Frey, A.: Absence of the epithelial glycocalyx as potential tumor marker for the early detection of colorectal cancer. PLoS ONE **11**, e0168801 (2016). https://doi.org/10.1371/journal.pone.0168801
25. Bullen, T.F., Forrest, S., Campbell, F., Dodson, A.R., Hershman, M.J., Pritchard, D.M., Turner, J.R., Montrose, M.H., Watson, A.J.M.: Characterization of epithelial cell shedding from human small intestine. Lab. Invest. **86**, 1052–1063 (2006). https://doi.org/10.1038/labinvest.3700464
26. Madara, J.L.: Maintenance of the macromolecular barrier at cell extrusion sites in intestinal epithelium: physiological rearrangement of tight junctions. J. Mem. Biol. **116**, 177–184 (1990)
27. Marchiando, A.M., Shen, L., Graham, W.V., Edelblum, K.L., Duckworth, C.A., Guan, Y., Montrose, M.H., Turner, J.R., Watson, A.J.M.: The epithelial barrier is maintained by in vivo tight junction expansion during pathologic intestinal epithelial shedding. Gastroenterology **140**, 1208–1218 (2011). https://doi.org/10.1053/j.gastro.2011.01.004
28. Watson, A.J.M., Chu, S., Sieck, L., Gerasimenko, O., Bullen, T., Campbell, F., McKenna, M., Rose, T., Montrose, M.H.: Epithelial barrier function in vivo is sustained despite gaps in epithelial layers. Gastroenterology **129**, 902–912 (2005). https://doi.org/10.1053/j.gastro.2005.06.015
29. Frey, A., Giannasca, K.T., Weltzin, R., Giannasca, P.J., Reggio, H., Lencer, W.I., Neutra, M.R.: Role of the glycocalyx in regulating access of microparticles to apical plasma membranes of intestinal epithelial cells: implications for microbial attachment and oral vaccine targeting. J. Exp. Med. **184**, 1045–1059 (1996). https://doi.org/10.1084/jem.184.3.1045
30. Pelasayed, T., Bergström, J.H., Gustafsson, J.K., Ermund, A., Birchenough, G.M.H., Schütte, A., van der Post, S., Svensson, F., Rodríguez-Piñeiro, A.M., Nyström, E.E.L., Wising, C., Johansson, M.E.V., Hansson, G.C.: The mucus and mucins of the goblet cells and enterocytes provide the first defense line of the gastrointestinal tract and interact with the immune system. Immunol. Rev. **260**, 8–20 (2014). https://doi.org/10.1111/imr.12182
31. Johansson, M.E.V., Sjövall, H., Hansson, G.C.: The gastrointestinal mucus system in health and disease. Nat. Rev. Gastroenterol. Hepatol. **10**, 352–361 (2013). https://doi.org/10.1038/nrgastro.2013.35
32. Neutra, M.R., Forstner, J.F.: Gastrointestinal mucus: synthesis, secretion, and function. In: Johnson, L.R. (ed.) Physiology of the Gastrointestinal Tract. Raven Press: New York, NY, U.S.A, (1987)
33. Johansson, M.E.V., Phillipson, M., Petersson, J., Velcich, A., Holm, L., Hansson, G.C.: The inner of the two MUC2 mucin-dependent mucus layers in colon is devoid of bacteria. Proc. Natl. Acad. Sci. U.S.A. **105**, 15064–15069 (2008). https://doi.org/10.1073/pnas.0803124105
34. Busch, A.E., Herzer, T., Waldegger, S., Schmidt, F., Palacin, M., Biber, J., Markovich, D., Murer, H., Lang, F.: Opposite directed currents induced by the transport of dibasic and neutral amino acids in Xenopus oocytes expressing the protein rBAT. J. Biol. Chem. **269**, 25581–25586 (1994)
35. Palacín, M., Kanai, Y.: The ancillary proteins of HATs: SLC3 family of amino acid transporters. Pflugers Arch. Eur. J. Physiol. **447**, 490–494 (2004). https://doi.org/10.1007/s00424-003-1062-7
36. Howard, A., Hirst, B.H.: The glycine transporter GLYT1 in human intestine: expression and function. Biol. Pharm. Bull. **34**, 784–788 (2011). https://doi.org/10.1248/bpb.34.784
37. Pramod, A.B., Foster, J., Carvelli, L., Henry, L.K.: SLC6 transporters: structure, function, regulation, disease association and therapeutics. Mol. Asp. Med. **34**, 197–219 (2013). https://doi.org/10.1016/j.mam.2012.07.002
38. Bröer, A., Klingel, K., Kowalczuk, S., Rasko, J.E.J., Cavanaugh, J., Bröer, S.: Molecular cloning of mouse amino acid transport system B0, a neutral amino acid transporter related to Hartnup Disorder. J. Biol. Chem. **279**, 24467–24476 (2004). https://doi.org/10.1074/jbc.M400904200

39. Takanaga, H., Mackenzie, B., Suzuki, Y., Hediger, M.A.: Identification of mammalian proline transporter SIT1 (SLC6A20) with characteristics of classical System Imino. J. Biol. Chem. **280**, 8974–8984 (2005). https://doi.org/10.1074/jbc.M413027200
40. Thwaites, D.T., Anderson, C.M.H.: The SLC36 family of proton-coupled amino acid transporters and their potential role in drug transport. Br. J. Pharmacol. **164**, 1802–1816 (2011). https://doi.org/10.1111/j.1476-5381.2011.01438.x
41. Douard, V., Ferraris, R.P.: Regulation of the fructose transporter GLUT5 in health and disease. Am. J. Physiol. **295**, E227–E237 (2008). https://doi.org/10.1152/ajpendo.90245.2008
42. Wright, E.M.: Glucose transport families SLC5 and SLC50. Mol. Asp. Med. **34**, 183–196 (2013). https://doi.org/10.1016/j.mam.2012.11.002
43. Wright, E.M., Turk, E.: The sodium/glucose cotransport family SLC5. Pflugers Arch. Eur. J. Physiol. **447**, 510–518 (2004). https://doi.org/10.1007/s00424-003-1063-6
44. Barley, N.F., Howard, A., O'Callaghan, D., Legon, S., Walters, J.R.F.: Epithelial calcium transporter expression in human duodenum. Am. J. Physiol. **280**, G285–G290 (2001). https://doi.org/10.1152/ajpgi.2001.280.2.G285
45. Vesey, D.A.: Transport pathways for cadmium in the intestine and kidney proximal tubule: focus on the interaction with essential metals. Toxicol. Lett. **198**, 13–19 (2010). https://doi.org/10.1016/j.toxlet.2010.05.004
46. Mackenzie, B., Hediger, M.A.: SLC11 family of H + -coupled metal-ion transporters NRAMP1 and DMT1. Pflugers Arch. Eur. J. Physiol. **447**, 571–579 (2004). https://doi.org/10.1007/s00424-003-1141-9
47. Hashimoto, A., Kambe, T.: Mg, Zn and Cu transport proteins: a brief overview from physiological and molecular perspectives. J. Nutr. Sci. Vitaminol. **61**, S116–S118 (2015). https://doi.org/10.3177/jnsv.61.S116
48. Voets, T., Nilius, B., Hoefs, S., van der Kemp, A.W.C.M., Droogmans, G., Bindels, R.J.M., Hoenderop, J.G.J.: TRPM6 forms the Mg^{2+} influx channel involved in intestinal and renal Mg^{2+} absorption. J. Biol. Chem. **279**, 19–25 (2004). https://doi.org/10.1074/jbc.M311201200
49. Reboul, E.: Vitamin E bioavailability: mechanisms of intestinal absorption in the spotlight. Antioxidants **6**, 95 (2017). https://doi.org/10.3390/antiox6040095
50. Reboul, E., Borel, P.: Proteins involved in uptake, intracellular transport and basolateral secretion of fat-soluble vitamins and carotenoids by mamalian enterocytes. Prog. Lipid Res. **50**, 388–402 (2011). https://doi.org/10.1016/j.plipres.2011.07.001
51. Anderson, C.M., Stahl, A.: SLC27 fatty acid transport proteins. Mol. Asp. Med. **34**, 516–528 (2013). https://doi.org/10.1016/j.mam.2012.07.010
52. Daniel, H., Kottra, G.: The proton oligopeptide cotransporter family SLC15 in physiology and pharmacology. Pflugers Arch. Eur. J. Physiol. **447**, 610–618 (2004). https://doi.org/10.1007/s00424-003-1101-4
53. May, J.M.: The SLC23 family of ascorbate transportes: ensuring that you get and keep your daily dose of vitamin C. Br. J. Pharmacol. **164**, 1793–1801 (2011). https://doi.org/10.1111/j.1476-5381.2011.01350.x
54. Yonezawa, A., Inui, K.: Novel riboflavin transporter family RFVT/SLC52: identification, nomenclature, functional characterization and genetic diseases of RFVT/SLC52. Mol. Asp. Med. **34**, 693–701 (2013). https://doi.org/10.1016/j.mam.2012.07.014
55. Zhao, R., Goldman, I.D.: Folate and thiamine transporters mediated by facilitative carriers (SLC19A1-3 and SLC46A1) and folate receptors. Mol. Asp. Med. **34**, 373–385 (2013). https://doi.org/10.1016/j.mam.2012.07.006
56. Ganapathy, V., Smith, S.B., Prasad, P.D.: SLC19: the folate/thiamine transporter family. Pflugers Arch. Eur. J. Physiol. **447**, 641–646 (2004). https://doi.org/10.1007/s00424-003-1068-1
57. Roth, M., Obaidat, A., Hagenbuch, B.: OATPs, OATs and OCTs: the organic anion and cation transporters of the SLCO and SLC22A gene superfamilies. Brit. J. Pharmacol. **165**, 1260–1287 (2012). https://doi.org/10.1111/j.1476-5381.2011.01724.x

58. Bargheer, D., Giemsa, A., Freund, B., Heine, M., Waurisch, C., Stachowski, G.M., Hickey, S.G., Eychmüller, A., Heeren, J., Nielsen, P.: The distribution and degradation of radiolabeled superparamagnetic iron oxide nanoparticles and quantum dots in mice. Beilstein J. Nanotechnol. **6**, 111–123 (2015). https://doi.org/10.3762/bjnano.6.11
59. Heinrich, H.C.: Diagnostik, Ätiologie und Therapie des Eisenmangels unter besonderer Berücksichtigung der 59Fe-Retentionsmessung im Gesamtkörper-Radioaktivitätsdetektor. Der Nuklearmediziner **137**, 137–269 (1983)
60. Bruns, O.T., Ittrich, H., Peldschus, K., Kaul, M.G., Tromsdorf, U.I., Lauterwasser, J., Nikolic, M.S., Mollwitz, B., Merkel, M., Bigall, N.C., Sapra, S., Reimer, R., Hohenberg, H., Weller, H., Eychmüller, A., Adam, G., Beisiegel, U., Heeren, J.: Real-time magnetic resonance imaging and quantification of lipoprotein metabolism in vivo using nanocrystals. Nat. Nanotechnol. **4**, 193–201 (2009). https://doi.org/10.1038/nnano.2008.405
61. Kottwitz, K., Laschinsky, N., Fischer, R., Nielsen, P.: Absorption, excretion and retention of ^{51}Cr from labelled Cr-(III)-picolinate in rats. Biometals **22**, 289–295 (2009). https://doi.org/10.1007/s10534-008-9165-4
62. Chen, N., He, Y., Su, Y., Li, X., Huang, Q., Wang, H., Zhang, X., Tai, R., Fan, C.: The cytotoxicity of cadmium-based quantum dots. Biomaterials **33**, 1238–1244 (2012). https://doi.org/10.1016/j.biomaterials.2011.10.070
63. Cho, S.J., Maysinger, D., Jain, M., Röder, B., Hackbarth, S., Winnik, F.M.: Long-term exposure of CdTe quantum dots causes functional impairments in live cells. Langmuir **23**, 1974–1980 (2007). https://doi.org/10.1021/la060093j
64. Hardman, R.: A toxicological review of quantum dots: toxicity depends on physicochemical and environmental factors. Environ. Health Perspect. **114**, 165–172 (2006). https://doi.org/10.1289/ehp.8284
65. Hoshino, A., Hanada, S., Yamamoto, K.: Toxicity of nanocrystal quantum dots: the relevance of surface modifications. Arch. Toxicol. **85**, 707–720 (2011). https://doi.org/10.1007/s00204-011-0695-0
66. Winnik, F.M., Maysinger, D.: Quantum dot cytotoxicity and ways to reduce it. Acc. Chem. Res. **46**, 672–680 (2013). https://doi.org/10.1021/ar3000585
67. Zheng, X., Tian, J., Weng, L., Wu, L., Jin, Q., Zhao, J., Wang, L.: Cytotoxicity of cadmium-containing quantum dots based on a study using a microfluidic chip. Nanotechnology **23**, 055102 (2012). https://doi.org/10.1088/0957-4484/23/5/055102
68. Loginova, Y.F., Dezhurov, S.V., Zherdeva, V.V., Kazachkina, N.I., Wakstein, M.S., Savitsky, A.P.: Biodistribution and stability of CdSe core quantum dots in mouse digestive tract following per os administration: Advantages of double polymer/silica coated nanocrystals. Biochem. Biophys. Res. Commun. **419**, 54–59 (2012). https://doi.org/10.1016/j.bbrc.2012.01.123
69. Mohs, A.M., Duan, H., Kairdolf, B.A., Smith, A.M., Nie, S.: Proton-resistant quantum dots: stability in gastrointestinal fluids and implications for oral delivery of nanoparticle agents. Nano Res. **2**, 500–508 (2009). https://doi.org/10.1007/s12274-009-9046-3
70. Mancini, M.C., Kairdolf, B.A., Smith, A.M., Nie, S.: Oxidative quenching and degradation of polymer-encapsulated quantum dots: new insights into the long term fate and toxicity of nanocrystals in-vivo. J. Am. Chem. Soc. **130**, 10836–10837 (2008). https://doi.org/10.1021/ja8040477
71. Smith, A.M., Duan, H., Rhyner, M.N., Ruan, G., Nie, S.: A systematic examination of surface coatings on the optical and chemical properties of semiconductor quantum dots. Phys. Chem. Chem. Phys. **8**, 3895–3903 (2006). https://doi.org/10.1039/b606572b
72. Min, K.S., Sano, E., Ueda, H., Sakazaki, F., Yamada, K., Takano, M., Tanaka, K.: Dietary deficiency of calcium and/or iron, an age-related risk factor for renal accumulation of cadmium in Mice. Biol. Pharm. Bull. **38**, 1557–1563 (2015)
73. Hauck, T.S., Anderson, R.E., Fischer, H.C., Newbigging, S., Chan, W.C.W.: In vivo quantum-dot toxicity assessment. Small **6**, 138–144 (2010). https://doi.org/10.1002/smll.200900626
74. Rzigalinski, B.A., Strobl, J.S.: Cadmium-containing nanoparticles: perspectives on pharmacology and toxicology of quantum dots. Toxicol. Appl. Pharmacol. **238**, 280–288 (2009). https://doi.org/10.1016/j.taap.2009.04.010

75. Tsoi, K.M., Dai, Q., Alman, B.A., Chan, W.C.: Are quantum dots toxic? Exploring the discrepancy between cell culture and animal studies. Acc. Chem. Res. **46**, 662–671 (2013). https://doi.org/10.1021/ar300040z
76. Liu, Y., Li, Y., Liu, K., Shen, J.: Exposing to cadmium stress cause profound toxic effect on microbiota of the mice intestinal tract. PLoS ONE **9**, e85323 (2014). https://doi.org/10.1371/journal.pone.0085323
77. Breton, J., Daniel, C., Dewulf, J., Pothion, S., Froux, N., Sauty, M., Thomas, P., Pot, B., Foligné, B.: Gut microbiota limits heavy metals burden caused by chronic oral exposure. Toxicol. Lett. **222**, 132–138 (2013). https://doi.org/10.1016/j.toxlet.2013.07.021
78. Zhai, Q., Yin, R., Yu, L., Wang, G., Tian, F., Yu, R., Zhao, J., Liu, X., Chen, Y.Q., Zhang, H., Chen, W.: Screening of lactic acid bacteria with potential protective effects against cadmium toxicity. Food Control **54**, 23–30 (2015). https://doi.org/10.1016/j.foodcont.2015.01.037
79. Breton, J., Massart, S., Vandamme, P., De Brandt, E., Pot, B., Foligné, B.: Ecotoxicology inside the gut: impact of heavy metals on the mouse microbiome. BMC Pharmacol. Toxicol. **14**, 62 (2013). https://doi.org/10.1186/2050-6511-14-62
80. Tiwari, R., Singh, R.D., Khan, H., Gangopadhyay, S., Mittal, S., Singh, V., Arjaria, N., Shankar, J., Roy, S.K., Singh, D., Srivastava, V.: Oral subchronic exposure to silver nanoparticles causes renal damage through apoptotic impairment and necrotic cell death. Nanotoxicology **11**, 671–686 (2017). https://doi.org/10.1080/17435390.2017.1343874
81. Nielsen, P.: Chelation therapy for heavy metals. In: Crichton, R., Ward, R.J., Hider, R.C., (eds.) Metal Chelation in Medicine. The Royal Society of Chemistry (2016). https://doi.org/10.1039/9781782623892
82. Lo, D.D.: Vigilance or subversion? Constitutive and inducible M cells in mucosal tissues. Trends Immunol. **39**, 185–195 (2017). https://doi.org/10.1016/j.it.2017.09.002
83. Mantis, N.J., Frey, A., Neutra, M.R.: Accessibility of glycolipid and oligosaccharide epitopes on rabbit villus and follicle-associated epithelium. Am. Physiol. **278**, G915–G923 (2000). https://doi.org/10.1152/ajpgi.2000.278.6.G915
84. Bonnardel, J., Da Silva, C., Henri, S., Tamoutounour, S., Chasson, L., Montaña-Sanchis, F., Gorvel, J.-P., Lelouard, H.: Innate and adaptive immune functions of Peyer's patch monocyte-derived cells. Cell Rep. **11**, 770–784 (2015). https://doi.org/10.1016/j.celrep.2015.03.067
85. Neutra, M.R., Frey, A., Kraehenbuhl, J.-P.: Epithelial M cells: gateways for mucosal infection and immunization. Cell **86**, 345–348 (1996). https://doi.org/10.1016/S0092-8674(00)80106-3
86. Rescigno, M., Urbano, M., Valzasina, B., Francolini, M., Rotta, G., Bonasio, R., Granucci, F., Kraehenbuhl, J.-P., Ricciardi-Castagnoli, P.: Dendritic cells express tight junction proteins and penetrate gut epithelial monolayers to sample bacteria. Nat. Immunol. **2**, 361–367 (2001). https://doi.org/10.1038/86373
87. Jung, C., Hugot, J.-P., Barreau, F.: Peyer's patches: the immune sensors of the intestine. Int. J. Inflamm. **2010**, 823710 (2010). https://doi.org/10.4061/2010/823710
88. Knoop, K.A., Kumar, N., Butler, B.R., Sakthivel, S.K., Taylor, R.T., Nochi, T., Akiba, H., Yagita, H., Kiyono, H., Williams, I.R.: RANKL is necessary and sufficient to initiate development of antigen-sampling M cells in the intestinal epitelium. J. Immunol. **183**, 5738–5747 (2009). https://doi.org/10.4049/jimmunol.0901563
89. Kanaya, T., Ohno, H.: The mechanisms of M cell differentiation. Biosci. Microbiota Food Health **33**, 91–97 (2014). https://doi.org/10.12938/bmfh.33.91
90. Jang, M.H., Kweon, M.-N., Iwatani, K., Yamamoto, M., Terahara, K., Sasakawa, C., Suzuki, T., Nochi, T., Yokota, Y., Rennert, P.D., Hiroi, T., Tamagawa, H., Iijima, H., Kunisawa, J., Yuki, Y., Kiyono, H.: Intestinal villous M cells: an antigen entry site in the mucosal epithelium. Proc. Natl. Acad. Sci. U.S.A **101**, 6110–6115 (2004). https://doi.org/10.1073/pnas.0400969101
91. Lelouard, H., Fallet, M., De Boris, B., Méresse, S., Gorvel, J.-P.: Peyer's patch dendritic cells sample antigens by extending dendrites through M-cell specific transcellular pores. Gastroenterology **142**, 592–601 (2012). https://doi.org/10.1053/j.gastro.2011.11.039
92. Pelasayed, T., Gustafsson, J.K., Gustafsson, I.J., Ermund, A., Hansson, G.C.: Carbachol-induced MUC-17 endocytosis is concomitant with NHE3 internalization and CFTR membrane

recruitment in enterocytes. Am. J. Physiol. **305**, C457–C467 (2013). https://doi.org/10.1152/ajpcell.00141.2013
93. Silveira, J.R., Raymond, G.J., Hughson, A.G., Race, R.E., Sim, V.L., Hayes, S.F., Caughy, B.: The most infectious prion particles. Nature **437**, 257–261 (2005). https://doi.org/10.1038/nature03989
94. Bade, S., Frey, A.: Potential of active and passive immunizations for the prevention and therapy of transmissible spongiform encephalopathies. Expert Rev. Vaccines **6**, 153–168 (2007). https://doi.org/10.1586/14760584.6.2.153
95. Donaldson, D.S., Kobayashi, A., Ohno, H., Yagita, H., Williams, I.R., Mabbott, N.A.: M cell-depletion blocks oral prion disease pathogenesis. Mucosal Immunol. **5**, 216–225 (2012). https://doi.org/10.1038/mi.2011.68
96. Donaldson, D.S., Sehgal, A., Rios, D., Williams, I.R., Mabbott, N.A.: Increased abundance of M cells in the gut epithelium dramatically enhances oral prion disease susceptibility. PLoS Pathog. **12**, e1006075 (2016). https://doi.org/10.1371/journal.ppat.1006075
97. Ermak, T.H., Dougherty, E.P., Bhagat, H.R., Kabok, Z., Papp, J.: Uptake and transport of copolymer biodegradable microspheres by rabbit Peyer's patch M cells. Cell Tissue Res. **279**, 433–436 (1995). https://doi.org/10.1007/BF00318501
98. Foged, C., Brodin, B., Frokjaer, S., Sundblad, A.: Particle size and surface charge affect particle uptake by human dendritic cells in an in vitro model. Int. J. Pharm. **298**, 315–322 (2005). https://doi.org/10.1016/j.ijpharm.2005.03.035
99. Gebert, A., Steinmetz, I., Fassbender, S., Wendlandt, K.-H.: Antigen transport into Peyer's patches: Increased uptake by constant numbers of M cells. Am. J. Pathol. **164**, 65–72 (2004). https://doi.org/10.1016/s0002-9440(10)63097-0
100. Jepson, M., Simmons, N.L., O'Hagan, D.T., Hirst, B.H.: Comparison of poly(DL-lactide-co-glycolide) and polystyrene microsphere targeting to intestinal M cells. J. Drug Target. **1**, 245–249 (1993). https://doi.org/10.3109/10611869308996082
101. Jepson, M.A., Simmons, N.L., Savidge, T.C., James, P.S., Hirst, B.H.: Selective binding and transcytosis of latex microspheres by rabbit intestinal M cells. Cell Tissue Res. **271**, 399–405 (1993). https://doi.org/10.1007/BF02913722
102. Pappo, J., Ermak, T.H.: Uptake and translocation of fluorescent latex particles by rabbit Peyer's patch follicle epithelium: a quantitative model for M cell uptake. Clin. Exp. Immunol. **76**, 144–148 (1989)
103. Berg, R.D.: Bacterial translocation from the gastrointestinal tract. Trends Microbiol. **3**, 149–154 (1995). https://doi.org/10.1016/S0966-842X(00)88906-4
104. Gewirtz, A.T., Navas, T.A., Lyons, S., Godowski, P.G., Madara, J.L.: Cutting edge: bacterial flagellin activates basolaterally expressed TLR5 to induce epithelial proinflammatory gene expression. J. Immunol. **167**, 1882–1885 (2001). https://doi.org/10.4049/jimmunol.167.4.1882
105. Husebye, E.: The pathogenesis of gastrointestinal bacterial overgrowth. Chemotherapy **51**(Suppl1), 1–22 (2005). https://doi.org/10.1159/000081988
106. Berkes, J., Viswanathan, V.K., Savkovic, S.D., Hecht, G.: Intestinal epithelial responses to enteric pathogens: effects on the tight junction barrier, ion transport, and inflammation. Gut **52**, 439–451 (2003). https://doi.org/10.1136/gut.52.3.439
107. Mukiza, C.N., Dubreuil, J.D.: Escherichia coli heat-stable toxin b impairs intestinal barrier function by altering tight junction proteins. Infect. Immun. **81**, 2819–2827 (2013). https://doi.org/10.1128/IAI.00455-13
108. Ugalde-Silva, P., Gonzalez-Lugo, O., Navarro-Garcia, F.: Tight junction disruption induced by type 3 secretion system effectors injected by enteropathogenic and enterohemorrhagic *Escherichia coli*. Front. Cell Infect. Mirobiol. **6**, 87 (2016). https://doi.org/10.3389/fcimb.2016.00087
109. Freeman, H.J.: Spontaneous free perforation of the small intestine in adults. World J. Gastroenterol. **20**, 9990–9997 (2014). https://doi.org/10.3748/wjg.v20.i29.9990
110. Laukoetter, M.G., Nava, P., Nusrat, A.: Role of the intestianal barrier in inflammatory bowel disease. World J. Gastroenterol. **14**, 401–407 (2008). https://doi.org/10.3748/wjg.14.401

111. Schmitz, H., Barmeyer, C., Fromm, M., Runkel, N., Foss, H.-D., Bentzel, C.J., Rieken, E.-O., Schulzke, J.-D.: Altered tight junction structure contributes to the impaired epithelial barrier function in ulcerative colitis. Gastroenterology **116**, 301–309 (1999). https://doi.org/10.1016/S0016-5085(99)70126-5
112. Lechuga, S., Ivanov, A.I.: Disruption of the epithelial barrier during intestinal inflammation: quest for new molecules and mechanisms. Biochim. Biophys. Acta **1864**, 1183–1194 (2017). https://doi.org/10.1016/j.bbamcr.2017.03.007
113. Lautenschläger, C., Schmidt, C., Lehr, C.-M., Fischer, D., Stallmach, A.: PEG-functionalized microparticles selectively target inflamed mucosa in inflammatory bowel disease. Eur. J. Pharm. Biopharm. **85**, 578–586 (2013). https://doi.org/10.1016/j.ejpb.2013.09.016
114. Champion, J.A., Mitragotri, S.: Role of target geometry in phagocytosis. Proc. Natl. Acad. Sci. U.S.A. **103**, 4930–4934 (2006). https://doi.org/10.1073/pnas.0600997103
115. Docter, D., Westmeier, D., Markiewicz, M., Stolte, S., Knauer, S.K., Staubert, R.H.: The nanoparticle biomolecule corona: lessons learned—challenge accepted? Chem. Soc. Rev. **44**, 6094–6121 (2015). https://doi.org/10.1039/c5cs00217f
116. Lundqvist, M., Stigler, J., Elia, G., Lynch, I., Cedervall, T., Dawson, K.A.: Nanoparticle size and surface properties determine the protein corona with possible implications for biological impacts. Proc. Natl. Acad. Sci. U.S.A. **105**, 14265–14270 (2008). https://doi.org/10.1073/pnas.0805135105
117. Saptarshi, S.R., Duschi, A., Lopata, A.L.: Interaction of nanoparticles with proteins: relation to bio-reactivity of the nanoparticle. J. Nanobiotech. **11**, 26 (2013). https://doi.org/10.1186/1477-3155-11-26
118. Parsons, B.N., Campbell, B.J., Wigley, P.: Soluble plantain nonstarch polysaccharides, although increasing caecal load, reduce systemic invasion of *Salmonella* gallinarum in the chicken. Lett. Appl. Microbiol. **60**, 347–351 (2014). https://doi.org/10.1111/lam.12377
119. Parsons, B.N., Wigley, P., Simpson, H.L., Williams, J.M., Humphrey, S., Salisbury, A.-M., Watson, A.J.M., Fry, S.C., O'Brien, D., Roberts, C.L., O'Kennedy, N., Keita, A.V., Söderholm, J.D., Rhodes, J.M., Campbell, B.J.: Dietary Supplementation with soluble plantain non-starch polysaccharides inhibits intestinal invasion of *Salmonella* typhimurium in the chicken. PLoS ONE **9**, e87658 (2014). https://doi.org/10.1371/journal.pone.0087658
120. Roberts, C.L., Keita, A.V., Duncan, S.H., O'Kennedy, N., Söderholm, J.D., Rhodes, J.M., Campbell, B.J.: Translocation of Crohn's disease Escherichia coli across M-cells: contrasting effects of soluble plant fibres and emulsifiers. Gut **59**, 1331–1339 (2010). https://doi.org/10.1136/gut.2009.195370
121. Roberts, C.L., Keita, A.V., Parsons, B.N., Prorok-Hamon, M., Knight, P., Winstanley, C., O'Kennedy, N., Söderholm, J.D., Rhodes, J.M., Campbell, B.J.: Soluble plantain fibre blocks adhesion and M-cell translocation of intestinal pathogens. J. Nutr. Biochem. **24**, 97–103 (2013). https://doi.org/10.1016/j.jnutbio.2012.02.013
122. Hochella Jr., M.F., Spencer, M.G., Jones, K.L.: Nanotechnology: nature's gift or scientists' brainchild? Environ. Sci. Nano **2**, 114–119 (2015). https://doi.org/10.1039/c4en00145a
123. Sharma, V.K., Filip, J., Zboril, R., Varma, R.S.: Natural inorganic nanoparticles—formation, fate, and toxicity in the environment. Chem. Soc. Rev. **44**, 8410–8423 (2015). https://doi.org/10.1039/c5cs00236b
124. Griffin, S., Masood, M.I., Nasim, M.J., Sarfraz, M., Ebokaiwe, A.P., Schäfer, K.-H., Keck, C.M., Jacob, C.: Natural nanoparticles: a particular matter inspired by Nature. Antioxidants **7**, 3 (2018). https://doi.org/10.3390/antiox7010003
125. Strambeanu, N., Demetrovici, L., Dragos, D.: Natural sources of nanoparticles. In: Lungu, M. et al. (eds.) Nanoparticles' Promises and Risks. Springer International Publishing Switzerland (2015). https://doi.org/10.1007/978-3-319-11728-7
126. Dykman, L.A., Khlebtsov, N.G.: Gold nanoparticles in biology and medicine: recent advances and prospects. Acta Naturae **3**, 34–55 (2011)
127. Zhang, X.F., Liu, Z.G., Shen, W., Gurunathan, S.: Silver nanoparticles: synthesis, characterization, properties, applications, and therapeutic approaches. Int. J. Mol. Sci. **17**, 1534 (2016). https://doi.org/10.3390/ijms17091534

128. Ali, A., Zafar, H., Zia, M., ul Haq, I., Phull, A.R., Ali, J.S., Hussain, A.: Synthesis, characterization, applications, and challenges of iron oxide nanoparticles. Nanotechnol. Sci. Appl. **9**, 49–67 (2016). https://doi.org/10.2147/NSA.S99986
129. Valizadeh, A., Mikaeili, H., Samiei, M., Farkhani, S.M., Zarghami, N., Kouhi, M., Akbarzadeh, A., Davaran, S.: Quantum dots: synthesis, bioapplications, and toxicity. Nanoscale Res. Lett. **7**, 480 (2012). https://doi.org/10.1186/1556-276X-7-480
130. Pan, K., Zhong, Q.: Organic nanoparticles in foods: fabrication, characterization and utilization. Annu. Rev. Food Sci. Technol. **7**, 245–266 (2016). https://doi.org/10.1146/annurev-food-041715-033215
131. Marcaccio, M., Paolucci, F., eds.: Making and exploiting fullerenes, graphene, and carbon nanotubes. Springer, Berlin, Heidelberg (2014). https://doi.org/10.1007/978-3-642-55083-6
132. Nasir, S., Hussein, M.Z., Zainal, Z., Yusof, N.A.: Carbon-based nanomaterials/allotropes: a glimpse of their synthesis, properties and some applications. Materials **11**, 295 (2018). https://doi.org/10.3390/ma11020295
133. Feltracco, M., Barbaro, E., Contini, D., Zangrando, R., Toscano, G., Battistel, D., Barbante, C., Gambaro, A.: Photo-oxidation products of α-pinene in coarse, fine and ultrafine aerosol: a new high sensitive HPLC-MS/MS method. Atmos. Environ. **180**, 149–155 (2018). https://doi.org/10.1016/j.atmosenv.2018.02.052
134. Kerminen, V.-M.: Roles of SO_2 and secondary organics in the growth of nanometer particles in the lower atmosphere. J. Aerosol Sci. **30**, 1069–1078 (1999). https://doi.org/10.1016/S0021-8502(98)00775-7
135. Tu, P., Johnston, M.V.: Particle size dependence of biogenic secondary organic aerosol molecular composition. Atmos. Chem. Phys. **17**, 7593–7603 (2017). https://doi.org/10.5194/acp-17-7593-2017
136. Lindner, K., Ströbele M., Schlick, S., Webering, S., Jenckel, A., Kopf, J., Danov, O., Sewald, K., Buj, C., Creutzenberg, O., Tillmann, T., Pohlmann, G., Ernst, H., Ziemann, C., Hüttmann, G., Heine, H., Bockhorn, H., Hansen, T., König, P., Fehrenbach, H.: Biological effects of carbon black nanoparticles are changed by surface coating with polycyclic aromatic hydrocarbons. Part. Fibre Toxicol. **14**, 8 (2017). https://doi.org/10.1186/s12989-017-0189-1
137. Ginoux, P., Chin, M., Tegen, I., Prospero, J.M., Holben, B., Dubovik, O., Lin, S.-J.: Sources and distributions of dust aerosols simulated with GOCART model. J. Geophys. Res. **106**, 20255–20273 (2001). https://doi.org/10.1029/2000JD000053
138. D'Andrea, S.D., Häkkinen, S.A.K., Westervelt, D.M., Kuang, C., Levin, E.J.T., Kanawade, V.P., Leaitch, W.R., Spracklen, D.V., Riipinen, I., Pierce, J.R.: Understanding global secondary organic aerosol amount and size-resolved condensational behavior. Atmos. Chem. Phys. **13**, 11519–11534 (2013). https://doi.org/10.5194/acp-13-11519-2013
139. Taghavi, S.M., Momenpour, M., Azarian, M., Ahmadian, M., Souri, F., Taghavi, S.A., Sadeghain, M., Karchani, M.: Effects of nanoparticles on the environment and outdoor workplaces. Electron. Physician **5**, 706–712 (2013). https://doi.org/10.14661/2013.706-712
140. Rivero, P.J., Urrutia, A., Goicoechea, J., Arregui, F.J.: Nanomaterials for functional textiles and fibers. Nanoscale Res. Lett. **10**, 501 (2015). https://doi.org/10.1186/s11671-015-1195-6
141. Blackford, D.B., Simons, G.R.: Particle size analysis of carbon black. Part. Charact. **4**, 112–117 (1987). https://doi.org/10.1002/ppsc.19870040123
142. ICBA International Carbon Black Association. Carbon Black User's Guide. www.carbon-black.org (2016)
143. SCCS Scientific Committee on Consumer Safety and Chaudhry Q. Opinion of the Scientific Committee on Consusmer Safety (SCCS)—Second revision of the opinion on carbon black, nano-form, in cosmetic products. Regul. Toxicol. Pharmacol. **79**, 103–104 (2016). https://doi.org/10.1016/j.yrtph.2016.02.021
144. Suryanto, B.H.R., Zhao, C.: Surface-oxidized carbon black as a catalyst for the water oxidation and alcohol oxidation reactions. Chem. Commun. **52**, 6439–6442 (2016). https://doi.org/10.1039/c6cc01319h
145. Yuan, L., Lu, X.-H., Xiao, X., Zhai, T., Dai, J., Zhang, F., Hu, B., Wang, X., Gong, L., Chen, J., Hu, C., Tong, Y., Zhou, J., Wang, Z.L.: Flexible solid-state supercapacitors based on carbon

nanoparticles/MnO_2 nanorods hybrid structure. ACS Nano **6**, 656–661 (2012). https://doi.org/10.1021/nn2041279
146. Yuan, L., Tao, Y., Chen, J., Dai, J., Song, T., Ruan, M., Ma, Z., Gong, L., Liu, K., Zhang, X., Hu, X., Zhou, J., Wang, Z.L.: Carbon nanoparticles on carbon fabric for flexible and high-performance field emitters. Adv. Funct. Mater. **21**, 2150–2154 (2011). https://doi.org/10.1002/adfm.201100172
147. Posthuma-Trumpie, G.A., Wichers, J.H., Koets, M., Berendsen, L.B.J.M., van Amerongen, A.: Amorphous carbon nanoparticles: a versatile label for diagnostic (immuno)assays. Anal. Bioanal. Chem. **402**, 593–600 (2012). https://doi.org/10.1007/s00216-011-5340-5
148. Rosic, J.S., Conte, M., Muncan, J., Matija, L., Koruga, D.: Characterization of fullerenes thin film on glasses by UV/VIS/NIR and opto-magnetic imaging spectroscopy. FME Trans. **42**, 172–176 (2014). https://doi.org/10.5937/fmet1402172S
149. Gatti, T., Menna, E., Meneghetti, M., Maggini, M., Petrozza, A., Lamberti, F.: The renaissance of fullerenes with perovskite solar cells. Nano Energy **41**, 84–100 (2017). https://doi.org/10.1016/j.nanoen.2017.09.016
150. Liu, L., Niu, Z., Chen, J.: Unconventional supercapacitors from nanocarbon-based electrode materials to device configurations. Chem. Soc. Rev. **45**, 4340–4363 (2016). https://doi.org/10.1039/c6cs00041j
151. Lv, T., Liu, M., Zhu, D., Gan, L., Chen, T.: Nanocarbon-based materials for flexible all-solid-state supercapacitors. Adv. Mater. **2018**, 1705489 (2018). https://doi.org/10.1002/adma.201705489
152. Yong, Y., Zhou, Q., Li, X., Lv, S.: The $H_{60}Si_6C_{54}$ heterofullerene as high-capacity storage medium. AIP Adv. **6**, 075321 (2016). https://doi.org/10.1063/1.4960330
153. Yoon, M., Yang, S., Hicke, C., Wang, E., Geohegan, D., Zhang, Z.: Calcium as the superior coating metal in functionalization of carbon fullerenes for high-capacity hydrogen storage. Phys. Rev. Lett. **100**, 206806 (2008). https://doi.org/10.1103/physrevlett.100.206806
154. Yoon, M., Yang, S., Wang, E., Zhang, Z.: Charged fullerenes as high-capacity hydrogen storage media. Nano Lett. **7**, 2578–2583 (2007). https://doi.org/10.1021/nl070809a
155. Al-Jumaili, A., Alancherry, S., Bazaka, K., Jacob, M.V.: Review on the antimicrobial properties of carbon nanostructures. Materials **10**, 1066 (2017). https://doi.org/10.3390/ma10091066
156. Teradal, N.L., Jelinek, R.: Carbon nanomaterials in biological studies and biomedicine. Adv. Healthc. Mater. **6**, 1700574 (2017). https://doi.org/10.1002/adhm.201700574
157. De Smet, R., Demoor, T., Verschuere, S., Dullaers, M., Ostroff, G.R., Leclerq, G., Allais, L., Pilette, C., Dierendonck, M., De Geest, B.G., Cuvelier, C.A.: β-Glucan microparticles are good candidates for mucosal antigen delivery in oral vaccination. J. Control Rel. **172**, 671–678 (2013). https://doi.org/10.1016/j.jconrel.2013.09.007
158. des Rieux, A., Fievez, A., Garinot, M., Schneider, Y.-J., Préat, V.: Nanoparticles as potential oral delivery systems of proteins and vaccines: a mechanistic approach. J. Control Rel. **116**, 1–27 (2006). https://doi.org/10.1016/j.jconrel.2006.08.013
159. Zhu, Q., Talton, J., Zhang, G., Cunningham, T., Wang, Z., Waters, R.C., Kirk, J., Eppler, B., Klinman, D.M., Sui, Y., Gagnon, S., Belyakov, I.M., Mumper, R.J., Berzofsky, J.A.: Large intestine-targeted, nanoparticle-releasing oral vaccine to control genitorectal viral infection. Nat. Med. **18**, 1291–1297 (2012). https://doi.org/10.1038/nm.2866
160. Fonte, P., Nogueira, T., Gehm, C., Ferreira, D., Sarmento, B.: Chitosan-coated solid lipid nanoparticles enhance the oral absorption of insulin. Drug Deliv. Transl. Res. **1**, 299–308 (2011). https://doi.org/10.1007/s13346-011-0023-5
161. Ren, T., Wang, Q., Xu, Y., Cong, L., Gou, J., Tao, X., Zhang, Y., He, H., Yin, T., Zhang, H., Zhang, Y., Tang, X.: Enhanced oral absorption and anticancer efficacy of cabazitaxel by overcoming intestinal mucus and epithelium barriers using surface polyethylene oxide (PEO) decorated positively charged polymer-lipid hybrid nanoparticles. J. Control Rel. **269**, 423–438 (2018). https://doi.org/10.1016/j.jconrel.2017.11.015
162. Sun, S., Liang, N., Gong, X., An, W., Kawashima, Y., Cui, F., Yan, P.: Multifunctional composite microcapsules for oral delivery of insulin. Int. J. Mol. Sci. **18**, 54 (2017). https://doi.org/10.3390/ijms18010054

163. Niu, Z., Conejos-Sánchez, I., Griffin, B.T., O'Driscoll, C.M., Alonso, M.J.: Lipid-based nanocarriers for oral peptide delivery. Adv. Drug Deliv. Rev. **106 Part B**, 337–354 (2016). https://doi.org/10.1016/j.addr.2016.04.001
164. Sheng, Y., He, H., Zou, H.: Poly(lactic acid) nanoparticles coated with combined WGA and water-soluble chitosan for mucosal delivery of β-galactosidase. Drug Deliv. **21**, 370–378 (2014). https://doi.org/10.3109/10717544.2014.905653
165. Yin, Y.S., Chen, D.W., Qiao, M.X., Wei, X.Y., Hu, H.Y.: Lectin-conjugated PLGA nanoparticles loaded with thymopentin: ex vivo bioadhesion and in vivo biodistribution. J. Control Rel. **123**, 27–38 (2007). https://doi.org/10.1016/j.jconrel.2007.06.024
166. Menzel, C., Bernkop-Schnürch, A.: Enzyme decorated drug carriers: targeted swords to cleave and overcome the mucus barrier. Adv. Drug Deliv. Rev. **124**, 164–174 (2018). https://doi.org/10.1016/j.addr.2017.10.004
167. Frøkjær, J.B., Drewes, A.M., Gregersen, H.: Imaging of the gastrointestinal tract-novel technologies. World J. Gastroenterol. **15**, 160–168 (2009). https://doi.org/10.3748/wjg.15.160
168. Stark, D.D., Weissleder, R., Elizondo, G., Hahn, P.F., Saini, S., Todd, L.E., Wittenberg, J., Ferrucci, J.T.: Superparamagnetic iron oxide: clinical application as a contrast agent for MR imaging of the liver. Radiology **168**, 297–301 (1988). https://doi.org/10.1148/radiology.168.2.3393649
169. Shokrollahi, H.: Contrast agents for MRI. Mater. Sci. Eng. C **33**, 4485–4497 (2013). https://doi.org/10.1016/j.msec.2013.07.012
170. Li, W., Tutton, S., Vu, A.T., Pierchala, L., Li, B.S.Y., Lewis, J.M., Prasad, P.V., Edelman, R.R.: First-pass contrast-enhanced magnetic resonance angiography in humans using ferumoxytol, a novel ultrasmall superparamagnetic iron oxide (USPIO)-based blood pool agent. J. Magn. Reson. Imaging **21**, 46–52 (2005). https://doi.org/10.1002/jmri.20235
171. Frisch, A., Walter, T.C., Hamm, B., Denecke, T.: Efficacy of oral contrast agents for upper gastrointestinal signal suppression in MRCP: A systematic review of the literature. Acta Radiol. Open **6**, 2058460117727315 (2017). https://doi.org/10.1177/2058460117727315
172. Maccioni, F., Bruni, A., Viscido, A., Colaiacomo, M.C., Cocco, A., Montesani, C., Caprilli, R., Marini, M.: MR imaging in patients with Crohn disease: value of T2- versus T1-weighted gadolinium-enhanced MR sequences with use of an oral superparamagnetic contrast agent. Radiology **238**, 517–530 (2006). https://doi.org/10.1148/radiol.2381040244
173. Gleich, B., Weizenecker, J.: Tomographic imaging using the nonlinear response of magnetic particles. Nature **435**, 1214–1217 (2005). https://doi.org/10.1038/nature03808
174. Salamon, J., Hofmann, M., Jung, C., Kaul, M.G., Werner, F., Them, K., Reimer, R., Nielsen, P., vom Scheidt, A., Adam, G., Knopp, T., Ittrich, H.: Magnetic particle/magnetic resonance imaging: In-Vitro MPI-guided real time catheter tracking and 4D angioplasty using a road map and blood pool tracer approach. PLoS ONE **11**, e0156899 (2016). https://doi.org/10.1371/journal.pone.0156899
175. Yu, E.Y., Chandrasekharan, P., Berzon, R., Tay, Z.W., Zhou, X.Y., Khandhar, A.P., Ferguson, R.M., Kemp, S.J., Zheng, B., Goodwill, P.W., Wendland, M.F., Krishnan, K.M., Behr, S., Carter, J., Conolly, S.M.: Magnetic particle imaging for highly sensitive, quantitative, and safe in vivo gut bleed detection in a murine model. ACS Nano **11**, 12067–12076 (2017). https://doi.org/10.1021/acsnano.7b04844
176. Gamboa, J.M., Leong, K.W.: In vitro and in vivo models for the study of oral delivery of nanoparticles. Adv. Drug Deliv. Rev. **65**, 800–810 (2013). https://doi.org/10.1016/j.addr.2013.01.003
177. Buhrke, T., Lengler, I., Lampen, A.: Analysis of proteomic changes induced upon cellular differentiation of the human intestinal cell line Caco-2. Dev. Growth Differ. **53**, 411–426 (2011). https://doi.org/10.1111/j.1440-169X.2011.01258.x
178. Hidalgo, I.J., Raub, T.J., Borchardt, R.T.: Characterization of the human colon carcinoma cell line (Caco-2) as a model system for intestinal epithelial permeability. Gastroenterology **96**, 736–749 (1989)
179. Sinnecker, H., Ramaker, K., Frey, A.: Coating with luminal gut-constituents alters adherence of nanoparticles to intestinal epithelial cells. Beilstein J. Nanotechnol. **5**, 2308-2315 (2014). https://doi.org/10.3762/bjnano.5.239

180. Béduneau, A., Tempesta, C., Fimbel, S., Pellequer, Y., Jannin, V., Demarne, F., Lamprecht, A.: A tunable Caco-2/HT29-MTX co-culture model mimicking variable permeabilities of the human intestine obtained by an original seeding procedure. Eur. J. Pharm. Biopharm. **87**, 290–298 (2014). https://doi.org/10.1016/j.ejpb.2014.03.017
181. Mahler, G.J., Shuler, M.L., Glahn, R.P.: Characterization of Caco-2 and HT29-MTX cocultures in an in vitro digestion/cell culture model used to predict iron bioavailability. J. Nutr. Biochem. **20**, 494–502 (2009). https://doi.org/10.1016/j.jnutbio.2008.05.006
182. Kernéis, S., Bogdanova, A., Kraehenbuhl, J.-P., Pringault, E.: Conversion by Peyer's patch lymphocytes of human enterocytes into M cells that transport bacteria. Science **277**, 949–952 (1997). https://doi.org/10.1126/science.277.5328.949
183. Ahmad, T., Gogarty, M., Walsh, E.G., Brayden, D.J.: A comparison of three Peyer's patch "M-like" cell culture models: particle uptake, bacterial interaction and epithelial histology. Eur. J. Pharm. Biopharm. **119,** 426–436 (2017). https://doi.org/10.1016/j.ejpb.2017.07.013
184. des Rieux, A., Fievez, V., Théate, I., Mast, J., Préat, V., Schneider, Y.-J.: An improved in vitro model of human intestinal follicle-associated epithelium to study nanoparticle transport by M cells. Eur. J. Pharm. Sci. **30**, 380–391 (2007). https://doi.org/10.1016/j.ejps.2006.12.006
185. Gullberg, E., Leonard, M., Karlsson, J., Hopkins, A.M., Brayden, D., Baird, A.W., Artursson, P.: Expression of specific markers and particle transport in a new human intestinal M cell model. Biochim. Biophys. Res. Commun. **279**, 808–813 (2000). https://doi.org/10.1006/bbrc.2000.4038
186. Schimpel, C., Teubl, B., Absenger, M., Meindl, C., Fröhlich, E., Leitinger, G., Zimmer, A., Roblegg, E.: Development of an advanced intestinal in vitro triple culture permeability model to study transport of nanoparticles. Mol. Pharm. **11**, 808–818 (2014). https://doi.org/10.1021/mp400507g
187. Hilgers, A.R., Conradi, R.A., Burton, P.S.: Caco-2 cell monolayers as a model for drug transport across the intestinal mucosa. Pharm. Res. **7**, 902–910 (1990). https://doi.org/10.1023/A:1015937605100
188. Beloqui, A., des Lieux, A., Préat, V.: Mechanisms of transport of polymeric and lipidic nanoparticles across the intestinal barrier. Adv. Drug Deliv. Rev. **106, Part B**, 242–255 (2016). https://doi.org/10.1016/j.addr.2016.04.014
189. He, B., Lin, P., Jia, Z., Du, W., Qu, W., Yuan, L., Dai, W., Zhang, H., Wang, X., Wang, J., Zhang, X., Zhang, Q.: The transport mechanisms of polymer nanoparticles in Caco-2 epithelial cells. Biomaterials **34**, 6082–6098 (2013). https://doi.org/10.1016/j.biomaterials.2013.04.053
190. Russel-Jones, G.J., Arthur, L., Walker, H.: Vitamin B12-mediated transport of nanoparticles across Caco-2 cells. Int. J. Pharm. **179**, 247–255 (1999). https://doi.org/10.1016/S0378-5173(98)00394-9
191. Sheng, J., Han, L., Qin, J., Ru, G., Li, R., Wu, L., Cui, D., Yang, P., He, Y., Wang, J.: N-Trimethyl chitosan chloride-coated PLGA nanoparticles overcoming multiple barriers to oral insulin absorption. ACS Appl. Mater. Interfaces **7**, 15430–15441 (2015). https://doi.org/10.1021/acsami.5b03555
192. Luo, Y., Teng, Z., Li, Y., Wang, Q.: Solid lipid nanoparticles for oral drug delivery: Chitosan coating improves stability, controlled delivery, mucoadhesion and cellular uptake. Carbohydr. Polym. **122**, 221–229 (2015). https://doi.org/10.1016/j.carbpol.2014.12.084
193. Araújo, F., Shrestha, N., Shahbazi, M.-A., Fonte, P., Mäkilä, E.M., Salonen, J.J., Hirvonen, J.T., Granja, P.L., Santos, H.A., Sarmento, B.: The impact of nanoparticles on the mucosal translocation and transport of GLP-1 across the intestinal epithelium. Biomaterials **35**, 9199–9207 (2014). https://doi.org/10.1016/j.biomaterials.2014.07.026
194. Lichtenstein, D., Ebmeyer, J., Meyer, T., Behr, A.-C., Kästner, C., Böhmert, L., Juling, S., Nieman, B., Fahrenson, C., Selve, S., Thünemann, A.F., Meijer, J., Estrela-Lopis, I., Braeuning, A., Lampen, A.: It takes more than a coating to get nanoparticles through the intestinal barrier in vitro. Eur. J. Pharm. Biopharm. **118**, 21–29 (2017). https://doi.org/10.1016/j.ejpb.2016.12.004
195. Giannasca, K.T., Giannasca, P.J., Neutra, M.R.: Adherence of *Salmonella* typhimurium to Caco-2 cells: identification of a glycoconjugate receptor. Infect. Immun. **64**, 135–145 (1996)

196. Jahn, K.A., Biazik, J.M., Braet, F.: GM1 Expression in Caco-2 cells: characterisation of a fundamental passage-dependent transformation of a cell line. J. Pharmaceut. Sci. **100**, 3751–3762 (2011). https://doi.org/10.1002/jps.22418
197. Behrens, I., Vila Pena, A.I., Alonso, M.J., Kissel, T.: Comparative uptake studies of bioadhesive and non-bioadhesive nanoparticles in human intestinal cell lines and rats: the effect of mucus on particle adsorption and transport. Pharm. Res. **19**, 1185–1193 (2002). https://doi.org/10.1023/A:10198543
198. Ke, Z., Guo, H., Zhu, X., Jin, Y., Huang, Y.: Efficient peroral delivery of insulin via vitamin B_{12} modified trimethyl chitosan nanoparticles. J. Pharm. Pharm. Sci. **18**, 155–170 (2015)
199. Yoshida, T., Yoshioka, Y., Takahashi, H., Misato, K., Mori, T., Hirai, T., Nagano, K., Abe, Y., Mukai, Y., Kamada, H., Tsunoda, S., Nabeshi, H., Yoshikawa, T., Higashisaka, K., Tsutsumi, Y.: Intestinal absorption and biological effects of orally administered amorphous silica particles. Nanoscale Res. Lett. **9**, 532–538 (2014). https://doi.org/10.1186/1556-276X-9-532
200. Wiwattanapatapee, R., Carreño-Gomez, B., Malik, N., Duncan, R.: Anionic PAMAM dendrimers rapidly cross adult rat intestine in vitro: a potential oral delivery system? Pharm. Res. **17**, 991–998 (2000). https://doi.org/10.1023/A:1007587523543
201. Lautenschläger, I., Dombrowski, H., Frerichs, I., Kuchenbecker, S.C., Bade, S., Schultz, H., Zabel, P., Scholz, J., Weiler, N., Uhlig, S.: A model of the isolated perfused rat small intestine. Am. J. Physiol. **298**, G304–G313 (2010). https://doi.org/10.1152/ajpgi.00313.2009
202. Sinnecker, H., Krause, T., Koelling, S., Lautenschläger, I., Frey, A.: The gut wall provides an effective barrier against nanoparticle uptake. Beilstein J. Nanotechnol. **5**, 2092–2101 (2014). https://doi.org/10.3762/bjnano.5.218
203. Bergin, I.L., Witzmann, F.A.: Nanoparticle toxicity by the gastrointestinal route: evidence and knowledge gaps. Int. J. Biomed. Nanosci. Nanotechnol. **3**, 163–210 (2013). https://doi.org/10.1504/ijbnn.2013.054515
204. Delie, F.: Evaluation of nano- and microparticle uptake by the gastrointestinal tract. Adv. Drug Deliv. Rev. **34**, 221–233 (1998). https://doi.org/10.1016/S0169-409X(98)00041-6
205. Bölke, T., Krapf, L., Orzekowsky-Schroeder, R., Vossmeyer, T., Dimitrijevic, J., Weller, H., Schüth, A., Klinger, A., Hüttmann, G., Gebert, A.: Data-adaptive image-denoising for detecting and quantifying nanoparticle entry in mucosal tissues through intravital 2-photon microscopy. Beilstein J. Nanotechnol. **5**, 2016–2025 (2014). https://doi.org/10.3762/bjnano.5.210
206. Lee, C.-M., Lee, T.K., Kim, D.-I., Kim, Y.-R., Kim, M.-K., Jeong, H.-J., Sohn, M.-H., Lim, S.T.: Optical imaging of absorption and distribution of RITC-SiO2 nanoparticles after oral administration. Int. J. Nanomed. **9**(Suppl 2), 243–250 (2014). https://doi.org/10.2147/ijn.s57938
207. Howe, S.E., Lickteig, D.J., Plunkett, K.N., Ryerse, J.S., Konjufca, V.: The uptake of soluble and particulate antigens by epithelial cells in the mouse small intestine. PLoS ONE **9**, e86656 (2014). https://doi.org/10.1371/journal.pone.0086656
208. Loeschner, K., Hadrup, N., Qvortrup, K., Larsen, A., Gao, X., Vogel, U., Mortensen, A., Lam, H.R., Larsen, E.H.: Distribution of silver in rats following 28 days of repeated oral exposure to silver nanoparticles or silver acetate. Part. Fibre Toxicol. **8**, 18 (2011). https://doi.org/10.1186/1743-8977-8-18
209. Jani, P., Halbert, G.W., Langridge, J., Florence, A.T.: Nanoparticle uptake by the rat gastrointestinal mucosa: quantitation and particle size dependency. J. Pharm. Pharmacol. **42**, 821–826 (1990). https://doi.org/10.1111/j.2042-7158.1990.tb07033.x
210. Geraets, L., Oomen, A.G., Krystek, P., Jaobsen, N.R., Wallin, H., Laurentie, M., Verharen, H.W., Brandon, E.F.A., de Jong, W.H.: Tissue distribution and elimination after oral and intravenous administration of different titanium dioxide nanoparticles in rats. Part. Fibre Toxicol. **11**, 30 (2014). https://doi.org/10.1186/1743-8977-11-30
211. Janer, G., Mas del Molino, E., Fernández-Rosas, E., Fernández, A., Vázquez-Campos, S.: Cell uptake and oral absorption of titanium dioxide nanoparticles. Toxicol. Lett. **228**, 103–110 (2014). https://doi.org/10.1016/j.toxlet.2014.04.014

212. Jovanovic, B.: Critical review of public health regulations of titanium dioxide, a human food additive. Integr. Environ. Assess. Manag. **11**, 10–20 (2015). https://doi.org/10.1002/ieam.1571
213. Böckmann, J., Lahl, H., Eckert, T., Unterhalt, B.: Titan-Blutspiegel vor und nach Belastungsversuchen mit Titandioxid. Pharmazie **55**, 140–143 (2000)
214. Jones, K., Morton, J., Smith, I., Jurkschat, K., Harding, A.-H., Evans, G.: Human in vivo and in vitro studies on gastrointestinal absorption of titanium dioxide nanoparticles. Toxicol. Lett. **233**, 95–101 (2015). https://doi.org/10.1016/j.toxlet.2014.12.005
215. Pele, L.C., Thoree, V., Bruggraber, S.F.A., Koller, D., Thompson, R.P.H., Lomer, M.C., Powell, J.J.: Pharmaceutical/food grade titanium dioxide particles are absorbed into the bloodstream of human volunteers. Part. Fibre Toxicol. **12**, 26 (2015). https://doi.org/10.1186/s12989-015-0101-9
216. Rompelberg, C., Heringa, M.B., van Donkersgoed, G., Drijvers, J., Roos, A., Westenbrink, S., Peters, R., van Bemmel, G., Brand, W., Oomen, A.G.: Oral intake of added titanium dioxide and its nanofraction from food products, food supplements and toothpaste by the Dutch population. Nanotoxicology **10**, 1404–1414 (2016). https://doi.org/10.1080/17435390.2016.1222457
217. Weir, A., Westerhoff, P., Fabricius, L., Hristovski, K., von Goertz, N.: Titanium dioxide nanoparticles in food and personal care products. Environ. Sci. Technol. **46**, 2242–2250 (2012). https://doi.org/10.1021/es204168d
218. Jani, P.U., McCarthy, D.E., Florence, A.: Titanium dioxide (rutile) particle uptake from the rat GI tract and translocation to systemic organs after oral administration. Int. J. Pharm. **105**, 157–168 (1994). https://doi.org/10.1016/0378-5173(94)90461-8
219. Hummel, T.Z., Kindermann, A., Stokkers, P.C.F., Benninga, M.A., ten Kate, F.J.W.: Exogenous pigment in Peyer's patches of children suspected of having IBD. J. Pediatr. Gastroenterol. Nutr. **58**, 477–480 (2014). https://doi.org/10.1097/MPG.0000000000000221
220. Shepherd, N.A., Crocker, P.R., Smith, A.P., Levison, D.A.: Exogenous pigment in Peyer's patches. Human Pathol. **18**, 50–54 (1987). https://doi.org/10.1016/S0046-8177(87)80193-4
221. Feliu, N., Docter, D., Heine, M., Del Pino, P., Ashraf, S., Kolosnjaj-Tabi, J., Macchiarini, P., Nielsen, P., Alloyeau, D., Gazeau, F., Stauber, R.H., Parak, W.J.: In vivo degeneration and the fate of inorganic nanoparticles. Chem. Soc. Rev. **45**, 2440–2457 (2016). https://doi.org/10.1039/C5CS00699F
222. Carambia, A., Freund, B., Schwinge, D., Bruns, O.T., Salmen, S.C., Ittrich, H., Reimer, R., Heine, M., Huber, S., Waurisch, C., Eychmüller, A., Wraith, D.C., Korn, T., Nielsen, P., Weller, H., Schramm, C., Lüth, S., Lohse, A.W., Heeren, J., Herkel, J.: Nanoparticle-based autoantigen delivery to Treg-inducing liver sinusoidal endothelial cells enables control of autoimmunity in mice. J. Hepatol. **62**, 1349–1356 (2015). https://doi.org/10.1016/j.jhep.2015.01.006
223. Jung, C.S.L., Heine, M., Freund, B., Reimer, R., Koziolek, E.J., Kaul, M.G., Kording, F., Schumacher, U., Weller, H., Nielsen, P., Adam, G., Heeren, J., Ittrich, H.: Quantitative activity measurements of brown adipose tissue at 7 T magnetic resonance imaging after application of triglyceride-rich lipoprotein 59Fe-superparamagnetic iron oxide nanoparticle: intravenous versus intraperitoneal approach. Invest. Radiol. **51**, 194–202 (2016). https://doi.org/10.1097/RLI.0000000000000235
224. Wang, Y., Zhao, Y., Cui, Y., Zhao, Q., Zhang, Q., Musetti, S., Kinghorn, K.A., Wang, S.: Overcoming multiple gastrointestinal barriers by bilayer modified hollow mesoporous silica nanocarriers. Acta Biomater. **65**, 405–416 (2018). https://doi.org/10.1016/j.actbio.2017.10.025
225. Bartelt, A., Bruns, O.T., Reimer, R., Hohenberg, H., Ittrich, H., Peldschus, K., Kaul, M.G., Tromsdorf, U.I., Weller, H., Waurisch, C., Eychmüller, A., Gordts, P.L.S.M., Rinninger, F., Bruegelmann, K., Freund, B., Nielsen, P., Merkel, M., Heeren, J.: Brown adipose tissue activity controls triglyceride clearance. Nat. Med. **17**, 200–205 (2011). https://doi.org/10.1038/nm.2297
226. Freund, B., Tromsdorf, U.I., Bruns, O.T., Heine, M., Giemsa, A., Bartelt, A., Salmen, S.C., Raabe, N., Heeren, J., Ittrich, H., Reimer, R., Hohenberg, H., Schumacher, U., Weller,

H., Nielsen, P.: A simple and widely applicable method to 59Fe-radiolabel monodisperse superparamagnetic iron oxide nanoparticles for in vivo quantification studies. ACS Nano **6**, 7318–7325 (2012). https://doi.org/10.1021/nn3024267

227. Kreyling, W.G., Hirn, S., Möller, W., Schleh, C., Wenk, A., Celik, G., Lipka, J., Schäffler, M., Haberl, N., Johnston, B.D., Sperling, R., Schmid, G., Simon, U., Parak, W.J., Semmler-Behnke, M.: Air-blood barrier translocation of tracheally instilled gold nanoparticles inversely depends on particle size. ACS Nano **8**, 222–233 (2014). https://doi.org/10.1021/nn403256v
228. Schleh, C., Semmler-Behnke, M., Lipka, J., Wenk, A., Hirn, S., Schäffler, M., Schmid, G., Simon, U., Kreyling, W.G.: Size and surface charge of gold nanoparticles determine absorption across intestinal barriers and accumulation in secondary target organs after oral administration. Nanotoxicology **6**, 36–46 (2012). https://doi.org/10.3109/17435390.2011.552811

Chapter 13
Interactions of Nanoparticles with Skin

Fanny Knorr, Alexa Patzelt, Martina Claudia Meinke, Anika Vogt, Ulrike Blume-Peytavi, Eckart Rühl and Jürgen Lademann

Abstract The interactions of nanoparticles with skin and skin cells are complex and depend on the nanoparticle type. The present work provides an overview on the interactions between solid nanoparticles including silica, titanium dioxide, and silver particulates and skin and skin cells on the basis of previous research results. Generally, nanoparticles applied to skin tend to remain on the skin surface and penetrate only into the upper layers of the stratum corneum and the follicular ducts. In very few cases, nanoparticles have been found in deeper skin layers, particularly if the skin barrier was previously disrupted. Increased nanoparticle penetration may result in biologically relevant effects, e.g. cytotoxic cellular effects induced by silver ions released from wound dressings incorporating silver nanoparticles.

13.1 Introduction

The skin represents an effective barrier that is able to protect the organism from physical, chemical, thermal, oxidative, UV, and microbial influences [1]. The penetration of topically applied drugs and cosmetics as well as environmental deposits on the skin is thus considerably impeded. It is assumed that the bioavailability of topically applied substances is often very low and not higher than 1–2% of the applied dose [2]. Topically applied substances can overcome the skin barrier via three possible pathways, i.e. the intercellular, the follicular, and the transcellular penetration routes (Fig. 13.1). The relevance of each penetration pathway for the percutaneous absorption process strongly depends on the physicochemical properties of the topically

F. Knorr · A. Patzelt · M. C. Meinke · A. Vogt · U. Blume-Peytavi · J. Lademann (✉)
Department of Dermatology, Venerology and Allergology, Charité – Universitätsmedizin Berlin, Chariteplatz 1, 10117 Berlin, Germany
e-mail: juergen.lademann@charite.de

F. Knorr
e-mail: Fanny.knorr@charite.de

E. Rühl
Physical Chemistry, Institute of Chemistry and Biochemistry, Free University of Berlin, Takustrasse 3, 14195 Berlin, Germany

P. Gehr and R. Zellner (eds.), *Biological Responses to Nanoscale Particles*, NanoScience and Technology, https://doi.org/10.1007/978-3-030-12461-8_13

applied substance [3]. However, for most topically applied substances it is assumed that at least two penetration pathways are used in parallel but to a different extent and speed.

It is accepted that the complex intercellular penetration pathway plays an important role in dermal penetration. Topically applied substances have been found to diffuse via complexly arranged lipid layers and overcome alternating hydrophilic and hydrophobic regions. The low bioavailability of most topically applied substances seems to be related to the complexity of this pathway and also to the relatively small active diffusion area as only the intercellular gap is accessible for the substance and not the large area of the corneocytes [4]. In contrast, the transcellular penetration pathway is of minor importance and its relevance is still under discussion. However, some authors suggest a transcellular transport for hydrophilic substances [5], others propose porous polar penetration pathways in the intercellular regions [6]. Although the follicular penetration pathway was considered to be of minor importance in the past, recent investigations could demonstrate its relevance for the penetration of topically applied substances and especially particulate substances [7]. Hair follicles, acting as shunt routes for topically applied nanoparticles (NPs), are widely accepted as sites of preferred agglomeration and deep penetration for a variety of particle types [8, 9]. They are an efficient reservoir for drug delivery as they are surrounded by a dense network of blood capillaries which play an important role in systemic drug delivery. In addition, hair follicles host stem cells, which are important for regenerative medicine, and the Langerhans cells that are responsible for immunomodulation.

While a number of commercially available products, such as drugs, food, cosmetics, and textiles include nanomaterials as active agents, little is known about the

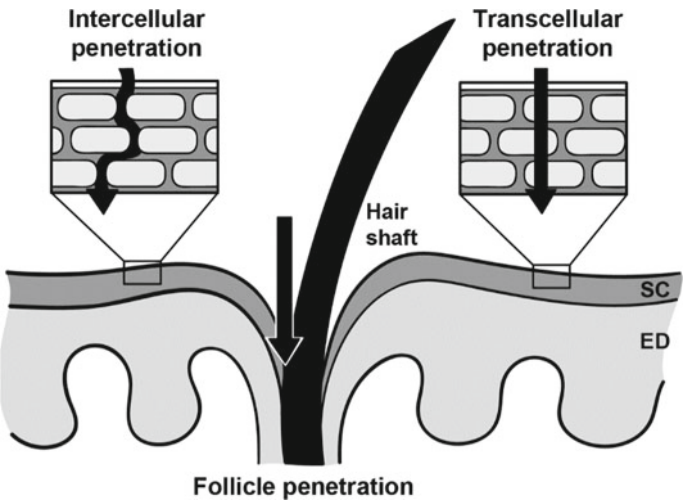

Fig. 13.1 Schematic overview of the three penetration pathways through the skin (SC: stratum corneum, ED: epidermis)

principles underlying NP translocation through the skin barrier as well as their possible interactions with biological processes and the mechanisms of cellular uptake. In the fields of cosmetology and dermatology, NPs are becoming increasingly important tools for the efficient and selective targeting of active agents to skin regions and skin cells. Evidence exists that NPs interact with biological systems differently than their corresponding bulk materials, and several studies have shown that particularly in the nanometer range, particulates may even become harmful [10, 11]. This is especially the case for metal particles, which are designed to exhibit toxic effects against microorganisms. In order to minimize the risks associated with NPs, it is therefore important to understand how their physicochemical properties can influence NP interactions with biological systems. The present overview focuses on studies examining solid NPs including silica (SiO_2), titanium dioxide (TiO_2), and silver (Ag) nanoparticles in particular as representative examples for insights on NP interactions with skin.

13.2 Penetration of NPs into Skin

Several reports suggest that deformable particles, such as liposomes or transferosomes, are able to translocate across the stratum corneum [12, 13]. In contrast, solid NPs administered to skin, e.g. metal particles, such as TiO_2 NPs above 40 nm in sunscreens, tend to remain in the uppermost layers of the stratum corneum as penetration through the intact horny layer and subsequent cellular uptake is highly limited for such particulates [14, 15], but they may lodge in the hair follicles [16]. For example, scanning transmission X-ray microscopy studies visualized 94 ± 6 and 161 ± 13 nm gold core particles with SiO_2 shells and 298 ± 11 nm SiO_2 particles coated with a gold shell in ultramicrotome sections of intact human skin samples on the outermost layers of the stratum corneum and on the epithelium in the upper regions of hair follicles at the single particle level [17]. In exceptional cases, very small particles may be found in the viable skin [18], e.g. Baroli et al. [19] showed that iron NPs smaller than 10 nm could penetrate the skin through the stratum corneum's lipid matrix and hair follicle orifices, reaching the deepest layers of the stratum corneum and less often the uppermost strata of the viable epidermis.

There is strong evidence that the extent of some solid NP penetration into the skin changes if the integrity of the skin barrier is disrupted for some NP types [20–22], such as after mechanical, physical, or chemical damage. When the skin barrier is partially damaged, particles can bypass the rate-limiting stratum corneum barrier and come into direct contact with the first layers of the keratinocytes [23], potentiating their bioavailability. In this context, the particle size is a major determinant for the extent of penetration and cellular uptake and the size limit seems to differ for different particle types.

Patzelt et al. [7] investigated the follicular penetration depth of different nanocarriers on histological sections by laser scanning microscopy (LSM) and could demon-

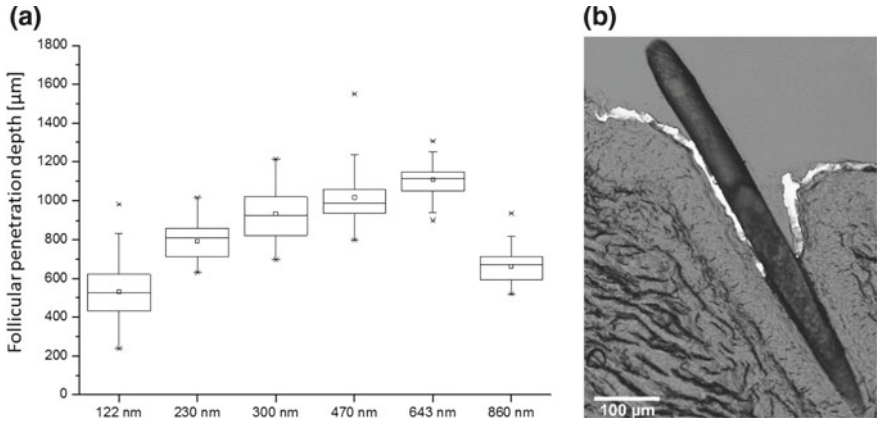

Fig. 13.2 **a** Nanocarriers with different sizes show different follicular penetration depths (data from Patzelt et al. [7]). The differences between the follicular penetration depths of the different nanocarriers were significantly different $p < 0.05$ (exception: 300 nm and 470 nm nanocarriers: $p > 0.05$). **b** Demonstrates a LSM image of a hair follicle showing the follicular penetration of a nanocarrier (size: 122 nm) labelled with a fluorescent dye

strate that nanocarriers with a size around 640 nm penetrated significantly deeper into the hair follicles than smaller or larger nanocarriers (Fig. 13.2).

Rancan et al. [24] used human skin explants pretreated with cyanoacrylate skin surface stripping (CSSS) to compare amorphous SiO_2 particulates of different sizes and surface charges with regard to skin penetration. SiO_2 NPs are promising inorganic NPs for various medical and non-medical applications, such as drug and gene delivery systems [25], and as additives, fillers, and rheological modifiers for food, cosmetics, paints, as well as other products [10], respectively. Deeper penetration through the stratum corneum into the viable epidermis could only partially be observed after mild skin barrier disruption. Abdel-Mottaleb et al. [26] similarly reported penetration and accumulation of polymeric particles sized approx. 100 nm into inflamed skin. Mortensen et al. [22] showed that UV-exposure facilitated penetration for rigid quantum dot NPs, which may cause particle disintegration and therefore an increased likelihood for penetration [27].

Most reports on TiO_2 NPs conclude that the particulates are generally unable to permeate human skin [28]. Their large size and tendency to form aggregates may impede penetration through the skin [29]. Few studies have evaluated TiO_2 penetration into damaged [30–32] and sunburnt or UV-irradiated [33] skin. Filipe et al. [31] examined the localization and skin penetration of TiO_2 and zinc oxide NPs included in two sunscreens in vivo in intact human skin as well as samples that were damaged by tape-stripping. TiO_2 was not detected in the subcorneal epidermis, i.e. the concentrations were below the detection limit in healthy and psoriatic skin. Miquel-Jeanjean et al. [34] found negligible quantities of TiO_2 in the viable epidermis and dermis in normal skin as well as damaged irradiated skin. In a study comparing TiO_2 penetration in healthy and psoriatic skin biopsies by scanning transmission

ion microscopy, Rutherford backscattering spectrometry, and particle-induced X-ray emission, it was reported that the permeation profile of TiO_2 was similar in normal and psoriatic skin despite the labile structure of the stratum corneum [32]. While TiO_2 reached deeper regions of the horny layer in psoriatic skin compared to healthy skin, in no cases did NPs reach the viable layers of the stratum granulosum or stratum spinosum [32]. Monteiro-Riviere et al. [33] attempted to determine whether skin damage by moderate UV-B radiation enhanced the penetration of TiO_2 in commercial sunscreen formulations. The application of TiO_2 was performed in vivo for 24 and 48 h and in vitro in flow-through experiments for 24 h. UVB-sunburnt skin showed a slightly enhanced in vitro or in vivo stratum corneum penetration of TiO_2 NPs. In their in vitro flow-through studies, nanosized TiO_2 was found to penetrate to a depth or 9 layers in the stratum corneum of normal skin and 17 layers in the stratum corneum of UVB-exposed skin. In vivo, TiO_2 penetrated deeper into the horny layer of non-UVB-exposed skin (20 cell layers) than in UVB-exposed skin (12–13 cell layers). This corroborates results by Miquel-Jeanjean et al. [34], which quantified bioavailable titanium at 0.02% of the deposited titanium in irradiated skin versus 0.19% in non-irradiated skin. These low levels in all skin samples confirmed that TiO_2 NPs did not penetrate intact or damaged irradiated pig skin in vitro to a significant degree, and it can therefore be assumed that they are unlikely to penetrate human skin.

The penetration depths of AgNPs into porcine ear skin, a model for human skin, were determined by Ahlberg et al. [35] using confocal Raman microscopy. In intact pig skin, the mean penetration depth was 4.4 ± 1.5 μm, whereby tape stripping and removal of about 70–80% of the stratum corneum prior to the experiment slightly increased the penetration depth to 5.1 ± 2.5 μm. However, results obtained from surface-enhanced Raman scattering (SERS), typical for AgNPs in this size range, showed that single AgNPs penetrated deeply into the stratum corneum in intact skin (19 ± 10 μm). In tape-stripped porcine skin, SERS due to silver nanoparticles was measured deep in the stratum corneum and in the stratum granulosum of the viable skin, indicating a deeper penetration in moderately disrupted skin. First results by Larese et al. [36] showed that, while topically applied AgNPs accumulated predominantly in the horny layer, small amounts of AgNP sized 25 nm passed the intact skin barrier and entered the upper layers of the epidermis. Higher amounts of AgNP came into contact with viable skin cells, such as keratinocytes, when the skin barrier was damaged. Vogt et al. [20] showed that 40 nm NPs, but not 750 or 1500 nm NPs, were able to penetrate the perifollicular dermis through the hair follicles in human skin explants pretreated with cyanoacrylate skin surface stripping (CSSS). Another study elucidated the relevance of shunt penetration in mice, where fluorescent polystyrene particles ranging from 40 to 200 nm in diameter were tracked in hair follicles and the surrounding dermis, as well as in draining lymph nodes and secondary lymphatic organs subsequent to topical administration and skin surface stripping [21]. Using polystyrene particles and Modified Vaccinia Ankara Virus as an example for biologically and immunologically relevant particulates in the context of transcutaneous vaccination, hair follicles were recently identified as sites of nanomaterial transloca-

tion into the viable tissue, particularly when tape stripping was performed to cause mild skin barrier disruption [20, 21].

13.3 Biological Effects and Cellular Uptake of NPs in Skin and Skin Cells

The first cell layers of the epidermis represent another barrier to NP translocation into the viable skin, which are interconnected by tight junctions. In order to penetrate the skin, particles must be sufficiently small to bypass the tight junctions (approx. 6 nm) or be internalized by cells [23]. Particularly for metal particles designed to exhibit toxic effects against microorganisms, collateral damage to healthy skin may become a limiting factor. Several studies have shown pro-inflammatory adjuvant effects of negatively charged SiO_2 NPs during ovalbumin or mite antigen-induced allergic dermatitis and allergic airway disease in cases where NP and antigen were administered simultaneously as an immunogenic challenge [37–40]. However, research has suggested that surface functionalization of SiO_2 NPs may reduce their in vitro and in vivo cytotoxicity considerably compared to unfunctionalized SiO_2 NPs [41]. In addition, positively charged *N*-(6-aminohexyl)-aminopropyltrimethoxysilane (AHAPS)-functionalization of SiO_2 NPs resulted in increased colloidal stability compared to unfunctionalized SiO_2 NPs and distinctly reduced their tendency to aggregate [42]. Ostrowski et al. [43] therefore investigated the topical effect of positively charged AHAPS-functionalized SiO_2 NP exposure in a murine model of acute oxazolone-induced allergic contact dermatitis. In contrast to previous investigations with negatively charged SiO_2 NPs, which had aggravated allergic reactions in the skin and airways using the same dosages [37–40], the functionalized NPs did not appear to have any effects on the quality or degree of inflammation in diseased tissue. Presumably, the AHAPS functionalized SiO_2 NPs did not penetrate beyond the stratum corneum, which is in accordance with an earlier study on the distribution and levels of penetration of AHAPS SiO_2 NPs [44]. Both, the failure to penetrate beyond the horny layer and the improved biocompatibility due to surface functionalization [41] may have prevented the aggravation of barrier defects and inflammatory response in previous work [43].

Several in vitro studies have reported oxidative stress induction and cell death in mammalian cells treated with TiO_2 NPs. Wright et al. [45] analyzed the effects of differently sized TiO_2 NPs on oxidative stress levels in human keratinocytes and observed a significant dose-response increase in superoxide levels and subsequent apoptosis in HaCaT cells, as also evidenced in other cell lines [46]. It was determined that UV-C exposure had no significant effect on TiO_2-induced apoptosis in HaCaT cells, however, this is in contrast to other reports that pre-exposing cells to UV radiation may enhance the cytotoxic effects of TiO_2 NPs [47–49]. A possible explanation may be the comparably weaker rays of UV-C radiation, which emit less

radiation than UV-A and UV-B. Furthermore, the various TiO_2 particles studied had no consistent effects on cell proliferation and viability of HaCaT keratinocytes.

In studies by Ahlberg et al. [35], possible noxious in vitro effects of spherical poly(*N*-vinylpyrrolidone)-coated AgNPs with a negative zeta potential of—20 mV and a metallic core of approx. 70 ± 20 nm on the human keratinocyte cell line HaCaT were investigated. Medical applications comprising AgNP, such as wound dressings and gels, are based on the antibacterial and anti-inflammatory potential of slowly released silver ions (Ag^+) [50–52]. However, AgNP-specific and Ag^+-specific cytotoxic effects have been reported [53].

The main mechanism of cytotoxicity appears to be the release of Ag^+ from AgNPs in the presence of oxygen, which can exert silver toxicity in bacteria and eukaryotic cells [54], resulting in DNA breakage, apoptosis, and necrosis [55]. Particularly when applied repetitively to burns or open lesions, direct AgNP exposure of vital epidermis cells and cellular uptake is likely to occur. Possible biological effects of such cellular uptake were investigated in in vitro experiments on AgNP-treated HaCaT cells by transmission electron microscopy (TEM) and the cell viability assay (XTT). Furthermore, the influence of fetal calf serum content in cell media on AgNP cytotoxicity was examined. TEM results confirmed the intracellular uptake of AgNP in cellular vesicles. The XTT signal increased in cells incubated with low concentrations of Ag, but it decreased for cells incubated with 40 μg/mL. A serum concentration in the cell culture media below the required amount of 9% resulted in a reduction in cell viability for all concentrations of AgNP. When toxic concentrations of AgNPs were applied to HaCaT cells, cell death occurred as a result of degeneration of the cell nuclei and cell membranes [35]. Electron paramagnetic resonance (EPR) spectroscopy, used to detect free radicals in cell suspensions, was implemented by using the spin probe TEMPO (2,2,6,6-tetramethylpiperidine-1-oxyl) to investigate the AgNP-mediated intracellular production of reactive oxygen species (ROS) in cells and whole skin. If radicals are present, the signal of the spin probe decreases. AgNPs reduced the TEMPO signal after 1 h incubation time in HaCaT cells, whereby the ROS production was dependent on the formation and storage condition of the AgNPs. AgNPs produced under ambient air conditions formed more ROS compared to AgNP produced and stored in an argon atmosphere, as the oxygen in the ambient atmosphere was responsible for the formation of silver ions (Ag^+) by oxidation of the AgNPs. These findings confirmed the role of Ag^+ ions in AgNP-mediated oxidative stress and cell damage as depicted in Fig. 13.3. Reactive-oxygen species-mediated DNA damage and apoptosis were similarly reported for epidermal cells in human skin after exposure to nickel NPs [56].

Cellular uptake by particles varies depending on the cell type, and immune cells are particularly specialized in taking up pathogens or proteins and other antigens via endocytosis, macropinocytosis, and phagocytosis [57]. Flow cytometry analysis of freshly isolated skin cells incubated with differently sized SiO_2 NPs by Rancan et al. [24] showed that the particle size, the degree of aggregation, and the surface charge influenced particle uptake by epidermal cells and Langerhans cells considerably. In skin explants pretreated by CSSS, a small number of keratinocytes and Langerhans cells that had internalized particles sized 42 nm, but not 75 or 291 nm, were isolated.

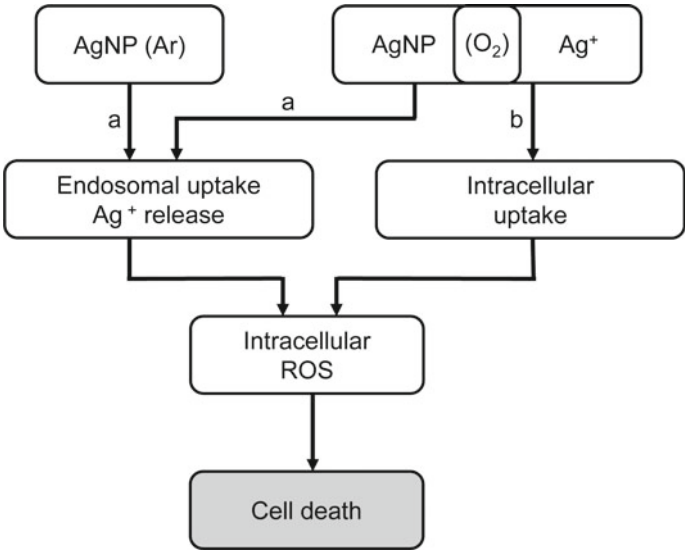

Fig. 13.3 Schematic picture of the uptake and cytotoxic effects of two different AgNP. AgNP (Ar) with low content of Ag^+ ions are taken up by endosomes (**a**), AgNP (O_2) can be likewise uptaken by endocytosis (**a**) and the Ag^+ ions by cells (**b**). The released ions induce intracellular ROS which can lead to cell death (modified according to [35])

In vitro, HaCaT cells and Langerhans cells took up particles with a diameter of 200 nm and larger aggregates via phagocytosis or macropinocytosis, while epidermis cells internalized NPs smaller than 200 nm by endocytosis. Under cell culture conditions, HaCaT cells and primary human keratinocytes showed an increased uptake of SiO_2 nanoparticles with positive surface charge due to positively charged ligands. This was contrasted by an increased tendency to form aggregates, which may explain why barrier translocation did not occur, in spite of increased cellular uptake [24]. However, results obtained from cell culture conditions are not always predictive for ex vivo or in vivo tissue studies, e.g. in a previous study using biodegradable poly(lactic acid) particles (228 and 365 nm) loaded with fluorescent dyes and human skin explants. It was found for mono-disperse and stable aqueous solutions, that skin contact with the NPs led to destabilization of the particles and a release of the dyes [58].

13.4 Conclusion

The aim of the present work was to provide a comprehensive overview of the complexities of NP-skin interactions, with a particular focus on SiO_2 NPs, TiO_2 NPs and AgNPs. Research on the dermal penetration of NPs has shown that the majority

of solid NPs remain on the skin surface under ex vivo conditions, whereby a small number may be found in deeper skin layers. The hair follicles play an important role as shunt routes, storage sites, and presumptive routes of entry. When the integrity of the skin barrier is disturbed, increased NP penetration may occur, resulting in biologically relevant effects. This is particularly the case when metal NPs are applied intentionally to inflamed or wounded skin. Secondary effects, induced by NP contact with the viable tissue, include Ag^+ release from AgNPs with resulting cytotoxic effects. Notably, biological effects resulting from NP interactions and cellular uptake of nanoparticles vary depending on experimental setups and the cell types examined.

Acknowledgements We thankfully acknowledge the Deutsche Forschungsgemeinschaft for their support of the Priority Program SPP 1313 "Biological Responses to Nanoscale Particles".

References

1. Menon, G.K., Kligman, A.M.: Barrier functions of human skin: a holistic view. Skin Pharmacol. Physiol. **22**(4), 178–189 (2009)
2. Hadgraft, J., Lane, M.E.: Advanced topical formulations (ATF). Int. J. Pharm. **514**(1), 52–57 (2016)
3. Patzelt, A., Lademann, J.: Drug delivery to hair follicles. Expert Opin. Drug Deliv. **10**(6), 787–797 (2013)
4. Albery, W.J., Hadgraft, J.: Percutaneous absorption: in vivo experiments. J. Pharm. Pharmacol. **31**(3), 140–147 (1979)
5. Barbero, A.M., Frasch, H.F.: Transcellular route of diffusion through stratum corneum: results from finite element models. J. Pharm. Sci. **95**(10), 2186–2194 (2006)
6. Sznitowska, M., Janicki, S., Williams, A.C.: Intracellular or intercellular localization of the polar pathway of penetration across stratum corneum. J. Pharm. Sci. **87**(9), 1109–1114 (1998)
7. Patzelt, A., et al.: Selective follicular targeting by modification of the particle sizes. J. Control. Release **150**(1), 45–48 (2011)
8. Toll, R., et al.: Penetration profile of microspheres in follicular targeting of terminal hair follicles. J. Invest. Dermatol. **123**(1), 168–176 (2004)
9. Lademann, J., et al.: Drug delivery with topically applied nanoparticles: science fiction or reality. Skin Pharmacol. Physiol. **26**(4–6), 227–233 (2013)
10. Napierska, D., et al.: The nanosilica hazard: another variable entity. Part. Fibre Toxicol. **7**(1), 39 (2010)
11. Shvedova, A.A., Kagan, V.E., Fadeel, B.: Close encounters of the small kind: adverse effects of man-made materials interfacing with the nano-cosmos of biological systems. Annu. Rev. Pharmacol. Toxicol. **50**, 63–88 (2010)
12. Cevc, G., Schätzlein, A., Richardsen, H.: Ultradeformable lipid vesicles can penetrate the skin and other semi-permeable barriers unfragmented. Evidence from double label CLSM experiments and direct size measurements. Biochim. Biophys. Acta **1564**(1), 21–30 (2002)
13. Schätzlein, A., Cevc, G.: Non-uniform cellular packing of the stratum corneum and permeability barrier function of intact skin: a high-resolution confocal laser scanning microscopy study using highly deformable vesicles (Transfersomes). Br. J. Dermatol. **138**(4), 583–592 (1998)
14. Lademann, J., et al.: Penetration of titanium dioxide microparticles in a sunscreen formulation into the horny layer and the follicular orifice. Skin Pharmacol. Appl. Skin Physiol. **12**(5), 247–256 (1999)
15. Sadrieh, N., et al.: Lack of significant dermal penetration of titanium dioxide from sunscreen formulations containing nano- and submicron-size TiO_2 particles. Toxicol. Sci. **115**(1), 156–166 (2010)

16. Lademann, J., et al.: Hair follicles—a long-term reservoir for drug delivery. Skin Pharmacol. Physiol. **19**(4), 232–236 (2006)
17. Graf, C., et al.: Qualitative detection of single submicron and nanoparticles in human skin by scanning transmission X-ray microscopy. J. Biomed. Opt. **14**(2), 021015 (2009)
18. Larese, F.F., et al.: Human skin penetration of cobalt nanoparticles through intact and damaged skin. Toxicol. In Vitro **27**, 121–127 (2013)
19. Baroli, B., et al.: Penetration of metallic nanoparticles in human full-thickness skin. J. Invest. Dermatol. **127**(7), 1701–1712 (2007)
20. Vogt, A., et al.: 40 nm, but not 750 or 1,500 nm, nanoparticles enter epidermal $CD1a^+$ cells after transcutaneous application on human skin. J. Invest. Dermatol. **126**(6), 1316–1322 (2006)
21. Mahe, B., et al.: Nanoparticle-based targeting of vaccine compounds to skin antigen-presenting cells by hair follicles and their transport in mice. J. Invest. Dermatol. **129**(5), 1156–1164 (2009)
22. Mortensen, L.J., et al.: In vivo skin penetration of quantum dot nanoparticles in the murine model: the effect of UVR. Nano Lett. **8**(9), 2779–2787 (2008)
23. Kubo, A., et al.: External antigen uptake by Langerhans cells with reorganization of epidermal tight junction barriers. J. Exp. Med. **206**(13), 2937–2946 (2009)
24. Rancan, F., et al.: Skin penetration and cellular uptake of amorphous silica nanoparticles with variable size, surface functionalization, and colloidal stability. ACS Nano **6**(8), 6829–6842 (2012)
25. Wang, L., Zhao, W., Tan, W.: Bioconjugated silica nanoparticles: development and applications. Nano Res **1**, 99–115 (2008)
26. Abdel-Mottaleb, M.M., et al.: Surface-charge-dependent nanoparticles accumulation in inflamed skin. J. Pharm. Sci. **101**(11), 4231–4239 (2012)
27. Bennett, S.W., et al.: Photoinduced disaggregation of TiO(2) nanoparticles enables transdermal penetration. PLoS ONE **7**(11), e48719 (2012)
28. Adachi, K., et al.: Subchronic exposure of titanium dioxide nanoparticles to hairless rat skin. Exp. Dermatol. **22**(4), 278–283 (2013)
29. Larese Filon, F., et al.: Nanoparticles skin absorption: New aspects for a safety profile evaluation. Regul. Toxicol. Pharmacol. **72**(2), 310–322 (2015)
30. Senzui, M., et al.: Study on penetration of titanium dioxide (TiO(2)) nanoparticles into intact and damaged skin in vitro. J. Toxicol. Sci. **35**(1), 107–113 (2010)
31. Filipe, P., et al.: Stratum corneum is an effective barrier to TiO_2 and ZnO nanoparticle percutaneous absorption. Skin Pharmacol. Physiol. **22**(5), 266–275 (2009)
32. Pinheiro, T., et al.: The influence of corneocyte structure on the interpretation of permeation profiles of nanoparticles across skin. Nucl. Instrum. Methods Phys. Res. Sect. B **260**(1), 119–123 (2007)
33. Monteiro-Riviere, N.A., et al.: Safety evaluation of sunscreen formulations containing titanium dioxide and zinc oxide nanoparticles in UVB sunburned skin: an in vitro and in vivo study. Toxicol. Sci. **123**, 264–280 (2011)
34. Miquel-Jeanjean, C., et al.: Penetration study of formulated nanosized titanium dioxide in models of damaged and sun-irradiated skins. Photochem. Photobiol. **88**(6), 1513–1521 (2012)
35. Ahlberg, S., et al.: Comparison of silver nanoparticles stored under air or argon with respect to the induction of intracellular free radicals and toxic effects toward keratinocytes. Eur. J. Pharm. Biopharm. **88**(3), 651–657 (2014)
36. Larese, F.F., et al.: Human skin penetration of silver nanoparticles through intact and damaged skin. Toxicology **255**(1–2), 33–37 (2009)
37. Brandenberger, C., et al.: Engineered silica nanoparticles act as adjuvants to enhance allergic airway disease in mice. Part. Fibre Toxicol. **10**, 26 (2013)
38. Hirai, T., et al.: Amorphous silica nanoparticles size-dependently aggravate atopic dermatitis-like skin lesions following an intradermal injection. Part. Fibre Toxicol. **9**, 3 (2012)
39. Hirai, T., et al.: Size-dependent immune-modulating effect of amorphous nanosilica particles. Pharmazie **66**(9), 727–728 (2011)
40. Yoshida, T., et al.: Promotion of allergic immune responses by intranasally-administrated nanosilica particles in mice. Nanoscale Res. Lett. **6**(1), 195 (2011)

41. Yoshida, T., et al.: Surface modification of amorphous nanosilica particles suppresses nanosilica-induced cytotoxicity, ROS generation, and DNA damage in various mammalian cells. Biochem. Biophys. Res. Commun. **427**(4), 748–752 (2012)
42. Graf, C., et al.: Surface functionalization of silica nanoparticles supports colloidal stability in physiological media and facilitates internalization in cells. Langmuir **28**(20), 7598–7613 (2012)
43. Ostrowski, A., et al.: AHAPS-functionalized silica nanoparticles do not modulate allergic contact dermatitis in mice. Nanoscale Res. Lett. **9**(1), 524 (2014)
44. Ostrowski, A., et al.: Skin barrier disruptions in tape stripped and allergic dermatitis models have no effect on dermal penetration and systemic distribution of AHAPS-functionalized silica nanoparticles. Nanomedicine **10**(7), 1571–1581 (2014)
45. Wright, C., et al.: Effects of titanium dioxide nanoparticles on human keratinocytes. Drug Chem. Toxicol. **40**(1), 90–100 (2017)
46. Niska, K., et al.: Titanium dioxide nanoparticles enhance production of superoxide anion and alter the antioxidant system in human osteoblast cells. Int. J. Nanomed. **10**, 1095–1107 (2015)
47. Cai, R., et al.: Induction of cytotoxicity by photoexcited TiO_2 particles. Cancer Res. **52**(8), 2346–2348 (1992)
48. Zhang, A.P., Sun, Y.P.: Photocatalytic killing effect of TiO_2 nanoparticles on Ls-174-t human colon carcinoma cells. World J. Gastroenterol. **10**(21), 3191–3193 (2004)
49. Kang, S.J., et al.: Cytotoxicity and genotoxicity of titanium dioxide nanoparticles in UVA-irradiated normal peripheral blood lymphocytes. Drug Chem. Toxicol. **34**(3), 277–284 (2011)
50. Ahamed, M., Alsalhi, M.S., Siddiqui, M.K.: Silver nanoparticle applications and human health. Clin. Chim. Acta **411**(23–24), 1841–1848 (2010)
51. Chernousova, S., Epple, M.: Silver as antibacterial agent: ion, nanoparticle, and metal. Angew. Chem. Int. Ed. Engl. **52**(6), 1636–1653 (2013)
52. Rai, M., Yadav, A., Gade, A.: Silver nanoparticles as a new generation of antimicrobials. Biotechnol. Adv. **27**(1), 76–83 (2009)
53. Chambers, B.A., et al.: Effects of chloride and ionic strength on physical morphology, dissolution, and bacterial toxicity of silver nanoparticles. Environ. Sci. Technol. **48**(1), 761–769 (2014)
54. Greulich, C., et al.: The toxic effect of silver ions and silver nanoparticles towards bacteria and human cells occurs in the same concentration range. RSC Adv. **2**(17), 6981–6987 (2012)
55. Foldbjerg, R., et al.: PVP-coated silver nanoparticles and silver ions induce reactive oxygen species, apoptosis and necrosis in THP-1 monocytes. Toxicol. Lett. **190**(2), 156–162 (2009)
56. Alarifi, S., et al.: Reactive oxygen species-mediated DNA damage and apoptosis in human skin epidermal cells after exposure to nickel nanoparticles. Biol. Trace Elem. Res. **157**(1), 84–93 (2014)
57. Coombes, J.L., Robey, E.A.: Dynamic imaging of host-pathogen interactions in vivo. Nat. Rev. Immunol. **10**(5), 353–364 (2010)
58. Rancan, F., et al.: Investigation of polylactic acid (PLA) nanoparticles as drug delivery systems for local dermatotherapy. Pharm. Res. **26**(8), 2027–2036 (2009)

Index

P. Gehr and R. Zellner (eds.), *Biological Responses to Nanoscale Particles*,
NanoScience and Technology, https://doi.org/10.1007/978-3-030-12461-8